STRENGTH CHARACTERISTICS OF POLYMER MODIFIED ASPHALT BINDERS AND MIXES

Ph.D. THESIS

by

NIKHIL SABOO

DEPARTMENT OF CIVIL ENGINEERING
INDIAN INSTITUTE OF TECHNOLOGY ROORKEE
ROORKEE – 247 667 (INDIA)
DECEMBER, 2015

STRENGTH CHARACTERISTICS OF POLYMER MODIFIED ASPHALT BINDERS AND MIXES

A THESIS

Submitted in partial fulfilment of the requirements for the award of the degree of

DOCTOR OF PHILOSOPHY

in

CIVIL ENGINEERING

by

NIKHIL SABOO

DEPARTMENT OF CIVIL ENGINEERING
INDIAN INSTITUTE OF TECHNOLOGY ROORKEE
ROORKEE – 247 667 (INDIA)
DECEMBER, 2015

INDIAN INSTITUTE OF TECHNOLOGY ROORKEE
ROORKEE

CANDIDATE'S DECLARATION

I hereby certify that the work which is being presented in the thesis entitled "**STRENGTH CHARACTERISTICS OF POLYMER MODIFIED ASPHALT BINDERS AND MIXES"**, in partial fulfilment of the requirements for the award of the Degree of Doctor of Philosophy and submitted in the Department of Civil Engineering of the Indian Institute of Technology Roorkee, Roorkee, is an authentic record of my own work carried out during the period from January, 2013 to December, 2015 under the supervision of Dr. Praveen Kumar, Professor, Civil Engineering Department, Indian Institute of Technology Roorkee, Roorkee, India.

The matter presented in this thesis has not been submitted by me for the award of any other degree of this or any other Institute.

(NIKHIL SABOO)

This is to certify that the above statement made by the candidate is correct to the best of my knowledge.

(PRAVEEN KUMAR)
Supervisor

Date:

Abstract

With the ever increasing demands of traffic and temperature imposed on highways, it has become mandatory to find alternative means, either in terms of design or use of better materials, to tackle these issues. Modification of bitumen is one of the simplest and most effective techniques which has been used over years to increase the strength and life of pavements. Out of various forms of modification, polymer modification has gained the most importance due to its capability to improve the viscoelastic response of the bitumen. It increases the stiffness of asphalt binder at higher temperature while maintains the flexibility at lower temperatures, thereby improving both the rutting and fatigue resistance of bitumen.

The study of viscoelastic response of bitumen is usually done using dynamic shear rheometer (DSR). DSR can capture various rheological aspects of bitumen at a wide range of frequency and temperature. The traditional Superpave parameters for characterization of rutting and fatigue resistance of bitumen ($G^*/\sin\delta$ and $G^*.\sin\delta$) has been criticized in many literatures and has been found inadequate, specially for modified binders. Improvement in the test methods came out in form of multiple stress creep and recovery (MSCR) and linear amplitude sweep (LAS) test for quantifying the rutting and fatigue characteristics of bitumen.

The study of binder alone is not sufficient for judging the performance of the pavement. Aggregate gradation also plays a vital role in describing the overall performance of the asphalt mixture. Asphalt mixture are usually dense graded, gap graded or open graded. The volumetrics of these different aggregate gradation along with the properties and amount of asphalt binder is responsible for total characterization of the asphalt mixture. In India, Marshall mix design is used for evaluation of optimum binder content. In order to evaluate the permanent deformation and fatigue characteristics of asphalt mixtures, tests like wheel rut test and four point beam bending test are the most common. Correlation between the binder and mix attributes is another important aspect for judging field performance of the asphalt mix.

This research outlines the study conducted on conventional and polymer modified asphalt binders and mixes. The conventional and rheological properties of the asphalt binders

are studied in detail at a temperature range of 10-70 ˚C. The performance of these binders with respect to fatigue and rutting is evaluated and the suitability of binder for different practical conditions is explored. The study also evaluates the performance of different aggregate gradations with use of tests like Marshall stability and flow, indirect tension test, wheel rut test and four point beam bending test. The correlation of binder properties with mix results are also taken up as a part of this research.

The study begins with finding the optimum blending requirements and optimum modifier content of two polymers i.e ethylene vinyl acetate (EVA) and styrene butadiene styrene (SBS). SBS was incorporated in VG 10 at five different modifier content of 1-5% while EVA was blended at 1-7%. The blending temperature, shear rate and time was varied from 160-200 ˚C, 300-1500 s^{-1} and 20-60 minutes respectively. Conventional binder like VG 10 and VG 30 were also used for comparison. Storage stability and fluorescence microscopy were used to find the optimum blending requirements and modifier content. From the analysis it was found that SBS could be incorporated in the base binder at a temperature of 180 °C using a high shear mixture operated at 1500 rpm for 60 minutes. The corresponding temperature, shear rate and time for EVA were 190 °C, 600 rpm and 30 minutes. Storage stability test showed that optimum modifier content for EVA is 5% while for SBS is 3%. This result was also validated by the study of morphology using Fluorescence microscopy. An interlocked bitumen-polymer phase is the most desirable for obtaining a homogenous blend.

The flow properties of the binders were evaluated using steady shear method. The viscosity versus shear rate for the binders were measured using DSR at a temperature range of 40-80 ˚C. Carreau-Yasuda (C-Y) equation was combined with the concept of rheogram to simulate the variation of viscosity versus shear rate. A new model was proposed which could be used to evaluate the mixing temperature of asphalt binder corresponding to the viscosity at any desired shear rate. The model was found to be critical to the value of zero shear viscosity (ZSV). At higher shear rates the viscosity of the modified binders were found to be even lower than the conventional binders owing to the shear thinning behavior, which indicated that lower mixing temperatures could be used for modified binders at practical shear rates.

The rheological measurements for all the binders were done using frequency sweep test at a temperature range of 10-70 ˚C. The linear viscoelastic (LVE) limits were evaluated as the initial part of the study. The effect of spindle geometry and plate gap was also evaluated. 25 mm and 8 mm diameter spindle were used. For 25 mm, three spindle gaps viz. 1 mm, 2 mm and 3 mm were used, while for 8 mm diameter 1 mm and 2 mm gap was employed. Master curves were constructed at three different reference temperatures of 20, 40 and 60 ˚C. Various shift factor methods were analyzed and a new method was proposed for the construction of master curves. The method was named as 'Equivalent Slope Method'. The complex modulus and phase angle master curves were modelled using the concept of rheogram and C-Y equation. At higher temperatures spindle diameter 8 mm gave higher values for complex modulus and phase angle of the asphalt binders as compared to 25 mm diameter spindle. At higher temperatures higher plate gap gave lower values of complex modulus as compared to lower gap width. The difference in the measurements decreased with decrease in temperature with similar values at intermediate temperatures. It was found that spindle geometry plays a crucial role in determination of rheological properties of both conventional and modified binders. The shift factor obtained by the equivalent slope method which was developed in the study gave the better results in plotting master curves as compared to WLF and Arrhenius equation. It was found that Cox-Merz rule can be successfully applied in the zero shear viscosity domain. The simple C-Y model was found to be successfully applicable in modelling the rheological properties of both conventional and modified bitumen. Phase angle was found to be sensitive to the type and chemical nature of bitumen.

The performance of the binder with respect to rutting and fatigue were evaluated using MSCR and LAS test. Multiple Stress Creep and Recovery (MSCR) test was conducted at three different temperatures (40, 50 and 60 °C) using Dynamic Shear Rheometer (DSR) operated in constant stress mode. Four different stress levels were chosen, viz. 100, 3200, 5000 and 10,000 Pa. The test was done using 25 mm sample geometry with 1 mm gap between the spindle and the base plate on RTFO aged samples. The strain response was modelled using Burgers four element model and power law model. Applicability of Boltzmann superposition principle was also checked in the study. Burger model was not able to model the delayed elastic response of asphalt binders. The power law model was modified

for the recovery domain to incorporate the effect of delayed elastic response. The model parameters were analyzed and were correlated with the conventional properties like softening point and ZSV of the binders. LAS test was conducted at 10, 20 and 30 ˚C to determine the fatigue lives of the asphalt binders. The parameters A and B were evaluated at different temperatures. LAS test was found to be more practical than the existing intermediate performance criteria of $G^*.sin\delta$. By LAS test it was possible to evaluate the complex behavior of the binder at a wide range of loading level. PMB (S) gave the best overall performance in both the test methods. PMB (E), though performs well at higher temperature, but at intermediate pavement temperature it may be susceptible to fatigue cracking attributed to higher sensitivity to strain amplitudes. Among the conventional binders both VG 10 and VG 30 were found to be suitable for resisting fatigue cracking at intermediate pavement temperatures. Nevertheless, at higher temperatures both VG 10 and VG 30 showed poor performance.

Marshall mix design was used for the preparation of asphalt mixtures with three different aggregate gradation viz. bituminous concrete (BC), dense bituminous macadam (DBM) and stone mastic asphalt (SMA). All the mixes were prepared at 4% target air void content. The moisture susceptibility of the mixtures were also evaluated using retained Marshall stability test and tensile strength ratio. The film thickness for these mixtures were also calculated. Modified mixtures were found to have higher strength than the mixes prepared with conventional binders. The Marshall stability and indirect tension strength of SMA was found to be lower than BC and DBM, however their retained Marshall stability and tensile strength ratio were higher indicating higher resistance to moisture damage. Moreover, the film thickness for SMA was found to be higher in comparison to BC and DBM, attributed to higher void in mineral aggregates (VMA). This indicated better durability for these mixtures.

The last part of the study dealt with the evaluation of rutting and fatigue performance of the asphalt mixtures. Rutting characteristics was evaluated using wheel rut testing at 60 ˚C. Fatigue performance of the mixes was evaluated using four point beam bending test (4PBBT). This test was performed at 20 ˚C at a strain level ranging from 200-1000 micro-strains. A new phenomenological model was proposed to characterize the variation of fatigue

life at different strain levels. Correlation of rutting and fatigue test with binder performance was also attempted. It was found that SMA had the highest rutting and fatigue life in comparison to BC and DBM. Plastomeric modified mixes were found to be highly susceptible to change in strain levels. In rut depth was found to correlate fairly well with the unrecoverable creep compliance from the MSCR test. The fatigue life of asphalt binders from LAS test showed linear correlation with the fatigue life from 4PBBT. The new phenomenological model proposed in the study correlated appreciably with the measured response.

ACKNOWLEDGEMENT

Though only my name appears on the cover of this dissertation, a great many people have contributed to its production. I owe my gratitude to all those people who have made this dissertation possible and because of whom my PhD experience has been one that I will cherish forever.

First and foremost, I thank the almighty God who showered his blessings, without which it would have not been possible for me to complete the dissertation in the present form.

My deepest gratitude is to my advisor, **Dr. Praveen Kumar, Professor IIT Roorkee**. I have been amazingly fortunate to have an advisor who gave me the freedom to explore on my own, and at the same time the guidance to recover when my steps faltered. He taught me how to question thoughts and express ideas. His patience and support helped me overcome many crisis situations and finish this dissertation. I hope that one day I would become as good an advisor to my students as Dr. Kumar has been to me.

I am grateful to **Dr. B.B Pandey, Emeritus Professor, IIT Kharagapur** and **Dr. Animesh Das, Professor, IIT Kanpur,** for their encouragement and practical advice. I am also thankful to them for commenting on my views and helping me understand and enrich my ideas.

I would also like to thank **Professor Satish Chandra,** and **Professor S.S Jain, IIT Roorkee** for providing all the lab and technical support while acting as the lab coordinators. I am thankful to other faculty members including **Professor M. Parida, Associate Professor Rajat Rastogi, Associate Professor Dr. G.D Ranjan,** and **Assistant Professor Dr. Indrajit Ghosh, IIT Roorkee** for their supporting attitude. A special thanks to my S.R.C Chairman, **Professor Mahender Singh,** internal S.R.C member, **Professor M. Parida** and external S.R.C member, **Professor Anil Kumar, IIT Rorkee,** for actively judging my work and providing useful feedback which made me improve my work.

I express my gratitude to the HOD's of Civil Engineering, **Professor A.K Jain, Professor P.K Garg and Professor C.S.P Ojha, IIT Roorkee,** for making available the departmental facilities during my research tenure.

I wish to convey my sincere thanks to **Mr. Pradeep Kumar**, Lab Incharge Transportation Engineering laboratory. Many thanks are also due to **Mr. Bhopal Singh, Mr. Rakesh Pundir, Mr. Raj Pal, Mr. Dal Singh, Mr.J.P. Mishra, Mr. Gyanendra**, **Mr. Pushpendra,** and **Mr. Mukesh,** for providing their assistance in laboratory for performing the tests.

I would like to acknowledge my friends **Bibekananda, Rajiv, Souvik, Preeti, Bhupender** and **Sumit** for their active discussion on my work and time to time support that helped me improve my knowledge in the area. Many friends have helped me stay sane through these difficult years. Their support and care helped me overcome setbacks and stay focused on my research study. I greatly value their friendship and I deeply appreciate their belief in me.

Most importantly, none of this would have been possible without the love and support of my family. I thank them for their unconditional trust, timely encouragement, and endless patience. It was their love that raised me up again when I got weary.

And to the rest, I am extremely thankful to those people, whose names have been unknowingly left, thank you very much for your support and prayers. It really helped me a lot.

Last but not the least, my special thanks and appreciation to the Ministry of Human Resource and Development, Government of India, for providing me financial help in the form of research fellowship and contingency grant for the study.

(NIKHIL SABOO)

TABLE OF CONTENTS

LIST OF FIGURES

LIST OF TABLES

NOMENCLATURE

AASHTO	American Association for State Highway and Transportation Officials
AC	Asphalt Concrete
ASCE	American Society of Civil Engineers
ASTM	American Society for Testing and Material
BBR	Bending Beam Rheometer
BC	Bituminous Concrete
BIS	Bureau of Indian Standards
BS	British Standard
CI	Colloidal Instability
CRCP	Continuously Reinforced Asphalt Concrete
C-Y	Carreau-Yasuda
DBM	Dense Bituminous Macadam
DMA	Dynamic Mechanical Analysis
DSC	Differential Scanning Calorimetry
DSR	Dynamic Shear Rheometer
EVA	Ethylene Vinyl Acetate
EBA	Ethylene Butyl Acrylate
EMA	Ethylene Methyl Acrylate
FHWA	Federal Highway Administration
FM	Fluorescence Microscopy
GDP	Gross Domestic Product
GEL	Gelatinous
HMA	Hot Mix Asphalt
Hz	Hertz
IR	Infrared
IRC	Indian Roads Congress
IS	Indian Standards
ITS	Indirect Tensile Strength

LAS	Linear Amplitude Sweep
LVDT	Linear Vertical Displacement Transducers
LVE	Linear Viscoelastic
MFI	Melt Flow Index
MoRTH	Ministry of Shipping, Road Transport & Highways
MSCR	Multiple Stress Creep and Recovery
NCAT	National Centre for Asphalt Technology
NCHRP	National Cooperative Highway Research Program
NR	Natural Rubber
OBC	Optimum Binder Content
PAV	Pressure Ageing Vessel
PB	Poly Butadiene
PE	Polyethylene
PG	Performance Grade
PI	Penetration Index
PP	Polypropylene
PS	Poly Styrene
PVC	Polyvinyl Chloride
PMB	Polymer Modified Bitumen
RCRT	Repeated Creep and Recovery Test
RMS	Retained Marshall Stability
RTFOT	Rolling Thin Film Oven Test
SBS	Styrene Butadiene Styrene
SBR	Styrene Butadiene Rubber
SHRP	Strategic Highway Research Program
SMA	Stone Mastic Asphalt
SOL	Solution
SS	Storage Stability
TRB	Transportation Research Board
TSR	Tensile Strength Ratio
TTSP	Time Temperature Superposition Principle

USA	United States of America
UV	Ultra-Violet
VECD	Viscoelastic Continuum Damage
VG	Viscosity Grade
VFB	Voids Filled with Bitumen
VMA	Voids in Mineral Aggregate
WLF	Williams-Landel-Ferry
ZSV	Zero Shear Viscosity
G*	Complex shear modulus,
δ	Phase angle
G”	Loss shear modulus
G’	Storage shear modulus
cP	centipoise
Pa.s	Pascal second
ε	Strain
σ	Stress
J	Creep Compliance
R	Relaxation Modulus
%R	Percent Recovery
J_{nr}	Non-recoverable Creep Compliance
ω	Angular Frequency
f	Frequency
η	Viscosity
η'	Storage Viscosity
η'’	Loss Viscosity
η*	Dynamic Viscosity
η_o	Zero Shear Viscosity
$\dot{\gamma}$	Shear Rate
$\dot{\gamma}_d$	Desired Shear Rate
a_T	Horizontal Shift Fatcor

b_T	Vertical Shift Factor
T_{ref}	Reference Temperature
T_g	Glass Transition Temperature
D	Damage
W	Materials Energy Potential

Chapter 1
Introduction

1.1 General

India has the second largest road network in the world, 2,914,133 mi (4,689,842 kilometers) as of 2013. Quantitatively India's road network density is equivalent to that of U.S.A (0.65), which is far higher with respect to other countries like Brazil (0.20) and China (0.16). However, qualitatively, India has a mix of unpaved narrow roads and modern highways which are being improved. As of 2011, India had about 54 %(2.53 million kilometers) of paved roads.

As of April 2015, over 24000 kilometers of 4 or 6 lane highways have been completed by India, which connects majority of its commercial, manufacturing and cultural centers. This increase in rate of highway construction accelerated after 1999. However, regulatory blocks and policy delays has slowed down this rate in recent years. National highway development program, which is a government initiative, controls the implementation of all the major projects in the country. Initiatives are also being taken by highway operators and private builders. For context, in U.S.A, the density of road network is about 21 kilometers per 1000 people while in France the figure is nearly 15 kilometers per 1000 people; predominantly high quality and paved in both the cases. In terms of all weather, 4 or more lane highways, these density figures of U.S.A and France is over 15 times as that of India.

According to a survey by Goldman Sachs, India will have to invest US$1.7 trillion on projects related to infrastructure before 2020, in order to meet the economic demands, a part of which would go in the development of the countries road network. Promoting foreign investments in road projects is another step taken by the Indian government, which has attracted 40 design/engineering consultants and 45 international contractors with U.S.A, United Kingdom, Malaysia and South Korea being the largest players.

India's economy is highly dependent on road transport. It aids the transportation sector of the country in contributing about 4.7% towards the gross domestic product (GDP), which is much higher than the other sectors like railways which contribute only about 1%.

Over the years, much importance has been given to road sector in comparison to railway and air, despite of significant inefficiencies and barriers in interstate passenger and freight movement. Various government authorities (given by India's federal form of government) administers India’s road network.

1.2 Background

Based on the structural performance, the pavements can be divided into two types: flexible pavements and rigid pavements. Flexible pavement functions by transferring wheel loads by grain to grain contact of the aggregates in the granular structure. Having less flexural strength, flexible pavements acts like a flexible sheet. In rigid pavements however, it is the flexural strength which transfers the wheel load to the subgrade soil through slab action and the pavement structure behaves like a rigid plate [76]. Composite pavements are also another available option. Example of an ideal pavement is a thin layer of flexible pavement over rigid pavement. This type of pavement possess the most desirable characteristics but are rarely used due to high cost of construction and complexity in its analysis.

In flexible pavements there is a wide distribution of the wheel loads acting on the pavement, where the stress reduces with depth. This stress distribution characteristic of flexible pavement makes it advantageous to be used in multiple layers. Hence, layered system concept is used for designing a flexible pavement. Among the different layers, the top layer is usually of the best quality which sustains the maximum compressive stress along with the wear and tear. Low quality materials can be used in lower layers, as it experiences lesser magnitude of strain. Bituminous materials are used for construction of flexible pavements. These can be either in the form of surface treatments (such as bituminous surface treatments generally found on low volume roads) or, asphalt concrete surface courses (generally used on high volume roads such as national highways). The layers in the flexible pavements reflect the deformation occurring in the lower layers to the surface (e.g. if there is any deformation in sub-grade then it will be transferred to the top layer). In case of flexible pavement the design is based on the design traffic which is denoted in terms of million standard axle (msa) loading and the stress should be kept below the allowable stress. Below is presented a typical schematic representation of a flexible pavement.

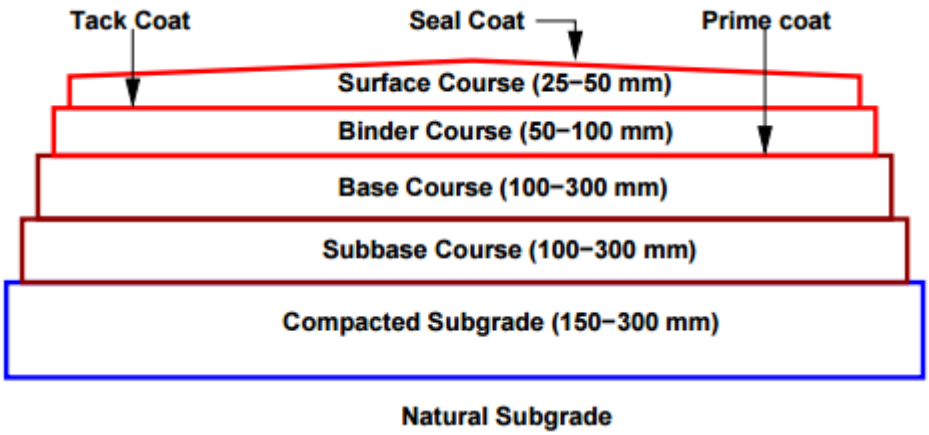

Figure 1.1 Typical example of a flexible pavement

In general, hot mix asphalt (HMA) can be defined as a mixtures of aggregate (mixed in a definite gradation) and asphalt cement (binder) produced at high temperatures (generally between 130-170 °C) in an asphalt plant. With the advent of time cold mix asphalt technology is also becoming popular [47]. Typically, HMA mixtures can be categorized into three different types: dense-graded; open-graded; and gap-graded which is as a function of gradation of the aggregates used in the mix. Mix design is done to incorporate a number of performance concerns in the finished mat of HMA. These include:

- **Resistance to Permanent Deformation.** The mix should be resistant to distortion and displacement. This resistance should be provided specially during summers having high temperatures. During this period the binder softens and the incoming loads are mainly carried by the aggregate structure.

  Resistance to permanent deformation is dependent on the properties of (crushed faces), the mix, and the grade and content of asphalt binder used [52, 90, 134].

- **Resistance to Fatigue and Reflective Cracking.** Resistance to fatigue and reflective cracking is inversely related to the stiffness of the mix. Though a stiffer mix is desirable for resistance to rutting, design for rut resistance alone may affect the all over performance of the pavement if reflective cracking or fatiguing occurs[15, 112, 115]. Stiff mixtures are desirable for use in thick HMA pavements and when used as a thin overlay on a continuously reinforced concrete pavement (CRCP).

Thin HMA mats placed on an unbound base or on surfaces prone to reflective cracking (e.g., jointed rigid pavements, bound bases subject to shrinkage cracking, etc.) should use a mix that strikes a better balance between rut and crack resistance. Fatigue and reflective crack resistance is primarily controlled by the proper selection of the asphalt binder. Application of a specially designed crack-resistant interlayer is another option for mitigating cracking.

- **Resistance to Low Temperature (Thermal) Cracking.** Cooler regions are particularly prone to thermal cracking concerns. Mitigation of thermal cracking can be achieved by the selection of an asphalt binder which is less susceptible to low temperature cracking[90, 129].
- **Durability.** Durability is a function of amount of asphalt cement such that an adequate film thickness is available around the aggregate particles. This helping minimizing the ageing and hardening of the asphalt binder during production and in service. Sufficient asphalt binder content will also help ensure adequate compaction in the field, keeping air voids within a range that minimizes permeability and ageing [14].
- **Resistance to Moisture Damage (Stripping)**. Loss of adhesion between the asphalt binder and the aggregate depends primarily on the characteristics of the aggregates [123, 133, 186]. A mix designer should assume that at some point of time moisture will eventually find its way into the pavement structure; and hence should design the mix, at any level of pavement structure, to resist stripping by using anti-stripping agents.
- **Workability.** Workability relates to the easiness of field compaction. Many a times it may be required to incorporate a slight change in the mix design so that the mix is properly placed without sacrificing the performance.
- **Skid Resistance.** This is a concern for surface mixtures that must have sufficient resistance to skidding, particularly under wet weather conditions. Aggregate properties such as texture, shape, size, and resistance to polish are all factors related to skid resistance [61].

Selection of a HMA mix or combination of mixes to use in a project should be a conscious decision made by the responsible engineer based on mix attributes (suitability as

part of the overall pavement design, existing pavement conditions, lift thickness, traffic loading characteristics), environment, past performance, local contractor experience, and economics.

Bitumen is a crucial component of asphalt - the most widely used material for constructing and maintaining roads in the world [83]. Asphalt mix is typically a mixture of approximately 95% aggregate particles and sand, and 5% bitumen, which acts as the binder, or glue. The viscous nature of the bitumen allows the asphalt mix to sustain significant flexibility, creating a very durable surface material. Bitumen is a civil engineering construction material manufactured from crude oil through a series of distillation processes undertaken during the refining of petroleum. One of the characteristics and advantages of bitumen as an engineering construction and maintenance material is its great versatility. The principle use of bitumen is as a binder in the road construction industry where it is mixed with graded aggregate to produce asphalt mixture. This mixture is then laid as the structural pavement layers of a road. As the mechanical properties of asphalt mixture are strongly dependent upon the properties of the binder, it has to fulfil certain mechanical and rheological requirements to ensure the integrity of the road. First, the bitumen must be fluid enough at high temperature (approximately160 °C) to be pumpable and workable to allow for a homogeneous coating of the aggregates upon mixing. Second, it has to become stiff enough at the highest pavement temperature to resist rutting deformation (approximately around 60 °C, depending on the local climate). Finally, it must remain soft enough at lower temperatures (down to -20 °C, depending on the local climate) to resist cracking. Therefore, it is difficult to obtain bitumen that would work under all possible climates. To surmount this problem, different types of bitumens including modified binders are available. The softer and harder binders are normally used for colder and hotter climate regions respectively.

The rheological properties of bituminous binders including bitumens are typically determined by means of dynamic mechanical analysis (DMA) using an oscillatory type, dynamic shear rheometer (DSR) tests [12, 55, 192]. In general, the test is conducted within the linear viscoelastic (LVE) region [11]. Research into the rheological properties of bitumen has been growing since the early 1990's, following the Strategic Highway Research Program (SHRP). The DSR instrument, however, does have its limitations where the measured rheological data are exposed to the measurement error particularly at low temperatures

and/or high frequencies. Alternatively, other equipment's such as a bending beam rheometer (BBR) and a direct tension test (DT) can be used at this region.

1.3 Problem Statement

Bitumen has been long used as an important binding material in pavement. When combined with a given aggregate gradation in appropriate quantity, it produces a mix structure which acts as load carrying component in highways. Bitumen is the only component of the pavement which displays thermo-mechanical behavior, making it a complex element to study. As bitumen acts as binding material in the pavement structure, the properties and performance of the pavement highly depend on the type, quality and amount of bitumen. Hence selection of appropriate bitumen for pavement construction is very vital for the structure to perform well.

For most of the purposes, conventional binders have tended to give adequate performance. But with the advent of time, the demand of highway has increased. Increase in traffic, introduction of new axle configuration and increase in temperature demands effective strengthening of pavements [111, 141, 200]. With the worst combination of these extreme conditions, early failure of pavement is becoming common with respect to permanent deformation and fatigue cracking. There are two basic methods which can be employed to counteract these issues:

-Improving the pavement design technique, and

-Use of better materials

Modification of bitumen is the simplest and one of the most effective ways which falls under the second category as mentioned above. Modification of different pavement layers also tend to improve the overall strength of pavement [74, 81, 82, 96, 153, 168]. In fact, modification of other type of pavements is also not new to research [93]. Construction also plays a crucial role in characterizing the strength of pavements [175].

Various modifiers have been used since decades for improving the viscoelastic response of bitumens, thereby increasing the strength of pavement structure [39, 154]. In general, modified bitumen increases the stiffness at higher temperature while maintains

adequate flexibility at low service temperatures [92, 124]. Modifiers can be categorized in a number of different ways including filler, polymers and chemical additives. Out of various modification technique, polymers have shown to give the best results [125, 149, 174, 176], improving the rheological characteristics of bitumen and reducing its temperature susceptibility.

A polymer (Greek poly-, "many" + -mer, "parts") is a large molecule, or macromolecule, composed of many repeated subunits. Because of their broad range of properties, both synthetic and natural polymers play an essential and ubiquitous role in everyday life. Polymers range from familiar synthetic plastics such as polystyrene to natural biopolymers such as DNA and proteins that are fundamental to biological structure and function. Polymers, both natural and synthetic, are created via polymerization of many small molecules, known as monomers. Their consequently large molecular mass relative to small molecule compounds produces unique physical properties, including toughness, viscoelasticity, and a tendency to form glasses and semi crystalline structures rather than crystals.

Polymers are basically divided into two broad categories depending on their response to external loads:plastomers and elastomers. An elastomer is a polymer with viscoelasticity (having both viscosity and elasticity) and very weak inter-molecular forces, generally having low Young's modulus and high failure strain compared with other materials. Each of the monomers which link to form the polymer is usually made of carbon, hydrogen, oxygen or silicon. Elastomers are amorphous polymers existing above their glass transition temperature, so that considerable segmental motion is possible. Styrene butadiene styrene (SBS), styrene butadiene rubber (SBR) and crumb rubber are the most common elastomers which have gained a lot of attention in the market of modified bitumen [22]. A plastomer on the other hand is a polymer material which combines qualities of elastomers and plastics, such as rubber-like properties with the processing ability of plastic. Polyethylene and ethylene vinyl acetate (EVA) are the most common palstomers which have been widely used to improve the strength of bitumen.

Modification of bitumen with polymers requires blending the polymer using high shear mixer following which the polymers swell and disperse in the maltene fraction of the

bitumen. The asphaltene and the polymer compete for the solvency power of the maltene fraction which leads to phase separation in the modified bitumen. This incompatibility is a resultant of difference in density and molecular weight of the polymer and the asphaltene. The chemical structure also plays a vital role in production of a homogenous blend with interlocked phases of polymer and bitumen.

Different agencies use different modification technique to produce bitumen satisfying the required specifications laid down by the government for modified binders. They do not mention the amount and type of modification technique employed for the production of the modified binder. The production, however, is highly dependent on the type of base binder and the amount and type of polymer. The three blending parameters influencing the modification technique are the temperature, shear rate and blending time employed for its production. Variation in these three parameters can greatly affect the quality of binder produced. Hence selection of appropriate combination of the blending parameters for different modifier is an important task to be achieved in laboratory for obtaining a storage stable blend before studying their rheological and mechanical properties.

Though polymers have shown to improve the viscoelastic response of the base binders to an appreciable degree, still the practitioners and contractors remain skeptical on its use, mainly due to the associated cost and high temperature requirements of mixing and compaction required for modified binders. Traditionally Brookfield viscometer is employed for finding the mixing and compaction temperature of bitumen in India. The mixing and compaction temperatures are determined by plotting the viscosity values in the log-log scale whereas the temperature on the log scale and assuming a straight line relationship. India follows the equiviscous concept, in which the mixing and compaction temperatures are defined corresponding to the viscosities of 0.17 ± 0.02 and 0.28 ± 0.03 Pa.s. But modified binders have been found to display shear thinning behavior even at high temperatures [18]. Shear thinning is a term used in rheology to describe non-Newtonian fluids which have decreased viscosity when subjected to shear strain. The term is sometimes considered to be a synonym for pseudo-plastic behavior, and is usually defined as excluding time-dependent effects, such as thixotropy. Moreover, the shear rate employed in Brookfield viscometer (6.8 s^{-1}) is very low when compared to the shear rate employed on mixing plants. This questions

the reliability of the procedure in predicting the mixing and compaction temperatures corresponding to practical conditions. Moreover the effect of shear rate has more influence on mixing rather than compaction, which depends on the vertical load of the rollers and not the shearing action.

So, studying the flow behavior of modified binders at a wide range of shear rate is very crucial in determining the rheological aspects of the bitumen which will throw light on the practical calculation and determination of viscosity corresponding to any shear rate and hence facilitate the procurement of appropriate mixing temperature for bitumen.

Bitumen is a viscoelastic material, whose behavior depends on both temperature and rate of loading (frequency) [31, 91, 128]. The study of viscoelastic behavior of bitumen can be done using two methods: transient and oscillatory. Creep and relaxation are the most common testing methods employed to assess the transient response and requires longer testing times. Oscillatory testing using dynamic shear rheometer (DSR) is more common to study the rheological aspects of bitumen at a wide range of temperature and frequency domain within a short period of time. Testing in DSR is accomplished by subjecting a bitumen sample to loading, where the bitumen sample is sandwiched between two plates, one fixed and the other rotating. Different sample geometry has been recommended based on the stiffness of the binder at a particular temperature and frequency. Rheological results are obtained using 25 mm diameter spindle geometry with 1 mm plate gap or 8 mm diameter spindle with 2 mm plate gap. The variation in results due to change in plate gap using these spindle geometries is one important aspect which has to be understood for appropriate evaluation of different rheological properties. It will also facilitate in gaining more confidence and reliability on the measured strength values by the DSR.

Predictive models and equations are excellent tools for quantifying the mechanical/rheological properties of any material. It is time saving, less laborious and doesn’t require any skilled operators. Since 1950’s researchers have tried to predict the linear viscoelastic characteristics of bitumen using nonlinear multivariable models, also known as nomographs. These nomographs were later replaced by empirical equations and the use of mechanical elements (spring and dashpot), for modelling the linear rheological properties. These techniques were mainly used for predicting variation of complex modulus and phase

angle master curves, at any desired reference temperature. Yusoff et al. [196] presented a brief overview of all the models developed over the past years. Most of the algebraic models consist of large number of model parameters which are empirical and does not have any physical significance. A more simple model is hence desired which can be directly related to the flow properties of the binder.

SUPERPAVE is the product of the asphalt research undertaken as part of the Strategic Highway Research Program (SHRP) and it integrates performance based specifications, test methods, equipment testing protocols, and a mixture design system. SHRP was established by the United States Congress in 1987 as a five-year, $150 million research program to improve the performance and durability of highways and to make them safer for motorists and highway workers. They sponsored $50 million of research on asphalt binders to relate the specifications to actual pavement performance. The outcome of the SHRP project was termed as Superpvae, initiated from the Superior Performance Asphalt Pavements. The new Performance Grade (PG) asphalt binder specifications measures physical properties of the material throughout its temperature range. PG graded asphalt binders are graded according to the climatic conditions they will endure in the roadway. A PG 64-22 will perform from a high pavement temperature of 64 °C to a low pavement temperature of -22 °C. This binder grading system requires testing of bitumen using DSR. The binder properties and grading system of Superpave is dependent on the value of complex modulus (G*) and phase angle (δ) of the binder for unaged and aged samples. The resistance to pavement deformation and fatigue cracking of the binder was related to the value of G*/sinδ and G*.sinδ at a particular temperature and a frequency of 10 rad/sec. The current Superpave specification for performance grading was developed mainly for unmodified binders and has been proved to be misleading for predicting rutting and fatigue properties of modified bitumen [71, 73, 84, 85, 199]. These tests were developed based on the speculation that binder in pavements functions mostly in the LVE range and is not likely to affect their properties. Such single value specifications cannot describe the actual complicated failure phenomena, in which the binder is exposed to higher strain levels and varied frequency levels. This led to the introduction of two new test methods for evaluating the binder performance with respect to rutting and fatigue cracking. Multiple stress creep and recovery (MSCR) test has been introduced to evaluate the permanent deformation characteristics of

asphalt binders while linear amplitude sweep (LAS) is recommended for quantifying the fatigue behavior of asphalt binders. As a new test methods, it is necessary to understand and explore the behavior of binders at different test conditions to gain more confidence on its use. Moreover, the correlation of the binder properties, evaluated using these test methods, with the mix performance is necessary to be established.

Binder alone cannot determine the performance of the pavement. Aggregate gradation plays an important role in judging the strength of the mix. The bituminous mix is composed of about 92 % of aggregates and having proper aggregate gradation is very crucial for determination of the mix characteristics in terms of its resistance to structural distresses. In India specifications laid out by Ministry of Roads Transport and Highways (MoRT&H) are followed for selection of mix gradation for bituminous pavements. Bituminous concrete (BC) and dense bituminous macadam (DBM) are the most commonly used gradations for surface and binder courses. Stone mastic asphalt (SMA) is a gap-graded mix which is also being used at locations with extreme traffic and temperature conditions. SMA has voids in mineral aggregates (VMA) of about 20%. For a fixed air void content of 4% high binder content (around 7% by weight of the mix) is usually required. SMA has been found to be a rut resistant mix due to the stone to stone contact generated by the gradation and also have high fatigue resistance attributable to the high binder content. Cellulose fibers are generally required to counteract the draindown issue in SMA mixes. As SMA is a gap graded mix, the binders are susceptible to flow out of the mix at high handling temperatures (near about 163 °C). This phenomena is known as draindown which should be less than 0.3% as per specification outlined in IRC SP-79 2008 [79]. This might be true for conventional binders having low viscosity, but modified binders might be able to resist the draindown without the use of any fibers attributable to higher viscosity.

Evaluation of mix performance and its correlation with binder properties is necessary to completely define the strength characteristics of the mix. Various test methods have been recommended for the evaluation of the rutting characteristics of asphalt mixes. Wheel rut test, however, has been found to be more suitable in accurately justifying the field results. Laboratory evaluation of fatigue performance of bituminous mixtures have been found to be very difficult, as fatigue is micro level deformation phenomena and is more complicated than

concept of permanent deformation. Out of the various recommended test techniques four point beam bending test (4PBBT) has been suggested by many research to give results which is a close representation of practical field data.

1.4 Goals and Objectives

The main objective of this study is to assess the effect of polymer modification on the rheological characteristics of asphalt binders and mixes. To achieve this objective following sub objectives have been defined.

1. To find the optimum blending requirements for different polymer modifier to be used and obtain the optimum modifier content for each of the modifiers.
2. To study the flow behavior of unmodified and modified binders at a wide range of temperature and shear rates and propose a new technique for calculation of appropriate mixing temperatures for these binders.
3. To study the rheological characteristics of all the binders using dynamic shear rheometer (DSR). This objective includes assessing the effect of spindle geometry on the rheological measurements for the binders, using master curves to define the rheological behavior at a wide range of frequency at different temperatures and attempting to provide a more simple modelling technique for the linear viscoelastic behavior of the binders.
4. To study the rutting and fatigue characteristics of binders at different temperature and stress conditions.
5. To study different mix gradations using these binders and evaluate the performance of the bituminous mixes using rut testing and four point beam bending test. This objective also includes obtaining correlation between binder and mix properties from the results obtained in this study.

1.5 Scope of the Work

The study evaluates the strength characteristics of four different asphalt binders and three different asphalt mixes. VG 10 and VG 30 are the viscosity graded binders. VG 10 is being polymer modified using styrene butadiene styrene (SBS) and ethylene vinyl acetate (EVA)

using the optimum modifier contents. The rheological and strength characteristics of the binders and the mixes are accomplished in the following parts:

a) Modification of bitumen using a high shear mixer and evaluation of optimum blending requirements and optimum modifier content corresponding to each modifier. The optimum modifier content so obtained is further used for testing and analysis.
b) Determination of physical and rheological properties of unmodified and modified bitumen using conventional and fundamental testing.
c) Evaluation of flow behavior of bitumen using steady shear tests in DSR. The viscosity versus shear rate is analyzed and a rheogram is plotted using the concept of rheogram. Carreau-Yasuda equation is used for modelling the variation of viscosity with shear rate. This model is used as the basis of calculating the mixing temperatures for different bitumen.
d) The rheological properties of the asphalt binders are evaluated with the aid of dynamic shear rheometer (DSR) for a temperature range of 10-70 °C and frequency varying from 0.1-100 rad/sec. Master curves are constructed at three different reference temperature to assess the rheological properties at a wide range of frequency. The shift factors are analyzed and a new technique has been proposed for construction of the master curves. Effect of spindle geometry on the value of complex modulus (G*) and phase angle (δ) are also explored. A simple model has been proposed to model the complex modulus and phase angle master curves.
e) The strength properties of the binders are evaluated at a temperature range of 10-60 ºC. The fatigue behavior of binders has been explored using linear amplitude sweep (LAS) test at three different temperatures of 10, 20 and 30 ºC. Similarly, multiple stress creep and recovery (MSCR) test is done to evaluate the performance of the binders in rutting at 40, 50 and 60 ºC. These temperatures corresponds to the high pavement temperatures at which rutting could be the predominant structure failure criteria. In MSCR test, four different stress levels are chosen, viz. 100, 3200, 5000 and 10,000 Pa. All the tests are performed using dynamic shear rheometer (DSR). For LAS, 8 mm plate diameter with 2 mm gap is used. All the binders are subjected to long term aging using pressure aging vessel (PAV) prior to testing. For MSCR

test, rolling thin film oven (RTFO) aged binders are used. 25 mm plate diameter using 1 mm gap setting is adopted.

The measured response in MSCR test is analyzed using two different modelling techniques. Changes in the suggested model is made to account for the non-linearity associated with the binders. The significance of model parameters, influencing the permanent deformation characteristics are evaluated. Critical values to these parameters are assigned and proposed as a performance measure, after comparison with the already existing PG plus specification. This may provide additional benefit in judging the relative performance of asphalt binders at high temperature. Correlation with conventional binder properties using the model parameters is evaluated. In LAS test the variation of model parameters with change in temperature is also assessed.

f) The performance of unmodified and modified asphalt mixes are quantified using wheel rut testing and four point beam bending test. Rut testing is conducted at 60 °C, while 4PBBT is conducted at 20 °C for strain amplitudes varying from 200-1000 micro strain. Tests like retained Marshall Stability and Indirect Tensile Strength (ITS) are also carried out to judge the mix performance. The suitability of different test methods for quantifying rutting is also presented and discussed. A new phenomenological model has been proposed to quantify the fatigue life of asphalt mixes. At the end correlation between fatigue and rutting of binders and mixes has been established.

All the tests were conducted in the Civil Engineering Department, IIT Roorkee. Fluorescence microscopy was conducted in the Biotechnology Department, IIT Roorkee. A few tests e.g. resilient modulus test on bituminous mixes, dynamic modulus of mixes and bending beam rheometer could not be conducted due to unavailability of the instrument at IIT Roorkee or any other nearby research laboratory.

1.6 Organization of the Thesis

The present research work has been documented in nine different chapters as follows:

Chapter 1: This is an introductory chapter which lays down the background of the study. The problem statement is defined along with the goals and objective of the research. The scope of the work is clearly defined and the layout of the thesis is stated.

Chapter 2: This chapter presents the literature review required for conducting the study. The literature behind the evaluation and testing of unmodified and modified bitumen is discussed. The need for modification and the studies conducted related to the effect of modification on the rheological properties of the binders is presented. The mix design of bituminous mixes along with the literature on their strength evaluation is laid out.

Chapter 3: This chapter discusses the method adopted for obtaining the optimum blending requirements and modifier content for the modified binders used in the study. The results obtained from fluorescence microscopy is also presented.

Chapter 4: The flow behavior of the unmodified and modified binders using steady shear test in DSR has been discussed in this chapter. It presents a new technique for the practical evaluation of mixing temperatures for different bitumen. A modelling technique to simulate the variation of viscosity with shear rate is also discussed.

Chapter 5: This chapter explains the various rheological aspects of the asphalt binders. The chapter comprises of evaluation of the linear viscoelastic region of the binders at different temperatures and frequencies. Effect of spindle geometry on the rheological results is discussed next. Further, results of master curves at three different reference temperatures are outlined. Lastly, the chapter presents a simple modelling technique for the complex modulus and phase angle master curves with a brief discussion on shift factors.

Chapter 6: In this chapter the strength characteristics of modified and unmodified binders have been determined using MSCR and LAS test methods at a temperature range of 10- 60 °C. This chapter outlines the various test parameters adopted and the

experimental results so obtained. The analysis of the test results along with the effect of temperature and stress/strain levels on the test parameters have been discussed and presented.

Chapter 7: The evaluation of asphalt concrete mixes has been detailed in this chapter. The properties of aggregates have been stated and the Marshall mix design procedure and the results obtained for the optimum binder content different mixes (BC, DBM and SMA) using various binders (VG 10, VG 30, PMB (S) and PMB (E)) have been presented. The strength tests conducted on Marshall specimens also forms the part of this chapter.

Chapter 8: This chapter presents the results of wheel rut testing and four point beam bending test (4PBBT). The suitability of different test methods for quantifying the rutting behavior of asphalt binders is also discussed. In addition, a new phenomenological method for evaluating the fatigue response of binders at different strain levels is also outlined. Finally the chapter establishes a correlation between the behavior of binders and mixes from the results obtained.

Chapter 9: Significant conclusions drawn from the different chapters are discussed in this study. The contribution of the work is also presented. Recommendations and the future scope of the study are also outlined.

Chapter 2
Literature Review

2.1 Introduction

This literature review covers different aspects related to physical and chemical properties of bitumen, its rheology, performance evaluation of bitumen and bituminous mixture characterization. The literature begins with the characterization of bitumen for paving application. The chemical nature of the bitumen is described in brief along with its importance in research application.

The second section describes the conventional and rheological tests for bitumen characterization. The review presents a brief description about the conventional tests like penetration, softening point and viscosity and its importance in judging the performance of bitumen. Further, dynamic mechanical analysis (DMA) of bitumen has been described along with the concept of viscoelasticity. Dynamic Shear Rheometer (DSR) has been introduced and the concepts underlining its working application has been presented. The use of DSR for evaluation of various rheological properties has been described along with the various ways of interpreting and analyzing the rheological data. New test methods like multiple stress creep and recovery (MSCR) and linear amplitude sweep (LAS) test used for the performance evaluation of asphalt binders has also been discussed.

The third section deals with the modification of bitumen. It begins with the studies related to need of bitumen modification and its importance. The various modification techniques adopted so far has been tabulated and the best forms of modification is identified. Further, different forms of polymer modification has been described with a detailed overview of elastomer styrene butadiene styrene (SBS) and ethylene vinyl acetate (EVA).

The last section of the literature review discusses the bituminous mixture characterization, mix design concepts and the various test methods for characterizing and evaluating the performance of bituminous mixtures. In the whole thesis the term ‘bitumen’ and ‘asphalt binder’ is used analogous to each other. The mixture is described using ‘bituminous mixture’ or ‘asphalt mixture’.

Individual literatures on the study of bitumen and asphalt mixtures are taken up as a part of different chapters and are not discussed here. This chapter outlines the overall concept on characterization of asphalt binders and mixes.

2.2 Bitumen

The term "bitumen" originated in ancient Hindu language Sanskrit, where the words "jatu" meaning pitch and "jatu-krit" meaning pitch creating, referred to the pitch produced by some resinous trees. The Latin equivalent is claimed to be originally "gwitu-men"/"pixtu-men", which was further shortened to "bitumen"[83]. The use of bitumen as an engineering material dates back to 3000 B.C, when surface seepages of "natural" bitumen were used as mortar for masonry and water proofing purposes [6] . The history of use of asphalt later shifted from use of lake asphalt to rock asphalt followed by consumption of gilsonite and later coal tar. The use of coal tar disappeared around 1975 and bitumen was used as the primary product for surfacing of roads.

Most of the current applications in asphalt pavements make use of bitumen manufactured from crude oil. The process involves distillation, blowing and blending. Fractional distillation is used to refine the bitumen and the crude is separated to liquid petroleum gas, naphtha, kerosene, gas oil and long residue (complex mixture of high molecular weight hydrocarbons). The long residue is then further subjected to vacuum distillation at high temperature (350 °C-400 °C), which produces short residue. The different grades of bitumen are obtained from this short residue. The short residue may be further modified by air blowing to change its physical properties.

The four principal crude oil producing areas in the world are the Middle East, U.S.A., Russia and the Caribbean countries. The physical and chemical properties varies depending on the crude source. Physically, they can be sorted as viscous black to free-flowing straw colored liquids. Chemically, they may be predominantly paraffinic, naphthenic or aromatic, with combinations of the first two being common [83].

It is estimated that the current world use of bitumen is approximately 102 million tonnes per year. Approximately 85% of all the bitumen produced is used as the binder in asphalt for roads. It is also used in other paved areas such as airport runways, car parks and

footways.

A further 10% of global bitumen production is used in roofing applications, where its waterproofing qualities are invaluable. The remaining 5% of bitumen is used mainly for sealing and insulating purposes in a variety of building materials, such as pipe coatings, carpet tile backing and paint. Bitumen when combined with properly graded aggregates produces asphalt mixture which serve as the load carrying component of asphalt pavement. Hence, it can be concluded that bitumen is not only a vital engineering material but also a vibrant component in pavement engineering.

2.2.1 *Bitumen constitution*

Bitumen is a complex chemical mixtures of molecules which are predominantly hydrocarbons with little amount of functional groups and heterocyclic species containing atoms of sulfur, nitrogen and oxygen. Trace amount of metals like vanadium, nickel, magnesium, iron and calcium can also be found. The proportion of these constituents vary greatly depending on the crude source and type. The average quantity are as follows:

- Carbon 82-88%
- Hydrogen 8-11%
- Sulfur 0-6%
- Oxygen 0-1.5%
- Nitrogen 0-1%

The chemical composition of bitumen is complex. Broadly, the bitumen can be separated to two main chemical groups called asphaltenes and maltenes. Maltenes can be further subdivided into saturates, aromatics and resins. Methods such as solvent extraction, adsorption by finely divided solids and removal of unabsorbed solution by filtration, chromatography and molecular distillation are available to separate bitumen into various fractions. Among these, chromatographic technique is most widely used for SARA (saturates, aromatics, resins and asphaltenes) analysis of bitumen.

2.2.1.1 Asphaltenes

Asphaltenes, which are insoluble in n-heptane are black or brown amorphous solids containing nitrogen, sulphur and oxygen in addition to carbon and hydrogen. They have high

molecular weight and are highly polar complex aromatic materials. Asphaltene constitutes 5-25% of the bitumen and have considerable effect on its rheological characteristics. The molecular weight ranges from 600-300000 depending on the separation technique. Increasing the asphaltene content produces a harder bitumen, with lower penetration, higher softening point and high viscosity. Figure 2.1 shows the typical structure of asphaltene.

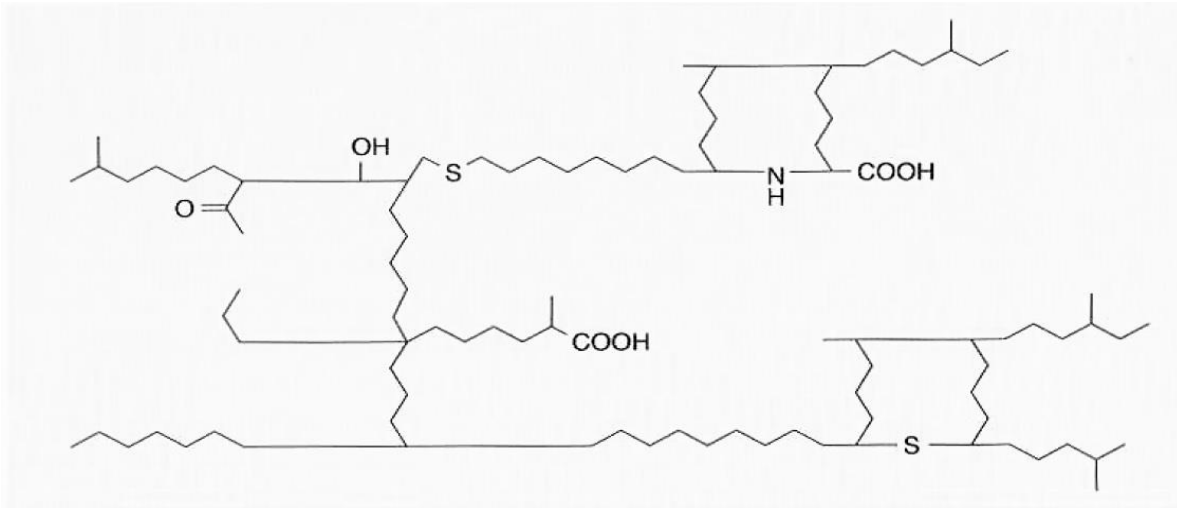

Figure 2.1 Asphaltene structure

2.2.1.2 Resins

Largely composed of hydrogen and carbon, resins are n-heptane soluble dispersing agents are peptisers for the asphaltenes. They are dark brown, solid or semi-solid polar compounds which are highly adhesive. Their molecular weight ranges from 500-50,000. The proportion of resins to asphaltenes governs the character of a bitumen being solution (SOL) or gelatinous (GEL) type [83]. Figure 2.2 (a,b) shows the two typical nature of bitumen depending on this ratio.

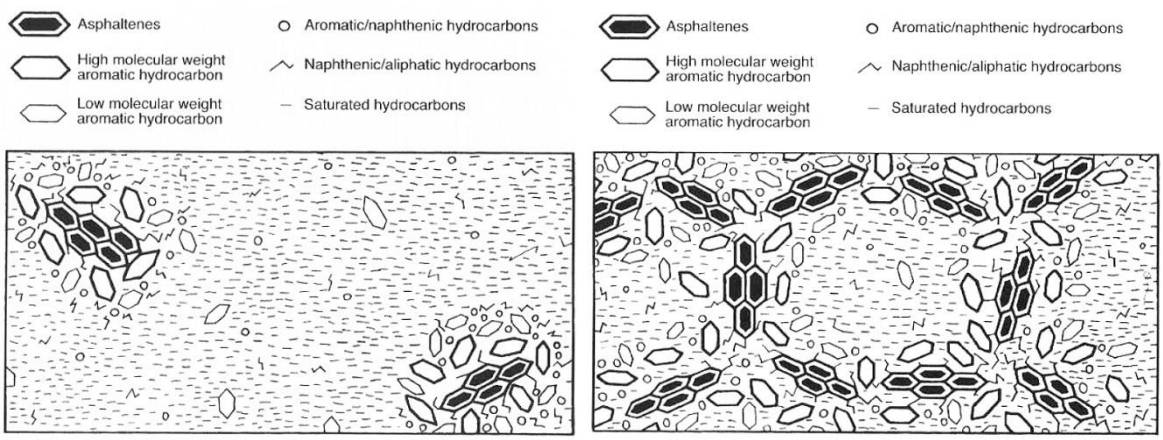

a b

Figure 2.2 (a,b) SOL and GEL type bitumen structure

2.2.1.3 Aromatics

Aromatics constitutes 40-65% of the bitumen and are dark brown viscous solids. Their average molecular weight varies from 300-2000. They are low molecular weight napthenic aromatic compounds which forms the dispersion medium for asphaltenes. They are non-polar and have high dissolving power for other higher molecular weight hydrocarbons [6]. The typical structure of aromatics is shown in Figure 2.3.

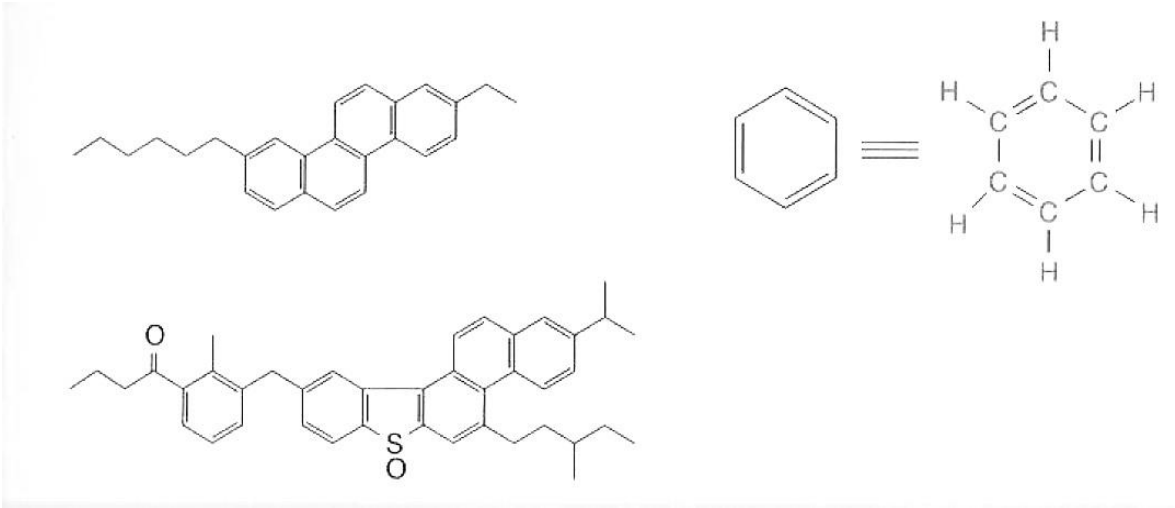

Figure 2.3 Aromatics structures

2.2.1.4 Saturates

Saturates are non-polar viscous oils which are white or straw in color. They form 5-20% of the bitumen and include both waxy and non-waxy saturates. Their molecular structure consist of straight and branched chained aliphatic hydrocarbons. Figure 2.4 presents a typical structures of saturates.

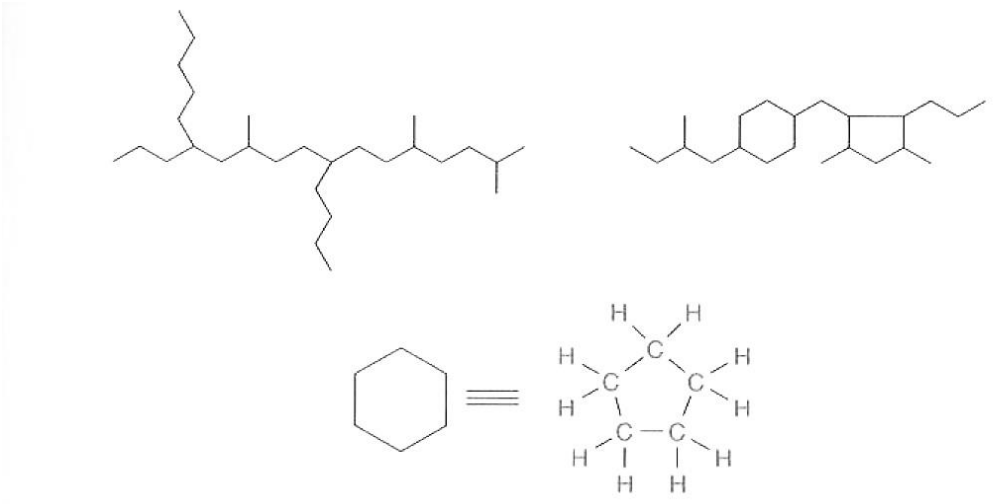

Figure 2.4 Saturate structures

The Colloidal Index (CI) also known as Gaestel Index, which is defined as the ratio of the amount of asphaltenes and saturates to the amount of resins and aromatics, is often used to assess the colloidal structure stability in bitumen [6]. A higher CI, indicates a GEL type bitumen while a lower value portrays a more stable colloidal structure, therefore the bitumen is regarded as SOL type bitumen [196]. The physical, mechanical and rheological properties of asphalt binders are defined and determined by both the chemical composition and the physical arrangement of the molecules in the material.

2.3 Conventional and Fundamental Testing of Bitumen

2.3.1 *Penetration test*

The penetration is a measure of the consistency of bitumen at 25 °C. The earlier grading system of bitumen as per IS 73:1992 specification was based on penetration values. The penetration value is defined as the distance in tenths of millimeter, a standard needle

penetrates a sample of bitumen under a load of 100 grams at a temperature of 25 °C for a known loading time of 5 seconds. For example, a 30/40 penetration grade bitumen has a penetration value at 25 °C ranging from 30 to 40 in units dmm. The test apparatus is shown in Figure 2.5. Typically the values for paving grade bitumen range between 15-200 dmm.

Figure 2.5 Penetration apparatus used in the study

2.3.2 *Ring and ball softening point test*

The ring and ball softening point test is an empirical way to determine the consistency of asphalt binders by measuring the equi-viscous temperature at the initiation of the fluidity of bitumens. In this test, a steel ball (3.5 g in weight) is placed on a bitumen sample contained in a brass ring. The sample is suspended in a water or glycerin bath. The temperature of the bath is raised at 5 °C per minute until the ball travels a specified distance of 2.5 cm. This temperature is considered as the softening point of the bitumen. Water is used for bitumen with a softening point of 80 °C or below. Meanwhile, glycerin is used for softening points greater than 80 °C. The test setup is shown in Figure 2.6.

Figure 2.6 Softening point test of asphalt binders

2.3.3 *Viscosity test*

Viscosity which is measured in units of pascal seconds (Pa.s), is a degree of the resistance to flow of a liquid which is defined as the ratio between the applied shear stress and the rate of shear strain. It is also a consistency indicator of bitumen which can be measured at a wide range of temperatures. In addition to absolute or dynamic viscosity, viscosity can also be measured as kinematic viscosity in units of mm^2/s which is equal to 1 centistoke (cSt). The viscosity of bitumen can be measured with a variety of devices in terms of its absolute and kinematic viscosities. In general, specifications are based on measurement of absolute viscosity at 60 °C and a minimum kinematic viscosity at 135 °C using atmospheric and vacuum capillary tube viscometers respectively. It determines the time required for bitumen to cross two pre-marked points. This time is multiplied by a calibration factor of the instrument to obtain the viscosity value. Absolute viscosity can also be measured using a sliding plate viscometer. The sliding plate test monitors force and displacement on a thin layer of bitumen contained between parallel metal plates at varying combinations of temperature and loading time [196].

Presently rotational viscometer test [3] is considered to be the most practical means of determining the viscosity of bitumen. The Brookfield rotational viscometer and thermocel system used in the study are shown in Figure 2.7. Measurements can be over a wide range of temperatures and shear rates. Rotational viscometers consist of one cylinder rotating

coaxially inside a second (static) cylinder containing the bitumen sample under a thermostatically contained chamber. The torque on the rotating cylinder or spindle is used to measure the relative resistance to rotation of the bitumen at a particular temperature and shear rate. The torque value is then changed using calibration factors to yield the viscosity of the bitumen. Viscosity is one of the most important parameter to describe the flow behavior of the binder [89, 105, 106, 192].

Figure 2.7 Brookfield viscometer used in the study

Bitumen being a viscoelastic material, its behavior under practical conditions are both temperature and time dependent and hence cannot be assessed using these conventional techniques. The increase in use of polymer modified bitumen required introduction of new test methods as conventional tests were proving to be inadequate. This led to the development of Performance Grade (PG) plus specifications to characterize the performance of binders. Multiple Stress Creep and Recover (MSCR) test [1, 4] and Linear Amplitude Sweep (LAS) are the latest techniques used for the evaluation of rutting and fatigue performance of asphalt binders. The Penetration and Softening Point tests are mostly empirical and hence are inadequate for characterizing the viscoelastic behavior of bitumen. Viscosity testing, although a more fundamental method of determining the rheological performance of a bitumen, does not provide information on the time dependency of bitumen [7].

2.3.4 *Dynamic shear rheometer*

The dynamic shear rheometer (DSR) test [2] is used to measure the elastic, viscous and viscoelastic properties of bituminous binders by applying a sinusoidal strain to a specimen and monitoring the resulting stress as a function of frequency. The test is conducted within the linear viscoelastic (LVE) region over a wide range of frequencies (time of loadings) and temperatures. The schematic diagram of DSR testing configuration is shown in Figure 2.8.

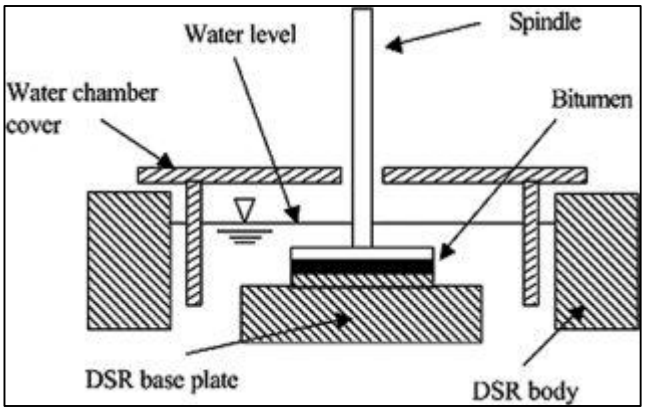

Figure 2.8 DSR testing configuration

The oscillatory-type test is conducted on binders at different temperature, frequency, stress and strain levels. The operational procedure consists of a bitumen sample sandwiched between two parallel plates which is subjected to a sinusoidal strain or a sinusoidal angular displacement of constant angular frequency. The amplitude of the responding stress is measured by determining the torque transmitted through the sample in response to the applied strain. The stress and strain parameters can be calculated as:

$$\sigma = \frac{2T}{\pi . r^3} \tag{2.1}$$

and

$$\gamma = \frac{\theta . r}{h} \tag{2.2}$$

Where, σ is a shear stress, T is a torque, r is radius of parallel discs, γ is shear strain, θ is deflection angle and h is the gap between parallel discs. They are shown in Figure 2.9.

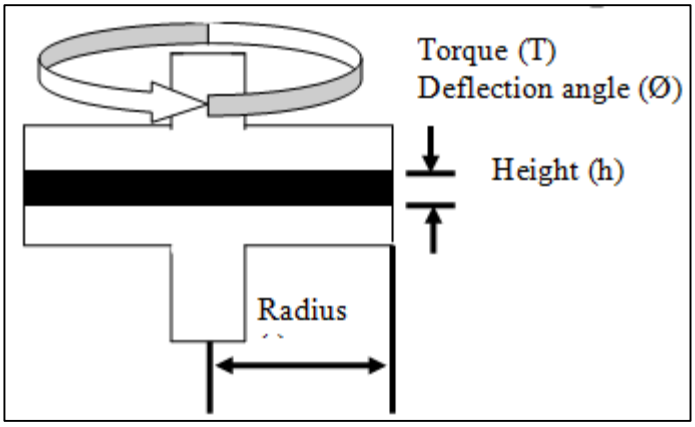

Figure 2.9 Bitumen sandwiched between base plate and spindle.

The shear stress and strain in Equations 2.1 and 2.2 are dependent on the radius of the parallel discs and vary in magnitude from the center to the perimeter of the disc. The shear stress, shear strain and complex modulus, which is a function of the radius to the fourth power, are calculated for the maximum value of radius. The phase angle, δ, is measured by the instrument by accurately determining the sine wave forms of the strain and torque.

The strains that are applied during the dynamic testing must be kept small to ensure that the test remains in the LVE region. Strain sweeps can be used to verify that testing occurs in the LVE region. In general, the strain must be less than 0.5 percent at low temperatures but can be increased at high temperatures. Various parallel disc sizes can be used during dynamic mechanical testing. The size of the disc that should be used to test the bitumen decreases as the expected stiffness of the bitumen increases. In other words, the lower the testing temperature, the smaller the diameter of the disc that needs to be used to accurately determine the dynamic properties of bituminous binders.

2.3.5 *Ageing of bitumen*

Bitumen, like many other organic compounds, is affected by the presence of ultraviolet radiations, oxygen and changes in temperature. During its service life bitumen undergoes ageing starting from its mixing with aggregates in mixing plants, during transportation and laying and finally under the influence of weather and traffic. Ageing leads to significant changes in physical and rheological properties of bitumen and is one of the major factors leading to deterioration of bituminous pavements [99, 102, 108, 120, 146]. It

leads to increase in stiffness of bitumen due to loss of volatiles and causes failure such as thermally induced cracking and ravelling. Ageing is primarily associated with the loss of volatile components and oxidation of the bitumen during asphalt mixture production (short-term ageing) and progressive oxidation of the in place material in the road (long-term ageing). Both factors cause an increase in viscosity (or stiffness) of the bitumen and consequential stiffening of the asphalt mixture.

During its service period, bitumen undergoes a gradual loss in its various mechanical and rheological properties such as cohesion, adhesion, waterproofing, self-healing, and resistance to abrasion. This reduction is mainly due to the exposure of the binder to continuous heat, light and moisture.

Based on the various physical hardening process the ageing of bitumen can be broadly classified into two main categories-

1. Short term ageing, and

2. Long term ageing

The earlier age-hardening of bitumen is usually simulated using short term ageing. Typically, these tests are used to simulate the relative hardening that occurs during the mixing and laying process (i.e. short-term ageing). The ageing is expected to start from the very first exposure of the bituminous binder to the plant burner and hot aggregates and continues to hauling and laying till the final compaction.

Long term ageing, on the other hand is a slow process of ageing to which the bitumen is exposed over its entire life period. Its effects in pavement depends on the prevailing traffic and environmental conditions.

Ageing of bitumen comprises of two main mechanisms [102]-

- The first mechanism is an irreversible process which is associated with the chemical changes inside the bitumen leading to changes in its mechanical and rheological properties. The processes behind the occurrence of this irreversible ageing includes loss of volatiles, oxidation and exudation which is the migration of oily components from the asphalt binder into the aggregates.

- The second ageing mechanism includes physical hardening which is a reversible process. Physical hardening is attributed to the reorganisation of the molecular structure of bitumen microstructure or bitumen molecules to attain a more stable and ideal thermodynamic state under the prevailing conditions.

The main reason behind the ageing of bitumen in its service life is the atmospheric oxidation of certain molecules which leads to the formation of highly polar and strongly interacting functional groups containing oxygen. A number of tests already exist to determine the effect of heat and air on bitumen and is discussed in the following sections.

2.3.5.1 Thin film oven test (TFOT)

The thin film oven test (TFOT) is a technique in which bitumen is aged by subjecting it to conditions as found during normal hot-mix plant operations. It can be conducted using ASTM Test Method D1754. Hot asphalt binder is placed in pans on a rotating shelf in an oven maintained at 163°C for five hours. The aged residue may be subjected to various tests to determine the effects of ageing.

2.3.5.2 Rolling thin film oven (RTFO) test

The rolling thin film oven test (RTFOT) can be conducted following ASTM Test Method D2872 [19]. It is an improvement of the TFOT. 35 gms of bitumen samples are poured on specially design glass bottles. The bottles are then placed horizontally into a vertically rotating rack inside the equipment which maintained at 163 °C for 75 minutes. As the bottles are rotated, fresh films of bitumen are exposed. During the test, the bitumen flows continuously around the inner surface of each container in relatively thin films of 1.25 mm. During each rotation, the opening of the bottle passes an air jet that purges accumulated vapors from the bottle and exposes the bitumen to additional air to intensify the ageing effect. The residue from the rolling thin film oven test is subsequently tested for the effects of ageing. Figure 2.10 shows the RTFOT bottles before and after the test. The chamber of the RTFOT used in the study is shown in Figure 2.11. The conditions in the test are not identical to those found in practice, but experience has shown that the amount of hardening in the RTFOT correlates reasonably well with that observed in a conventional batch mixer.

Figure 2.10 RTFOT bottle before and after the test

Figure 2.11 Inside chamber of the RTFOT used in the study

2.3.5.3 Pressure ageing vessel (PAV) test

The long-term in-service oxidative ageing in field is simulated using the pressure ageing vessel (PAV) [20]. The equipment used in the study is shown in figure below. The

RTFO ageing is followed by ageing in PAV and the samples are then subjected to different testing to assess the effect of long term ageing on the properties of the bitumen. The testing procedure entails ageing 50 g of asphalt binder in a 140 mm diameter pan (approximately 3.2 mm binder film thickness) within a heated vessel. The vessel is pressurized with to 2.1 MPa of air for 20 hours at temperatures of 90, 100 and 110 °C. The ageing temperature depends on the in service conditions where the bitumen is likely to be used and is selected from the SHRP specification manual. The PAV test accounts for temperature effects but is not intended to account for mixture variables such as air voids, type of aggregates and as well as aggregate adsorption [132].Schematic figures of PAV pans and chamber is shown in figure 2.12 (a,b).

(a) (b)

Figure 2.12 (a, b) Schematic figure of PAV pans and chamber

2.4 Viscoelastic Nature of Bitumen

Asphalt Binders are viscoelastic materials. Behavior of these materials, therefore is a combination of elastic and viscous parts. Elastic materials return to their initial state after the removal of applied loads, whereas in viscous materials permanent deformations persists even after the removal of loads. Several factors affect the behavior of viscoelastic materials, among which temperature is one of the most critical parameter. The second parameter, which has an effect on viscoelastic materials, is frequency (loading time) or the rate of loading. At

lower temperatures and higher frequency the behavior is elastic while at higher temperature and low frequencies the material displays a Newtonian fluid type behavior. The range of temperatures and loading times between these two extremes, at which the viscoelastic behavior occurs, represents the typical conditions experienced in service[31, 109].

Transient methods, e.g. creep loading, stress relaxation, and constant rate of loading, and Dynamic (oscillatory) test methods are the two most commonly used methods of determining viscoelastic properties. Amongst the two, dynamic (oscillatory) testing is usually considered more appropriate as in a relatively short testing time it covers a wide range of temperature and loading conditions. The viscoelastic behavior of bitumen, based on standard creep testing, is represented in Figure 2.13. Three regions of bitumen behavior can be seen in the figure: elastic, delayed elastic and viscous. The non-recoverable deformation is due to the viscous portion which the bitumen or the asphalt mixture incorporating the bitumen experiences under loading. Nevertheless, the elastic and delayed elastic strain are can be recovered completely after the load and applied stress are removed [83]. The elastic response dominates the asphalt binder at low temperatures and/or short loading times. Meanwhile, at high temperatures and/or intermediate loading times, the delayed response rules. The delayed elastic and the purely viscous components governs the time dependent deformation in the viscoelastic material [6]. The shape of the creep curve changes depending on the relative magnitude of these three components. These descriptions for elastic, viscous and viscoelastic nature of bitumen are for a linear response which means that the deformation at any temperature and time should be directly proportional to the applied load. It is enormously difficult to characterize the non-linear response for viscoelastic materials in the laboratory [16]. To confirm that the testing remains within this linear viscoelastic region, the strain/deformation to be applied to the bitumen should remain within limits.

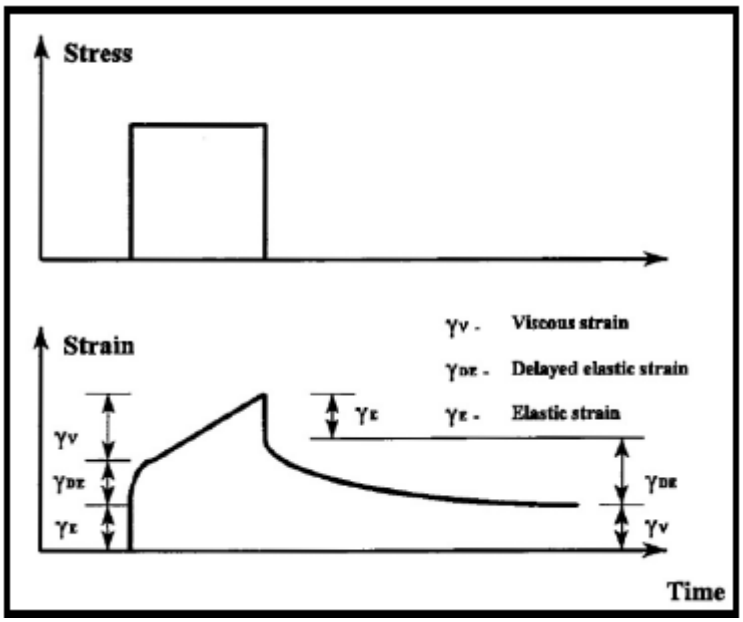

Figure 2.13 Response of a viscoelastic material in creep

2.5 Theory of Linear Viscoelasticity

The response of a linear elastic material is not time dependent. In other words, if a constant load is suddenly applied to it, it will deform immediately, maintain a constant deformation and return to its initial shape after the removal of the load. However, in a viscous material, according to Newton's law, stress is time dependent and is directly proportional to the rate of strain but independent of strain itself.

The behavior of linear viscoelastic materials combine both linear elastic and linear viscous behavior. If a constant strain is applied to this material, the stress, which is required to maintain this deformation, decreases gradually or relaxes. Also, when a constant stress is applied, deformation increases slowly with time or creeps. Under oscillatory testing, the stress in a viscoelastic material is not exactly in phase with strain (pure elastic solid), and also not 90 ° out of phase with strain (pure viscous fluid) but is between these two extremes. The difference between linear viscoelastic and non-linear viscoelastic materials is that in linear viscoelastic materials the ratio of stress and strain is a function of time (or frequency) and temperature but not of stress magnitude.

It is very important to understand the concept of linear viscoelasticity before moving forward for the evaluation of viscoelastic parameters. In a linear viscoelastic material the stress and strain is a function of time (frequency) and temperature, but is independent of the stress magnitude. This assumption of bitumen being a linear viscoelastic material is true for lower ranges of strain values which varies for different bitumen at different temperatures and makes the analysis easier and convenient as compared to nonlinear analysis.
The two common methods of determining viscoelastic properties are [137]

1. Transient methods: Creep, Relaxation, constant rate Loading, and
2. Dynamic or oscillatory methods.

Dynamic methods (shear rheometers) are most widely used because of their ability to incorporate wide range of loading and temperature conditions in a short time span [144].

2.5.1 *Creep:*

Creep is defined as the response of the material when subjected to a constant load (σ_o) over a time period t (Figure 2.14). The strain varies as a function of time. The viscoelastic parameter used to define creep is Creep Compliance J and is defined as the ratio of strain to stress.

$$J(t) = \grave{o}(t)/\sigma_o \tag{2.3}$$

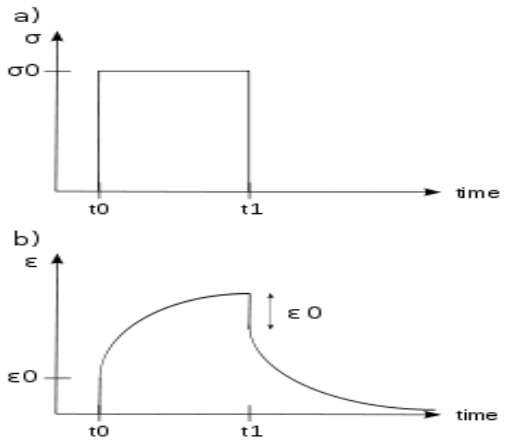

Figure 2.14 (a, b) Stress strain Variation for Creep

2.5.2 *Relaxation:*

Relaxation can be defined as the response of the material subjected to constant strain (ϵ_o) over a time period t (Figure 2.15 a, b). The stress relaxes as a function of time. Relaxation modulus R is used to define this process and is the ratio of stress and strain.

$$R(t) = \sigma_t / \dot{o}_o \tag{2.4}$$

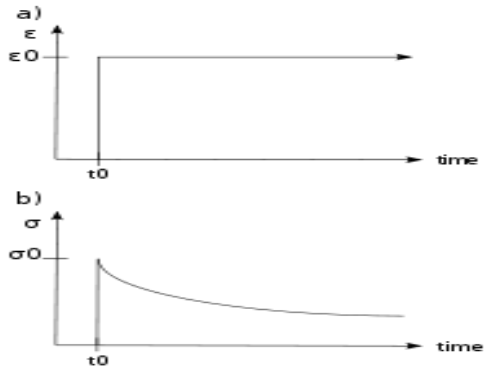

Figure 2.15 (a, b) Stress Strain Variation for Relaxation

Relation between stress and strain using Creep compliance and Relaxation modulus for a cubical element is as follows:

$$\varepsilon(t) = \int_0^t J(t-T).\frac{d\sigma(t)}{dt}.dt \tag{2.5}$$

$$\sigma(t) = \int_0^t R(t-T).\frac{d\dot{o}(t)}{dt}.dt \tag{2.6}$$

2.5.3 *Dynamic/Oscillatory testing*

The viscoelastic behavior of bitumen (especially polymers) can be characterized using Dynamic Mechanical Analysis (DMA) with the help of Dynamic shear rheometer (DSR) having parallel plate geometry. It can be operated in stress as well as strain controlled modes [132]. Controlled Strain mode is normally used to determine dynamic mechanical properties of bitumen [194]. A sinusoidal stress or strain amplitude is applied to a sample sandwiched between two plates with the lower plate fixed and the upper plate applying the oscillatory

load. Figure 2.16 (a-c) shows the variation of stress and strain for dynamically loaded sample for different materials.

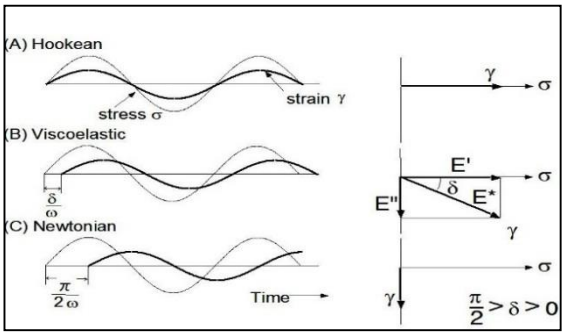

Figure 2.16 (a-c) variation of stress and strain

For a controlled strain mode the following equations defines the evaluation for the viscoelastic parameters [137]

$$\gamma = \gamma_o \sin \omega t \tag{2.7}$$

$$\dot{\gamma} = \gamma_o \omega \cos \omega t \tag{2.8}$$

From stress relaxation equation:

$$\sigma(t) = \int_0^t R(t-T).\frac{d\dot{o}(t)}{dt}.dt \tag{2.9}$$

Taking $\sigma\ (t) = \ \tau$ and R = G and t-T = s we get,

$$\tau(t) = \int_0^\infty G(s).\gamma_o \omega \cos\left[\ \omega(t-s)\right] ds \tag{2.10}$$

$$\tau(t) = \int_0^\infty G(s).\gamma_o \omega \sin(\omega t)\sin(\omega s) + \int_0^\infty G(s).\gamma_o \omega \cos(\omega s)\cos(\omega t) \tag{2.11}$$

$$\tau(t) = \gamma_{max}\left[\int_0^\infty G(s)\omega \sin(\omega s)\right]\sin(\omega t) + \gamma_{max}\left[\int_0^\infty G(s)\omega \cos(\omega s)\right]\cos(\omega t) \tag{2.12}$$

Replacing the first bracket by G‘ (ω) and the second bracket by G‘‘ (ω) we get

$$\tau(t) = \gamma_{max} G'(\omega)\sin(\omega t) + \gamma_{max} G''(\omega)\cos(\omega t) \tag{2.13}$$

As the corresponding stress will be in lag with the strain by let us say δ, therefore,

$$\tau(t) = \tau_{max}\, sin(\omega t + \delta) \tag{2.14}$$

$$\tau(t) = \tau_{max}\, sin\omega t\, cos\delta + \tau_{max} cos\omega t\, sin\delta \tag{2.15}$$

From the above equations,

$$G'(\omega) = \left(\frac{\tau_{max}}{\gamma_{max}}\right) cos\delta \tag{2.16}$$

$$G''(\omega) = \left(\frac{\tau_{max}}{\gamma_{max}}\right) sin\delta \tag{2.17}$$

G′ and G′′ are the storage and the loss modulus which provides an insight about the stored and dissipated energy by the sample. Storage modulus is associated with the stiffness while loss modulus gives information about the internal friction [80]. The loss modulus is also referred to as the viscous modulus or the viscous component of the complex modulus. The loss tangent is defined as the ratio of the viscous and elastic components of the complex modulus or simply the tangent of the phase angle.

$$\delta = \tan^{-1}\left(\frac{G''}{G'}\right) \tag{2.18}$$

The phase angle δ defines the comparative elastic and viscous behavior. For a complete viscous material the phase angle is equal to 90˚ while for a pure elastic material it equals to 0˚ (Figure 2.17). Complex modulus (G*) on the other hand is a measure of overall resistance to deformation and is defined as the ratio of maximum stress to maximum strain.

$$G^* = \left(\frac{\tau_{max}}{\gamma_{max}}\right) \tag{2.19}$$

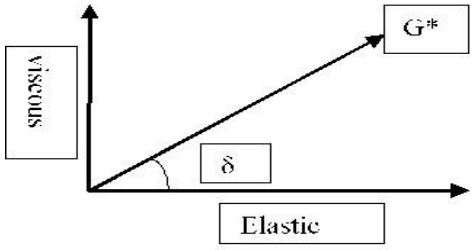

Figure 2.17 Representation of Complex Modulus

In addition, a viscosity value for the bitumen can also be obtained from dynamic oscillatory test. The viscosity is known as the complex viscosity (Pa.s) and is defined as the ratio of the complex modulus and the angular frequency:

$$\eta^* = \frac{|G^*|}{\omega} \tag{2.20}$$

Since the complex viscosity is a function of complex number pair, a real and an imaginary part of the complex viscosity can also be defined. The real part of the η^* is termed the dynamic viscosity and defined as:

$$\eta' = \frac{G''}{\omega} \tag{2.21}$$

Where, η' is dynamic viscosity (Pa.s) and the other parameters are as previously defined. The imaginary part of the η^* is called out-of-phase component of η^* and defined as:

$$\eta'' = \frac{G'}{\omega} \tag{2.22}$$

Where, η'' is out of phase component of η^* (Pa.s).

2.6 Time-Temperature Superposition Principle

Time temperature superposition (TTSP) is a competent tool for describing the viscoelastic behavior of linear polymers over a broad range of time and frequency, by shifting data obtained at several temperatures to a common reference temperature[6, 30, 59]. A single rheometer can be operated to give values only over a range of three to four decades at a

particular temperature[48]. For bitumen and modified binders comprising polymers, this data is insufficient to describe the complete rheological and viscoelastic response from the high frequency end of the plateau zone to the low-frequency terminal zone. In linear polymers viscoelasticity arises from a molecular rearrangement process, which occurs from a stress or from a diffusion process under stress. The speed of these processes depends on the speed of molecular motion where temperature is a measure. In such materials all the processes contributing to the viscoelasticity of a material are accelerated to the same extent by temperature rise [95]. Thus, by obtaining data at several temperatures for a measurable range of frequency, a master curve could be plotted at a single reference temperature that could cover many decades of frequency/time. A material to which this technique is applicable is said to be thermorheologically simple[6, 109].

Temperature dependent shift factors are used for the magnitude of stresses (vertical shift) and time/frequency (horizontal shift) on log-log plots of material functions, like complex modulus, phase angle and creep compliance. The temperature dependent, vertical shift factor b_T multiplies a stress, determined at temperature T to yield a "reduced stress", that is the value at the reference temperature chosen. Similarly, the horizontal shift factor a_T divides a time or multiplies a frequency to yield a reduced frequency/time scale of ωa_T or t / a_T. This principle can be mathematically written as

$$b_T E(\omega a_T, T) = E(\omega, T_0) \tag{2.23}$$

2.6.1 *Thermorheological simplicity*

TTSP is applicable only for "linear viscoelastic materials" which are "thermorheologically simple". How does one know if the material under consideration is thermorheologically simple? Thermorheological simplicity is attained when all the contributing retardation or relaxation mechanisms of the material and its stress magnitude at all times or frequencies have the same temperature dependence.

To experimentally determine if a material is thermorheologically simple, one may perform a set of creep or relaxation tests at different temperatures, and plot the results. If these curves can be overlapped by horizontal and vertical shifts, on the log-time axis the

material is said to be thermorheologically simple[95, 194]. If a smooth curve cannot be obtained the material is “thermorheologically complex”.

Different material functions describe different form of behavior for the same material. Bitumen complex modulus G^* is mainly associated with the physical aspect of the material whereas the phase angle δ is associated with its chemical nature. Hence in an attempt to construct master curves using TTSP different shift factors can be obtained for same temperature. Moreover predicting the behavior of the binder using only one of these parameter is questionable. So, while studying the viscoelastic behavior of the bitumen using master curves it is necessary that both these parameters be taken into consideration.

According to Airey [1997], modulus curves at low temperatures crowd together at high frequency/low temperature values and at very high frequencies they nearly all coincide with one horizontal asymptote. At this region, the modulus is called the glassy modulus, G_g. Under viscous conditions, however, there is no convergence to a single viscous asymptote as viscosity depends on temperature and therefore each temperature gives rise to a separate viscous flow asymptote. This is shown in Figure 2.18.

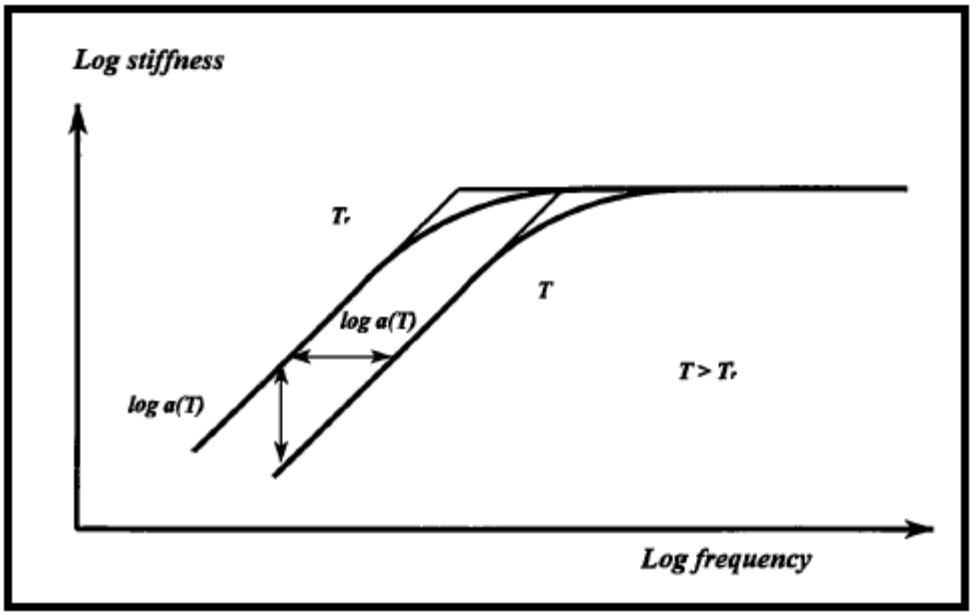

Figure 2.18 Viscous asymptote for asphalt binders.

Airey [1997] also noted that because the limiting viscous behavior is strongly temperature dependent and the elastic behavior is not, it is possible to separate the influence of frequency and temperature. The concept of time-temperature superposition (Figure 2.18) which shows an asymptote pair for an arbitrary reference temperature, T_{ref} (or T_r). If the temperature is increased from T_{ref} to T there is a decrease in viscosity by a factor a_T. Therefore, the viscous asymptote at T lies an amount of log a_T below that of T_{ref}. However, the elastic asymptote is negligibly changed during the temperature rise. The result is that the asymptote pair appears to be shifted a distance log a_T along the log ω axis, because the viscous asymptote has unit slope. The viscoelastic response of a bitumen is a transition between the asymptotic viscous and elastic response and is represented by the curve for T_{ref}. If a change in temperature causes the modulus curve to shift together with its asymptotes over the same distance log a_T, the material behaves as a thermorheologically simple one.

A reference temperature can be chosen and the next higher modulus curve shifted coincides with the reference temperature curve to obtain a value for the horizontal shift factor log a_T and a more extended modulus curve. This procedure is repeated for all curves in succession to obtain a master curve. The effect of temperature on complex modulus is, therefore, to shift the curve of log $|G^*|$ versus log ω axis without changing its shape. This permits the reduction of isotherms of log $|G^*|$ versus log ω measured over a wide range of temperatures to a single master curve.

The extended frequency scale used in a master curve is referred to as the reduced frequency scale and defined as:

$$\log f_r = \log f + \log a_T \tag{2.24}$$

Where, f_r is reduced frequency (Hz), f is frequency (Hz) and a_T is the shift factor. The amount of shifting required at each temperature to form the master curve is called the shift factor, a_T. A log a_T plot versus temperature with respect to the reference temperature curve is generally prepared in conjunction with a master curve. This plot gives a visual indication of how the properties of viscoelastic material change with temperature [104]. Figure 2.19 shows the process involved in constructing a master curve.

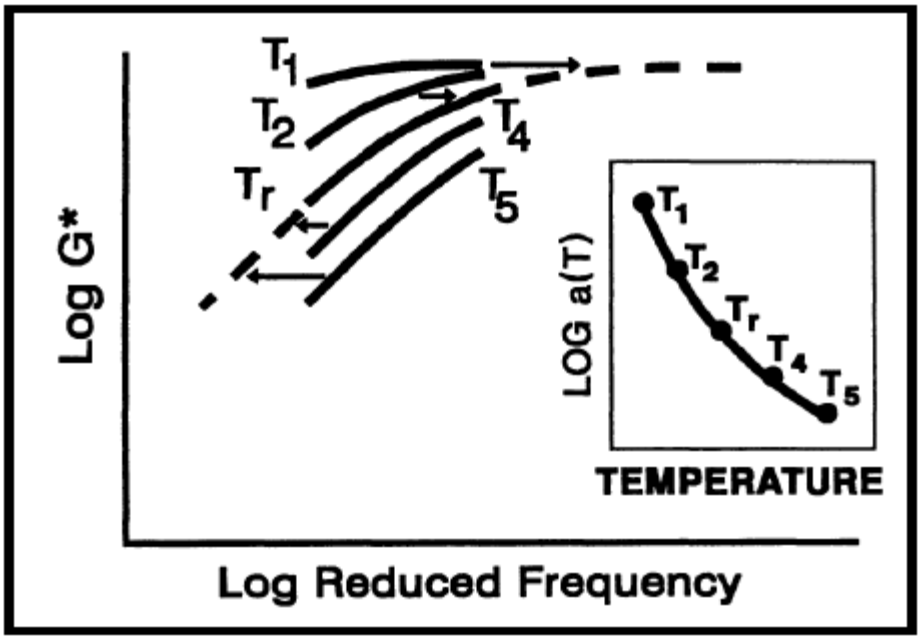

Figure 2.19 Process for construction of master curve.

2.6.2 *Shift factors*

2.6.2.1 Vertical shift factor

Research has shown that stress functions of linear viscoelastic materials are proportional to the product of density and temperature. The vertical shift factor represents temperature induced density changes and involves shift along the modulus or stress function axis. This implies that the vertical shift factor can be written as

$$b_T = (T_0\rho_0)/(T\rho) \tag{2.25}$$

Where, T_0 is the reference temperature, T is the temperature at which shift factor has to be applied, ρ_0 and ρ are the corresponding densities.

The vertical shift factor is also sometimes determined directly from the variation with temperature of a distinctive value of a modulus or compliance, such as a maximum or minimum in loss modulus. Plateau of the material functions can also be used. Determining horizontal shift of loss angle in loss angle versus log G* plot (Van Gurp-Palmen plot) is another way of determining vertical shift factor that is independent of time or frequency shift.

However, most of the research to date on binders and bituminous materials mastercurve construction does not normally consider vertical shift and it is assumed to be unity [6].

2.6.2.2 Horizontal shift factor

Horizontal shift factor a_T is a number which is required to be multiplied to the time/ frequency to shift data at a particular temperature T to the reference temperature T_0. Different researches had been done in finding a suitable value of a_T for bituminous materials which could be employed based on its thermal behavior. These studies focuses from the physical molecular aspect of the binder to its chemical behavior.

2.6.2.2.1 Shift based on viscosity

Viscosity is a parameter which comprises of stress and time. It requires the application of both the shift factors. If complex viscosity η^* is used as the rheological parameter then the master curve for complex viscosity is plotted between $\frac{b_T}{a_T}|\eta^*|(T)$ and ωa_T. This implies that if zero shear viscosity is taken into consideration one can write,

$$\frac{b_T(T)}{a_T(T)}\eta_0(T) = \eta_0(T_0) \tag{2.26}$$

Considering the vertical shift factor as unity, vertical shift factor can be written as,

$$a_T(T) = \frac{\eta_0(T)}{\eta_0(T_0)} \tag{2.27}$$

2.6.2.2.2 Arrhenius equation

Observation of the dependence of viscosity of liquids on temperature led to the empirical Arrhenius relationship that can be expressed as

$$a_T(T) = \exp[\frac{E_a}{2.303R}(1/T - 1/T_R)] \tag{2.28}$$

Where E_a is called the activation energy, typically 250 kJ/mol for bituminous binders. It is the minimum energy required for any intermolecular movement. R is the universal gas

constant 8.314 J/˚K-mol. Arrhenius equation has been found to fit data at the terminal and plateau zones for linear polymers as long as the temperature is well above the glass transition temperature T_g. Also meaningful activation energy has not been defined so far. Variation in E_a with frequency and modulus has also been reported. So a logical value must be chosen which could have some significance regarding the physical and/or chemical nature of bitumen.

2.6.2.2.3 William-Landel-Ferry (WLF) equation

This equation is based on the free volume concept of Doolittle. It has been widely used to describe relation between a_T and temperature dependency of bitumens.

$$\log a_T = \frac{-C_1(T - T_{ref})}{C_2 + (T - T_{ref})} \tag{2.29}$$

Where, C_1 and C_2 are empirical constants. The implication of this model lies in the determination of these constants. Moreover this equation has been mainly found suitable when reference temperature is close to T_g. Many universal constants have been proposed based on the reference temperature. The most famous and frequently used values are8.86 and 101.6 for C_1 and C_2 as proposed by Williams et al. These values have shown good fit when $T\text{-}T_r > -20^oC$. Another values proposed by Anderson were 19 and 92 which were based on some defining temperature T_d. This defining temperature is not very clear and is bitumen specific [6].

Williams et al. proposed that the reference temperature is related to glass transition temperature as

$$T_r - T_g = 50^0 C \tag{2.30}$$

But master curve should be such that, one must be able to view the rheological behavior at any reference temperature desired. This limits the use of WLF equation which has strong dependence on the selection of reference temperature.

2.6.2.2.4 Manual shift procedure

This is a simple procedure in which the data are shifted manually in MS EXCEL or similar workbook till a best and smooth fit is obtained. The smoothness of the curved is judged visually. If smooth curve cannot be obtained, it implies that the binder is not thermorheologically simple.

2.7 Rheological Data Representation

The DSR data obtained need to be represented in a useful form to enable study on the rheological properties of bituminous binders.

2.7.1 *Isochronal plots*

It is the representation of any viscoelastic function (complex modulus, phase angle etc.) verses temperature at constant frequency or loading time. Therefore, viscoelastic data can be presented over a range of temperatures at a given frequency using an isochronal plot. The simplest benefit of isochronal plots is the comparison of complex modulus or phase angle at different temperatures. Moreover, several properties of bitumens, such as temperature susceptibility, can be interpreted from this type of plot.

Temperature susceptibility, which is often a major performance criterion for bitumens, may be defined as the change in consistency, stiffness or viscosity, as a function of temperature. Temperature susceptibility should be based on measurements at different temperatures but similar loading times as the rheological properties of bitumens are a function of both time and temperature. The general shape of an isochronal plot at a constant frequency is shown in Figure 2.20.

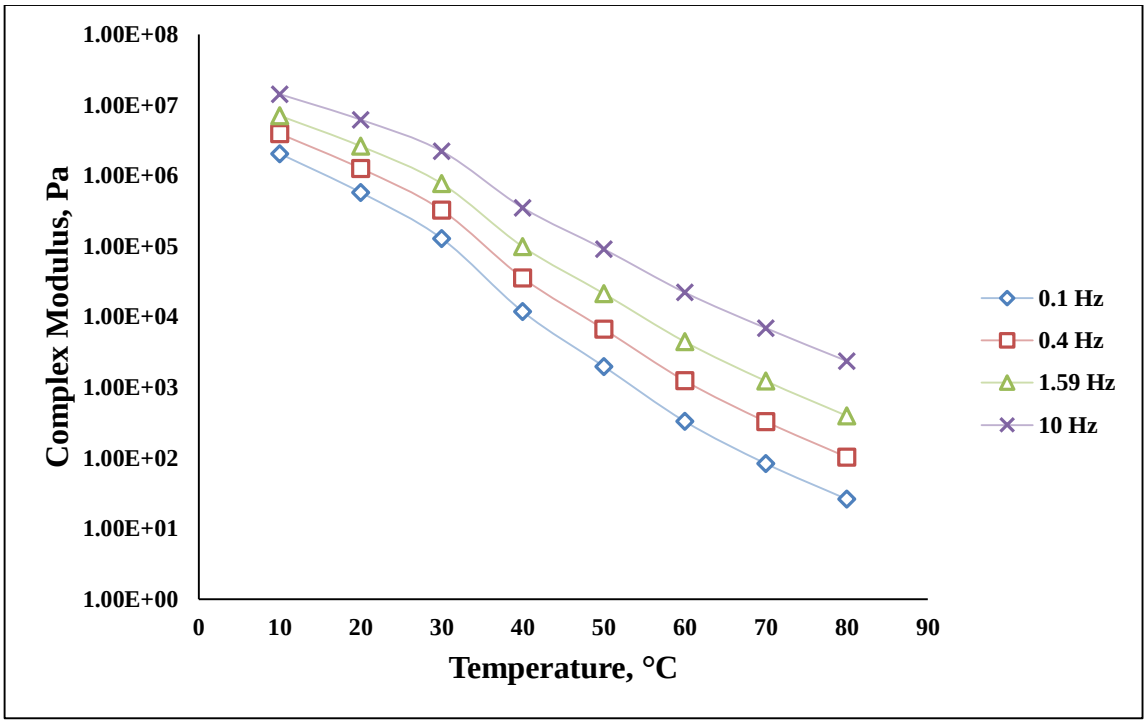

Figure 2.20 Example of isochronal plot at different frequencies

2.7.2 *Isothermal plots*

It is the plot (Figure 2.21) of some viscoelastic function (complex modulus, phase angle etc.) verses frequency at any particular temperature. In this plot, viscoelastic data, at a given temperature, is plotted over a range of frequencies or loading times. Therefore, this plot can be used to compare different viscoelastic functions at different loading times at a constant temperature. In addition, it can be used to study the time dependency of materials.

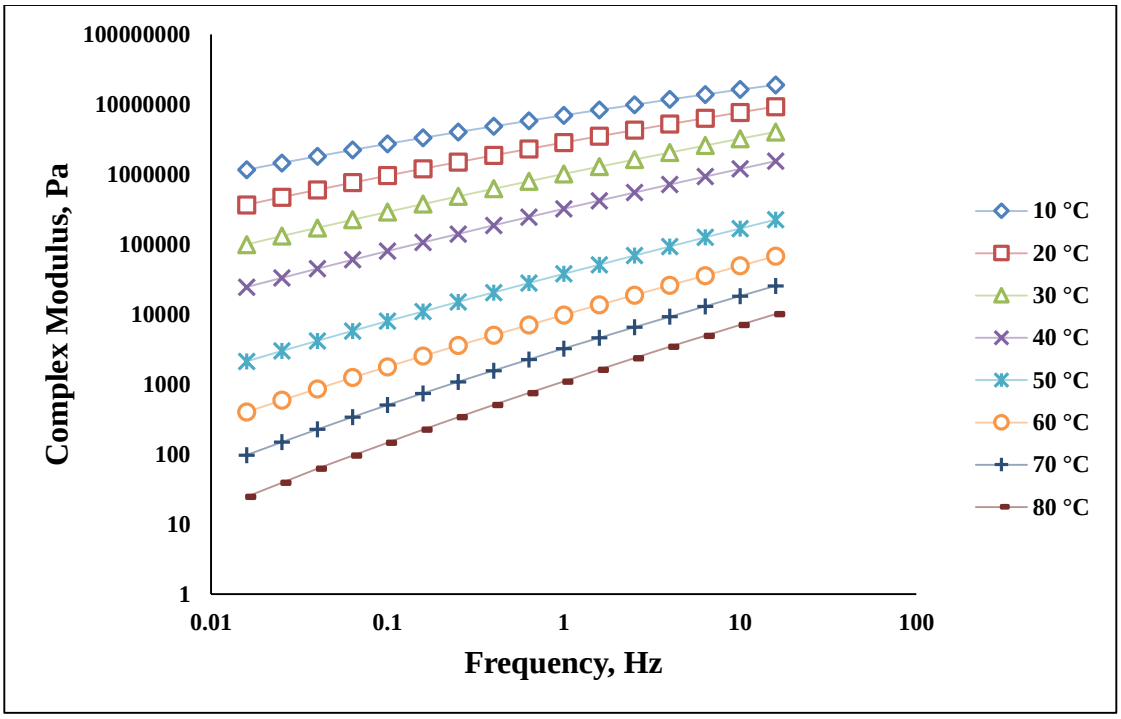

Figure 2.21 Example of isothermal plot at different temperatures

2.7.3 *Black diagrams*

It is the plot of complex modulus verses phase angle. It is very useful in judging measurement errors, change in composition or structure of bitumen. So indirectly it can be used for presenting the effect of aging or modification in bitumen. An example of the plot is shown in Figure 2.22.

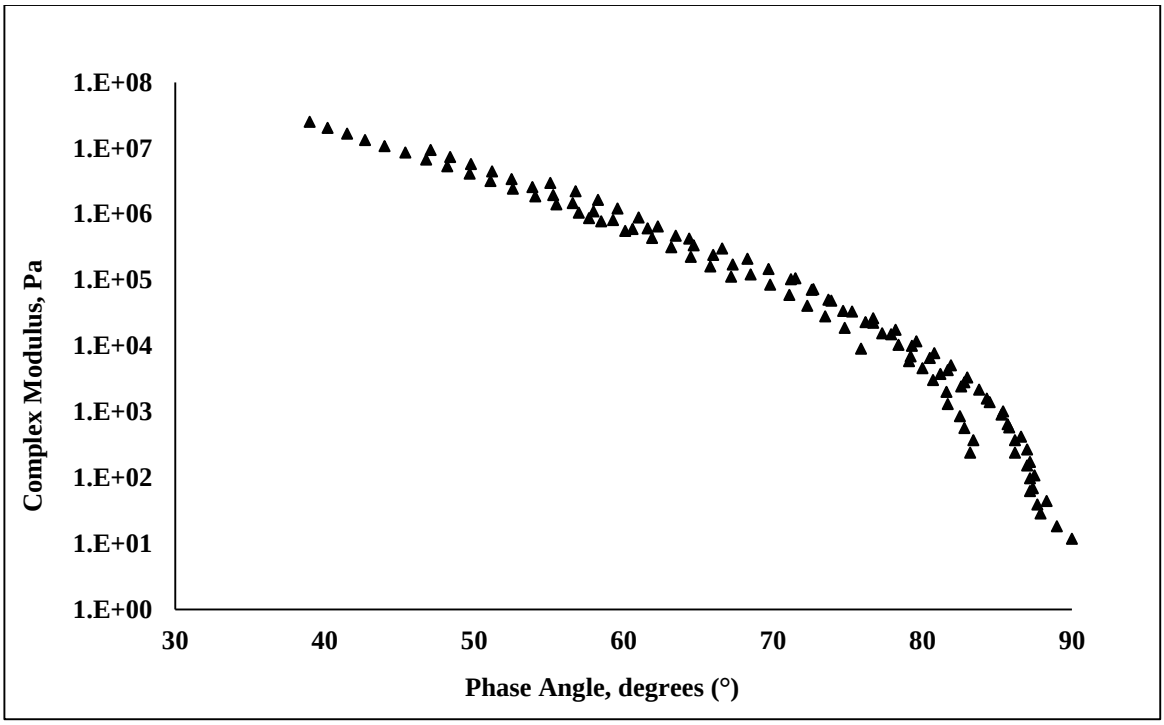

Figure 2.22 Example of black diagram

2.8 Tests on Performance Evaluation of Asphalt Binders

2.8.1 *Evaluation of rutting*

Various test methods have evolved over years for predicting the rutting susceptibility of unmodified and modified bitumen [69, 86, 117, 135, 138, 147, 163, 180]. Various tests and researches have indicated the superiority of one test method over the other. The first criteria/parameter to catch the rutting sensitivity of bitumen was $|G^*|/\sin\delta$, an outcome of the Strategic Highway Research Program (SHRP)'s Superpave binder grading protocol. The specification is laid out in American Association of State Highway and Transportation Officials (AASHTO) M 320. This parameter is a resultant of the dissipated energy concept, where the inverse of loss compliance (1/J'') is used [17]. It is based on the assumption that rutting is caused by the total energy dissipated per cycle of loading [135]. For a sinusoidal wave, typical in dynamic shear rheometer (DSR), it can be determined that

$$W_D = \pi.\tau_{\max}{}^2.\frac{1}{|G^*|/\sin\delta} \tag{2.31}$$

Where, W_D = energy loss per cycle or dissipated energy; τ_{max} = maximum shear stress; $|G^*|$ = shear complex modulus and δ = phase angle.

As can be seen in equation 2.31 that an increase in $|G^*|/\sin\delta$ causes the total dissipated energy to decrease. This in turn leads to the reduction of the rutting susceptibility. For this reason $|G^*|/\sin\delta$ was used for high temperature performance grading of paving asphalts in Superpave specification to rank asphalt binders based on their rutting resistance. This parameter correlated well with the rutting behavior of mixes in the studies done by Dongre [53] and Stuart [166].

In Europe, zero-shear viscosity (ZSV) was adopted as a standard parameter to judge the rutting performance of various binders. Different studies proved the validation of this parameter as a rutting predicting tool for bituminous mixes [143, 169, 178, 179, 203]. There are various methods by which the ZSV can be determined [34]. In this study steady shear creep test using DSR was used to evaluate the variation of viscosity with shear rate. This variation was modelled using Carreau-Yasuda equation using the following mathematical form.

$$\frac{\eta-\eta_\infty}{\eta_0-\eta_\infty}=\left[1+\left(\lambda\dot{\gamma}\right)^a\right]^{(n-1)/a} \tag{2.32}$$

Where η is the viscosity of the fluid, η_0 and η_∞ are the zero and infinite shear viscosity, $\dot{\gamma}$ is the shear rate, λ , n and a are the shape parameters. $1/\lambda$ is the critical shear rate at which the viscosity starts to decrease.

Shenoy [157] later introduced another rheological term which was an advancement of the traditional Superpave parameter. This term, according to studies done by Shenoy was proved to be more fundamental and accurate in judging the rutting resistance of mixes [158]. Using fundamentals of rheological equations he found that the percent unrecovered strain ($\%\gamma_{unr}$) can be written as

$$\%\gamma_{unr}=\frac{100.\tau_0}{|G^*|}\left(1-\frac{1}{\tan\delta\sin\delta}\right) \tag{2.33}$$

He concluded that, to minimize the permanent deformation, the term $\frac{|G^*|}{(1-1/\tan\delta\sin\delta)}$ should be maximized. Hence higher the value of this term, more rut resistant the binder will be.

During the same time, repeated creep-recovery test (RCRT) was suggested by Bahia et al [25]. This was the outcome of National Cooperative Highway Research Program (NCHRP) (NCHRP 459). Large number of mixes were found to correlate well with the results of RCRT. In order to introduce the non-linearity associated with modified binders and to make RCRT more rudimentary , multiple stress creep and recovery (MSCR) test was proposed by D'Angelo [44, 45, 53]. Various laboratory and field investigations have proved this method to be applicable for both unmodified and modified binders. This method has been introduced as a part of new Superpave grading system (AASHTO MP 19-10) and is accepted in standard form. MSCR test is conducted in accordance to AASHTO TP 70. DSR is used for conducting the test using 25 mm diameter spindle with 1mm gap. The binder is subjected to creep loading and unloading cycle of 1 second and 9 second respectively, at stress levels of 0.1 kPa and 3.2 kPa. Ten cycles of loading is given at each stress level. The non-recoverable creep compliance (J_{nr}) and percent recovery (% rec) are the two main parameters which are calculated from the test results to evaluate the rutting susceptibility of asphalt binders. The difference in J_{nr} between the two stress levels, expressed as percentage ($J_{nr,diff}$) is also calculated to determine the stress sensitivity of the bitumen. The test is typically conducted at 64 °C on rolling thin film oven (RTFO) samples. Figure 2.23 shows a classical creep and recovery curve for a single cycle and the corresponding calculations. However, the average of all the ten cycles at each stress level is used in practice. Table 2.1 and Table 2.2 presents the desired specification values for different traffic conditions as outlined by the Asphalt Institute (AI).

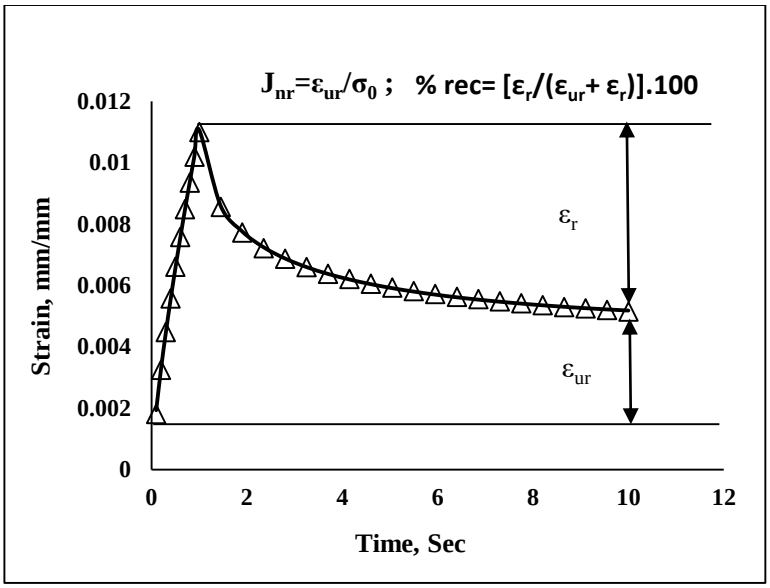

Figure 2.23 Schematic representation of creep and recovery.

Table 2.1 Specification for maximum J_{nr} at different traffic level

Type of Grade	$J_{nr,3.2kPa}$, kPa^{-1} Maximum	$J_{nR,diff}$ %, max
S	4	75
H	2	
V	1	
E	0.5	

Note: S-Slow; H-Heavy; V-Very heavy; E-Extremely heavy

Table 2.2 Specification for minimum % recovery for different J_{nr}

$J_{nr,3.2kPa}$, kPa^{-1}	Minimum % Recovery
2.0-1.01	30
1.0-0.51	35
0.5-0.251	45
0.25-0.125	50

2.8.1.1Calculations

The creep strain at the beginning and end of each creep cycle was denoted as ε_0 and ε_c. The strain at the end of each recovery cycle was symbolized as ε_r. The following calculations according to ASTM D7405-10a [21] were made for analyzing the results

obtained from the MSCR test. The calculations were made corresponding to each creep and recovery cycle (N=1 to 10).

$$\varepsilon_1 = \varepsilon_c - \varepsilon_0 \tag{2.34}$$

$$\varepsilon_{10} = \varepsilon_r - \varepsilon_0 \tag{2.35}$$

The average percent recovery at all the stress levels was calculated as

$$R(\sigma) = sum(\varepsilon_r(\sigma, N)) / 10 \tag{2.36}$$

Where,

$$\varepsilon_r(\sigma, N) = \frac{(\varepsilon_1 - \varepsilon_{10}).100}{\varepsilon_1} \tag{2.37}$$

Similarly the average percent non-recoverable creep compliance was calculated as

$$J_{nR}(\sigma) = sum(J_{nR}(\sigma, N)) / 10 \tag{2.38}$$

Where,

$$J_{nR}(\sigma, N) = \varepsilon_{10} / \sigma \tag{2.39}$$

2.8.2 *Evaluation of fatigue*

The current Superpave specification for performance grading was developed mainly for unmodified binders and has been proved to be misleading for predicting rutting and fatigue properties of modified bitumen [71, 73, 84, 85, 199]. The method employs the parameter G*.sin δ to quantify the asphalt binder fatigue resistance. It is based on the concept that lower dissipated energy per loading cycle ($\pi.\gamma_0^2.G^*.\sin\delta$) will lead to lower distress accumulation. Hence the intermediate temperature is determined such that G*.sinδ be less than 5000 kPa [17]. This stiffness based parameter, which is a development of Strategic Highway Research Program (SHRP), is measured at a fixed frequency (10 rad/sec) ensuring the strain to be below the linear viscoelastic regime of the bitumen. The recommended strain value is 1-2%. The test was developed based on the speculation that binder in pavements

functions mostly in the linear viscoelastic range and is not likely to affect their properties. This simple test cannot describe the actual complicated fatigue phenomena in which the binder is exposed to higher strain levels and varied frequency levels.

Several testing methods have been developed to describe fatigue properties of bitumen and modified binders, among which, the time sweep testing method, which was developed during NCHRP Project 9-10, is one of the most accurate in providing fatigue properties of bituminous binders [25]. However, Bahia et al. (2001) found that DSR-based time sweep testing was not suitable for characterizing the fatigue behavior of bitumen as a result of its unstable flow and edge fracture effects [199]. In this regard, Johnson (2010) developed a new testing method, named the linear amplitude sweep (LAS) test, which was used to investigate the fatigue properties of bitumen and polymer modified binders [46, 73, 199]. Good correlation with long-term pavement performance (LTPP), field fatigue cracking data, and shorter testing time (310 s) were some notable advantages of this testing method [73]. In this study hence LAS test has been used to evaluate the fatigue performance of asphalt binders.

2.8.2.1 Test procedure of linear amplitude sweep

Linear amplitude sweep (LAS) test following AASHTO TP 101-14 is conducted to determine the parameter A and B, to assess the fatigue life of the binders at different strain levels. The test requires conducting a frequency sweep test followed by a linear amplitude sweep. The frequency sweep is conducted at a very low strain level of 0.1% to obtain undamaged material properties (α), which is used as an input in the analysis of amplitude sweep test. The amplitude sweep test is conducted by linearly varying strain from 0-30%, through 3100 loading cycles at a fixed frequency of 10 Hz as shown in Figure 2.24. The test begins with 100 cycles of sinusoidal loading at 0.1% strain followed by incremental load steps of 100 cycles each, at a rate of 1% increment in strain level.

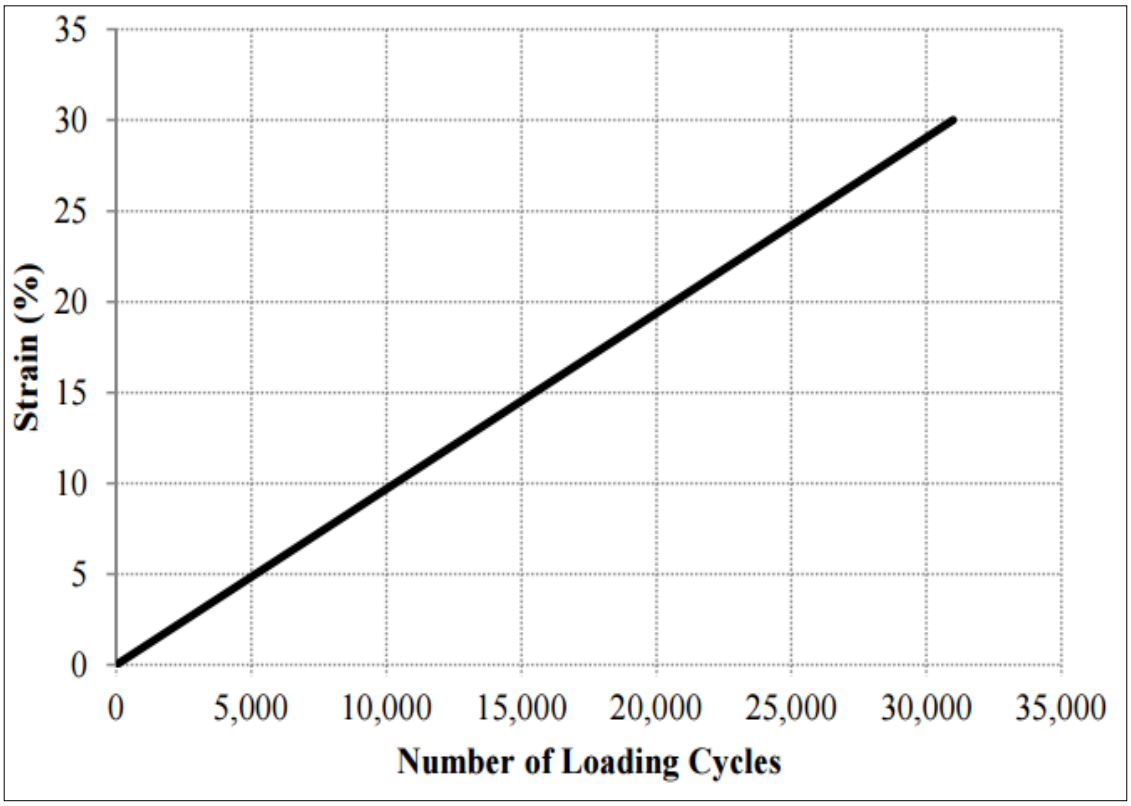

Figure 2.24 Strain sweep in LAS test

The frequency sweep test (0.2-30 Hz) is used for the determination of the parameter alpha (α) which is later used in the analysis of strain sweep data. α is the reciprocal of the straight line slope (m) of log G$^{'}$ (ω) versus log ω curve. Frequency sweep is conducted at a strain level of 0.1%, so as to ensure the linear viscoelastic range for the bitumen.

$$\alpha = 1/m \tag{2.40}$$

Amplitude or strain sweep test is conducted at a frequenof 10 Hz, with loading increasing from zero to 30% over the course of 3100 cycles of loading. The damage accumulation in the specimen is calculated using the formulae,

$$D(t) \cong \sum_{i=1}^{N} \left[\pi \gamma_0^{\,2} (C_{i-1} - C_i) \right]^{\frac{\alpha}{1+\alpha}} (t_i - t_{i-1})^{\frac{1}{1+\alpha}} \tag{2.41}$$

Where, *C(t)* is the ratio of $|G^*|(t)$ to $|G^*|_{initial}$, which are the value of complex shear modulus at any time t and the initial undamaged $|G^*|$.

Further, the calculated *C(t)* and *D(t)* are used to fit a relation of the form,

$$C_t = C_0 - C_1(D)^{C_2} \tag{2.42}$$

Where C_0, $C_1$and C_2 are evaluated using curve fitting. *C* at peak stress is used to calculate the value of *D(t)* at failure (D_f) using the above equation.

The binder fatigue life N_F is calculated using the equation

$$N_F = A(\gamma_{\max})^B \tag{2.43}$$

Where, *A* and *B* are evaluated using the following equations

$$A = \frac{f(D_f)^k}{k(\pi C_1 C_2)^\alpha} \tag{2.44}$$

$$B = 2\alpha \tag{2.45}$$

In the above equations, *f* is the frequency (10 Hz) and *k* is calculated as follows

$$k = 1 + (1 - C_2)\alpha \tag{2.46}$$

The above method for characterizing the fatigue is generated from the viscoelastic continuum damage (VECD) principle, which starts from the basic Schapery's equation for damage (*D*) rate, written as [127]

$$\frac{dD}{dt} = -\frac{\partial W}{\partial D} \tag{2.47}$$

The above equation for viscoelastic materials was modified to obey power law based on Paris Law of crack growth

$$\frac{dD}{dt} = (-\frac{\partial W}{\partial D})^\alpha \tag{2.48}$$

W is the materials energy potential, while α is the exponent determining the energy release rate.

Further the work done by Kim and co-workers [127] for monotonic loading was implemented for harmonic loading as typical in flexible pavements. For strain controlled

cyclic shear loading the dissipated energy during each cycle was used in place of *W* in equation 2.48[73]. The dissipated energy is derived from the work done per unit volume by the material, when subjected to cyclic loading. It could be written as

$$W = \pi.\gamma_0^{\,2}.\left|G^*\right|.\sin\delta \tag{2.49}$$

Using this equation in 2.48 yields the solution as

$$D(t) \cong \sum_{i=1}^{N}\left[\pi\gamma_0^{\,2}(\left|G^*\right|\sin\delta_{i-1} - \left|G^*\right|\sin\delta_i)\right]^{\frac{\alpha}{1+\alpha}}(t_i - t_{i-1})^{\frac{1}{1+\alpha}} \tag{2.50}$$

Further using equation 2.42 in equation 2.49 will give

$$\frac{dW}{dD} = -\pi C_1 C_2 (D)^{C_2-1}(\gamma_{\max})^2 \tag{2.51}$$

Equations 2.51 and 2.48 creates a differential equation, which on solving will give

$$D(t) = \left[\frac{1}{(-\alpha C_2 + \alpha + 1)t}\right]^{\left(\frac{1}{(\alpha C_2 - \alpha - 1)}\right)} \cdot \left[\frac{1}{(\pi C_1 C_2 \pi^2)}\right]^{\left(\frac{\alpha}{(\alpha C_2 - \alpha - 1)}\right)} \tag{2.52}$$

This equation is finally transformed to equation 2.43.

2.9 Bitumen Modification

On the majority of roads, conventional binders perform well. However, increasing demand of traffic, introduction of new axle configuration requires effective strengthening of pavements [83]. To assist the Highway Engineer to meet this growing challenge, there now exists a wide range of proprietary asphalts made with polymer modified bitumens.

Good basic design, stage construction and timely maintenance enable asphalt roads not only to withstand all the demands that are made of them but also to provide the high standards of safety and comfort that have become synonymous with bitumen-bound road materials. However, there exists sections which are more highly stressed. These areas requires special attention if the entire network is to perform well. It is better that maintenance and strengthening work be done at a particular point of time instead of correcting few sections repeatedly. Also, disruption of traffic during frequent maintenance will add more

cost unnecessarily. Use of better materials, such as modified binder offers a better solution of reducing the frequency of maintenance work and improving the life and strength of pavement for a longer period of time.

2.9.1 *Role of bitumen modifiers*

As asphalt binder is responsible for the thermos-rheological properties of asphalt mixes, it plays a vital role in determining many aspects including the permanent deformation and fatigue cracking. A proportion of induced strain in asphalt is attributable to viscous flow which is non-recoverable and gradually increases with both loading time and temperature. The change in strain with time is due to the viscous behavior of the material. On removal of the load, the elastic strain is recovered and some additional recovery occurs with time which is known as delayed elasticity. Finally a residual strain remains which is unrecoverable and is caused by the viscous behavior of the binder.

One of the primary role of the modifier is to increase the resistance of asphalt to permanent deformation at high road temperatures without affecting the properties at other temperatures. This can be achieved by either stiffening the bitumen or by increasing the elastic component of the bitumen. The stiffening will reduce the total visco-elastic response while increasing the elastic component will reduce the viscous component. Increasing the stiffness will also tend to increasing the dynamic stiffness of the asphalt mix which will lead to better load spreading capacity, increasing the structural strength and life of pavement. Increasing the elastic component will lead to better flexibility and will be beneficial when high tensile strains are induced on the structure [83].

2.9.2 *Desired properties of a modifier*

A plethora of studies have been conducted using different modifiers including filler, mineral fibres and rubbers. Use of various bitumen modifiers to be used in pavement construction has also been studied by many researchers. Table 2.3 details the most common modifier and additives.

Table 2.3 Different types of modifier

Type of Modifier	Example
Thermoplastic Elastomers	Styrene-butadiene-styrene (SBS) Styrene-butadiene-rubber (SBR) Natural rubber Crumb tyre rubber Polyisoprene
Thermoplastic Polymers	Ethylene vinyl acetate (EVA) Polyethylene (PE) Polypropylene (PP) Polyvinyl chloride (PVC)
Thermosetting Polymers	Epoxy resin Acrylic resin Phenolic resin
Chemical Modifiers	Sulfur Lignin
Fibres	Cellulose Glass fibre Polyester Polypropylene
Adhesion improvers	Organic amines Amides
Antioxidants	Amines Phenols
Natural Asphalts	Trinidad lake asphalt Gilsonite Rock asphalt
Fillers	Carbon black Hydrated lime Lime Flyash

Various types of polymer and additives are available but only a few are suitable for polymer modification. When used for bitumen modification a polymer must be capable to resist degradation at high temperature and should maintain the desirable properties during storage and handling. The polymer should also form a compatible system with the bitumen and should be capable enough so that it can be processed with conventional laying/mixing equipment and also should be cost effective [6]. The following table presents the benefit gained by different types of modifier as per work done by various researchers.

Table 2.4 Benefits with various modifiers.

Modifier	Permanent Deformation	Thermal Cracking	Fatigue Cracking	Moisture Damage	Ageing
Elastomer	✓	✓	✓		✓
Plastomer	✓				
Tyre rubber		✓	✓		
Carbon black	✓				✓
Lime				✓	✓
Sulphur	✓				
Chemical modifier	✓				
Antioxidants					✓
Adhesion improvers				✓	✓
Hydrated lime				✓	✓

To gain practical and economic benefit from the modifiers it should

- Be readily available
- Resist degradation of asphalt at mixing temperature
- Easily mix with bitumen
- Increase the resistance to deformation at high pavement temperatures, and improve the flexibility at lower temperatures
- Be cost effective

Once blended with bitumen, the modifier should maintain its premium properties during storage and in-service applications. Most importantly it should be physically and chemically stable during storage and should not separate from the base binder.

2.9.3 *Polymer modified binders*

Polymer modification is the incorporation of polymers in asphalt binders using mechanical stirrers or through chemical reactions. Traditionally polymers have been used to improve the temperature susceptibility of asphalt binders by increasing its stiffness at higher temperatures, while maintaining adequate flexibility at lower temperatures [28, 59]. Since 1970's a number of research articles have concentrated on use and benefits of polymer modification for bitumen. Among the various modification techniques use of plastomers and thermoplastic elastomers have gained lot of attention [100, 101]. An effective polymer

modification leads to a thermodynamically unstable but kinetically stable system in which the polymers are partially swollen by the light components of bitumen. The change in rheological properties of bitumen due to polymer modification is a function of many factors which includes amount and type of polymer, type of base binder and the mixing process. As the polymer content increases the bitumen slowly transfers from a bitumen dominant phase to a polymer dominant phase [6]. However, an ideal modified microstructure includes two interlocked continuous phase. The polymer content at which this interlocked phase is achieved is the optimum polymer content for bitumen modification. This interlocked phase leads to better performance with respect to rheological properties, storage stability and cost-effectiveness.

Although polymers tend to improve the performance of the virgin binder, but various challenges have been encountered while modifying bitumen with polymers. Compatibility between polymer and bitumen is one of the main issues which impose challenge on its use. The poor storage stability results from poor compatibility due to difference in densities and molecular weight of the bitumen and polymer. The difference in polarity and solubility is also one of the prime reason for the incompatibility. The asphaltene and polymer compete for the solubility in the maltene fraction which results in separation of the two phases [28, 83]. Higher cost, high temperature sensitivity and low ageing resistance has also been reported in many studies imposing challenge on the use of polymer modified bitumen.

Polymers are generally categorized as plastomers and elastomers. Plastomers form a tough, three dimensional rigid network to resist deformation, while elastomers are characterized for having high elastic response and can resist permanent deformation by stretching and elastically recovering their initial shape [83]. Plastomers have no or little elastic component, resulting in their quick early strength under load. Thermoplastic elastomers on the other hand soften on heating and hardens on cooling and have been found to be more successful than plastomers as bitumen modifiers.

2.9.3.1 Thermoplastic polymers

Thermoplastics are characterized by softening on heating and hardening on cooling. Polypropylene (PP), polyethylene (PE), polyvinyl chloride (PVC), polystyrene (PS) and various ethylene copolymers (semi-crystalline polymers), such as ethylene vinyl acetate (EV

A), ethylene butyl acrylate (EBA and ethylene methyl acrylate (EMA), are the principal thermoplastic polymers. These polymers increase the stiffness and viscosity of bitumen at normal service temperatures. They tend to influence the penetration more than the softening point. EVA polymers have been widely used in the road construction industry for more than 20 years, where they improve both the workability of the asphalt during compaction and its deformation resistance in service. EVA polymers improve the bitumen properties significantly but to a different extent depending on the bitumen source and the polymer characteristics [64, 65, and 124].

EVA copolymers consist of random chains of ethylene-vinyl acetate chain produced by the copolymerization of ethylene and vinyl acetate. The structure of the EVA copolymer is shown in Figure 2.25 and consists of the closely packed, regular polyethylene segments that form the crystalline regions, and the bulky vinyl acetate groups, which constitutes the non-crystalline or amorphous rubbery regions [83]. The presence of polar acetate groups as short branches in EVA disrupts the closely packed crystalline microstructure of the ethylene-rich segments which leads to reduction in the degree of crystallinity, increasing the polarity of the polymer. This is beneficial in terms of storage stability for the modified bitumen. The properties of EVA copolymers are classified by the molecular weight and vinyl acetate content of the polymer. The molecular weight of the polymer is measured using its melt flow index (MFI), which is inversely related to molecular weight. The proportion of vinyl acetate in the copolymer determines whether the behavior of the EVA will be more crystalline, stiff and reinforcing in character or more amorphous and rubbery. When vinyl-acetate content is low, the degree of crystallinity is high and the properties of the EVA is analogues to low density polyethylene. As the vinyl-acetate content increases, EVA shows a biphasic microstructure where the polyethylene (PE) segments imparts crystallinity and the vinyl acetate content provides the amorphous behavior.

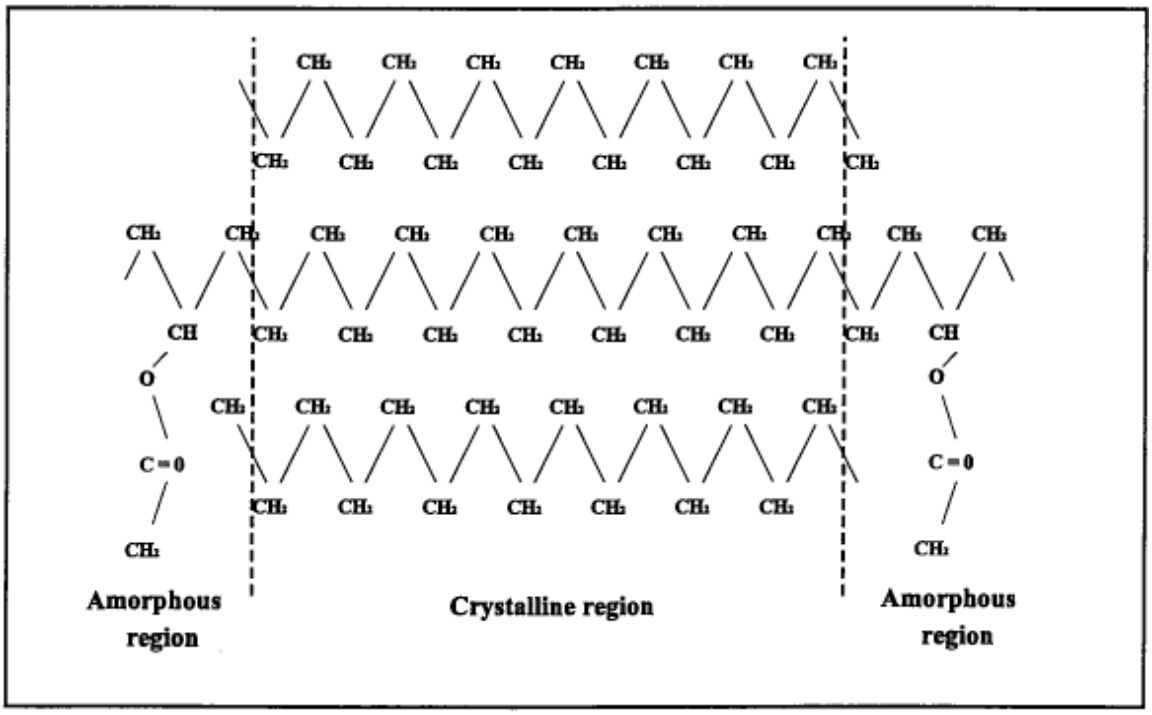

Figure 2.25 Structure of Ethylene Vinyl Acetate (EVA)

EVA copolymers are easily dispersed in and have good compatibility with most available bitumens and are thermally stable at normal mixing and handling temperatures. When the EVA copolymer is blended with the base bitumen, portions of the "oil fraction" of the bitumen are absorbed by the amorphous phase causing the polymer to swell. At low EVA concentrations, a dispersed EVA-rich phase can be observed within a continuous bitumen-rich phase. As the EVA concentration increases, phase inversion occurs in modified bitumen and the EVA-rich phase becomes a continuous phase. Only the amorphous, low molecular weight fractions of the polymer are involved in this dissolution reaction between the bitumen and the polymer. EVA copolymers with a low vinyl acetate content and high molecular weight, therefore do not absorb "oil" significantly, due to their high crystallinity. If two interlocked continuous phases form in the modified bitumen, and the properties of bitumen could be improved to a large extent. EVA was found to form a tough and rigid network in modified bitumen to resist deformation, which means that EVA modified bitumen has an improved resistance to rutting at high temperatures [6, 150].

The quantity and chemical composition of the "oil fraction" of the bitumen and the crystallinity of the semi-crystalline polymer are critical in determining the rheological

character of ethylene copolymer modified bitumen. Highly crystalline polymers, that do not absorb sufficient quantities of oil, do not swell and therefore tend to behave simply as fillers in the modified bitumen, therefore reproducing a generally bitumen-like rheological character. At the same time, polymers that dissolve too easily in the PMB matrix, lose their mechanical characteristics resulting in a blend that again shows a bitumen-like behavior. Too high a degree of compatibility will therefore mask the properties of the EVA copolymer, and hence a certain degree of incompatibility is required to produce an optimum blend. Although some properties of bitumen are enhanced by EVA modification, there are still some problems limiting its application. One large limitation is the fact that EVA cannot much improve the elastic recovery of bitumen due to the plastomer nature of EVA. Furthermore, the glass transition temperature (Tg) of EVA copolymers, which strongly depends on the vinyl acetate content, is not low enough to significantly improve the low-temperature properties of bitumen. It was reported that Tg of EVA copolymers with 28.4 wt% of vinyl acetate is -19.9 ℃, which is even quite close to Tg of some base bitumen. As a result, EVA's ability to improve the low-temperature properties of bitumen is rather limited, especially at high EVA concentrations. According to a research, bitumen's resistance to low temperature cracking was increased to some extent by addition of 2 wt% or 4 wt% of EVA, while the resistance to low-temperature cracking was decreased when adding 6 wt%.

2.9.3.2 Elastomers

Thermoplastic elastomers are usually more effective than plastomers for bitumen modification. Elastomers such as natural rubber (NR), polybutadiene (BR), polyisoprene (IR), isobutene isoprene copolymer (IIR), polychloroprene (CR), styrene butadiene rubber (SBR) and styrenic block copolymers have been used to modify bitumen. The most popular thermoplastic elastomers as bitumen modifiers are SBS copolymers and SIS copolymers. Styrenic block copolymers, commonly termed thermoplastic rubbers (TR) due to their ability to combine both elastic and thermoplastic properties, may be produced by a sequential operation of successive polymerization of styrene-butadiene-styrene (SBS) or styrene-isoprene-styrene (SIS). Alternatively, a di-block precursor can be produced by successive polymerization of styrene and mid-block monomer, followed by a reaction with a coupling agent. Therefore, not only linear copolymers but multi-armed copolymers, known as star-

shaped, radial or branched copolymers, can be produced. The structure of a SBS copolymer is shown in Figure 2.26 and consists of styrene-butadiene- styrene tri-block chains, having a two phase morphology of spherical polystyrene block domains within a matrix of polybutadiene.

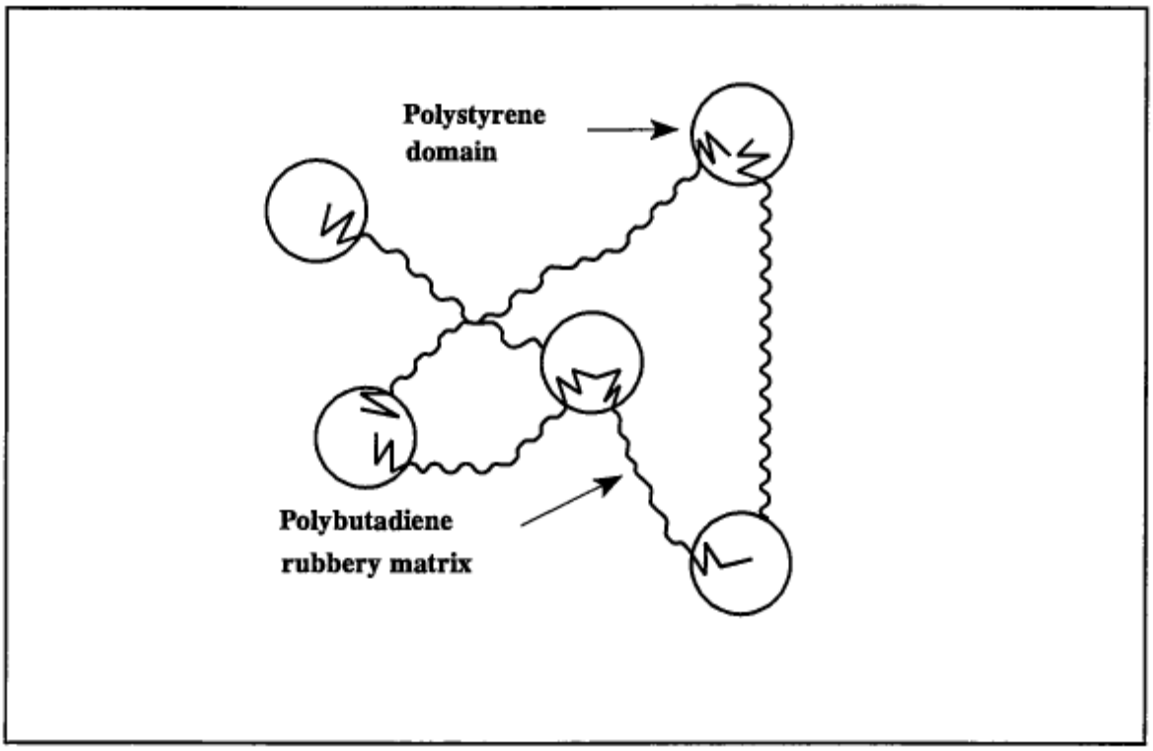

Figure 2.26 Structure of styrene butadiene styrene (SBS) copolymer.

SBS copolymers derive their strength and elasticity from physical cross-linking of the molecules into a three-dimensional network. The polystyrene (PS) end-blocks impart the strength to the polymer and the polybutadiene (PB) or polyisoprene rubbery matrix mid-blocks give the material its exceptional elasticity [22, 23, 99, and 182]. The chemical linkages between PS and PB blocks can immobilize domains in the matrix. Tg of PS blocks is around 95 °C and Tg of PB blocks is around 80 °C. Under the usual service temperatures of paving bitumen, PS blocks are glassy and contribute to the strength of SBS while PB blocks are rubbery and offer the elasticity. The effectiveness of these cross-links diminishes rapidly above the glass transition temperature of polystyrene of approximately 100 °C, but the polystyrene domains will reform, and the strength and elasticity will be restored on cooling as shown in Figure 2.27 (a-c) below.

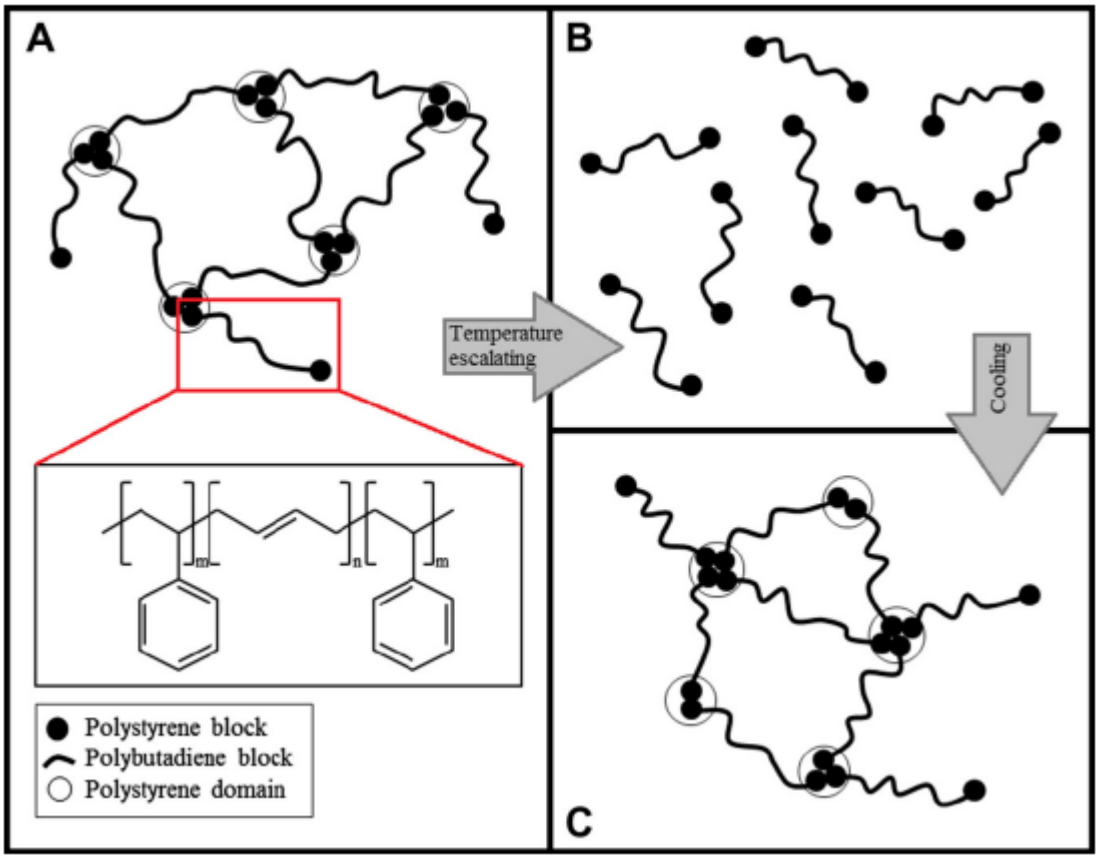

Figure 2.27 (a-c) Phase transition in styrene butadiene styrene (SBS) with change in temperature.

When SBS is blended with the base bitumen, the elastomeric phase of the SBS copolymer absorbs maltenes (oil fractions) from the bitumen and swells up to nine times its initial volume. At suitable SBS concentrations, a continuous polymer network (phase) is formed throughout the PMB, significantly modifying the bitumen properties [23, 182]. As thermoplastic rubbers have molecular weights similar to or higher than that of asphaltenes, they compete for the solvency power of the maltene phase and phase separation can occur if insufficient maltenes are available. This phase separation is an indication of the incompatibility of the base bitumen and the polymer and care should be taken when blending thermoplastic rubber PMB's. The compatibility of the SBS - bitumen blend can be improved through the addition of aromatic oils. However, too high an aromatic content in the blend will dissolve the polystyrene blocks and destroy the benefits of the SBS copolymer in the PMB.

2.10 Characterization of Asphalt Mixtures

2.10.1 *Mix design of asphalt mixture*

Binder alone cannot judge the performance of the mix. The aggregate gradation combined with the bitumen as the binding material has to perform together for complete characterization of the properties of the topmost pavement layer, also known as hot mix asphalt (HMA). The two basic ingredients of HMA are: aggregates and bitumen. Mix design of HMA is the process of determining the properties and blending of different size of aggregates, selection of appropriate binder and finally finding the optimum dosage of the binder to be combined with the selected aggregate gradation.

HMA is a complex material upon which many different, and sometimes conflicting, performance demands are placed. It must resist deformation and cracking, be durable over time, resist water damage, provide a good tractive surface, and yet be inexpensive, readily made and easily placed. In order to meet these demands, the mix designer can manipulate all of three variables:

a) Aggregate: Attributes such as source (type), size, strength (in terms of abrasion and toughness), gradation, texture and shape as well as durability and resistance to can be measured, judged and altered to some degree.
b) Asphalt binder: The rheology of the binder, its type as well its modification technique (if any) is measurable and can be judged and altered as required.
c) Proportion of asphalt binder to aggregate: The optimum asphalt binder is expressed in terms of total weight of the HMA or by total weight of the aggregate. The selection of this ratio has considerable effect on the mechanical response of the mix and is the most important parameter of mix design. The proportion of asphalt binder can be varied widely, due to the considerable difference between the aggregate specific gravity.

2.10.1.1 Basic procedure

Irrespective of the method used for mix design of asphalt mixture, the basic procedure remains the same. The three basic steps involved in the mix design procedure are as follows:

a) Selection of aggregate: Aggregate acceptance is different for various agencies/owners. Usually the aggregates are subjected to different physical tests and are checked against the specification laid down by the state agencies/government. The proper aggregate gradation depending on the mix design are specified. It may be required to procure the aggregates from more than one quarry stockpile in order to meet the required gradation criteria.
b) Asphalt binder selection. The selection and grading of asphalt binder also varies from country to country. In India viscosity graded (VG) binder is used for the construction of flexible pavement. Countries like USA follows the Superpave PG specification. Separate protocol is used for modified binders.
c) Determination of optimum binder content: Determination of optimum binder content is a function of the mix design method adopted. The process can be viewed in the following steps:
    - Prepare several trial mixes with varying asphalt contents.
    - Compact the trial mixes in the laboratory so as to roughly simulate the field compaction.
    - Measure the key sample characteristics using different laboratory techniques.
    - Adopt the asphalt binder content which satisfies the mix design objectives.

2.10.1.2 Different mix design methods

There are several methods which can be used for the mix design of asphalt mixtures. However, three methods as follows are the most common among all:

a) Hveem mix design
b) Marshall mix design, and
c) Superpave mix design

These methods have been discussed in brief in this section.

2.10.1.2.1 Hveem mix design

This method was developed in the late 1920s and 1930s by Francis Hveem, who was a resident engineer for the California division of highways. The method can be divided into three basic steps as follows:

1. Selection of aggregates: This procedure is similar to the other methods as discussed above.
2. Selection of asphalt binders: This is a function of the state design catalogs and special design requirements, if any.
3. Determination of optimum asphalt binder content: For the Hveem method this step can be divided further to five more substeps.
   a) Multiple initial samples are prepared at different asphalt binder content by the dry weight.
   b) These samples are compacted using the California kneading compactor (Figure 2.28). This is a specific type of compactor for Hveem mix design method.
   c) Hveem stabilometer and cohesiometer is employed for evaluating the stability and cohesion of the samples. Depending upon the mix class being evaluated the passing values of stability and cohesion are checked.
   d) The density and other volumetric properties of these samples are determined next.
   e) Finally the optimum binder content is selected corresponding to 4% air void content. His binder content should pass both the cohesion and stability test values.

Figure 2.28 California kneading compactor

2.10.1.2.2 Marshall mix design method

This method is most commonly used by most of the laboratories as this method is proven and relatively light, inexpensive and portable equipment is required. This method and its underlying concepts were developed by Bruce Marshall who worked for Mississippi highway department around 1939 and was later refined by U.S Army.

Like Hveem mix design, Marshall mix design procedure can also be divided into three basic steps out of which the first two are the same. The selection of optimum binder content in the Marshall mix design can be divided into five sub-steps as follows:

a) A series of initial samples are prepared at different asphalt contents. Two to three samples are typically made corresponding to each binder content. Two samples above and two samples below the optimum are usually prepared.
b) Marshall drop hammer is used to compact these samples. The drop height and weight of the hammer is specific for the method.
c) Stability and flow values for the compacted samples are evaluated further with use of Marshall equipment as shown in Figure 2.29.
d) The density and other volumetric properties are measured and calculated.
e) Finally the optimum binder content is selected corresponding to 4% air void content as long as it passes other volumetric requirements.

Figure 2.29 Example of Marshall test apparatus

2.10.1.2.3 Superpave mix design

Similar to Hveem and Marshall mix design methods, Superpave mix design has been proved to produce high quality hot mix asphalt from which long-lasting pavement can be constructed. Just like the other design methods the mix design in Superpave method can be divided into three steps as follows:

1. Selection of aggregates: There are three different ways in which the aggregate is specified. First, restrictions are specified on aggregate gradation by use of gradation specifications. Secondly, specification are imposed on physical properties of aggregate angularity, flat and elongated particles and clay content. Lastly, aggregate properties such as durability and soundness are specified, which is also known as 'source properties' by the Asphalt Institute.
2. Selection of asphalt binder: In this method PG binders according to Superpave are selected depending upon the expected pavement temperature.
3. Determination of optimum asphalt binder content: This step is broken up into four sub steps in the Superpave method.
    a) Several samples are prepared initially, usually two at the proposed design asphalt content and four other samples, two at 0.5% above and two at 0.5% below the design asphalt content.
    b) Superpave gyratory compactor (Figure 2.30) is employed for the compaction of these samples. The compactor is specific to the design method.
    c) The density and other volumetric properties are determined next.
    d) Finally, the optimum asphalt binder content is selected corresponding to 4% air void content.

No accepted standard performance test, typical to Hveem and Marshall mix design method, is used in Superpave mix design method. In this study, Marshall mix design procedure is used for preparation, testing and analysis of various asphalt mixtures.

Figure 2.30 Example of Superpave gyratory compactor

2.10.2 *Performance test of hot mix asphalt*

The laboratory mix design can be related to the actual field performance by use of different performance tests. Just like the characterization of asphalt binders, the task in HMA performance testing is the development of those physical tests which can successfully quantify the key performance parameters in HMA and how there are changes in these parameters throughout the life of a pavement. The following are those key parameters.

a) Rutting (deformation resistance): This is one of the key performance parameters for characterizing the permanent deformation behavior of the asphalt mix/pavement. It depends largely on the mix design, type and gradation of aggregates and the rheological aspects of the bitumen used to prepare the mix.
b) Fatigue life: This is also one of the key parameters describing the resistance of the asphalt mix to repetitive loading. Its dependency on structural design and subgrade support is higher than the mix design of the asphalt.
c) Tensile strength: Tensile strength is an indication of pavement cracking at low temperatures. It depends mostly on the properties of the binder.

d) Stiffness: The stiffness describes the stress-strain relationship of the HMA by use of elastic or resilient modulus. The variation of the elastic and resilient nature of the HMA with change in temperature is important for a detailed characterization of the mix.

e) Moisture susceptibility: Certain combinations of asphalt binder and aggregate can be prone to moisture damage. There are various tensile strength and deformation resistance tests that can be employed for the evaluation of the moisture susceptibility of a HMA mixture.

2.10.2.1 Rutting

Ongoing research into what type of test could more accurately predict the permanent deformation of HMA has yielded many test methods which can be broadly categorized as follows:

I. Static creep test: A load is applied to a sample and it measures the recovery on the removal of the load. Though this test provide an indication of the permanent deformation but correlates poorly with the actual field results.

II. Repeated load tests: A repeated load is applied to a test specimen at a constant frequency for more than 1000 repetitions and the specimen's permanent deformation and recoverable strain is measured. This test method has been found to give better field prediction as compared to static creep test results.

III. Dynamic modulus tests: A repeated load is applied to a test specimen at varying frequencies over a relatively short period of time and the specimen's permanent deformation and recoverable strain is measured. The viscous properties of the material can also be measured using some dynamic modulus test where the lag between the peaks applied stress and the peak resultant strain is obtained. Fair correlations with in-service rutting measurement can be obtained using these tests but the test is more complicated and difficult to run.

IV. Empirical test: Traditional tests using Hveem and Marshall apparatus can also be used to predict the permanent deformation characteristics of HMA. These tests however do not provide insight about any of the fundamental material parameter.

V. Simulative tests: Laboratory wheel tracking devices falls under this category. Research have shown that results using this test method correlates fairly well with field rutting measurements.

In this study wheel rut testing was used for the evaluation of permanent deformation characteristics of asphalt mixtures.

2.10.2.2 Fatigue life

Fatigue cracking is one of the principle modes of HMA pavement failure and hence the accurate evaluation/prediction of fatigue life can be useful in judging the overall life of pavement. Flexure test is one of the typical ways of estimating the in-place fatigue properties of HMA. In this test method small rectangular HMA beams are subjected to repeated loading until the failure. Failure is usually defined as 50% reduction in stiffness of the sample. Results are plotted in the form of fatigue life versus the applied stress/strain. In this study four point beam bending test (4PBBT) was used for the estimation of fatigue life of asphalt mixes. A schematic representation of the testing apparatus is shown in Figure 2.31.

Figure 2.31 Schematic representation of four point beam bending test

2.10.2.3 Tensile strength

Tensile strength of HMA is a good indicator of its potential to cracking. An asphalt mixture with high tensile strain at failure can be said to be resistant to cracking as it could undergo larger deformations before failure. Measuring the tensile strength before and after

water conditioning can also give indications about the moisture susceptibility of the mixture. If the asphalt mix retains higher tensile strain at failure relative to the unconditioned specimen, it would indicate greater potential to resist moisture damage. The tensile strength is usually measured using the following two tests:

I. Indirect tension test: The test setup is similar to the diametral repeated load test. A constant rate of vertical deformation is applied till failure of the specimen.
II. Thermal cracking test: Thermal cracking test measures the tensile load in the test specimen which is cooled at a constant rate while being restrained from contraction and determines the tensile strength and temperature at fracture of the sample. The test is terminated after the failure of the specimen.

In this study indirect tension test was used for reporting the tensile strength of different asphalt mixtures prepared using various binders.

2.10.2.4 Stiffness tests

The elastic or resilient modulus of HMA can be determined using stiffness tests. The primary use of this test methods can be appreciated when the values are evaluated at different test temperatures. Standard values already exists for different mixes at a standard temperature. Change in temperature has been found to considerably effect the elastic and resilient modulus of HMA.

2.10.2.5 Moisture susceptibility tests

Any test in which the performance can be evaluated on wet and dry samples can be used to see the effect of moisture on HMA. Various tests has been used for the same but none has attained any broad acceptance. Out of all, modified Lottman test has been recommended the most. In this test the indirect tensile strength of unconditioned and conditioned samples are compared by taking their ratio. This ratio is called the tensile strength ratio (TSR) which should be typically 0.80 or higher for better resistance to moisture. In this study the moisture susceptibility of the asphalt mixtures were determined by using TSR and retained Marshall stability test.

Chapter 3

Modification of Asphalt Binder

3.1 Introduction

Polymers are usually provided in the form of pellets or powder which can be subsequently diluted to the required polymer content by blending with base bitumen by using low to high shear mixer. Blending pellets of polymer with base bitumen results in a special polymer concentration suitable for different applications [150]. When a polymer is mixed in bitumen, compatibility due to difference in polarity, molecular weight and typical structure of polymer and base bitumen plays a critical role [65, 121, 182]. Also the competency of the polymer and asphaltene for the solvency of maltene fraction in the bitumen may disturb the polymer-bitumen system leading to phase separation [83, 101, 119, 200]. Various researchers have used different methods for modifying bitumen using polymers [36, 65, 124, 150]. The main difference is found in use of different mixing temperature, blending time and shear rate for producing the PMB. In spite of the significant research which has been carried out related to the SBS and EVA modified PMBs in road applications, more studies have to be undertaken on the compatibility and in the interaction between the SBS, EVA polymer and the base bitumen.

3.2 Materials Used

Modified binders were produced using the following materials:

1. VG 10, viscosity graded bitumen, collected from Mathura refinery. This was the base binder which was used for modification.

2. EVA copolymer (Evatane®) supplied in pellet form of 2-3mm in size. Evatane® 2805 which contains vinyl acetate content of 27–29% is a highly flexible plastomer designed for bitumen modification and especially for road paving. Modification was done using different percentage of EVA varying from 1-7%.

3. The SBS polymer used was Kraton D-1101 which is a linear SBS polymer in powder form that consists of different combinations made from blocks polystyrene (31%) and

polybutadiene of a very precise molecular weight [150]. These blocks are either sequentially polymerized from styrene and butadiene and/or coupled to produce a mixture of these chained blocks. Modification was done using different percentage of SBS varying from 1-5%.

The properties of Evatane® and Kraton D-1101 are presented in Table 3.1

Table 3.1 Properties of Evatane® and Kraton D-1101[160]

Composition	Specification	Evatane®	Kraton D-1101
Molecular structure	-	Linear	Linear
Specific gravity	ASTM D792	0.92	0.94
Shore hardness (A)	ASTM D2240	82	71
Melt index	ASTM D1238	5-8	<1
Elongation at break (%)	ASTM D412	700-1000	875
Tensile strength at break (MPa)	ASTM D412	33	31.8

3.3 Optimum Blending Requirements

The first part of this study focusses on obtaining optimum blending requirements for EVA and SBS modified binder by varying the mixing temperature, blending time and the shear rate. Modification was done at four different mixing temperatures (160˚ to 190˚C with increment of 10˚C), four different mixing time (20, 30, 40 and 60 minutes) and five altered shear rate (300, 600, 900, 1200 and 1500 rpm). A total of 80 combinations were obtained for each modifier. The range of values for different parameters were selected after reviewing various literatures.

Storage stability (SS) value (Separation test) as mentioned in IRC SP 53-2010 [78] was used as the variable for achieving the goal. It is believed that at higher temperatures the modifier tends to separate from the base bitumen which could be influenced by inappropriate blending requirements used for modification. An aluminum tube, 25.4 mm diameter and 136.7 mm height is filled with hot modified bitumen and is kept vertically at 163˚C for 48

hours. It is then immediately transferred to a freezer having temperature of 6.7 ± 5˚C and left for 4 hours to solidify. The tube is cut into three equal parts and ring and ball softening point test is conducted on the bitumen sample obtained from the top and bottom parts. The difference in softening point temperature should not be more than 3˚C for the modified binder to be storage stable.

Tables 3.2 and 3.3 shows the values obtained for different combinations of the blending parameters. Figures 3.1 (a-u) and 3.2 (a-o) presents the variation of storage stability for both EVA and SBS modified binders at different combinations of modifier content and the blending parameters.

In general, higher temperature, longer blending time and higher shear rate gave the least storage stability values for both EVA and SBS modification, indicating a better mix. Few values were found to be unexpected and may be attributed to measurement errors. These values can be ignored as we have a large number of data set. The storage stability values were higher than 3 °C for modifier content higher than 5% in case of EVA and 3% in case of SBS, irrespective of any combination of blending parameters. It can be seen (from the slope of the curves) that for EVA modification temperature plays the most crucial role. Shear rate has the minimum effect on the values of SS. The effect of shear rate became significant as the percent of modifier increased, showing maximum influence for 7% modification. However for SBS, shear rate had considerable effect on modification. It was found that a storage stable modified binder was obtained only at higher shear rates in case of SBS. It was not possible to obtain a storage stable mix for either of the modifier at temperatures below 170 °C. Blending time also plays a crucial role as sufficient time is required for the swelling of polymers in hot bitumen for proper dispersion.

Table 3.2 Storage stability values for EVA modification

S.No.	Temperature (°C)	Mixing time (minutes)	Shear Rate (s^{-1})	Percentage of Modifier						
				1%	2%	3%	4%	5%	6%	7%
1	160	20	300	3.9	4.2	5.3	5.3	5.5	6.0	7.2
2	160	30	300	3.2	3.5	5.2	5.3	5.4	5.9	6.5
3	160	40	300	3.2	3.3	5.2	5.2	5.4	6.0	6.6
4	160	60	300	2.9	3.2	5	5.1	5.2	5.9	6.2
5	160	20	600	3.7	4	4.8	5.2	5.4	6.2	6.8

6	160	30	600	3.1	3.4	4.7	5.1	5.3	5.9	6.6
7	160	40	600	2.8	3.1	4.7	5.2	5.3	5.8	6.5
8	160	60	600	2.7	3.1	4.5	4.7	4.9	5.7	6.5
9	160	20	900	3.5	4.1	4.7	4.8	5	5.8	6.7
10	160	30	900	3.1	3.4	4.6	4.6	4.8	5.5	6.6
11	160	40	900	3.0	3.3	4.7	4.5	4.7	5.4	6.2
12	160	60	900	3.1	3.3	4.3	4.3	4.5	5.4	5.9
13	160	20	1200	3.5	4	4.5	4.7	4.9	5.6	6.2
14	160	30	1200	3.1	3.4	4.2	4.7	4.9	5.4	6.1
15	160	40	1200	3.0	3.3	4.2	4.6	4.8	5.4	6.1
16	160	60	1200	2.9	3.2	3.9	4.3	4.7	5.3	5.8
17	160	20	1500	3.9	4.2	4.2	4.5	4.6	5.4	5.9
18	160	30	1500	3.1	3.4	3.6	3.9	3.9	5.2	5.9
19	160	40	1500	2.8	3.4	3.5	3.9	4.1	4.8	5.7
20	160	60	1500	2.6	3.1	3.3	3.9	4	4.6	5.6
21	170	20	300	3.1	3.5	3.8	3.7	4.1	5.5	5.7
22	170	30	300	2.9	3.2	3.5	3.7	3.9	5.1	5.4
23	170	40	300	2.8	3.1	3.5	3.6	3.9	4.9	5.4
24	170	60	300	2.7	3.1	3.3	3.4	3.6	4.9	5.4
25	170	20	600	3.0	3.3	3.5	3.5	3.7	4.2	5.6
26	170	30	600	2.2	2.5	3.1	3.2	3.4	3.9	5.1
27	170	40	600	1.6	1.9	2.8	2.8	3	3.8	4.9
28	170	60	600	1.2	1.5	2.6	2.7	2.7	4.1	4.9
29	170	20	900	2.9	3.2	3.1	3.1	3.3	4.5	5.3
30	170	30	900	2.1	2.4	3	2.9	3.1	4.1	5.3
31	170	40	900	1.6	1.9	2.5	2.4	2.6	3.7	5.1
32	170	60	900	1.6	1.9	2.6	2.4	2.6	3.5	4.6
33	170	20	1200	2.5	3	2.8	3.0	3.2	3.7	4.9
34	170	30	1200	1.5	1.8	2.6	2.7	2.9	3.4	4.7
35	170	40	1200	1.3	1.8	2.6	2.2	2.4	2.9	4.1
36	170	60	1200	1.2	1.5	2.4	2.1	2.4	2.9	3.9
37	170	20	1500	2.8	3.1	3.3	2.6	2.8	3.3	5.1
38	170	30	1500	1.8	2.1	3	3.0	3.1	3.6	4.8
39	170	40	1500	1.3	1.6	2.6	2.5	2.5	3.0	4.5
40	170	60	1500	0.9	1.2	2.1	2.4	2.6	3.1	4.4
41	180	20	300	2.7	3	3.4	3.4	3.6	4.1	4.7
42	180	30	300	2.4	2.7	3.2	3.1	3.3	3.8	4.6
43	180	40	300	2.0	2.3	3.2	3.3	3.2	3.7	3.9
44	180	60	300	1.9	2.2	3.1	2.8	2.9	3.4	4.1
45	180	20	600	3.0	3.2	3.1	3.0	3.1	3.6	4.5
46	180	30	600	2.1	2.4	2.6	3.0	2.7	3.7	3.8
47	180	40	600	0.8	1.1	2.3	2.4	2.6	3.1	3.6
48	180	60	600	0.7	1	2.1	2.5	2.6	3.1	3.7

49	180	20	900	2.6	2.9	3	3.0	3.2	3.7	4.5
50	180	30	900	1.6	1.9	1.9	2.7	2.9	3.4	4.2
51	180	40	900	0.8	1.1	1.5	2.3	2.5	3.0	4.2
52	180	60	900	0.6	0.8	1.5	2.3	2.4	2.9	3.8
53	180	20	1200	2.6	2.9	2.9	2.9	3	3.5	4.1
54	180	30	1200	0.8	1.2	2.1	2.4	2.8	3.3	3.9
55	180	40	1200	0.8	1	1.6	2.4	2.5	3.0	3.9
56	180	60	1200	0.7	0.9	1.6	2.0	2.1	2.6	3.6
57	180	20	1500	2.8	3.1	2.8	2.5	2.8	3.3	4.8
58	180	30	1500	1.7	2	1.7	2.5	2.7	3.2	3.6
59	180	40	1500	1.0	1.3	1.5	1.9	2.3	2.8	3.6
60	180	60	1500	0.9	1.1	1.6	2.1	2.2	2.7	3.8
61	190	20	300	2.6	2.9	3.3	3.0	3.2	3.7	4.1
62	190	30	300	1.8	2.2	3.2	3.1	3.2	3.7	4.1
63	190	40	300	1.2	1.5	3.1	3.0	3	3.5	4.2
64	190	60	300	1.1	1.4	3	2.9	3.1	3.6	3.8
65	190	20	600	2.5	2.8	2.9	2.8	2.9	3.4	4.2
66	190	30	600	1.4	1.7	2.2	2.6	2.8	3.3	3.7
67	190	40	600	1.3	1.6	1.9	2.3	2.5	3.0	3.6
68	190	60	600	0.8	1.1	1.7	2.4	2.5	3.0	3.6
69	190	20	900	2.3	2.7	2.8	2.9	3.1	3.6	3.7
70	190	30	900	1.2	1.5	2.5	2.7	2.9	3.4	3.5
71	190	40	900	0.7	1.1	2.1	2.4	2.6	3.1	3.4
72	190	60	900	0.5	0.8	2.1	2.5	2.6	3.1	3.4
73	190	20	1200	2.5	2.8	3	2.7	2.9	3.4	3.5
74	190	30	1200	2.2	2.5	2.6	2.6	2.8	3.3	3.5
75	190	40	1200	1.3	1.6	1.8	2.5	2.6	3.1	3.2
76	190	60	1200	0.6	0.9	1.9	2.3	2.5	3.0	3.2
77	190	20	1500	2.4	2.7	2.7	2.6	2.8	3.3	3.4
78	190	30	1500	1.5	1.9	2.5	2.5	2.7	3.2	3.1
79	190	40	1500	1.0	1.3	2.5	2.3	2.5	3.0	3
80	190	60	1500	0.7	0.7	1.6	2.0	2.2	2.7	3.1

Table 3.3 Storage stability values for SBS modification

S. No.	Temperature (°C)	Mixing time (minutes)	Shear Rate (s^{-1})	Storage Stability (ΔT), °C				
				1%	2%	3%	4%	5%
1	160	20	300	3.6	4.1	4.2	4.5	5.7
2	160	30	300	3.6	3.8	4.2	4.5	5.5
3	160	40	300	3.5	3.9	4.1	4.4	5.6
4	160	60	300	3.5	3.9	4.2	4.5	5.5
5	160	20	600	3.6	4	4.1	4.4	5.6

6	160	30	600	3.5	4.1	4.1	4.3	5.3
7	160	40	600	3.5	3.8	4	4.4	5.3
8	160	60	600	3.4	3.8	4	4.3	5.2
9	160	20	900	3.5	3.9	4.2	4.4	5.5
10	160	30	900	3.4	3.8	4.1	4.3	5.5
11	160	40	900	3.5	3.8	4.1	4.3	5.2
12	160	60	900	3.3	3.9	4	4.1	5.1
13	160	20	1200	3.4	3.8	4.2	4.2	5.5
14	160	30	1200	3.2	3.7	4.1	4.3	5.2
15	160	40	1200	3.2	3.8	4.2	4.3	5.3
16	160	60	1200	3.3	3.8	4	4.2	5.2
17	160	20	1500	3.3	3.9	4.1	4.1	5.3
18	160	30	1500	3.2	3.7	4.1	4	5.2
19	160	40	1500	3.3	3.7	3.9	4.2	5.2
20	160	60	1500	3.2	3.8	4	4	5.1
21	170	20	300	3.5	4.1	4.1	4.4	5.6
22	170	30	300	3.6	4	4	4.3	5.5
23	170	40	300	3.5	4.1	3.9	4.3	5.3
24	170	60	300	3.4	4	3.9	4.1	5.3
25	170	20	600	3.3	4	4.2	4.3	5.5
26	170	30	600	3.2	3.9	4.1	4.2	5.4
27	170	40	600	3.2	3.9	3.9	4.2	5.4
28	170	60	600	3.1	3.8	4	4.1	5.3
29	170	20	900	3.2	3.8	4.1	4.1	5.4
30	170	30	900	3.1	3.7	3.9	4.2	5.3
31	170	40	900	3	3.7	3.8	4	5.2
32	170	60	900	2.8	3.5	3.8	4	5.2
33	170	20	1200	3.1	3.5	3.9	4.3	5.4
34	170	30	1200	2.9	3.3	3.9	3.9	5.1
35	170	40	1200	2.7	3.1	3.8	4	5.2
36	170	60	1200	2.8	2.9	3.7	3.9	5.2
37	170	20	1500	3	2.9	3.8	4.2	5.4
38	170	30	1500	2.5	3	3.7	4.1	5.3
39	170	40	1500	2.3	2.7	3.7	3.9	5.2
40	170	60	1500	1.3	2.7	3.7	3.8	5.1
41	180	20	300	3.5	3.4	3.6	4.3	5.5
42	180	30	300	3.5	3.5	3.5	4.3	5.4
43	180	40	300	3.4	3.4	3.4	4.1	5.4
44	180	60	300	3.4	3.3	3.4	4.1	5.3
45	180	20	600	3.2	3.5	3.4	4.2	5.4
46	180	30	600	3.1	3.4	3.3	4.1	5.3
47	180	40	600	3.1	3.4	3.4	4.2	5.4

48	180	60	600	3	3.2	3.3	4	5.1
49	180	20	900	2.9	3.2	3.2	3.8	5.1
50	180	30	900	2.9	3.1	3.1	3.7	4.9
51	180	40	900	2.7	2.9	3	3.7	4.7
52	180	60	900	2.6	2.8	3	3.6	4.8
53	180	20	1200	2.9	2.7	2.9	3.7	5
54	180	30	1200	2.7	2.6	2.8	3.5	4.8
55	180	40	1200	2.4	2.3	2.6	3.6	4.8
56	180	60	1200	1.2	1.7	2.6	3.4	4.6
57	180	20	1500	2.8	2.5	2.6	3.5	4.7
58	180	30	1500	2.4	2.6	2.5	3.5	4.5
59	180	40	1500	2.1	1.8	2.2	3.3	4.5
60	180	60	1500	0.8	1.5	1.9	3.4	4.3
61	190	20	300	3.3	3.3	3.5	4.1	5.3
62	190	30	300	3.1	3.4	3.3	4	5.3
63	190	40	300	3	3.3	3.3	4.1	5.3
64	190	60	300	3	3.3	3.2	4.2	5.4
65	190	20	600	3.2	3.4	3.3	4	5.2
66	190	30	600	3.1	3.4	3.1	3.9	5.1
67	190	40	600	2.9	3.3	3.2	3.8	5
68	190	60	600	2.8	3.2	3.1	3.8	4.9
69	190	20	900	3	3.1	3	3.7	4.9
70	190	30	900	2.7	3	3	3.6	4.8
71	190	40	900	2.6	3	2.9	3.5	4.7
72	190	60	900	2.6	2.6	2.7	3.5	4.6
73	190	20	1200	2.8	2.7	2.8	3.5	4.6
74	190	30	1200	2.5	2.5	2.8	3.5	4.7
75	190	40	1200	2.1	2.1	2.6	3.4	4.6
76	190	60	1200	0.7	1.5	2.4	3.4	4.5
77	190	20	1500	2.7	2.4	2.8	3.4	4.6
78	190	30	1500	2.2	2.4	2.3	3.3	4.1
79	190	40	1500	1.5	1.5	2	3.3	4.1
80	190	60	1500	0.7	1.2	1.7	3.2	3.9

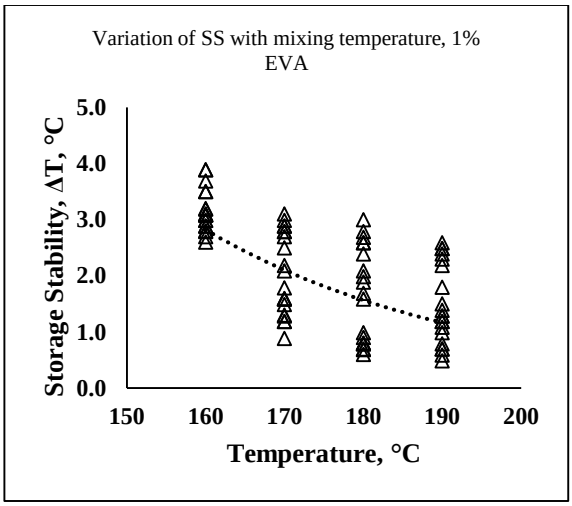
Variation of SS with mixing temperature, 1% EVA
Storage Stability, ΔT, °C
5.0
4.0
3.0
2.0
1.0
0.0
150
160
170
180
190
200
Temperature, °C

a

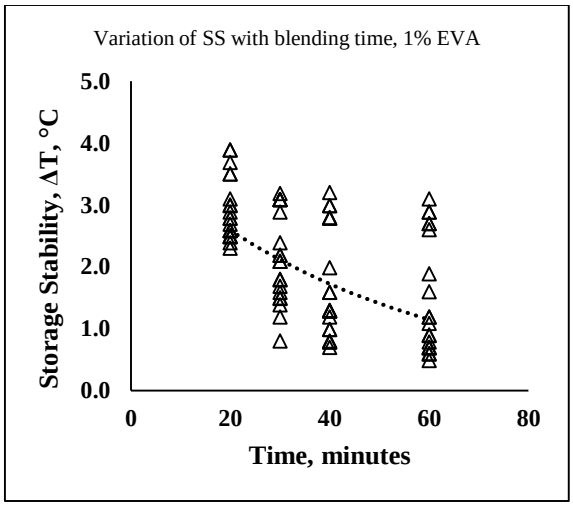
Variation of SS with blending time, 1% EVA
Storage Stability, ΔT, °C
5.0
4.0
3.0
2.0
1.0
0.0
0
20
40
60
80
Time, minutes

b

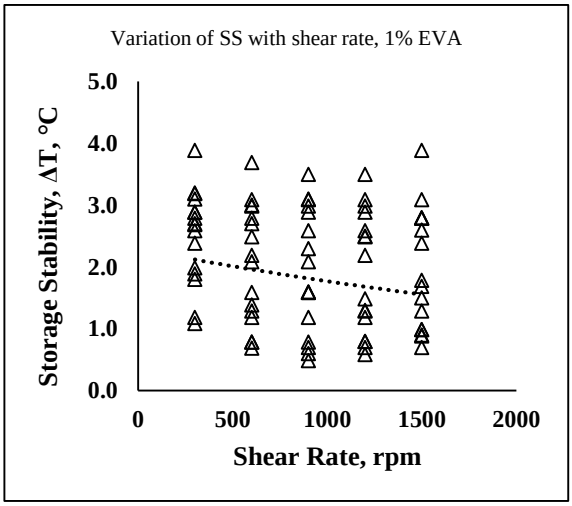
Variation of SS with shear rate, 1% EVA
Storage Stability, ΔT, °C
5.0
4.0
3.0
2.0
1.0
0.0
0
500
1000
1500
2000
Shear Rate, rpm

c

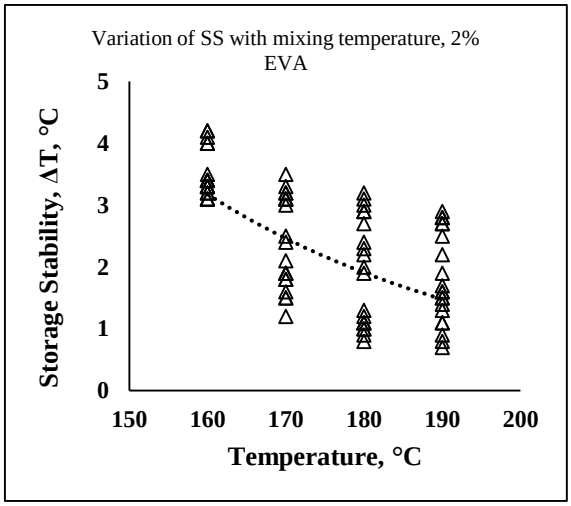
Variation of SS with mixing temperature, 2% EVA
Storage Stability, ΔT, °C
5
4
3
2
1
0
150
160
170
180
190
200
Temperature, °C

d

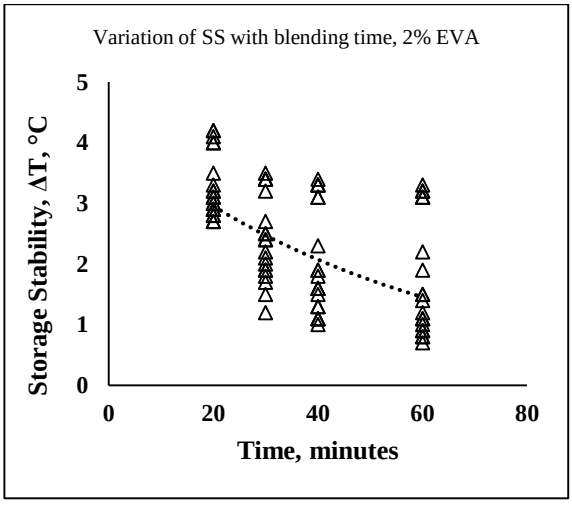
Variation of SS with blending time, 2% EVA
Storage Stability, ΔT, °C
5
4
3
2
1
0
0
20
40
60
80
Time, minutes

e

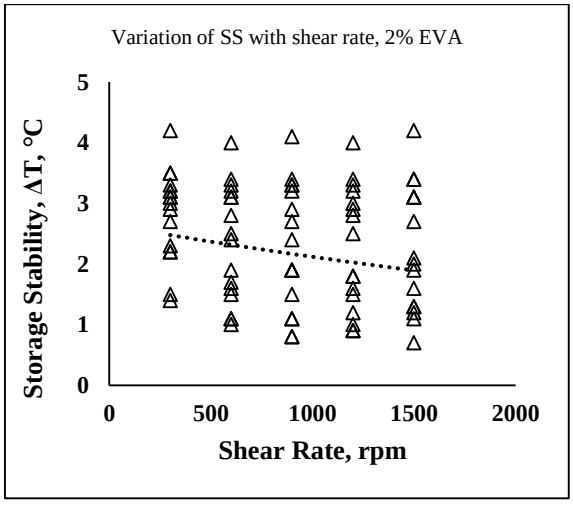
Variation of SS with shear rate, 2% EVA
Storage Stability, ΔT, °C
5
4
3
2
1
0
0
500
1000
1500
2000
Shear Rate, rpm

f

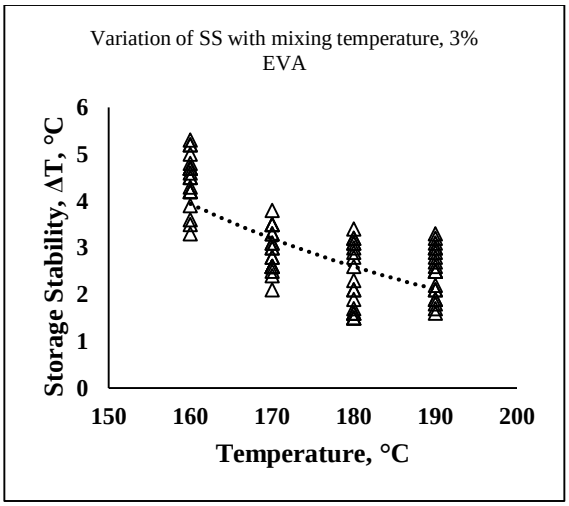
Variation of SS with mixing temperature, 3% EVA
Storage Stability, ΔT, °C
Temperature, °C
150
160
170
180
190
200

g

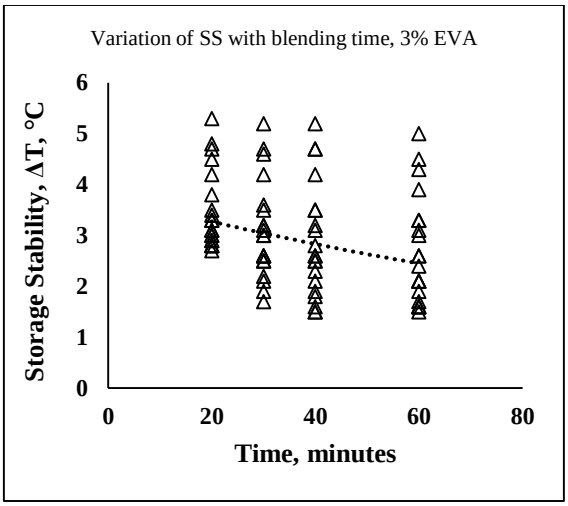
Variation of SS with blending time, 3% EVA
Storage Stability, ΔT, °C
Time, minutes
0
20
40
60
80

h

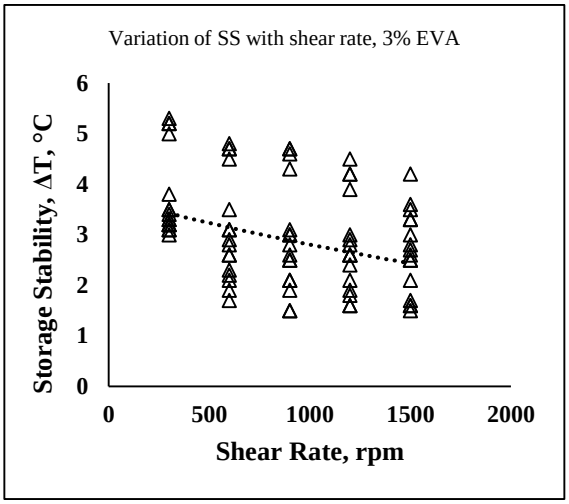
Variation of SS with shear rate, 3% EVA
Storage Stability, ΔT, °C
Shear Rate, rpm
0
500
1000
1500
2000

i

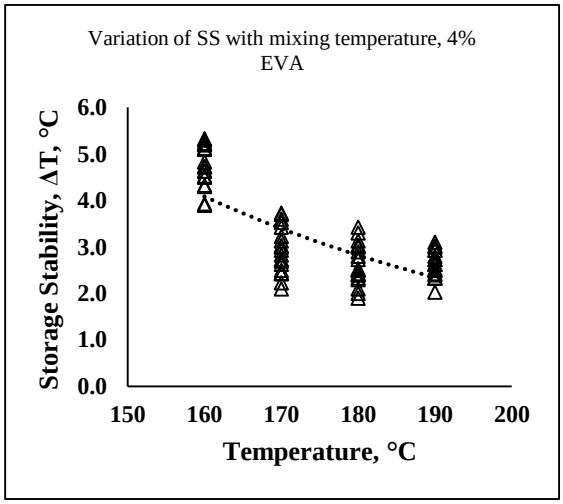
Variation of SS with mixing temperature, 4% EVA
Storage Stability, ΔT, °C
Temperature, °C
150
160
170
180
190
200

j

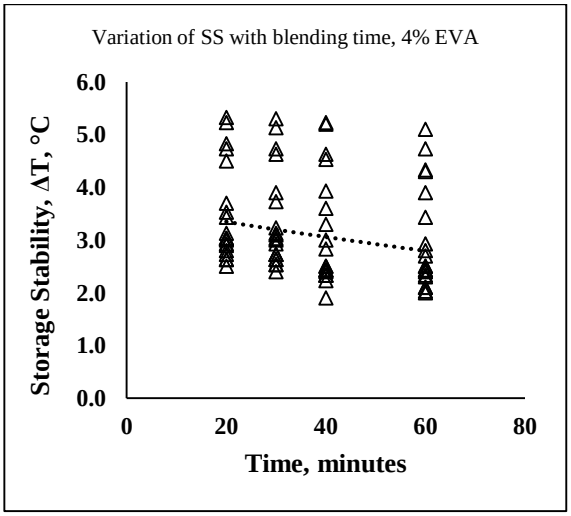
Variation of SS with blending time, 4% EVA
Storage Stability, ΔT, °C
Time, minutes
0
20
40
60
80

k

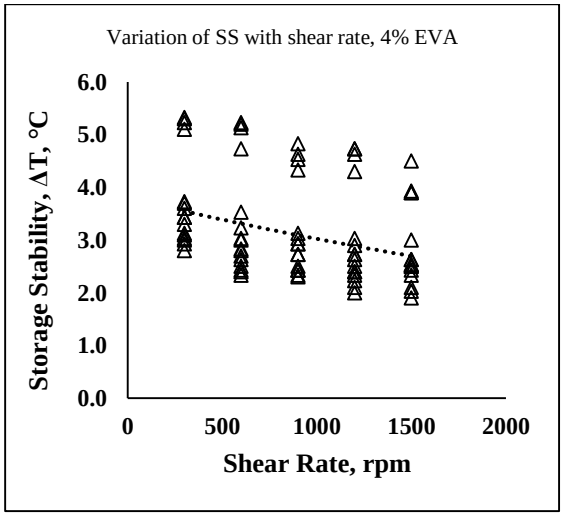
Variation of SS with shear rate, 4% EVA
Storage Stability, ΔT, °C
Shear Rate, rpm
0
500
1000
1500
2000

l

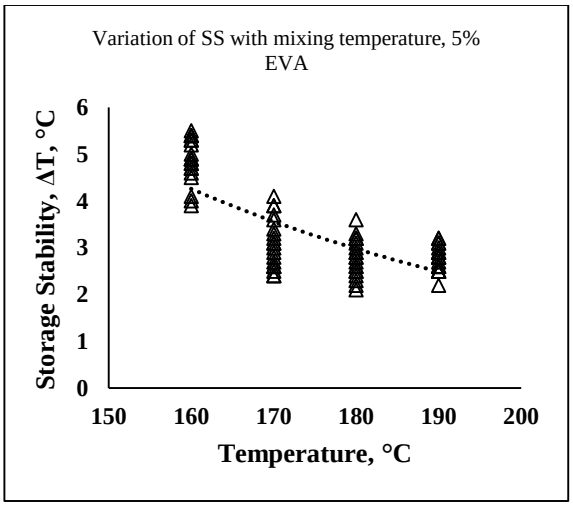
Variation of SS with mixing temperature, 5% EVA
Storage Stability, ΔT, °C
Temperature, °C
0
1
2
3
4
5
6
150
160
170
180
190
200

m

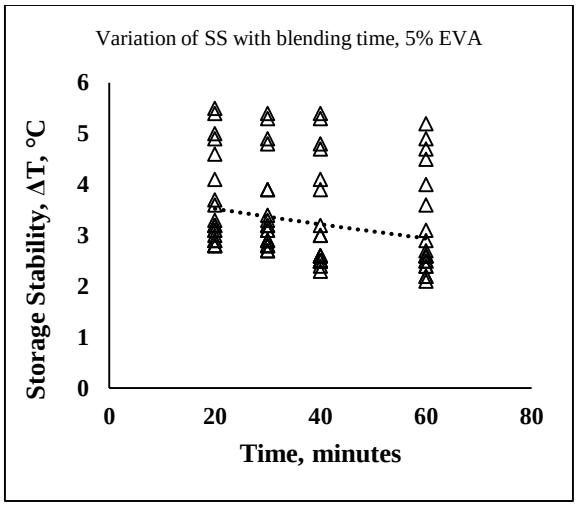
Variation of SS with blending time, 5% EVA
Storage Stability, ΔT, °C
Time, minutes
0
1
2
3
4
5
6
0
20
40
60
80

n

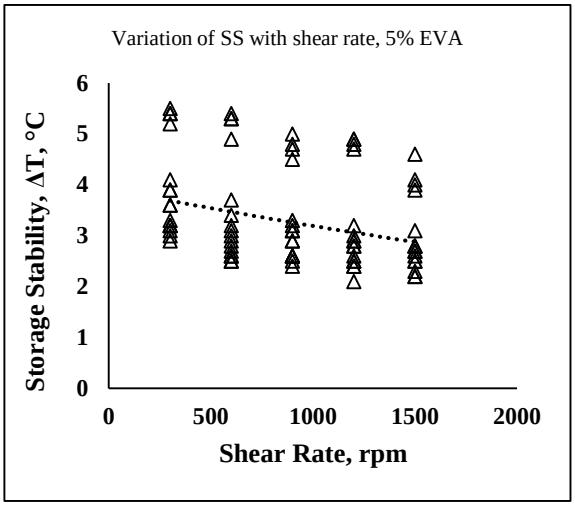
Variation of SS with shear rate, 5% EVA
Storage Stability, ΔT, °C
Shear Rate, rpm
0
1
2
3
4
5
6
0
500
1000
1500
2000

o

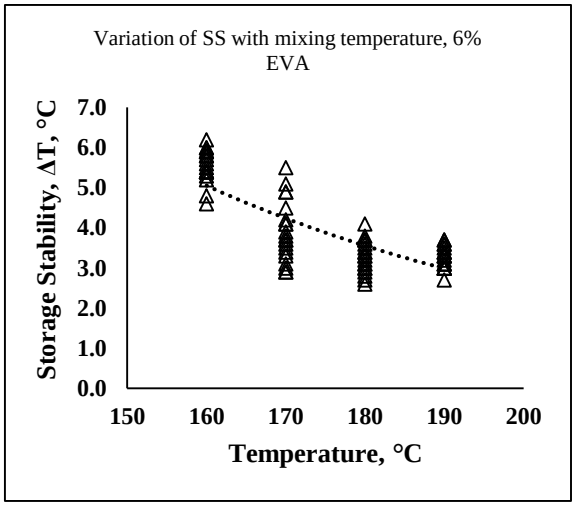
Variation of SS with mixing temperature, 6% EVA
Storage Stability, ΔT, °C
Temperature, °C
0.0
1.0
2.0
3.0
4.0
5.0
6.0
7.0
150
160
170
180
190
200

p

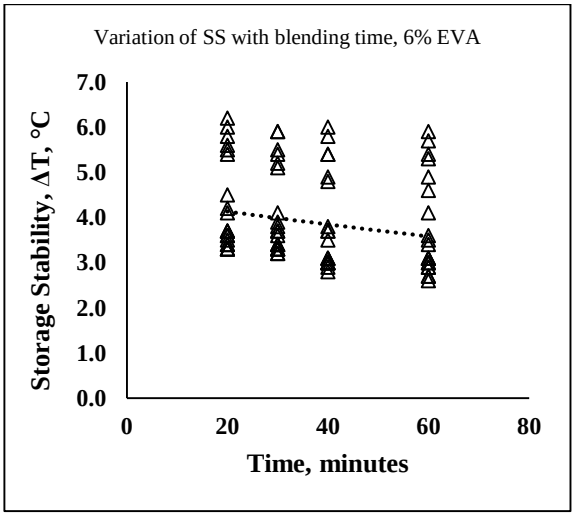
Variation of SS with blending time, 6% EVA
Storage Stability, ΔT, °C
Time, minutes
0.0
1.0
2.0
3.0
4.0
5.0
6.0
7.0
0
20
40
60
80

q

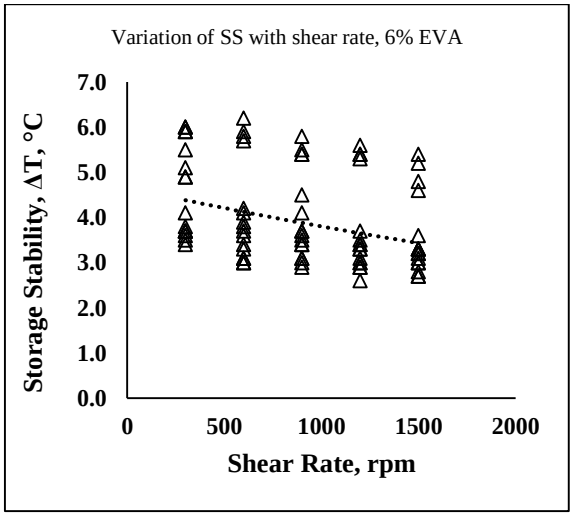
Variation of SS with shear rate, 6% EVA
Storage Stability, ΔT, °C
Shear Rate, rpm
0.0
1.0
2.0
3.0
4.0
5.0
6.0
7.0
0
500
1000
1500
2000

r

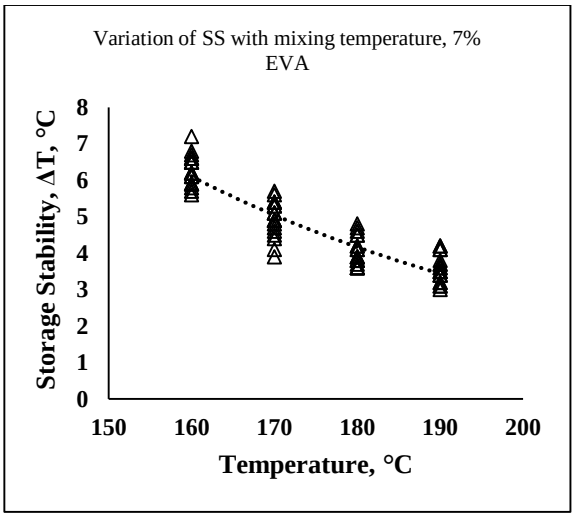

s

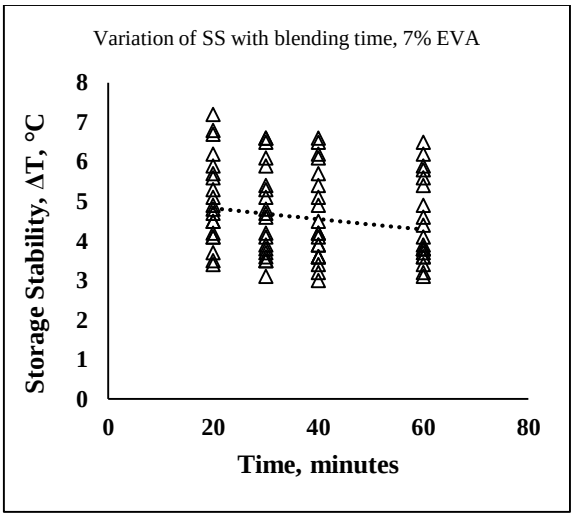

t

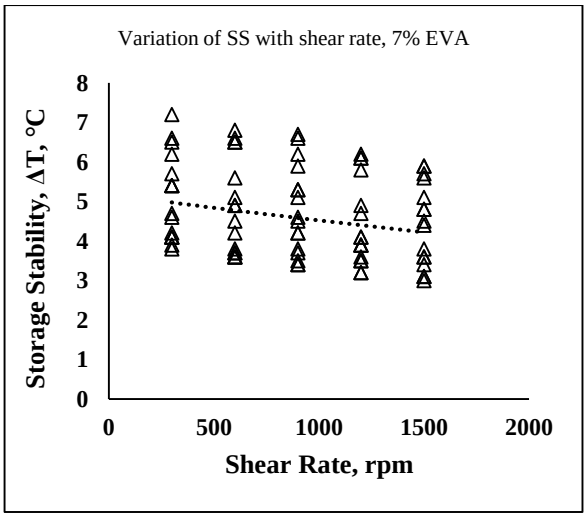

u

Figure 3.1(a-u) Variation of storage stability values with different blending parameters for EVA.

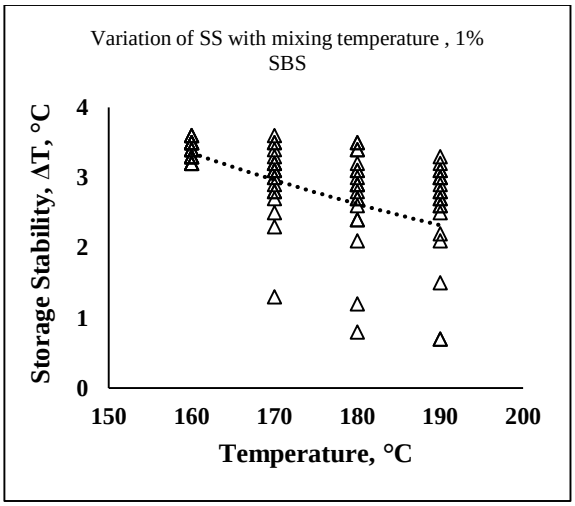
Variation of SS with mixing temperature , 1% SBS
Storage Stability, ΔT, °C
Temperature, °C
0
1
2
3
4
150
160
170
180
190
200

a

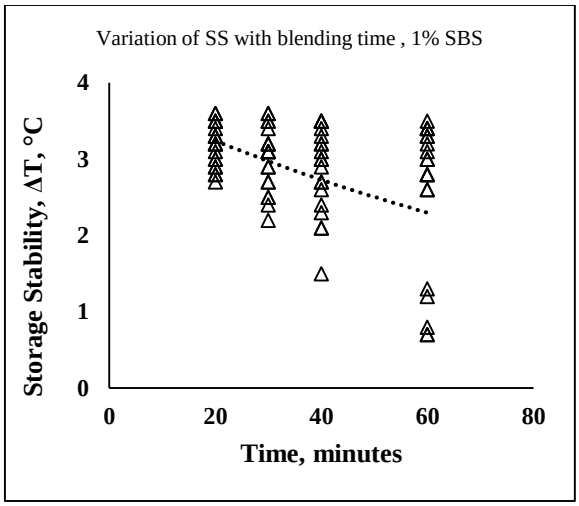
Variation of SS with blending time , 1% SBS
Storage Stability, ΔT, °C
Time, minutes
0
1
2
3
4
0
20
40
60
80

b

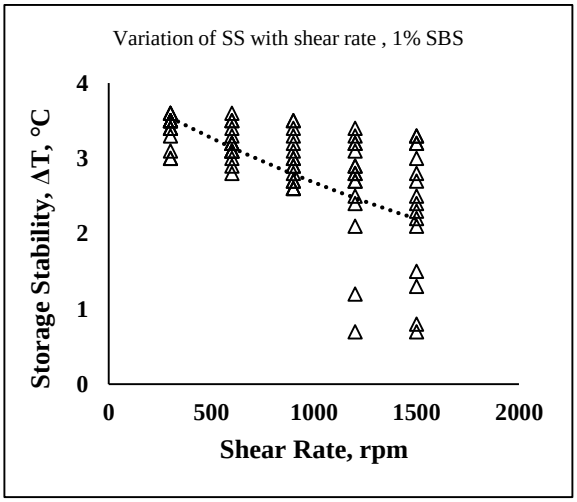
Variation of SS with shear rate , 1% SBS
Storage Stability, ΔT, °C
Shear Rate, rpm
0
1
2
3
4
0
500
1000
1500
2000

c

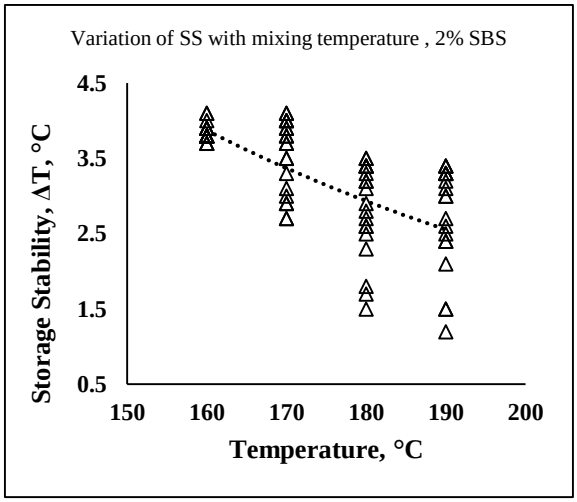
Variation of SS with mixing temperature , 2% SBS
Storage Stability, ΔT, °C
Temperature, °C
0.5
1.5
2.5
3.5
4.5
150
160
170
180
190
200

d

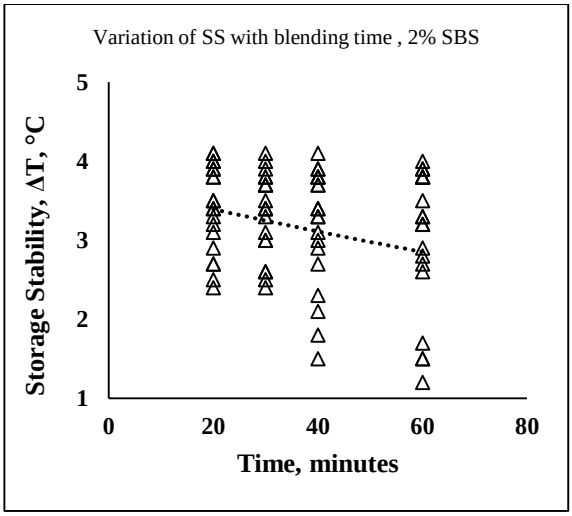
Variation of SS with blending time , 2% SBS
Storage Stability, ΔT, °C
Time, minutes
1
2
3
4
5
0
20
40
60
80

e

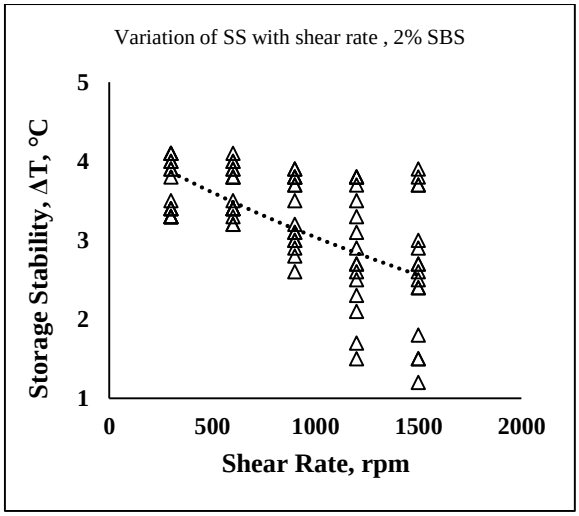
Variation of SS with shear rate , 2% SBS
Storage Stability, ΔT, °C
Shear Rate, rpm
1
2
3
4
5
0
500
1000
1500
2000

f

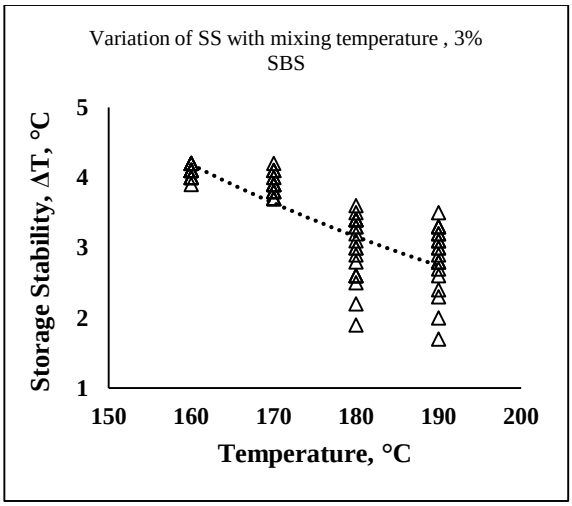
Variation of SS with mixing temperature , 3% SBS
Storage Stability, ΔT, °C
Temperature, °C
150 160 170 180 190 200
1 2 3 4 5

g

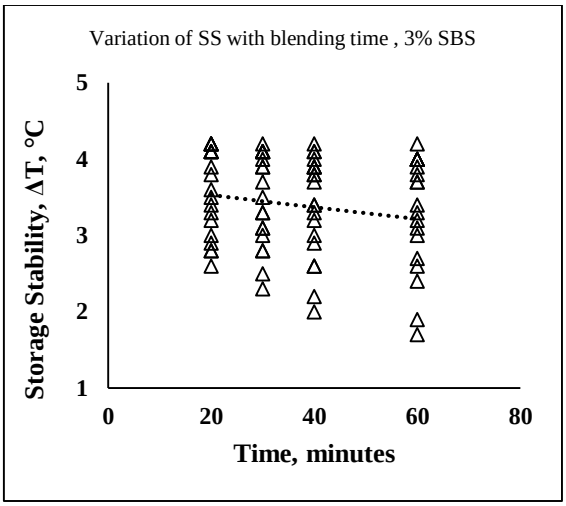
Variation of SS with blending time , 3% SBS
Storage Stability, ΔT, °C
Time, minutes
0 20 40 60 80
1 2 3 4 5

h

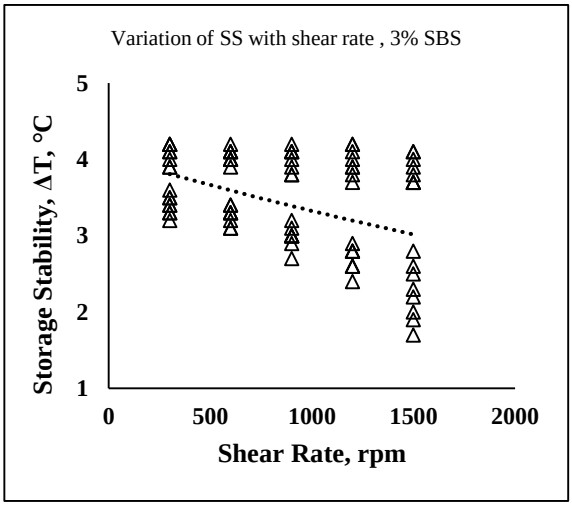
Variation of SS with shear rate , 3% SBS
Storage Stability, ΔT, °C
Shear Rate, rpm
0 500 1000 1500 2000
1 2 3 4 5

i

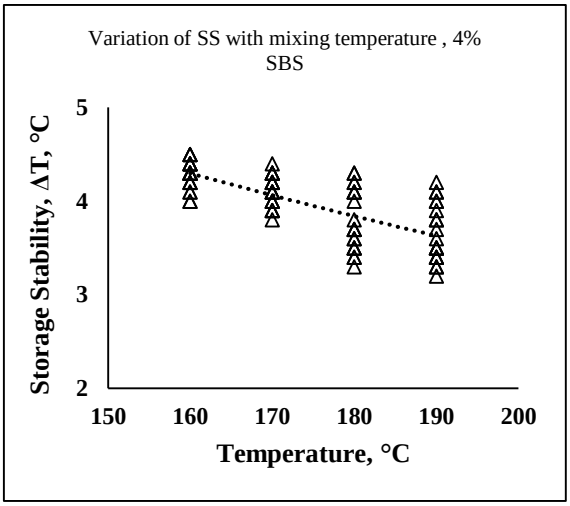
Variation of SS with mixing temperature , 4% SBS
Storage Stability, ΔT, °C
Temperature, °C
150 160 170 180 190 200
2 3 4 5

j

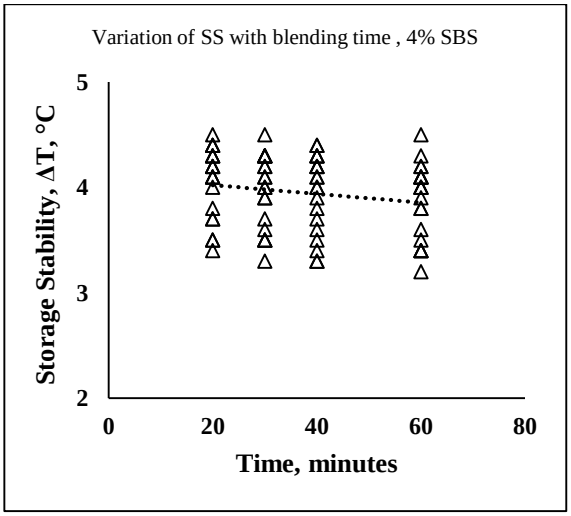
Variation of SS with blending time , 4% SBS
Storage Stability, ΔT, °C
Time, minutes
0 20 40 60 80
2 3 4 5

k

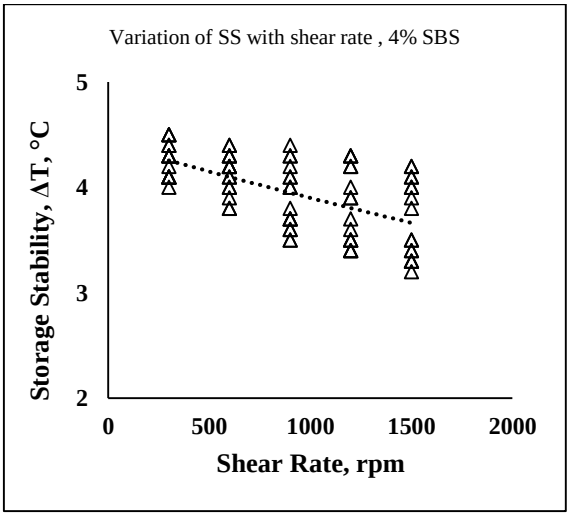
Variation of SS with shear rate , 4% SBS
Storage Stability, ΔT, °C
Shear Rate, rpm
0 500 1000 1500 2000
2 3 4 5

l

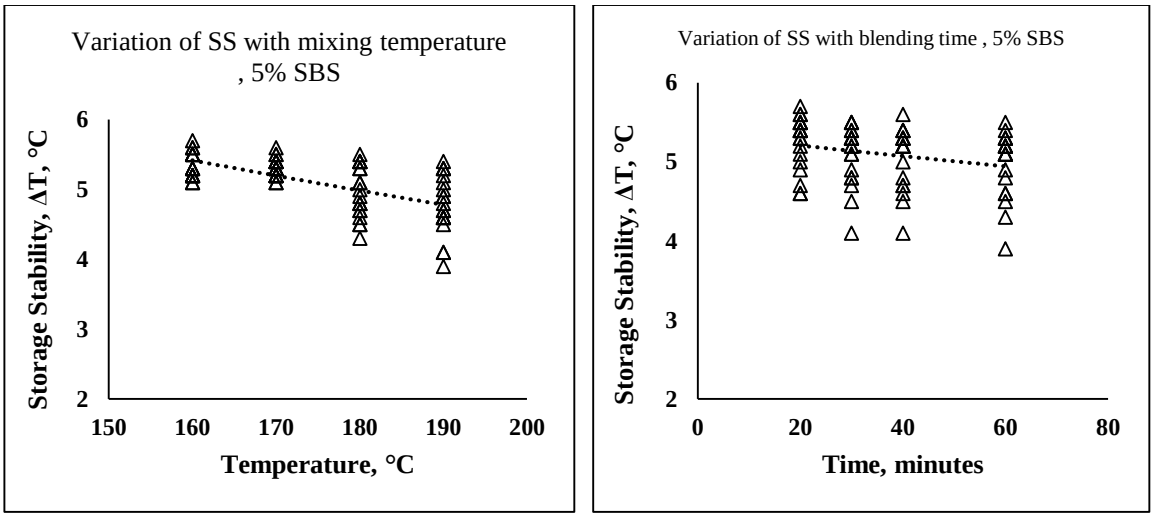

m n

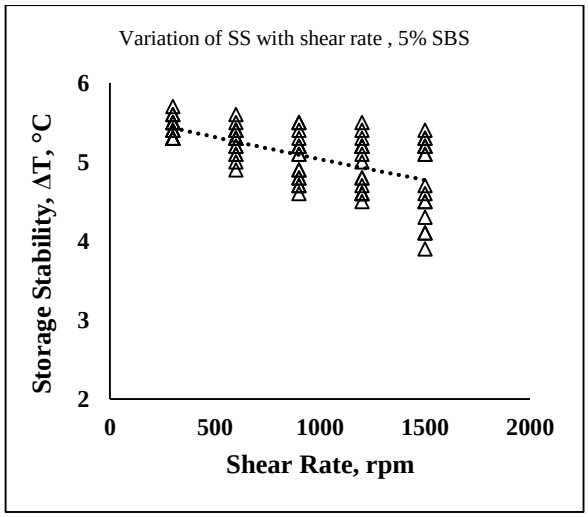

o

Figure 3.2(a-o) Variation of storage stability values with different blending parameters for SBS.

It is clear from the discussion above that an optimum combination of all the three blending parameter is desired to obtain a storage stable modified binder. Non-linear regression technique using SOLVER function in MS Excel was used to establish the correlation between SS and all the three parameters used. The following linear relationship was assumed between the dependent and independent variables.

$$SS = k + a_1.MixingTemperature + b_1.Blending\ Time + c_1.Shear\ Rate \quad (0.1)$$

Where, k= Constant;

a_1, b_1 and c_1 = coefficients of the equation.

Table 3.4 and Table 3.5 depict the values of the constant and the coefficients obtained for both the polymer modifiers. As was discussed above, that irrespective of any blending combinations the storage stability values was not lower than 3 °C for modification level higher than 5% in case of EVA and 3% in case of SBS. Hence the calculations were not made for those higher percentage levels.

Equation 3.1 was used to find the optimum blending requirement for each percent of modifier used and a constraint was set such that the SS value should be less than 3. The respective values can be seen in Table 3.6 and 3.7. Examining the values for each percent modification a common blending requirement was set, irrespective of the percent modifier used. SBS was incorporated in the base binder at a temperature of 180 °C using a high shear mixture operated at 1500 rpm for 60 minutes. The corresponding temperature, shear rate and time for EVA were 190 °C, 600 rpm and 30 minutes.

Table 3.4 Coefficients obtained using Solver function of EVA modification

Percent modifier (%)	k	a_1	b_1	c_1
1	13.246	0.055	0.033	0.000
2	13.873	0.056	0.035	0.000
3	15.972	0.066	0.019	0.001
4	15.794	0.065	0.013	0.001
5	16.045	0.066	0.014	0.001

Table 3.5 Coefficients obtained using Solver function of SBS modification

Percent modifier (%)	k	a_1	b_1	c_1
1	9.347	0.029	0.016	0.001
2	10.083	0.001	0.009	0.001
3	12.336	0.046	0.007	0.001

Table 3.6 Values of the optimum blending parameters for EVA modification

Percent modifier (%)	Mixing Temperature (°C)	Blending Time (minutes)	Shear Rate (s^{-1})
1	170	20	600
2	175	20	600
3	180	25	600
4	185	30	600
5	190	30	600

Table 3.7 Values of the optimum blending parameters for SBS modification

Percent modifier (%)	Mixing Temperature (°C)	Blending Time (minutes)	Shear Rate (s^{-1})
1	170	40	1200
2	180	40	1200
3	180	60	1500

3.4 Optimum Modifier Content

Once the blending requirement was set, PMB's at different percent of modifier were produced maintaining the obtained values of mixing parameters. Next, the objective was to obtain the optimum modifier content for producing a homogenous mix which would be stable at high temperatures. Storage stability test and Fluorescence microscopy was used to achieve the second objective. Conventional test like penetration and softening point were also carried out to see the effect of modification on the consistency of bitumen.

The results obtained from penetration and softening point test were used to determine the temperature susceptibility of the base and modified binders. It provides a mean to assess the change in behavior of material response at varying temperature conditions. It is defined as the change in consistency parameter as a function of temperature. A classical approach as given in Shell Bitumen Handbook [83]was used to calculate the value of Penetration index (PI).

$$PI = \frac{1952 - 500 \log\left(Pen_{25}\right) - 20 \times SP}{50 \log\left(Pen_{25}\right) - SP - 120} \quad (0.2)$$

Where, Pen_{25} is the penetration at 25˚C and SP is the softening point temperature of the PMB. The value of PI ranges from -3 for highly temperature susceptible bitumen's to +7 for low temperature susceptible and highly blown bitumen[83]

3.4.1 *Change in conventional properties*

The effect of polymer modification on VG 10 can be seen from Table 3.8 and Table 3.9 as a decrease in penetration and increase in softening point. Figure 3.3 (a,b) and Figure 3.4 (a,b) show the variation of penetration and softening point as a function of modifier percentage for both EVA and SBS. From Figure below it can be seen that there is a sudden decrease in penetration after 2 % modification in case of EVA and 1% modification for SBS. This may be considered as the threshold percentage after which polymer network start dominating the bitumen-polymer system. Decrease in penetration and increase in softening point indicate increased stiffness and hardness of the binder after modification. In addition to this there is an increase in PI values as the percentage of modifier increases, indicating reduction in temperature susceptibility due to polymer modification.

3.4.2 *Storage stability values*

Storage stability is a measure of homogeneity at high temperatures. From Table 3.8 it can be seen that in case of EVA, after 5% modification the difference in ring and ball softening point for the top and bottom samples in separation test exceeds 3˚C indicating phase separation. This may be due to the absence of adequate amount of maltene fraction to satisfy the demand of asphaltene and polymer solubility after EVA percentage exceeds this value. Similar result is found for SBS after 3% modifier content (see Table 3.9). At low polymer content there is practically no phase separation, hence it can be viewed as a bitumen (asphaltene) rich phase with polymer being dispersed thoroughly. So for EVA modified binder, 5% can be considered as the optimum percentage for modification of VG 10 considered in the study. Similarly for SBS the optimum modifier content is found to be 3%.

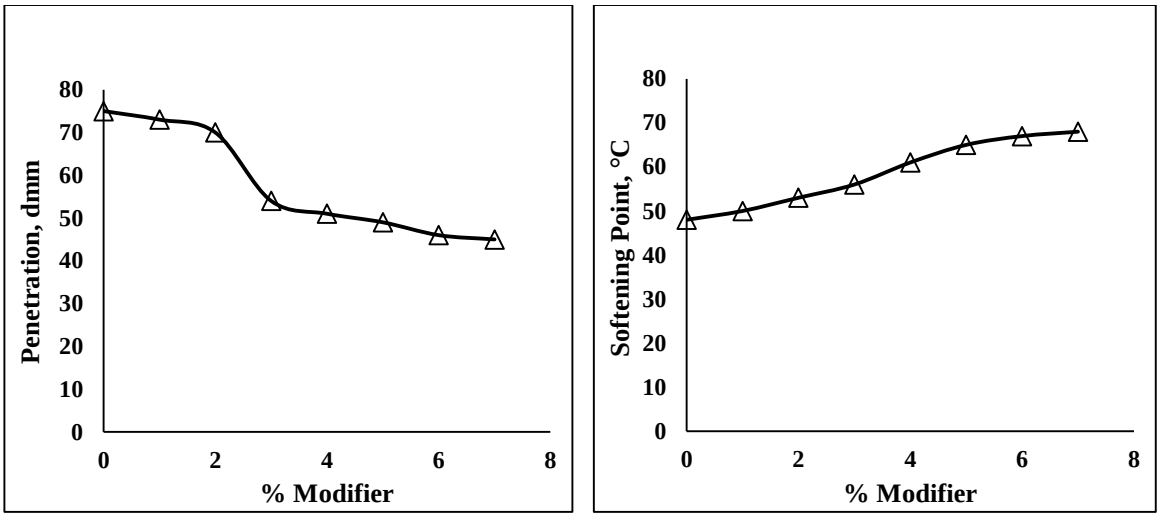

a b

Figure 3.3 (a,b) Change in penetration and softening point with increase in modifier content for EVA

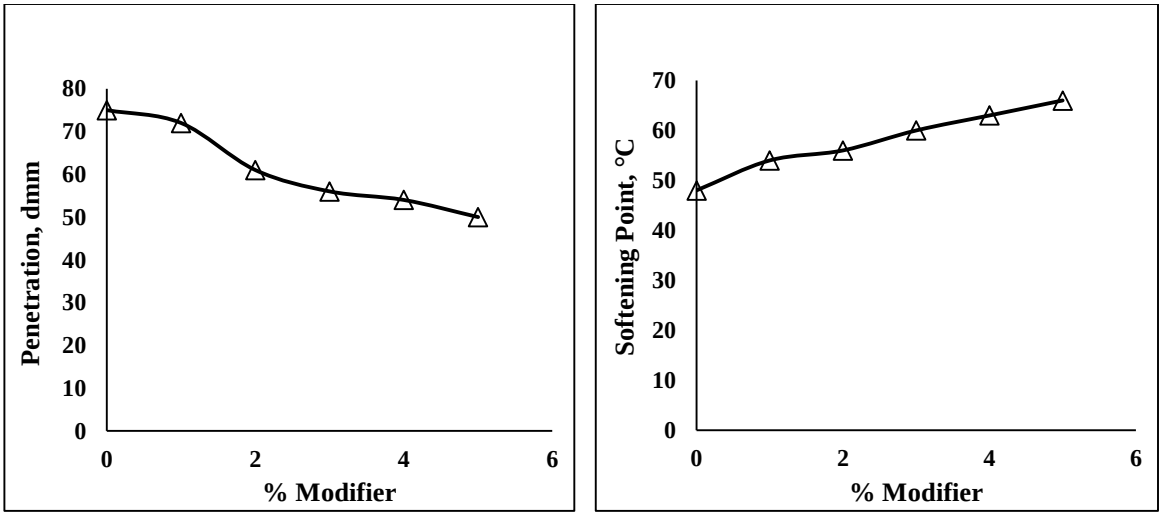

a b

Figure 3.4 (a,b) Change in penetration and softening point with increase in modifier content for SBS

Table 3.8 Variation of physical properties due to EVA modification

Properties	Standard	Percentage of EVA							
		0	**1**	**2**	**3**	**4**	**5**	**6**	**7**
Penetration	ASTM D5	75	73	70	54	51	49	46	45
Softening point	ASTM D36	48	50	53	56	61	65	67	68
Specific Gravity	ASTM D70	1.01	1.01	1.01	1	1	1	0.99	0.99
Penetration Index		-0.73	-0.26	0.38	0.38	1.27	1.92	2.11	2.23
Storage Stability (ΔT)	IRC SP53 2010	0	0.2	0.7	0.9	1.7	2.2	3.3	5.2

Table 3.9 Variation of physical properties due to SBS modification

Properties	Standard	Percentage of SBS					
		0	**1**	**2**	**3**	**4**	**5**
Penetration	ASTM D5	75	72	71	56	54	50
Softening point	ASTM D36	48	54	56	60	63	66
Specific Gravity	ASTM D70	1.01	1.01	1	0.99	1	0.99
Penetration Index		-0.73	0.70	1.12	1.32	1.81	2.15
Storage Stability (ΔT)	IRC SP53 2010	0	1.1	1.7	2.3	3.2	4.9

3.4.3 *Fluorescence microscopy*

Morphology of the polymer modified binders were studied using Fluorescence Microscopy (FM). The nature and quality of dispersion of the modifier in the bitumen was assessed using this technique. It is based on the principle that polymers swell due to absorption of some of the light fractions of bitumen (mainly maltene fraction) and hence fluoresce in ultraviolet (UV) light. This fluorescence is due to the aromatic oils absorbed by the polymer. It is by far one of the most valuable methods to study the phase morphology of modified bitumen and assessing the homogeneity and the structure in raw state. The sample preparation method involves diluting the bitumen and preparing it over glass slide so that the beam could pass through the sample. The samples were examined using a Nikon Eclipse LV 100 microscope using appropriate magnification. High pressure Xenon lamp was used for excitation and the wavelength was maintained between 510-560 nm. The Fluorescence Microscope used in the study is shown in Figure 3.5 (a,b).

From Figures 3.6 (a-h) and 3.7 (a-e), it can be seen that the morphology of the bitumen changes as the polymer content increases. At 0% modification level there is no fluorescence effect and the image appears to be single dark. Till 3% EVA it can be seen that the modification produces a bitumen rich phase (with the darker side dominating) with polymer being dispersed in it. 5% EVA produces an interlocked phase which is considered to be the most desirable morphology for modification. Higher percentages clearly demonstrates a polymer rich phase with large amount of fluorescence effect caused by the swelled polymer. This supports the result obtained in the separation test where 5% EVA content was found to be optimum for modification. In case of SBS it can be seen that till 2% modification the bitumen phase dominates till 2% modification level. At 3% the polymer phase (shown in white) dominates and is dispersed uniformly. At higher percentages the polymer fraction becomes coarser indicating a phase separated mix. Hence 3% SBS is best suited for obtaining a homogenous blend. Fluorescence microscopy also acts as a validation of storage stability result. It should be mentioned that the optimum modifier content obtained are with respect to the base binder, VG 10. The result are subjected to changes if the base binder is changed.

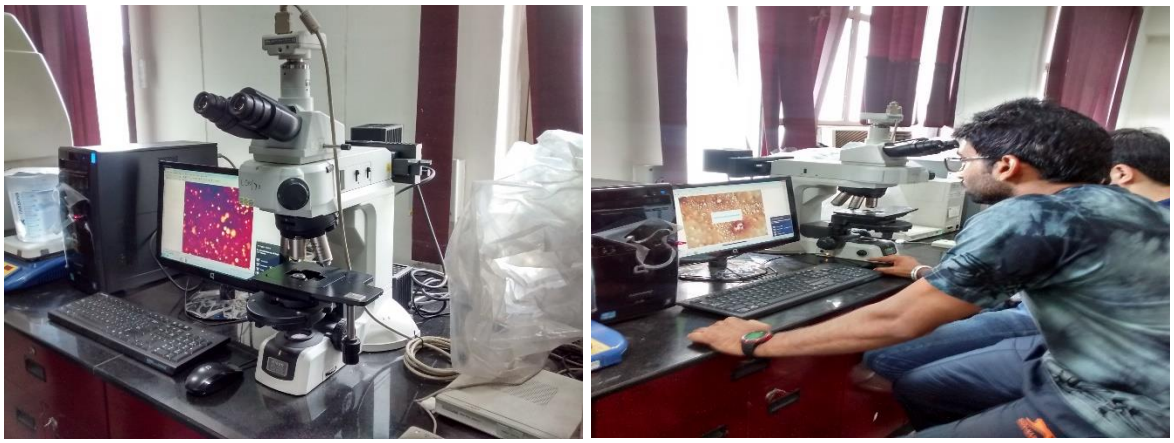

a b

Figure 3.5 (a,b) Fluorescence Microscope used in the study.

a

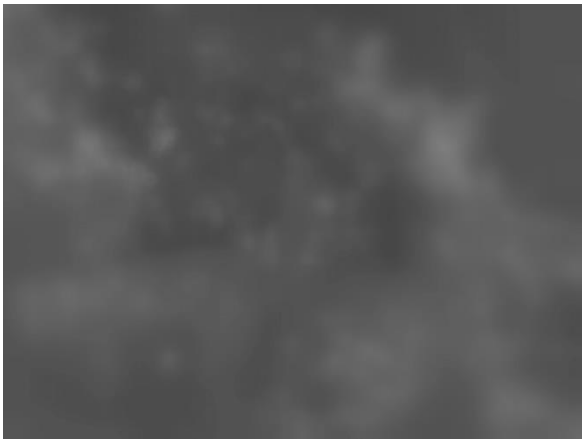

b

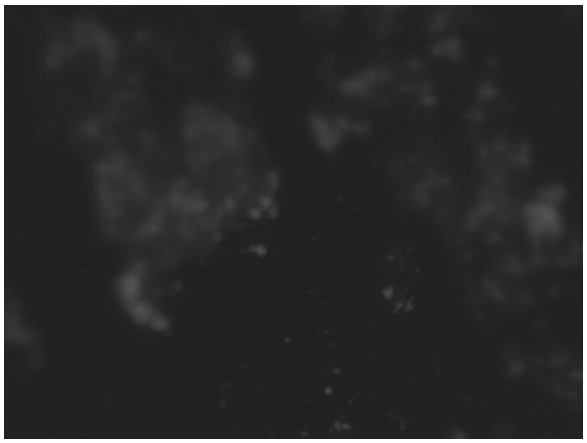

c

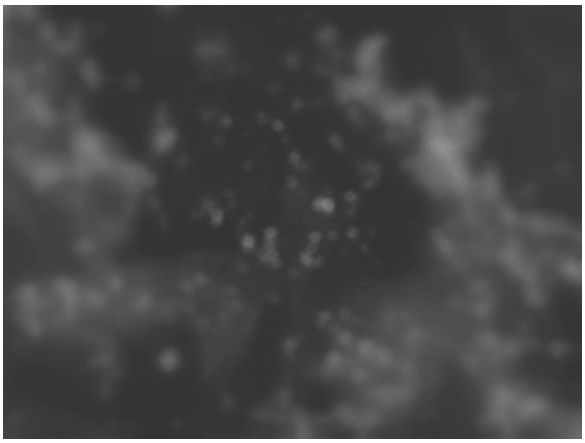

d

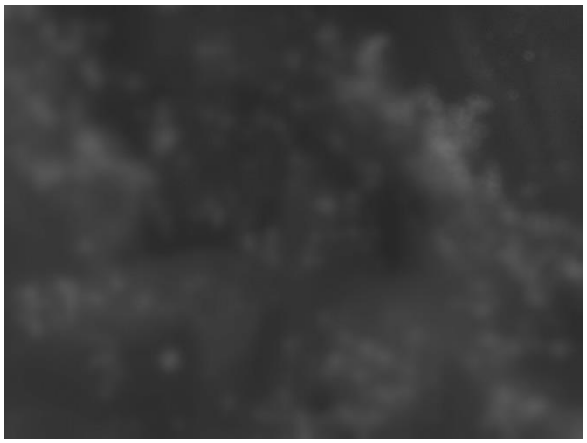

e

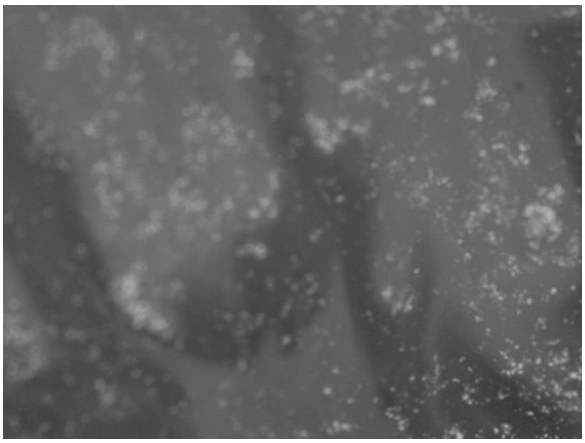

f

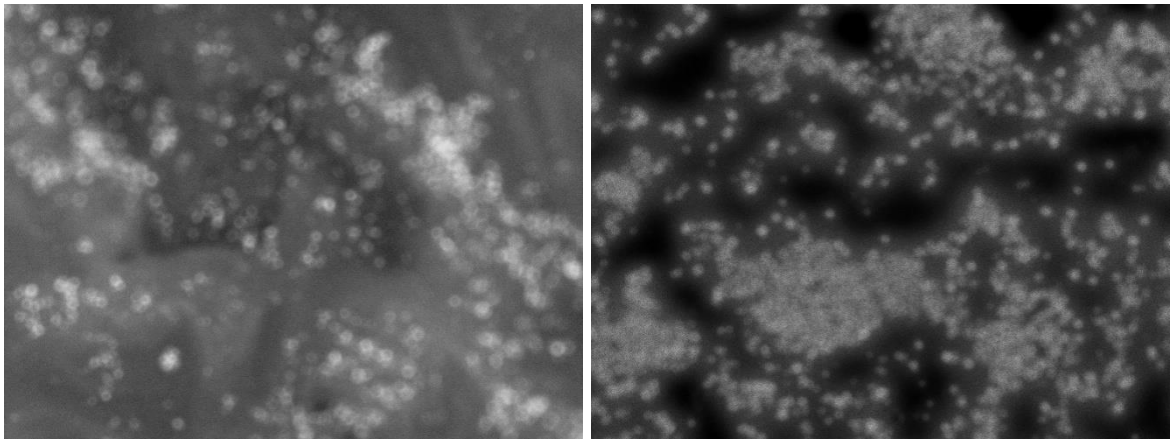

g h

Figure 3.6(a-h) Fluorescence microscopy results for EVA at modifier content of (a) 0%, (b) 1%, (c) 2%, (d) 3%, (e) 4%, (f) 5%, (g) 6%, (h) 7%

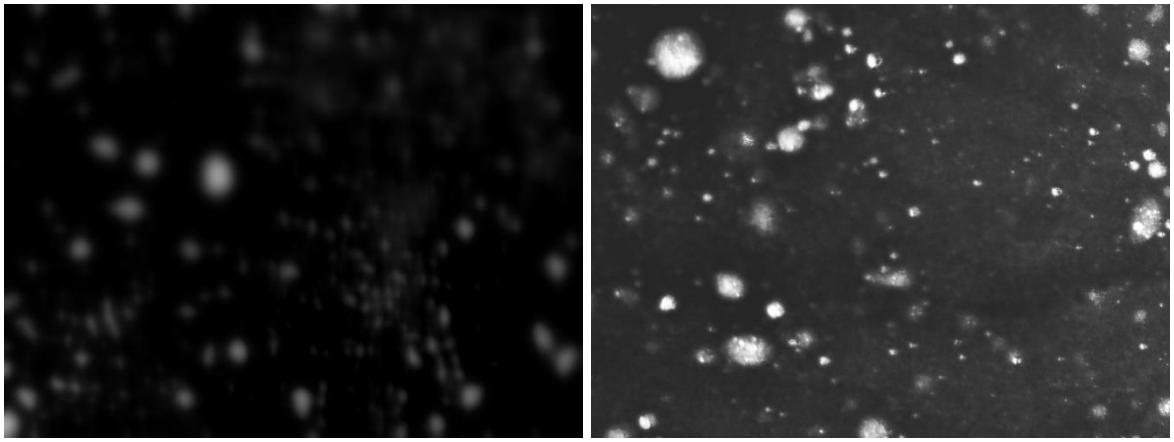

a b

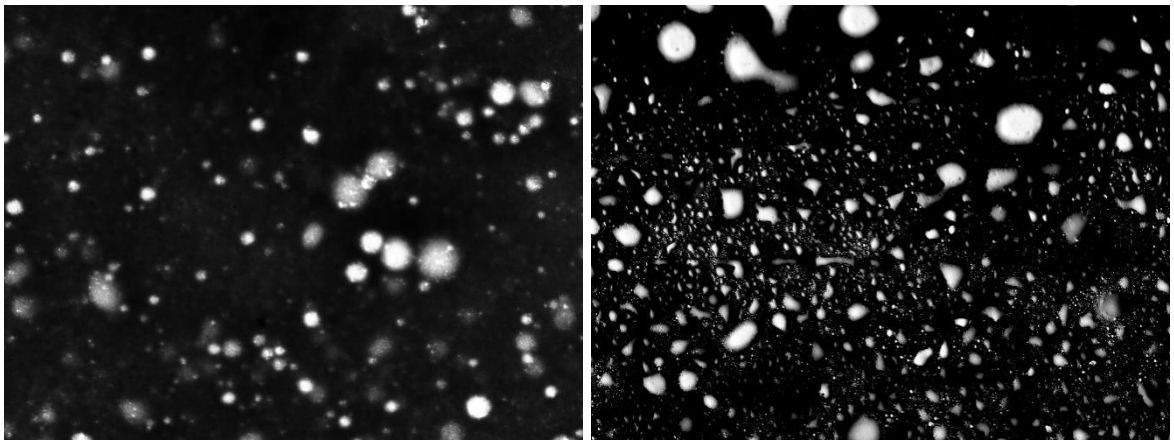

c d

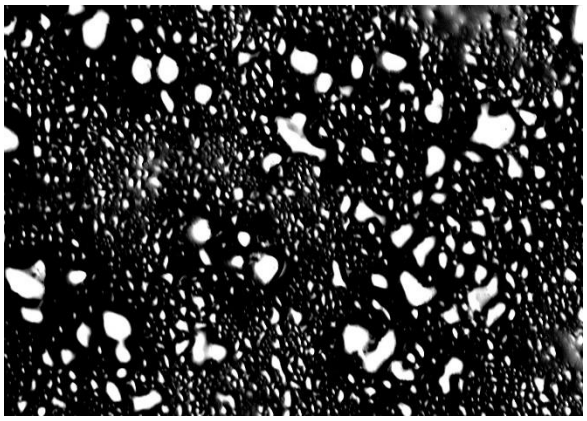

e

Figure 3.7(a-e) Fluorescence microscopy results for SBS at modifier content of (a) 1%, (b) 2%, (c) 3%, (d) 4%, (e) 5%

3.5 Conclusions

From the test and analysis done for the modification of asphalt binder, the following conclusions were drawn.

1. It is important to obtain the proper blending requirement for modifying bitumen with any additive. The importance of different blending parameters depends on the type of modifier used. It was found that for EVA modification temperature plays the most crucial role while for SBS the effect of shear rate is crucial.
2. Nonlinear regression technique was employed to find the optimum blending requirements for EVA and SBS modified bitumen. From the analysis it was found that SBS could be incorporated in the base binder at a temperature of 180 °C using a high shear mixture operated at 1500 rpm for 60 minutes. The corresponding temperature, shear rate and time for EVA were 190 °C, 600 rpm and 30 minutes.
3. There was a decrease in penetration and increase in softening point with increase in modifier content for both SBS and EVA modified binder. Storage stability test showed that optimum modifier content for EVA is 5% while for SBS is 3%. This result was also validated by the study of morphology using Fluorescence microscopy. An interlocked bitumen-polymer phase is the most desirable for obtaining a homogenous blend.

Chapter 4

Mixing and Compaction Temperature for Asphalt Binders

4.1 Introduction

Modification of bitumen is one of the several techniques to improve the structural performance of bituminous mix [6, 28, 80, 100]. Polymer modified binders have been successfully used to ameliorate the viscoelastic response of bitumen, especially at higher temperatures [6, 65, 150]. When it comes to applicability, contractors and practitioners remain skeptical, mostly due to the high mixing and compaction temperature requirements for these binders. Increase in cost is another main concern. Traditionally, Rotational Viscometer is used for evaluating the mixing and compaction temperature of bitumen. The viscometer applies 6.8 s^{-1} (20 rpm) shear rate and the resulting torque is utilized to calculate the viscosity of the binder at different temperatures. The log-log plot of viscosity versus temperature is used to find the temperatures corresponding to 0.17±0.02 Pa.s and 0.28±0.03 Pa.s. These temperatures are used for mixing and compaction of bituminous mix.

NCHRP report 648 [183] presented new methods for evaluating the mixing and compaction temperatures for modified binders, which resulted in reduction of temperature requirement by 20-30 ℃, as compared to the conventional method. In the first method named as "Phase Angle Method", the mixing and compaction temperature are established by construction of phase angle master curve at 80 ℃. Phase angle is more sensitive to chemical changes, as found in modified binders [6]. So it is rather difficult to construct a smooth master curve for phase angle, which results in a "wavy nature" (attributable to the transition and plateau regions) [6, 28, 100, 141, 150, 184]. Further in the method, the frequency corresponding to 86° phase angle is noted down and is used in an empirical equation to evaluate the mixing and compaction temperature of the binder. The use of frequency corresponding to this phase angle seems to have no practical significance. In the second method named as "Steady Shear Viscosity Method", Dynamic Shear Rheometer (DSR) is employed for finding the viscosity at 500 Pa shear stress at different temperatures. These viscosities values are plotted against temperature. Extrapolation of the viscosity data is made

for predicting the mixing and compaction temperature corresponding to a standard viscosity range similar to that of equiviscous method. The extrapolation of viscosity by using a straight line is questionable as the rheology of modified binder has high dependence on the molecular structure, which in turn is temperature sensitive [28, 63, 141, 150, 182].

The literature behind the new methods for finding out mixing and compaction temperatures for modified binder lies behind the concept that modified binders behave as a shear thinning fluid at higher shear rates which is practical in field conditions[42, 98, 159, 165, 177, 192]. Shear thinning behavior of any fluid is defined as the decrease in viscosity with increase in shear rate. But the concept of shear thinning and the reduction in viscosity could be applicable only when there is higher role of shear rate, typically found in mixing. But compaction (as in Marshall Compactor or field roller), has very little dependence on shear rate. Rather it is the normal force and energy which has higher dominance. So reduction in compaction temperature with these literature background of shear thinning behavior is again not valid. The literature mentions that, for batch and continuous mixing plants, the shear rate applied at the time of mixing are typically of the order of $6x10^4$ to $1x10^5$ s^{-1} [183]. If the role of shear rate is considered, then the viscosity at such higher shear rate will be even lower than predicted and hence even lower mixing temperatures can be suggested. But the same is not true for compaction temperature as there is no primary role of shear rate. A plethora of studies [14, 24, 77, 162, 183] have been done, where the change in density and strength of bituminous mixes have been evaluated by varying the compaction temperature, but no explicit study has been done by varying mixing temperatures. The main objective of the study is to evaluate the flow behavior of various binders at different shear rate and temperatures, and to establish a more practical way of finding the mixing temperatures for these binders.

4.2 Experimental Investigation

Steady shear viscosity was evaluated for all the binders using Dynamic Shear Rheometer (DSR). Testing was done at a shear rate of 0-100 s^{-1} for a temperature range of 40-80 °C. 25mm spindle geometry was used with 500 μm gap. The temperature of the assembly was set to 80 °C and was gradually reduced at an interval of 10 °C. 30 minutes conditioning time at each temperature was given before starting the test. High temperature

viscosity was measured using Brookfield viscometer (AASHTO 2013) using spindle no. 21 at 20 rpm standard rotational speed. Measurements were taken at 135 °C and 165 °C.

4.3 Results and Analysis

The viscosity versus shear rate behavior for all the binders have been studied at different temperatures. The Carreau-Yasuda (C-Y) is further used to model the viscosity master curve plotted using the concept of rheogram. Finally, the zero shear viscosity (ZSV) measured in the steady shear test is best fitted to a suitable model. A new technique has been proposed to evaluate the viscosity at any desired shear rate, which in turn can be used to predict the mixing temperature of bitumen.

4.3.1*Viscosity versus shear rate*

To study the influence of shear rate, steady shear viscosity test was carried out using DSR. In the oscillation mode, frequency sweep is usually done for a strain level which is well below the linear viscoelastic (LVE) range of the binder. But in the steady shear rate method no such control is monitored and the binder undergoes deformation until failure. So the data prior to failure should only be used for comparison with that in the oscillatory mode. The deviation from linearity in the stress versus shear rate graph is an indication of the failure of the specimen. Moreover, the same sample can be used in oscillation test for obtaining data at different temperatures. But in steady state mode, a single run on the sample damages it and hence the sample should be changed for the next test temperature, or else the viscosity value obtained using the same sample in the next successive temperature will be lower than the true viscosity, obtainable with the changed binder. The unmodified and modified binders were subjected to steady shear viscosity test at five different temperatures. Figure 4.1(a-d) shows the variation of viscosity of different binders with shear rate at different temperatures. Due to delamination of the binder with the spindle at 80 °C, only readings up to 70 °C are shown for VG 10. It can be seen that normal binders (VG 10 and VG 30) behaves closely as Newtonian fluids at temperature above 50 °C. It was observed that even at higher temperatures there was some evidence of shear thinning behavior for very high shear rates. For VG 10 and VG 30 there was a sharp decrease in viscosity with increase in shear rate at 40 °C. However the critical shear rate at which the change in behavior started was different

for both the binders. This sharp decrease is due to the sudden loosening of molecular networks. At this temperature, due to the higher stiffness, the binder behaves as a shear thinning fluid. After 50 °C, this shear thinning effect gradually reduces with smooth transitions with increase in shear rates, attributed to the dominance of Newtonian behavior. Modified binders, on the contrary, displayed shear thinning behavior at all temperatures. This characteristic was more dominant for plastomeric EVA polymer modified binder (PMB). For PMB (E), after 50 °C, a sharp decrease in viscosity beyond the critical shear rate was observed. This can be attributed to the melt of EVA crystallites at higher temperature, making bitumen phase more dominant as compared to the polymer phase. This argument is based on the work done by Airey [6] on polymer modified binders. A study on the change of molecular level of different binders at different temperatures will through more light on approving such behaviors. This study however deals only with the physical characteristics of binder. The onset of shear thinning behavior for modified binders occurred at lower shear rates (critical shear rate) as compared to normal binders, especially at higher temperatures. Asphaltenes are mainly responsible for the non-Newtonian behavior of the bitumen, whereas maltene governs the Newtonian flow [159]. The increase in non-Newtonian behavior of PMB may be attributed to the decrease in effective maltene fraction which are used by polymers for dispersion. The aspect to be noted is that, for all binders the critical shear rate were higher than 6.8 s^{-1} (shear rate used in Brookfield viscometer), and it increased at higher temperatures. This viscosity hence, is the zero shear viscosity (ZSV), also considered as low shear Newtonian viscosity. Two things have to be understood here. First, 6.8 s^{-1} is not the practical shear rate the binder experiences at the time of mixing an asphalt concrete. Secondly, it is due to this fact that higher mixing temperatures are obtained for modified binders, displaying high shear thinning behavior.

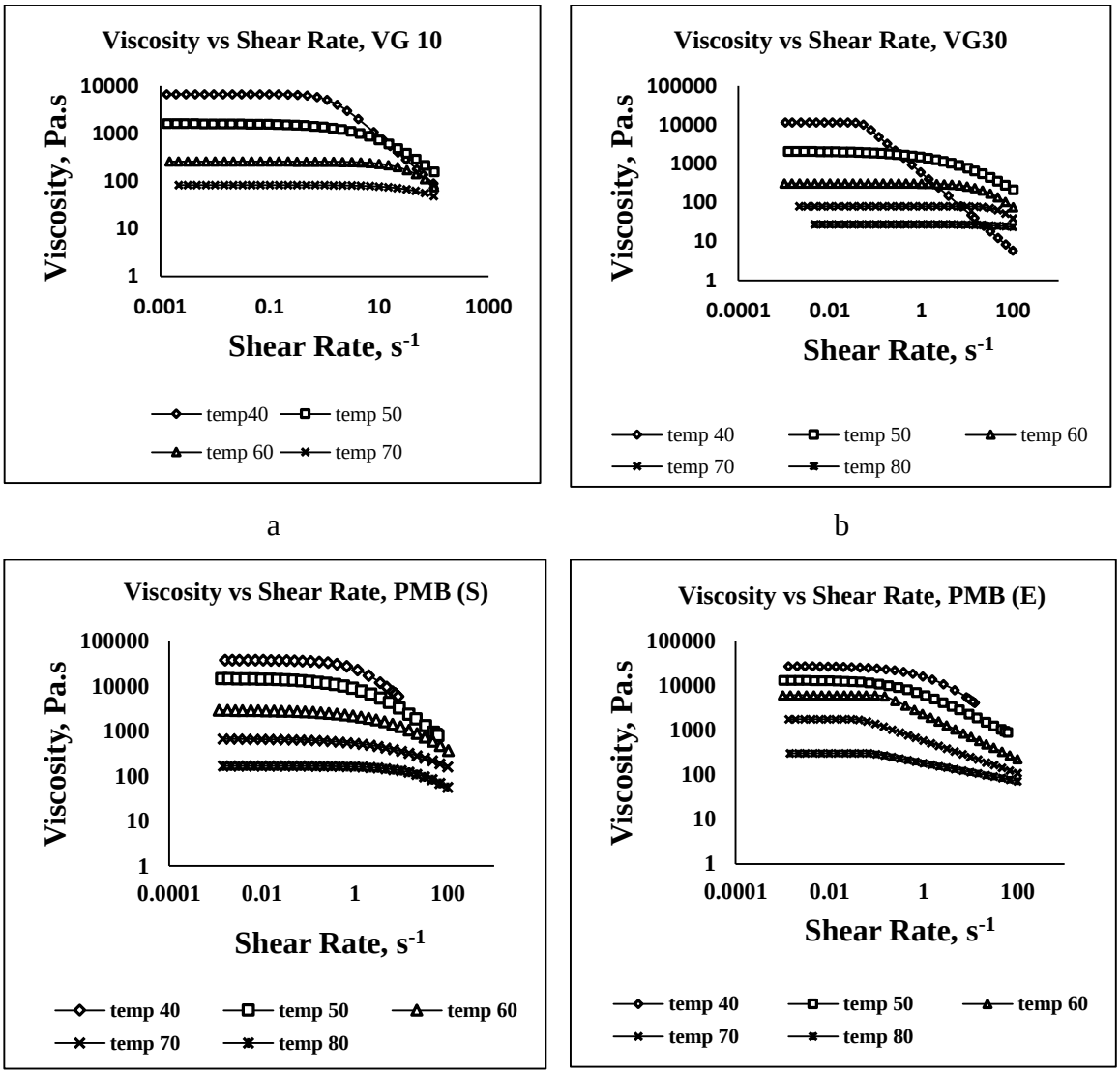

Figure 4.1 (a-d) Viscosity versus Shear Rate at different temperatures

4.3.2 *Construction and modelling of rheogram*

Shenoy [159] proposed a method of unifying the viscosity versus shear rate data at various temperatures for a number of asphalt grades. He presented the concept of Rheogram, through construction of master curve, which is independent of temperature and asphalt grade. The master curve is a plot of η/η_0 versus $\eta_0 \cdot \dot{\gamma}$, where η and η_0 are the corresponding viscosity and zero shear viscosity of the polymer. Melt flow index (MFI) has also been used

in place of η_0 for such construction. Thus by knowing the ZSV at different temperatures η can be evaluated for any desired shear rate.

Shear rate dependency of non-Newtonian (shear thinning) fluid can be evaluated using various models [33, 42, 57]. Carreau Yasuda (C-Y) model [33], however has been found to be successfully applicable to polymers such as bitumen [29, 64]. The model can be mathematically written as

$$\frac{\eta-\eta_\infty}{\eta_0-\eta_\infty}=\left[1+\left(\lambda\dot{\gamma}\right)^a\right]^{(n-1)/a} \tag{4.1}$$

Where η is the viscosity of the fluid, η_0 and η_∞ are the zero and infinite shear viscosity, $\dot{\gamma}$ is the shear rate, λ ,n and a are the shape parameters. $1/\lambda$ is the critical shear rate at which the viscosity starts to decrease.

Considering η/η_0 as the desired viscosity, η_d and $\eta_0\cdot\dot{\gamma}$ as the desired shear rate, $\dot{\gamma}_d$, the combination of equation (4.1) and the concept of Rheogram would yield,

$$\eta_d=\eta_{\infty d}+(\eta_{0d}-\eta_{\infty d})\left[1+(\lambda_d.\dot{\gamma}_d)^a\right]^{(n-1)/a} \tag{4.2}$$

Keeping all the parameters of (4.1) same, the above equation has been reconstructed to be applicable for the master curve.

Figure 4.2 (a-d) shows the fit of C-Y model to the master curve for all the binders. It can be seen that the concept of Rheogram stands true for the binders considered, although little deviation for PMB (E) could be seen. This is indicative of the change in polymer structure within the bitumen-polymer system with change in temperature. Using such plot the critical shear rate for any binder at any temperature could be easily appraised, provided ZSV at that temperature is acquired.

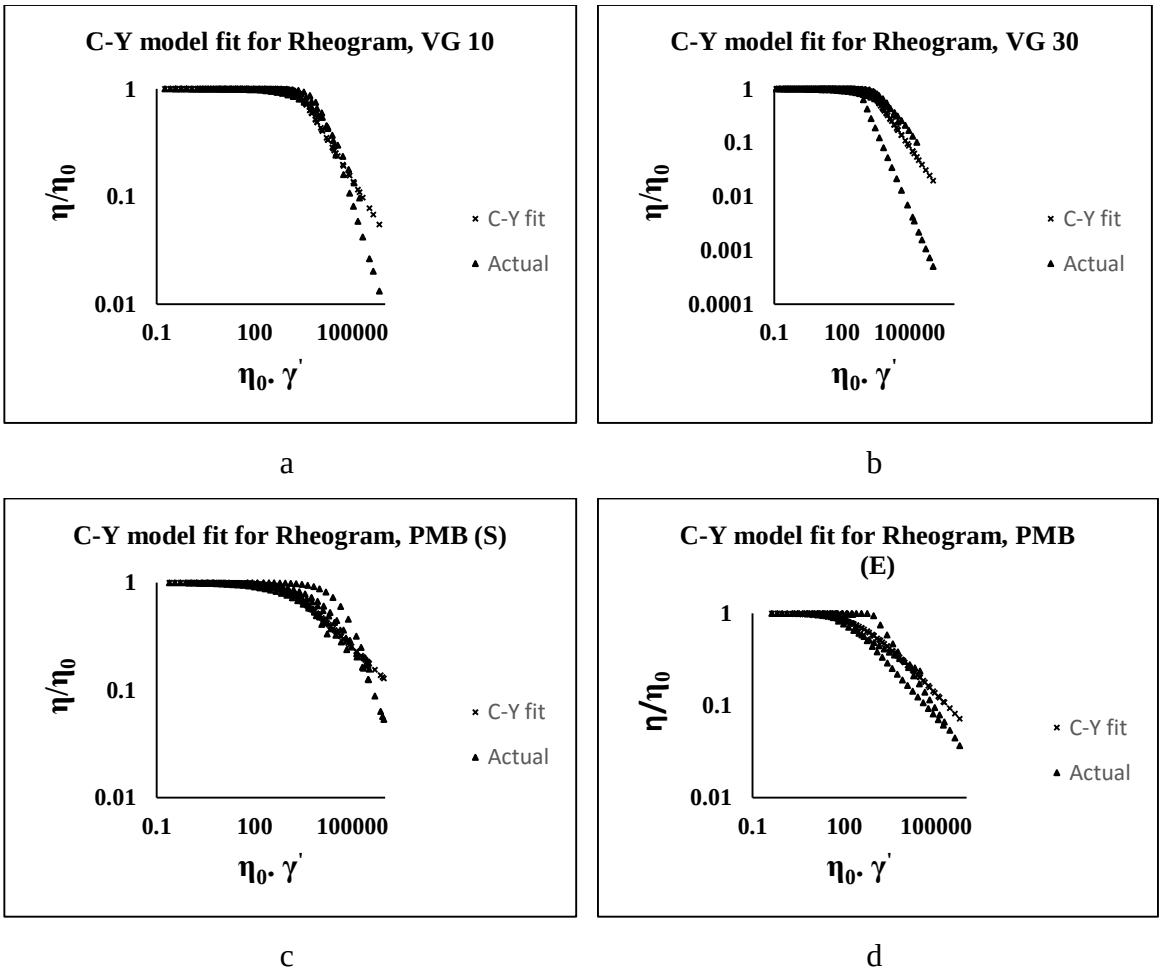

Figure 4.2(a-d) C-Y model fit with the master curves for different binders.

Table 4.1 shows the value of the C-Y parameters obtained for all the binders. The parameter of interest is the desired critical shear rate ($1/\lambda_d$). It can be seen that the critical shear rate decreases as we move from normal to modified binders. The practicality of this value could be appreciated for calculation of the minimum shear rate, which should be applied to the binder for onset of non-Newtonian flow. This is done by substituting the following in equation(4.2).

$$\eta_d \equiv \eta/\eta_0; \qquad \dot{\gamma}_d \equiv \eta_0 \cdot \dot{\gamma} \tag{4.3}$$

So the desired critical shear rate ($1/\lambda_d$) will be substituted by $\eta_0 . \dot{\gamma}_c$, where $\dot{\gamma}_c$ represents the critical shear rate.

Table 4.1 C-Y Model Parameters for Different Binders

Binder	Carreau-Yasuda Model Parameters					
	λ_d (s)	n	η_{0d} (Pa.s)	$\eta_{\infty d}$ (Pa.s)	a	$1/\lambda_d$ (s^{-1})
VG 10	0.0005	0.5	1	0	4	2000
VG 30	0.0006	0.4	1	0	3	1666.667
PMB (S)	0.001	0.7	1	0	1	1000
PMB €	0.003	0.65	1	0	0.7	333.3333

The most paramount use of such plot and the corresponding equation can be justified as follows. In equation (4.2) considering η_{0d} and $\eta_{\infty d}$ to be 1 and 0, the equation can be rewritten as

$$\eta_d = \left[1+\left(\lambda_d.\dot{\gamma}_d\right)^a\right]^{(n-1)/a} \tag{4.4}$$

$$\eta = \eta_0\left[1+(\lambda_d.\dot{\gamma}.\eta_0)^a\right]^{(n-1)/a} \tag{4.5}$$

Substituting λ_d, n and a in the above equations, which depends on the property of binder, viscosity parallel to any ZSV could be assessed. In other words it could be said that by knowing ZSV at any temperature, the viscosity of the binder can be easily forecasted. In turn these viscosities can then be used to determine the mixing temperatures corresponding to any chosen shear rate for different asphalt binders.

4.3.3 *Modeling zero shear viscosity (ZSV)*

Brookfield viscometer [3] was used to measure the viscosities at the two mentioned temperatures. Traditionally, the Brookfield viscometer for bitumen is used mainly for determination of mixing and compaction temperature of bituminous mixes. The test is carried out at 20 rpm (6.8 s^{-1}) using a spindle geometry such that the torque percentage remains in the range of 5-100%. A similar procedure was adopted in the study. The values of the viscosities obtained for all the binders are shown in Table 4.2 below, with the corresponding

mixing and compaction temperatures in Table 4.3. The mixing and compaction temperatures were obtained by plotting the viscosity values in the log-log scale whereas the temperature on the log scale and assuming a straight line relationship. India follows the equiviscous concept, in which the mixing and compaction temperatures are defined corresponding to the viscosities of 0.17 ± 0.02 and 0.28 ± 0.03 Pa.s. As can be seen in the Table 4.3, the mixing and compaction temperatures for modified bitumen are considerably higher as compared to the conventional binders.

The use of the viscosity values from the Brookfield viscometer for predicting the mixing and compaction temperatures has been long debated owing to the shear thinning behavior, typical for modified bitumen. The actual value of shear rate at the mixing plant is of higher order [183], which might have high influence on the viscosity values. Numerous study has been done to evaluate the ZSV of asphalt binders [103, 116, 128, 143, 169, 202]. Out of various models used, exponential model of Arrhenius type has shown good correlation for polymers. The viscosity versus shear rate at each temperature was modelled using Carreau-Yasuda equation and the value of ZSV was obtained. It was found that the variation of ZSV with temperature follows exponential law behavior for all the binders. The corresponding equation can be written in the following form

$$ZSV = A.e^{BT} \tag{4.6}$$

Where, *ZSV* stands for zero shear viscosity while *T* is the shear rate. *A* and *B* are model constants and are binder specific. Figure 4.3 (a-d) shows the model fit obtained for all the four binders. This model was also used to predict the viscosities at 135˚ C and 165˚C. A comparison of the viscosity values so obtained was made with the corresponding values obtained earlier. The exponential law gave excellent fit for all the binders. It was found that the predicted viscosities were in good agreement to the modeled viscosity as can be seen in figure below. This finding led to the conclusion that the viscosity values obtained using the Brookfield viscometer are corresponding to the shear rate which remains below the critical shear rate, and is a representation of the ZSV. 6.8 s^{-1} is a very low shear rate for representing the true viscosity at the time of mixing.

The ZSV calculated using equation (4.6) was used as an input to equation (4.5) to predict the viscosity at higher temperatures and different shear rates. This was finally used to judge the mixing temperature for different binders.

Table 4.2 Result of Brookfield viscometer test

Temperature	Brookfield Viscosity (Pa.s)			
	VG 10	VG 30	PMB (S)	PMB (E)
135	6.5E-01	7.7E-01	9.9E-01	1.7E+00
165	1.1E-01	1.5E-01	2.9E-01	5.7E-01

Table 4.3 Mixing and compaction temperatures for different binders

Binder	Mixing Temperature, °C	Compaction Temperature, °C
VG 10	154	145
VG 30	160	150
PMB (S)	170	160
PMB (E)	190	178

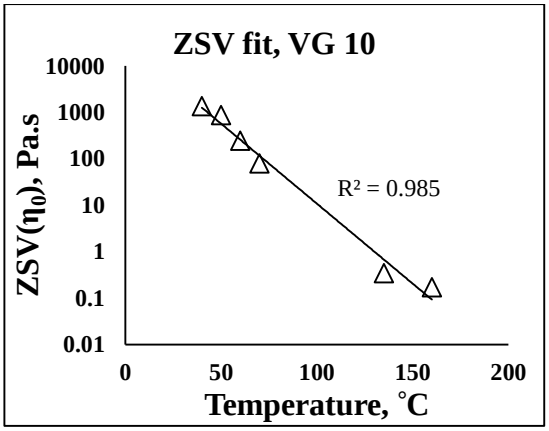

a

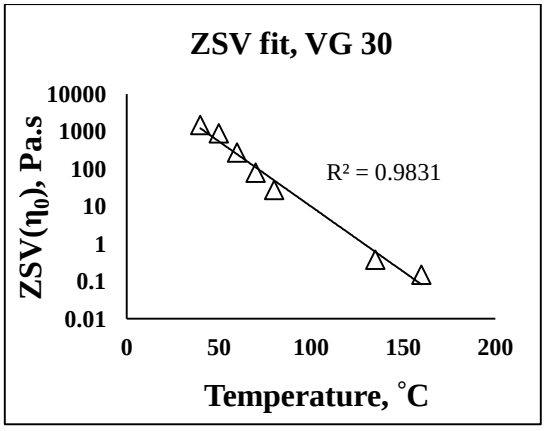

b

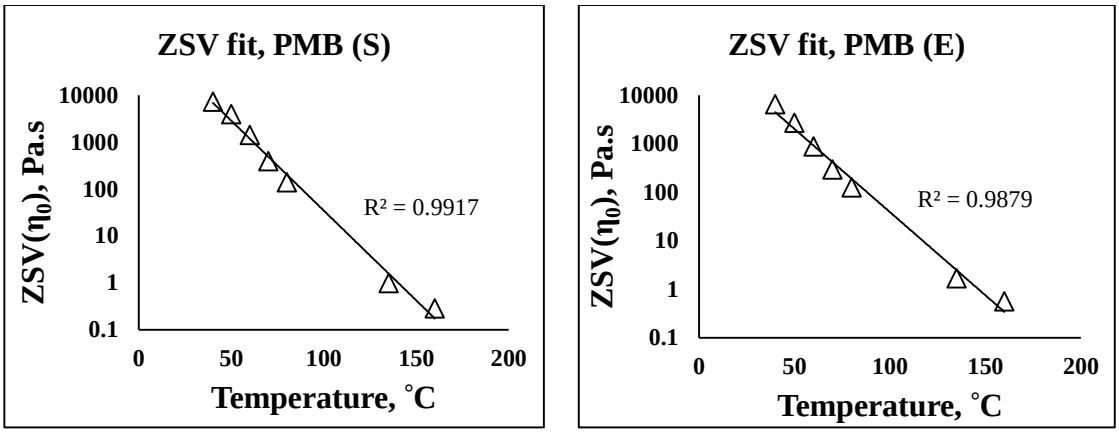

c d

Figure 4.3 (a-d) Exponential fit for Zero Shear Viscosity (ZSV).

4.3.4 *Comparison with the traditional method*

In order to present an explicit description of the effect of shear rate on mixing temperature, calculations were done using the concept of Rheogram and exponential model, as described earlier, to evaluate the viscosities at three different temperatures (100, 130 and 160^0C) and three different shear rates (1000, 10000 and 100000s^{-1}). These shear rates are good approximation of those used from laboratory to mixing plant. Further, plots were made to predict the mixing temperature corresponding to viscosity of 0.17 Pa.s. Figure 4.4 (a-c) and Table 4.4 presents the mixing temperature corresponding to different shear rates. It can be seen that modified binders are more sensitive to shear rate than the conventional binders. This indicates higher degree of non-Newtonian behavior in polymer modified bitumen. Among the modified binders, PMB (S) shows lesser sensitivity as compared to PMB (E). This can be attributed to the formation of tough three dimensional network in PMB (E) which makes it stiffer as compared to SBS PMB, increasing its shear thinning behavior.

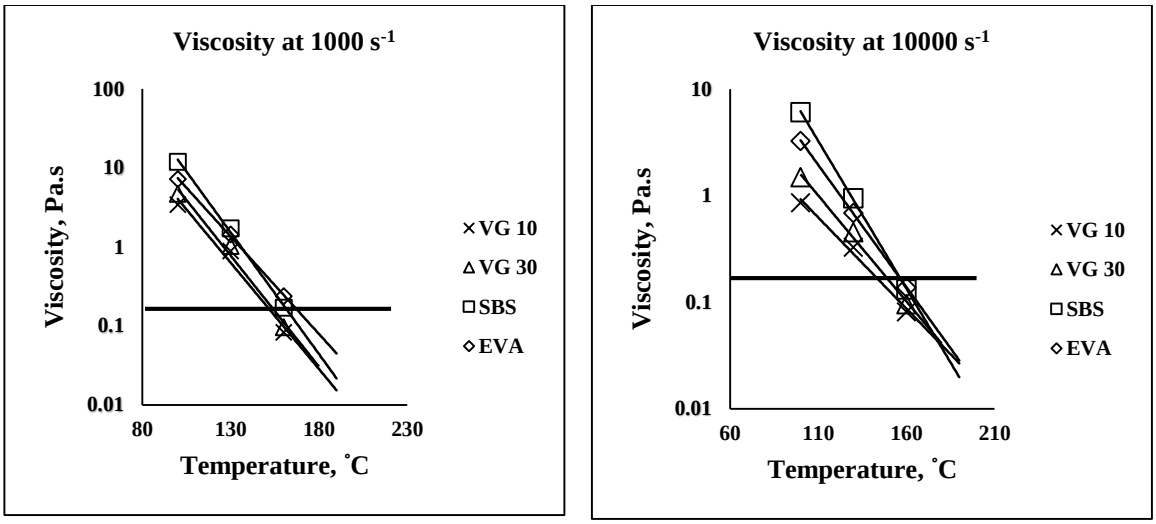

a b

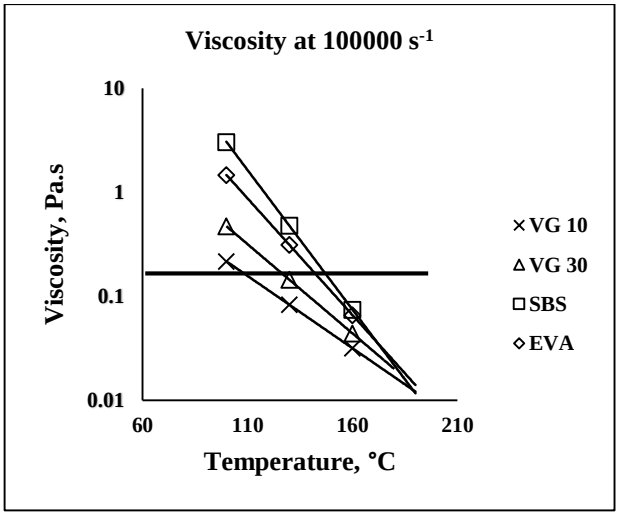

c

Figure 4.4 (a-c) Mixing temperatures corresponding to 0.17 Pa.s for different bitumen at different shear rates

Table 4.4 Mixing and compaction temperatures at different shear rates and temperatures

Shear rate,s^{-1}	Mixing temperatures for different binders, °C			
	VG 10	**VG 30**	**PMB (S)**	**PMB (E)**
1000	152	154	160	165
10000	144	149	156	156
100000	108	126	148	144

The mixing temperatures for modified binder were found to be higher than normal binders considering all binders to a certain degree behaves as a non-Newtonian fluid. The Brookfield viscometer predicts very high mixing temperatures, as the effect of practical shear rate is compounded. Increase in shear rate yielded much lower mixing temperatures, even for modified binders. This would in turn lead to higher energy savings and also would reduce the potential degradation of binders subjected to such high temperatures. The fact has to be appreciated that, laboratory mixing temperatures may be higher than those for field application. Compaction temperatures on the other hand will be higher for modified binders due to diminishing role of shear rate. Obviously, a field and laboratory check of the work is required in order to gain more confidence on such evaluations.

4.4 Conclusions

Four binders including two normal and two polymer modified were used in the study. The steady shear flow behavior for these binders were measured using DSR and Brookfield viscometer for a wide range of temperature and shear rate. The applicability of the use of Rheogram was studied. C-Y and exponential model were used to predict different flow properties for the binders. Using these techniques it was attempted to calculate the mixing temperatures of bitumen for different shear rates.

Based on the experimental results and analysis, the following conclusions can be drawn

- Polymer modified binders are more shear thinning as compared to normal binders as shown by the viscosity-shear rate plot at different temperatures. At higher temperatures, normal binders also show tendency of shear thinning, but at very high shear rates. The critical shear rate for modified binders are lower than the normal binders for all range of temperatures. This behavior could be attributed to the lowering of effective maltene fraction which are used for swelling of polymers.
- The concept of Rheogram for plotting master curve of viscosity versus shear rate is applicable to all the binders, with little deviation observed for PMB (E). C-Y model fits well with the master curve of all the binders.
- Steady shear viscosity measurement using DSR and Brookfield viscometer are found to be in good agreement with each other. Variation in ZSV with temperature can be described well with the exponential law model.

- Mixing temperature for modified binder are found to be lower for practical shear rates varying from laboratory to field. The mixing temperature requirements decreases with increase in shear rate.

Chapter 5

Rheological Characterization of Asphalt Binders

5.1 Introduction

Bitumen is the only component in the pavement showing thermo-mechanical behavior. It is characterized typically as a viscoelastic material whose properties are dependent on both time (rate of loading) and temperature. At high temperature bitumen behaves as a Newtonian fluid while at lower temperatures it displays characteristics of an elastic solid. In between these two extreme behaviors it exhibits viscoelastic response [9, 58, 108, 145].

Bitumen is a complex hydrocarbon which is traditionally regarded as a colloidal system consisting of high molecular weight asphaltenes dispersed in a lower molecular weight maltenes. The C-H bond are mainly arranged in branched, cyclic or aromatic fashion and the variation of these molecules and structural arrangement imparts intrinsic mechanical properties to the respective binder [128, 197]. The viscoelastic characteristic of bitumen can be determined either by transient or oscillatory type of testing. Oscillatory testing, using Dynamic Shear Rheometer (DSR) is currently recommended, as it is less time consuming and can be successfully used to determine the elastic, viscous and viscoelastic properties of bitumen [195].

While analyzing the material response of asphalt binders using dynamic testing, two behavioral domain appears: linear and non-linear. Nonlinearity implies the dependence of the viscoelastic properties (such as complex modulus and creep compliance.) of the asphalt binder to the magnitude of stress/strain in addition to temperature and time (frequency) of loading. Evaluation of this boundary limit is important for complete rheological characterization of any viscoelastic material [10].

This chapter focusses on assessing the linear viscoelastic (LVE) limits of different asphalt binders at varying frequencies (time of loading) and temperatures. Further the linear rheological characteristics of these binders are evaluated and discussed.

5.2 Materials Used

The previous chapter focused on obtaining the modified binders for the study, following which four asphalt binders were used. The study used two viscosity graded (VG) binders; VG 10, VG 30, and two polymer modified binders designated as PMB (S) and PMB (E). 'S' and 'E' exemplifies styrene–butadiene-styrene (SBS) and ethylene vinyl acetate (EVA). These two are the most common elastomer and plastomer used for polymeric modification of bitumen. Viscosity grade is defined based on the viscosity of the bitumen at 60 °C. This is different from the performance grade (PG) specification where the requirement of physical property remain same for all the grades, but the temperature at which these properties must be achieved varies depending on the climate in which the binder is to be used. VG 10 was the base binder used for the purpose of modification. The conventional binder properties for all the binders can be seen in Table 5.1. The high temperature PG grade and the true intermediate grade temperature are also listed.

Table 5.1 Properties and processing variables of binders used in the study.

Properties/Processing Variables	VG 10	VG 30	PMB (S)	PMB (E)
Penetration, dmm	75	62	56	49
Softening Point, °C	47	49	60	65
Penetration Index	-1.01	-0.95	1.31	1.92
Viscosity @ 60 °C, Pa.s	258	375	2120	6120
Storage Stability, ΔSoft. Point, °C	-	-	1.5	1.3
High Temperature PG Grade	PG 58-XX	PG 64-XX	PG 70-XX	PG 76-XX
True Grade, Intermediate Temperature, °C	25.3	20.1	15.7	12.2
Mixing Temperature , °C	-	-	180	190
Blending Time, minutes	-	-	60	30
Shear Rate, rpm	-	-	1500	600

5.3 Experimental Investigation

5.3.1 *Instrumentation*

Dynamic mechanical analysis was performed using a (DSR) having parallel plate geometry in oscillatory shear mode. Operation of the rheometer and temperature control unit, along with the data acquisition and analysis were controlled using a computer. Figure 5.1 (a,b) presents schematic picture of the DSR used in the study.

a b

Figure 5.1 (a, b) Schematic representation of DSR

5.3.2 *Sample handling and preparation*

The asphalt binders were stored in containers of 5 Kg. The bitumen were heated until they became sufficiently fluid to pour. Silicone mould method which is based on method B of specification for highway works, Method B of the IP standard, Method 2 of SHRP DSR protocol and alternative 2 of AASHTO standard (AASHTO 1994) was used for preparation of the DSR samples. Hot bitumen was poured into the silicone mould having diameter 8 mm/ 25 mm to a height of approximately 1.5 times the recommended gap requirement for the respective geometries (3 mm and 1.5 mm for 8 and 1 mm gap). The bitumen was cooled using short refrigeration and was placed between the spindle and the base plate. The upper plate is lowered to the required gap plus 50 μm. The extra bitumen is trimmed off once the desired gap is obtained. For lower temperatures the trimming was done at a temperature of 60 ℃ after which the temperature was reduced to the desired value.

5.3.3 *Testing procedure*

This chapter comprises two types of dynamic shear testing:

a) Strain sweep test, and
b) Frequency sweep test

Strain sweep test was carried out to evaluate the linear viscoelastic limits for the asphalt binders. After the determination of LVE range, frequency sweep test was done to evaluate the various rheological aspects of the asphalt binders at different temperature and frequencies. The effect of spindle geometry on the rheological measurements was also

assessed using the frequency sweep test. Frequency sweep test was done at a strain level below the LVE range of the binders, as determined in the first stage.

5.3.3.1 Strain sweep test

The strain sweep test was carried out to establish the LVE limits of asphalt binders. The test was done at temperatures varying 10-70°C with 10 degree increment. Four different frequencies of 0.2, 2, 5, 10 Hz was adopted to assess the effect of loading rate on LVE limits. The strain was varied for 0-100% to ensure that the sweep was well into the non-linear region. As each run of strain sweep test will tend to deform the sample, all the test were done on fresh samples for each loading combination. 8 mm diameter with 2 mm plate gap was used for temperatures between 10-30 °C, while 25 mm diameter with 1 mm plate gap was used for temperatures between 40-70 °C. The LVE limit was defined in accordance with the SHRP study as the strain level at which the complex modulus of the bitumen is 95 percent of its initial linear viscoelastic modulus. Below is presented a schematic representation of a typical curve obtained in strain sweep test (Figure 5.2). The modulus remains constant till a particular strain level and further reduces with increase in amplitude. The initial constant modulus G_0 is the linear viscoelastic modulus. γ_1 is the strain at which the modulus starts decreasing and can be considered as the point for the onset of non-linear behavior. γ_2 on the other hand is the strain corresponding to the 95 percent of the initial modulus. As per specification this strain level is considered as the linear viscoelastic region for the asphalt binder.

5.3.3.2 Frequency sweep test

After finding the LVE limits of all the binders, frequency sweep test were performed at the following test conditions:

- Mode of loading: Controlled strain,

- Temperatures: 10, 20, 30, 40, 50, 60 and 70 °C

- Frequencies: from 0.1-100 rad/second

All the tests were done at strain below the LVE limits determined earlier. The initial testing's were done by varying the spindle geometry and gap width to determine its effect on the rheological measurements. The following geometries were adopted for the study:

- 25 mm diameter with 1 mm gap
- 25 mm diameter with 2 mm gap
- 25 mm diameter with 3 mm gap
- 8 mm diameter with 1 mm gap
- 8 mm diameter with 2 mm gap

The most appropriate geometry for rheological measurements was also evaluated. Following this study frequency sweep test was used for determination and comparison of various rheological properties of unmodified and modified asphalt binders. Further, master curves were developed at different temperatures and the shift factors used for the construction of master curve were analyzed. Master curves allows the rheological data to be presented over a wide range of frequency and temperature in one plot [6].

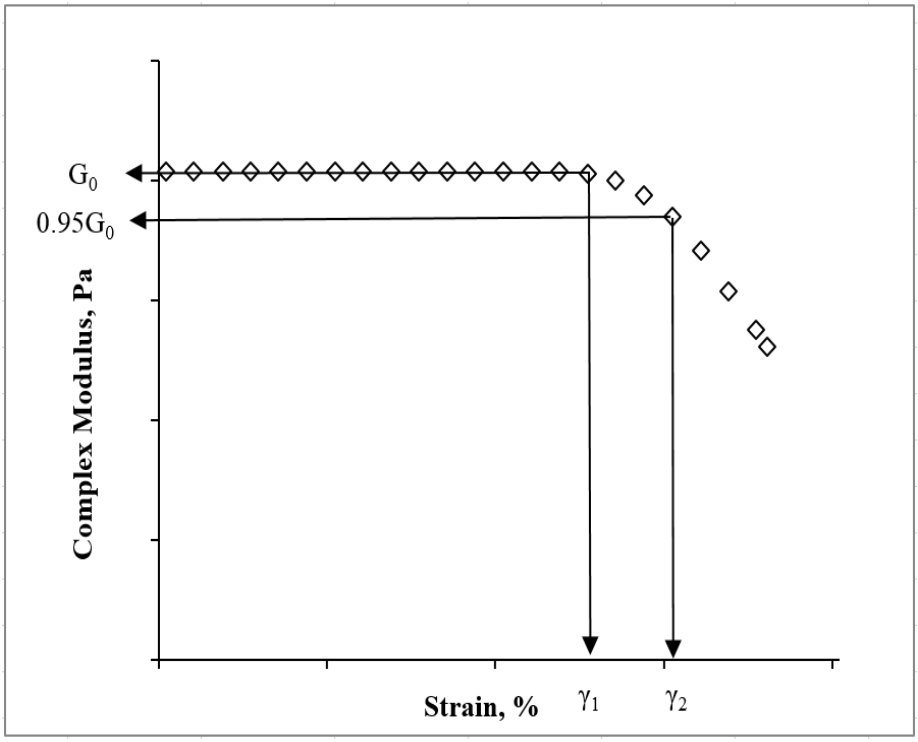

Figure 5.2 Schematic representation of amplitude sweep test

5.4 Linear Viscoelastic (LVE) Limits

Table 4.2-4.5 present the LVE strain limit in percentage for different asphalt binders at varying temperature and frequency. The variation can also be seen from Figure 4.3 (a-d). In general, the LVE strain increases with increase in temperature and reduction in frequency. At high temperature and low frequency the bitumen is less stiff and hence higher strain levels are required to push the binder in the non-linear region. At higher frequency and for low temperatures the LVE strain limits are low, owing to the higher stiffness of bitumen. The LVE limits of strain for modified bitumen were found to be lower than for conventional bitumen. The lowest LVE strain were found for PMB (E) due to its higher stiffness compared to other binders. The variation of LVE strain with frequency was not as much significant as with temperature. It was also found that PMB (S) gave more stable values with variation in both frequency and temperature. This strain susceptibility was found highest for PMB (E).

Strategic Highway Research Program (SHRP)'s Superpave binder grading criteria empirically suggests 10-12 % strain for test carried out using 25 mm diameter spindle, whereas 1-2 % strain for test done using 8 mm diameter spindle geometry as the LVE region for asphalt binders [17]. These values were based on tests carried out on a large number of unmodified bitumen. The following equations are suggested to find the linear viscoelastic domain of asphalt binders.

$$\gamma = \frac{12}{\left|G^*\right|^{0.29}} \tag{5.1}$$

$$\tau = \frac{0.12}{\left|G^*\right|^{0.71}} \tag{5.2}$$

Where, $\left|G^*\right|$ is the magnitude of the complex modulus; γ and τ are the linearity limits for strain and stress. The above equations suggests that the linearity limits are a function of stiffness of the binder at a particular temperature and frequency.

The LVE strain obtained from the tests were compared with those simulated using equation (5.1). Figure 5.4 presents an example for comparison. It was found that the LVE

limits as obtained from the measurements were higher than the values obtained using equation (5.1).

Table 5.2 LVE limit strain (%) for VG 10

Temperature	Frequency (Hz)			
	0.2	**2**	**5**	**10**
10	2.10E+00	1.10E+00	5.00E-01	3.00E-01
20	5.70E+00	2.30E+00	7.00E-01	6.00E-01
30	1.45E+01	1.00E+01	5.40E+00	2.10E+00
40	1.87E+01	1.48E+01	8.50E+00	4.90E+00
50	3.15E+01	2.16E+01	1.32E+01	5.30E+00
60	5.77E+01	4.65E+01	3.17E+01	1.48E+01
70	7.98E+01	6.85E+01	4.13E+01	3.67E+01

Table 5.3 LVE limit strain (%) for VG 30

Temperature	Frequency (Hz)			
	0.2	**2**	**5**	**10**
10	1.20E+00	9.00E-01	4.00E-01	3.00E-01
20	5.50E+00	1.10E+00	6.10E-01	5.20E-01
30	1.01E+01	4.65E+00	2.30E+00	1.60E+00
40	2.17E+01	1.01E+01	6.73E+00	3.80E+00
50	3.11E+01	1.47E+01	7.80E+00	4.70E+00
60	4.65E+01	2.17E+01	1.46E+01	5.20E+00
70	6.75E+01	3.17E+01	2.05E+01	1.13E+01

Table 5.4 LVE limit strain (%) for PMB (S)

Temperature	Frequency (Hz)			
	0.2	**2**	**5**	**10**
10	4.20E+00	3.80E+00	2.50E+00	1.70E+00
20	6.40E+00	5.75E+00	4.65E+00	2.80E+00
30	8.20E+00	6.73E+00	6.10E+00	5.60E+00
40	1.75E+01	1.48E+01	1.04E+01	6.20E+00
50	3.15E+01	2.17E+01	1.57E+01	1.31E+01
60	3.57E+01	2.17E+01	2.15E+01	1.46E+01
70	3.87E+01	3.17E+01	2.74E+01	2.17E+01

Table 5.5 LVE limit strain (%) for PMB (E)

Temperature	Frequency (Hz)			
	0.2	2	5	10
10	9.00E-01	5.00E-01	1.00E-01	
20	2.30E+00	1.10E+00	4.60E-01	1.00E-01
30	7.20E+00	3.18E+00	1.40E+00	8.00E-01
40	1.47E+01	6.86E+00	2.60E+00	1.10E+00
50	2.17E+01	1.48E+01	4.80E+00	2.40E+00
60	4.15E+01	3.16E+01	8.20E+00	3.70E+00
70	5.81E+01	3.16E+01	1.48E+01	5.70E+00

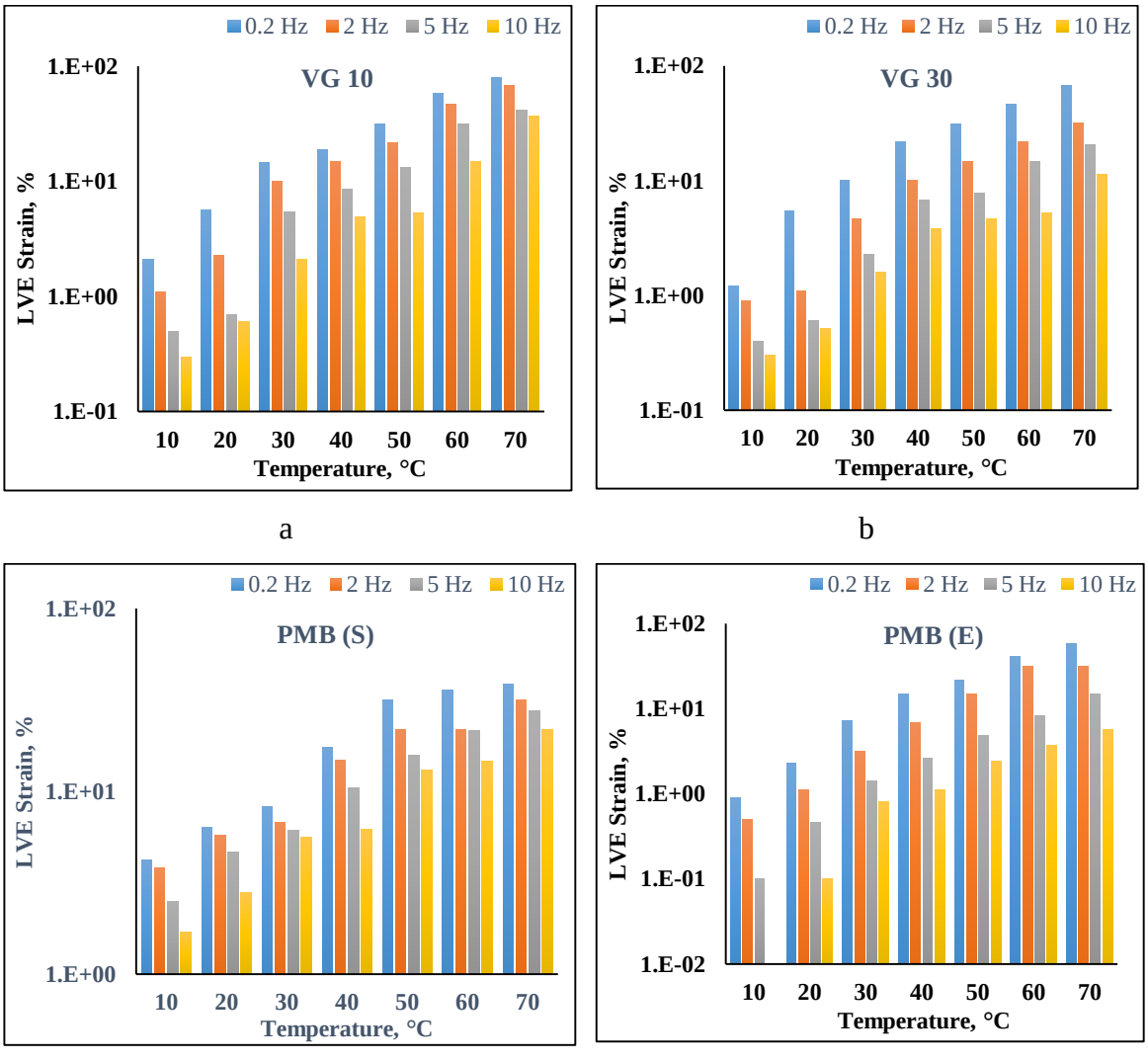

Figure 5.3 (a-d) LVE strain (%) limit for different asphalt binders

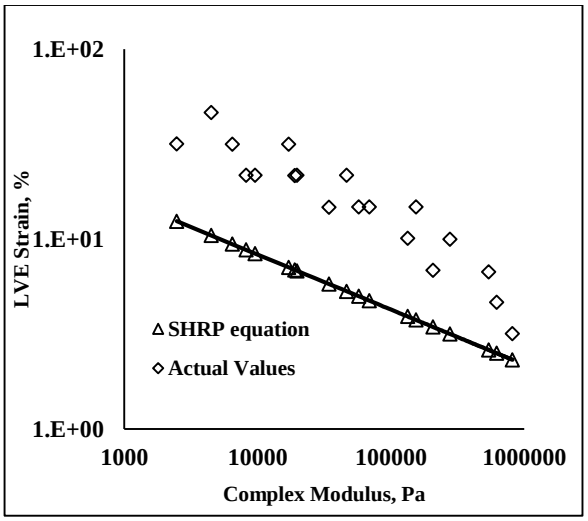

Figure 5.4 LVE strain comparison with SHRP equation

5.5 Evaluation of Frequency Sweep Test

5.5.1 *Effect of spindle geometry and gap height*

The DSR records only two measurements, i.e. torque and angular rotation, all other results are calculated using these two parameters. The following equations are used to calculate the stress and strain during the DSR measurement.

$$\tau = \frac{2T}{\pi . r^3} \tag{5.3}$$

$$\gamma = \frac{\theta . r}{h} \tag{5.4}$$

$$\tau = G . \gamma \tag{5.5}$$

Where, τ = stress; T = torque; r = spindle radius; γ = strain; θ = rotational angle of spindle; h = bitumen thickness and G = shear modulus.

In general two testing (plate) geometries are commonly used with the DSR, namely an 8 mm diameter spindle with a 2 mm testing gap and a 25 mm diameter spindle with 1 mm testing gap. The selection of the testing geometry is based on the operational conditions with the 8 mm plate geometry generally being used at low temperatures (-5°C to 20°C) and the

25 mm geometry at intermediate to high temperatures (20°C to 80°C). However, it is possible to use the 8 mm geometry between -5°C and 60°C, although the precision of the results may be limited at high temperatures as a result of a reduction in precision with which the torque can be measured. DSR testing can be conducted for a wide range of temperature and frequency. Different plate diameters are used for different testing conditions depending on the stiffness of the binder. Disk diameters suggested by SHRP [66] are in Table 5.5.

Table 5.6 Specification of spindle geometry.

Disk Diameter	Testing Temperature Range	Typical G* range
8 mm	0˚ to +40˚	10^5 to 10^7 Pa
25 mm	+40˚ to +80˚	10^3 to 10^5 Pa
40 mm	>80˚	<10^3 Pa

A research was also carried out by Airey [8] to see the effect of spindle geometry on the rheological measurement. Nevertheless, in his study the spindle gap was limited to 1 mm and 2 mm and the overlapping temperatures were less.

5.5.1.1 Effect of spindle diameter

To assess the effect of spindle diameter graphical plots for complex modulus and phase angle at each temperature was drawn, corresponding to 8 mm and 25 mm keeping the gap width to be 1 mm. Figure 5.5 (a-g) to Figure 5.12 (a-g) present the phase and complex modulus plot for all the binders from 10- 70 °C. As seen in the phase angle plots for all the binders, 8 mm diameter spindle gave erroneous results, mostly at lower frequencies. This may attribute to the lesser contact area of the spindle with the bitumen, which at higher temperatures, owing to the low viscosity of the binders tends to delaminate from the spindle. Also edge effects are much more pronounced with the use of 8 mm spindle. This discrepancy in the phase angle curves were more pronounced for conventional binders. This change should not be confused with the thermorheological complexity of the binders which also forms ‘wavy’ nature of curves. Hence, deviations in rheological results may also result from choice of spindle geometry rather than the type and properties of binders.

It can be seen that at intermediate temperatures (typically from 30- 50 °C) similar values of phase angles were measured, irrespective of the spindle diameter. At lower

temperatures, however, 25 mm spindle generated lower values of phase angles as compared to 8 mm diameter. This findings were consistent for all the binders used in the study.

The discrepancy in the measurements at higher temperatures as found in the phase angle curves were not found in the complex modulus curves. The complex modulus curves were rather smooth. At higher temperatures spindle diameter 8 mm gave higher values. This difference reduced with reduction in temperature with the curves coinciding at intermediate temperatures. With further reduction (at lower temperatures) the curve reversed its direction with 8 mm diameter tending to give lower values than 25 mm spindle diameter. Similar to phase angles these results were consistent for all the binders.

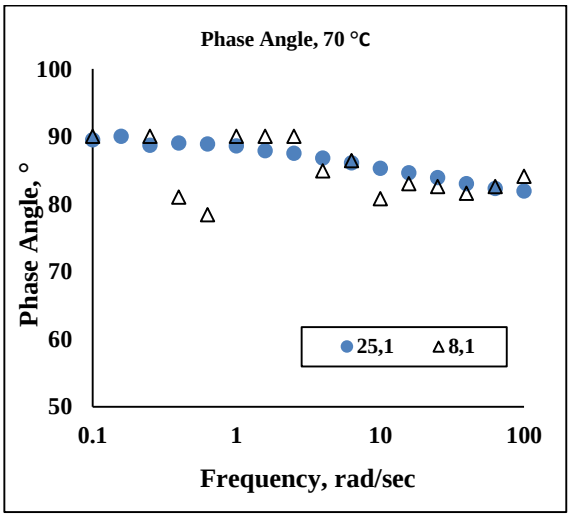

a

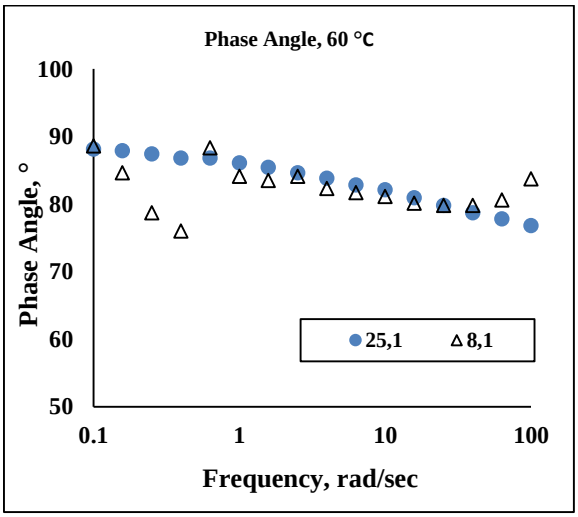

b

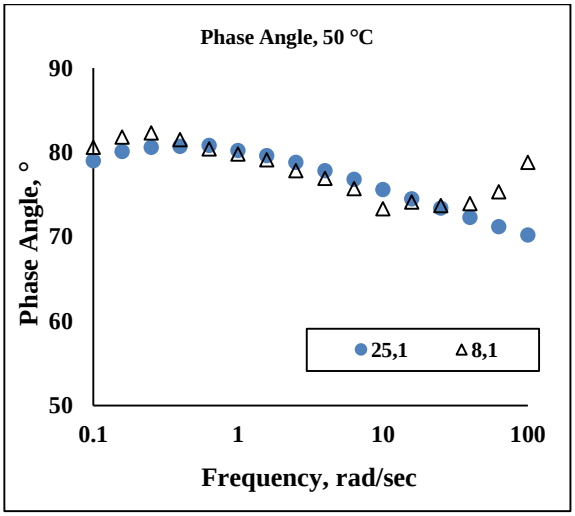

c

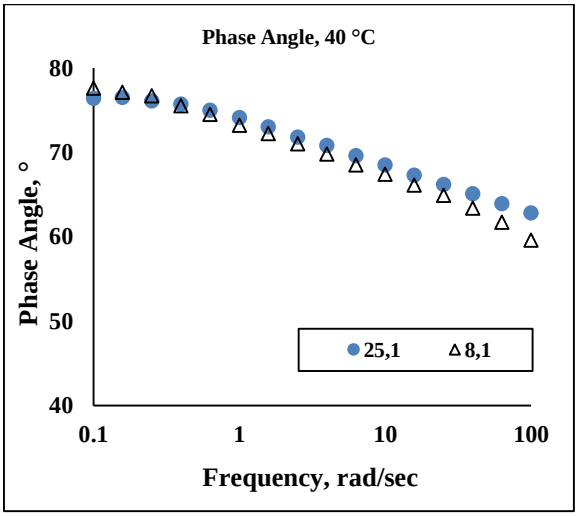

d

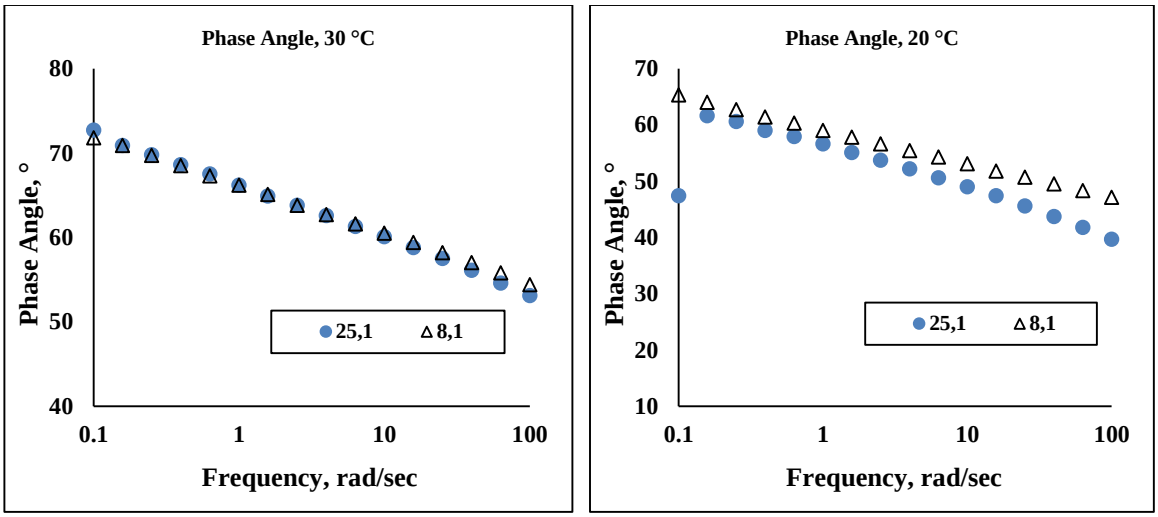

e

f

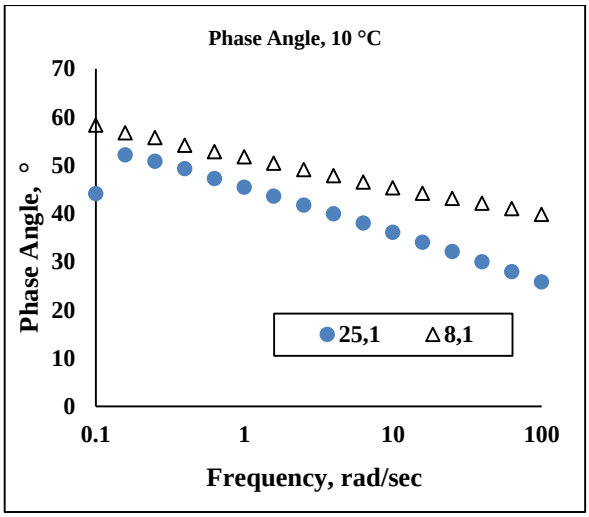

g

Figure 5.5 (a-g) Phase angle curves for VG 10 for 25 mm and 8 mm plate diameter corresponding to 1 mm plate gap.

(Note: 25, 1 represents spindle diameter of 25 mm with 1 mm plate gap; 8, 1 represents spindle diameter of 8 mm with 1 mm plate gap.)

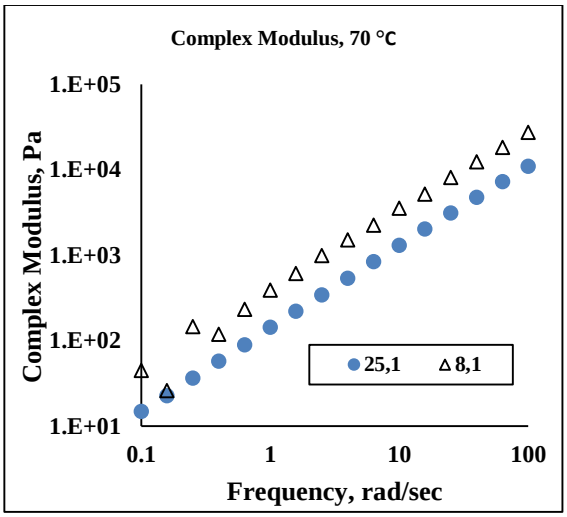
Complex Modulus, 70 °C
Complex Modulus, Pa
1.E+05
1.E+04
1.E+03
1.E+02
1.E+01
0.1
1
10
100
Frequency, rad/sec
25,1
8,1

a

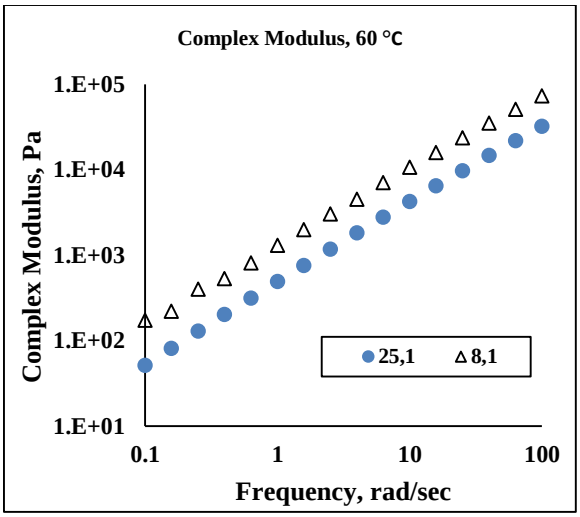
Complex Modulus, 60 °C
Complex Modulus, Pa
1.E+05
1.E+04
1.E+03
1.E+02
1.E+01
0.1
1
10
100
Frequency, rad/sec
25,1
8,1

b

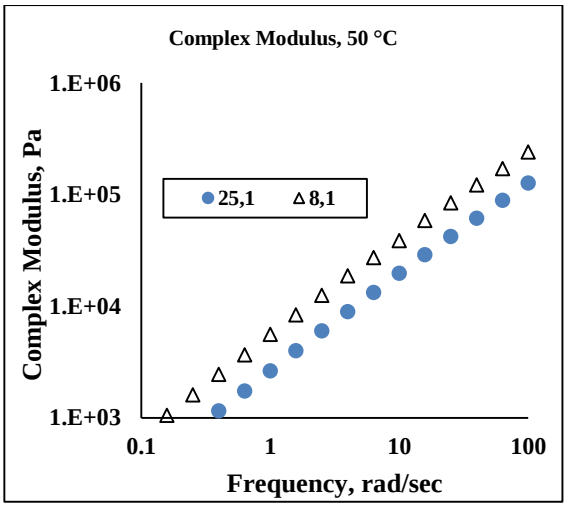
Complex Modulus, 50 °C
Complex Modulus, Pa
1.E+06
1.E+05
1.E+04
1.E+03
0.1
1
10
100
Frequency, rad/sec
25,1
8,1

c

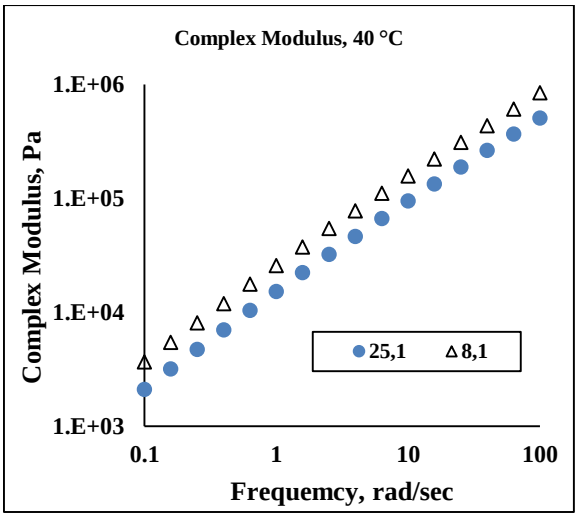
Complex Modulus, 40 °C
Complex Modulus, Pa
1.E+06
1.E+05
1.E+04
1.E+03
0.1
1
10
100
Frequemcy, rad/sec
25,1
8,1

d

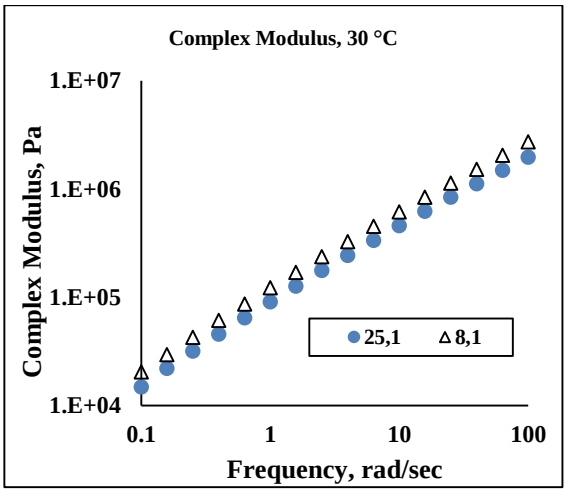
Complex Modulus, 30 °C
Complex Modulus, Pa
1.E+07
1.E+06
1.E+05
1.E+04
0.1
1
10
100
Frequency, rad/sec
25,1
8,1

e

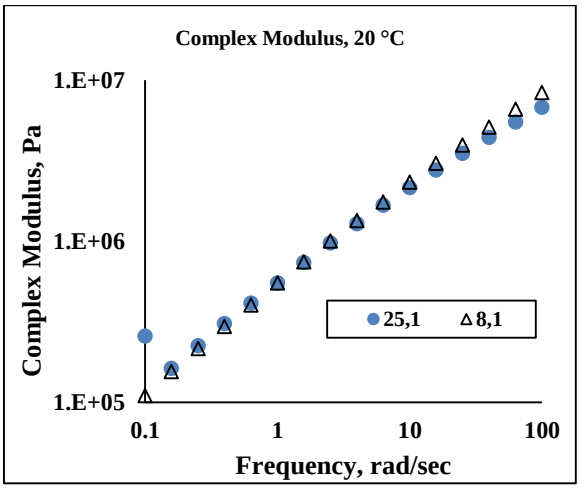
Complex Modulus, 20 °C
Complex Modulus, Pa
1.E+07
1.E+06
1.E+05
0.1
1
10
100
Frequency, rad/sec
25,1
8,1

f

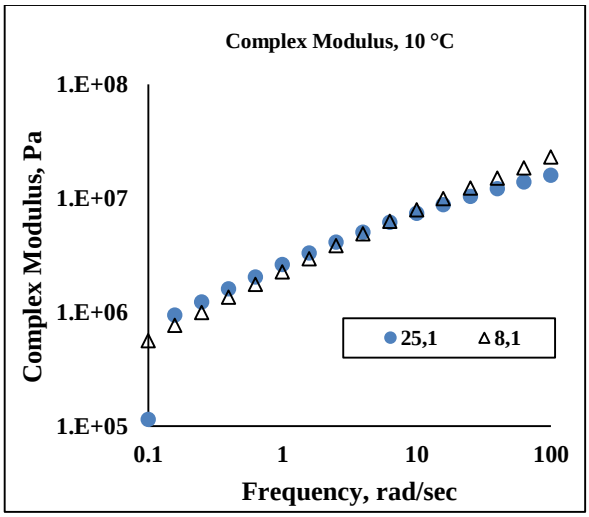

g

Figure 5.6 (a-g) Complex modulus curves for VG 10 for 25 mm and 8 mm plate diameter corresponding to 1 mm plate gap.

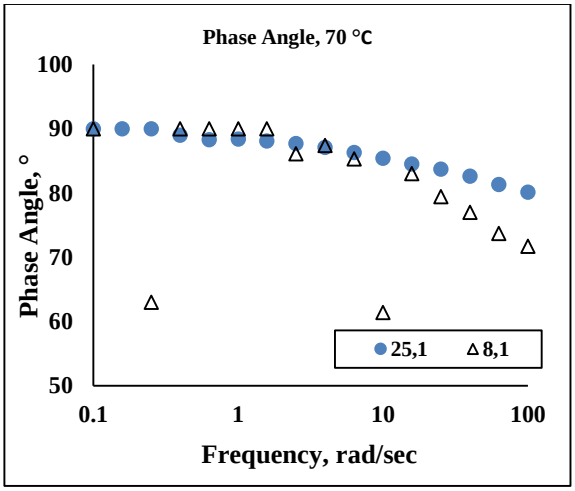

a

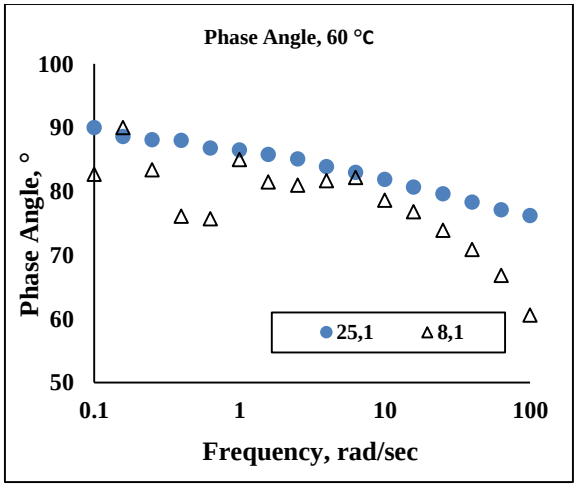

b

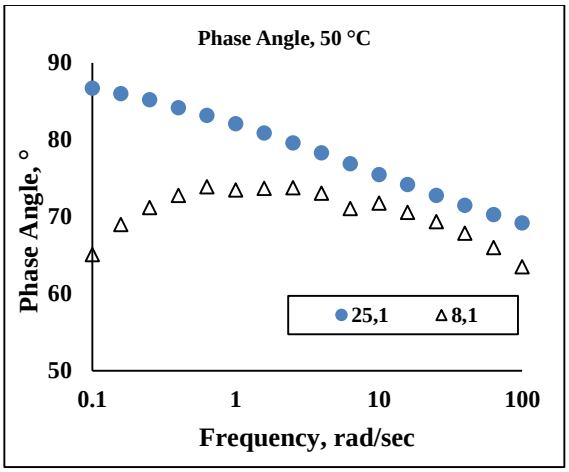

c

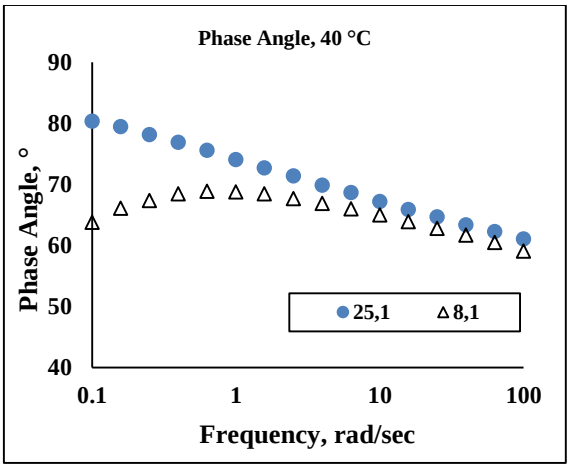

d

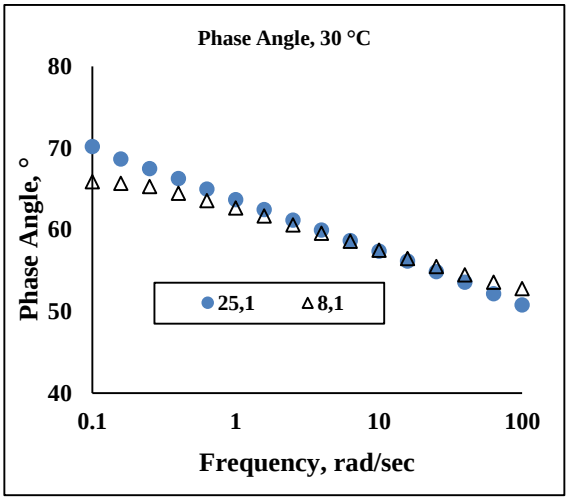

e

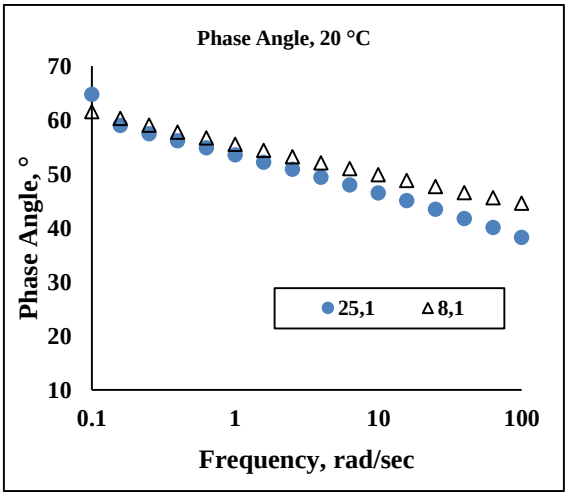

f

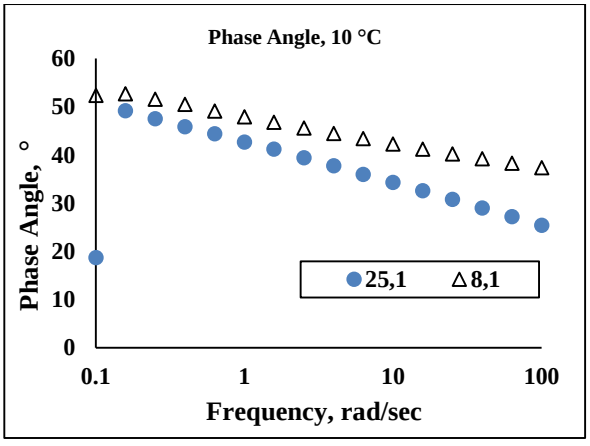

g

Figure 5.7 (a-g) Phase angle curves for VG 30 for 25 mm and 8 mm plate diameter corresponding to 1 mm plate gap.

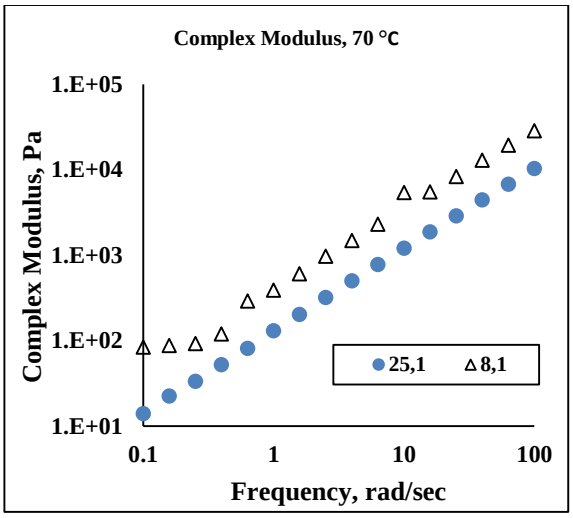
Complex Modulus, 70 °C
Complex Modulus, Pa
1.E+05
1.E+04
1.E+03
1.E+02
1.E+01
0.1
1
10
100
Frequency, rad/sec
25,1
8,1

a

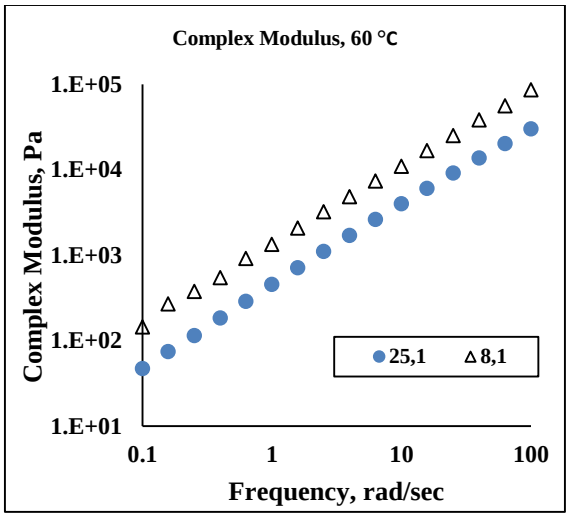
Complex Modulus, 60 °C
Complex Modulus, Pa
1.E+05
1.E+04
1.E+03
1.E+02
1.E+01
0.1
1
10
100
Frequency, rad/sec
25,1
8,1

b

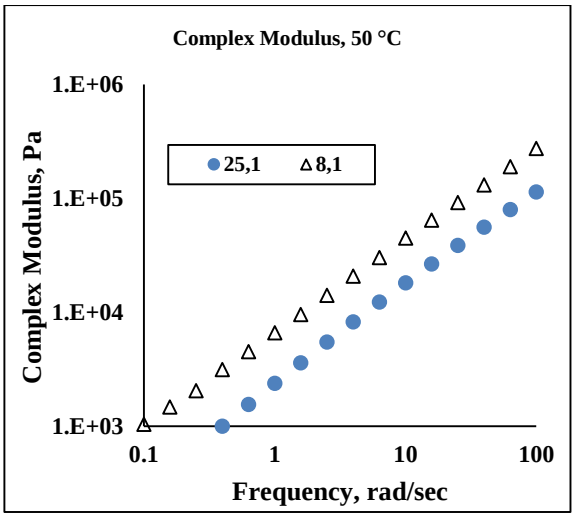
Complex Modulus, 50 °C
Complex Modulus, Pa
1.E+06
1.E+05
1.E+04
1.E+03
0.1
1
10
100
Frequency, rad/sec
25,1
8,1

c

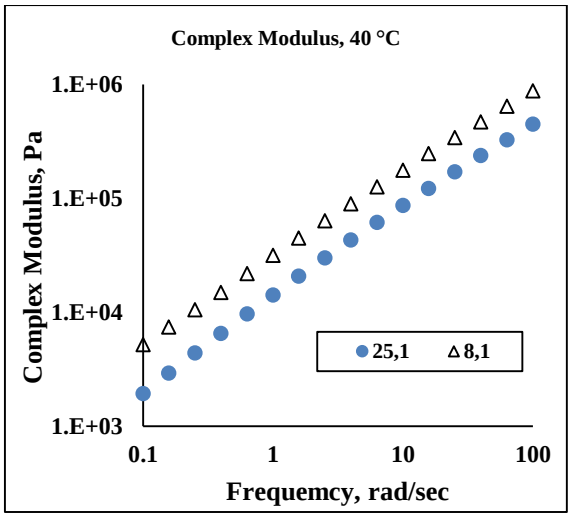
Complex Modulus, 40 °C
Complex Modulus, Pa
1.E+06
1.E+05
1.E+04
1.E+03
0.1
1
10
100
Frequemcy, rad/sec
25,1
8,1

d

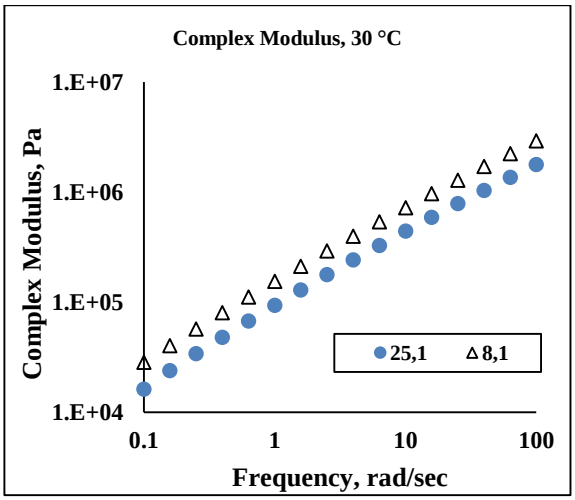
Complex Modulus, 30 °C
Complex Modulus, Pa
1.E+07
1.E+06
1.E+05
1.E+04
0.1
1
10
100
Frequency, rad/sec
25,1
8,1

e

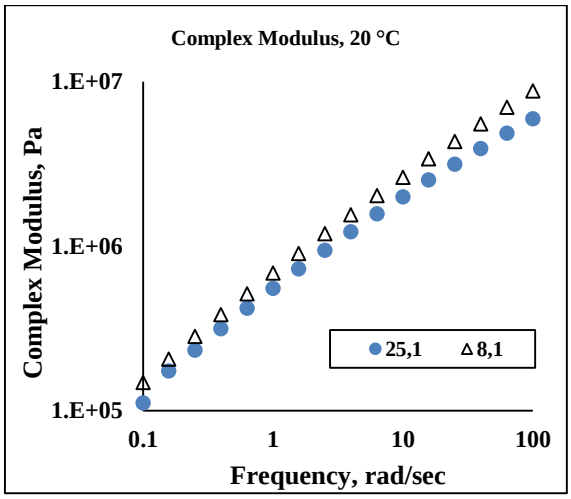
Complex Modulus, 20 °C
Complex Modulus, Pa
1.E+07
1.E+06
1.E+05
0.1
1
10
100
Frequency, rad/sec
25,1
8,1

f

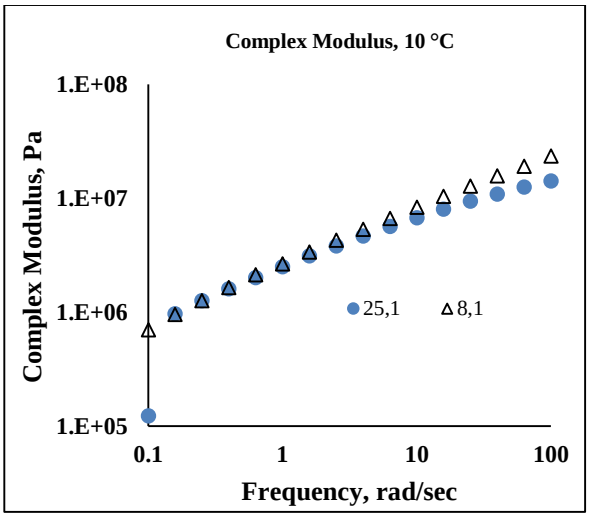

g

Figure 5.8 (a-g) Complex modulus curves for VG 30 for 25 mm and 8 mm plate diameter corresponding to 1 mm plate gap.

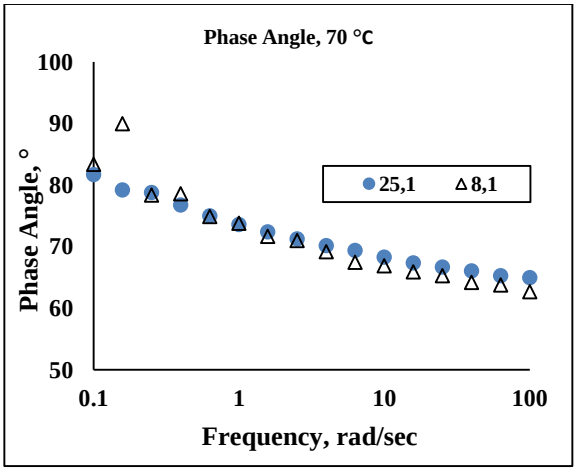

a

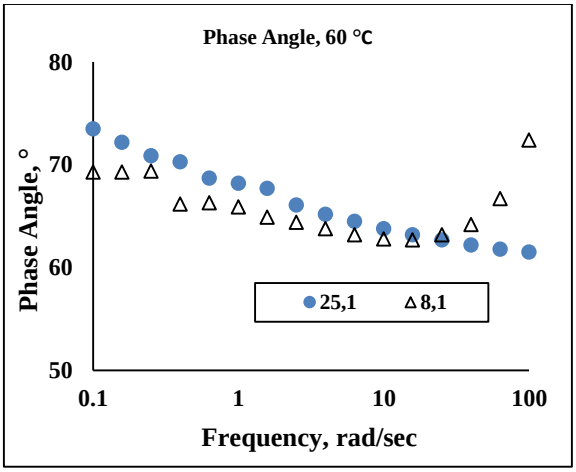

b

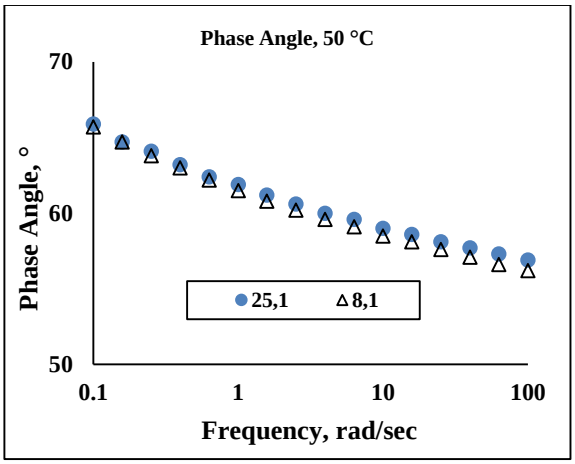

c

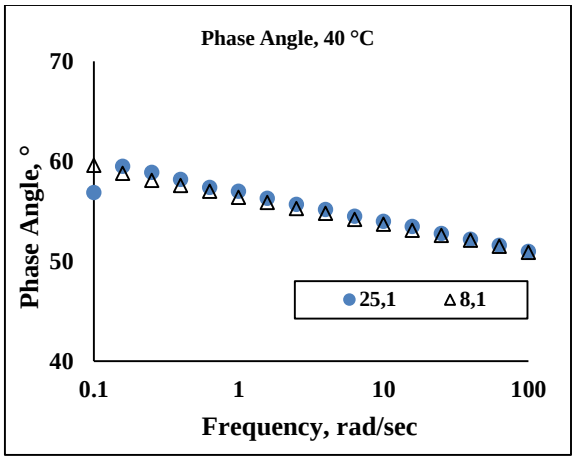

d

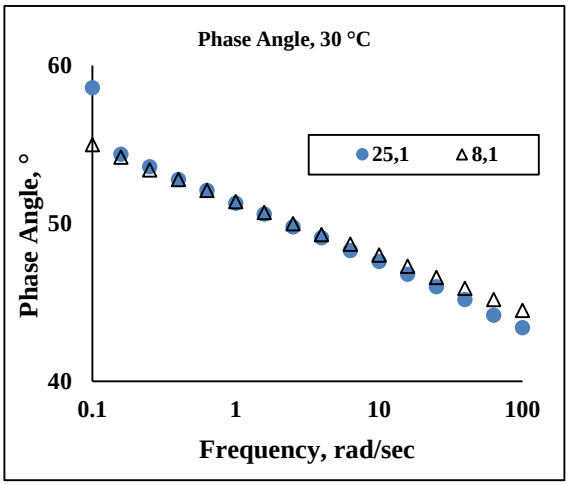

e

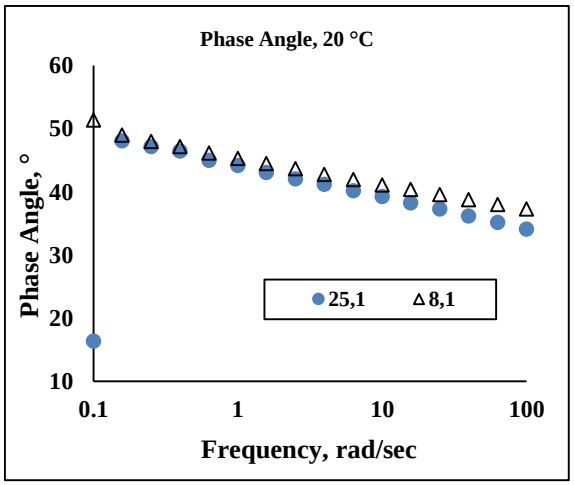

f

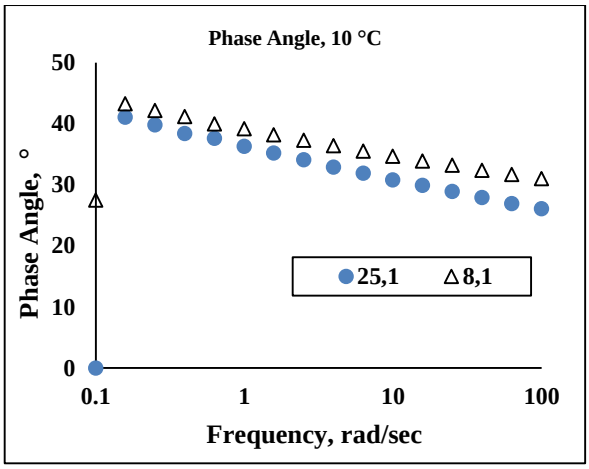

g

Figure 5.9 (a-g) Phase angle curves for PMB (S) for 25 mm and 8 mm plate diameter corresponding to 1 mm plate gap.

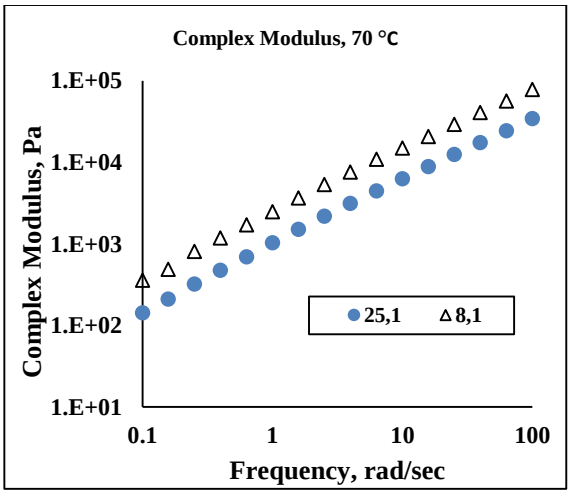
Complex Modulus, 70 °C
Complex Modulus, Pa
1.E+05
1.E+04
1.E+03
1.E+02
1.E+01
0.1
1
10
100
Frequency, rad/sec
25,1
8,1

a

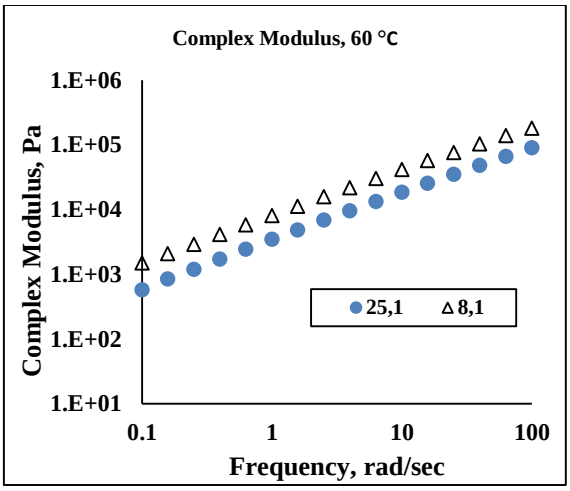
Complex Modulus, 60 °C
Complex Modulus, Pa
1.E+06
1.E+05
1.E+04
1.E+03
1.E+02
1.E+01
0.1
1
10
100
Frequency, rad/sec
25,1
8,1

b

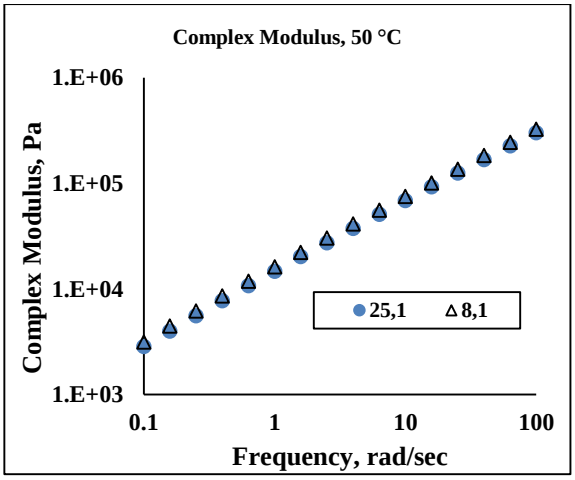
Complex Modulus, 50 °C
Complex Modulus, Pa
1.E+06
1.E+05
1.E+04
1.E+03
0.1
1
10
100
Frequency, rad/sec
25,1
8,1

c

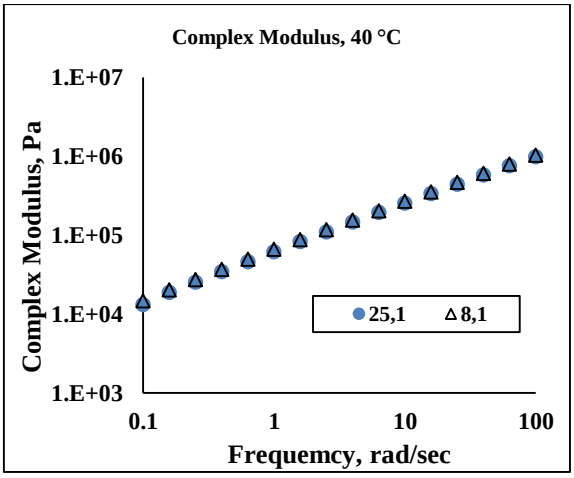
Complex Modulus, 40 °C
Complex Modulus, Pa
1.E+07
1.E+06
1.E+05
1.E+04
1.E+03
0.1
1
10
100
Frequemcy, rad/sec
25,1
8,1

d

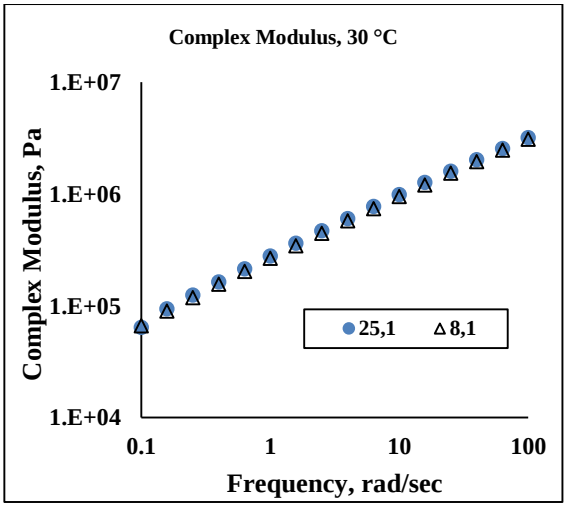
Complex Modulus, 30 °C
Complex Modulus, Pa
1.E+07
1.E+06
1.E+05
1.E+04
0.1
1
10
100
Frequency, rad/sec
25,1
8,1

e

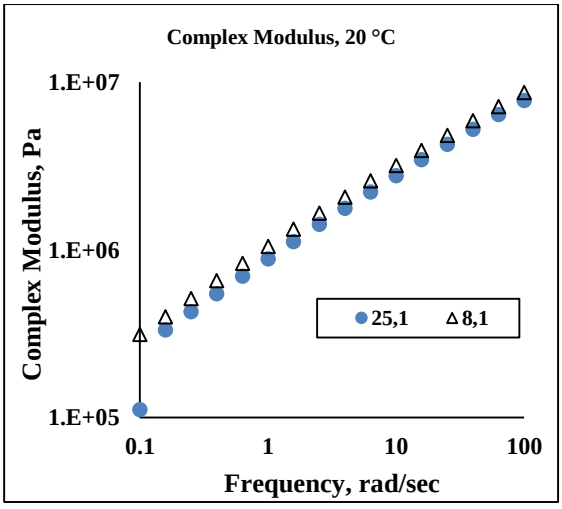
Complex Modulus, 20 °C
Complex Modulus, Pa
1.E+07
1.E+06
1.E+05
0.1
1
10
100
Frequency, rad/sec
25,1
8,1

f

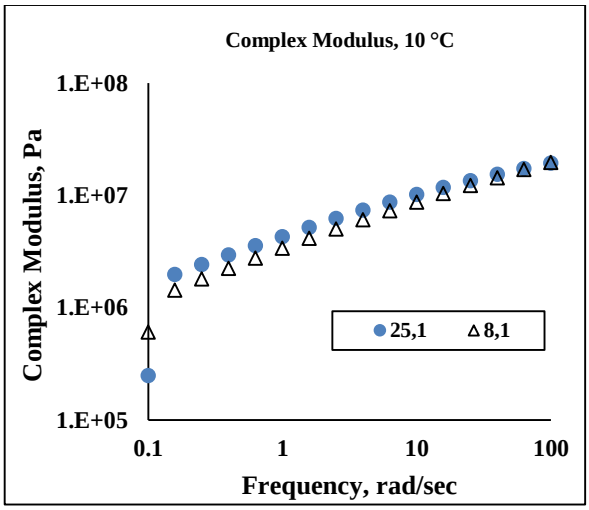

g

Figure 5.10 (a-g) Complex modulus curves for PMB (S) for 25 mm and 8 mm plate diameter corresponding to 1 mm plate gap.

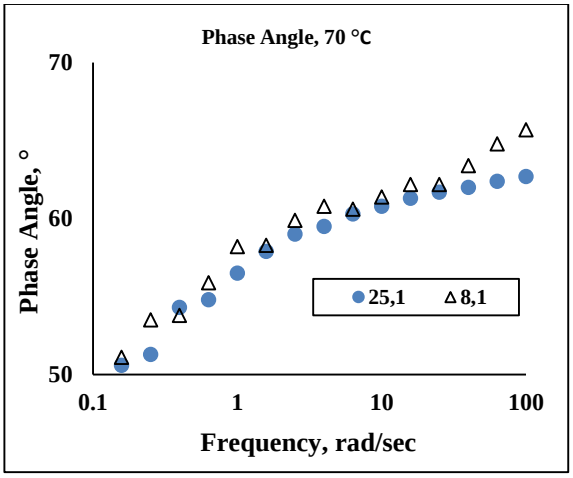

a

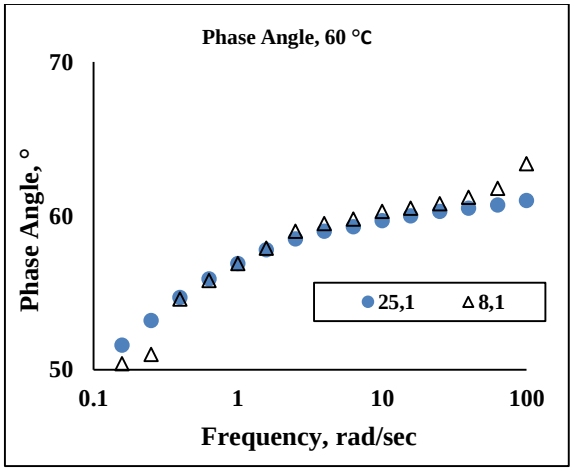

b

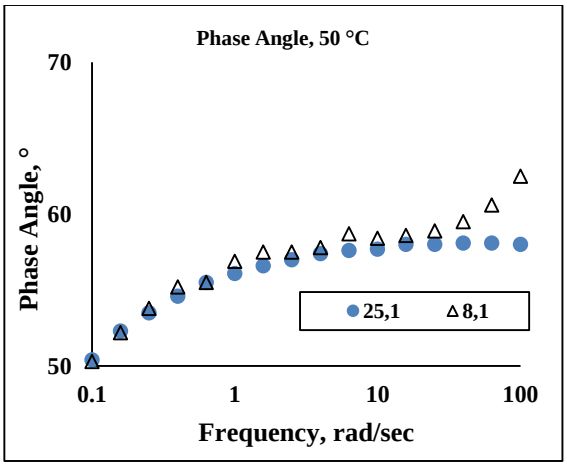

c

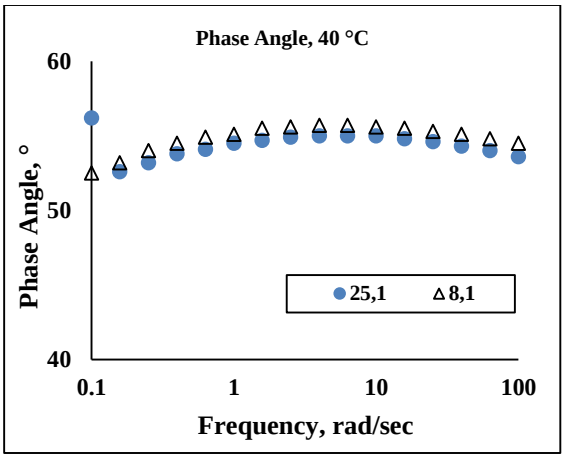

d

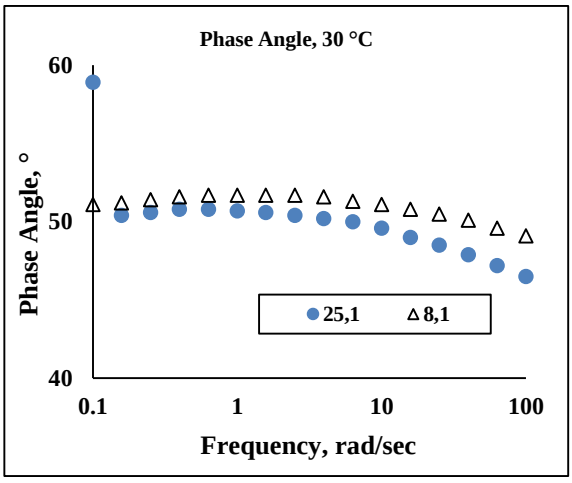

e

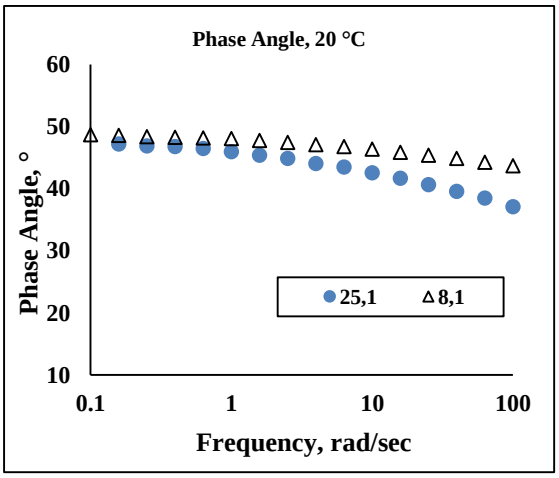

f

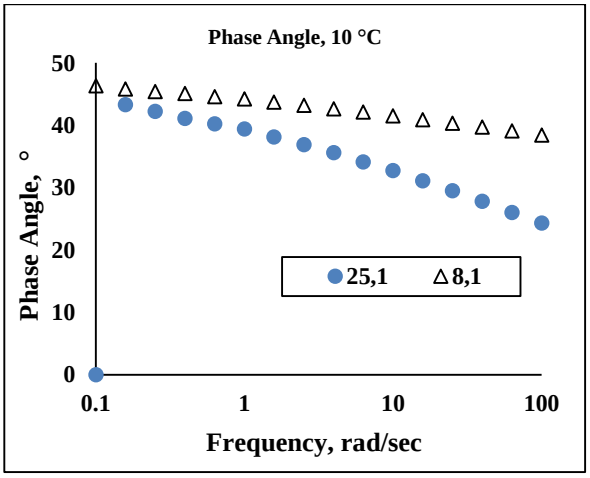

g

Figure 5.11 (a-g) Phase angle curves for PMB (E) for 25 mm and 8 mm plate diameter corresponding to 1 mm plate gap.

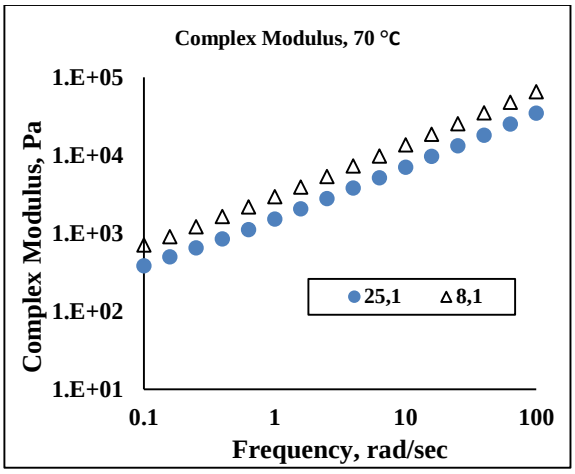
Complex Modulus, 70 °C
Complex Modulus, Pa
1.E+05
1.E+04
1.E+03
1.E+02
1.E+01
0.1
1
10
100
Frequency, rad/sec
25,1
8,1

a

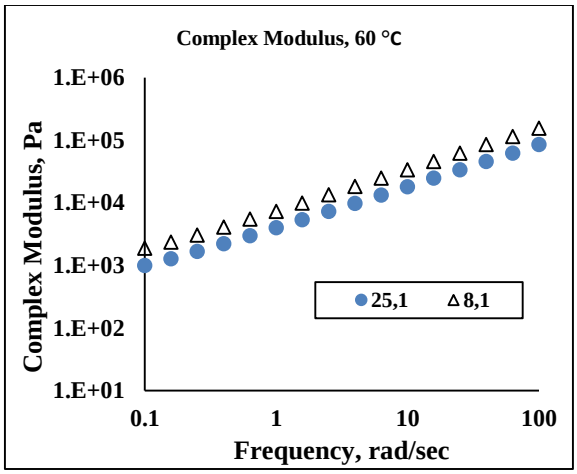
Complex Modulus, 60 °C
Complex Modulus, Pa
1.E+06
1.E+05
1.E+04
1.E+03
1.E+02
1.E+01
0.1
1
10
100
Frequency, rad/sec
25,1
8,1

b

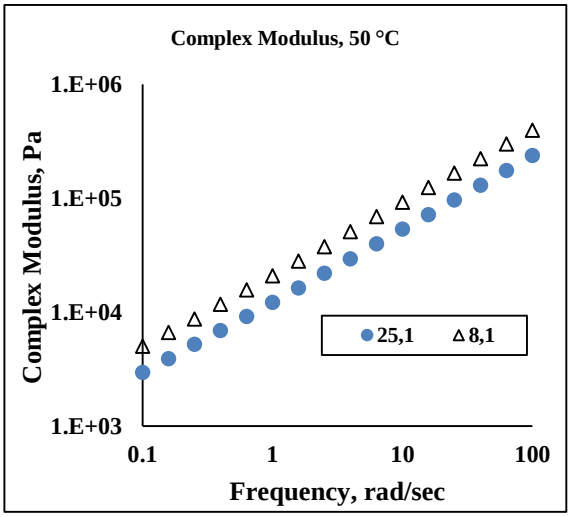
Complex Modulus, 50 °C
Complex Modulus, Pa
1.E+06
1.E+05
1.E+04
1.E+03
0.1
1
10
100
Frequency, rad/sec
25,1
8,1

c

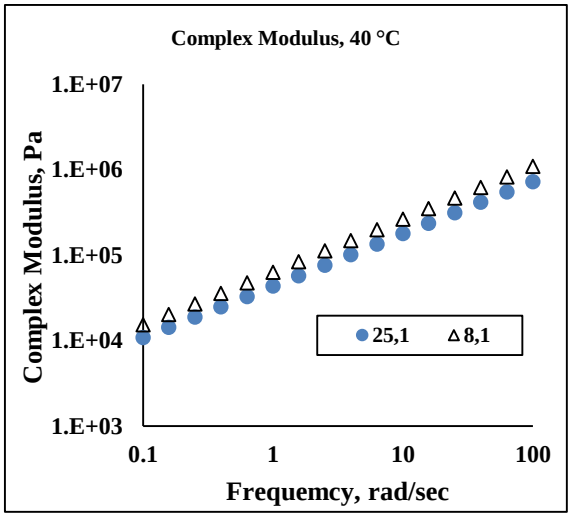
Complex Modulus, 40 °C
Complex Modulus, Pa
1.E+07
1.E+06
1.E+05
1.E+04
1.E+03
0.1
1
10
100
Frequemcy, rad/sec
25,1
8,1

d

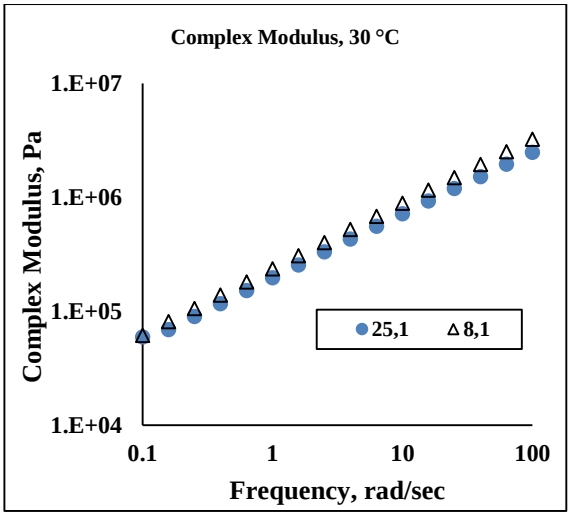
Complex Modulus, 30 °C
Complex Modulus, Pa
1.E+07
1.E+06
1.E+05
1.E+04
0.1
1
10
100
Frequency, rad/sec
25,1
8,1

e

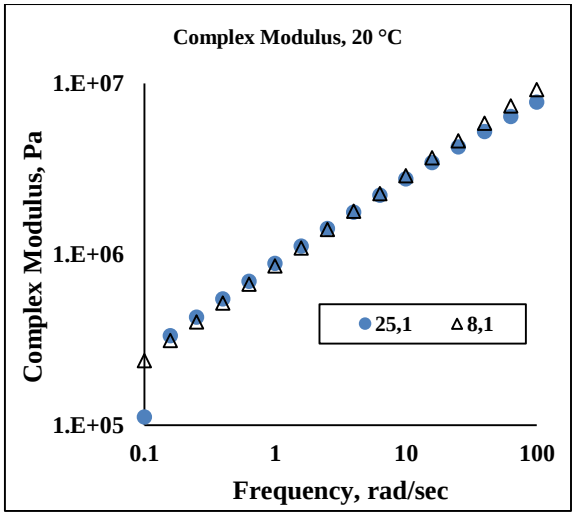
Complex Modulus, 20 °C
Complex Modulus, Pa
1.E+07
1.E+06
1.E+05
0.1
1
10
100
Frequency, rad/sec
25,1
8,1

f

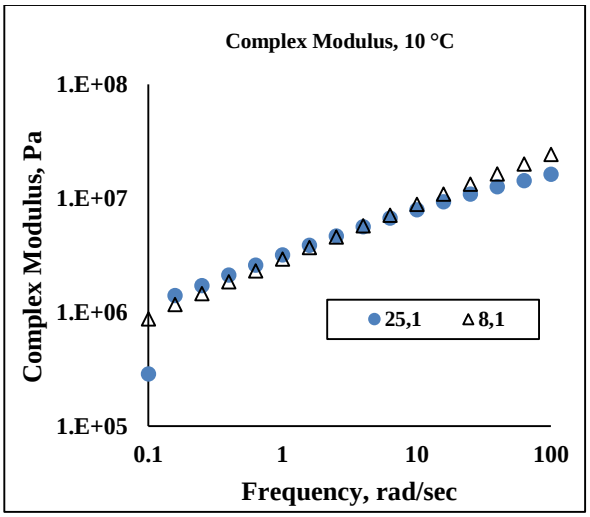

g

Figure 5.12 (a-g) Complex modulus curves for PMB (E) for 25 mm and 8 mm plate diameter corresponding to 1 mm plate gap.

5.5.1.2 Effect of plate gap

Figure 5.13 (a-g) to Figure 5.28 (a-g) presents the effect of plate gap on the measurements of phase angle and complex modulus from 10- 70 °C for all the binders. Curves corresponding to 25 mm and 8 mm spindle diameter are shown separately.

At higher temperatures higher plate gap gave lower values of complex modulus as compared to lower gap. The difference in the measurements decreased with decrease in temperature with similar values at intermediate temperatures. At lower temperatures smaller gap width gave higher values. The trend in the results were consistent for all the binders and both spindle diameters (8 mm and 25 mm). The difference in the results were more significant at lower frequencies for all the binders. In terms of viscoelastic nature of the asphalt binders it can be said that higher plate gap gave higher elastic behavior at higher temperatures, while at lower temperatures smaller gap width displayed stronger elastic nature.

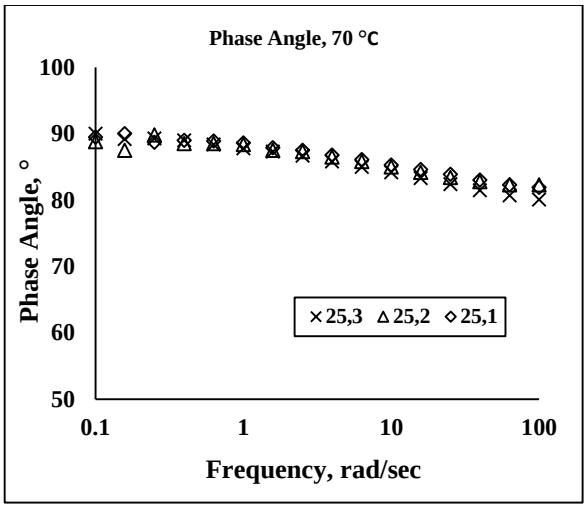
Phase Angle, 70 °C
Phase Angle, °
100
90
80
70
60
50
0.1
1
10
100
Frequency, rad/sec
×25,3 △25,2 ◇25,1

a

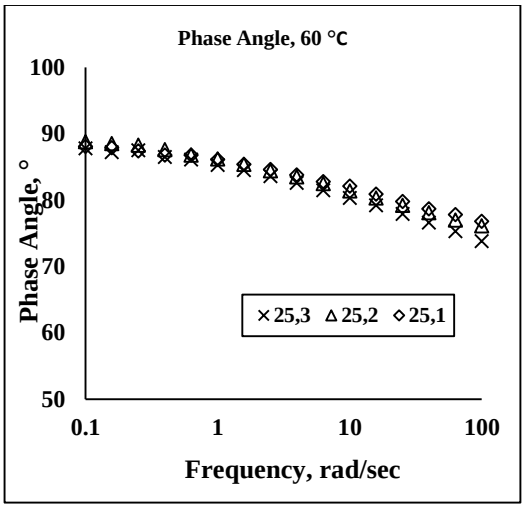
Phase Angle, 60 °C
Phase Angle, °
100
90
80
70
60
50
0.1
1
10
100
Frequency, rad/sec
×25,3 △25,2 ◇25,1

b

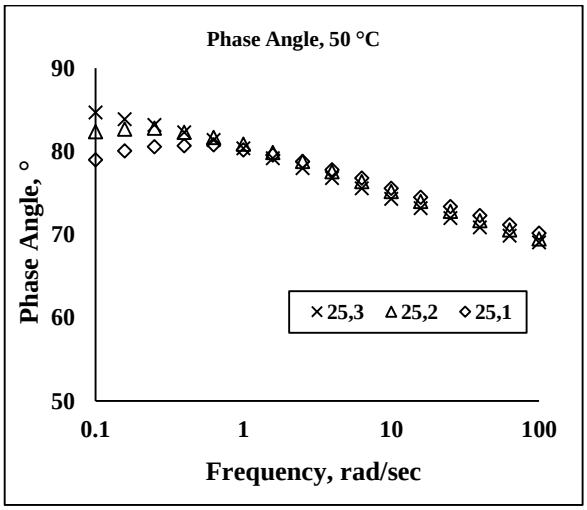
Phase Angle, 50 °C
Phase Angle, °
90
80
70
60
50
0.1
1
10
100
Frequency, rad/sec
×25,3 △25,2 ◇25,1

c

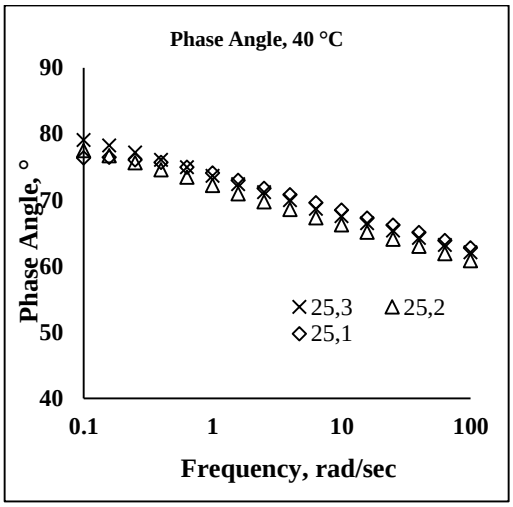
Phase Angle, 40 °C
Phase Angle, °
90
80
70
60
50
40
0.1
1
10
100
Frequency, rad/sec
×25,3 △25,2
◇25,1

d

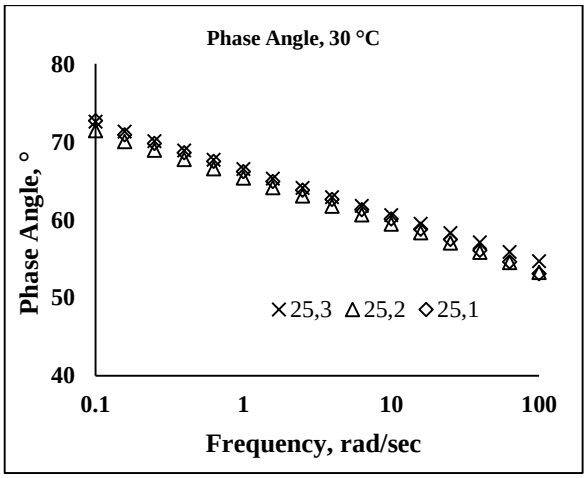
Phase Angle, 30 °C
Phase Angle, °
80
70
60
50
40
0.1
1
10
100
Frequency, rad/sec
×25,3 △25,2 ◇25,1

e

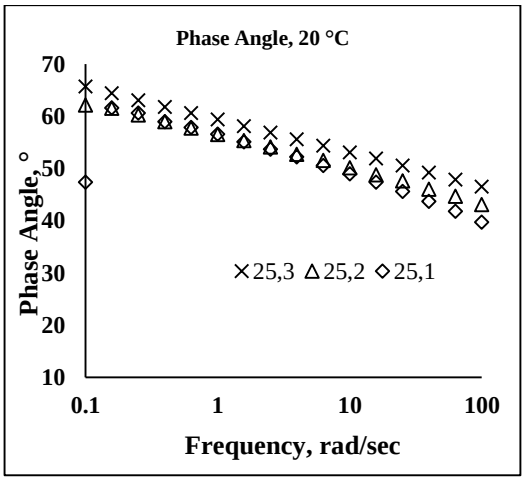
Phase Angle, 20 °C
Phase Angle, °
70
60
50
40
30
20
10
0.1
1
10
100
Frequency, rad/sec
×25,3 △25,2 ◇25,1

f

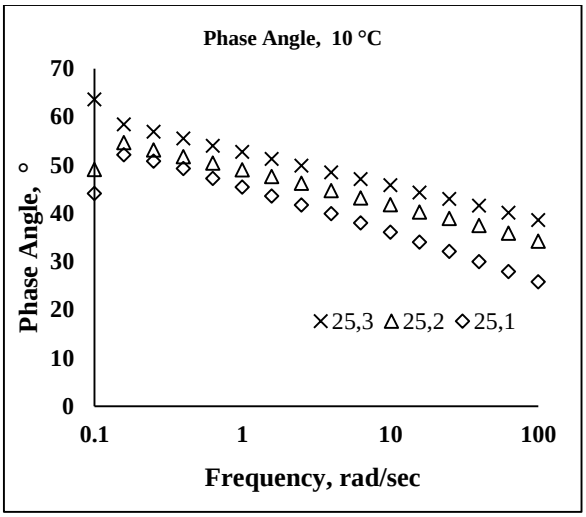

g

Figure 5.13 (a-g) Phase angle curves for VG 10 for 25 mm plate diameter corresponding to different gap width.

(Note: 25, 3; 25, 2; and 25, 1 represents spindle diameter of 25 mm with 1 mm, 2 mm and 3 mm plate gap.)

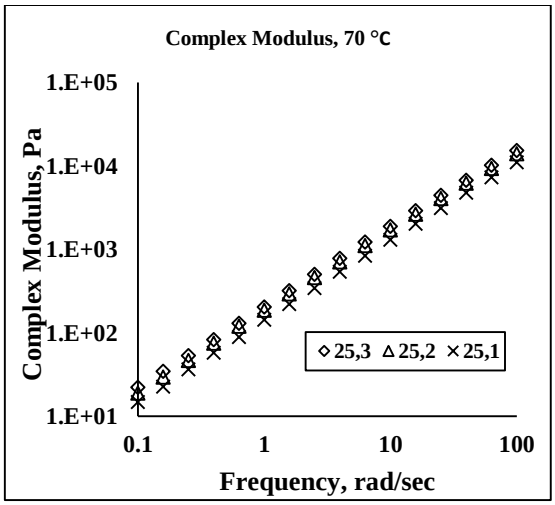

a

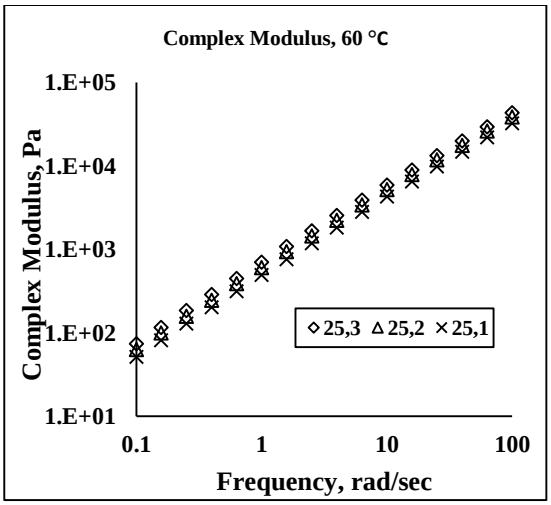

b

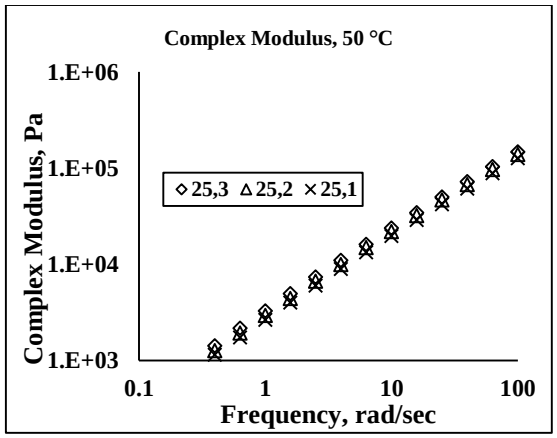

c

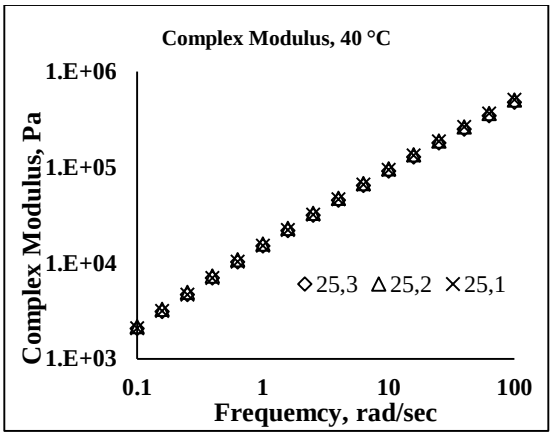

d

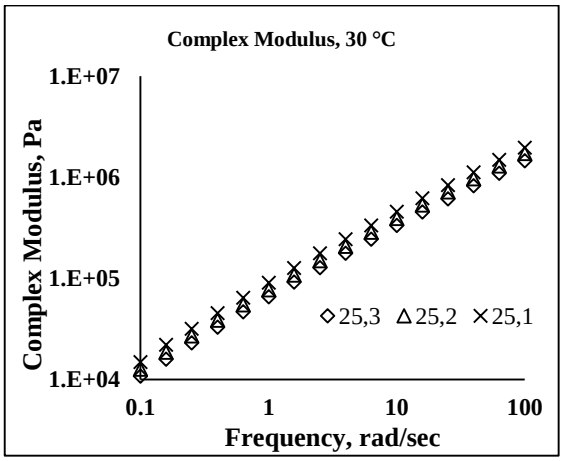

e

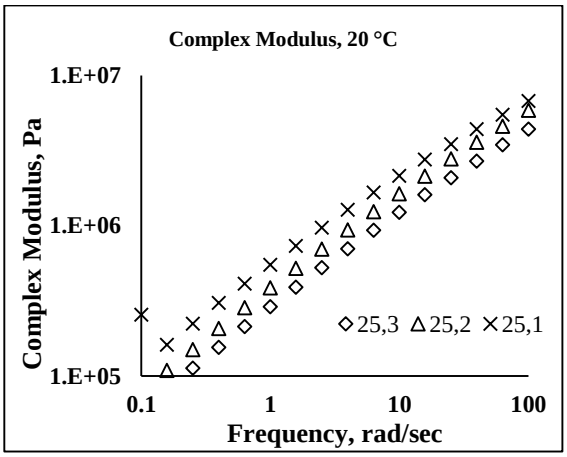

f

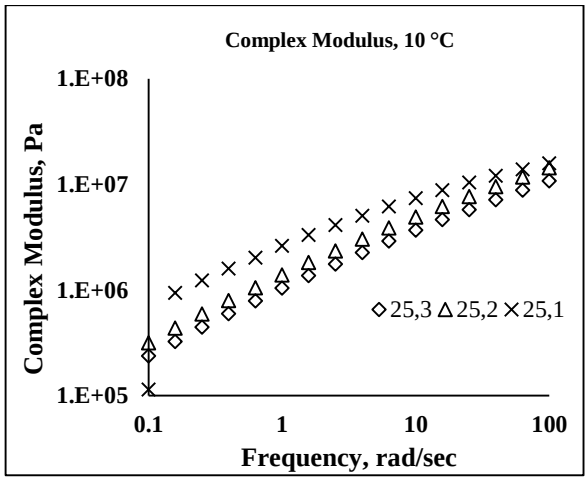

g

Figure 5.14 (a-g) Complex modulus curves for VG 10 for 25 mm plate diameter corresponding to different gap width.

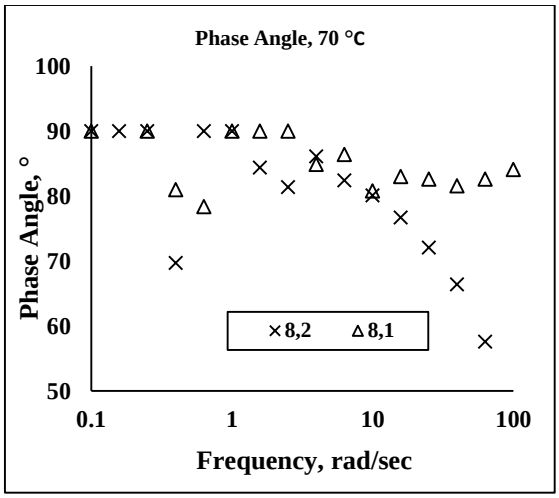
Phase Angle, 70 °C
Phase Angle, °
100
90
80
70
60
50
0.1
1
10
100
Frequency, rad/sec
×8,2
△8,1

a

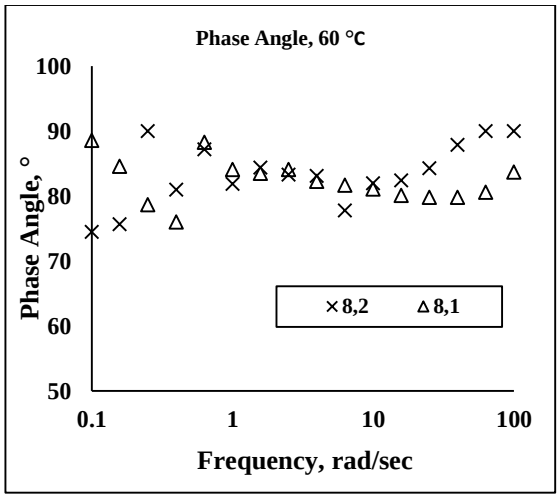
Phase Angle, 60 °C
Phase Angle, °
100
90
80
70
60
50
0.1
1
10
100
Frequency, rad/sec
×8,2
△8,1

b

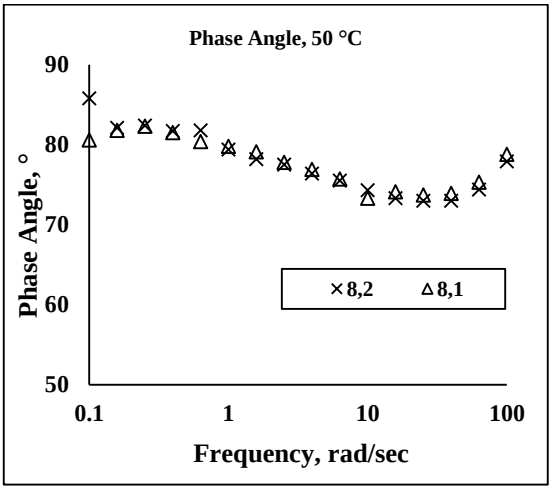
Phase Angle, 50 °C
Phase Angle, °
90
80
70
60
50
0.1
1
10
100
Frequency, rad/sec
×8,2
△8,1

c

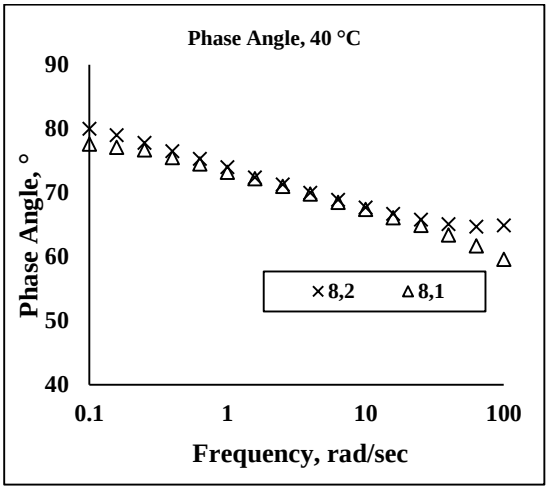
Phase Angle, 40 °C
Phase Angle, °
90
80
70
60
50
40
0.1
1
10
100
Frequency, rad/sec
×8,2
△8,1

d

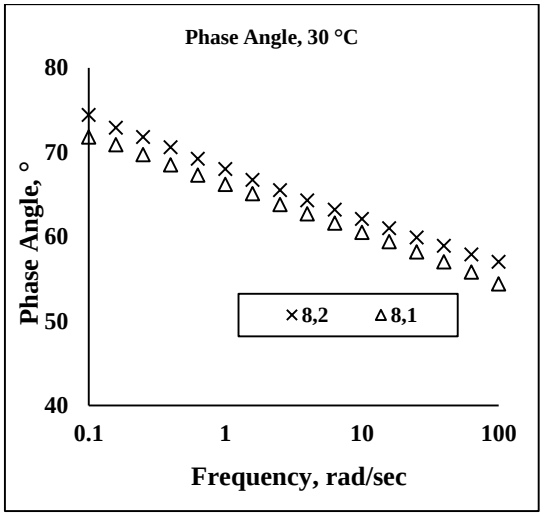
Phase Angle, 30 °C
Phase Angle, °
80
70
60
50
40
0.1
1
10
100
Frequency, rad/sec
×8,2
△8,1

e

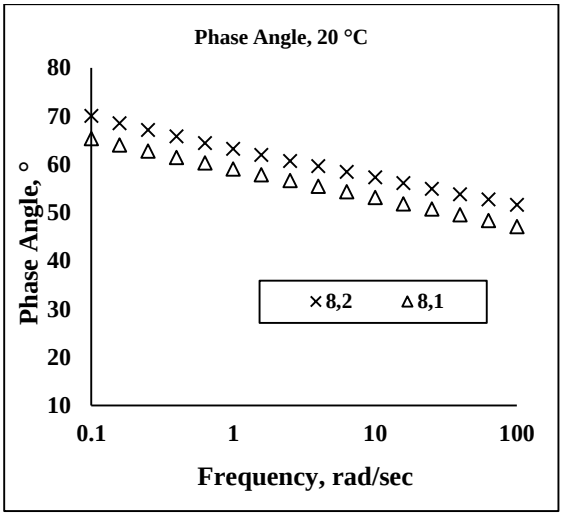
Phase Angle, 20 °C
Phase Angle, °
80
70
60
50
40
30
20
10
0.1
1
10
100
Frequency, rad/sec
×8,2
△8,1

f

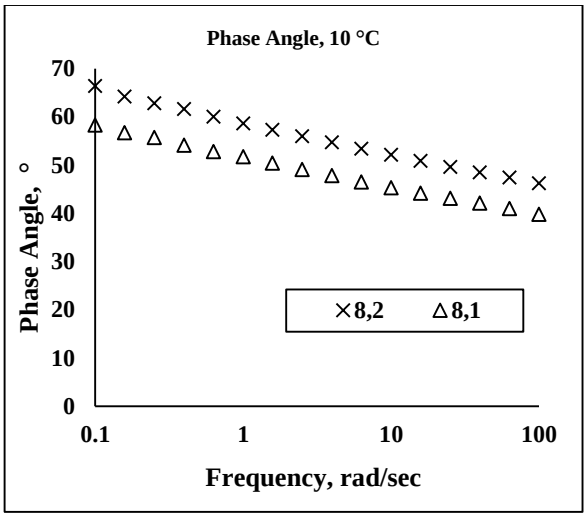

g

Figure 5.15 (a-g) Phase angle curves for VG 10 for 8 mm plate diameter corresponding to different gap width.

(Note: 8, 2 and 8, 1 represents spindle diameter of 8 mm with 2 mm and 3 mm plate gap.)

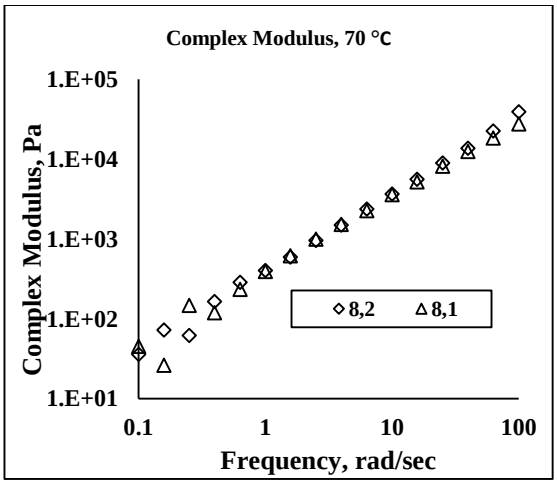

a

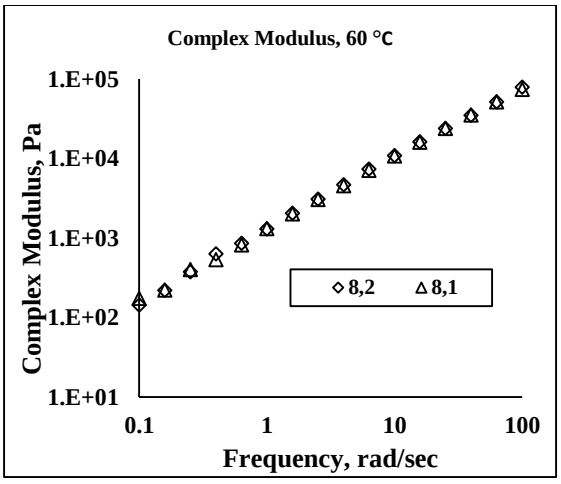

b

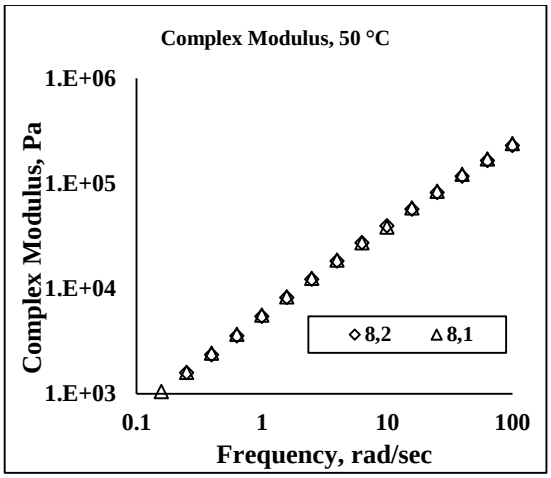

c

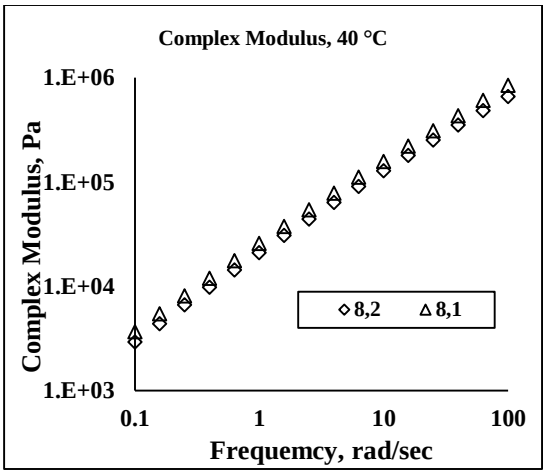

d

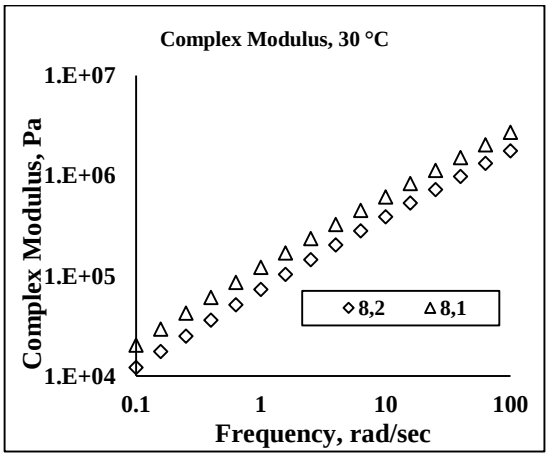

e

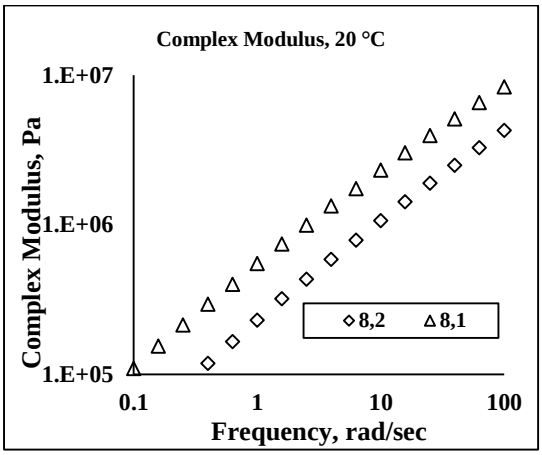

f

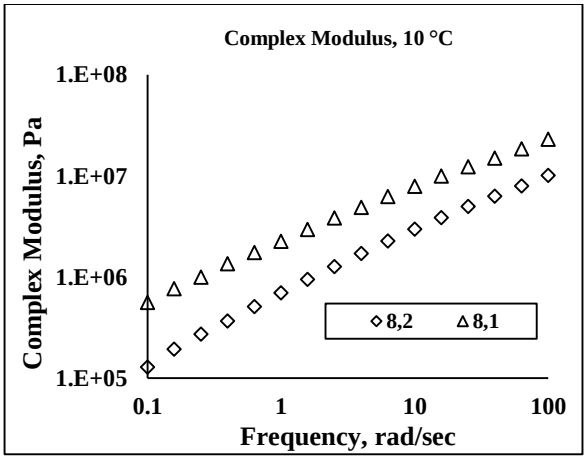

g

Figure 5.16 (a-g) Complex modulus curves for VG 10 for 8 mm plate diameter corresponding to different gap width.

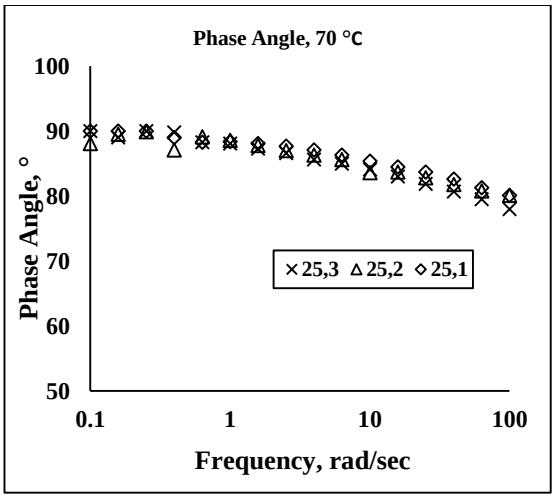
Phase Angle, 70 °C
Phase Angle, °
100
90
80
70
60
50
0.1
1
10
100
Frequency, rad/sec
×25,3 △25,2 ◇25,1

a

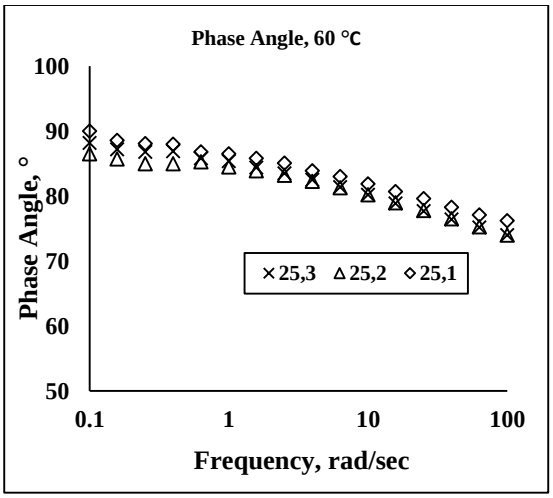
Phase Angle, 60 °C
Phase Angle, °
100
90
80
70
60
50
0.1
1
10
100
Frequency, rad/sec
×25,3 △25,2 ◇25,1

b

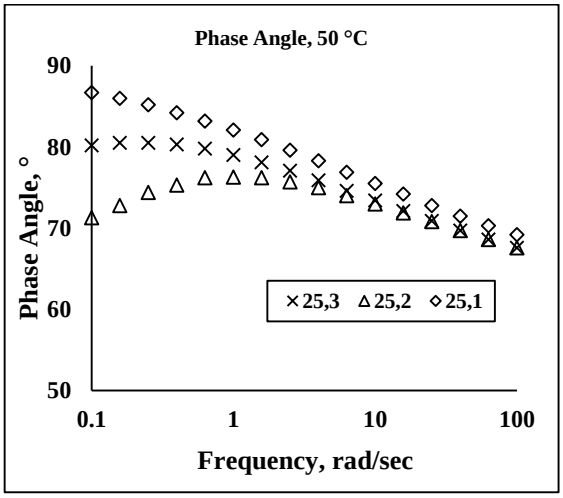
Phase Angle, 50 °C
Phase Angle, °
90
80
70
60
50
0.1
1
10
100
Frequency, rad/sec
×25,3 △25,2 ◇25,1

c

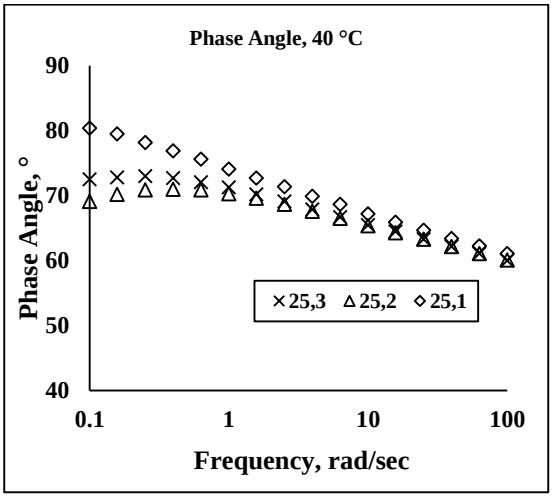
Phase Angle, 40 °C
Phase Angle, °
90
80
70
60
50
40
0.1
1
10
100
Frequency, rad/sec
×25,3 △25,2 ◇25,1

d

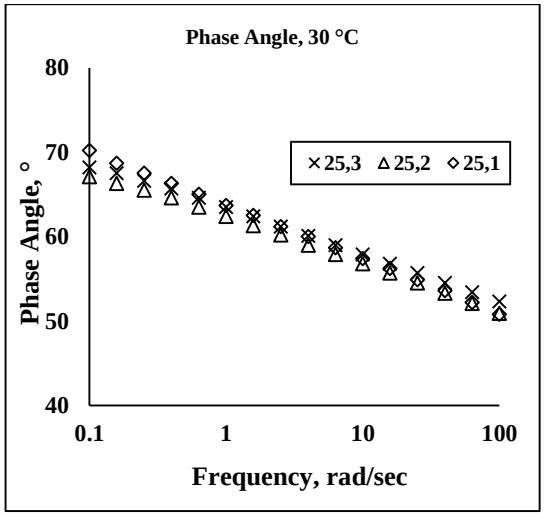
Phase Angle, 30 °C
Phase Angle, °
80
70
60
50
40
0.1
1
10
100
Frequency, rad/sec
×25,3 △25,2 ◇25,1

e

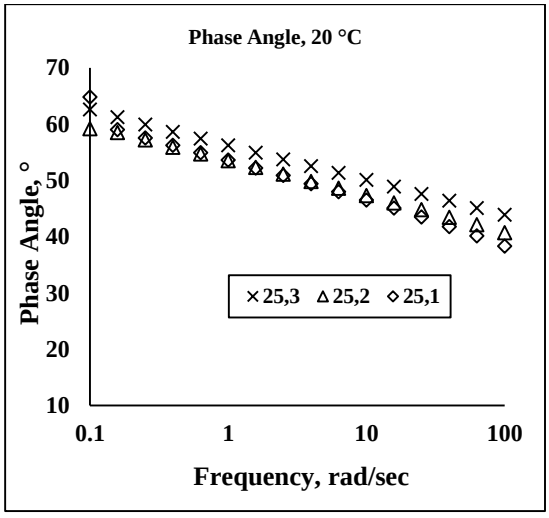
Phase Angle, 20 °C
Phase Angle, °
70
60
50
40
30
20
10
0.1
1
10
100
Frequency, rad/sec
×25,3 △25,2 ◇25,1

f

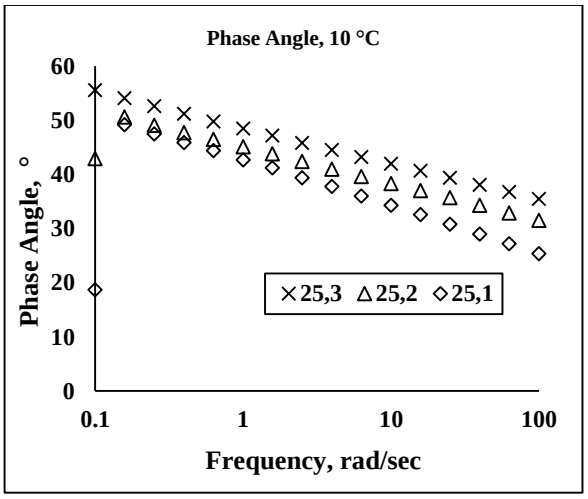

g

Figure 5.17 (a-g) Phase angle curves for VG 30 for 25 mm plate diameter corresponding to different gap width.

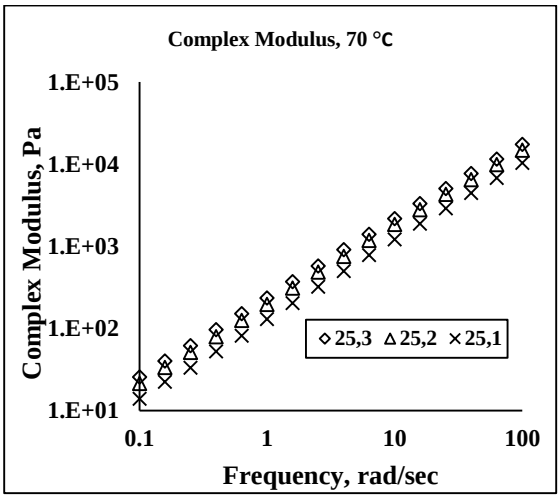

a

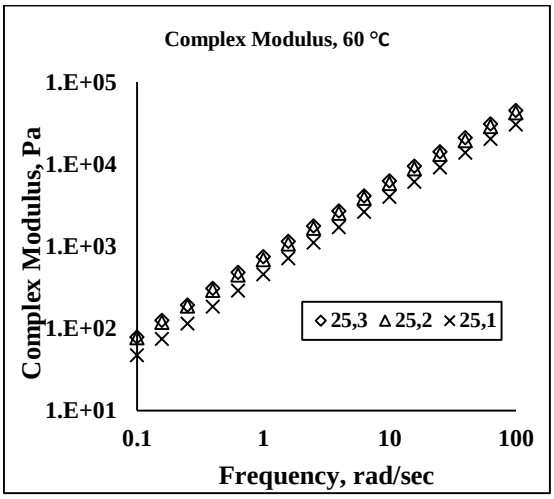

b

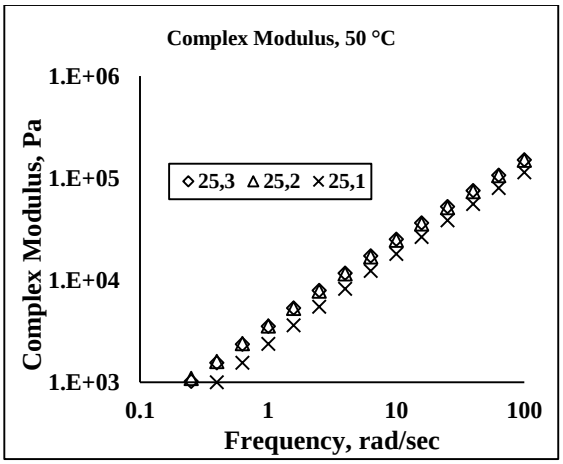

c

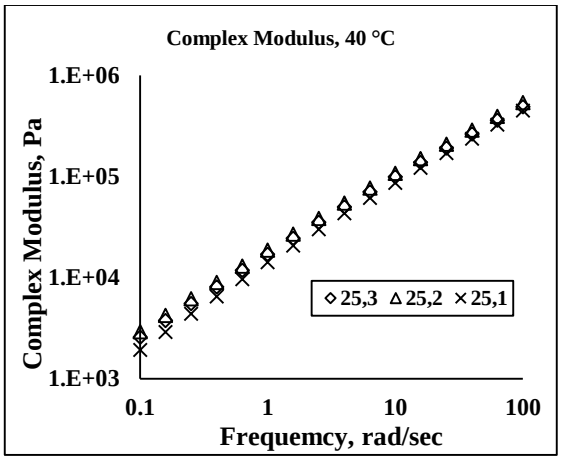

d

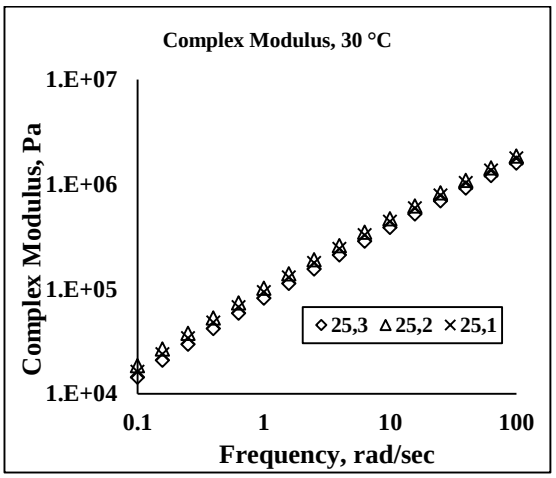

e

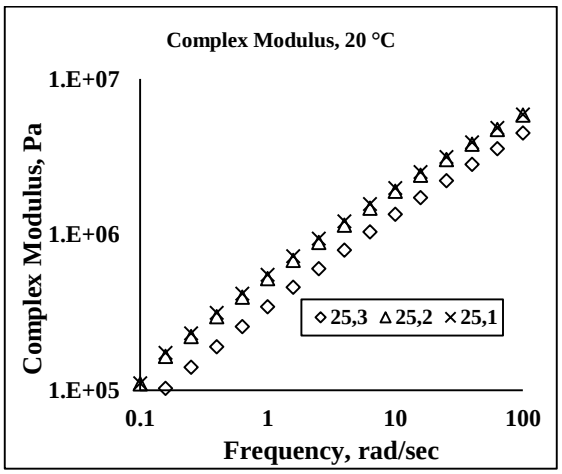

f

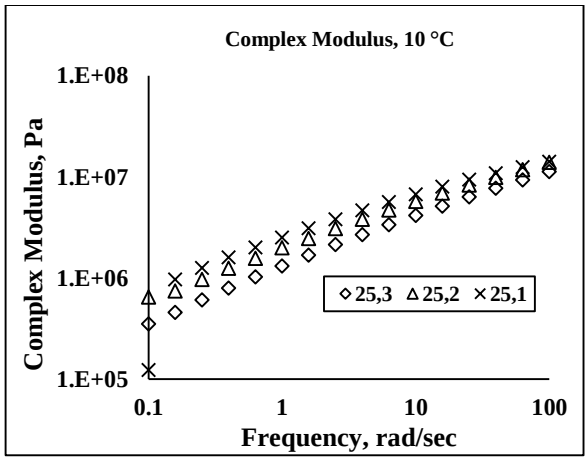

g

Figure 5.18 (a-g) Complex modulus curves for VG 30 for 25 mm plate diameter corresponding to different gap width.

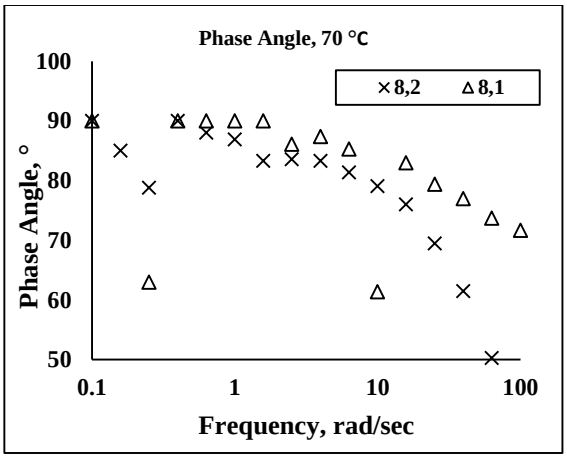
Phase Angle, 70 °C
Phase Angle, °
100
90
80
70
60
50
0.1
1
10
100
Frequency, rad/sec
×8,2
△8,1

a

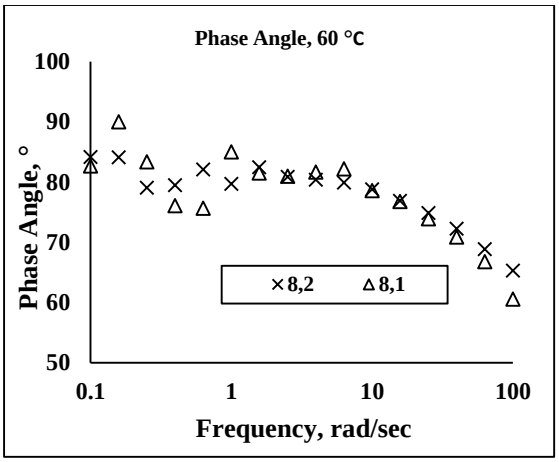
Phase Angle, 60 °C
Phase Angle, °
100
90
80
70
60
50
0.1
1
10
100
Frequency, rad/sec
×8,2
△8,1

b

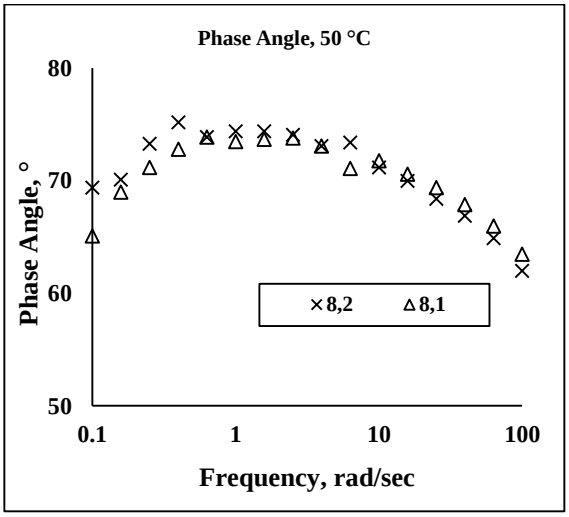
Phase Angle, 50 °C
Phase Angle, °
80
70
60
50
0.1
1
10
100
Frequency, rad/sec
×8,2
△8,1

c

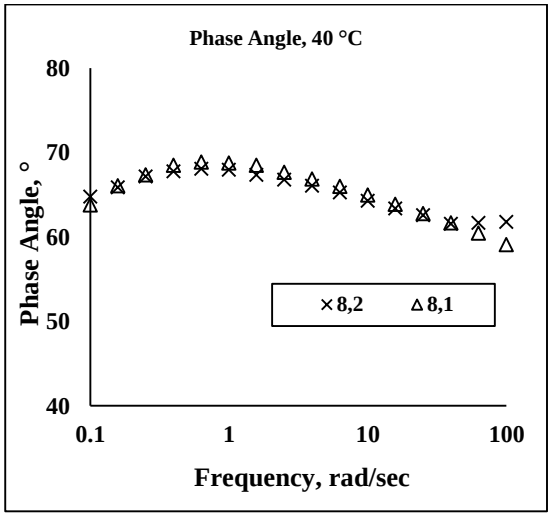
Phase Angle, 40 °C
Phase Angle, °
80
70
60
50
40
0.1
1
10
100
Frequency, rad/sec
×8,2
△8,1

d

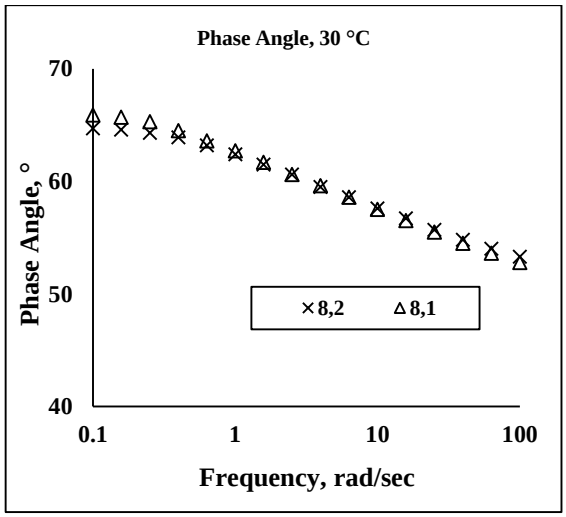
Phase Angle, 30 °C
Phase Angle, °
70
60
50
40
0.1
1
10
100
Frequency, rad/sec
×8,2
△8,1

e

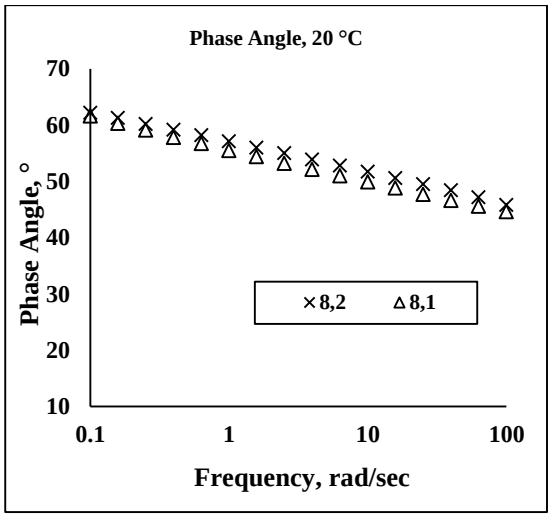
Phase Angle, 20 °C
Phase Angle, °
70
60
50
40
30
20
10
0.1
1
10
100
Frequency, rad/sec
×8,2
△8,1

f

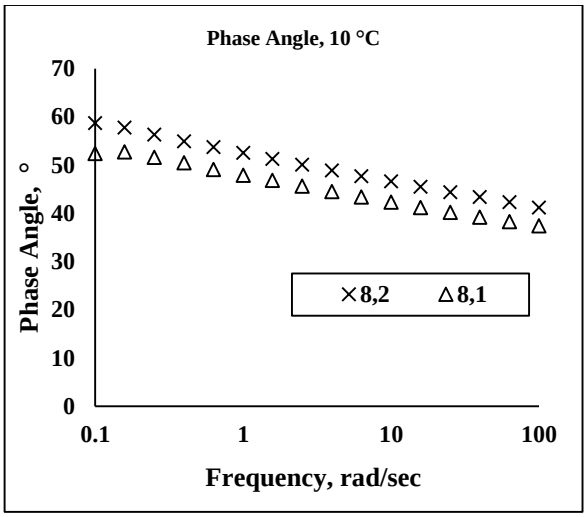

g

Figure 5.19 (a-g) Phase angle curves for VG 30 for 8 mm plate diameter corresponding to different gap width.

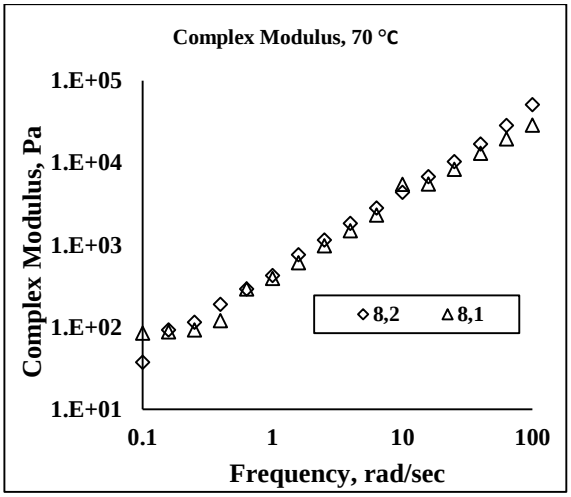

a

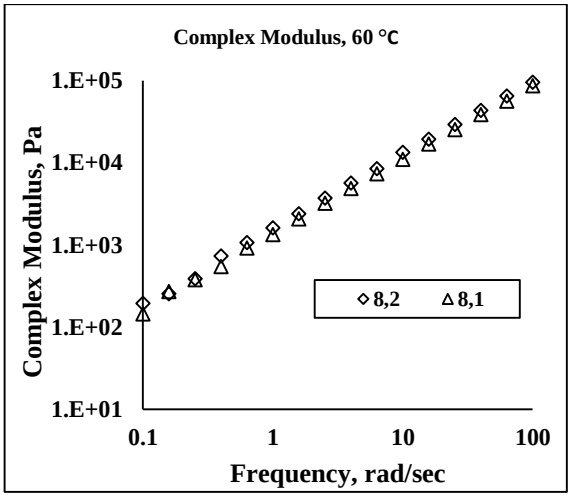

b

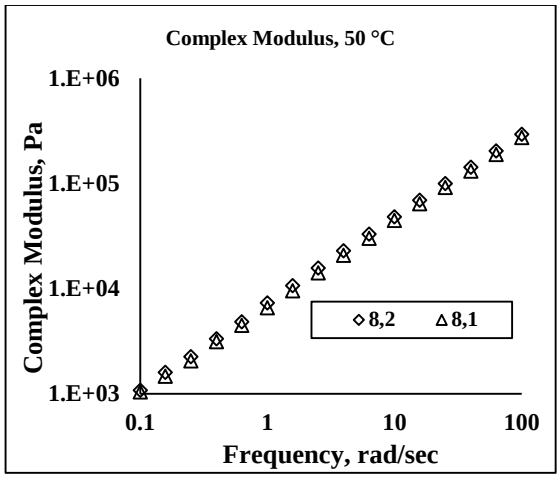

c

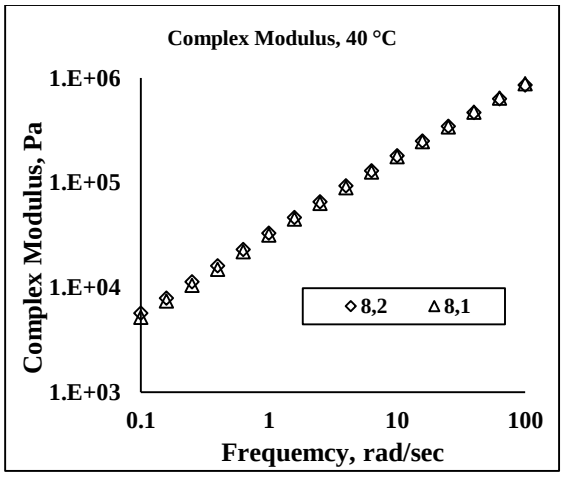

d

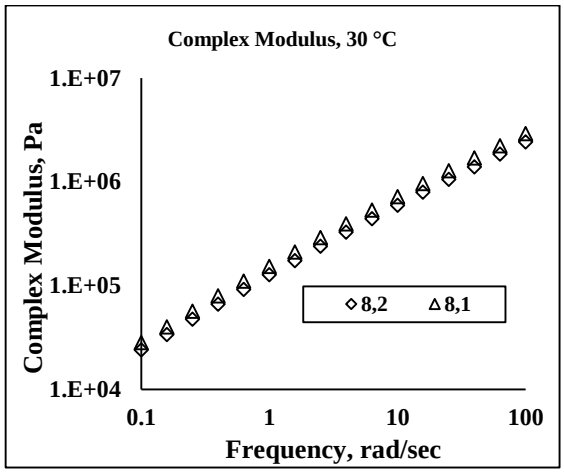

e

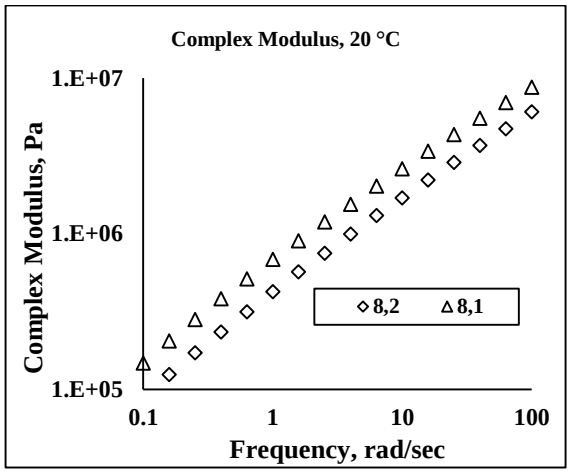

f

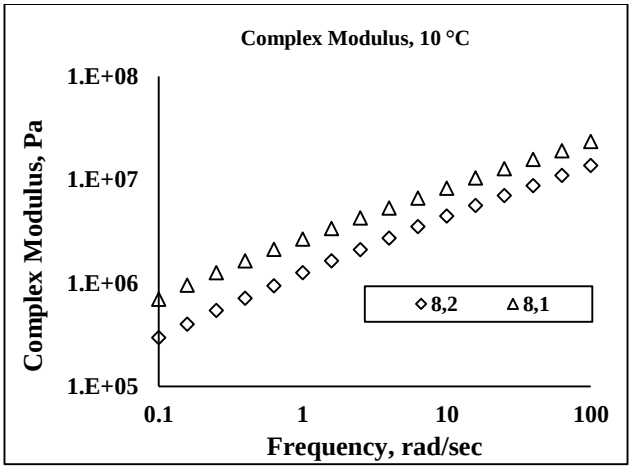

g

Figure 5.20 (a-g) Complex modulus curves for VG 30 for 8 mm plate diameter corresponding to different gap width.

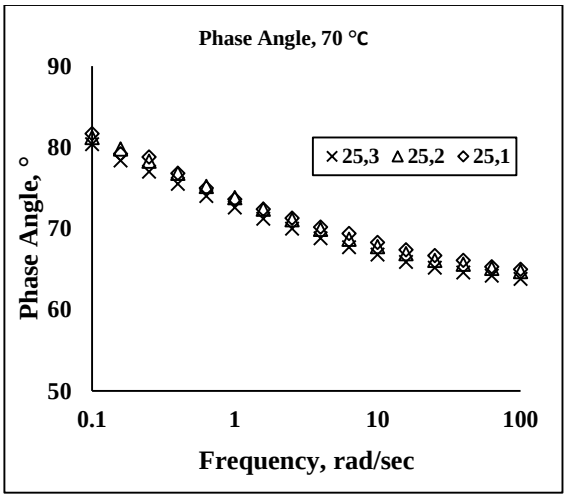
Phase Angle, 70 °C
Phase Angle, °
90
80
70
60
50
0.1
1
10
100
Frequency, rad/sec
×25,3 △25,2 ◇25,1

a

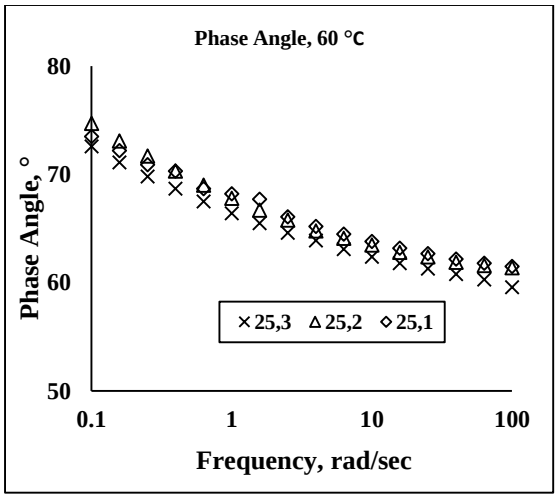
Phase Angle, 60 °C
Phase Angle, °
80
70
60
50
0.1
1
10
100
Frequency, rad/sec
×25,3 △25,2 ◇25,1

b

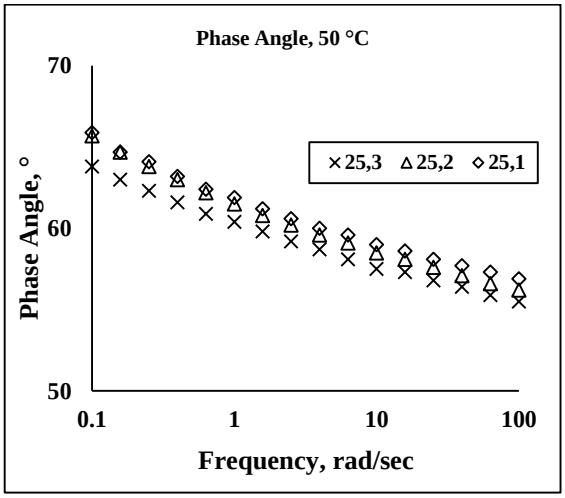
Phase Angle, 50 °C
Phase Angle, °
70
60
50
0.1
1
10
100
Frequency, rad/sec
×25,3 △25,2 ◇25,1

c

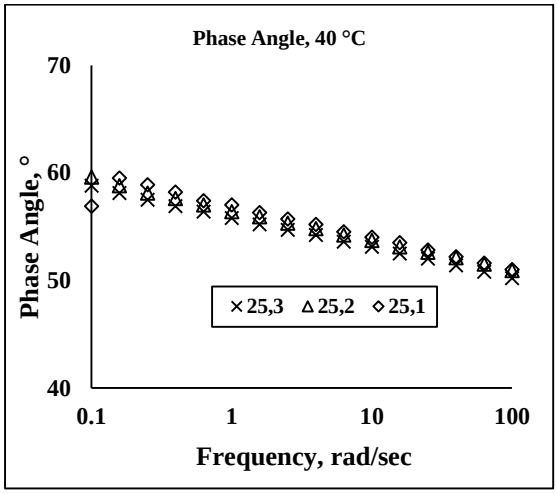
Phase Angle, 40 °C
Phase Angle, °
70
60
50
40
0.1
1
10
100
Frequency, rad/sec
×25,3 △25,2 ◇25,1

d

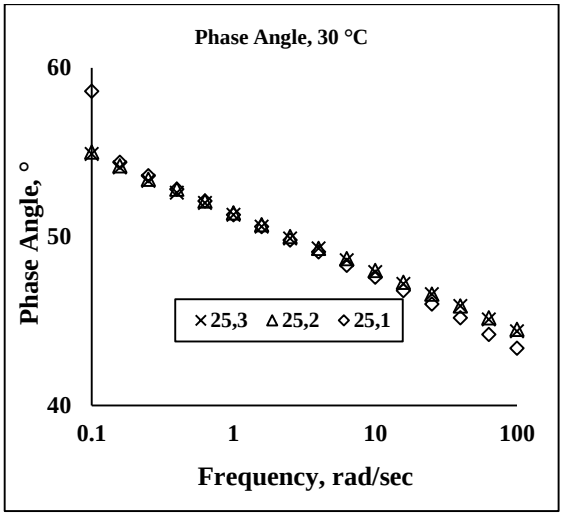
Phase Angle, 30 °C
Phase Angle, °
60
50
40
0.1
1
10
100
Frequency, rad/sec
×25,3 △25,2 ◇25,1

e

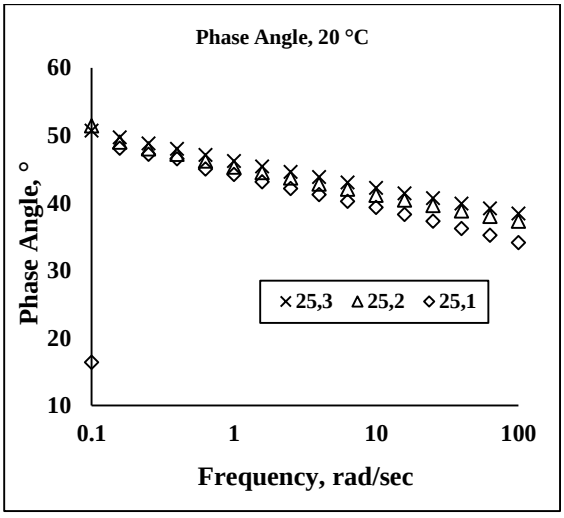
Phase Angle, 20 °C
Phase Angle, °
60
50
40
30
20
10
0.1
1
10
100
Frequency, rad/sec
×25,3 △25,2 ◇25,1

f

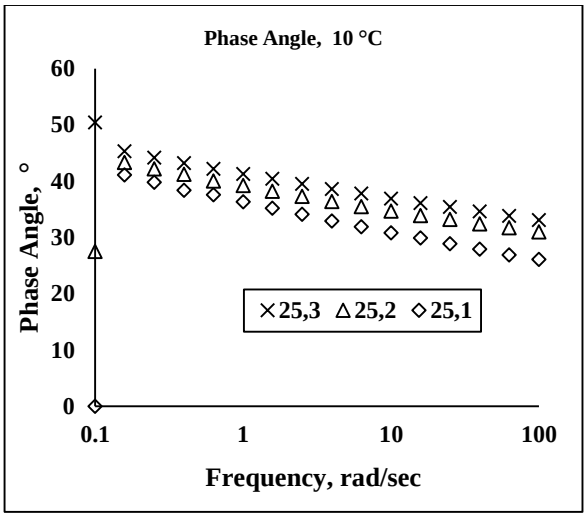

g

Figure 5.21 (a-g) Phase angle curves for PMB (S) for 25 mm plate diameter corresponding to different gap width.

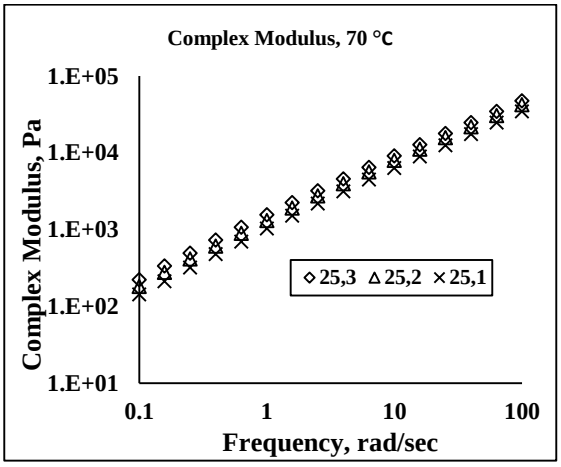

a

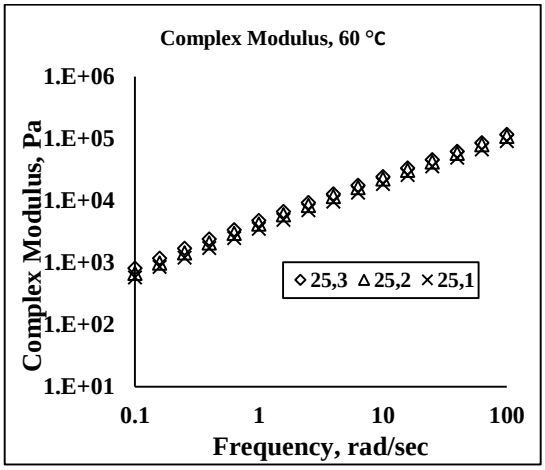

b

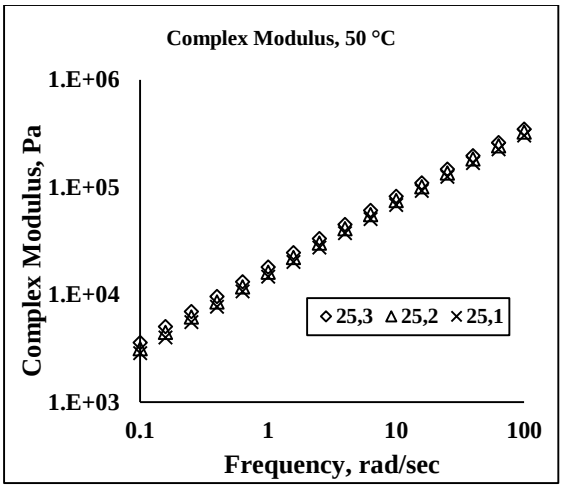

c

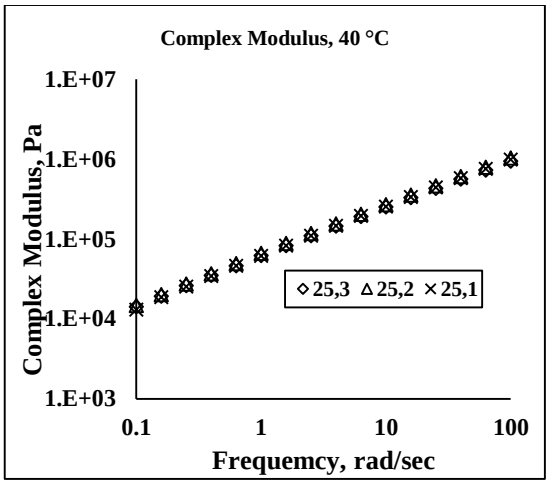

d

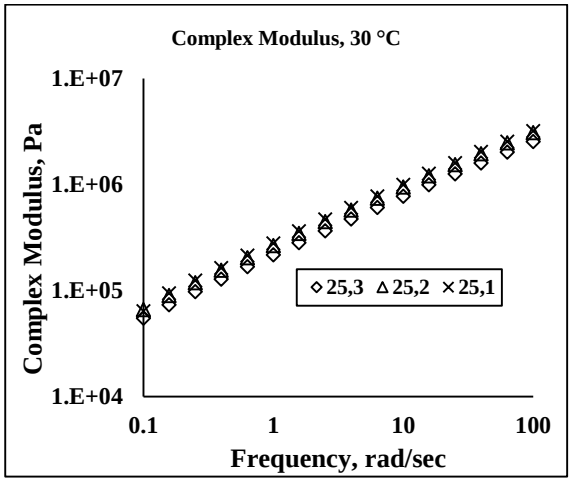

e

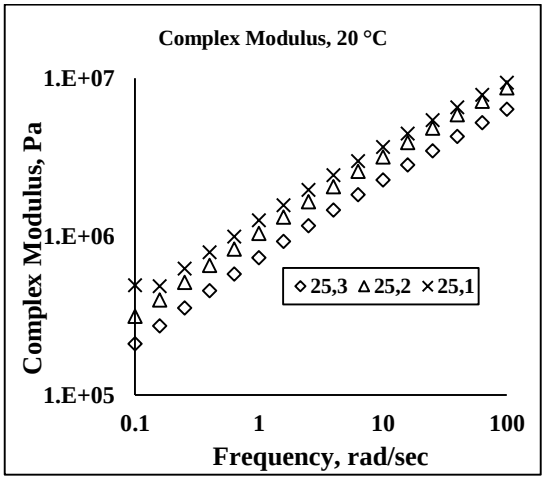

f

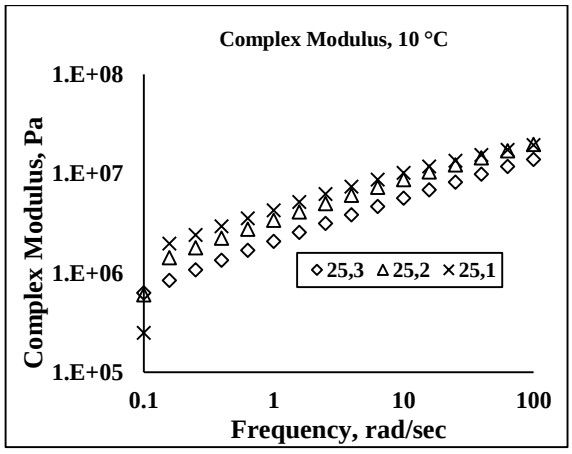

g

Figure 5.22 (a-g) Complex modulus curves for PMB (S) for 25 mm plate diameter corresponding to different gap width.

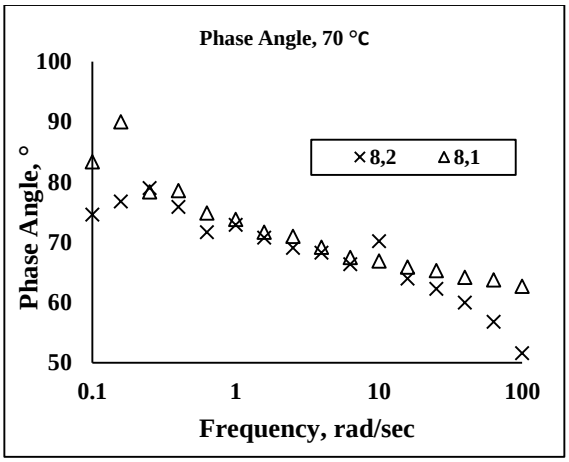
Phase Angle, 70 °C
Phase Angle, °
100
90
80
70
60
50
0.1
1
10
100
Frequency, rad/sec
×8,2
△8,1

a

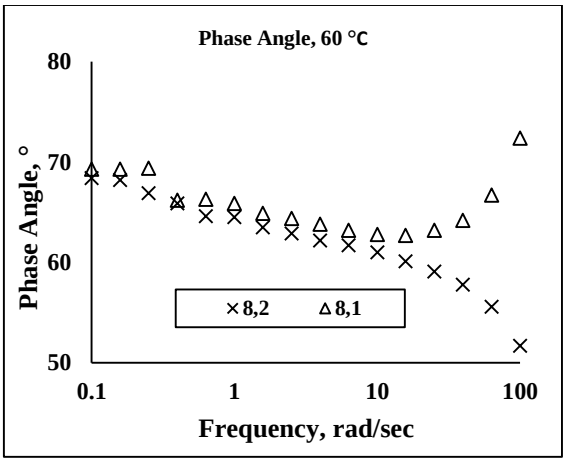
Phase Angle, 60 °C
Phase Angle, °
80
70
60
50
0.1
1
10
100
Frequency, rad/sec
×8,2
△8,1

b

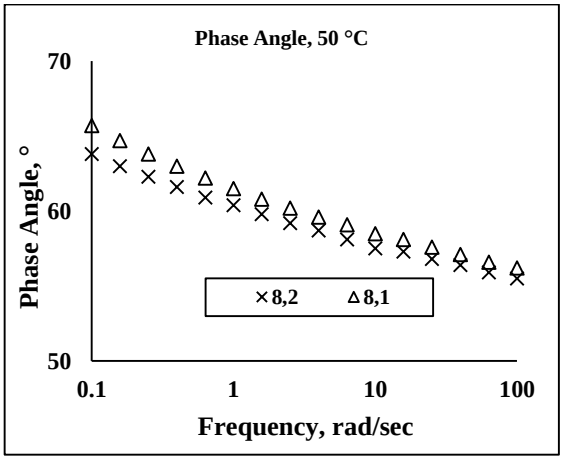
Phase Angle, 50 °C
Phase Angle, °
70
60
50
0.1
1
10
100
Frequency, rad/sec
×8,2
△8,1

c

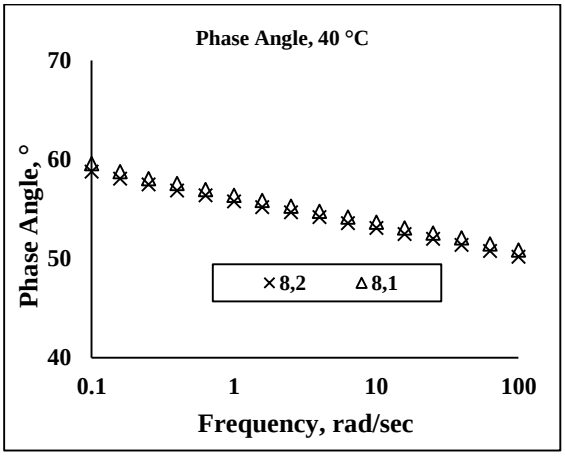
Phase Angle, 40 °C
Phase Angle, °
70
60
50
40
0.1
1
10
100
Frequency, rad/sec
×8,2
△8,1

d

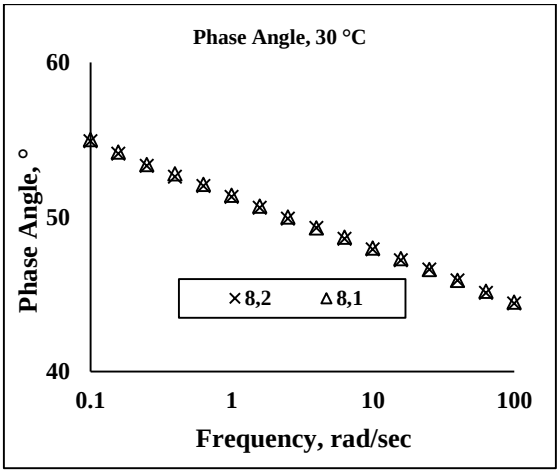
Phase Angle, 30 °C
Phase Angle, °
60
50
40
0.1
1
10
100
Frequency, rad/sec
×8,2
△8,1

e

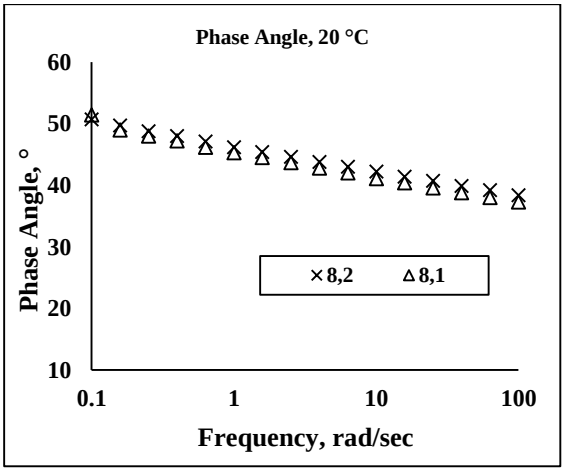
Phase Angle, 20 °C
Phase Angle, °
60
50
40
30
20
10
0.1
1
10
100
Frequency, rad/sec
×8,2
△8,1

f

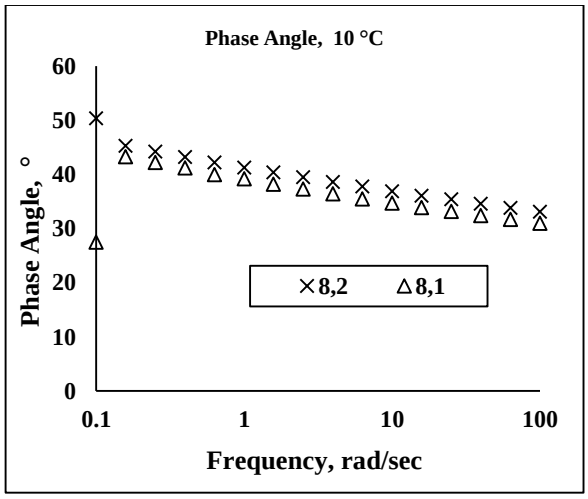

g

Figure 5.23 (a-g) Phase angle curves for PMB (S) for 8 mm plate diameter corresponding to different gap width.

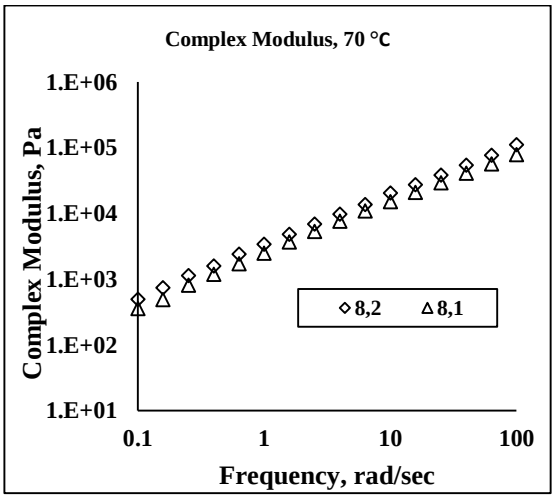

a

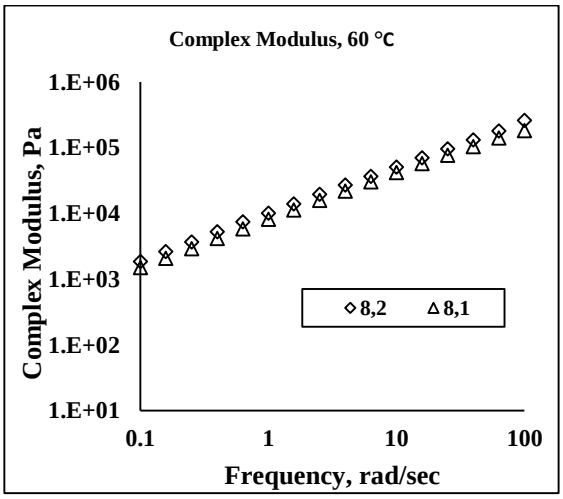

b

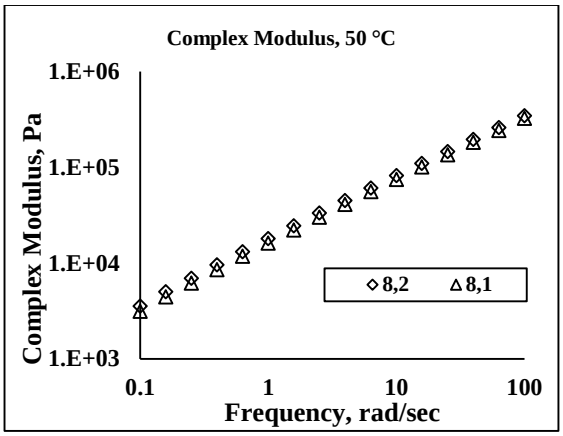

c

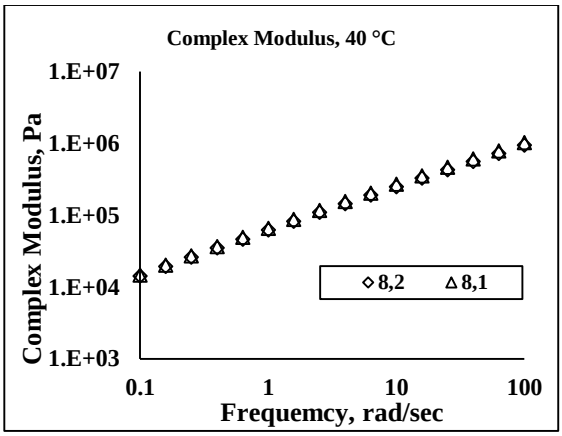

d

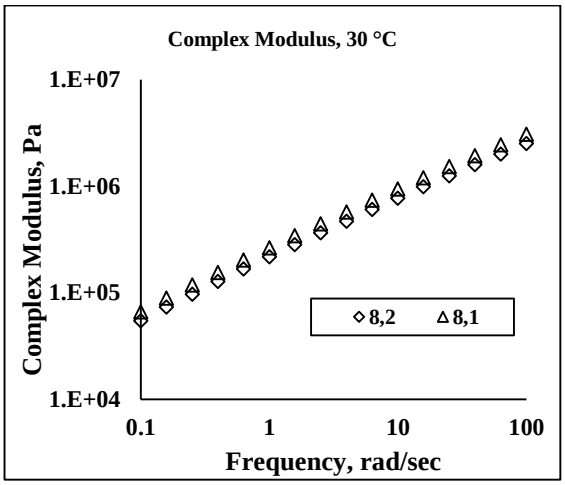

e

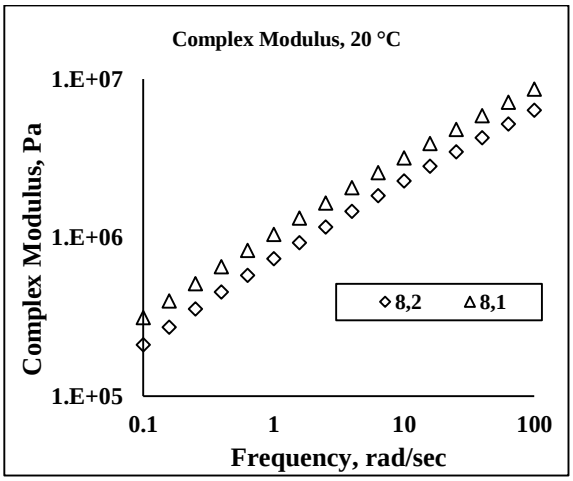

f

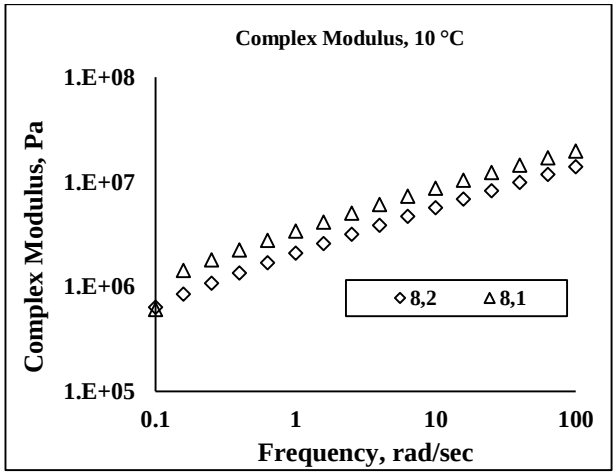

g

Figure 5.24 (a-g) Complex modulus curves for PMB (S) for 8 mm plate diameter corresponding to different gap width.

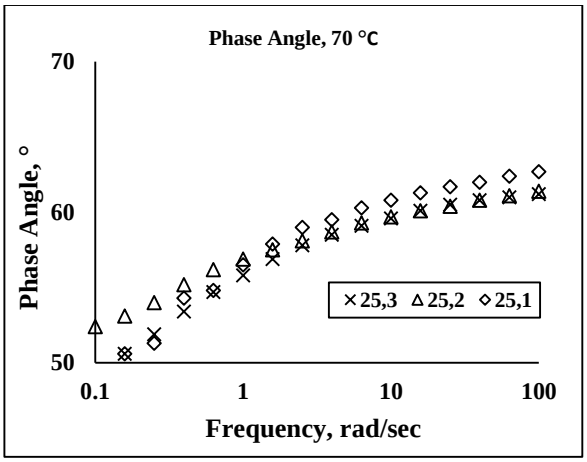
Phase Angle, 70 °C
Phase Angle, °
70
60
50
0.1
1
10
100
Frequency, rad/sec
×25,3 △25,2 ◇25,1

a

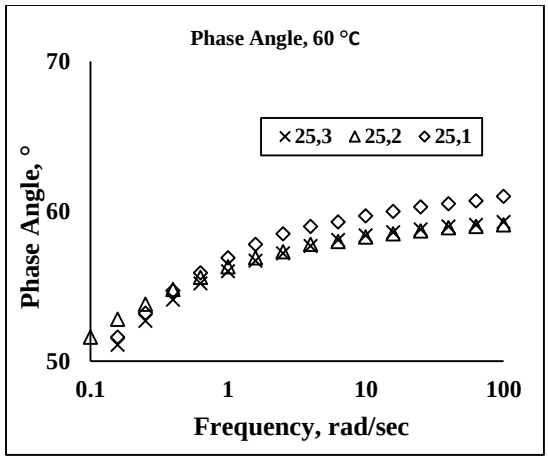
Phase Angle, 60 °C
Phase Angle, °
70
60
50
0.1
1
10
100
Frequency, rad/sec
×25,3 △25,2 ◇25,1

b

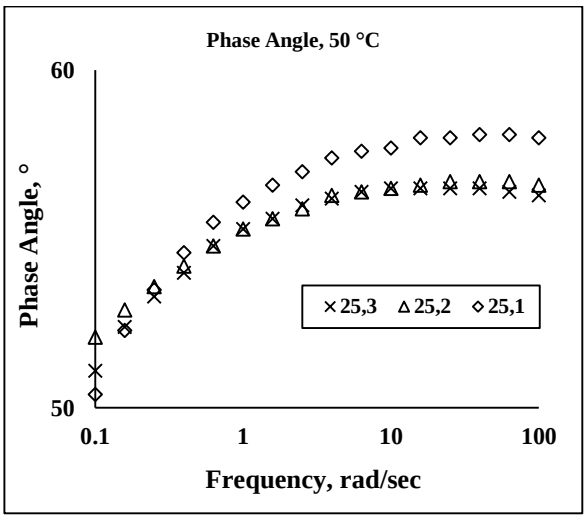
Phase Angle, 50 °C
Phase Angle, °
60
50
0.1
1
10
100
Frequency, rad/sec
×25,3 △25,2 ◇25,1

c

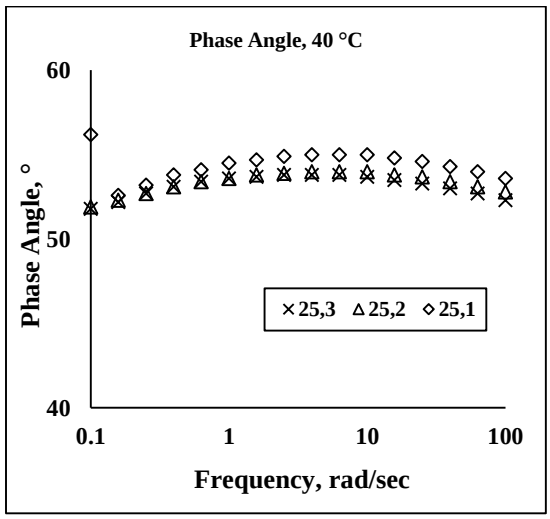
Phase Angle, 40 °C
Phase Angle, °
60
50
40
0.1
1
10
100
Frequency, rad/sec
×25,3 △25,2 ◇25,1

d

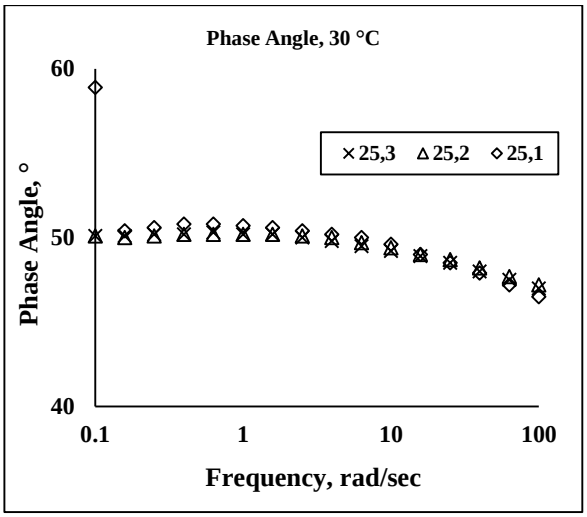
Phase Angle, 30 °C
Phase Angle, °
60
50
40
0.1
1
10
100
Frequency, rad/sec
×25,3 △25,2 ◇25,1

e

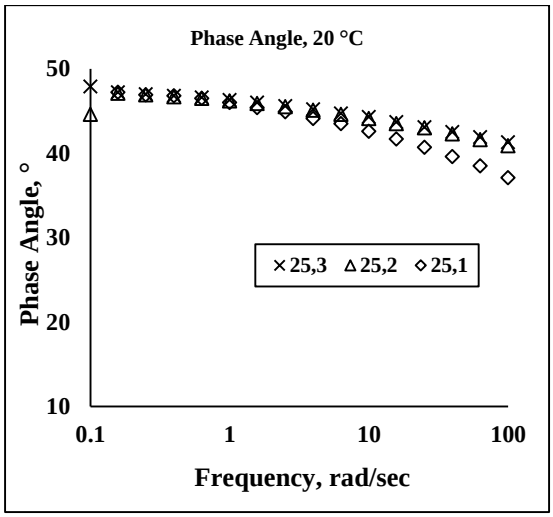
Phase Angle, 20 °C
Phase Angle, °
50
40
30
20
10
0.1
1
10
100
Frequency, rad/sec
×25,3 △25,2 ◇25,1

f

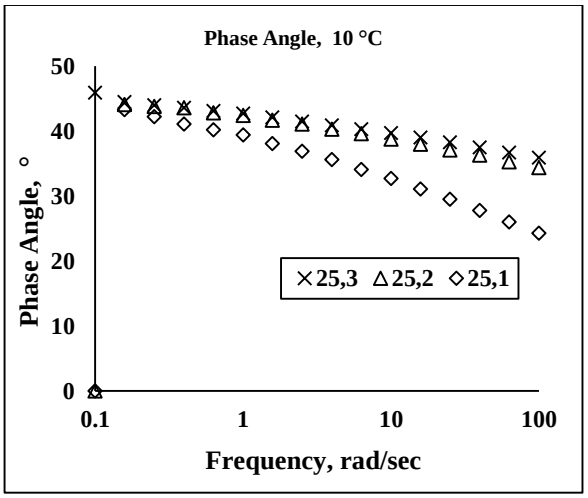

g

Figure 5.25 (a-g) Phase angle curves for PMB (E) for 25 mm plate diameter corresponding to different gap width.

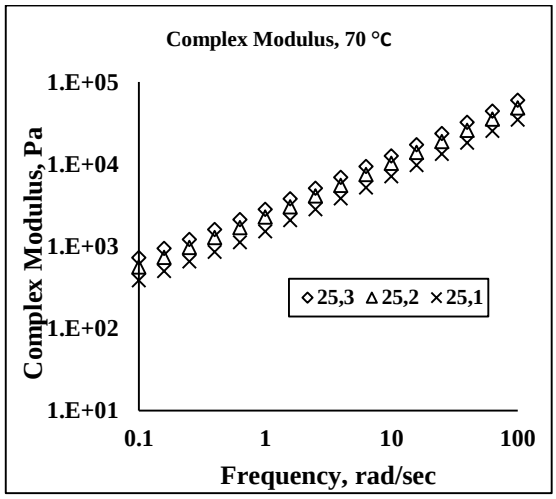

a

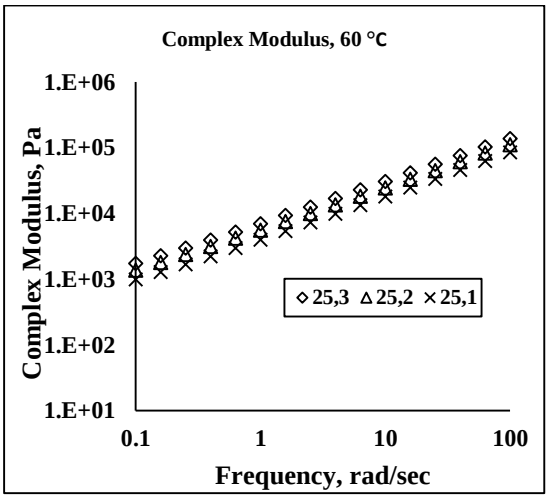

b

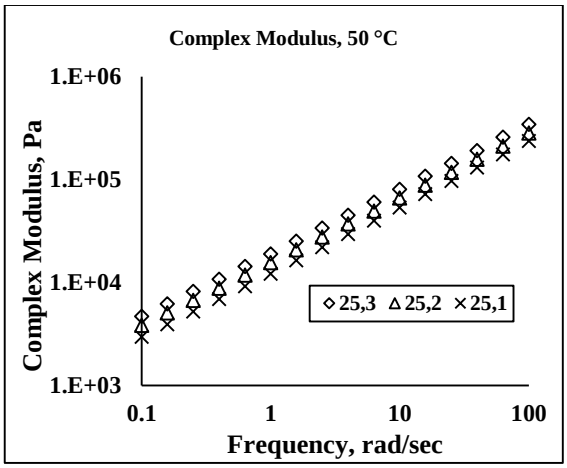

c

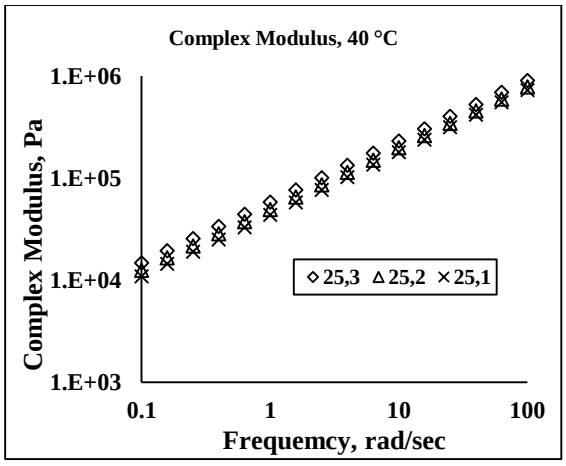

d

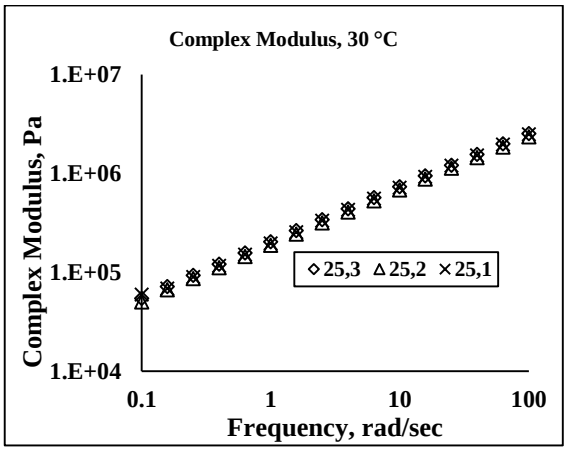

e

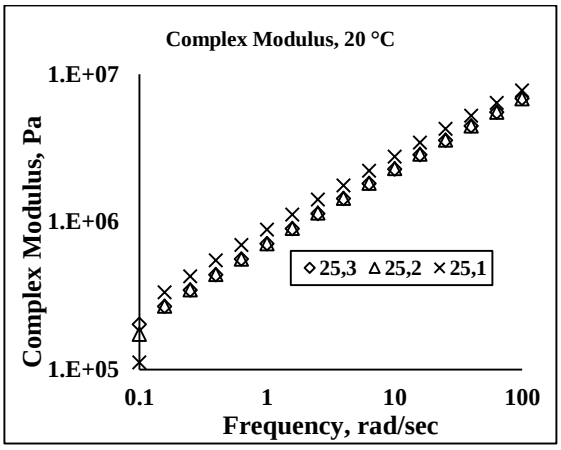

f

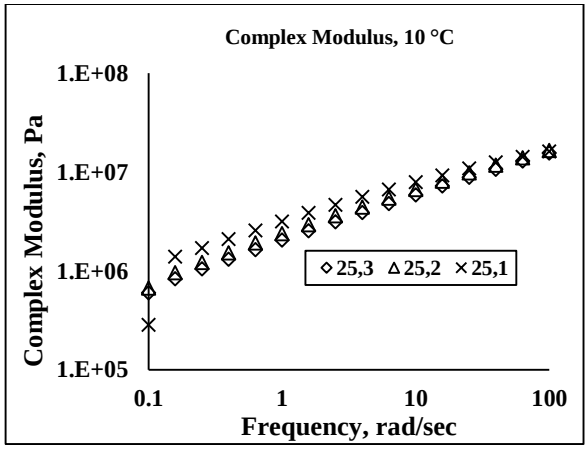

g

Figure 5.26 (a-g) Complex modulus curves for PMB (E) for 25 mm plate diameter corresponding to different gap width.

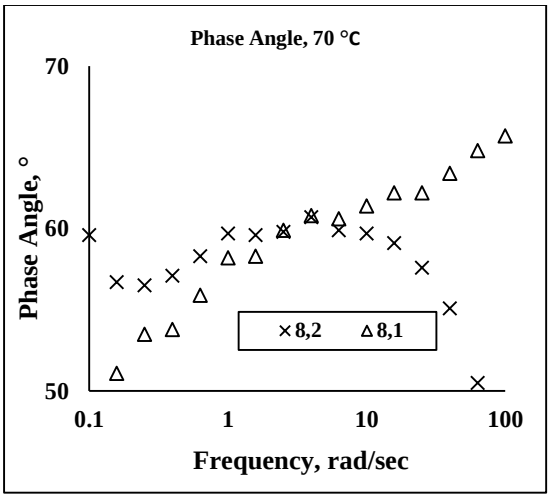
Phase Angle, 70 °C
Phase Angle, °
70
60
50
0.1
1
10
100
Frequency, rad/sec
×8,2 △8,1

a

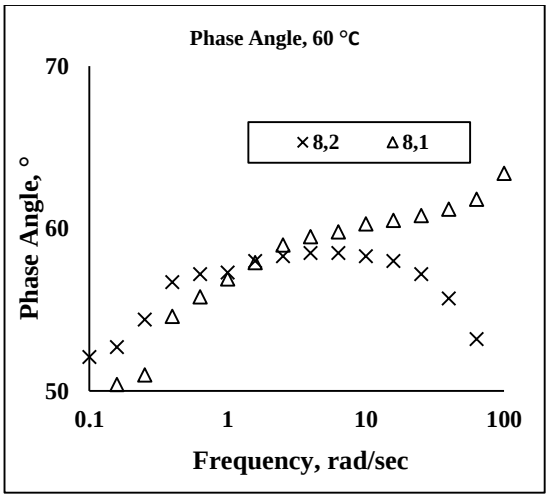
Phase Angle, 60 °C
Phase Angle, °
70
60
50
0.1
1
10
100
Frequency, rad/sec
×8,2 △8,1

b

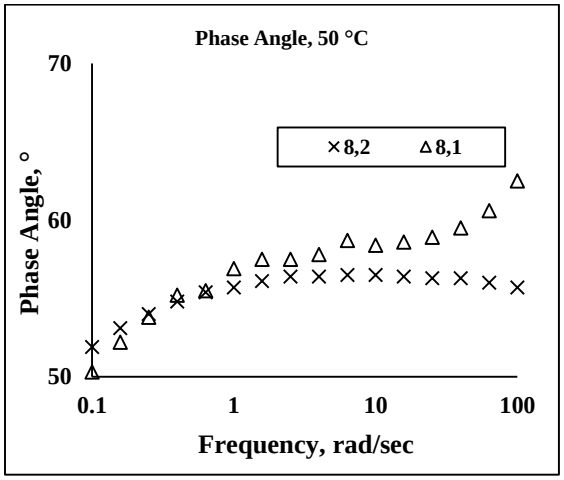
Phase Angle, 50 °C
Phase Angle, °
70
60
50
0.1
1
10
100
Frequency, rad/sec
×8,2 △8,1

c

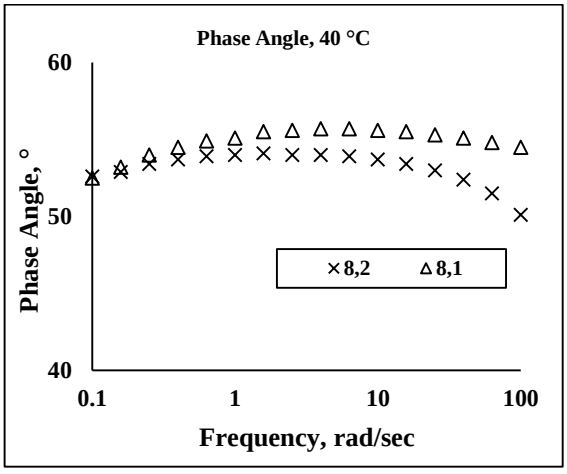
Phase Angle, 40 °C
Phase Angle, °
60
50
40
0.1
1
10
100
Frequency, rad/sec
×8,2 △8,1

d

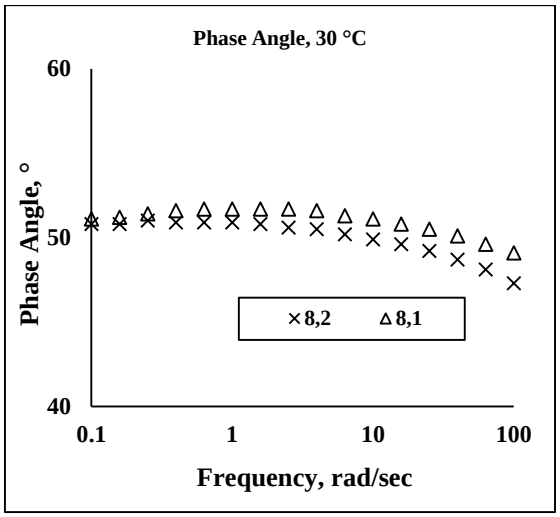
Phase Angle, 30 °C
Phase Angle, °
60
50
40
0.1
1
10
100
Frequency, rad/sec
×8,2 △8,1

e

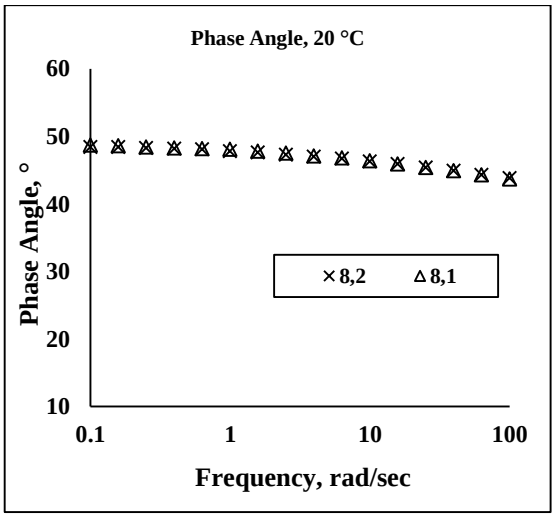
Phase Angle, 20 °C
Phase Angle, °
60
50
40
30
20
10
0.1
1
10
100
Frequency, rad/sec
×8,2 △8,1

f

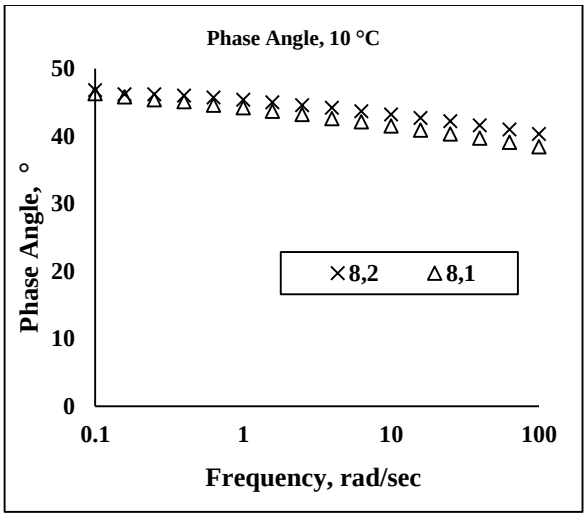

g

Figure 5.27 (a-g) Phase angle curves for PMB (E) for 8 mm plate diameter corresponding to different gap width.

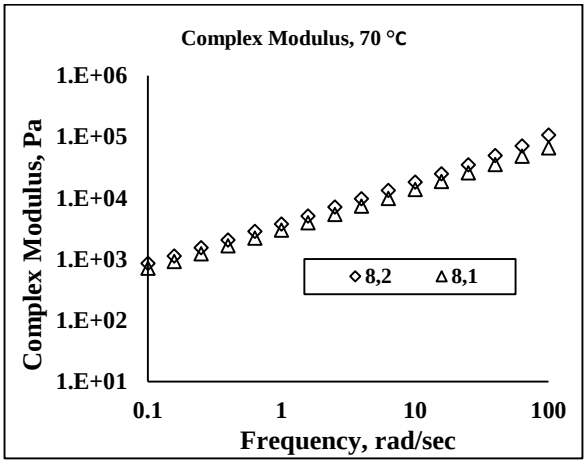

a

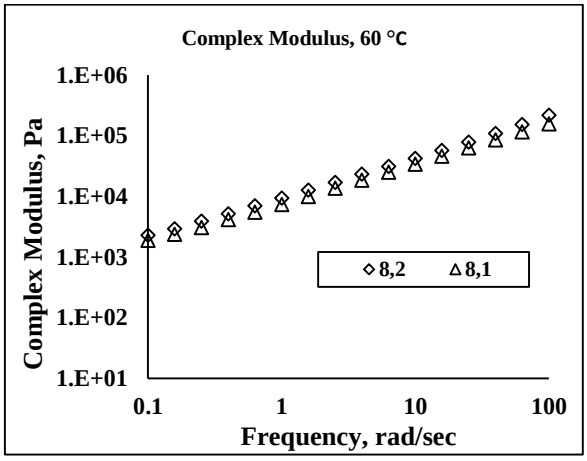

b

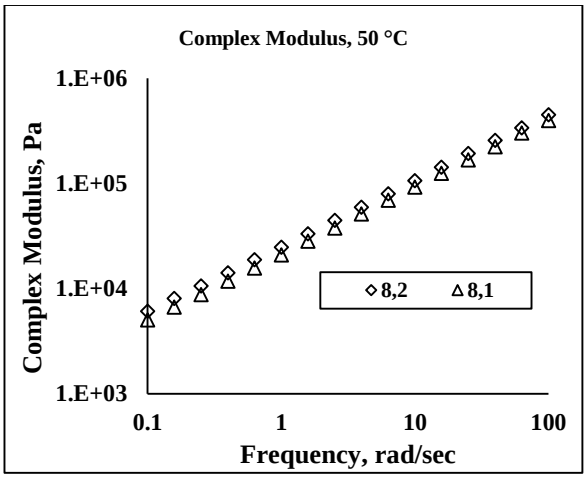

c

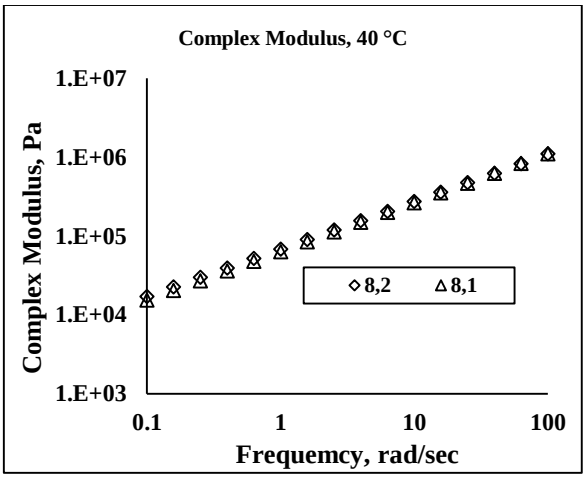

d

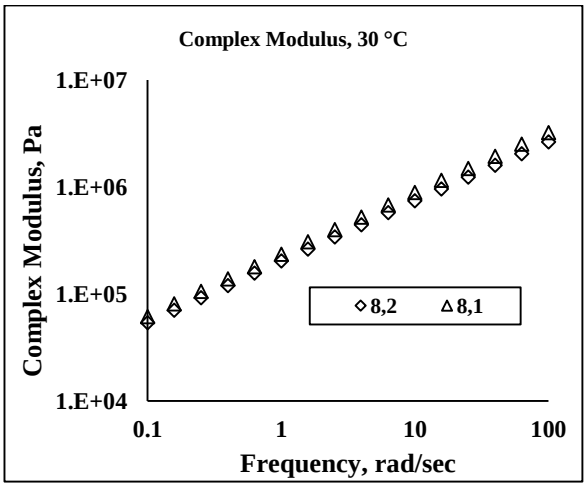

e

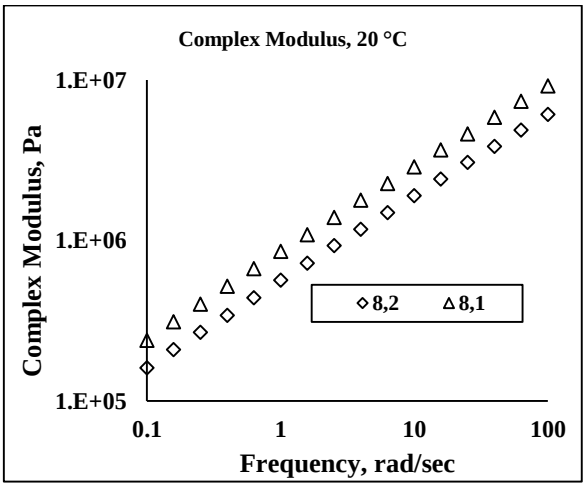

f

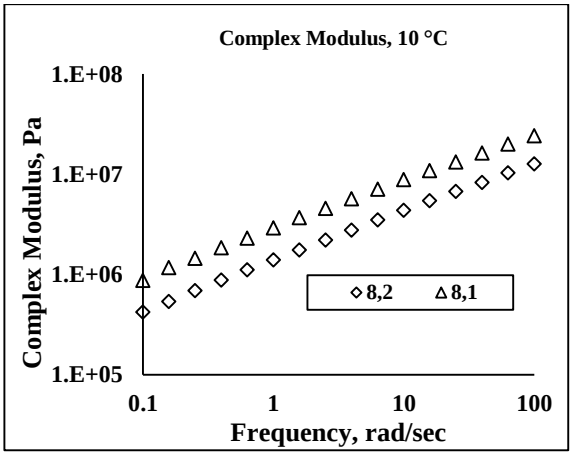

g

Figure 5.28 (a-g) Complex modulus for PMB (E) for 8 mm plate diameter corresponding to different gap width.

It can be seen that spindle geometry plays a crucial role in determination of rheological properties of both conventional and modified binders. A change in spindle diameter and plate gap changes the value of the rheological parameter. The changes are more pronounced at lower and higher temperatures. One conclusion which could be drawn from the study is that 8 mm spindle geometry cannot be used for higher temperatures and is suitable for temperature range of 10- 30 °C typically. The question to be answered is that which plate gap for 8 mm diameter spindle is suitable for characterizing the true rheological behavior of the binders at lower temperatures. Another question which arises is that what plate gap for 25 mm is suitable and can 25 mm spindle be used at all temperatures.

Asphalt binder exists in thin films in an asphalt mix. With variation in film thickness the response of the binder to applied shear stress changes and hence the difference in rheological properties are obtained. Another aspect is that larger diameter is more suitable as it will have larger contact area and lower edge effects as compared to 8 mm spindle diameter. The choice of spindle gap should be consistent for a study. DSR can be said to accurately quantify the "relative" rheological behavior of the binders. The term 'relative' is important as the values obtained may not be the true value.

5.5.2 *Master curves*

5.5.2.1 Rheological investigation

The previous section demonstrated the effect of spindle geometry on the rheological measurements of asphalt binders. In this section the rheological properties are investigated for each binder using master curves. From 10- 30 °C, 8 mm spindle with 2 mm gap was used, whereas 25 mm spindle diameter with 1 mm plate gap was employed from 40- 70 °C.

After obtaining the values of the rheological functions like complex modulus (G*) and phase angle (δ), isothermal plots were plotted. Comparison of different isothermal plots for different temperature is a clumsy task. Moreover isothermal plots for small range of frequency do not provide a complete description of the viscoelastic behavior of bitumen. So G* and δ master curves were further plotted at reference temperatures of 20, 40 and 60 °C.

Manual shift was employed first at each reference temperature to obtain a smooth curve (if possible). Next, different shift factors as mentioned above were also used to make

a comparison and their validation in obtaining master curves at any reference temperature chosen. Variation of shift factor was found by plotting the manual shift factors as the abscissa and the shift factors of various other models as ordinate. Deviation from the equality line would mean poor correlation.

5.5.2.1.1 Isothermal plots

Figure 5.29 (a-h) shows the isothermal plots of complex modulus and phase angle at different temperatures. It can be seen in complex modulus curves that the stiffness of PMB (E) is highest followed by PMB (S), VG 30 and VG 10. All the stiffness curves are consistent at all the temperatures. In general the stiffness of the binder increases with increase in frequency and reduction in temperature. The rate of change of modulus with change in frequency was found lower for modified binders (as can be seen by the slope) indicating lower susceptibility to loading rate. The curve describes the dominance of modification at higher temperature and lower frequency, where due to the reduction in viscosity of the base binder, the polymer network controls the viscoelastic response of the binder. On the other hand at lower temperatures and higher frequency the stiffness of the base binder is high enough which suppresses the control of polymer with regard to the rheological properties of the binder.

The phase angle is more sensitive to changes in chemical aspects of the binder. Modification with elastomers tends to increase the elastic component of the binder, as seen by the reduction in phase angle. Furthermore, polymer modified binder is less susceptible to frequency as seen by the slope of the curves in which the reduction in phase angle due to increase in frequency is least in EVA modified binder. A noticeable fact was seen in the phase angle plots at higher temperatures. After 40 °C, PMB (E) shows increase in phase angle, this phenomena being more dominant at lower frequency. This may be strongly attributed to the melt of EVA crystallites, which tend to shift its behavior towards the base binder. This change in property was not given by the complex modulus curves. Therefore the study of phase angle was found to be an important tool in broadly classifying the performance of modified binders. A conclusion based on complex modulus alone, which is a replica of the physical aspects of the binders, can be misleading and questionable. PMB (S) was found to be least susceptible to temperature among all the binders considered. Also

'wavy' nature of curves for modified binders at higher temperatures gave strong evidence of the dominative polymer network. These wavy natures are consistent with the findings done by Airey [6].

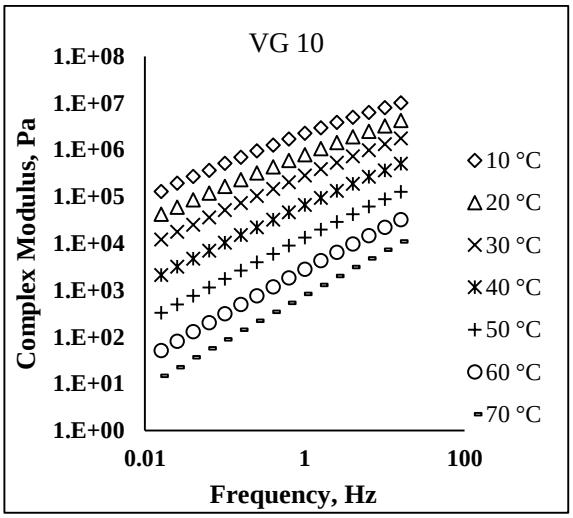

a

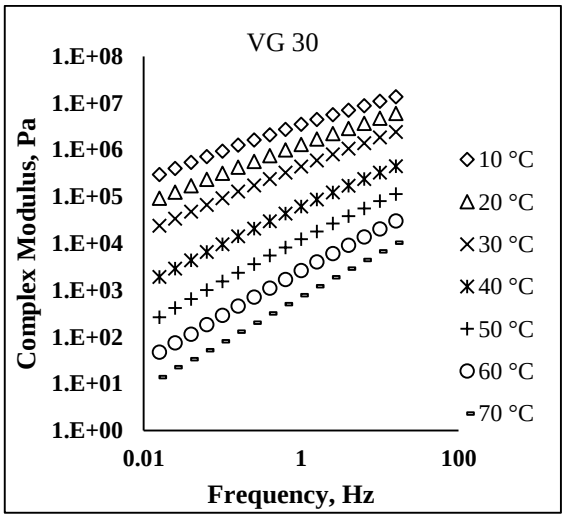

b

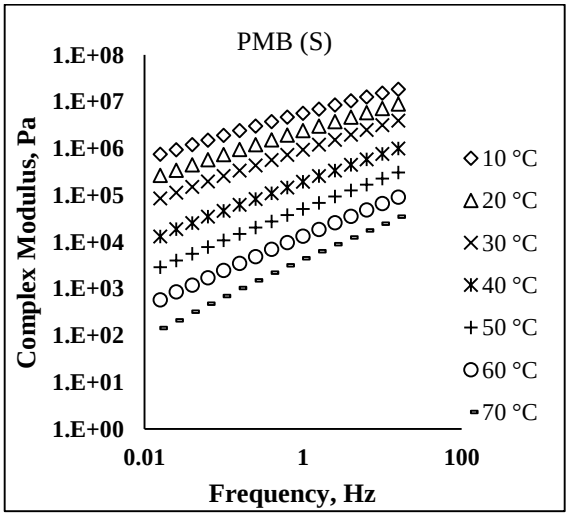

c

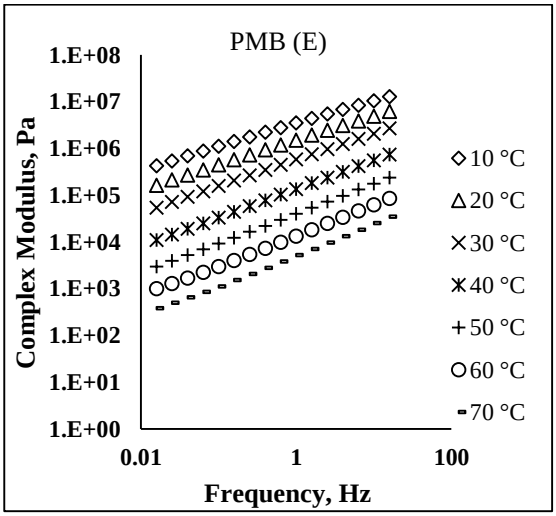

d

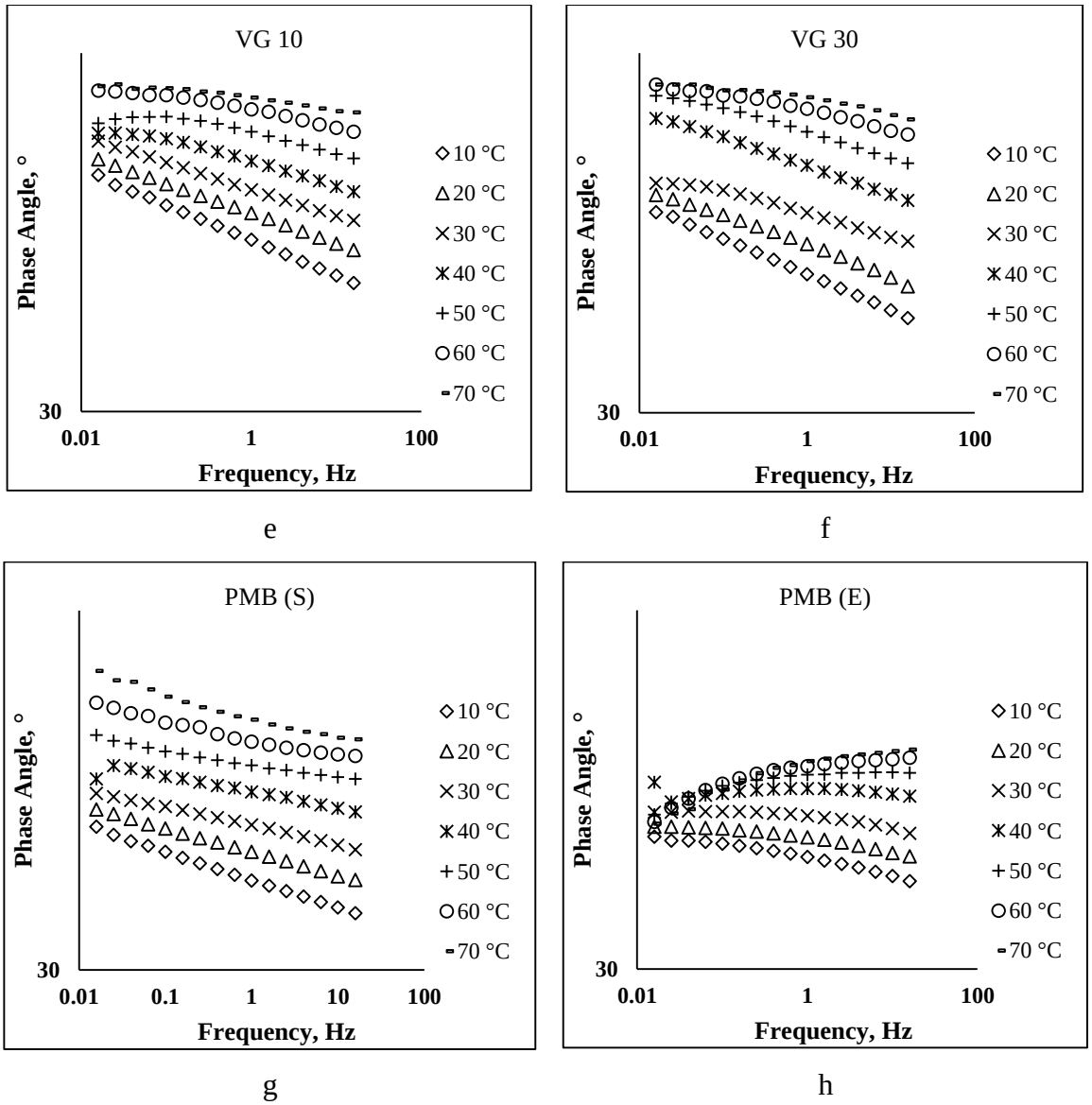

Figure 5.29 (a-h) Complex modulus and phase angle master curves

Figures 5.30 to Figure 5.33 shows the complex modulus and phase angle master curves drawn for all the binders at three different reference temperatures of 20, 40 and 60 °C. Complex modulus for all binders decreases with increase in temperature. The curves for modified binders are less steep than the conventional binders, indicating lesser susceptibility of modified binders with respect to temperature and frequency. It can be seen that at very low frequency the curves at all the reference temperature tend to merge to a single asymptotic value. This is also known as the 'Glassy Modulus' for bitumen which is independent of the temperature chosen.

Phase angle master curves gave diverse results. It was not possible to construct a smooth phase angle master curve for PMB (E). This may be attributed to the deviation from thermorheological simplicity for this binder. This difference was not revealed by complex modulus master curves, which produced smooth curves irrespective of the type of binder (as can be seen below). The phase angle is more sensitive to changes in chemical aspects of the binder, which might be the sole reason for occurrence of 'wavy' phase angle master curves mostly at higher temperature and lower frequency. Conventional binders, on the other hand produced smooth phase angle master curves at all the reference temperatures. As the frequency increases the elastic component of the binder increases, as seen by the reduction in phase angle. At around 60 °C, VG-10 and VG-30 almost behave like a Newtonian fluid with phase angle very close to 90˚.

The study showed that there stands a difference when viewing and comparing the viscoelastic properties of binders with respect to its physical and chemical nature. Though phase angle master curve plots for modified binders were not smooth yet complex modulus master curves can be plotted for the same. So it can be assumed that there are two thermorheological simplicity existence- one in its physical state as given by complex modulus master curves, and the other which describes changes in the chemical state, i.e. as given by the phase angle master curve. A binder may be thermorheologically simple in its physical state, but at the same time it may be complex in its chemical state. So the conclusion of thermorheological simplicity cannot be made only on the basis of complex modulus master curves.

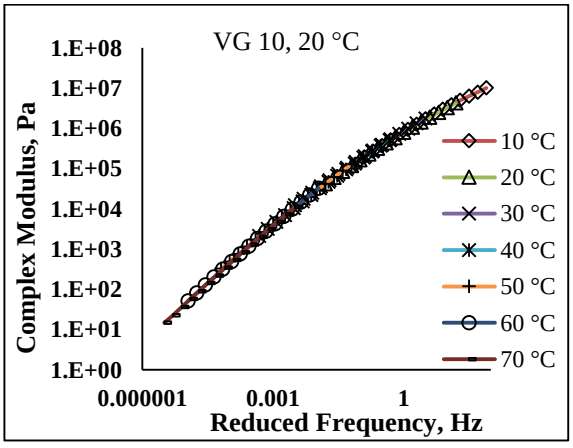

a

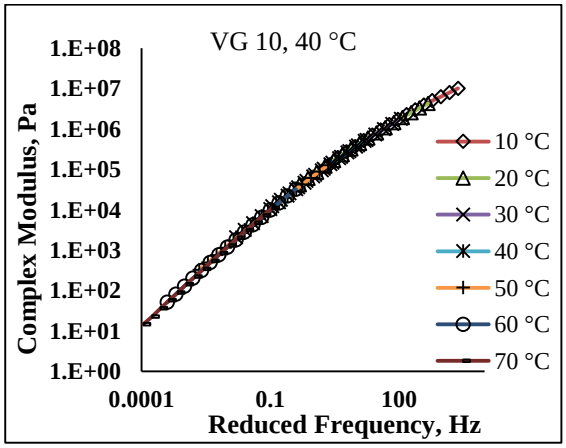

b

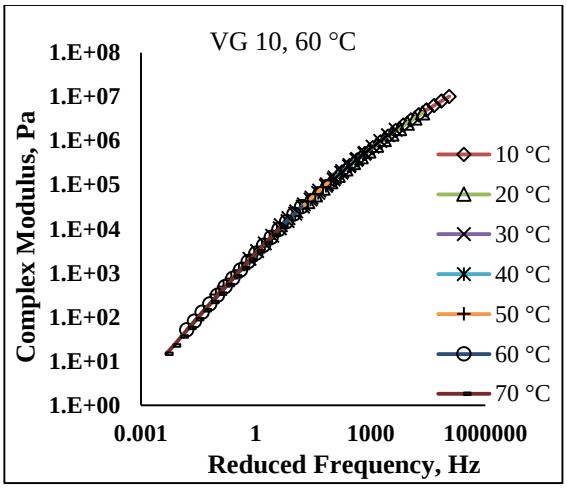

c

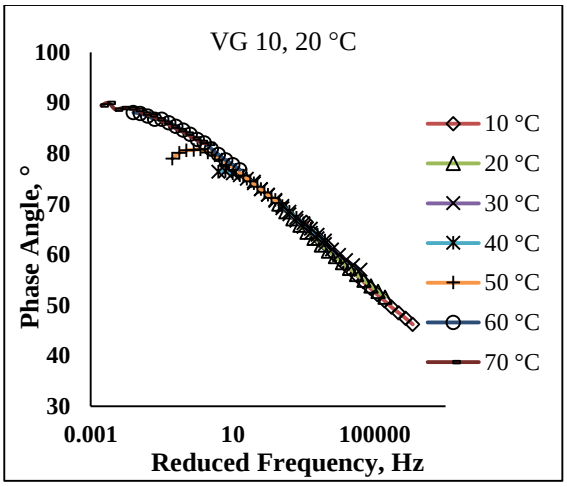

d

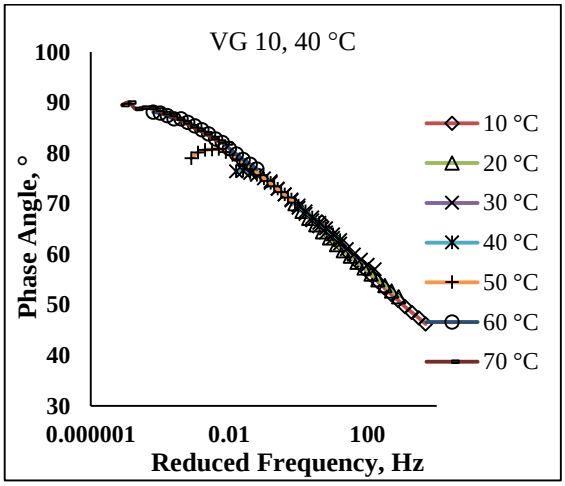

e

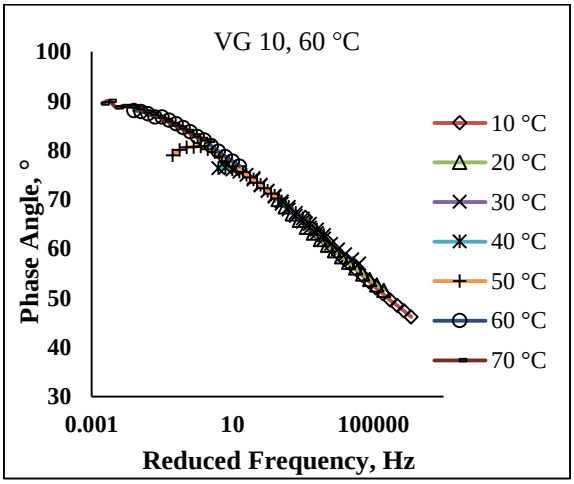

f

Figure 5.30 (a-f) Complex modulus and phase angle master curves for VG 10

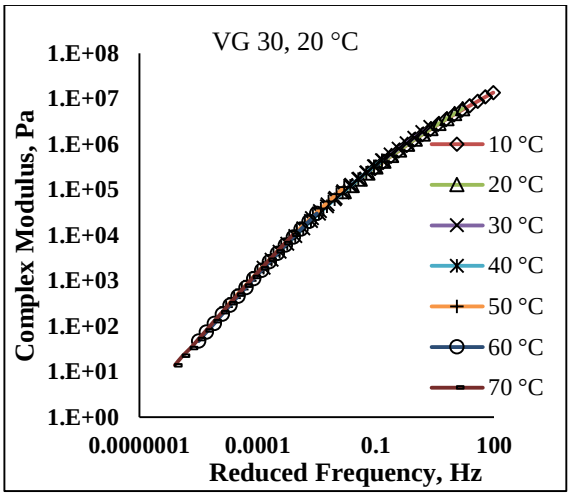

a

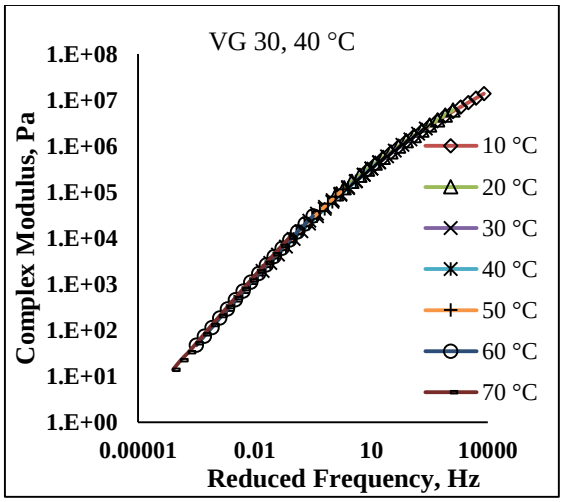

b

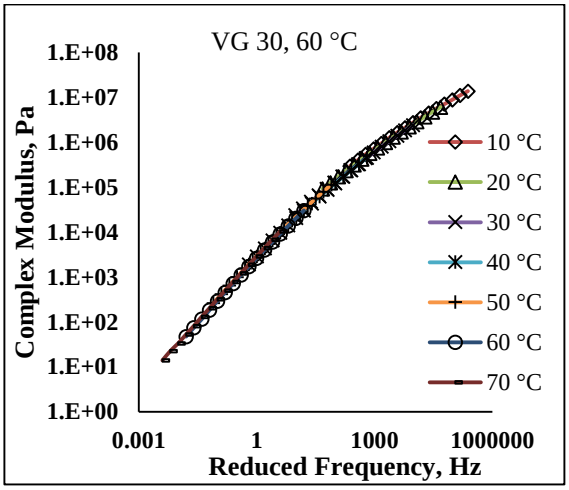

c

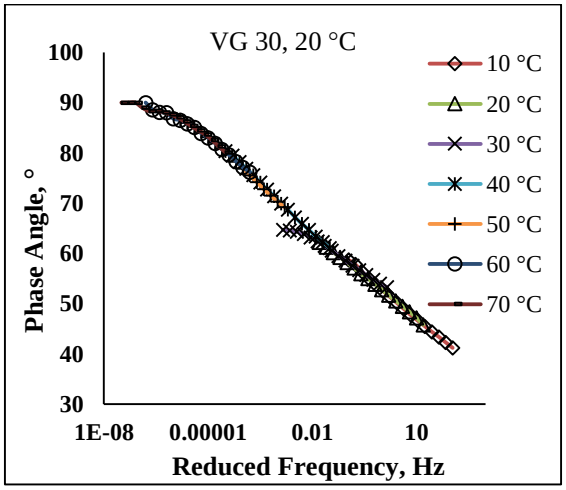

d

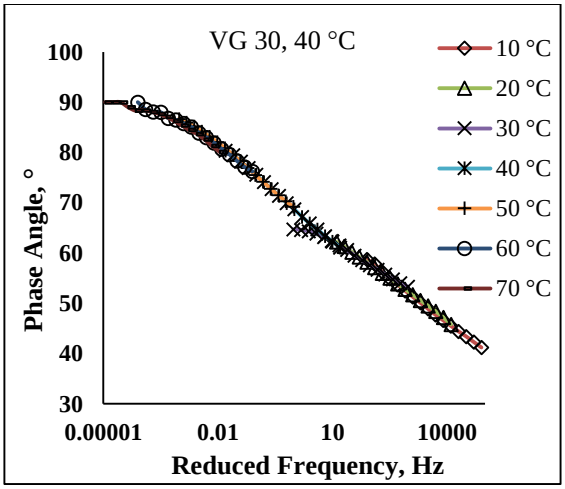

e

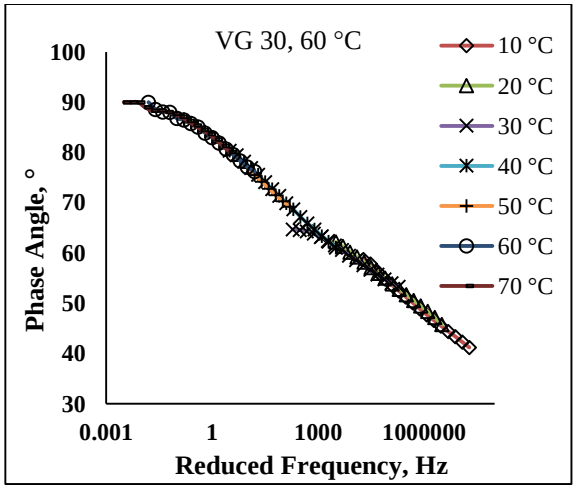

f

Figure 5.31 (a-f) Complex modulus and phase angle master curves for VG 30

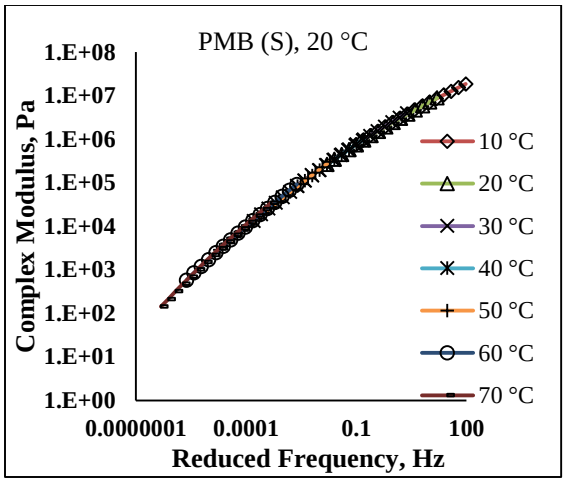

a

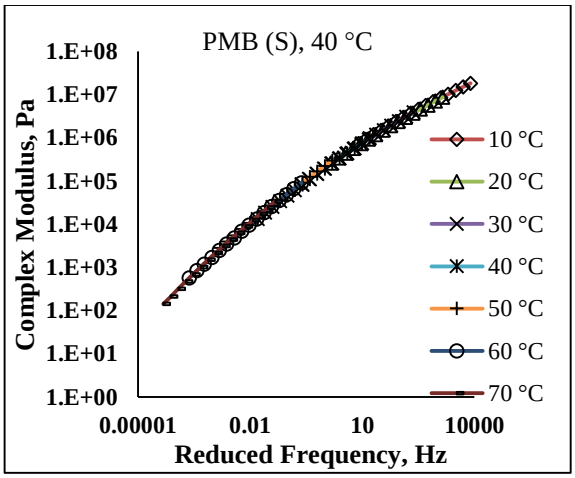

b

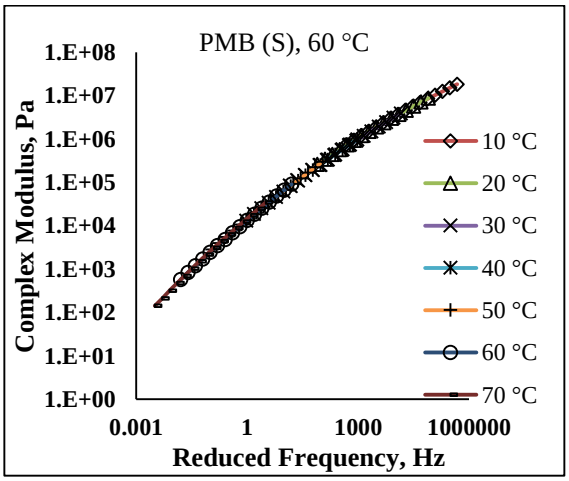

c

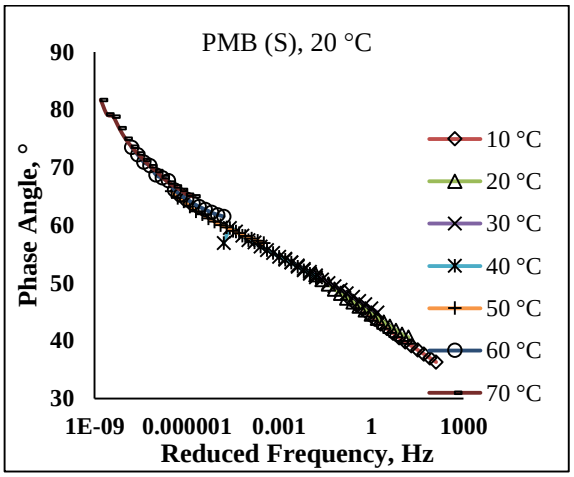

d

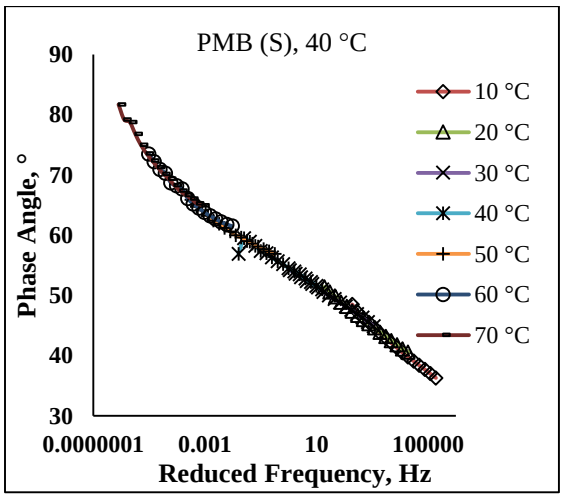

e

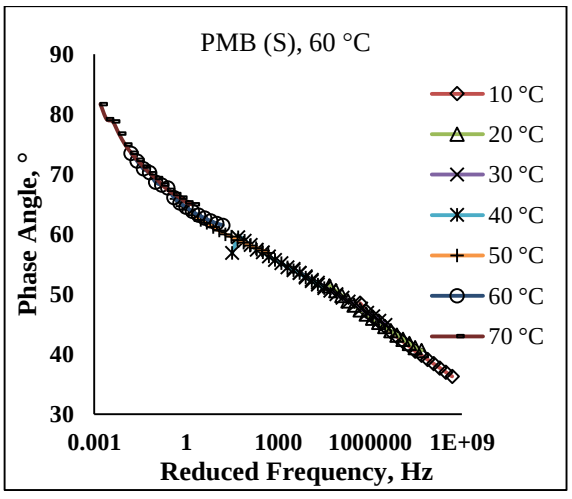

f

Figure 5.32 (a-f) Complex modulus and phase angle master curves for PMB (S)

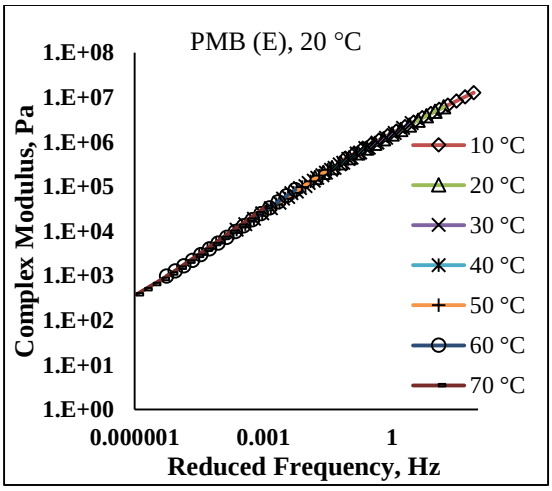

a

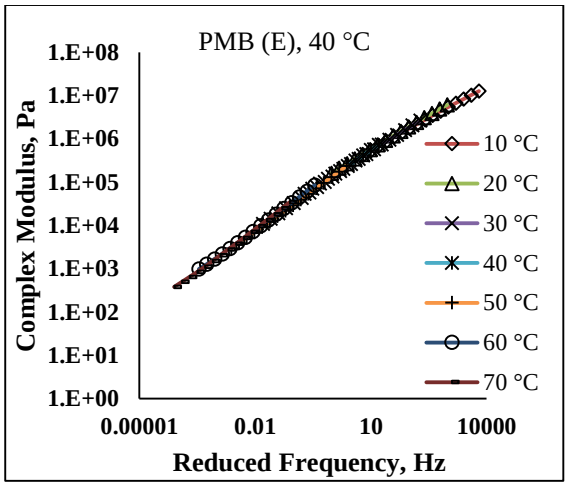

b

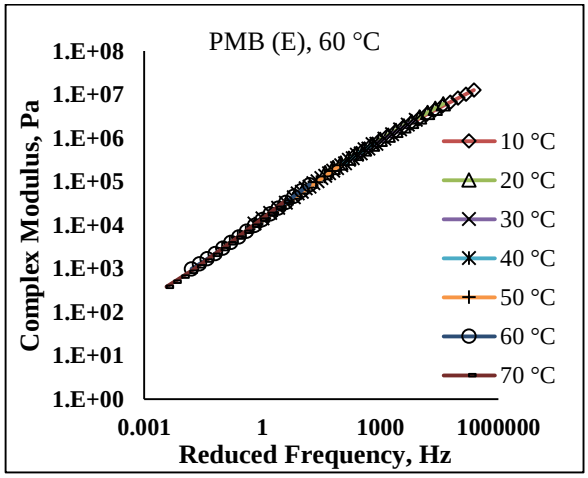

c

Figure 5.33 (a-c) Complex modulus master curves for PMB (E)

5.5.2.2 Shift factor analysis

Considering the drawbacks of WLF and Arrhenius equations for obtaining the shift factors (discussed in chapter 2), a new method was proposed for automatically obtaining the shift procedure. The procedure is explained in the following section.

5.5.2.2.1 New method proposed

Appreciating the fact that thermorheological simplicity can be validated if a smooth curve is obtained after shifting the data at a particular reference temperature, it would be more convenient to introduce a process which will shift the data till a best fit is obtained and

will return the shift factors once shifting is accomplished. Finally the graph so obtained can be analyzed visually to see if the material obeys time temperature superposition principle.

A new procedure was hence introduced and was programmed using MATLAB. The method is named as 'Equivalent Slope Method' and could be used to plot master curve for any rheological parameter requiring horizontal shift at any reference temperature. The base behind the development of this procedure is that stress function for two different temperatures merges to a single or nearly similar value, but at different frequency. So shifting the curve till the slope at few desired points become similar would yield a smooth master curve, provided thermorheological simplicity prevails.

The algorithm adopted for preparing the program for obtaining shift factor is presented in Figure 5.34. Few terms are defined formerly to understand the procedure.

$$i \rightarrow Frequency, i \in [1, k]$$
$$j \rightarrow Temperature,\ j \in [10, 70]$$
$$T_R \rightarrow Reference\ Temperatrure, R \subset j$$
$$Y_{i,j} \rightarrow Value\ of\ Y\ variable\ at\ Frequency\ i\ and\ Temperature\ j$$

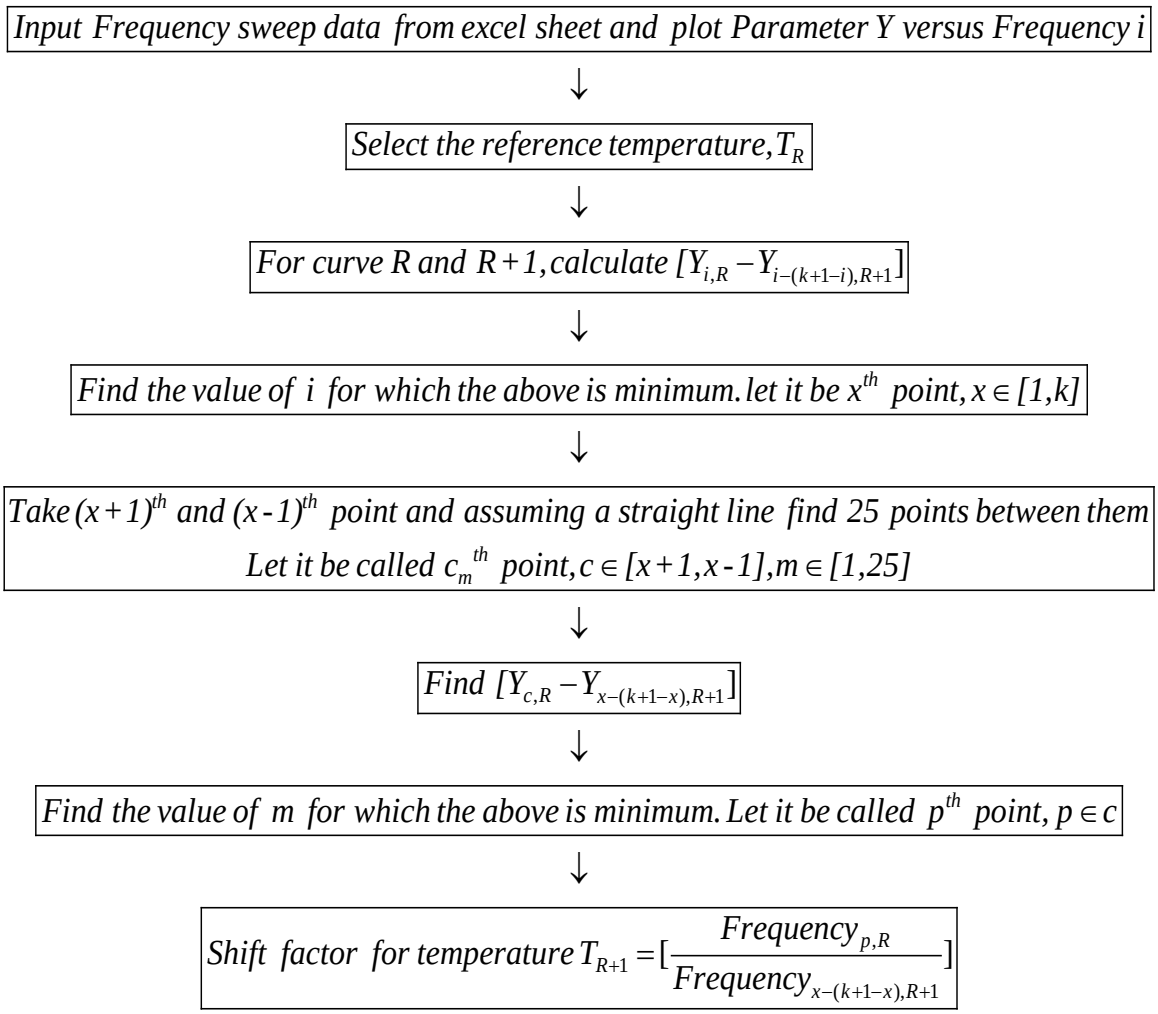

Figure 5.34 Algorithm adopted for preparing the program for obtaining shift factor

The above concept is extended similarly for other temperatures, below and above the reference temperature. This method can be used to construct master curve for stress functions in which horizontal shift is required.

Figure 5.35 (a-f) shows the graphical representation of various shift factor laws plotted against manual shift factors for VG 10 and PMB (E) at reference temperatures of 20, 40 and 60 °C. Manual shift factors were obtained by manually shifting all the isothermal plots to a single reference temperature to obtain a smooth fit. Higher deviation from the equality line would indicate a poor correlation of the shift factor in obtaining the master curve. WLF, Arrhenius and equivalent slope shift factors were considered for correlation. C_1

and C_2 value in WLF were considered to be 8.86 and 101.6 as given by William et.al. The value of E_a in Arrhenius equation was found by optimizing the sum of least squares with respect to manual shift using SOLVER function in MS EXCEL.

It was found that different shift factors for phase angle and complex modulus are required at the same reference temperature for obtaining a smooth master curve. A single set of shift factor cannot be used to describe the master curve for these two parameters as both represent different aspects of the same binder. Moreover, for modified binders it was not possible to obtain phase angle master curve due to the deviation from chemical thermorheological simplicity, as mentioned earlier.

The WLF equation had very poor correlation at all the reference temperatures chosen in the study as shown in figures below. It was found that WLF equation yielded similar shift factor as that with the manual shift for temperature lower than the reference temperature. For higher temperatures, it produced very high values. At a reference temperature of 60 ℃ very poor shift was obtained by using WLF equation. This may be due to the William's constant used in the study. Optimizing the constants could give a more accurate value, but was out of the scope of the study.

Analysis using Arrhenius constants gave several outcomes. First, the E_a values obtained for PMB (E) was highest followed by PMB (S), VG-30 and VG 10. This should be true, as higher stiffness of PMB (E) will require higher energy for starting molecular movements. Arrhenius constants gave poor correlation with the manual shift for complex modulus, but were rational in describing the master curve for phase angle. Good correlation of Arrhenius equation with phase angle master curve indicated that the Arrhenius equation is better in describing the chemical aspects of the binder rather than its physical nature.

The shift factor obtained by the equivalent slope method which was developed in the study gave the best results. It was obvious as the method considered minimization of the slope of the isothermal plots, so that a smooth curve can be obtained. This method was also found useful in describing the thermorheological complexity of the binder and will yield 'no' result for thermorheological complex binder, as the software will not be able to plot a smooth curve. Figure 5.36 (a-c) shows the complex modulus master curve obtained for VG-10 at all the temperatures using this method.

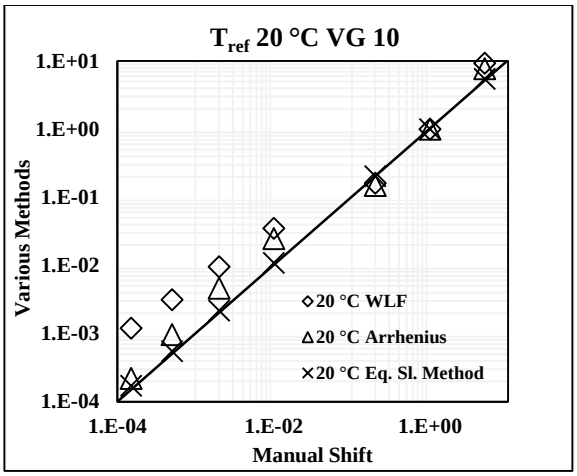

a

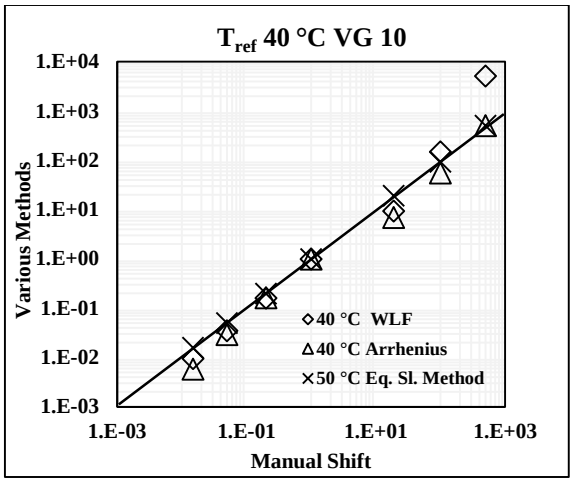

b

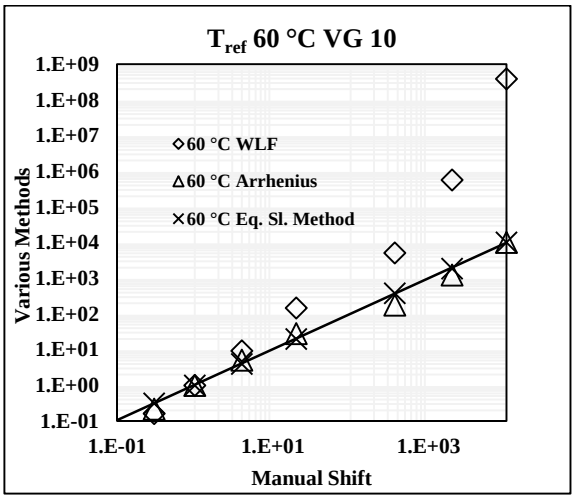

c

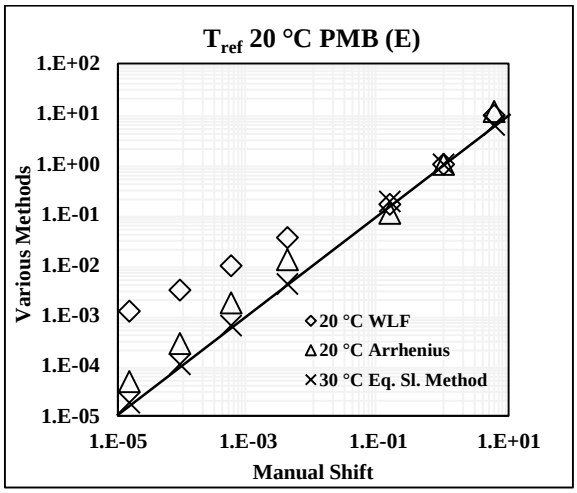

d

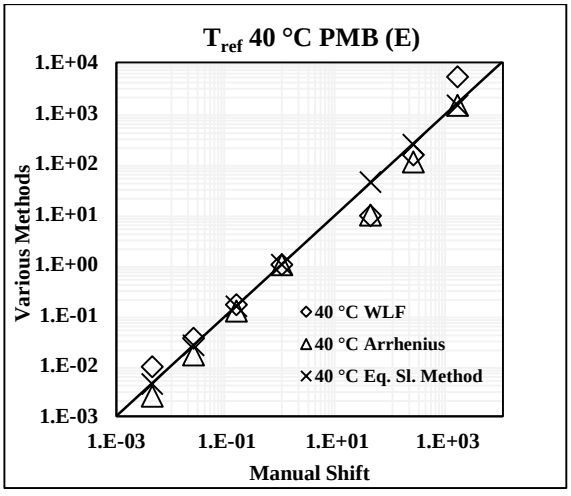

e

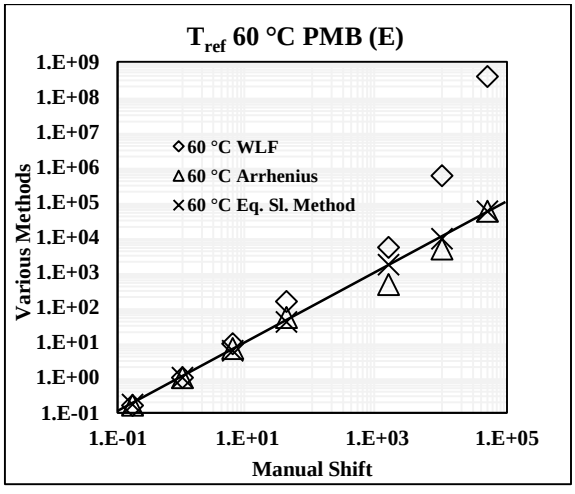

f

Figure 5.35 (a-f) Shift factors using different methods for VG 10 and PMB (E)

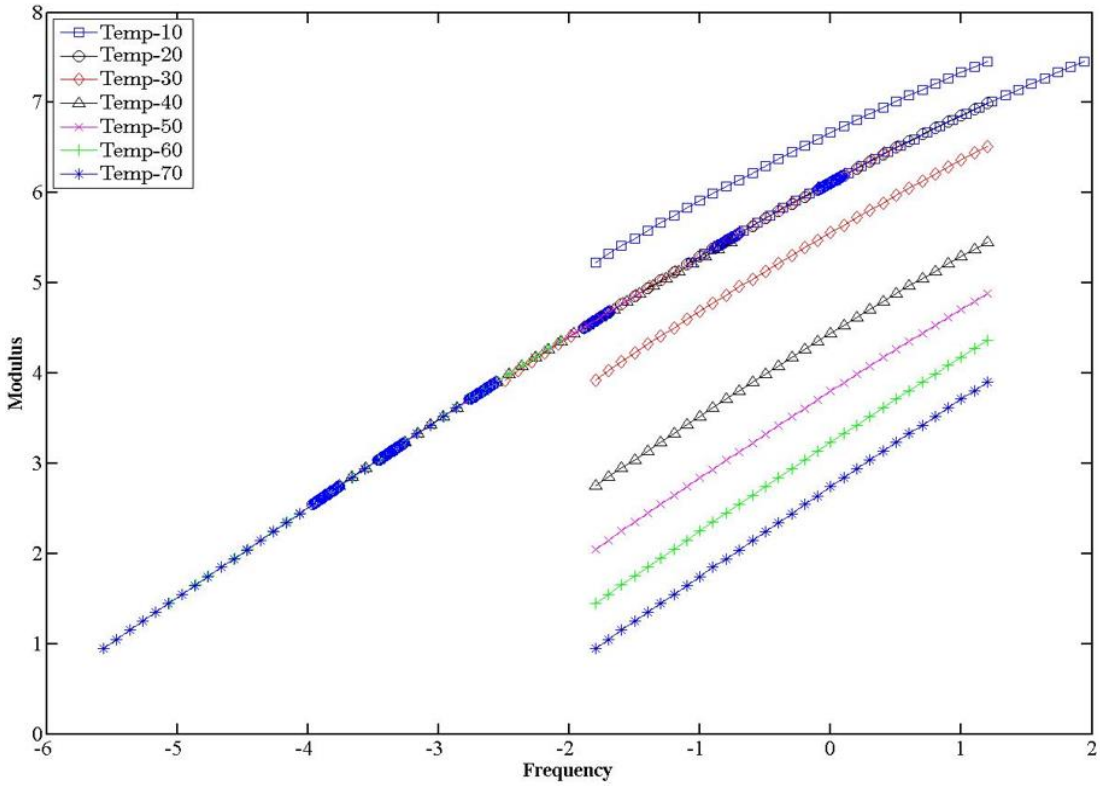
Temp-10
Temp-20
Temp-30
Temp-40
Temp-50
Temp-60
Temp-70
Modulus
Frequency
0
1
2
3
4
5
6
7
8
-6
-5
-4
-3
-2
-1
0
1
2

a

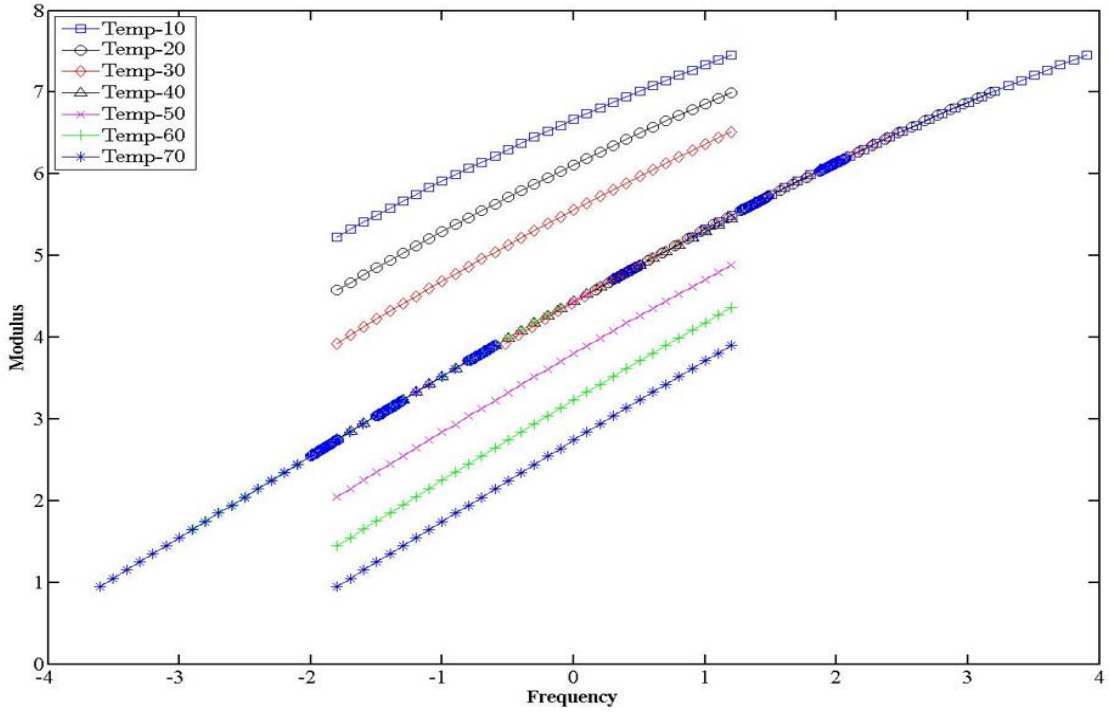
Temp-10
Temp-20
Temp-30
Temp-40
Temp-50
Temp-60
Temp-70
Modulus
Frequency
0
1
2
3
4
5
6
7
8
-4
-3
-2
-1
0
1
2
3
4

b

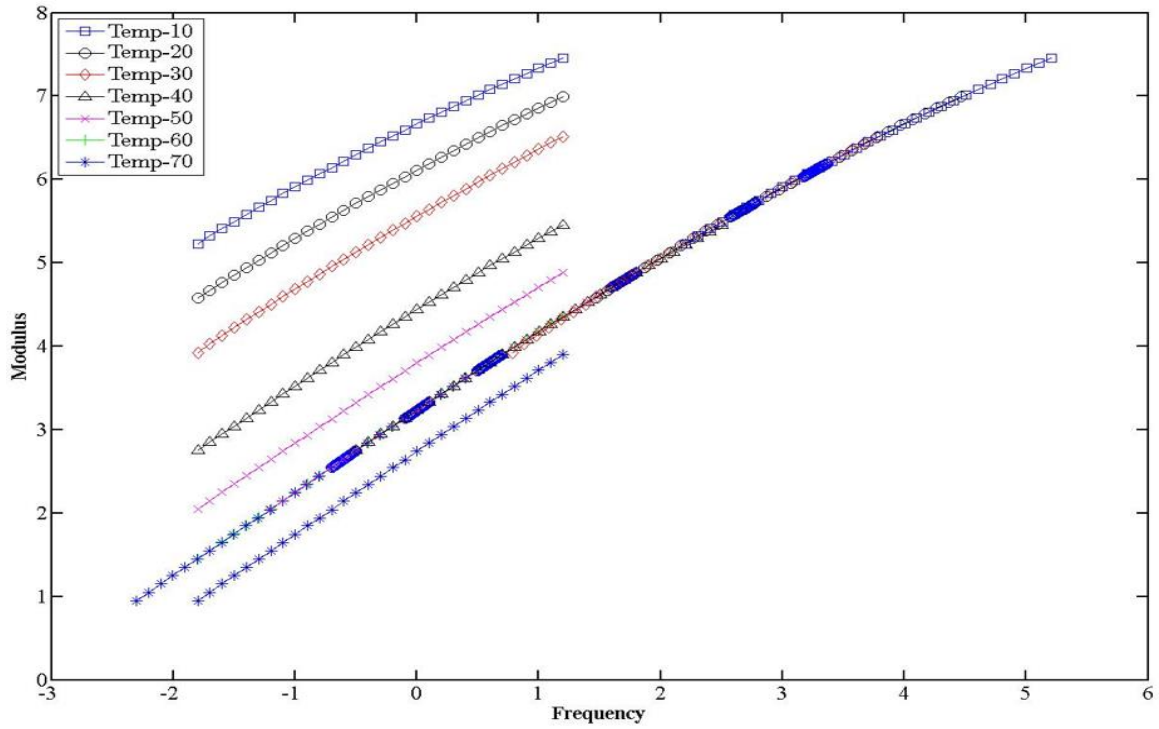

c

Figure 5.36 (a-c) Simulated curves in MATLAB using equivalent slope method for VG 10

5.5.2.2.2 Modelling shift factors

The shift factor for all the binders at different reference temperature was found to obey exponential law of the form

$$a_T = A.\exp^{(-B.T)} \tag{5.6}$$

where, *A* and *B* are the model parameters, dependent on the reference temperature and the type of binder. *'A'* increases with increase in the reference temperature, whereas B for a particular binder was found to be invariable irrespective of any reference temperature. The value of 'B' roughly was found to be nearly 0.2 for all the binders. The value of *'A'* for a particular reference temperature was higher for stiffer binder, PMB (E) having the highest value whereas VG 10 having the least. As an example, Figure 5.37 (a-l) shows the variation of a_T with temperature for all the binders at reference temperatures of 20, 40 and 60 °C and the corresponding exponential fit. Very high coefficient of determination (R^2) was found for

all the binders. Variation at other reference temperatures, though not shown, follows similarly.

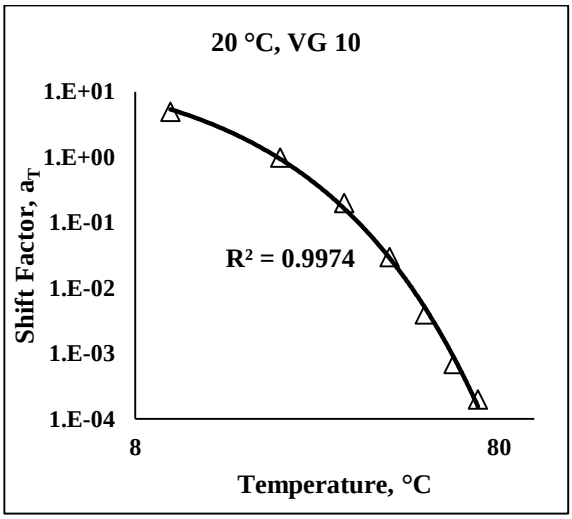

a

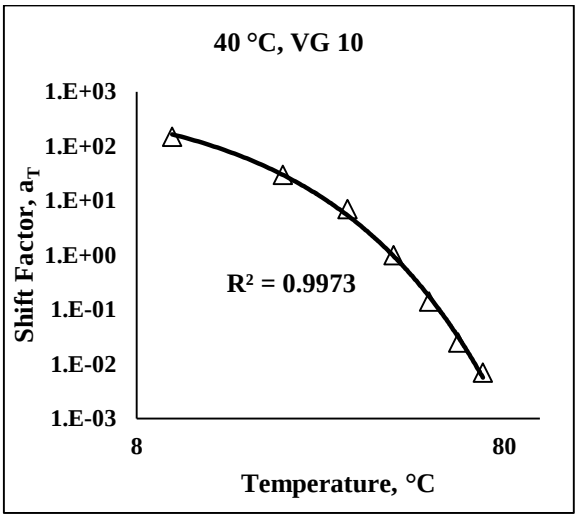

b

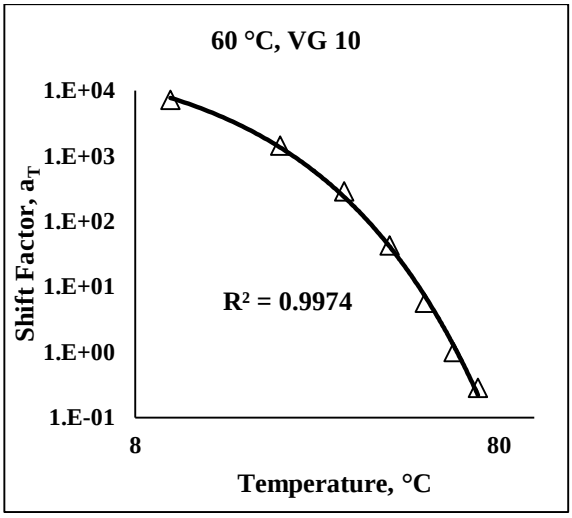

c

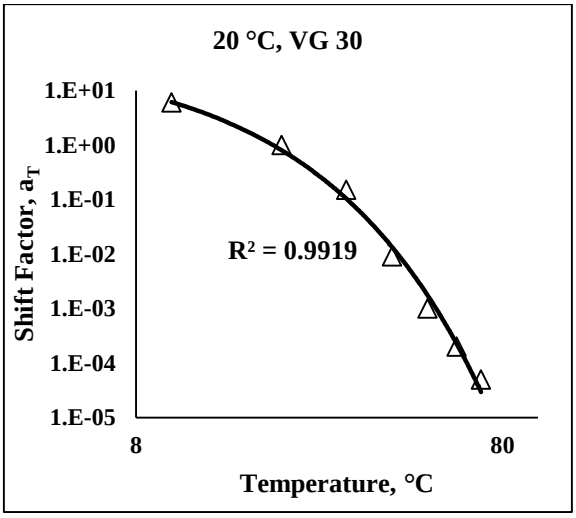

d

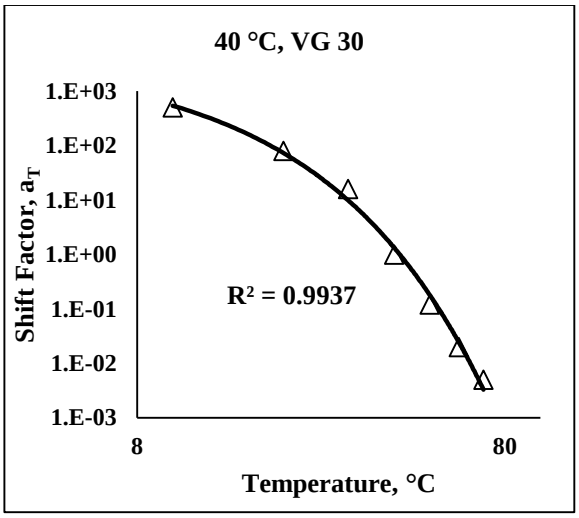
40 °C, VG 30
1.E+03
1.E+02
1.E+01
1.E+00
1.E-01
1.E-02
1.E-03
Shift Factor, a_T
R² = 0.9937
8
80
Temperature, °C

e

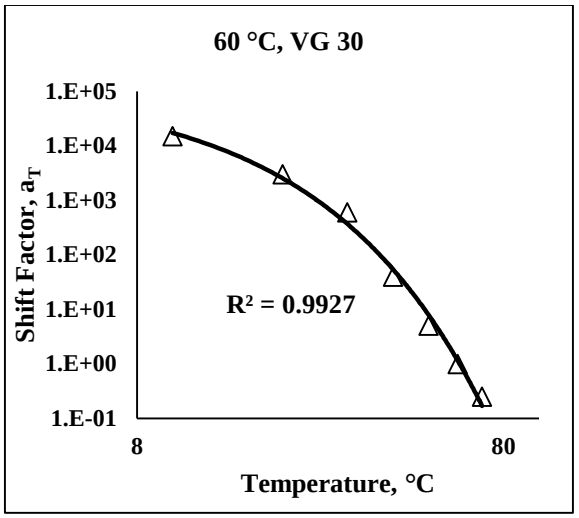
60 °C, VG 30
1.E+05
1.E+04
1.E+03
1.E+02
1.E+01
1.E+00
1.E-01
Shift Factor, a_T
R² = 0.9927
8
80
Temperature, °C

f

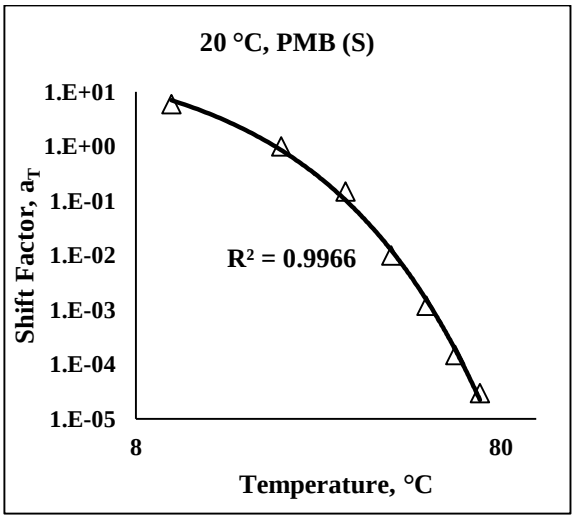
20 °C, PMB (S)
1.E+01
1.E+00
1.E-01
1.E-02
1.E-03
1.E-04
1.E-05
Shift Factor, a_T
R² = 0.9966
8
80
Temperature, °C

g

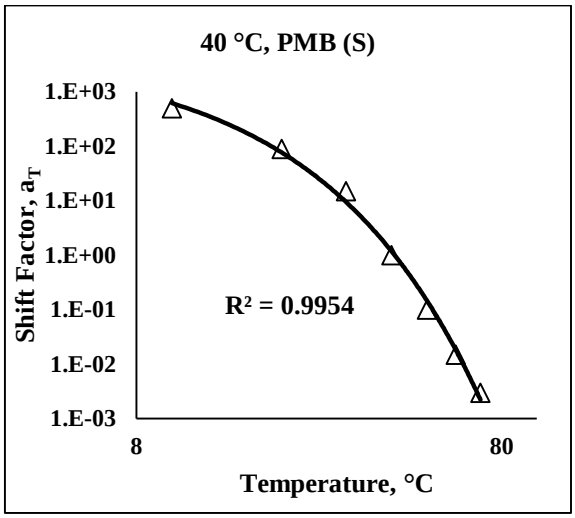
40 °C, PMB (S)
1.E+03
1.E+02
1.E+01
1.E+00
1.E-01
1.E-02
1.E-03
Shift Factor, a_T
R² = 0.9954
8
80
Temperature, °C

h

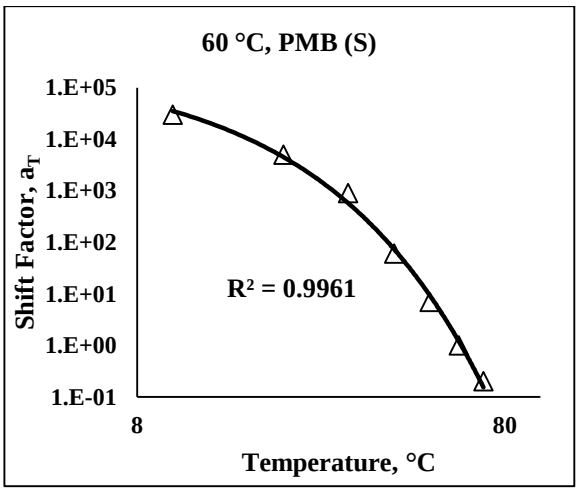
60 °C, PMB (S)
1.E+05
1.E+04
1.E+03
1.E+02
1.E+01
1.E+00
1.E-01
Shift Factor, a_T
R² = 0.9961
8
80
Temperature, °C

i

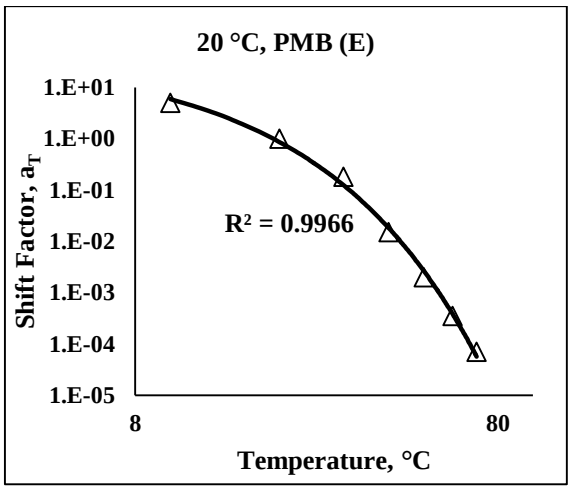
20 °C, PMB (E)
1.E+01
1.E+00
1.E-01
1.E-02
1.E-03
1.E-04
1.E-05
Shift Factor, a_T
R² = 0.9966
8
80
Temperature, °C

j

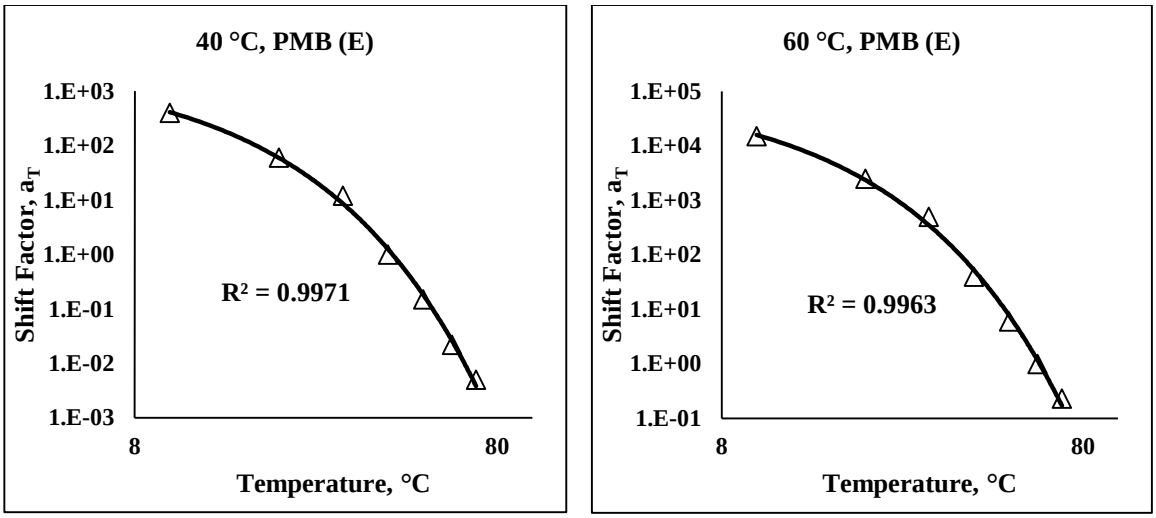

k l

Figure 5.37 (a-l) Exponential fitting of shift factors for different binders.

5.5.3 *Modelling the LVE master curves*

Predictive models and equations are excellent tools for quantifying the mechanical/rheological properties of any material. It is time saving, less laborious and doesn't require any skilled operators. Since 1950's researchers have tried to predict the linear viscoelastic characteristics of bitumen using nonlinear multivariable models, also known as nomographs. These nomographs were later replaced by empirical equations and the use of mechanical elements (spring and dashpot), for modelling the linear rheological properties. These techniques were mainly used for predicting variation of complex modulus and phase angle master curves, at any desired reference temperature. Yusoff et al. [196] presented a brief overview of all the models developed over the past years. Most of the algebraic models consist of large number of model parameters which are empirical and does not have any physical significance. A more simple model is hence desired which can be directly related to the flow properties of the binder.

5.5.3.1 Cox-Merz principle

The study of asphalt binder in dynamic and steady-state state are usually done separately. Researchers found that the association between these two states stands important for arriving at the rheological curves and mathematical interrelationships [27, 131, 152, 204].

Cox-Merz relationship is one such tool which connects the dynamic and steady-state properties [54, 185]. Cox-Merz relationship is an empirical relationship relating dynamic and steady-state viscosities applicable mainly to polymer melts. Cox and Merz [41] were the first researchers who observed that, the steady-state viscosity at some shear rate ($\dot{\gamma}$) can be successfully related to the dynamic complex viscosity as follows

$$\left|\eta^*(\omega)\right| = \eta(\dot{\gamma}) \tag{5.7}$$

$|\eta^*(\omega)|$ is the absolute value of complex viscosity at a frequency ω equal to the shear rate $\dot{\gamma}$. As an empirical relationship, its applicability as a general rule stands debatable [54, 152, 185]. Shan et al. [152] found that Cox-Merz relationship for bitumen is applicable in the shear-thinning region and is not always true in the zero-shear-rate-limiting viscosity region. Modifications and changes to the principle have also be done to relate the dynamic and steady state relationships.

5.5.3.2 Modeling complex viscosity/modulus master curves

Frequency sweep test was carried from 0.1-20 Hz from 10-70 ˚C, with temperature increment of 10 ˚C. The concept of rheogram as discussed in section 1.2 was used and master curves, independent of temperature, for all the binders were potted using the ZSV as obtained in the steady shear test. This was a form of validation of the relationship between the dynamic and the steady-state platform. If a smooth master curve could be produced, it would imply the applicability of Cox-Merz rule at least in the zero-shear domain. The rheogram for all the binders at all the three reference temperatures are shown in Figure 5.38 (a-d). It was found that excellent fit was obtained using the ZSV from the steady state as a shift factor for plotting the master curves. This led to the conclusion that Cox-Merz principle holds true for asphalt binders in the zero shear region and ZSV from steady state test can be successfully used as shift factors for construction of master curves in dynamic domain.

Similarly, complex modulus master curves using the same concept were plotted using the relationship:

$$\left|\eta^*\right| = \left|G^*\right| / \omega \tag{5.8}$$

Figure 5.39 (a-d) shows the complex modulus master curves for all the binders. Similar to complex viscosity, smooth master curves for complex modulus were also obtained. It has to be mentioned that these master curves are independent of temperature, and the strength of a particular binder could be obtained at any desired frequency and temperature, provided the ZSV is accurately known.

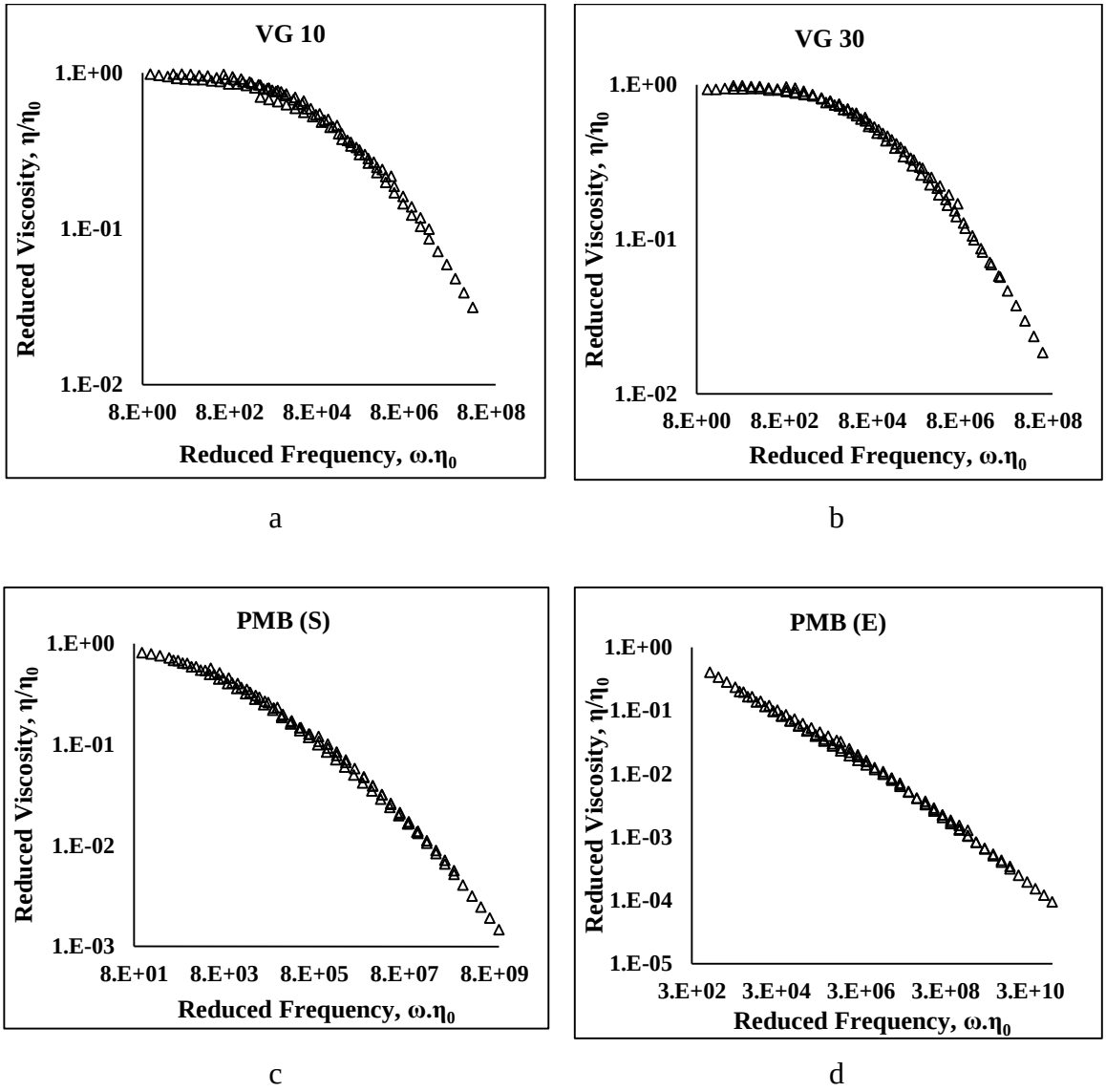

Figure 5.38 (a-d) Complex viscosity rheogram showing the validity of Cox-Merz principle.

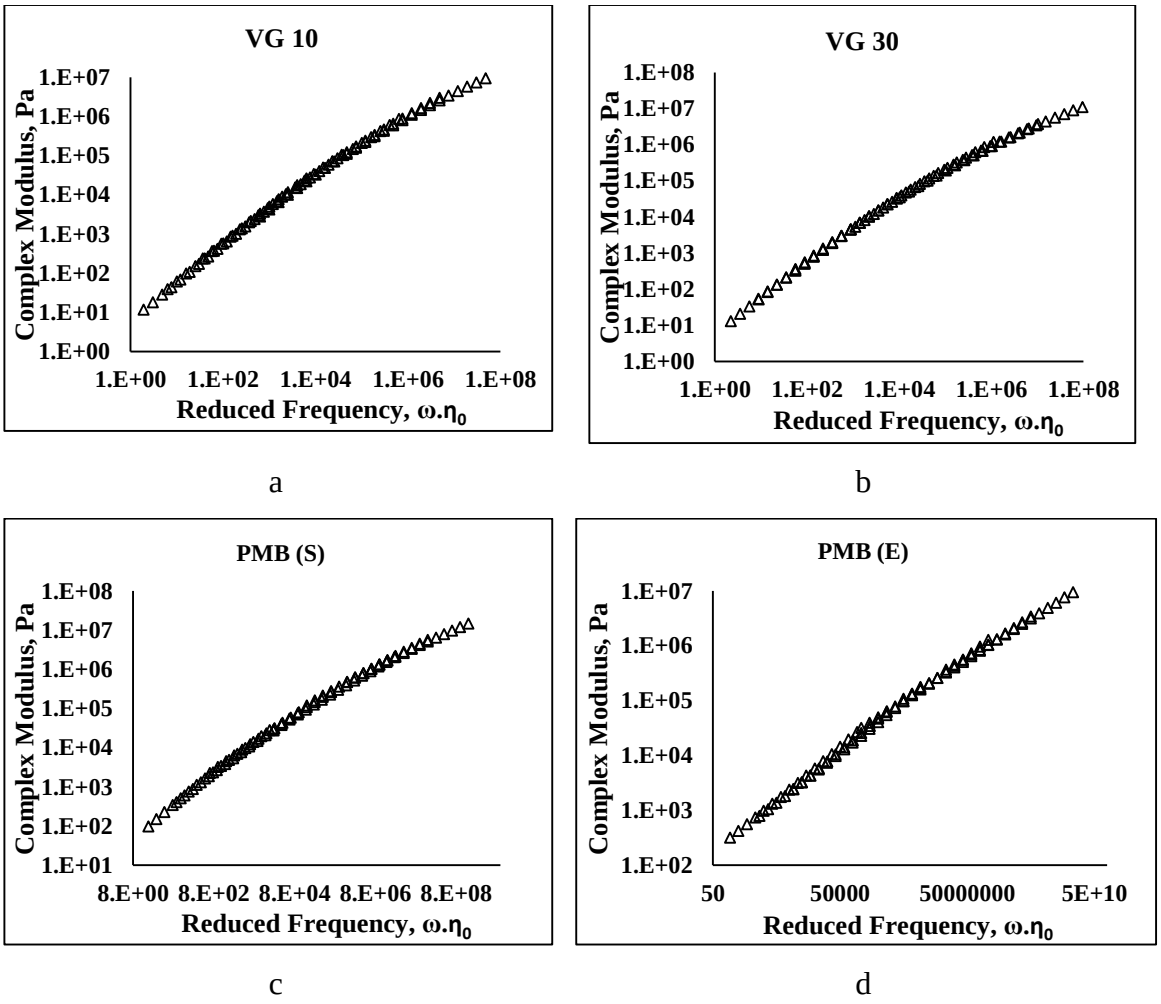

Figure 5.39 (a-d) Complex modulus master curves

Following the concept of rheogram and the Carreau-Yasuda equation, the following equation was fitted for all the binders.

$$\left|\eta^*\right| = \eta_0^* \left[1+(\lambda^*.\omega_{red})^{a^*}\right]^{\left(\frac{n^*-1}{a^*}\right)} \tag{5.9}$$

$$\left|G^*\right| = \omega_{red}.G_0^* \left[1+(\lambda^*.\omega_{red})^{a^*}\right]^{\left(\frac{n^*-1}{a^*}\right)} \tag{5.10}$$

The Star (*) notation implies the parameter pertaining to the oscillation mode. The physical significance of the parameters remains the same as described in chapter 4.

It can be seen from Figure 5.40 (a-d) that very successfully can the equation be used to model the variation of reduced complex viscosity versus the reduced frequency. This plot can be of great use in determining the viscosity corresponding to any shear rate (frequency) provided the ZSV is known at the desired temperature. The values of model parameters are presented below in Table 5.6. It can be seen that the critical shear rate ($1/\lambda^*$) for modified binders are much lower than for conventional binders. This is an indication of greater shear thinning behavior and hence, higher dependence of viscosity on shear rate. Table 5.7 shows the variation of viscosity with shear rate for all the binders at a temperature of 160 ˚C. It can be seen that for conventional binders the percentage change in viscosity is only about 25% when the shear rate varies from 50 s^{-1} to 100000 s^{-1}. The corresponding change in PMB (S) and PMB (E) is 59 and 83 %. Hence, shear rate definitely plays a crucial role in influencing the flow behavior of binder even at higher temperatures. The table also depicts that at higher shears rates of the order of 10^5 s^{-1}, the viscosities of modified binders are even lower than the conventional binders. Hence, even lower mixing and compaction temperatures could be obtained as compared to the conventional binders. The authors also feel that the effect of shear rate is higher at the time of mixing rather than for compaction. During compaction the vertical load of the roller is the primary parameter influencing the compaction. So, though the mixing temperature of modified binders will be lower than the conventional binders, the compaction temperature might remain same or be slightly higher, owing to lesser effect of shear rate at the time of compaction.

Similar fit were obtained for complex modulus master curves using the equation above. The plots are not shown for brevity. Hence C-Y model proves to be an excellent tool for modelling the rheological properties of both conventional and modified bitumen with high degree of accuracy. This simple equation is more fundamental as it delineates the use of greater number of model parameters, which has no significance to material characteristics. The critical frequency turns out to be an important parameter describing the intrinsic change in flow behavior of different binders. The equation is sensitive to only one parameter, i.e. the ZSV of the bitumen at different temperature. If the ZSV of the binder is determined accurately, the above model will give satisfactory results.

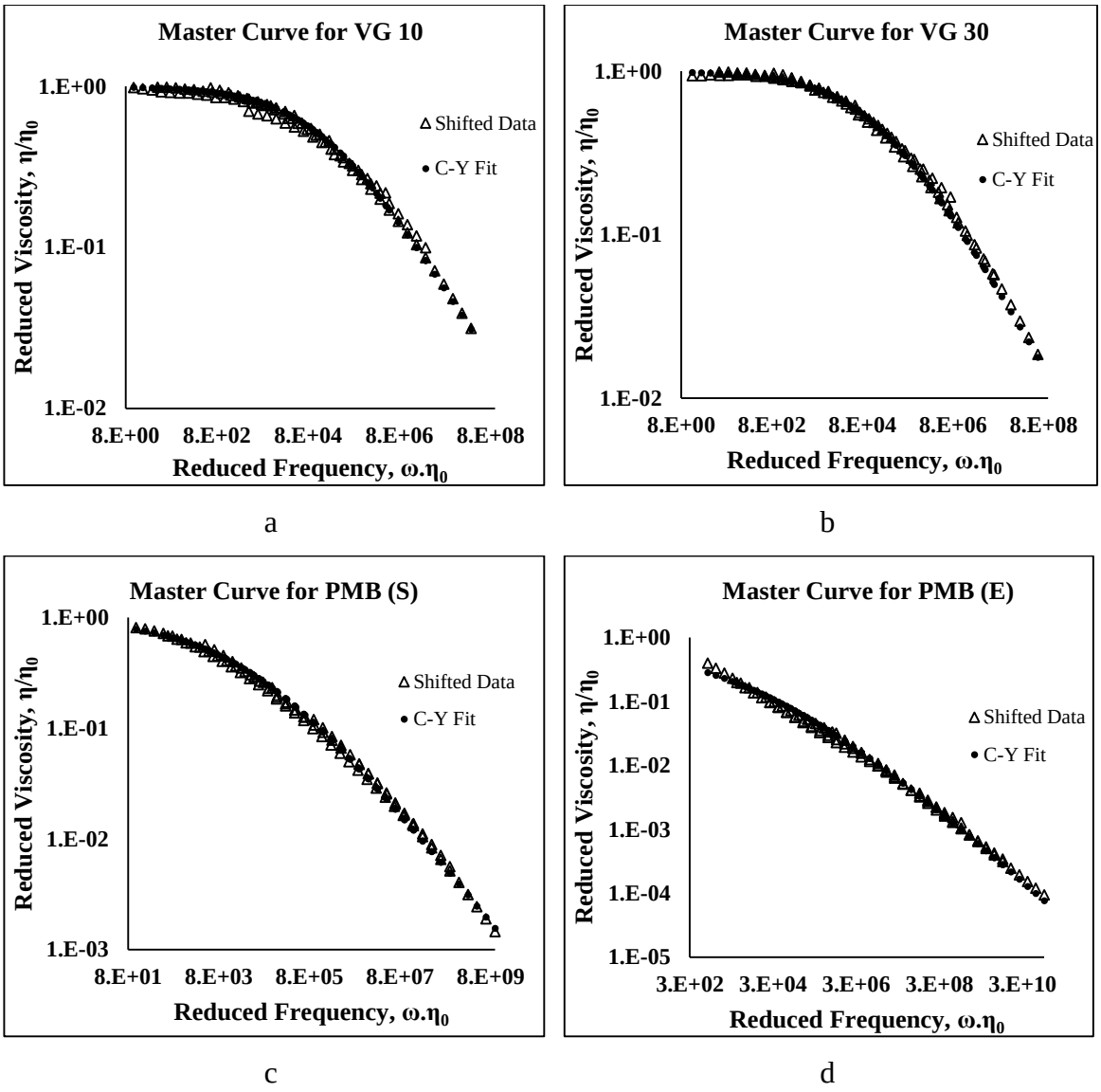

Figure 5.40 (a-d) C-Y model fit for complex viscosity master curves

Table 5.7 Carreau-Yasuda model parameters for different bitumen

Binder	Carreau-Yasuda					
	λ	n	η_0	η_∞	a	1/λ
VG 10	0.000007	0.55	1.00	0	0.45	142857.1
VG 30	0.000007	0.52	1.00	0	0.45	142857.1
PMB (S)	0.00003	0.49	1.00	0	0.32	33333.33
PMB (E)	0.00008	0.41	1.00	0	0.21	12500

Table 5.8 Shear rate dependence at 160 °C for different bitumen

Shear rate	Viscosity, Pa.s			
	VG 10	**VG 30**	**PMB (S)**	**PMB (E)**
50	0.124	0.126	0.210	0.370
100	0.124	0.126	0.204	0.335
500	0.122	0.122	0.186	0.255
1000	0.120	0.119	0.176	0.222
10000	0.112	0.113	0.134	0.126
50000	0.101	0.101	0.100	0.077
100000	0.094	0.094	0.085	0.061

5.5.3.3 Modelling phase angle master curves

The above mentioned procedure of using C-Y equation for modelling the dynamic viscosity and complex modulus master curves (rheogram) can also be applied to phase angle master curves. The interrelationship between complex modulus and phase angle can be mathematically written as

$$\left|G^*\right| = \left|G''\right| \sin\delta \tag{5.11}$$

Where, G^*, G'' and δ are the complex modulus, loss modulus and phase angle of the binder.

As G^* is modelled using (5.10), it can be assumed that G'' can also be modelled using a similar form of equation with changed model parameters. As an example, temperature independent G'' master curves for PMB (S) and VG 30 is shown in Figure 5.41. The master curves were also fitted with a similar form of equation as used for G^*. It was found that the model gave excellent fit for all the binders (Figure 5.41). It was also found that the G'' master curve could be modelled using the same equation as that used for G^* just by varying the parameter 'n'. There is no need to change any other model parameters. This result was found to be consistent for all the binders. So, the equation for modelling G'' master curves can be written as

$$\left|G''\right| = \omega_{red}.G_0'' \left[1+(\lambda^*.\omega_{red})^{a^*}\right]^{\left(\frac{\bar{n}^*-1}{a^*}\right)} \tag{5.12}$$

Where $\bar{n}^*$ is applicable to G'' master curve, all the other parameters remaining same as used in (5.10).

Dividing (5.10) by (5.12) and using (5.11) we get

$$\sin\delta = \left[1+(\lambda^*.\omega_{red})^{a^*}\right]^{\left(\frac{\bar{n}^*-n^*}{a^*}\right)} \tag{5.13}$$

$$\delta = \sin^{-1}\left[1+(\lambda^*.\omega_{red})^{a^*}\right]^{\left(\frac{\bar{n}^*-n^*}{a^*}\right)} \tag{5.14}$$

Equation (5.14) was used to model the phase angle rheogram. First, the phase angle master curves were plotted and then was fitted with the above equation to check its validity. It was found that smooth phase angle master curves couldnot be obtained for PMB (E), as can be seen in Figure 5.42. This is attributed to the presence of crystallites in PMB (E) which induces the inapplicability of TTSP for these binders. Similar results were obtained by Airey [8] for modified binders. This breakdown of TTSP can also be appreciated through black diagrams, which are a plot of complex modulus versus phase angle. Such plot delineates the use of frequency or temperature, which allows all the dynamic data to be presented in one plot without the need to perform TTSP manipulations of the raw data [8]. A smooth curve indicates the applicability of TTSP for any polymer. Figure 5.43 clearly explains the deviations observed for phase angle master curve of PMB (E). For all the other binders smooth master curves were obtained and the above mentioned model gave excellent fit. It is worth mentioning that phase angle is more sensitive to the type and chemical nature of the binder. Such sensitivity is not displayed in complex modulus master curves, which was the reason that smooth master curves were obtained even for PMB (E).

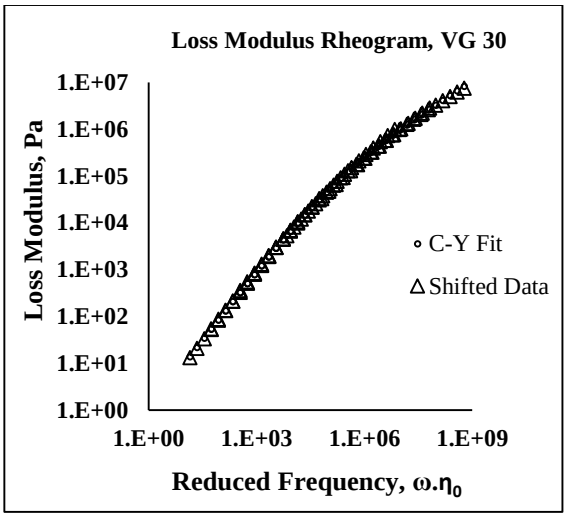

a

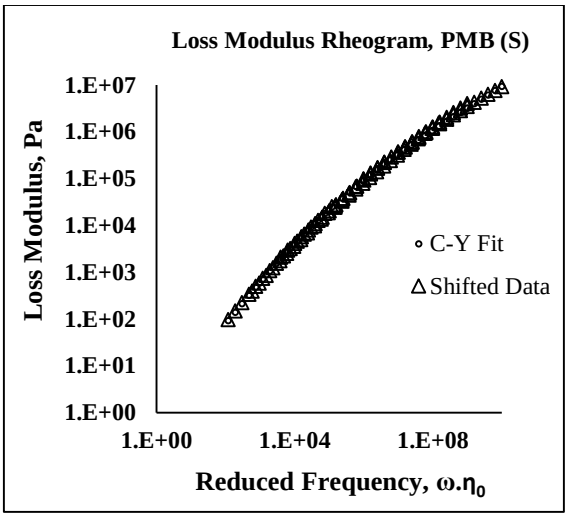

b

Figure 5.41 (a,b) Loss modulus master curves fitted with C-Y equation

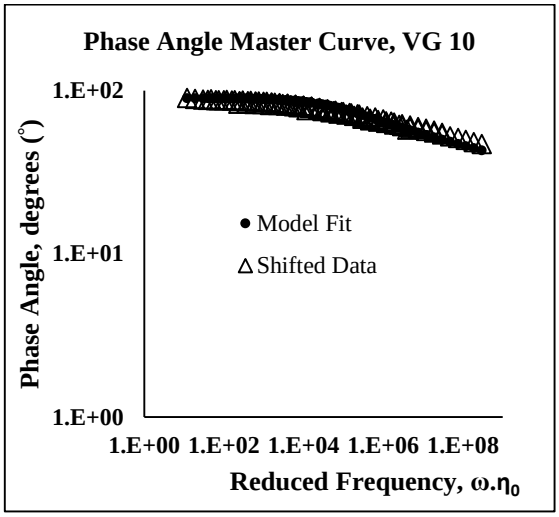

a

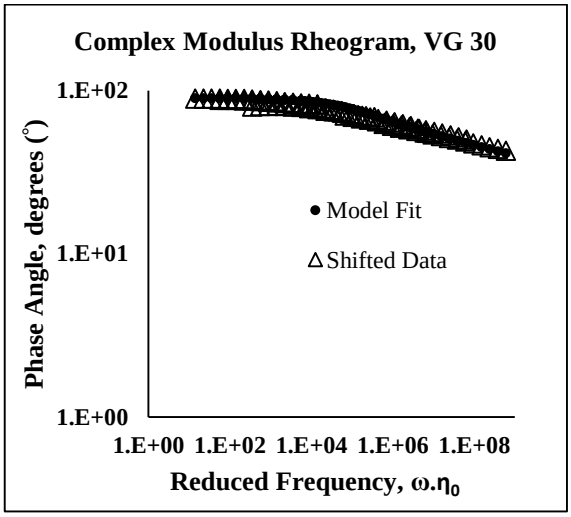

b

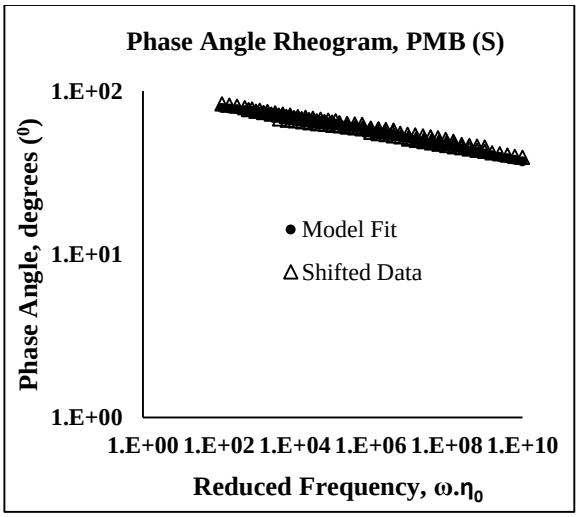

c

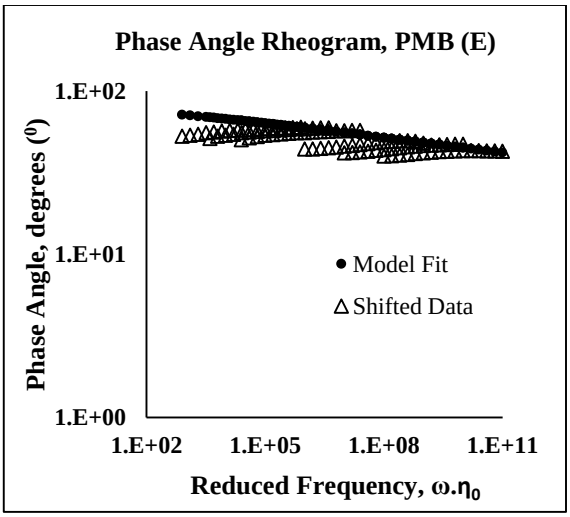

d

Figure 5.42 (a-d) Phase angle master curves fitted with the suggested model

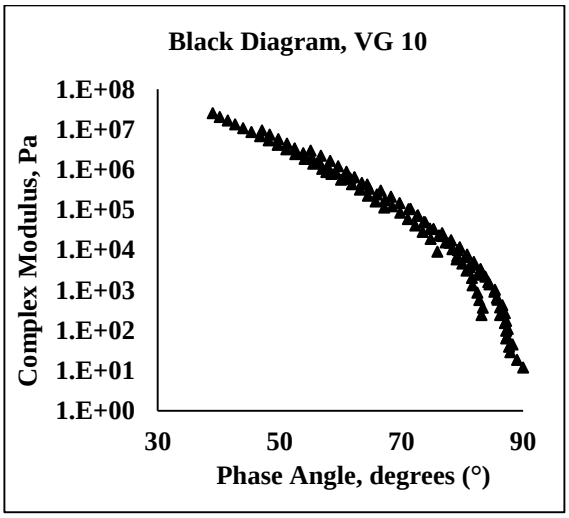

a

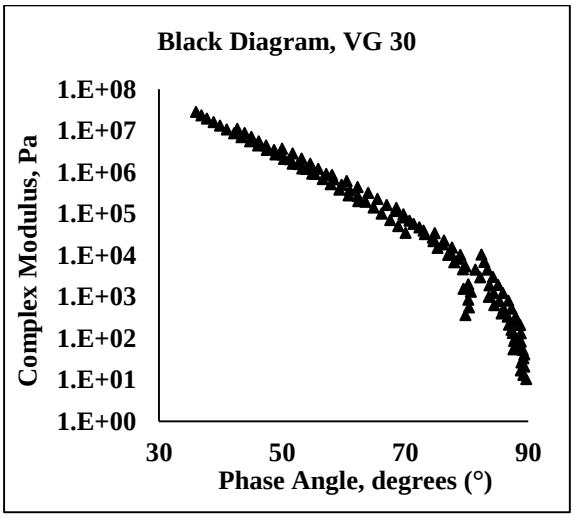

b

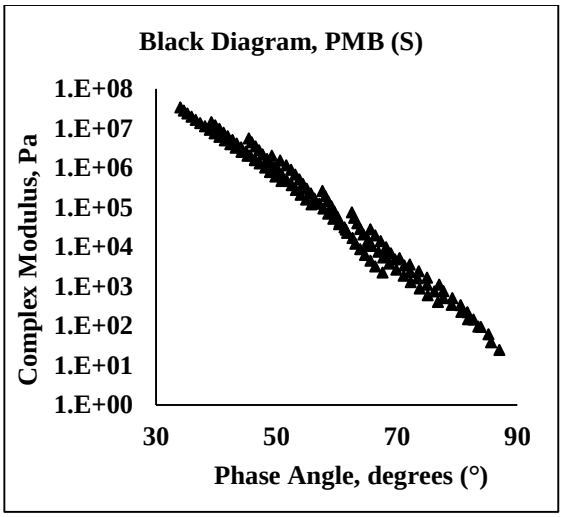

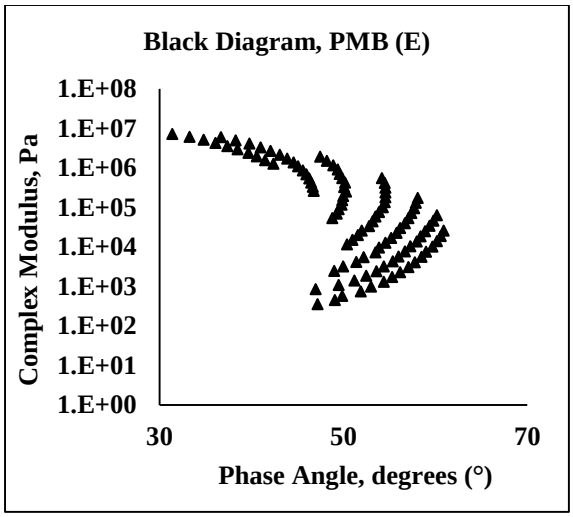

c d

Figure 5.43 (a-d) Black diagrams for all the binders

5.6 Conclusions

The LVE strain increased with increase in temperature and reduction in frequency. At higher frequency and for low temperatures the LVE strain limits were low, owing to the higher stiffness of bitumen. The LVE limits of strain for modified bitumen was found to be lower than for conventional bitumen. The lowest LVE strain were found for PMB (E) due to its higher stiffness compared to other binders. The variation of LVE strain with frequency was not as much significant as with temperature. It was also found that PMB (S) gave more stable values with variation in both frequency and temperature. This strain susceptibility was found highest for PMB (E).

At higher temperatures spindle diameter 8 mm gave higher values for complex modulus and phase angle of the asphalt binders as compared to 25 mm diameter spindle. This difference reduced with reduction in temperature with the curves coinciding at intermediate temperatures. With further reduction (at lower temperatures) the curve reversed its direction with 8 mm diameter tending to give lower values than 25 mm spindle diameter. At higher temperatures higher plate gap gave lower values of complex modulus as compared to lower gap width. The difference in the measurements decreased with decrease in temperature with similar values at intermediate temperatures. At lower temperatures smaller

gap width gave higher values. It was found that spindle geometry plays a crucial role in determination of rheological properties of both conventional and modified binders. A change in spindle diameter and plate gap changes the value of the rheological parameter. The changes are more pronounced at lower and higher temperatures. One conclusion which could be drawn from the study 8 mm spindle geometry cannot be used for higher temperatures and is suitable for temperature range of 10- 30 °C typically.

Complex modulus for all binders decreases with increase in temperature. The curves for modified binders were less steep than the conventional binders, indicating lesser susceptibility of modified binders with respect to temperature and frequency. It was not possible to construct a smooth phase angle master curve for PMB (E). A conclusion was made that the study of thermorheological simplicity cannot be made only on the basis of complex modulus master curves. Phase angle curves are more sensitive to change in chemical nature of the bitumen.

The shift factor obtained by the equivalent slope method which was developed in the study gave the better results in plotting master curves as compared to WLF and Arrhenius equation. The shift factor for all the binders at different reference temperature was found to obey exponential law.

It was found that Cox-Merz rule can be successfully applied in the zero shear viscosity domain. Using the concept of rheogram, complex viscosity master curves were plotted for all the binders for the data obtained in frequency sweep test conducted using dynamic shear rheometer. The shift factor employed was the ZSV from steady state experiments. Smooth master curves, independent of temperature were obtained for all the binders.

Master curves of complex viscosity were converted to complex modulus master curves. Carreau –Yasuda (C-Y) equation was used to model the complex viscosity master curve. Excellent fit was obtained for all the binders. The critical shear rate was lower for modified binders, which indicated higher dependence of modified binders on shear rate. The same equation can also be used to find the mixing and compaction temperature of different binders at the practical shear rates. At very high shear rate of the order of 10^5 s^{-1}, the viscosity of modified binders were found to be lower than the conventional binder.

The simple C-Y model was found to be successfully applicable in modelling the rheological properties of both conventional and modified bitumen. The model however is sensitive to the determination of ZSV values. So, accurate determination of ZSV is recommended to gain more confidence in using the equation.

The C-Y equation for modelling complex modulus was modified for phase angle rheograms. Excellent fit using the suggested model was obtained. TTSP principle breakdown for PMB (E) resulted in wavy nature of phase angle master curves. Phase angle was found to be sensitive to the type and chemical nature of bitumen. Such sensitivity and the TTSP breakdown cannot be witnessed by using complex modulus master curves.

Chapter 6

Performance Evaluation of Asphalt Binders

6.1 Introduction

Fatigue and rutting are two of the three (rutting, fatigue cracking and low temperature cracking) major failure modes in flexible pavements which results in degradation of the pavement materials and finally the pavement structure [201]. The materials in pavement are subjected to short time load amplitudes upon passage of a vehicle. Higher amplitudes of this repeated loading causes distributed micro cracking which leads to an effective reduction in material stiffness and its subsequent accumulation with time may lead to complete failure [32]. Fatigue failure occurs at intermediate pavement temperatures at which the stiffness of the binder is high, making it susceptible to fatigue damage [23, 37, 170, 198]. Moreover, the failure is more likely to occur after subsequent aging of the pavement. Rutting is one of the high temperature distresses, which leads to permanent deformation of pavements. The resistance of asphalt mixture to permanent deformation depends on many factors, including stiffness of bitumen, mix volumetrics and bonding between aggregate and bitumen [203].

The inability of Superapave specification of $G^*/\sin\delta$ to characterize permanent deformation behavior of bitumen has been reported in many studies [34, 43, 44, 46]. This applies mainly to the modified binders, attributed to the non-linearity associated at high temperatures and stress levels. Nonlinearity implies the dependence of the viscoelastic properties (such as complex modulus, creep compliance etc.) of the asphalt binder to the magnitude of stress/strain in addition to temperature and time (frequency) of loading. In lieu to this, performance grade (PG) plus specification has been introduced, which requires conducting multiple stress creep and recovery (MSCR) test on binder at stress levels of 0.1 and 3.2 kPa. This method has been introduced as a part of new Superpave grading system (AASHTO MP 19-10) and is accepted as a standard. MSCR test is conducted in accordance to AASHTO TP 70. The details of the experimental procedure are already discussed in Chapter 2.

Results have shown that, the unrecoverable creep compliance (J_{nR}) at 3.2 kPa, measured using this test method, correlates fairly well with the actual field performance [25, 44, 46]. A lot of research has been done and is still ongoing to understand more about the permanent deformation characteristics of binder using this method [51, 56, 69, 75, 136, 147, 190]. Modelling the response of any material to the imposed stress/strain is one of the popular technique to study and quantify their physical and mechanical properties [172]. Many researchers have tried to model the creep and recovery behavior of bitumen using different mathematical and rheological models [26, 38, 49, 51, 110, 118, 191]. Among the mechanical models, generalized Kelvin and four element Burger's model have shown to give good experimental fit [34, 38]. Mathematically, Boltzmann superposition principle is widely used and the concept has been extended for non-linear models through Schapery's equation [26, 148, 191]. Numerous modifications to these models have also been attempted, to include various viscoelastic and viscoplastic characteristics, mostly for modified bitumen.

The current Superpave specification for performance grading was developed mainly for unmodified binders and has been proved to be misleading for predicting rutting and fatigue properties of modified bitumen [71, 73, 84, 85, 199]. The method employs the parameter $G^*.sin\,\delta$ to quantify the asphalt binder fatigue resistance. It is based on the concept that lower dissipated energy per loading cycle $(\pi.\gamma_0^2.G^*.sin\delta)$ will lead to lower distress accumulation. Hence the intermediate temperature is determined such that $G^*.sin\delta$ be less than 5000 kPa [17]. This stiffness based parameter, which is a development of Strategic Highway Research Program (SHRP), is measured at a fixed frequency (10 rad/sec), ensuring the strain to be below the linear viscoelastic (LVE) regime of the bitumen. The recommended strain value is 1-2%. The test was developed based on the speculation that binder in pavements functions mostly in the LVE range and is not likely to affect their properties. This simple test cannot describe the actual complicated fatigue phenomena, in which the binder is exposed to higher strain levels and varied frequency levels. Efforts placed on development of new technique to more accurately quantify the fatigue behavior of asphalt binder led to the introduction of Linear Amplitude Sweep (LAS) test. It is based on the principal of continuum viscoelastic damage and has been standardized as AASHTO TP 101-14. A plethora of studies have indicated its superiority over the traditional methods for evaluating

the fatigue damage of asphalt binders [15, 72, 73]. The details of the test method has been discussed in chapter 2.

This chapter focusses on quantifying the performance of unmodified and modified asphalt binders using MSCR and LAS test methods at varying temperatures and stress/strain levels. The effect of polymer modification on the values of different test parameters has also been evaluated and discussed. The suitability of different asphalt binders in actual field conditions is also established which can help the practitioners in choosing the appropriate binder. The measured response in MSCR test was analyzed using two different modelling techniques. Changes in the suggested model were made to account for the non-linearity associated with the binders. The significance of model parameters, influencing the permanent deformation characteristics were evaluated. Critical values to these parameters were assigned and proposed as a performance measure, after comparison with the already existing PG plus specification. This may provide additional benefit in judging the relative performance of asphalt binders at high temperature.

6.2 Experimental Investigation

6.2.1 *Multiple stress creep and recovery test*

Multiple Stress Creep and Recovery (MSCR) test [1] was conducted at three different temperatures (40, 50 and 60 °C) using Dynamic Shear Rheometer (DSR) operated in constant stress mode. Four different stress levels were chosen, viz. 100, 3200, 5000 and 10,000 Pa. Studies [50, 68] have shown that the non-linearity in creep compliance usually starts beyond 3.2 kPa at higher temperatures. So two additional stress levels (5 and 10 kPa) were used to evaluate the performance in the non-linear domain. The test was done using 25 mm sample geometry with 1 mm gap between the spindle and the base plate on RTFO aged samples. Samples were prepared using silicon mold method (alternative 2 of AASHTO standard, 1994). The temperature was allowed to equilibrate for 30 minutes before starting the test. All the results in this chapter are average of three test carried out in each mode. This was done to check for the repeatability of the instrument.

First cycle of each stress level at a particular temperature was chosen to model creep and recovery response for the binder. It was hence necessary to bring the data on a single

scale of time. The creep and recovery of the first cycle at stress level of σ_{i+n} was converted to the scale of σ_i by subtracting each value of strain for creep and recovery of σ_{i+n} by the last strain value of σ_{i+n-1}. Figure 6.1 shows the procedure of shifting the axis. Applicability of Boltzmann superposition principle was checked for the final shifted data. If Boltzmann superposition is assumed to be applicable, then

$$\varepsilon_{i+k} = \left(\sigma_{i+n} / \sigma_i\right).\varepsilon_i \tag{6.1}$$

Where, '*i*' is the known data and '*n*' is the point for which the applicability has to be checked. Checking this applicability using such technique would automatically enclose the effect of cycle on creep and recovery, as the data for σ_{i+k} are shifted from higher cycle numbers.

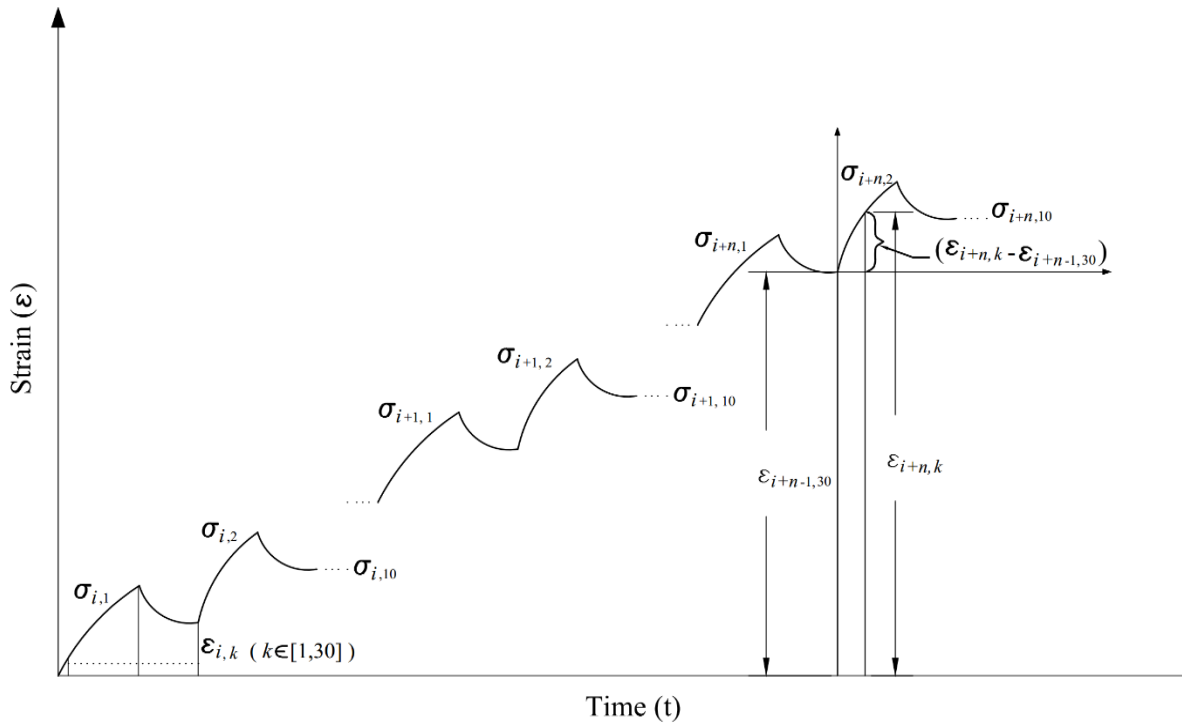

Figure 6.1 Shifting of creep and recovery data to a single scale

Though the specifications (as discussed in chapter 2) are given only for two stress levels of 0.1 and 3.2 kPa, in this study the calculations were done for all the four stress levels.

6.2.1.1 Modelling the strain response of asphalt binders

Boltzmann superposition principle has been widely used to define the linear rheological characteristics of polymers. This principle states that the creep strain in a material is affected by its loading history and the strains due to multiple load steps are additive and independent. The hereditary integral representation of this principle is as follows [181]:

$$\varepsilon(t) = D_0\sigma + \int_0^t \Delta D(t-\tau)\frac{d\sigma}{d\tau}d\tau \tag{6.2}$$

Where, D_0 is the instantaneous creep compliance, $\Delta D(t)$ is the transient creep compliance, σ is the applied stress, and τ is a variable introduced into the integral in order to account for the stress history of the material. This principle has been found to serve well for low stress levels, or in the linear viscoelastic region of bitumen.

For the associated non-linearity, such as in modified bitumen, Schapery's principle [148] based on irreversible thermodynamics has been recommended which could be written as

$$\varepsilon(t) = g_0 D_0\sigma + g_1\int_{0^-}^t \Delta D(\psi - \psi')\frac{dg_2\sigma}{d\tau}d\tau \tag{6.3}$$

Where, D_0 and $\Delta D(\Psi)$ are the instantaneous and transient linear viscoelastic creep compliance, and Ψ is the reduced-time which is defined by:

$$\psi = \int_0^t \frac{dt'}{a_\sigma[\sigma(t')]}(a_\sigma > 0) \tag{6.4}$$

$$\psi' = \int_0^\tau \frac{dt'}{a_\sigma[\sigma(t')]} \tag{6.5}$$

The factors g_0, g_1, g_2 and a_σ in the model are all stress dependent nonlinearity parameters. The g_0 term indicates the nonlinearity in the instantaneous elastic compliance due to varying stress and temperature, and can therefore be a measure of the stiffness of the material. Factor g_1 has a similar interpretation but acts on the transient creep compliance, and g_2 shows the nonlinearity effects of loading rate. The parameter a_σ is a time shift factor that is both stress and temperature dependent [126]. Though a very effective technique to model the non-linear

viscoelasticity in polymers, too many model parameters tends to involve complexity in relating them to the measured performance.

6.2.1.2 Burger's four element model

Of the various rheological models, Burger's four element model had been very promising in characterizing the creep and recovery of viscoelastic materials [34, 38]. Burger's model consists of four mechanical components as shown below in Figure 6.2. It consists of a Maxwell and a Kelvin unit connected in series. The constitutive equation for a Burger's model can be derived by considering the strain response under constant stress of each coupled element in series as depicted in Figure 6.2. The total strain ε_B at time t is a sum of the strains in these three elements, where the spring and dashpot in the Maxwell model are considered as two elements. The subscripts B, M, and K indicate Burger's model, Maxwell and Kelvin elements, respectively; ε_{M1}, ε_{M2}, and ε_K are the strains of the Maxwell spring, Maxwell dashpot, and Kelvin unit, respectively.

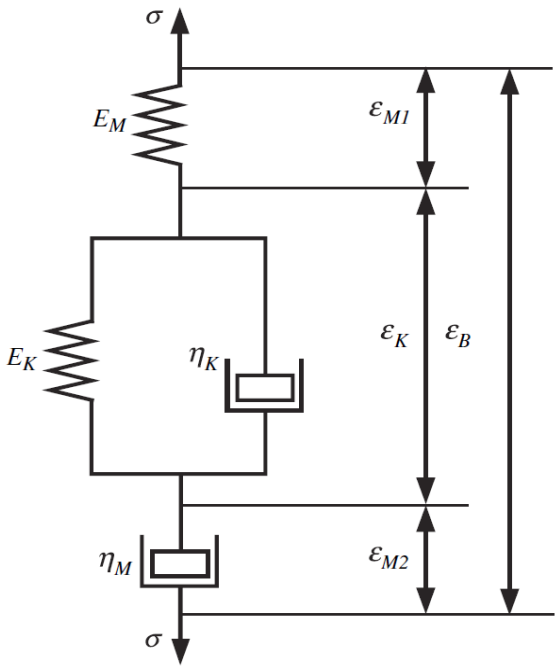

Figure 6.2 Schematic representation of Burger's four element model

For creep and recovery loading the strain response can be written as follows,

$$\varepsilon(t) = \sigma_0 / E_M + \sigma_0 t / \eta_M + \sigma_0 / E_K (1 - e^{-E_K t/\eta_K}) \quad (6.6)$$

for creep phase, and

$$\varepsilon(t) = \sigma_0 t / \eta_M + \frac{\sigma_0}{E_K} e^{-E_K t/\eta_K} (e^{E_K \tau/\eta_K} - 1) \quad (6.7)$$

for recovery stage, considering that the load is removed at t = τ.

E_M, η_M, E_K, and η_K are the model parameters pertaining to modulus and viscosity of Maxwell and Kelvin elements respectively. η_M characterizes the viscous flow behavior of the bitumen and is considered as an important parameter to describe the rutting potential of different binders. The creep and recovery of all the four binders were fitted with the help of this model and the model parameter η_M, was analyzed. The data fitting was done using the non-linear least square technique.

6.2.1.3 Power law model

The transient creep compliance function, *ΔD(t)*, is often given the form of a Power law or a Prony series in viscoelastic modeling. In this study Power law was used to model the strain response of the binder in creep. It could be mathematically written as

$$\varepsilon(t) = K + A.\mathrm{t}^B \quad (6.8)$$

K is the assumed elastic response and the second term is the time dependent viscoelastic response. *A* and *B* are the model shape parameters. If Boltzmann superposition is to be valid for both creep and recovery phenomena, then the recovery could be written as

$$\varepsilon_r(t) = \varepsilon(t) - \varepsilon(t - t') \quad (6.9)$$

First, a verification was done, if modelled values obeyed Boltzmann superposition principle and further changes in the equations were made accordingly to account for the nonlinearity.

6.2.2 *Linear amplitude sweep (LAS) test*

Linear amplitude sweep test following AASHTO TP 101-14 was conducted to determine the parameter *A* and *B*, to assess the fatigue life of the binders at different strain levels. The test requires conducting a frequency sweep test followed by a linear amplitude sweep. The frequency sweep is conducted at a very low strain level of 0.1% to obtain undamaged material properties (α), which is used as an input in the analysis of amplitude sweep test. The amplitude sweep test is conducted by linearly varying strain from 0-30%, through 3100 loading cycles at a fixed frequency of 10 Hz. The test begins with 100 cycles of sinusoidal loading at 0.1% strain followed by incremental load steps of 100 cycles each, at a rate of 1% increment in strain level.

The binder fatigue life N_F is calculated using the equation (details given in chapter 2)

$$N_F = A(\gamma_{\max})^B \tag{6.10}$$

6.3 Results and Analysis

6.3.1 *Experimental results of MSCR test*

The average unrecoverable creep compliance (J_{nR}) and average percent recover (R) at the three test temperatures are shown in Figure 6.3 (a-d) and Figure 6.4 (a-d). In general, modified binders outperformed the conventional binders at all the temperatures and stress levels. The value of J_{nR} was found to be lowest for PMB (E), followed by PMB (S) at all the test conditions. For locations with heavy traffic, which requires the maximum value of J_{nR} to be 2 kPa, according to specifications given by Asphalt Institute (Table 2.1), the binder VG 10 is not suitable. Even VG 30 could be used only for low stress levels (<3.2 kPa), above which the performance degrades. Both modified binders were found to be apposite for resisting permanent deformation at all the conditions studied. It is worth mentioning that according to the traditional Superpave grading system, VG 10 and VG 30 are supposed to perform well at regions where the average maximum seven day temperatures are 58 °C and 64 °C respectively (Table 5.1). But the MSCR result clearly demonstrates that VG 10 and VG 30 are not very suitable at such high temperature conditions. Hence use of the traditional

Superpave grading protocol as a standard for characterizing permanent deformation of binders is misleading.

Modified binders had considerably higher percent recovery *(R)* than the conventional binders. *R* for PMB (E) was found to be higher than PMB (S) below the stress level of 10 kPa. At 10 kPa for the temperature of 50 and 60 °C, PMB (S) showed higher recovery. This is attributed to the interlocked polymer network in PMB (S), which makes it capable to resist higher stresses, without accumulating any permanent strain. EVA on the other hand imparts high rigidity to the binder, which increases the stiffness, but the flexibility reduces when subjected to worst combination of temperature and stress i.e. at high strain levels. At 60 °C and for stress levels greater than 100 Pa, both the normal binders showed negative percent recovery. This is due to the tertiary creep flow in these binders, even after removal of load. Moreover, the drop in percent recovery with increase in temperature and stress levels, were found to be higher for normal binders, making them both temperature and stress sensitive. Use of these binders at locations with high temperature and heavy traffic should hence be avoided. Furthermore, none of the conventional binder satisfied the minimum percent recovery criteria mentioned in Table 2.2 for temperatures greater than 40 °C. This proves the absence of delayed elastic response in these binders, making them highly rut susceptible. It was also found that if any binder has at least 20% recovery, irrespective of any stress level or temperature, it will indicate the presence of delayed elastic behavior. Table 6.1 presents the suitability of all the binders at 60 °C for different stress levels based on the recommended maximum J_{nR} values. In the Table 'Y' represents the suitability and 'N' denotes that it is not suitable.

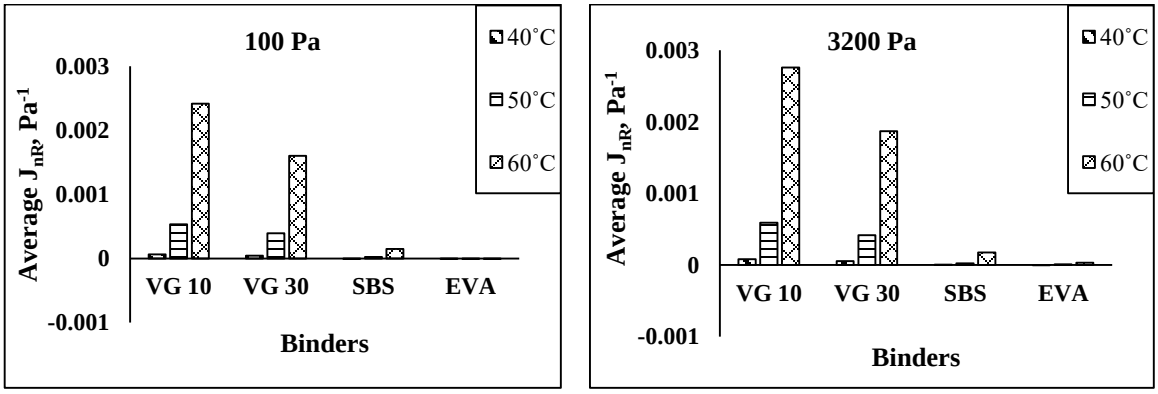

a b

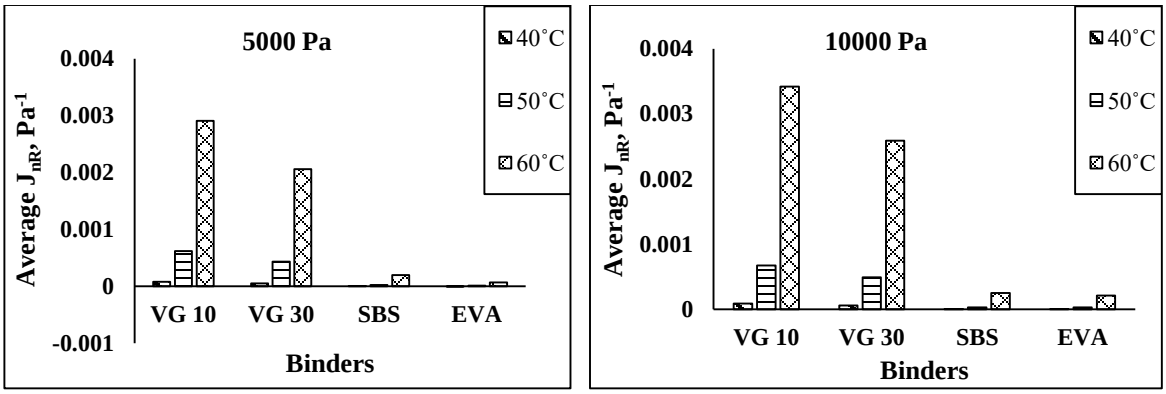

c d

Figure 6.3(a-d) Average unrecoverable creep compliance *(J_{nR})* for different binders

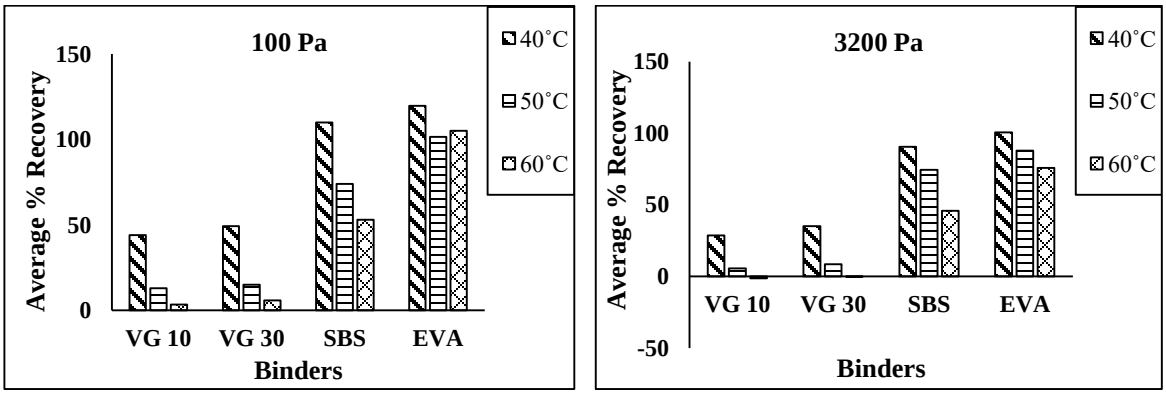

a b

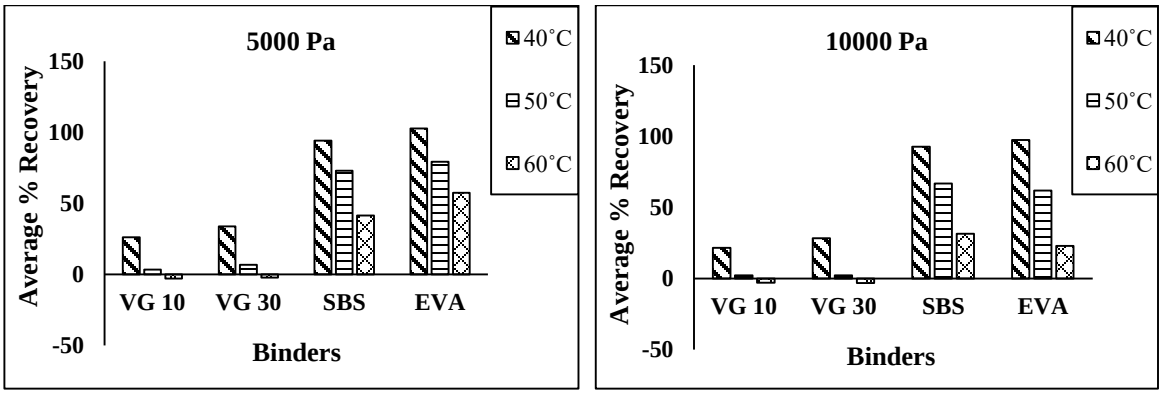

c d

Figure 6.4 (a-d) Average percent recovery for different binders

Table 6.1 Suitability of different binders at 60 °C

Type of Grade	J_{nR} Maximum	0.1 kPa				3.2 kPa				5 kPa				10 kPa			
		VG 10	VG 30	PMB (S)	PMB (E)	VG 10	VG 30	PMB (S)	PMB (E)	VG 10	VG 30	PMB (S)	PMB (E)	VG 10	VG 30	PMB (S)	PMB (E)
S	4	Y	Y	Y	Y	Y	Y	Y	Y	Y	Y	Y	Y	Y	Y	Y	Y
H	2	N	Y	Y	Y	N	Y	Y	Y	N	N	Y	Y	N	N	Y	Y
V	1	N	N	Y	Y	N	N	Y	Y	N	N	Y	Y	N	N	Y	Y
E	0.5	N	N	Y	Y	N	N	Y	Y	N	N	Y	Y	N	N	Y	Y

*S: Slow; H: Heavy; V: Very Heavy; E: Extremely Heavy (each denotes the traffic loading conditions)

6.3.2 *Modelling creep and recovery*

6.3.2.1 Modelling using Burger's four element model

The representative creep and recovery curves for the stress level of 3.2 kPa at 50 °C are presented in Figure 6.5 (a-d). The simulated curves using Burger's model are drawn in solid lines. It could be seen that the modelling curves are in good agreement with the experimental data for conventional binders. Deviation were found particularly for modified binders, at the lower temperatures (40 and 50 °C) and stress levels (0.1 and 3.2 kPa). The recovery portion deviated from Burger's fitting, for these binders. The marked circles represents the area where the model deviated from the experimental results. The model was not able to simulate the delayed elastic response, typical in polymer modified binders. Out of the four Burger model parameters, η_M accounts for the viscous strain after the recovery and is considered to describe the permanent deformation characteristics of asphalt binders. Researchers [34] have found it close to the zero shear viscosity (ZSV) of the bitumen. A higher value of η_M would mean better resistance to rutting. The values for different binders obtained in the study are shown in Table 6.2. The values of all the model parameters at different test conditions are also presented in Table 6.3. In general, the value of η_M were found to be higher for modified binders, PMB (E) giving the highest value. The values at all the stress levels decreased with increase in temperature. However the rate of decrease was higher in conventional binders. This portrays the higher temperature susceptibility for these binders in comparison to modified binders. It was also found that the value of η_M is affected by the level of stress only after a certain temperature. This temperature is binder specific and was found to be the point from where the viscous flow dominates. For VG 10 this temperature was found to be 40 °C, for VG 30 it was 50 °C and for modified binders the change in η_M with stress level dominated after attaining 60 °C. The parameter η_M, was found

to give good correlation with the unrecoverable creep compliance, J_{nR} and the value of R, as can be seen in Figure 6.6 (a-b). It is worth noting that both J_{nR} and η_M are affected by stress levels only at viscous temperatures, contrary to the average % recovery, which is sensitive to stress levels at all temperatures.

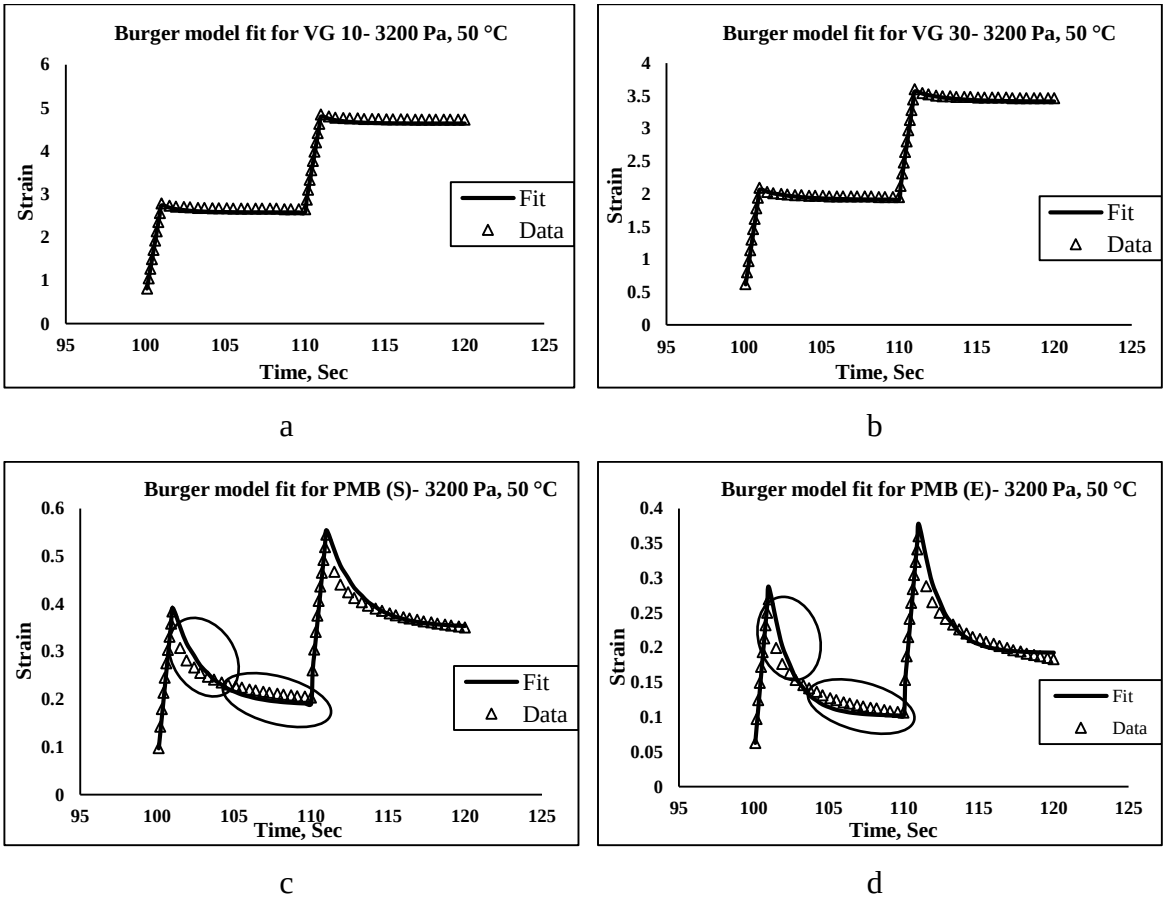

Figure 6.5 (a-d) Burger's model fit at 50 °C for different binders

Table 6.2 Maxwell dashpot element (η_M) for all the binders at different stress levels and temperatures.

Binder	Stress (kPa)	η_M (Pa.s)		
		40^{0}C	**50^{0}C**	**60^{0}C**
VG 10	**0.1**	7500	1500	360
	3.2	7500	1500	330
	5	7500	1400	310
	10	7500	1350	290
VG 30	**0.1**	11000	2000	550
	3.2	11000	2000	490

	5	11000	2000	450
	10	11000	1850	395
PMB (S)	**0.1**	46000	10000	2900
	3.2	44000	10000	2900
	5	44000	10000	2750
	10	44000	10000	2550
PMB (E)	**0.1**	50000	13000	9000
	3.2	48000	13000	7500
	5	48000	13000	6000
	10	48000	13000	4000

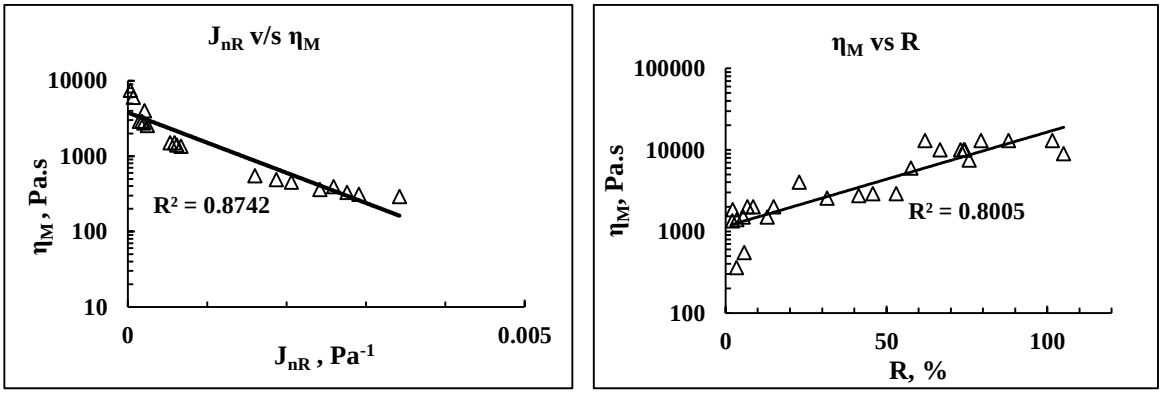

a b

Figure 6.6 (a, b) Correlation between η_M with J_{nR} and % Recovery (R)

It was attempted to assign a critical values to η_M, so that it could be used to characterize the rutting resistance of any binder. These values were assigned after careful examination of all the values of J_{nR} and the corresponding ZSV values. These minimum values corresponds to the PG plus specification for different traffic conditions. Table 6.4 presents the recommended values, independent of the type of binder. The binder should possess these minimum values when tested at the average maximum temperature of the area of interest. Also, if a minimum recovery of 20% is assigned for the presence of delayed elastic response, then irrespective of any stress level and temperature, a minimum value of 2000 Pa.s is recommended for η_M.

Table 6.4 Recommended minimum values of η_M for different traffic levels

Type of Grade	Traffic Level (ESAL, millions)	$J_{nR,3.2kPa}$, Maximum, kPa^{-1}	$\eta_{M\ critical}$(min), Pa.s
S	<3	4	200
H	3-10	2	800
V	10-30	1	2000
E	>30	0.5	4000

6.3.2.2 Modelling using Power law model

The strain response of the binders in creep and recovery were fitted with the Power law model as described by equation 6.8. It was found that this model gave excellent fit in creep for all the binders at all temperatures and stress levels. The value of parameter *K* was found to be 'zero' for all the considered cases. This means that there is no dominance of the elastic response of the binder at temperatures greater than 40 °C. Figure 6.7 (a-l) shows the plot of strain versus the shifted time for all the stress levels, and the corresponding superimposed data calculated using equation 6.1 with respect to 100 Pa as the reference point '*i*'. The jump in strain was found to be higher when moving from 1 kPa to 3.2 kPa after which the change in it reduces. Boltzmann superposition principle was found to be applicable for all the binders at all the temperatures. Deviations were observed for higher stress levels at higher temperatures. This is an indication of non-linearity at stress levels higher than 5000 Pa. These deviations were higher for modified binders at 60 °C, especially for PMB (E). Also the success of superposition implied independence from the effect of number of cycles, at all temperatures and stresses.

Table 6.3 Burger's four element model parameters

Binder	Stress (kPa)	40^{0}C				50^{0}C				60^{0}C			
		E_M (Pa)	η_M (Pa.s)	E_K (Pa)	η_K (Pa.s)	E_M (Pa)	η_M (Pa.s)	E_K (Pa)	η_K (Pa.s)	E_M (Pa)	η_M (Pa.s)	E_K (Pa)	η_K (Pa.s)
VG 10	**0.1**	1.0E+07	7.5E+03	2.0E+04	2.5E+04	1.0E+07	1.5E+03	2.0E+04	2.5E+04	1.0E+07	3.6E+02	4.0E+04	3.0E+04
	3.2	1.0E+07	7.5E+03	3.0E+04	2.5E+04	1.0E+07	1.5E+03	2.0E+04	2.5E+04	1.0E+07	3.3E+02	4.0E+04	3.0E+04
	5	1.0E+07	7.5E+03	3.0E+04	2.5E+04	1.0E+07	1.4E+03	2.5E+04	3.0E+04	1.0E+07	3.1E+02	4.0E+04	3.0E+04
	10	1.0E+07	7.5E+03	3.0E+04	2.5E+04	1.0E+07	1.4E+03	4.0E+04	3.0E+04	1.0E+07	2.9E+02	4.0E+04	3.0E+04
VG 30	**0.1**	1.0E+07	1.1E+04	2.8E+04	4.2E+04	1.0E+07	2.0E+03	2.0E+04	4.0E+04	1.0E+07	5.5E+02	4.0E+04	4.0E+04
	3.2	1.0E+07	1.1E+04	4.0E+04	5.0E+04	1.0E+07	2.0E+03	2.0E+04	4.0E+04	1.0E+07	4.9E+02	4.0E+04	4.0E+04
	5	1.0E+07	1.1E+04	4.0E+04	5.0E+04	1.0E+07	2.0E+03	4.0E+04	4.0E+04	1.0E+07	4.5E+02	4.0E+04	4.0E+04
	10	1.0E+07	1.1E+04	4.0E+04	5.0E+04	1.0E+07	1.9E+03	4.0E+04	4.0E+04	1.0E+07	4.0E+02	4.0E+04	4.0E+04
PMB (S)	**0.1**	1.0E+07	4.6E+04	4.5E+04	1.0E+05	1.0E+07	1.0E+04	1.5E+04	3.0E+04	1.0E+07	2.9E+03	6.8E+03	8.0E+03
	3.2	1.0E+07	4.4E+04	6.5E+04	6.0E+04	1.0E+07	1.0E+04	1.5E+04	3.0E+04	1.0E+07	2.9E+03	8.0E+03	1.0E+04
	5	1.0E+07	4.4E+04	5.5E+04	8.0E+04	1.0E+07	1.0E+04	1.5E+04	3.0E+04	1.0E+07	2.8E+03	8.0E+03	1.0E+04
	10	1.0E+07	4.4E+04	5.5E+04	8.0E+04	1.0E+07	1.0E+04	1.5E+04	3.0E+04	1.0E+07	2.6E+03	9.0E+03	1.0E+04
PMB (E)	**0.1**	1.0E+07	5.0E+04	1.6E+04	2.5E+04	1.0E+07	1.3E+04	1.6E+04	2.5E+04	1.0E+07	9.0E+03	1.0E+04	1.5E+04
	3.2	1.0E+07	4.8E+04	1.7E+04	2.5E+04	1.0E+07	1.3E+04	1.7E+04	2.5E+04	1.0E+07	7.5E+03	1.2E+04	1.5E+04
	5	1.0E+07	4.8E+04	1.7E+04	2.5E+04	1.0E+07	1.3E+04	1.7E+04	2.5E+04	1.0E+07	6.0E+03	1.1E+04	1.5E+04
	10	1.0E+07	4.8E+04	2.5E+04	2.0E+04	1.0E+07	1.3E+04	2.5E+04	2.0E+04	1.0E+07	4.0E+03	1.5E+04	1.5E+04

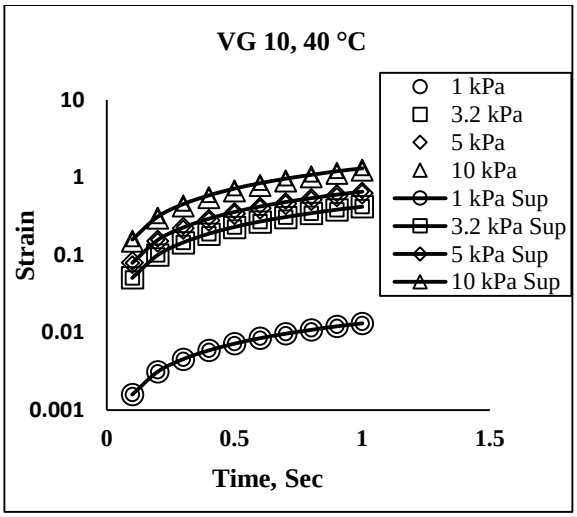
VG 10, 40 °C
Strain
Time, Sec
1 kPa
3.2 kPa
5 kPa
10 kPa
1 kPa Sup
3.2 kPa Sup
5 kPa Sup
10 kPa Sup

a

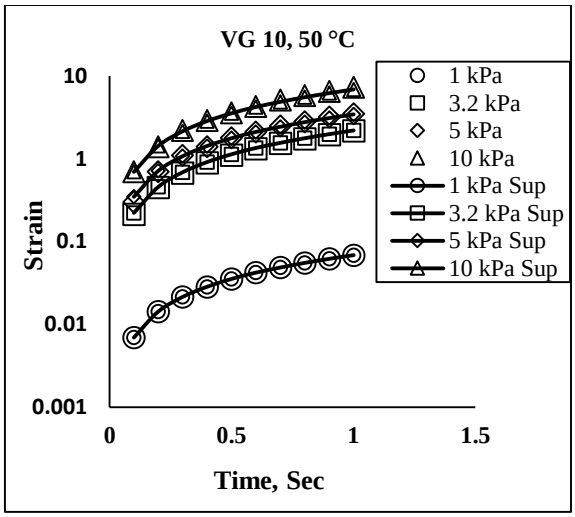
VG 10, 50 °C
Strain
Time, Sec
1 kPa
3.2 kPa
5 kPa
10 kPa
1 kPa Sup
3.2 kPa Sup
5 kPa Sup
10 kPa Sup

b

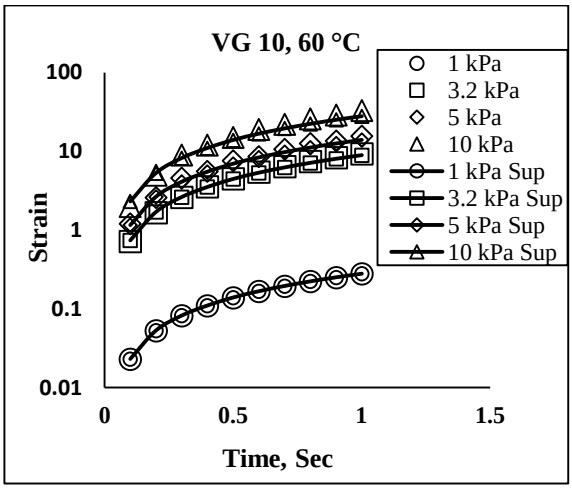
VG 10, 60 °C
Strain
Time, Sec
1 kPa
3.2 kPa
5 kPa
10 kPa
1 kPa Sup
3.2 kPa Sup
5 kPa Sup
10 kPa Sup

c

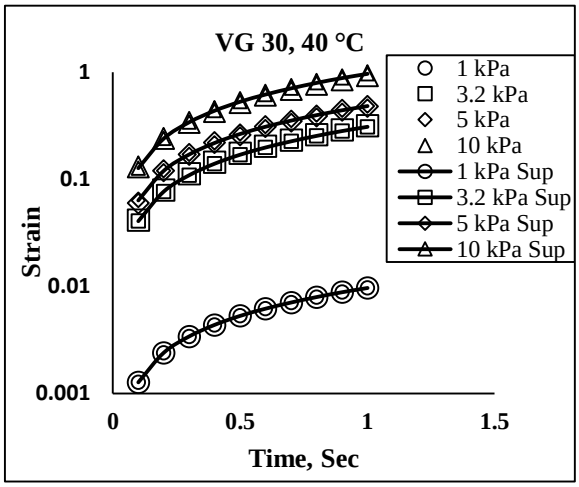
VG 30, 40 °C
Strain
Time, Sec
1 kPa
3.2 kPa
5 kPa
10 kPa
1 kPa Sup
3.2 kPa Sup
5 kPa Sup
10 kPa Sup

d

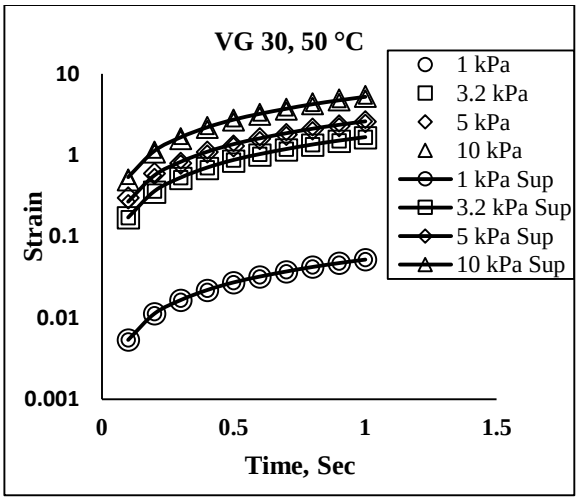
VG 30, 50 °C
Strain
Time, Sec
1 kPa
3.2 kPa
5 kPa
10 kPa
1 kPa Sup
3.2 kPa Sup
5 kPa Sup
10 kPa Sup

e

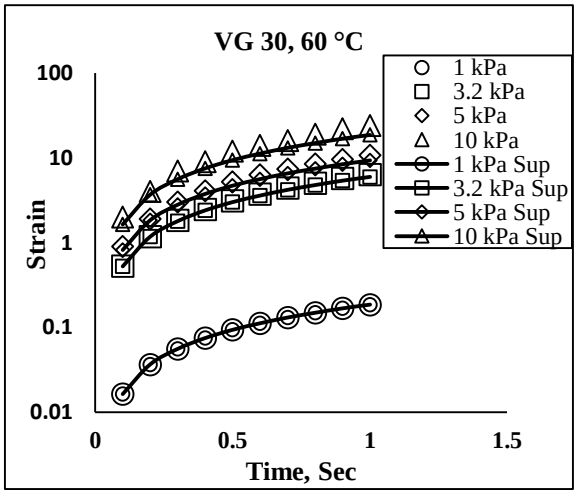
VG 30, 60 °C
Strain
Time, Sec
1 kPa
3.2 kPa
5 kPa
10 kPa
1 kPa Sup
3.2 kPa Sup
5 kPa Sup
10 kPa Sup

f

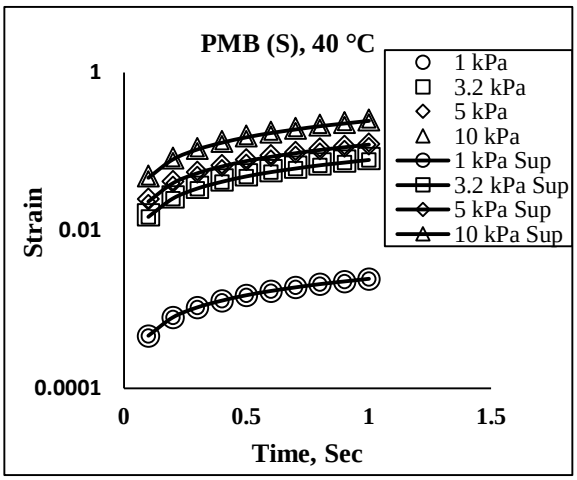

g

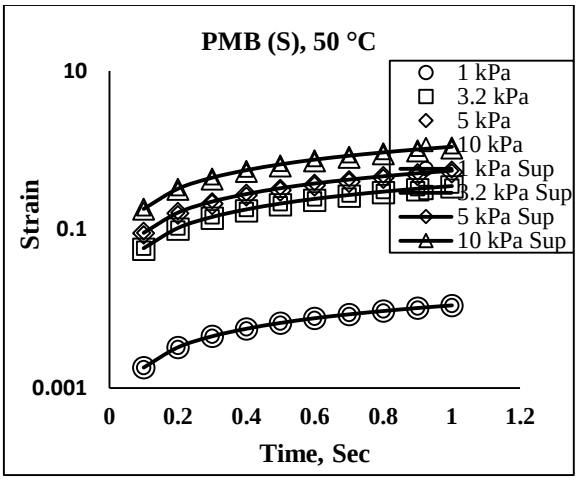

h

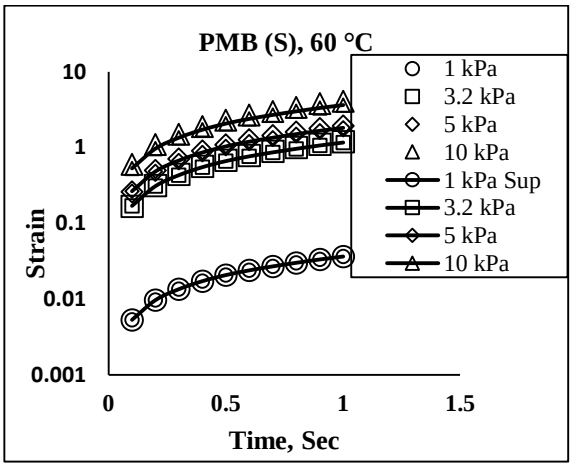

i

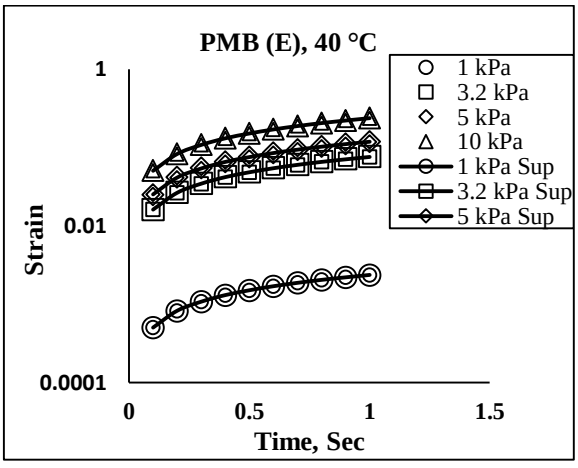

j

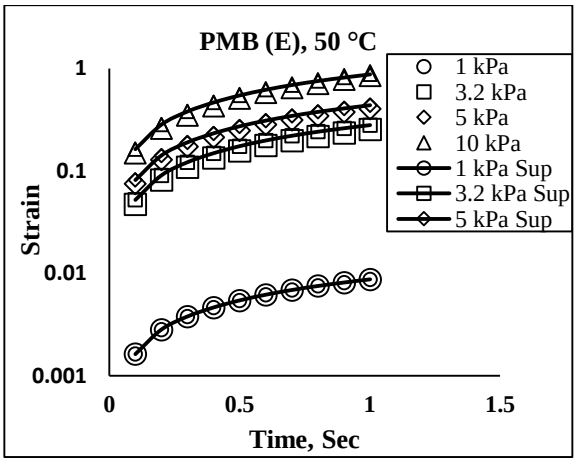

k

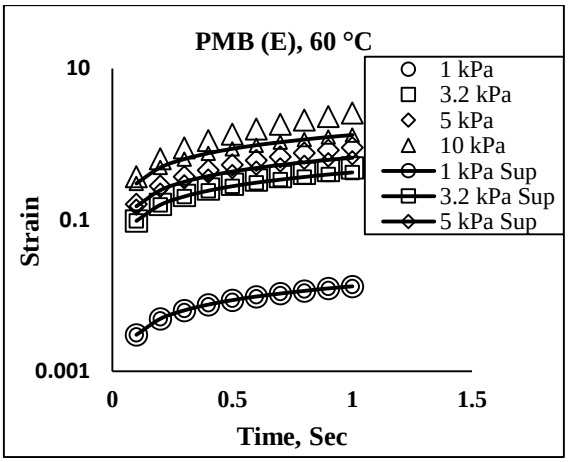

l

Figure 6.7(a-l) Validating Boltzmann superposition principle for different bitumen. (*Sup- Superimposed)

If Boltzmann superposition is to be valid for both creep and recovery phenomena, then the recovery could be written as

$$\varepsilon_r(t) = \varepsilon(t) - \varepsilon(t - t') \tag{6.11}$$

Where, the suffix *'r'* denotes the recovery region and *t'* is the time at which the load is removed. Applying this principle on the measured data, it was found that the data fitted poorly for all types of binder. However, good fit were observed for low stress level (100 Pa), higher temperatures (60 °C) and only for the conventional binders. In Figure 6.8 (a-h), the marked circles shows the deviation of model fit with measured results. As an example, plot for VG 30 and PMB (S) is shown for stress levels of 100 Pa and 5000 Pa at 40 °C and 60 °C.

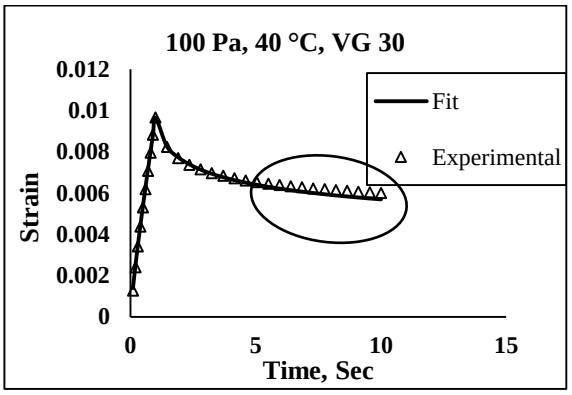

a

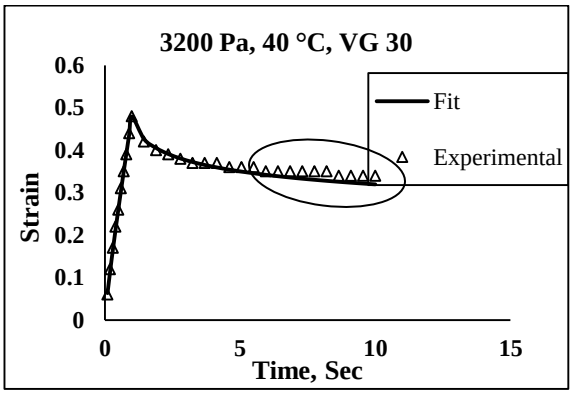

b

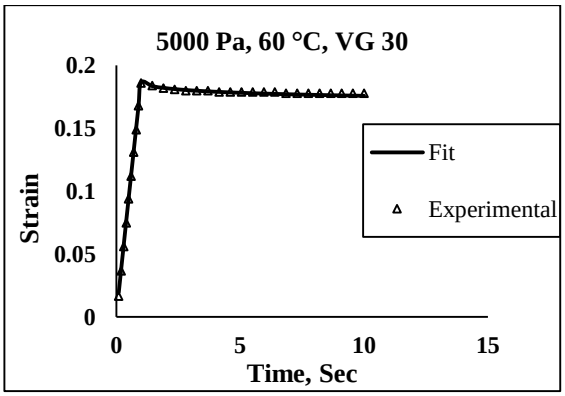

c

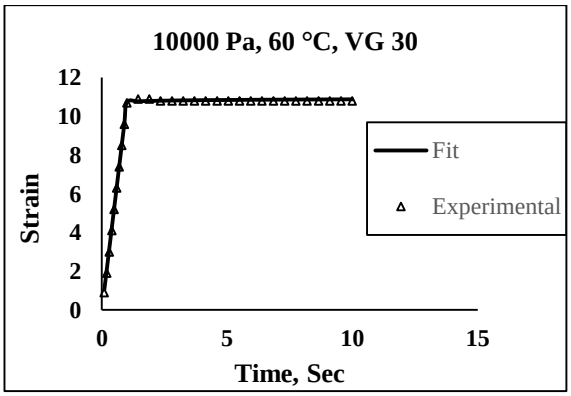

d

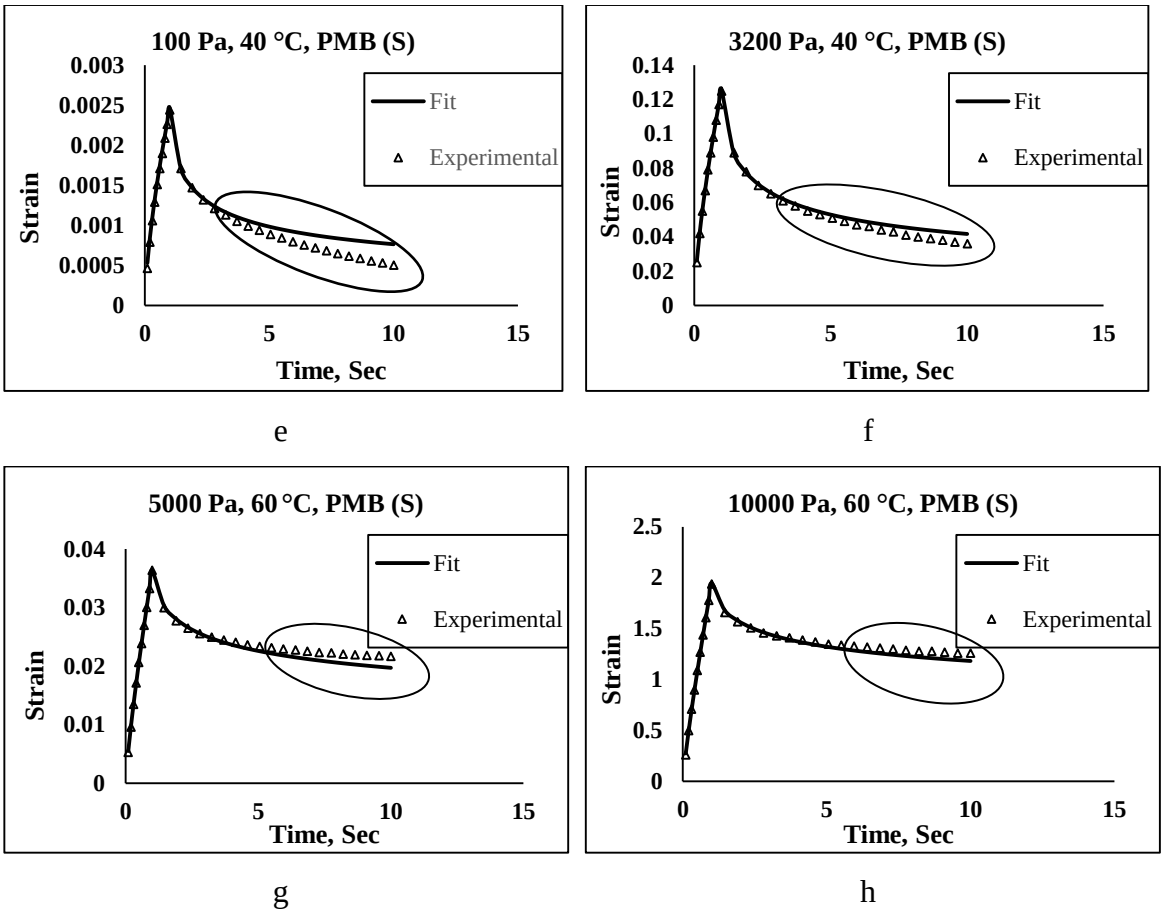

Figure 6.8(a-h) Power model plot for VG 30 and PMB (S) at 40 °C and 60 °C

6.3.2.3 Modification of Power model in recovery

To remove the small deviations between the modelled and experimental data observed in the Power law model, a factor *'n'* was introduced as a multiple of *B*, for modelling the recovery domain. The modified expression can be mathematically represented as

$$\varepsilon_r(t) = A.t^B - A.(t-t')^{B.n} \tag{6.12}$$

The factor *'n'* accounted for the nonlinearity associated with the asphalt binder. For linear materials the factor will be equal to 1. It was found that the above model gave excellent fit for all the binders, at all temperatures and stress levels. As an example, the model fit for PMB (S) and VG 30 is shown Figure 6.9 (a-h). It can be seen that the anomalies in Figure 6.8 are now removed by the application of the new recovery model. Similar results were

obtained for other binders at all the test temperatures and stress levels as can be seen in Figure 6.10 (i-xxxvi). It was found that the factor *B.n* (considered as α), correlated well with the J_{nR} and excellently with the average % recovery value for all the binders, as shown in Figure 6.11 (a,b). It increased with increase in J_{nR} and decreased with increase in average % recovery. A high value would indicate poor behavior in rutting. This parameter was further used to characterize the permanent deformation behavior of asphalt binders corresponding to different traffic level and temperature. After careful examination of the relationship between J_{nR} and the factor α (*B.n*), maximum values were assigned for different traffic level, beyond which the performance of the binder will degrade, and will make it rut susceptible. Table 6.5 presents the assigned values. To achieve a minimum value of 20% recovery, as recommended by the study, the value of α should never be greater than 0.92, irrespective of any stress level.

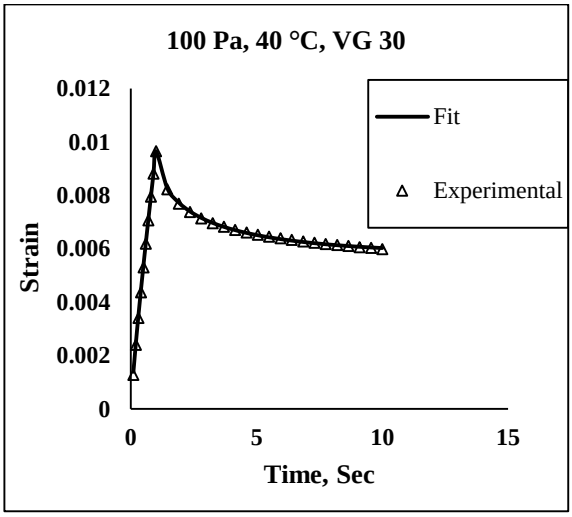

a

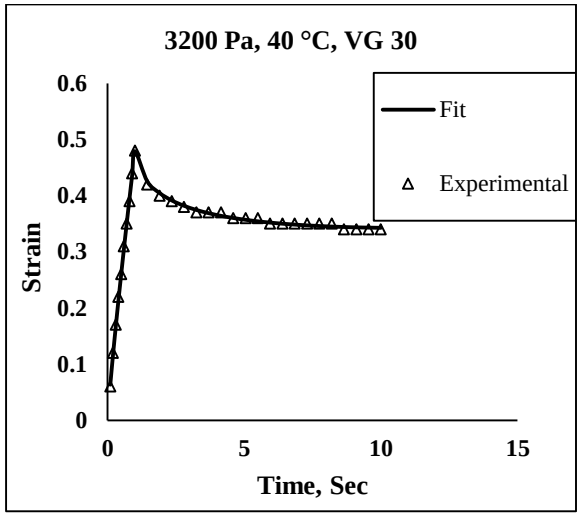

b

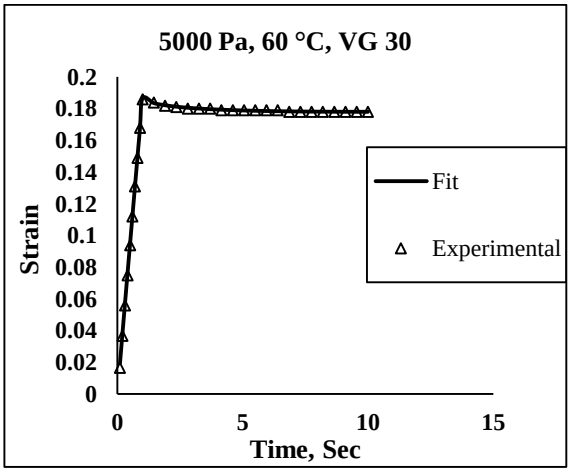

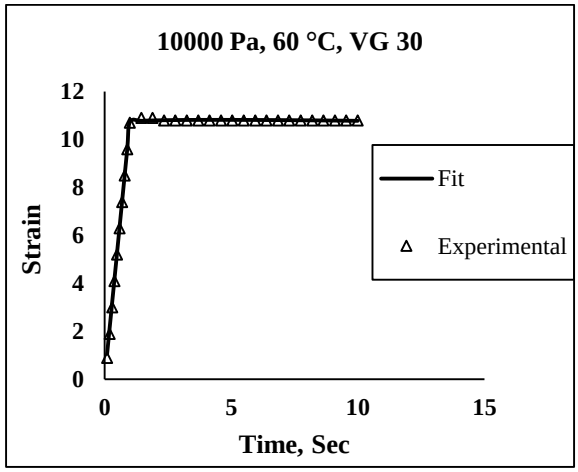

c

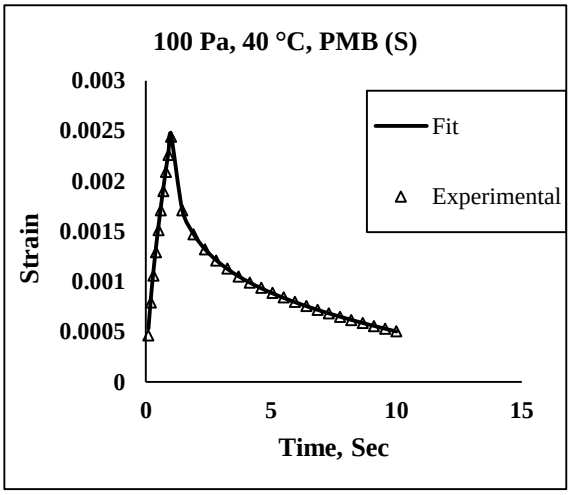

d

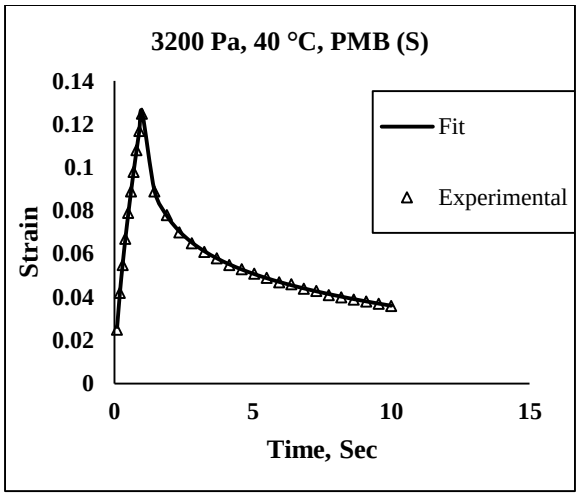

e

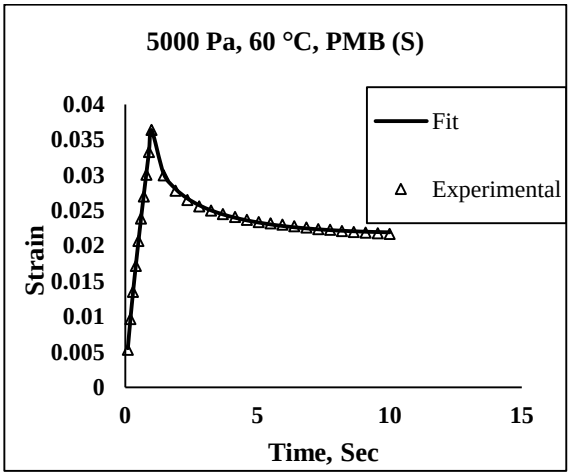

f

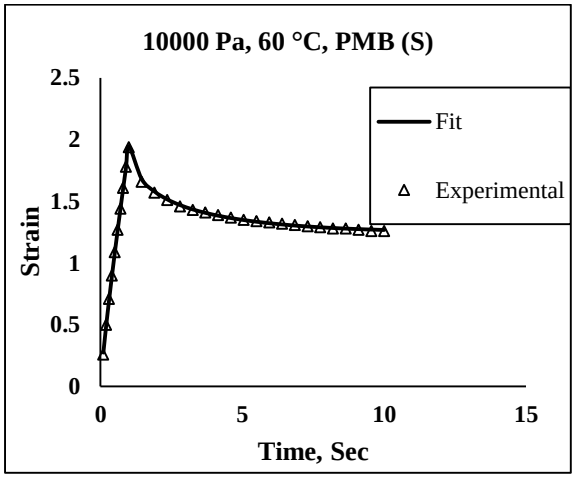

g h

Figure 6.9(a-h) Modified power model fit for VG 30 and SBS at 40 and 60 °C.

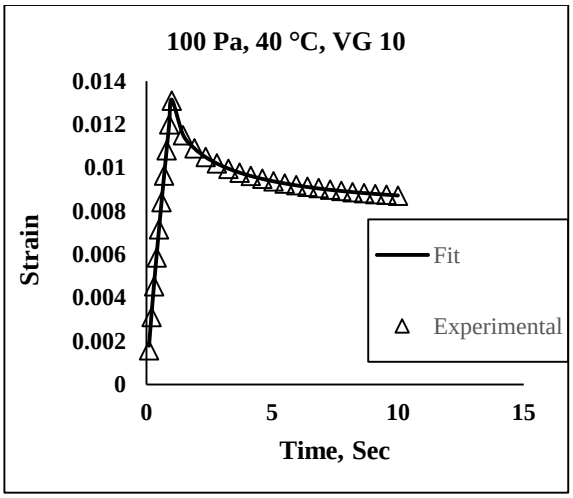

i

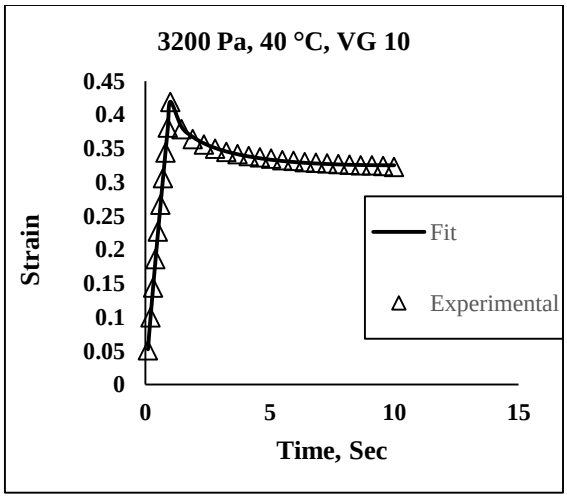

ii

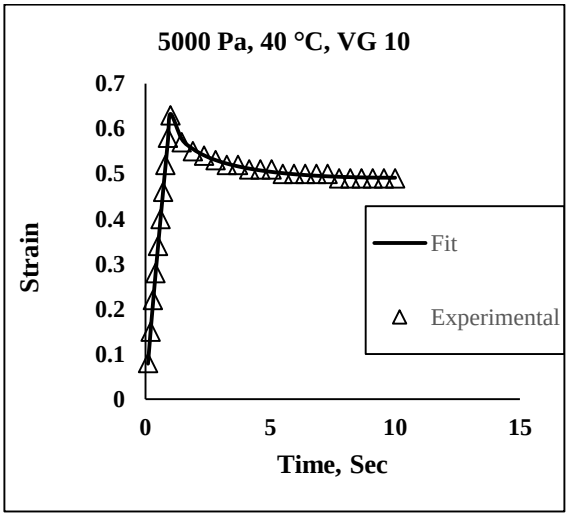

iii

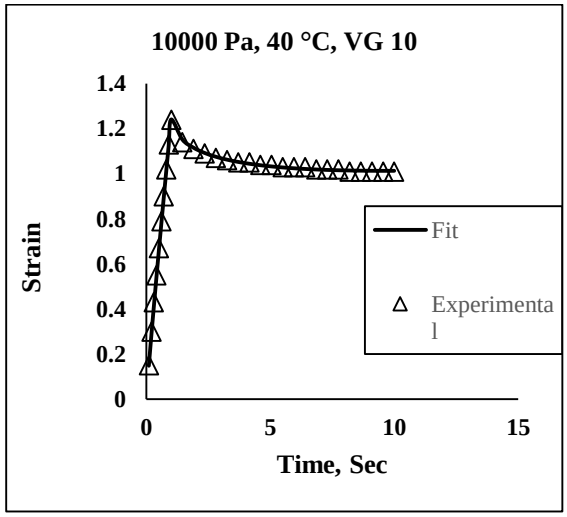

iv

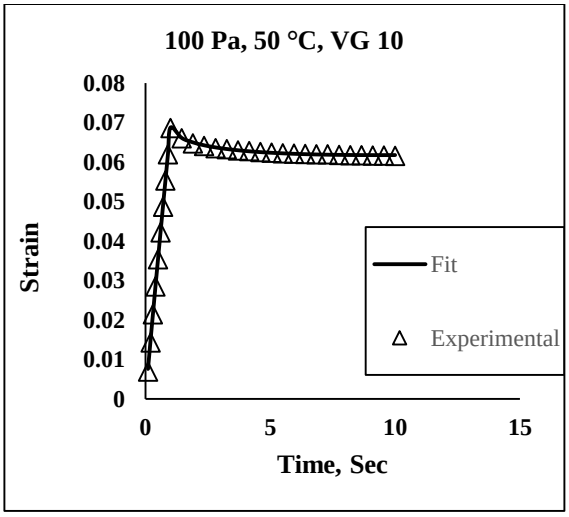

v

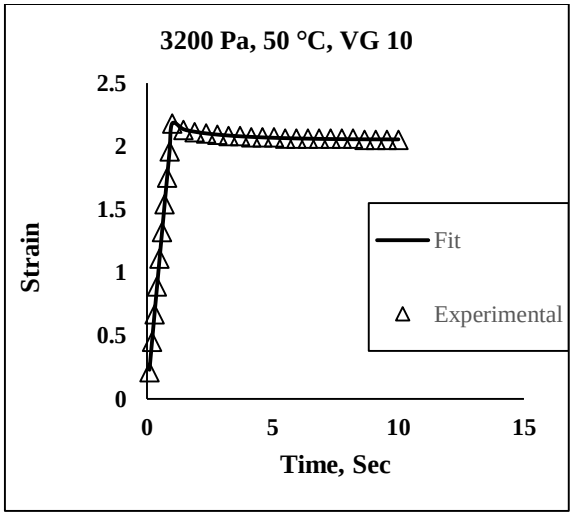

vi

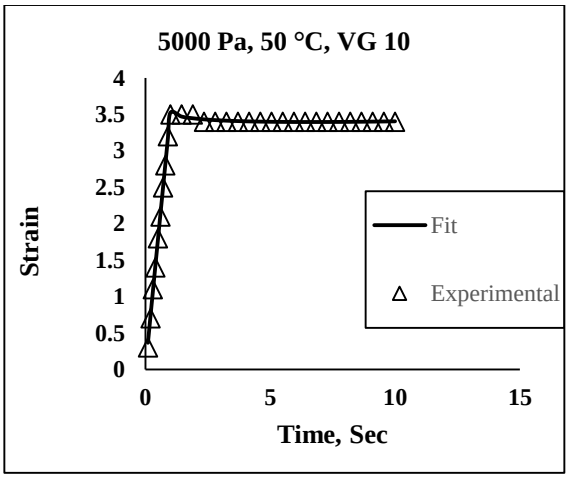

vii

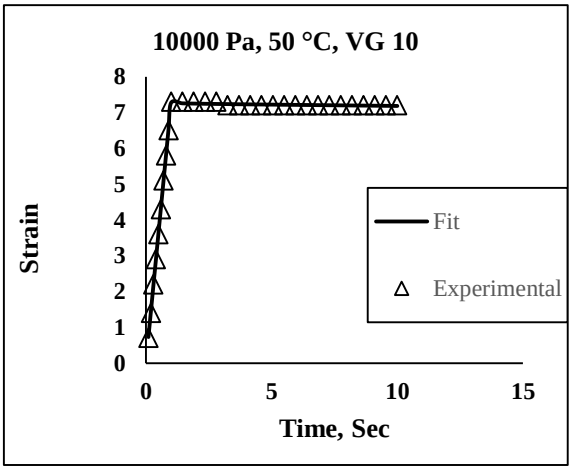

viii

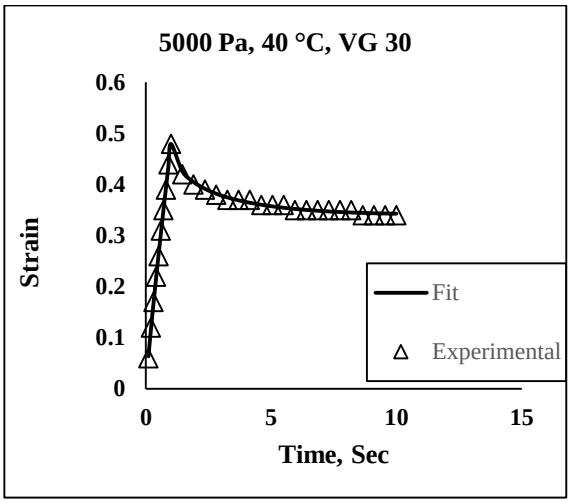

ix

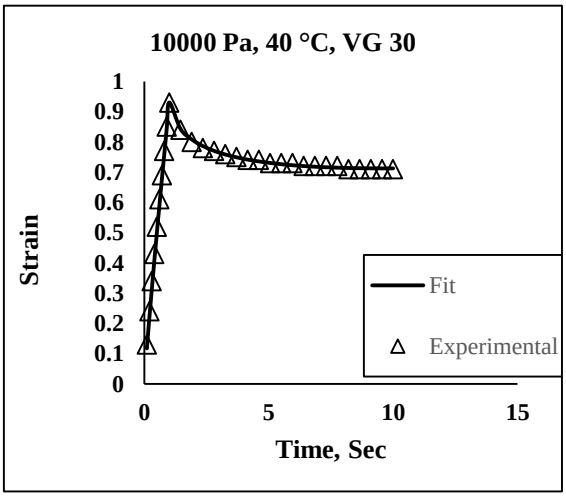

x

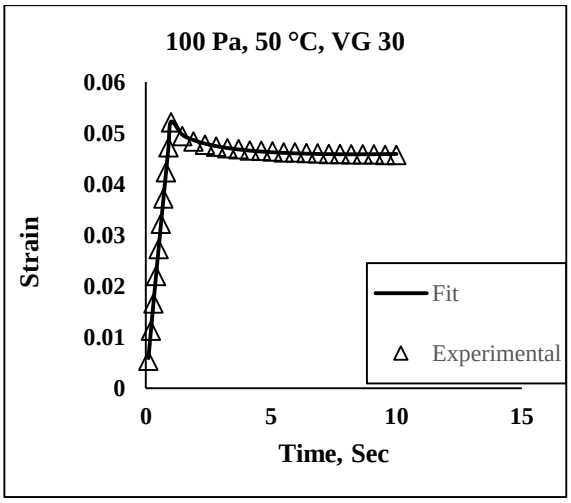

xi

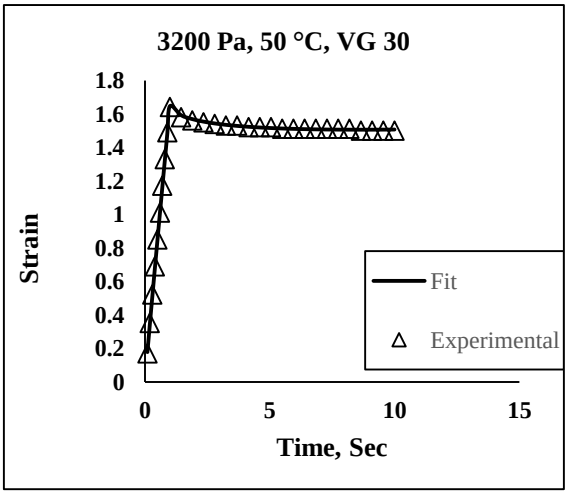

xii

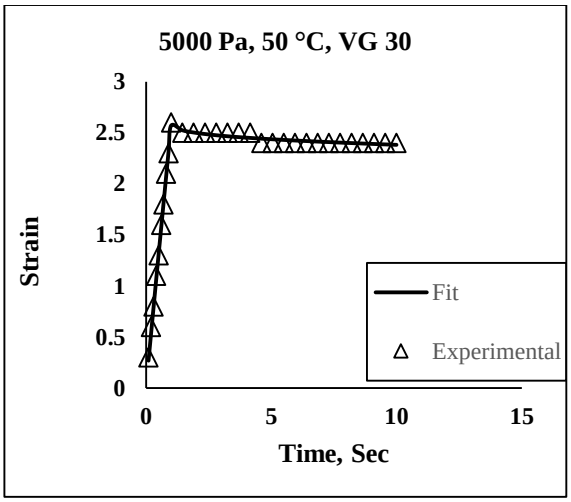

xii

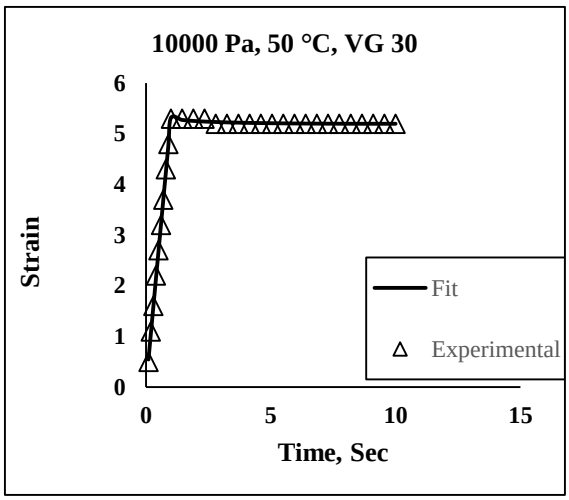

xiv

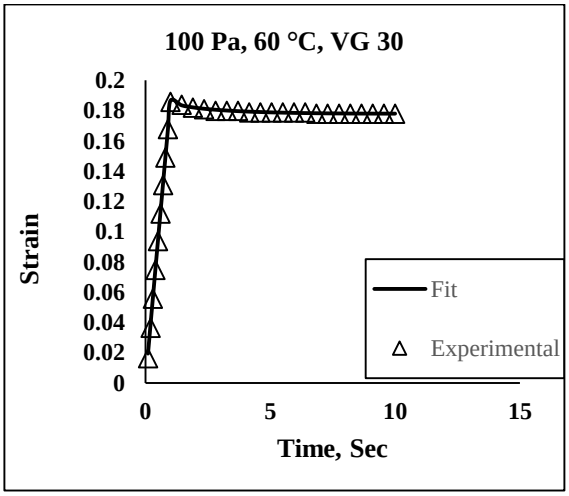

xv

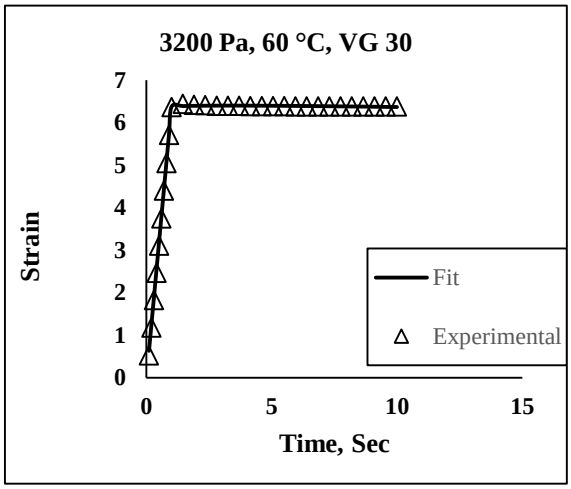

xvi

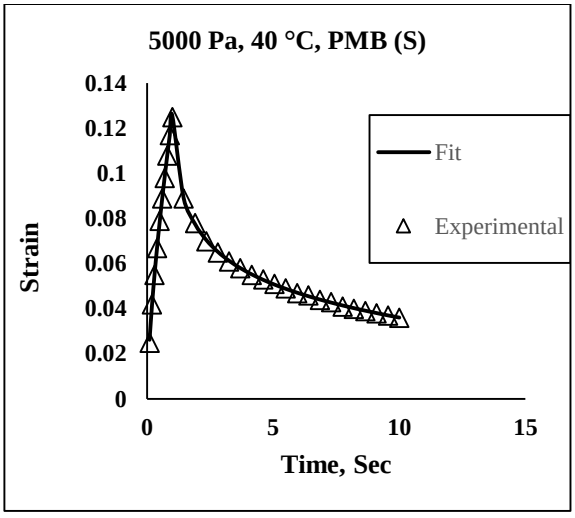

xvii

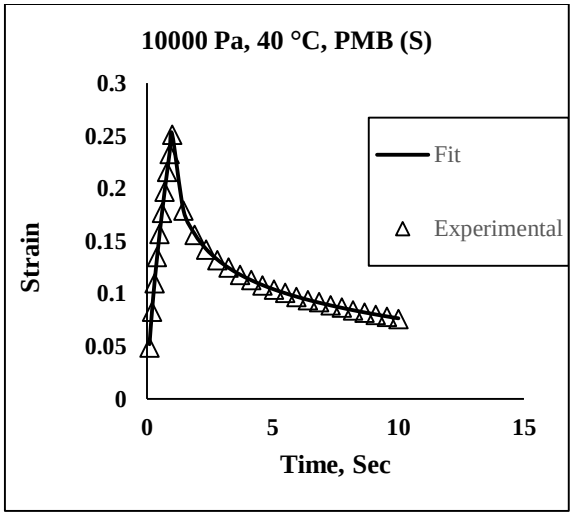

xviii

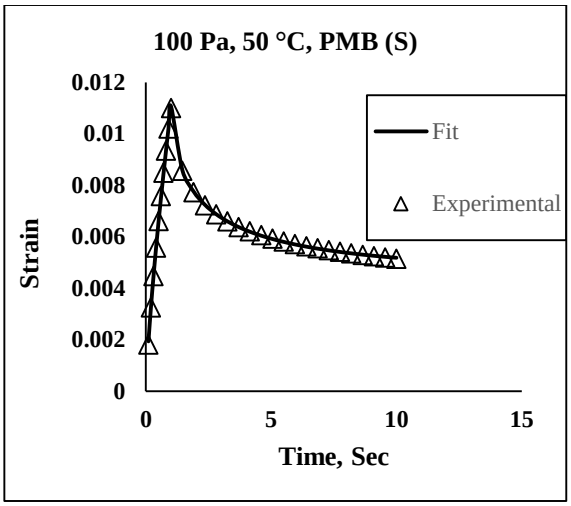

xix

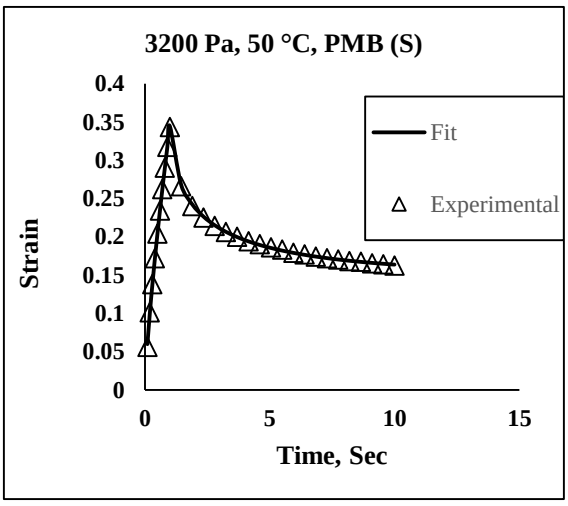

xx

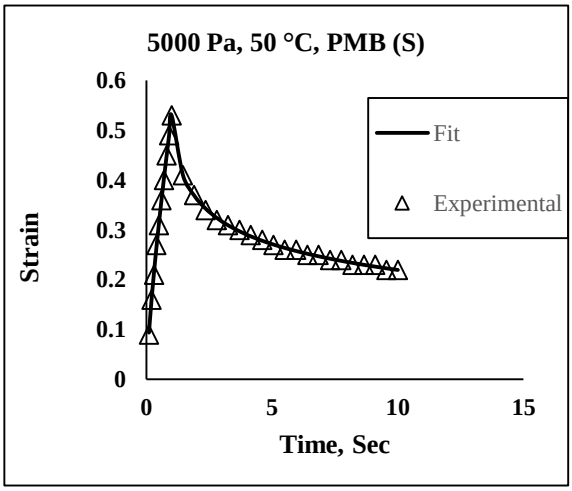

xxi

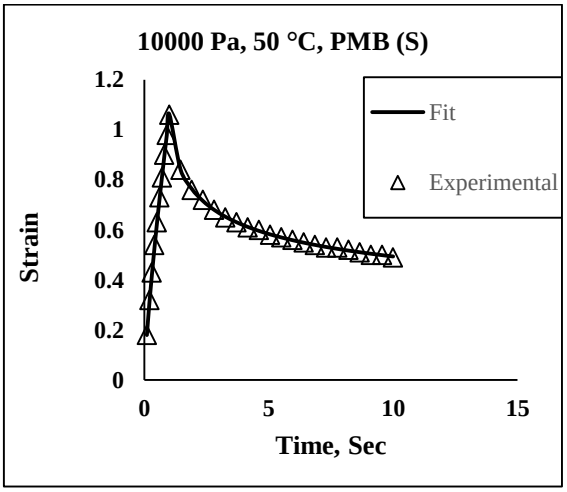

xxii

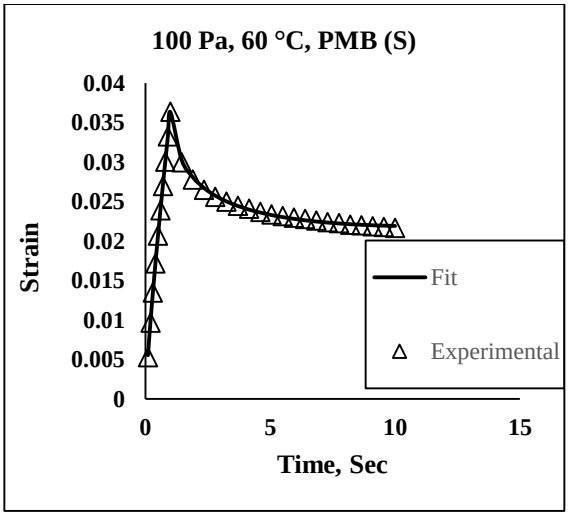

xxiii

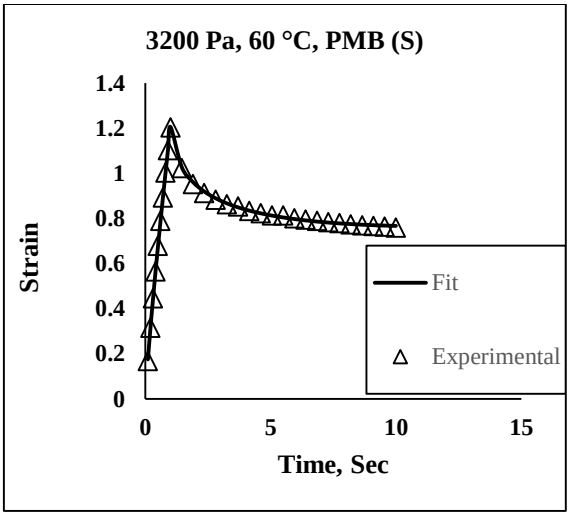

xxiv

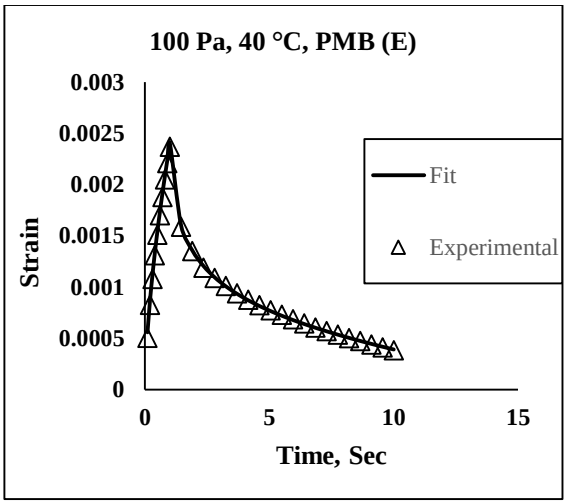

xxv

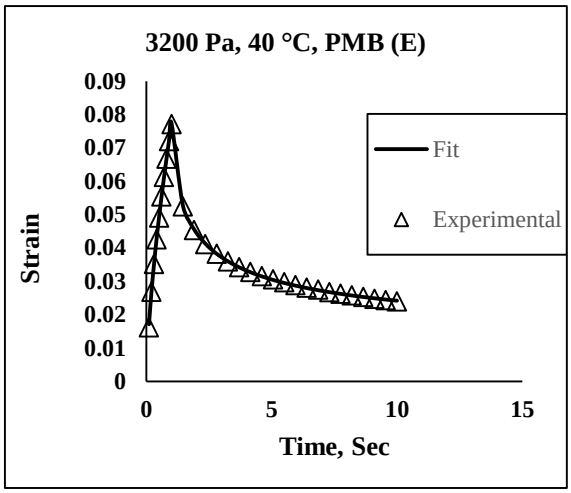

xvi

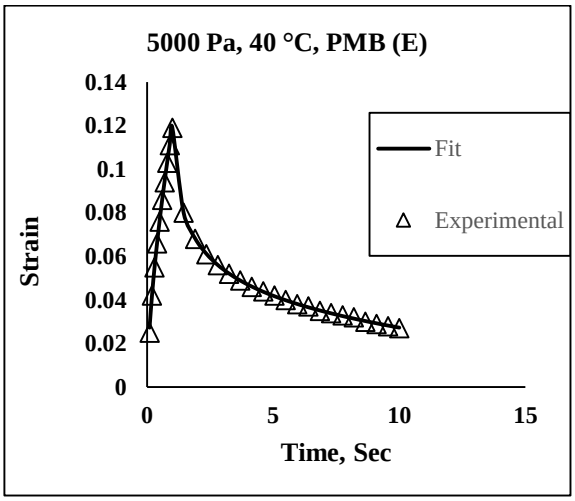

xvii

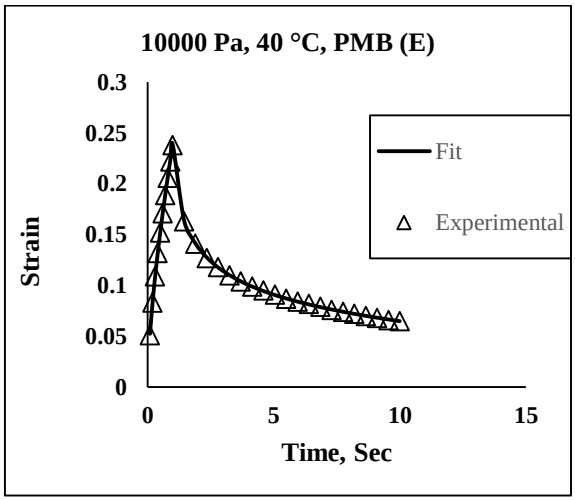

xviii

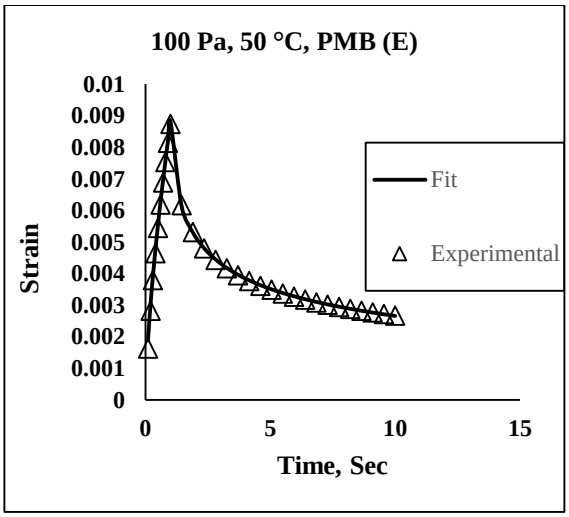

xix

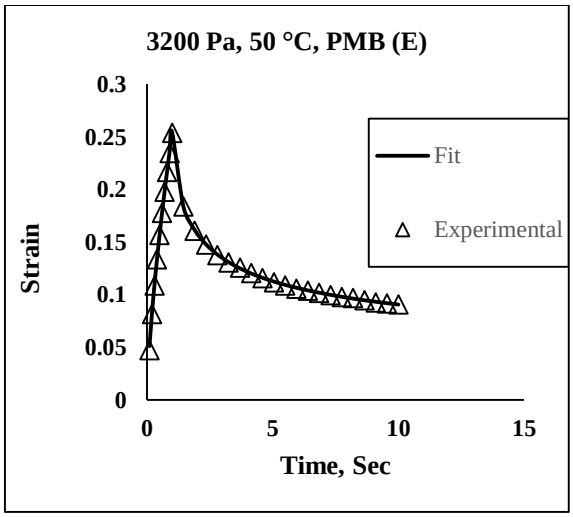

xxx

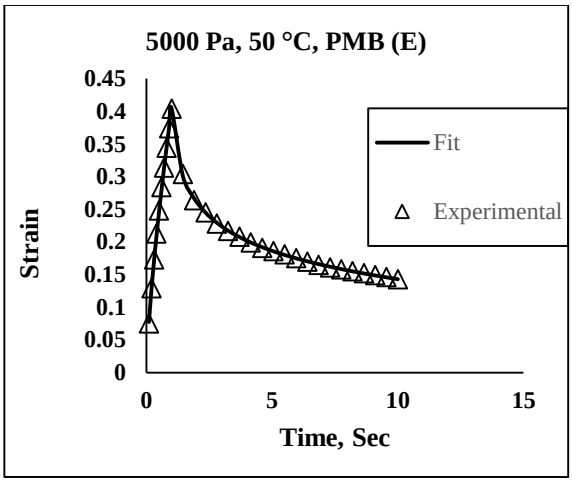

xxxi

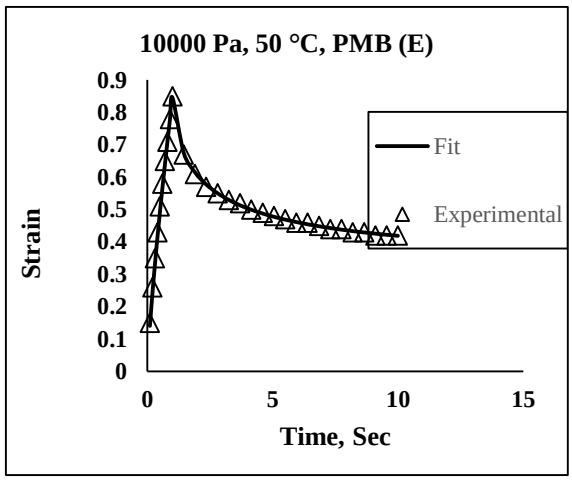

xxxii

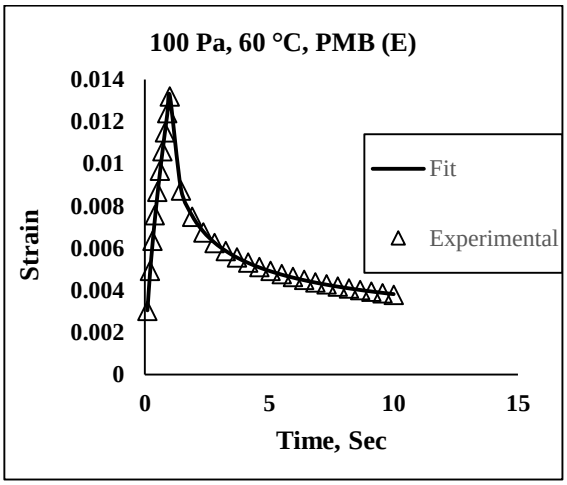

xxxiii

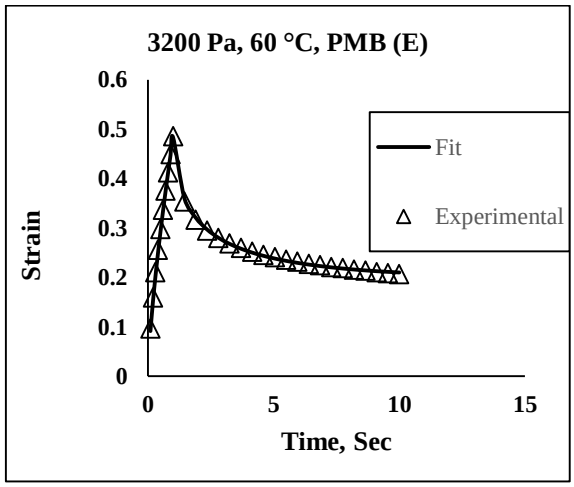

xxxiv

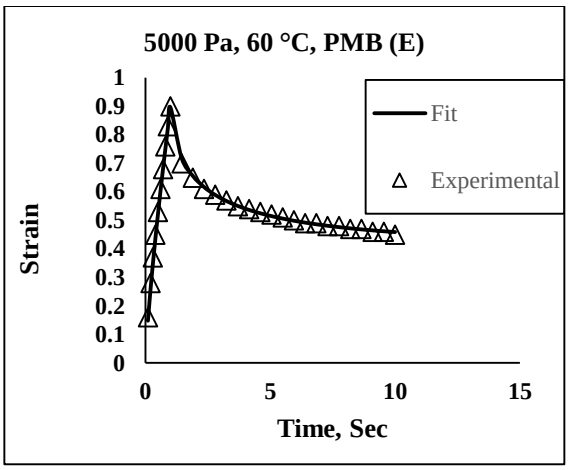

xxxv

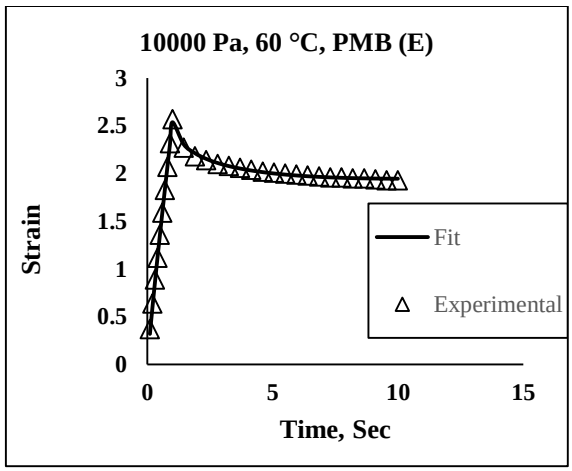

xxxvi

Figure 6.10 (i-xxxvi) Modified power model fit for all the binders.

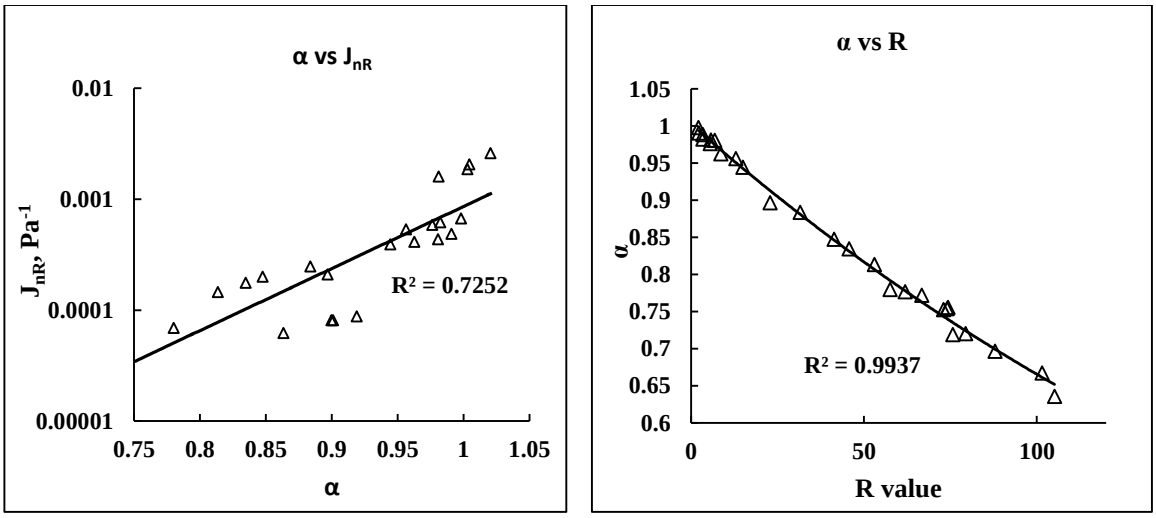

a b

Figure 6.11(a, b) Correlation between α with J_{nR} and % recovery

Table 6.5 Recommended maximum values of α for different traffic levels

Type of Grade	Traffic Level (ESAL, millions)	$J_{nR,3.2kPa}$, Maximum, kPa^{-1}	$\alpha_{critical}$(max)
S	<3	4	1
H	3-10	2	0.97
V	10-30	1	0.94
E	>30	0.5	0.91

6.3.2.4 Analysis of parameter B

The parameter *B* was found to be independent of the stress level at each temperature. However, it showed a linear relationship with temperature. Table 6.6 presents the average values obtained for all the type of binders at different test conditions. An interesting fact to be noted was that, the ratio of their averages, was almost constant irrespective of any temperature, as can be seen in Table 6.7. The ratio was taken corresponding to VG 10, just for referencing. This ratio was found to be same as the ratio of the corresponding softening point for the binders. Figure 6.12 shows the correlation.

Table 6.6 Average values of parameter B at different temperatures

Temp (°C)	VG 10	VG 30	PMB (S)	PMB (E)
40	0.89	0.86	0.69	0.64
50	0.99	0.96	0.76	0.71
60	1.07	1.04	0.83	0.78

Table 6.7 Ratio of B with respect to VG 10

Temperature (°C)	VG 30	PMB (S)	PMB (E)
40	0.97	0.78	0.72
50	0.97	0.77	0.72
60	0.97	0.78	0.73

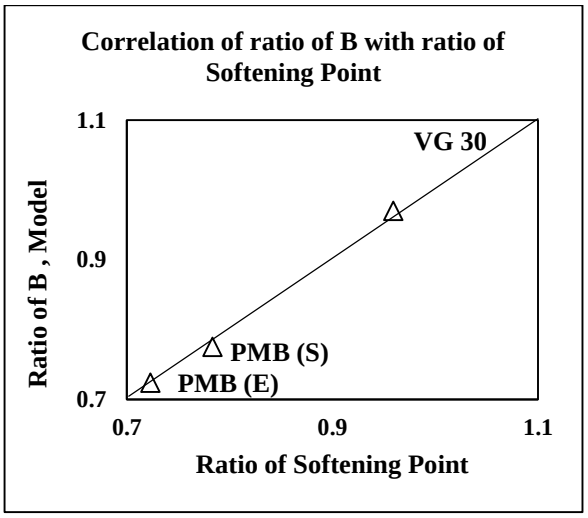

Figure 6.12 Correlation of ratio of B with the ratio of softening point.

Appreciating the above mentioned fact, the result can be now mathematically written as

$$B_{\psi,T} = \frac{SP_k}{SP_\psi} B_{k,T} \tag{6.13}$$

Where, ψ is any binder for which the value is to be determined, provided value of B is known for binder k at temperature T.

6.3.2.5 Analysis of Parameter A

The parameter A was found to be function of both stress level and the temperature. It was found to obey a power law behavior with respect to the stress level as shown in Figure 6.13 (a-c). Mathematically,

$$A = M\sigma_i^N \tag{6.14}$$

N represents the dependence of strain on the stress level. For linear behavior it remains close to 1. It was found close to 1 except for stress levels higher than 5000 Pa.

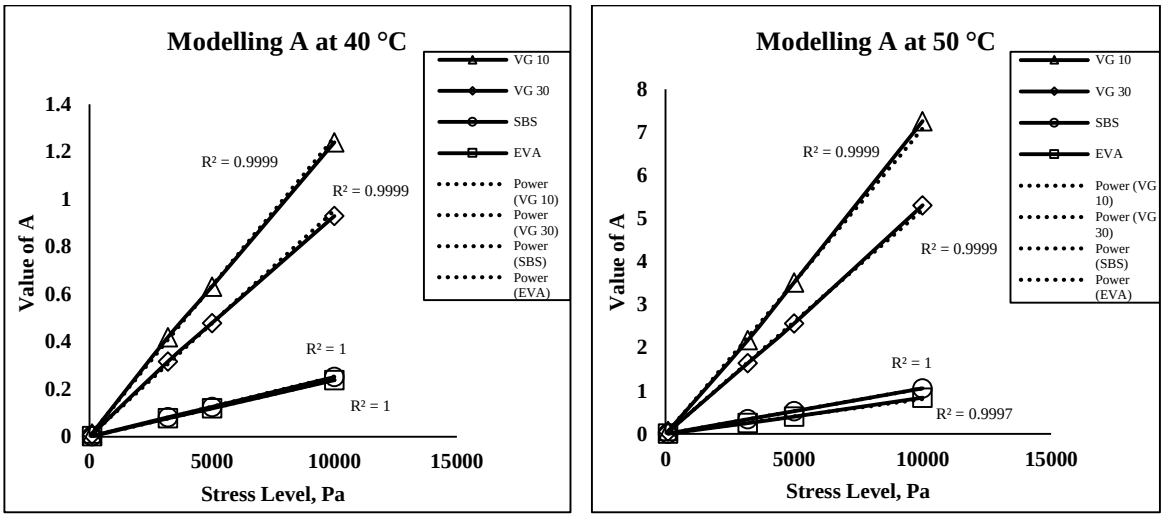

a b

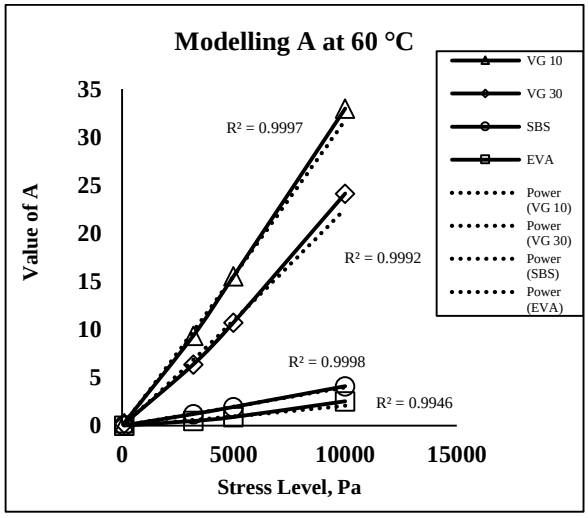

c

Figure 6.13(a-c) Power law fit for A.

Instead of going into the details of too many values obtained for different binders at various stress levels and temperatures, ratio of *A* of VG 30, PMB (S) and PMB (E) were taken with respect to VG 10. For a particular temperature this ratio was found to be invariant with stress level. Table 6.8 presents the average value obtained for all the binders.

Table 6.8 Average value of ratio of *A* taken with respect to VG 10

Temperature (^{0}C)	VG 30	PMB (S)	PMB (E)
40	1.33	5.11	5.35
50	1.34	6.51	8.43
60	1.44	7.87	17.72

The ratio, at a particular temperature showed excellent correlation with the inverse of the ratio of Zero Shear Viscosity (ZSV) of the binders. This portrays the temperature sensitivity of PMBs in comparison to the virgin binders. It can be seen that the increase in the ratio is higher for PMB (E), especially at higher temperature. At 40 °C the value of PMB (S) and PMB (E) is almost close to each other, but as the temperature increases, the corresponding values differ to a very high degree. This shows the shift of behavior of other binders towards more viscous regime, while EVA maintains a higher degree of stiffness with increase in temperature. Figure 6.14 (a-c) shows the plot of both the ratios at the three temperatures studied.

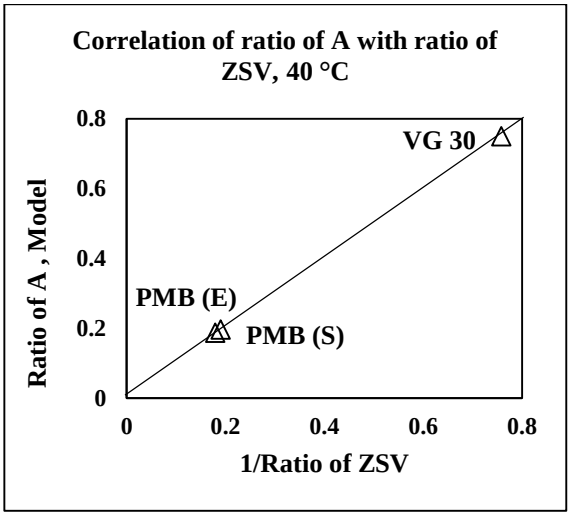

a

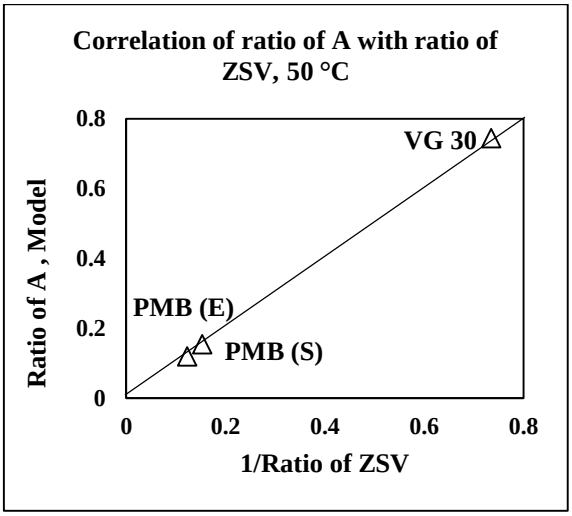

b

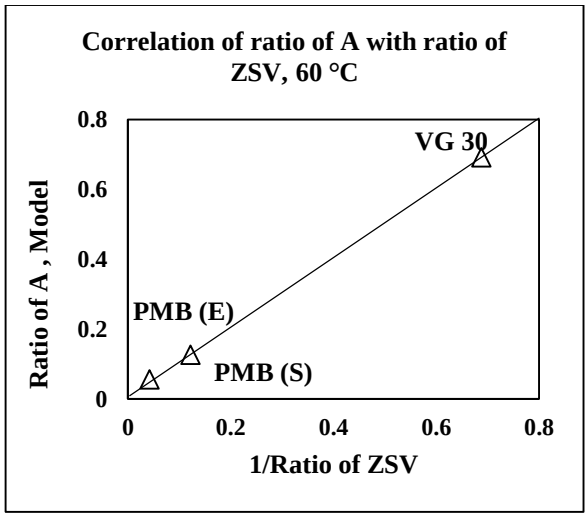

c

Figure 6.14(a-c) Correlation of ratio of A with inverse ratio of ZSV.

The result can hence be summarized as

$$\left[A_{\psi,T}\right]_{\sigma_i} = \frac{ZSV_{\psi,T}}{ZSV_{k,T}} A_{k,T} \tag{6.15}$$

So, if the value of A and B for any binder 'k' is known, the corresponding values for any other binder 'ψ' can be calculated using the above relationship.

The whole model of creep can now be written as

$$\left[\varepsilon(t)\right]_{T,\sigma_i,\psi} = \frac{\left[ZSV\right]_{\psi,T}}{\left[ZSV\right]_{k,T}} A_{k,T} t^{(\frac{SP_k}{SP_\psi})B_k} \tag{6.16}$$

6.3.2.6 Analysis of Parameter α

The parameter *B.n* (considered as α) was found to have similar correlation as the factor *B*. so, the factor α could be written as

$$\alpha_{\psi,T} = \frac{SP_k}{SP_\psi}\alpha_{k,T} \tag{6.17}$$

The model of recovery for any binder ψ, provided the model parameters of binder k is known, can be written as

$$\left[\varepsilon(t)\right]_{T,\sigma_i,\psi} = \frac{\left[ZSV\right]_{\psi,T}}{\left[ZSV\right]_{k,T}} A_{k,T} t^{(\frac{SP_k}{SP_\psi})B_k} - \frac{\left[ZSV\right]_{\psi,T}}{\left[ZSV\right]_{k,T}} A_{k,T}(t-t')^{(\frac{SP_k}{SP_\psi})\alpha_k} \tag{6.18}$$

6.3.3 *Variation of fatigue life with strain*

Figure 6.15 (a-c) shows the comparison of fatigue lives for all the binders at the three temperatures considered in the study. It can be seen that PMB (S) outperforms all the binders irrespective of any test temperatures. At 10 and 20 ºC, for low strain levels, PMB (E) had higher fatigue life than VG 10 and VG 30. As the strain level increased (typically after 10%) the fatigue life decreased steeply for PMB (E), giving lower values than the conventional binders. This describes the higher strain susceptibility for plastomeric PMB (E). Due to higher stiffness at lower temperature, PMB (E) tends to undergo brittle failure when strained to higher strain amplitudes. This is attributed to the crystalline nature of the polyethylene segment in EVA, which imparts brittle nature to the binder at lower temperatures. However at 30 ºC, the fatigue life of PMB (E) was found to be higher than VG 30. The conventional binders displayed interesting behavior. VG 10 and VG 30 had lower fatigue lives at lower strain amplitudes. But the rate of decrease in fatigue life with increase in strain level was lower than the polymer modified binders. VG 10 had the lowest strain susceptibility and gave better results than PMB (E) and VG 30 at higher strain amplitudes. As can be seen in Table 5.1 that the true intermediate temperature, for $G^*.sin\delta$ to be lower than 5000 kPa, is lowest for PMB (E), indicating that it would perform better than all other binders. This is in contrary to the ranking of binder as demonstrated by LAS test results. Moreover, in the traditional method, the wide spectrum of fatigue behavior with change in strain level cannot be evaluated. Hence LAS test is a better way of judging the relative fatigue performance of different binders. Figure 6.16 (a-l) shows the stress strain curve generated through the amplitude sweep test. It can be seen that the slope of the curve first increases and after

reaching a particular strain level it starts decreasing indicating fatigue failure of the asphalt binder. The strain at which the slope decreases is found to be binder and temperature dependent. A higher area under the stress strain curve is an indication of better performance in fatigue. For all the binders this area increases with increase in temperature. Moreover for PMB (S), the wide areal distribution at all the temperatures indicates its superiority over other binders in fatigue. The damage intensity curve fit as described by equation 2.41 in chapter 2 is also presented in Figure 6.17 (a-l). It is found that the experimental data and the curve fit simulated using the equation are in good agreement with each other. This is an indication of the accuracy of LAS test in simulating the damage growth in asphalt binders

6.3.3.1 Analysis of test parameters

The fatigue life for all the binders using LAS method was found to be sensible to the value of α and *A*. A lower value of α and a higher value of *A* is desirable for superior performance in fatigue. 'α' indicates the rate of reduction in fatigue life with increase in strain amplitude. A lower value would indicate lower strain susceptibility. In general, α decreases and *A* increases with increase in temperature for all the binders. But the change in the respective values with change in temperature is different for each binder. Also, it is observed that the value of α has dependence on the stiffness of binder. The value increased with increase in stiffness, with PMB (E) having the highest value. Table 6.9 presents the values of the *A* and α at all the test temperatures.

6.3.3.2 Effect of temperature on fatigue life

Variation of fatigue life with temperature was also evaluated corresponding to two different strain levels as can be seen in Figure 6.18 (a,b). Usually, it is assumed that the strain in the binder is about 50 times than that in the mixture [107]. Hence the fatigue life at two strain levels were evaluated for comparison. 2.5% and 5% corresponding to 500 micro strain and 1000 micro strain was reported. In general, the fatigue life increase with increase in temperature for all the binders. The increase in fatigue life with increase in temperature was highest for VG 10, indicating higher temperature susceptibility.

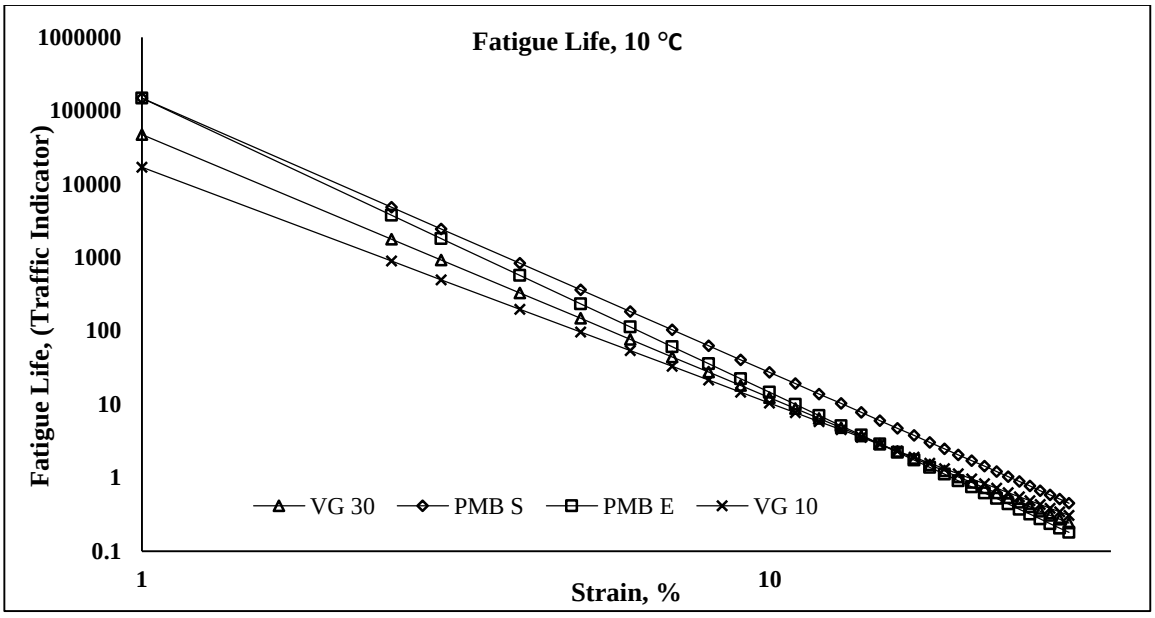
Fatigue Life, 10 °C
Fatigue Life, (Traffic Indicator)
1000000
100000
10000
1000
100
10
1
0.1
VG 30
PMB S
PMB E
VG 10
1
10
Strain, %

a

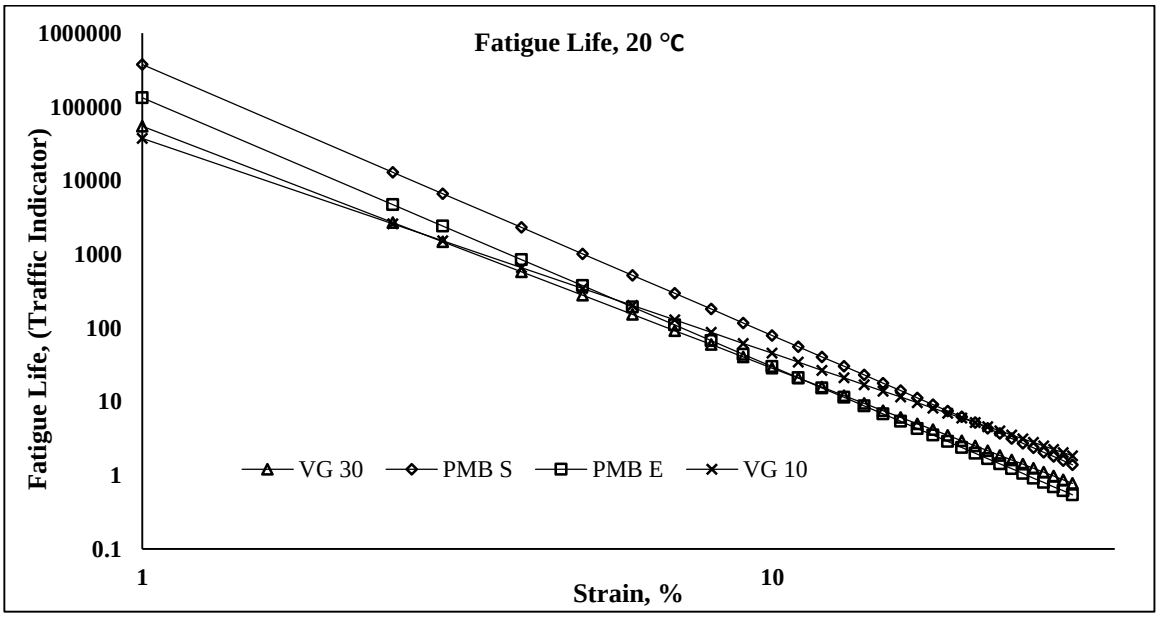
Fatigue Life, 20 °C
Fatigue Life, (Traffic Indicator)
1000000
100000
10000
1000
100
10
1
0.1
VG 30
PMB S
PMB E
VG 10
1
10
Strain, %

b

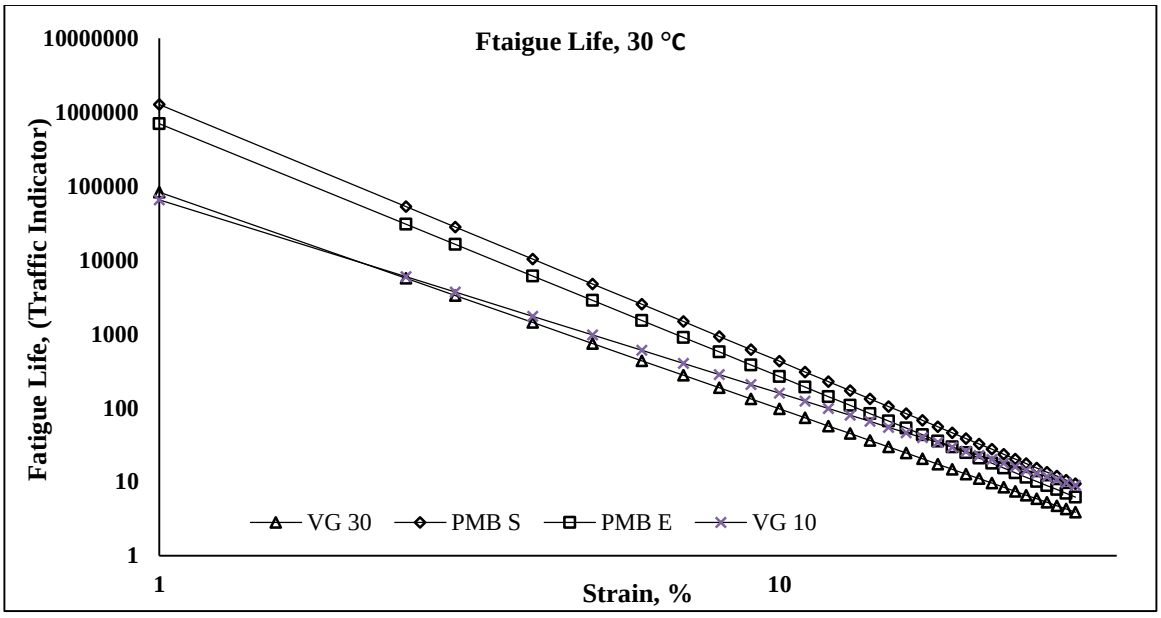

c

Figure 6.15 (a-c) Variation of fatigue life at different temperatures.

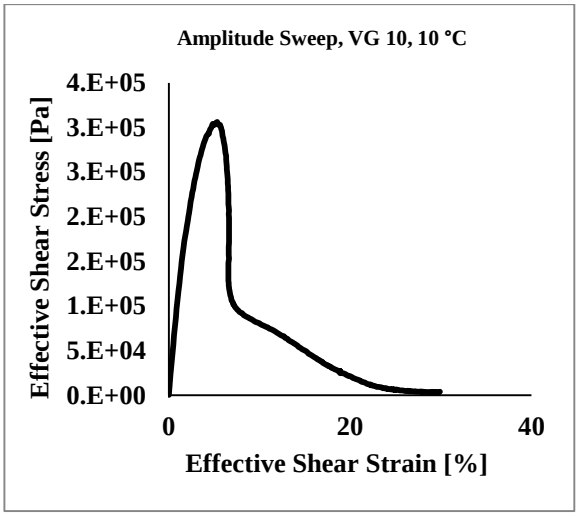

a

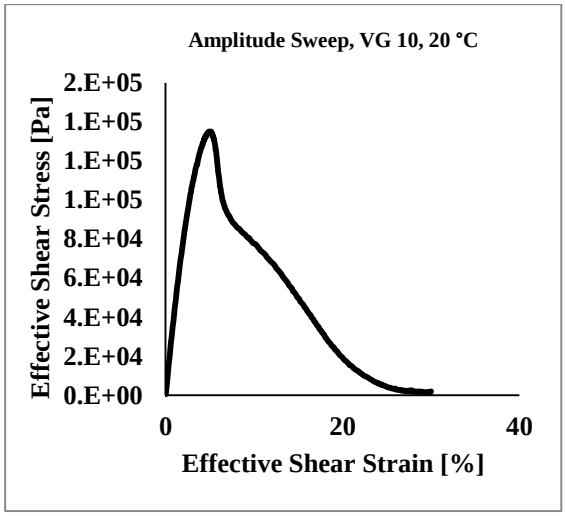

b

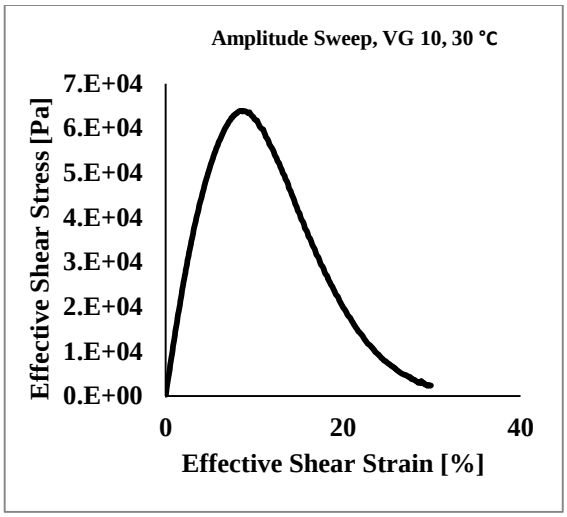
Amplitude Sweep, VG 10, 30 °C
Effective Shear Stress [Pa]
7.E+04
6.E+04
5.E+04
4.E+04
3.E+04
2.E+04
1.E+04
0.E+00
0
20
40
Effective Shear Strain [%]

c

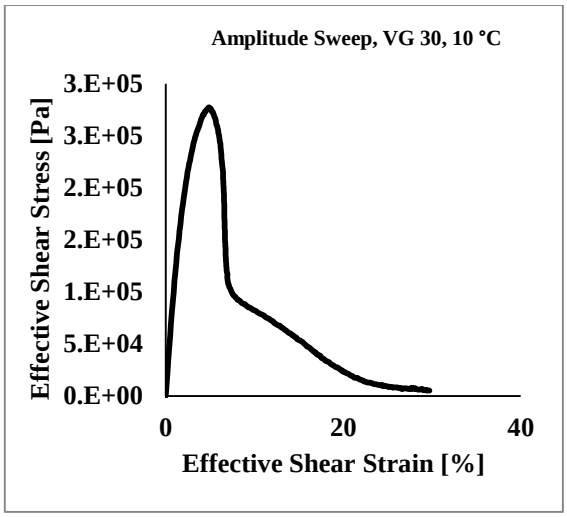
Amplitude Sweep, VG 30, 10 °C
Effective Shear Stress [Pa]
3.E+05
3.E+05
2.E+05
2.E+05
1.E+05
5.E+04
0.E+00
0
20
40
Effective Shear Strain [%]

d

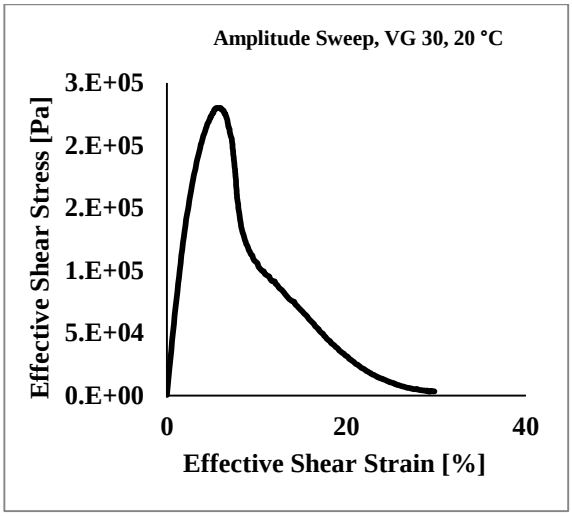
Amplitude Sweep, VG 30, 20 °C
Effective Shear Stress [Pa]
3.E+05
2.E+05
2.E+05
1.E+05
5.E+04
0.E+00
0
20
40
Effective Shear Strain [%]

e

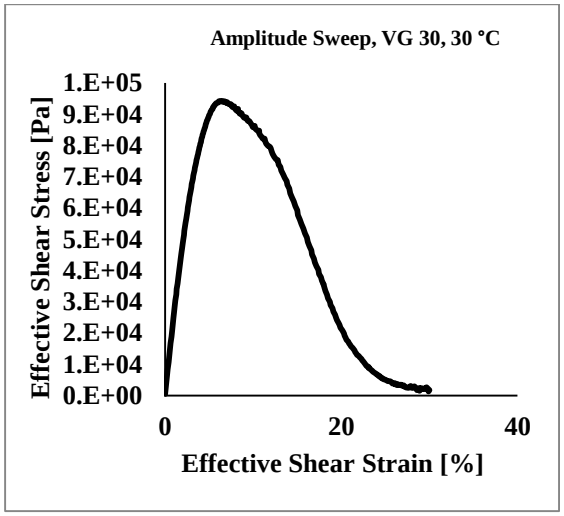
Amplitude Sweep, VG 30, 30 °C
Effective Shear Stress [Pa]
1.E+05
9.E+04
8.E+04
7.E+04
6.E+04
5.E+04
4.E+04
3.E+04
2.E+04
1.E+04
0.E+00
0
20
40
Effective Shear Strain [%]

f

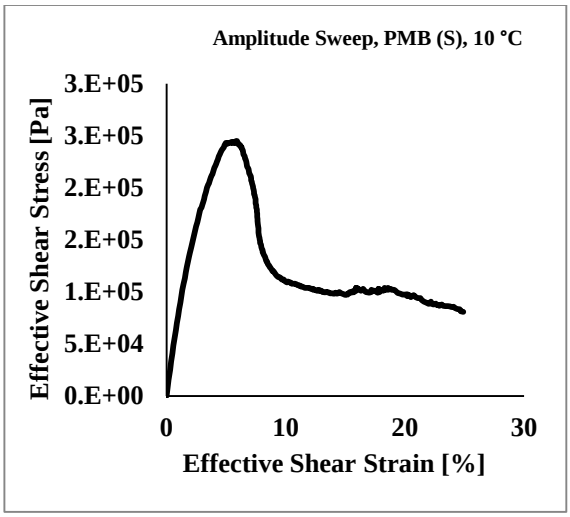
Amplitude Sweep, PMB (S), 10 °C
Effective Shear Stress [Pa]
3.E+05
3.E+05
2.E+05
2.E+05
1.E+05
5.E+04
0.E+00
0
10
20
30
Effective Shear Strain [%]

g

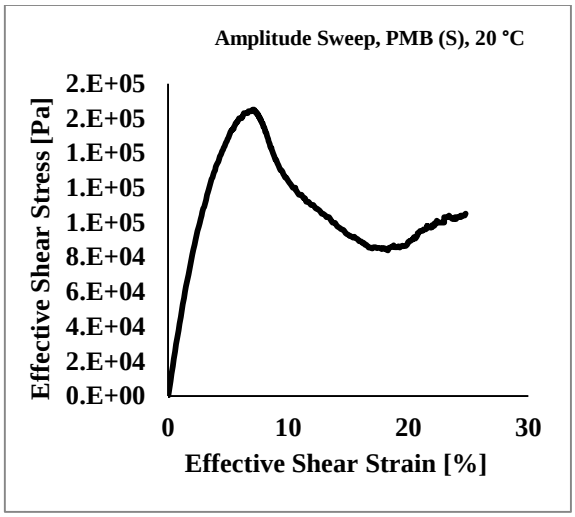
Amplitude Sweep, PMB (S), 20 °C
Effective Shear Stress [Pa]
2.E+05
2.E+05
1.E+05
1.E+05
1.E+05
8.E+04
6.E+04
4.E+04
2.E+04
0.E+00
0
10
20
30
Effective Shear Strain [%]

h

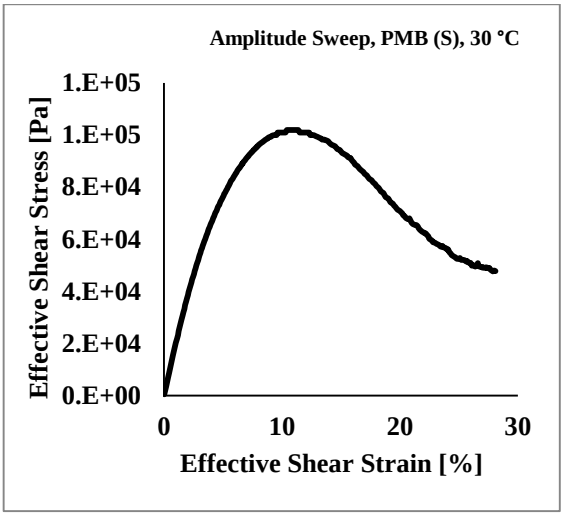
Amplitude Sweep, PMB (S), 30 °C
Effective Shear Stress [Pa]
1.E+05
1.E+05
8.E+04
6.E+04
4.E+04
2.E+04
0.E+00
0
10
20
30
Effective Shear Strain [%]

i

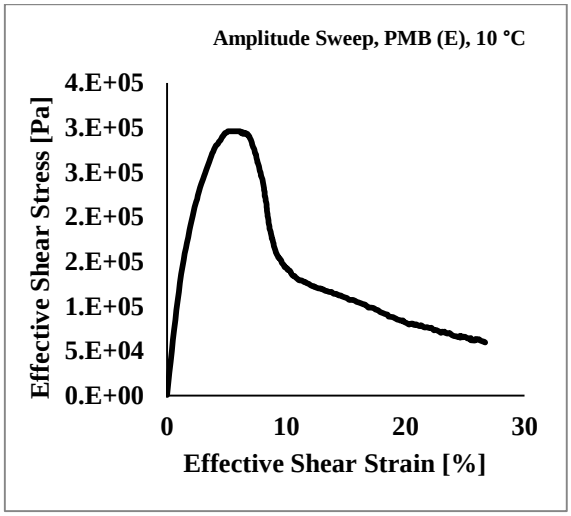
Amplitude Sweep, PMB (E), 10 °C
Effective Shear Stress [Pa]
4.E+05
3.E+05
3.E+05
2.E+05
2.E+05
1.E+05
5.E+04
0.E+00
0
10
20
30
Effective Shear Strain [%]

j

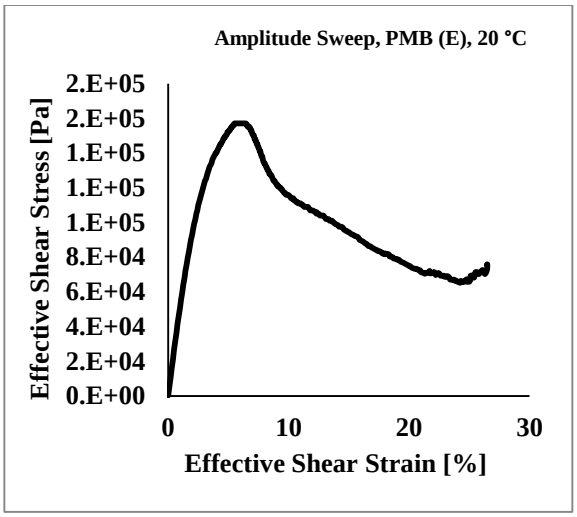

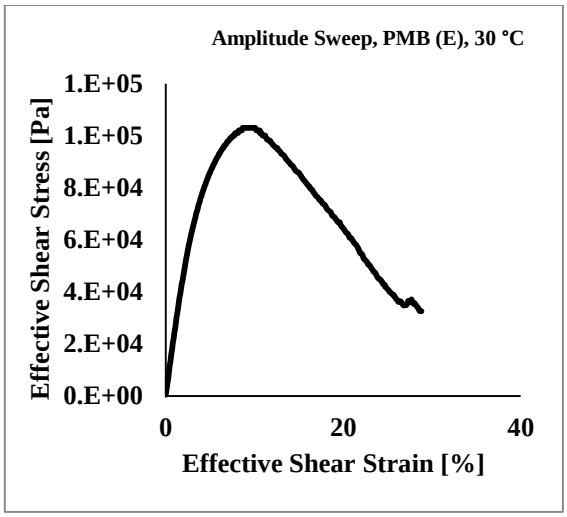

k l

Figure 6.16(a-l) Stress strain curve from amplitude sweep test

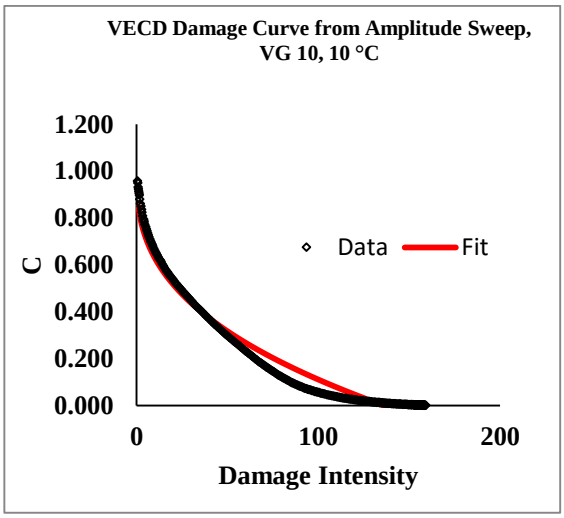

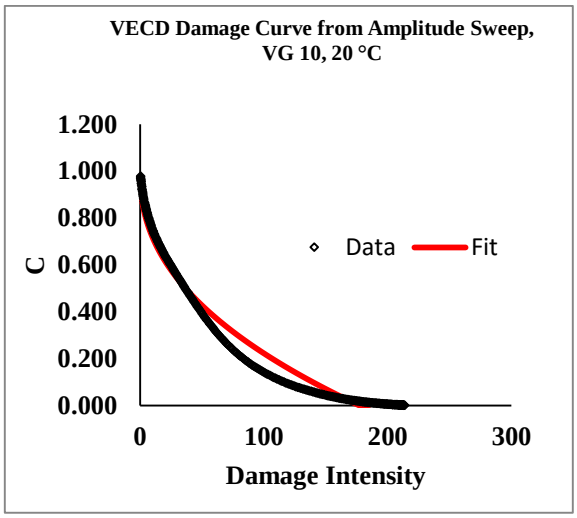

a b

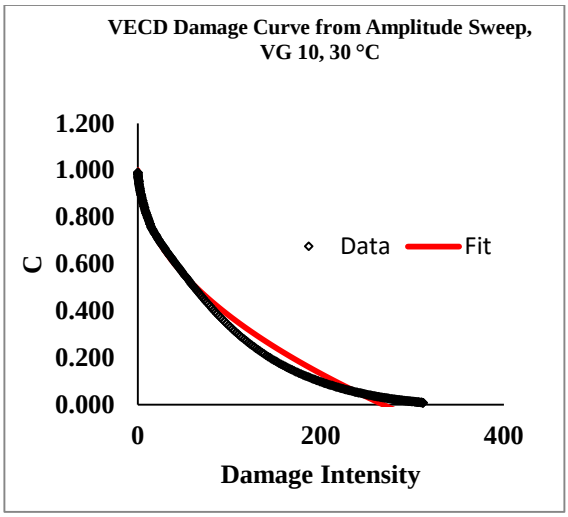
VECD Damage Curve from Amplitude Sweep, VG 10, 30 °C
C
1.200
1.000
0.800
0.600
0.400
0.200
0.000
Data
Fit
0
200
400
Damage Intensity

c

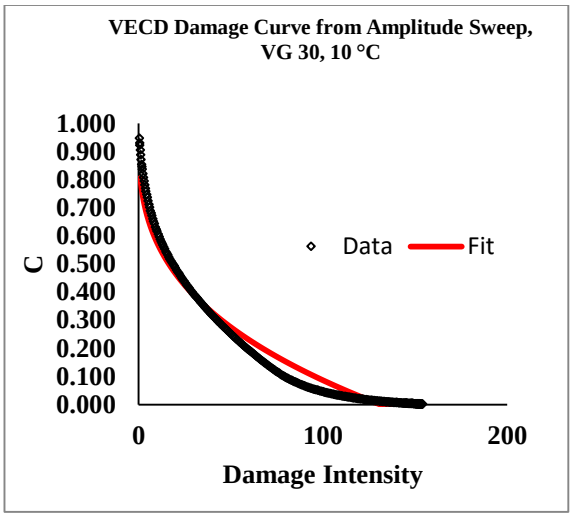
VECD Damage Curve from Amplitude Sweep, VG 30, 10 °C
C
1.000
0.900
0.800
0.700
0.600
0.500
0.400
0.300
0.200
0.100
0.000
Data
Fit
0
100
200
Damage Intensity

d

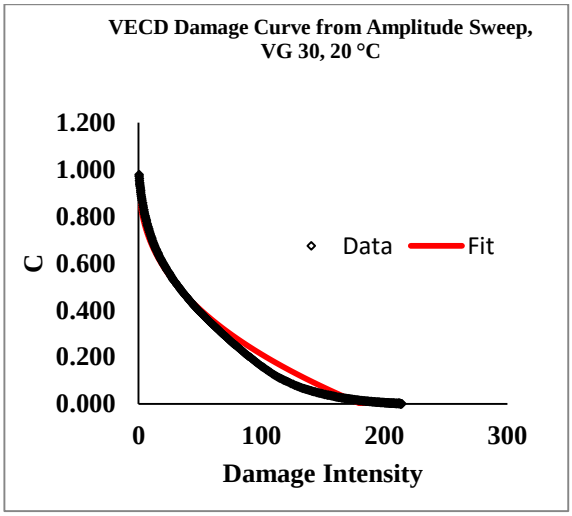
VECD Damage Curve from Amplitude Sweep, VG 30, 20 °C
C
1.200
1.000
0.800
0.600
0.400
0.200
0.000
Data
Fit
0
100
200
300
Damage Intensity

e

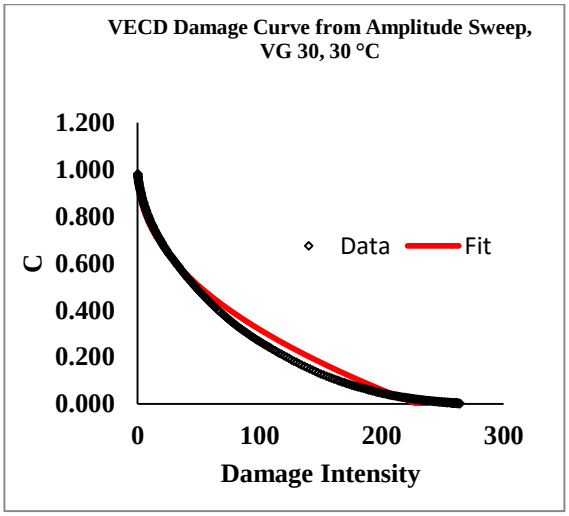
VECD Damage Curve from Amplitude Sweep, VG 30, 30 °C
C
1.200
1.000
0.800
0.600
0.400
0.200
0.000
Data
Fit
0
100
200
300
Damage Intensity

f

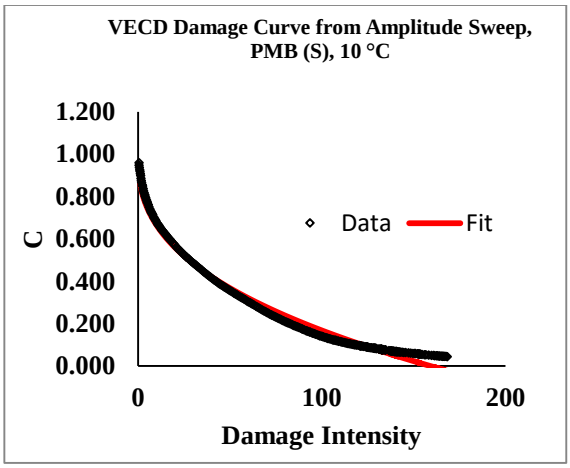

g

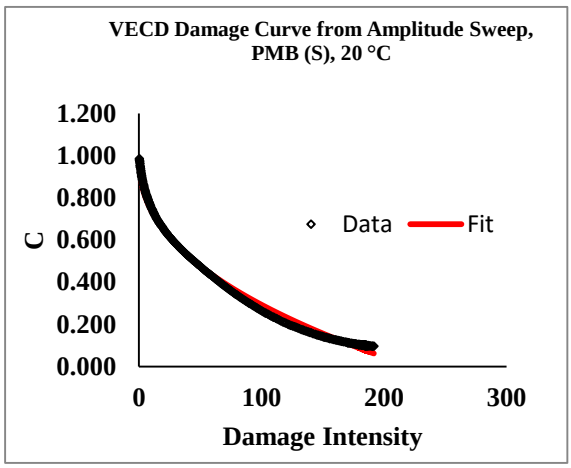

h

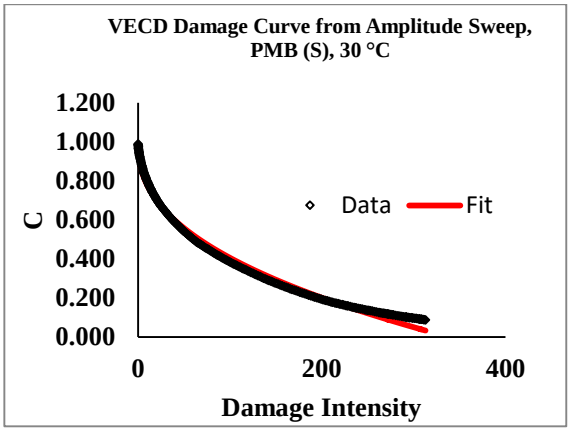

i

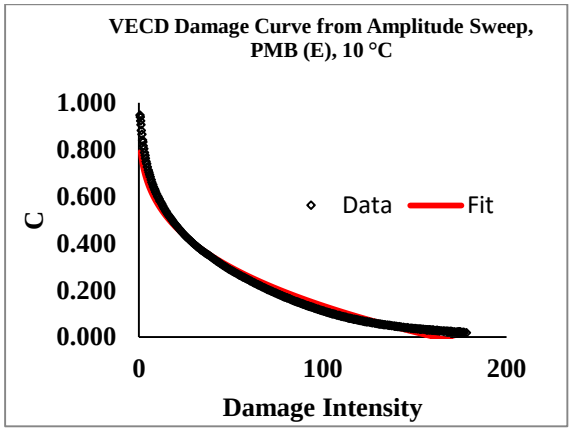

j

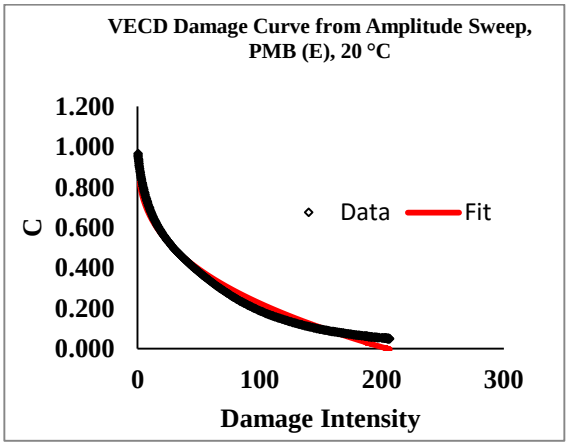

k

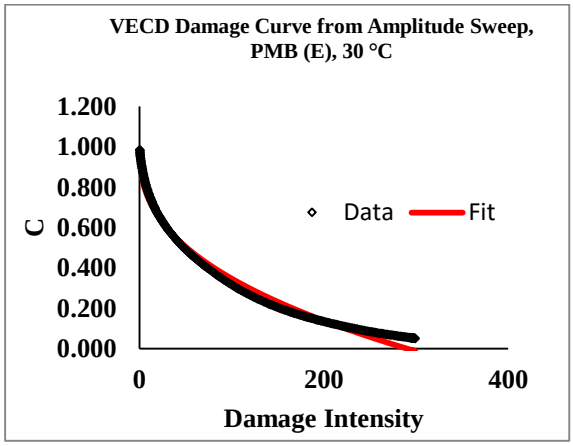

l

Figure 6.17(a-l) Damage curve fit at different temperatures

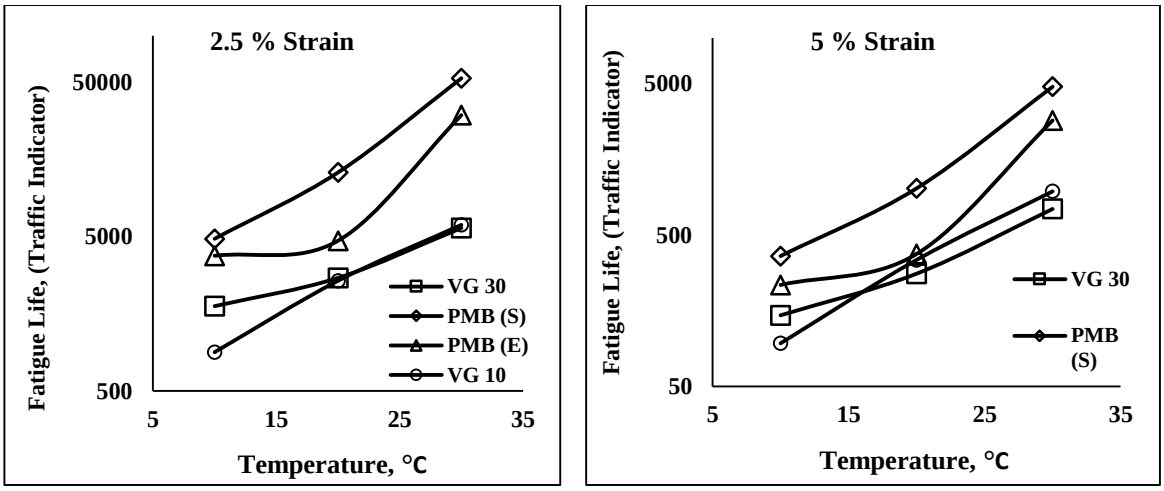

a b

Figure 6.18(a, b) Variation of fatigue life with temperature at two different strain levels.

Table 6.9 Values of fatigue parameter α and A

Binders	α			A		
	10 ˚C	20 ˚C	30 ˚C	10 ˚C	20 ˚C	30 ˚C
VG 10	1.6048405	1.4582551	0.3822351	16892.32	37431.015	65396.962
VG 30	1.7922338	1.6402502	0.3409223	47259.719	54534.01	83388.288
PMB (S)	1.8680149	1.8391338	0.2876897	148400.75	378251.85	1279936.4
PMB (E)	2.0018136	1.8236637	0.2922775	147129.68	132799.17	702093.28

6.4 Conclusions

The study focused on quantifying and comparing the performance of different conventional and polymer modified binders using MSCR and LAS tests at a temperature range of 10- 60 ºC. The effect of stress/strain levels on the test parameters was also evaluated.

It was found that the conventional binders are highly sensitive to change in stress level and temperatures and are not suitable at locations with extreme temperature and loading conditions. The average percent recovery of modified binders were subsequently higher than the conventional binders. PMB (S) showed higher recovery than PMB (E) at 60 °C for higher stress levels, attributed to the highly elastic network, which increases the flexibility of the bitumen.

Burger's model was found to be weak in characterizing the delayed elastic response of modified bitumen. The model parameter η_M had good correlation with the unrecoverable

creep compliance J_{nR} and the average % recovery. The value of η_M was affected by the level of stress only after a certain temperature. This temperature was binder specific and was found to be the point from where the viscous flow dominates. The Boltzmann superposition was not valid for recovery portion of MSCR test. The deviations mainly occurred at lower stress levels and temperatures. The power law was modified to include the nonlinearity associated with bitumen. The factor α correlated well with the J_{nR} and average % recovery. Critical values of η_M and α were assigned, which should be achieved at the desired temperature of study. This temperature should correspond to the maximum average temperature of the study area. A minimum value of 2000 Pa.s and a maximum value of 0.92 was assigned for J_{nR} and α, so as to trace the presence of delayed elastic response in any bitumen.

The parameter *B* of the power law model showed a linear relationship with temperature. The ratio of the averages, was almost constant irrespective of any temperature. The ratio was found to be same as the ratio of the corresponding softening point for the binders. The parameter *A* was found to be function of both stress level and the temperature. It displayed a power law behavior with respect to the stress level. For a particular temperature the ratio of *A* was found to be invariant with stress level. This ratio was at a particular temperature showed excellent correlation with the inverse of the ratio of Zero Shear Viscosity (ZSV) of the binders. The parameter *B.n* (considered as α) in the recovery model was found to have similar correlation as the factor *B*. The equations relating the model parameters with the intrinsic binder properties is presented and could be very useful to establish the creep and recovery behavior of any binder through simple measurements of conventional properties.

LAS test was found to be more practical than the existing intermediate performance criteria of $G^*.sin\delta$. By LAS test it was possible to evaluate the complex behavior of the binder at a wide range of loading level. Elastomeric polymer modified binder (PMB (S)) displayed the highest fatigue life at all the test temperatures. PMB (E) was found to susceptible to strain amplitudes at 10 and 20 ºC at which the performance degraded at higher strain levels. VG 10 and VG 30 had lower fatigue lives at lower strain amplitudes. But the rate of decrease in fatigue life with increase in strain level was lower than the modified binders. VG 10 had the lowest strain susceptibility and gave better results than PMB (E) and

VG 30 at higher strain amplitudes. However at 30 ºC PMB (E) performed better than the conventional binders. A lower value of α and a higher value of A is desirable for superior performance in fatigue. The increase in fatigue life with increase in temperature was found to be highest for VG 10.

PMB (S) gave the best overall performance in both the test methods. PMB (E), though performs well at higher temperature, but at intermediate pavement temperature it may be susceptible to fatigue cracking attributed to higher sensitivity to strain amplitudes. Among the conventional binders both VG 10 and VG 30 were found to be suitable for resisting fatigue cracking at intermediate pavement temperatures. Nevertheless, at higher temperatures both VG 10 and VG 30 showed poor performance. These detailed information about the performance of the binders are impeded in the traditional Superpave performance criteria. Hence the study finds both LAS and MSCR to be more fundamental in characterizing the rutting and fatigue performance of asphalt binders. It has to be mentioned that the results of this study are based solely on binder testing and must be verified using validation with mixture performance testing.

Chapter 7

Marshall Mix Design of Bituminous Mixes

7.1 Introduction

The experimental program included in this research was aimed to study the effect of SBS and EVA on the mechanical properties of asphalt concrete mixtures. This chapter provides detailed information about raw materials (used to prepare specimens) such as: aggregates and type of mix used in this research. The mix design procedure along with the calculation of optimum binder content is also described. In addition, this chapter presents the results of tests carried out on Marshall Specimens for evaluating the strength characteristics of different asphalt mixes.

Asphalt concrete mix design methods attempt to balance the composition of aggregate and asphalt binder to achieve long lasting performance in a pavement structure [142]. It is known that asphalt concrete mixture consists primarily of mineral aggregates, asphalt cement, and air. The main purpose of a mix design is to produce mixtures with high resistance to deformation and cracking. In addition, for the wearing surface, it is also necessary to provide surface texture and skid resistance. The properties of the produced mixtures depend on the physical and chemical properties of the used materials. Each of the component materials needs to be carefully selected and controlled to ensure that they are of a suitable quality for the asphalt mixtures and the expected performance [113].

7.2 Materials

7.2.1 *Aggregates*

Aggregates are the building blocks of the pavement structure. The pavement undergoes large amount of abrasive action and stress from moving loads (traffic) during its life time. For acceptable functioning of the pavement, the road aggregates should possess better engineering properties. Various tests were performed in the study to assess the quality of aggregates. Following are the description of the tests performed on the aggregates.

7.2.1.1 Water absorption and aggregate specific gravity

The porosity of the aggregates can be judged from water absorption test. Highly porous aggregates are unacceptable for the pavements and tends to degrade its performance. Specific gravity is also one of the important properties of aggregates. It finds it main use in determination of volumetric properties of asphalt mixture. Specific gravity also gives an indication of strength of aggregates. This test was performed following the procedure laid out in with IS: 2386 (part III) - 1963.

7.2.1.2 Aggregate impact test

The toughness of the road aggregates is determined using the aggregate impact test. This test is a measure of resistance of the aggregates to breakdown under the impact of heavy loads/traffic. Test procedure given in IS: 2386 (part IV) – 1963 was adopted.

7.2.1.3 Crushing test of aggregate

Road aggregates should be capable enough to resist the crushing load imposed by heavy vehicles. This resistance to crushing of aggregates under the influence of gradually applied compressive load is represented as “Aggregate Crushing Value”. Procedure laid out in IS: 2386 (part IV) – 1963 was used in this study. ‘Ten percent fine value’ is used if aggregate crushing value is found to be 30% or higher.

7.2.1.4 Test for flakiness and elongation index

Better interlocking between aggregates can be achieved using angular aggregates. Flakiness and elongation index describes the shape of the aggregates. IS: 2386 (part I) – 1963 was adopted for conducting this test. Determination of the combined index has been suggested by MoRT&H.

Table 7.1 presents the results obtained for the aggregates used in the study.

Table 7.1 Properties of the aggregates used in the study

Parameters	Specification (MORT&H)	Test result
Water absorption	Max. 2%	0.6%
Specific gravity (CA)[1]	-	2.702
Specific gravity (FA)[2]	-	2.711
Specific gravity (filler)	-	2.720
Impact value of aggregate	Max. 18%	12.8 %
Los Angeles abrasion value	Max. 25%	14.7 %
Crushing value of aggregate	-	15.3 %
Combined flakiness and elongation index	Max. 30%	21.5 %

[1]CA= coarse aggregate, [2]FA= fine aggregate.

7.2.2 *Bitumen*

Four different bitumen, viz. VG 10, VG 30, PMB (S) and PMB (E) were used to prepare all the mixes. The properties of these binders have already been discussed in Chapter 5.

7.2.3 *Aggregate Gradation*

Three gradations, viz. bituminous concrete (BC), dense bituminous macadam (DBM) and stone mastic asphalt (SMA) were adopted in the study. The requirements for these gradations are as per MoRT&H. BC and DBM are amongst the most commonly used dense graded mixes in India for the surface and binder courses respectively. SMA on the other hand, is a gap-graded mix used as a wearing course with high rut resistant properties. Typically, SMA is used at places with extreme conditions of temperature and loading. Table 7.2 and Figure 7.1 demonstrate the mid-point aggregate size distribution for the respective mixes. For SMA, the draindown test was carried out using all the binders. Owing to the gap gradation, the binders in SMA are susceptible to flow out of the mix at high handling temperatures (near about 163 °C). This phenomena is known as draindown which as per specification outlined in IRC SP-79 2008 [79] should be less than 0.3%. In the draindown test, about 1200 ± 200 g of freshly prepared un-compacted asphalt mix is transferred to a

pre-weighted wire basket. The sample is not consolidated while transferring. The basket is transferred to an oven maintained at 175 °C and placed over an empty catch plate for 1 hr. After the specified time the basket is removed from the oven and the value of the drain down is calculated using equation 7.1, expressed as a percentage of the original weight of the sample.

$$Draindown\ (\%) = \frac{D-C}{B-A}.100 \tag{7.1}$$

Where, A = mass of empty wire basket, gm; B = mass of basket with the bituminous mix, gm; C = mass of the empty catch plate, gm and D = mass of the drained material plus the catch plate.

Drain down test was carried out using Schellenberg method. It was found that, only the modified binders (PMB (S) and PMB (E)) satisfied the maximum draindown criteria. So VG 10 and VG 30 were not used for preparing SMA samples. Table 7.3 presents the results of the draindown test.

Table 7.2 Gradation of aggregates adopted in this study

IS Sieve size (mm)	**Cumulative % passing by weight**		
	BC	**DBM**	**SMA**
	NMAS (mm)		
	19	26.5	19
37.5	100	100	100
26.5	100	95	100
19	95	83	95
13.2	69	68	57.5
9.5	62	-	42.5
4.75	45	46	24
2.36	36	35	20
1.18	27	-	17
0.600	21	-	15
0.300	15	14	15
0.150	9	-	-
0.075	5	5	10

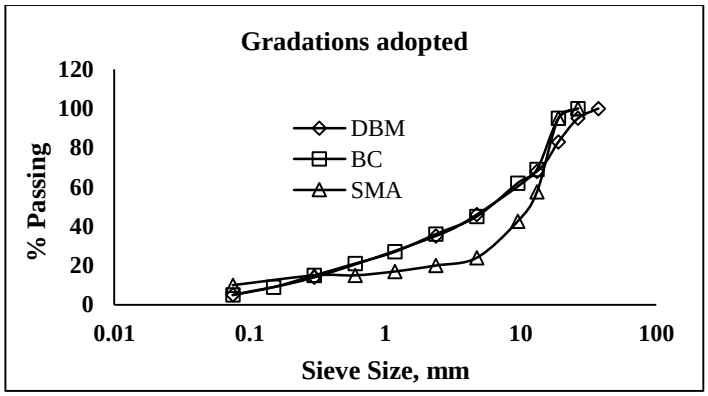

Figure 7.1 Aggregate gradation adopted in the study.

Table 7.3 Drain down test results

Type of mix	**Draindown in SMA (%)**			
Type of binder	VG 10	VG 30	PMB (S)	PMB (E)
Drain down (%), max 0.3	0.57	0.43	0.28	0.26

7.3 Tests on Bituminous Mixes

7.3.1 *Volumetrics of mix design*

Determination of various volumetric parameter of a bituminous mixture play a vital role in characterizing the performance of the mix. The probable durability and strength of the asphalt mixes used in the study were determined through the analysis of various mix volumetric parameters including maximum theoretical specific gravity, G_{mm}, the bulk specific gravity of the asphalt mix, G_{mb}, percent air voids bin the total mix, V_v, percentage volume of bitumen, V_b, voids in mineral aggregates, VMA and voids filled with bitumen, VFB. The phase diagram showing various weight and volumetric components of a standard asphalt mix can be seen in Figure 7.2. Inaccurate determination of these volumetric parameter while designing an asphalt mixture may impose negative impact on its in-service performance.

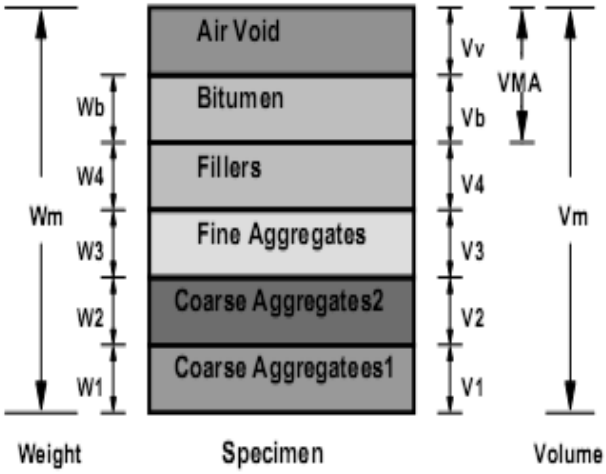

Figure 7.2 Phase diagram of a bituminous mix

7.3.1.1 Theoretical maximum specific gravity of the asphalt mix, (G_{mm})

Theoretical specific gravity $G_{mm,}$ is the specific gravity without considering air voids, and is given by:

$$G_{mm} = \frac{100}{\frac{W_1}{G_c} + \frac{W_2}{G_f} + \frac{W_3}{G_d} + \frac{W_b}{G_b}} \quad (7.2)$$

Where,

W_1 is the total weight of the coarse aggregates

W_2 is the total weight of the fine aggregates

W_3 is the mass of the fillers

W_b represents the weight of the bitumen

G_c represents the apparent specific gravity of the coarse aggregates

G_f denotes the apparent specific gravity of fine aggregates

G_d denotes the apparent specific gravity of filler

G_b represents the apparent specific gravity of bitumen.

7.3.1.2 Bulk specific gravity of the asphalt mix, (G_{mb})

The bulk specific gravity (also known as the actual specific gravity) of the asphalt mix, G_{mb}, is the specific gravity including the air voids and is calculated using the following formulae:

$$G_{mb} = \frac{W_{ma}}{W_{ma} - W_{mw}} \tag{7.3}$$

Where, W_{ma} is the weight of bituminous mix sample in air, W_{mw} is the weight of the asphalt mix suspended in water and (W_{ma}- W_{mw}) is a representation of the volume of the asphalt mix sample. Sometimes when the surface air voids is more (as in stone mastic asphalt), the specimen is coated with thin film of paraffin wax, for accurate calculation of the specific gravity. This however requires considering the volume and weight of wax in the calculations.

7.3.1.3 Percentage volume of bitumen in the asphalt mix (V_b)

The volume of bitumen V_b , expressed as a percentage of the total volume is given by:

$$V_b = \frac{(\frac{W_b}{G_b})}{(\frac{W_1 + W_2 + W_3 + W_b}{G_{mb}})} \tag{7.4}$$

Where, W_b is the weight of bitumen in the total mix, G_b is the apparent specific gravity of bitumen, W_1 , W_2, and W_3 are the weight of coarse aggregate, fine aggregate and filler in the total mix, and G_{mb} is the bulk specific gravity of mix.

7.3.1.4 Voids in mineral aggregates (VMA)

Voids in mineral aggregates (*VMA*) can be defined as the volume of intergranular void space between the aggregate particles of a compacted paving mixture that includes the air voids and volume of the asphalt not absorbed into the aggregates.

It is calculated as the sum of air voids and volume of bitumen. Mathematically it can be expressed as

$$VMA = V_v + V_b \tag{7.5}$$

Where

VMA = voids in the mineral aggregates (% of bulk volume).

V_v = air voids in the mix expressed as percentage, and

V_b = percent bitumen content in the mix

VMA is the total volume of voids within the mass of the compacted aggregate. This total amount of voids significantly affects the performance of a mixture because if the *VMA* is too small, the mix may suffer durability problems, and if the *VMA* is too large, the mix may show stability problems and be uneconomical to produce. Normally as the maximum particle size decreases, the minimum *VMA* increases. This occurs because the total void space between small particles is greater than that between large particles [142]. Therefore, the optimum asphalt content for a dense-graded aggregate mixture with a maximum aggregate size of 2 inches (50 mm) may be as low as 3.0 to 3.5 percent while for a 3/8 inch (9.5 mm) maximum aggregate size the asphalt content may be as high as 7.0 to 7.5 percent. The *VMA* for any given mix must be sufficiently high to ensure that there is room for the asphalt cement plus the required air voids.

The *VMA* has two components: the volume of the voids that is filled with asphalt and the volume of voids remaining after compaction that is available for thermal expansion of asphalt cement during hot weather. The volume of the asphalt cement is critical for durability of the asphalt mixture. This asphalt cement volume along with the aggregate gradation determines the thickness of the asphalt film around each aggregate particle. Without adequate film thickness, the asphalt cement can be oxidized faster, the films are more easily penetrated by water, and the tensile strength of the mixtures are adversely affected. Normally, the *VMA* decreases with increase in asphalt content to a minimum value. After a certain point with the increase in asphalt content, the *VMA* starts increasing because of the displacement of relatively more dense material (aggregates) which is pushed apart by the bitumen which is a less dense material. The asphalt content on the “wet” side of *VMA* curve is usually avoided, even if the criteria for minimum air void and *VMA* is met [161]. Plastic flow and bleeding is likely to occur in field conditions if the design asphalt contents in this range is used.

7.3.1.5 Air voids, Vv

The volume of the small air pockets within the coated particles of aggregates in a compacted asphalt mixture is called the air voids which is expressed as a percentage of the bulk volume of the mixture. Mathematically it can be written as:

$$V_v = 100.(G_{mm} - G_{mb})/G_{mm} \quad (7.6)$$

Where,

Vv = percent air voids in the compacted mixture.

G_{mm} = Theoretical maximum specific gravity of the asphalt mix.

G_{mb} = Bulk specific gravity of the compacted asphalt mix.

The air voids in the compacted dense-graded HMA specimen at optimum asphalt content are suggested by most agencies to lie between 3 and 5 percent. There are a number of reasons for recommending this void content range. However, this air void content is for laboratory compacted samples and should not be confused with field compacted samples. This void content must be approached during construction through the application of compactive effort and not by adding asphalt cement to fill up the voids [142]. HMA pavement layers transfer the load from the surface to underlying layers through intergranular contact and resistance to flow of the binder matrix; therefore, high shear resistance must be developed in the HMA layers if adequate performance is to be achieved. This high shear resistance must be present to prevent additional compaction under traffic which could result in rutting in the wheel paths or flushing and bleeding of the asphalt cement at the surface.

In addition, the dense-graded HMA wearing course must provide a surface that is relatively impermeable to both air and water. If the in-place air void content is only slightly higher than the 3 to 5 percent range, both the air and water permeabilities should be quite low-because the voids which are present are not interconnected but rather are isolated individual voids within the aggregate and asphalt mass. Low air void contents minimize the aging of the asphalt cement films within the aggregate mass and also minimize the possibility that water can get into the mix, penetrate the thin asphalt cement film, and strip the asphalt

cement off the aggregates. It is very important that the HMA be compacted to a laboratory density that approximates the ultimate density achieved under traffic and at the same time have an air void content in the 3 to 5 percent range. The in-place air void content should initially be slightly higher than 3 to 5 percent to allow for some additional compaction. In this study the air void content of the asphalt mix was set to 4%.

7.3.1.6 Voids filled with bitumen (VFB)

Voids filled with bitumen is the volume of the inter-granular void space which is effectively occupied by bitumen. This mean that it is the total volume voids minus the air voids. It is expressed as a percentage of VMA of the mix. Mathematically it can be represented as:

$$VFB = 100.\frac{(VMA - V_v)}{VMA} \tag{7.7}$$

Where,

VFB = voids filled with bitumen, expressed as percentage of VMA.

VMA = voids in the mineral aggregates as described above.

Vv = air voids in the compacted sample of asphalt mix.

The specification ranges of the values of different volumetric parameters and their values as obtained in the study are discussed in the following sections.

7.3.2 *Preparation of Mixes*

All the bituminous mixes in the study were prepared using Marshall mix design procedure. The procedure as recommended by National Association of Pavement Association (NAPA) was adopted for the evaluation of the optimum binder content (OBC) [142]. According to the method, the binder content corresponding to 4% air void (by weight of the mix) is determined first and this binder content is adopted for the determination of Marshall stability, voids in mineral aggregates (VMA), flow and percent voids filled with bitumen (VFB). The values so obtained are compared with the specified value corresponding to that property. If all the values are found to be within the range of specification, the asphalt

content corresponding to 4 percent air void is considered to be the optimum. After determination of the OBC corresponding to 4% air void, three more samples at that binder content were prepared for Marshall testing.

7.3.3 *Marshall Mix Design of Bituminous Mixtures*

For the determination of the optimum binder content of the mixes considered in this study, Marshall mix design procedure was followed. Procedure stated in Asphalt Institute MS-2 is considered. About 1200 g of aggregate (of the desired gradation) is taken and mixed with the different percentage of bitumen. The aggregate and bitumen is heated to the required temperature such that at no time the difference between their temperatures exceeds 14˚C. The mixing is done at a suitable predetermined temperature for the preparation one Marshall sample. The mixture is then transferred to a pre-heated Marshall mould having a height of 63.5 mm and diameter of 102 mm. A mechanical hammer of standard weight is used to compact the sample at a suitable compaction temperature. The preheated hammer was placed in position and the mix was compacted by applying 75 blows on each face for BC and DBM. For SMA, 50 blows of Marshall compaction was provided. It was found that additional compaction result in breaking of aggregate particles. Samples were prepared at five different binder content for each type of mix. Three identical samples were prepared at each binder content. The compacted samples were allowed to cool at room temperature overnight.

The extracted samples were used for the determination of the bulk specific gravity (G_{mb}) as per ASTM D1188 (for BC & DBM) or ASTM D2726 (for SMA). The samples were then transferred to a pre-heated water bath having a temperature of 60 °C for 30 to 40 minutes. Marshall Stability and flow test was performed on these samples following the specification laid out in ASTM D6927. According to the test procedure, the Marshall sample is placed below the Marshall testing head. Compressive load is applied at a constant rate of 51 mm/minutes until the failure of the specimen. Marshall stability is the value of the maximum load at failure while the flow value the amount of deformation undergone by the sample as given by the reading of the flow meter. The tested sample is loosened by application of heat and is used for the determination of the theoretical maximum specific gravity (G_{mm}) as per ASTM D2041. Similarly the whole procedure is repeated at other binder contents and a series of Marshall stability, flow, G_{mm}, G_{mb}, percent air voids (V_a), and density

values were obtained. Separate graphical plots of each parameter was made against different binder contents. In this study the binder content with respect to 4 % air void was considered as the optimum and the other obtained parameters like VMA, stability, unit weight, and flow values were checked to be under the specified limits as per MoRT&H. Table 7.4 shows the required specifications of the mixes as per MoRT&H. It has to be mentioned that the requirements of minimum binder content mentioned in MoRT&H are for aggregates having specific gravity of 2.7. For higher specific gravity binder content has to be reduced proportionately. The requirement of minimum VMA are based on nominal maximum size of the aggregate and varies as per grade of the mix. Figure 7.3 (a and b) shows some of the representative Marshall samples obtained in the study. Figure 7.4 presents the laboratory experimental setup for conducting the test.

Table 7.4 Requirements of mix design as per MoRT&H

Parameters	**Type of Asphalt Mix**		
	BC	**DBM**	**SMA**
Level of compaction	75 blows on each face		50 blows on each face
Percent binder content (by wt. of mix)	5.2%	4.5%	5.8%
Percent air void content	3-5%		4%
Stability (minimum), at 60 ^{o}C (Kg)	900 (Viscosity graded binder) 1200 (modified binder)		-
Marshall Flow (mm)	2 – 4 (Viscosity graded binder) 2.5 – 4 (modified binder)		-
Voids filled with bitumen (%)	65 - 75		-
Percent VMA (minimum)	12		17
Marshall quotient	2-5 for viscosity grade binder 2.5-5 for modified binder		

a b

Figure 7.3 (a) Marshall Samples of BC, DBM & SMA; (b) Wax coated SMA mixes

Figure 7.4 Marshall stability and flow test

7.3.3.1 Stability correction

The standard specification of the height of the Marshall specimen is 63.5 mm. It may happen that during lab compaction the height of the compacted specimen deviate from the standard height. To reduce the effect of this height variation on the stability values, correction factors should be applied to the measured values. The factors which are needed to be multiplied are stated in Table 7.5.

Table 7.5 Correction factors for Marshall stability values

Volume of the specimen (cm^3)	Thickness of the specimen (mm)	Correction factor
457 - 470	57.1	1.19
471 - 482	68.7	1.14
483 - 495	60.3	1.09
496 - 508	61.9	1.04
509 - 522	63.5	1.00
523 - 535	65.1	0.96
536 - 546	66.7	0.93
547 - 559	68.3	0.89
560 - 573	69.9	0.86

Table 7.6 presents the result of the optimum binder content and the corresponding Marshall mix parameters. The stability of mixes prepared with modified binders were higher than those prepared with conventional binders. Figure 7.5 presents the graphical representation of the Marshall stability and flow values obtained in the study. Amongst different mixes, SMA had the lowest stability values attributed to higher VMA and binder content. PMB (S) had 25% higher stability values than VG 10 for BC and 23% for DBM. Mixes prepared with PMB (E) showed 34% and 35% higher stability values for BC and DBM as compared to the mixes prepared using VG 10. A comparison with VG 30 showed that PMB (S) had 18 % and 12 % higher stability values for BC and DBM, while PMB (E) gave 26 and 22% higher values respectively. Use of PMB (E) for SMA mixtures yielded a 7% increment in stability when compared with PMB (S).

Table 7.6 Marshall mix design results

Mix Properties	BC				DBM				SMA	
	VG 10	VG 30	PMB (S)	PMB (E)	VG 10	VG 30	PMB (S)	PMB (E)	PMB (S)	PMB (E)
G_{sb}	2.712				2.712				2.710	
G_b	1.02	1.02	1.03	1.04	1.02	1.02	1.03	1.04	1.03	1.04
G_{mb}	2.454	2.458	2.451	2.452	2.455	2.458	2.462	2.459	2.324	2.325
G_{mm}	2.556	2.562	2.554	2.556	2.558	2.561	2.565	2.561	2.422	2.423

OBC, %	4.9	5.1	5.1	5.1	4.7	4.7	4.8	4.8	6.7	6.7
$V_{a,\%}$	3.99	4.06	4.03	4.07	4.03	4.02	4.02	3.98	4.05	4.04
VMA, %	13.9	14.0	14.2	14.2	13.7	13.6	13.6	13.7	20.0	19.9
VFB, %	71.4	71.0	71.7	71.3	70.7	70.5	70.4	70.9	79.8	79.7
Stability, Kg	1255.6	1333.7	1576.3	1684.4	1157.8	1273.1	1424.7	1561.9	990	1060.9
Flow, mm	3.1	2.9	3.2	3.4	3.6	3.4	3.1	3.1	3.8	3.7
Marshall quotient	4.1	4.7	4.9	4.9	3.3	3.7	4.7	5.1	2.5	2.7

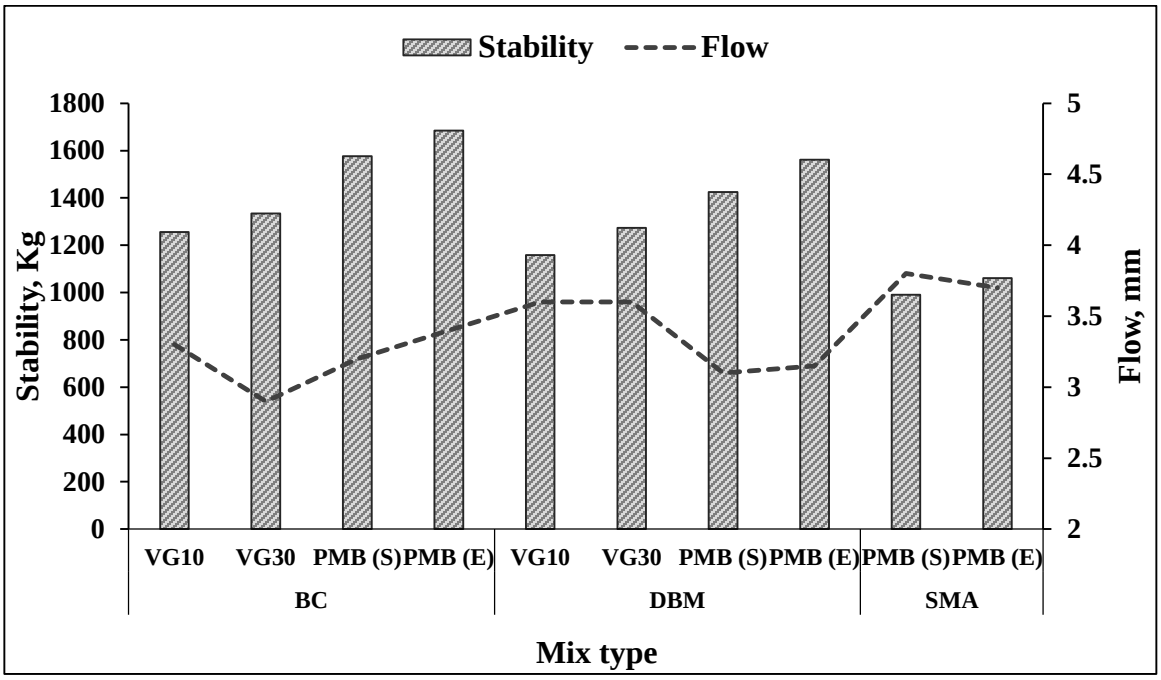

Figure 7.5 Graphical representation of Marshall stability and flow values

7.3.4 *Retained Marshall stability test*

The durability of an asphalt mixture can be indirectly assessed by its susceptibility to moisture. Retained Marshall Stability test was carried out to evaluate the susceptibility of the asphalt mixes to moisture. For each type of mix six different specimens having the same bulk specific were prepared and divided into two groups having three specimens. Group 1 specimens were subjected to conditioning by immersing them in a water bath maintained at 60 °C for a period of 24 hours. On the other hand, specimens of group two were kept unconditioned following the normal immersing of specimens for 30 minutes at a temperature

of 60 °C. All the samples were tested in a Marshall stability testing machine until failure by application of load at a constant deformation rate of 51 mm per minute. The average stability values for each group was calculated and the retained Marshall stability were determined using the following equations.

$$\text{Retained Stability} = \frac{\text{Marshall Stability of conditioned specimen}}{\text{Marshall Stability of standard specimen}} .100 \quad (7.8)$$

Presence of moisture in a bituminous mix can lead to early failure of flexible pavements and can be a major hazard. The durability of asphalt mixture can also be evaluated by studying the susceptibility of asphalt mixtures to moisture. The loss of adhesion between the bitumen and aggregates was studied by utilising the retained Marshall stability test. A higher value of retained Marshall stability indicates lower moisture susceptibility and vice-versa. Table 7.7 presents the result of the retained Marshall stability.

Table 7.7 Retained stability of mixes

Mix	Binder type	Stability (kg)		Retained stability (%)
		Standard	Conditioned	
BC	VG-10	1255.63	1013.41	80.71
	VG-30	1333.75	1176.50	88.21
	PMB (S)	1576.25	1451.25	92.07
	PMB (E)	1684.38	1632.83	96.94
DBM	VG-10	1157.81	901.36	77.85
	VG-30	1273.13	1046.76	82.22
	PMB (S)	1424.69	1294.33	90.85
	PMB (E)	1561.88	1479.72	94.74
SMA	PMB (S)	990.00	848.53	85.71
	PMB (E)	1060.94	932.88	87.93

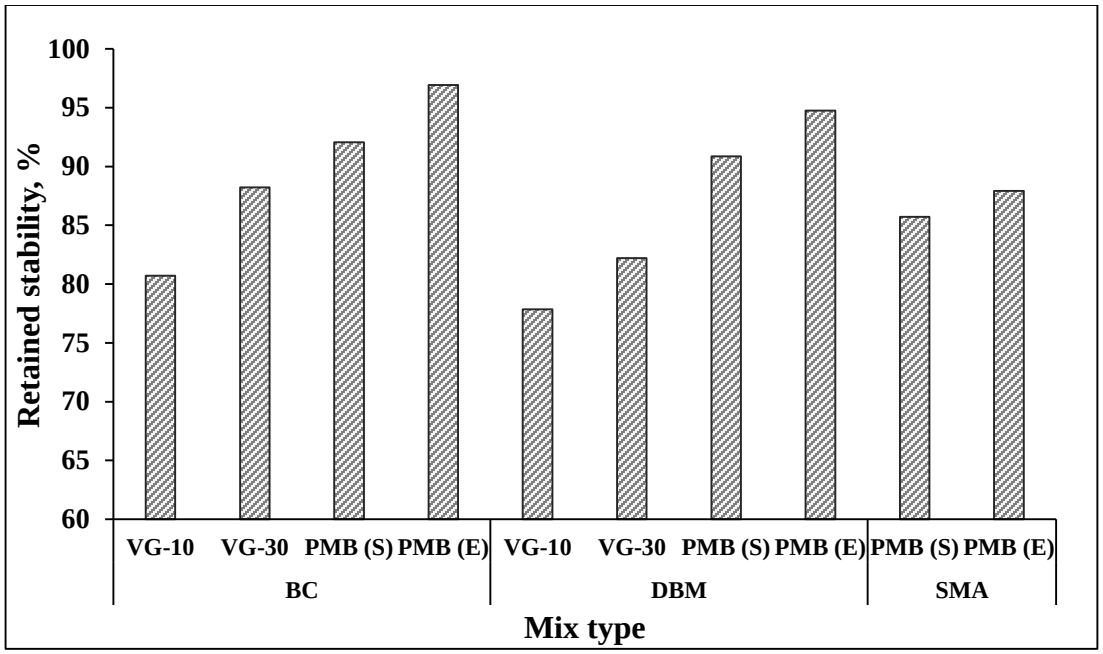

Figure 7.6 Retained satiability of the mixes

Results clearly showed that mixes prepared using modified binders had higher retained Marshall stability than the conventional binder implying that the modified binders are less susceptible to moisture damage. Of all the three mixes, BC with PMB (E) had the best retained Marshall stability. In case of DBM mix prepared using VG10, retained stability value was less than 80 %, so it is not suitable for use in heavy rainfall areas. Figure 7.6 compares the retained Marshall stability values of the different mixes prepared using conventional and modified binders.

The retained Marshall stability values were found to be higher for mixes prepared with modified binders. Moreover, amongst all the mixes, SMA had the highest retained stability value. Two outcomes can be derived from this observation. First, the modified binders have lower temperature susceptibility and secondly higher binder content (as in SMA mixes) tends to increase the film thickness making the mix more durable and resistant to moisture damage.

7.3.5 *Indirect tensile strength (ITS) test*

Indirect Tensile Test (ASTM D 6931-12) involves the application of load to a cylindrical specimen along its vertical diametrical plane as shown in Figure 7.7 (a). Load is

applied through two curved strips whose radius of curvature is the same as that of the specimen. A nearly uniform tensile stress is developed normal to the direction of the applied load along the same vertical plane causing the specimen to fail by splitting along the vertical diameter as represented in Figure 7.7 (b).

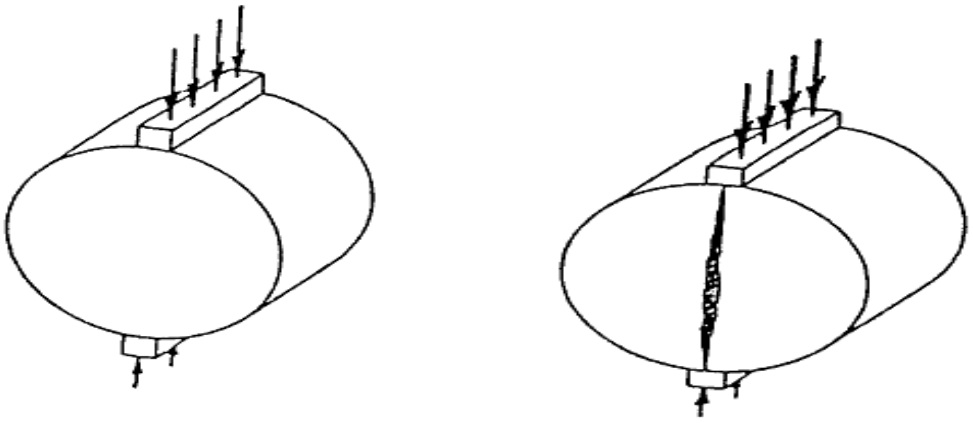

a b

Figure 7.7 Load Configurations and Failure of the Specimen in Indirect Tensile Strength Test

Indirect tensile strength test procedure consists of applying a load along cylindrical specimen's diametrical axis at a fixed deformation rate of 5.1cm/min until failure and determining the total vertical load at failure of the specimen at 25 °C. Failure is defined as the point after which there is no increase in load. While conducting this test it should be ensured that two loading strips remain parallel to each other during testing. ITS test was carried out using a 12.7 mm wide loading strip in a Marshall testing head until failure.

The maximum load sustained by the specimen is used to calculate the indirect tensile strength with the help of the following expression.

$$S_T = \frac{2F}{3.14(hd)} \quad (7.9)$$

Where:-

S_T = Indirect tensile strength,

F = Total applied vertical load at failure, N.

h = Height of specimen, mm.

d = Diameter of specimen, mm.

The use of indirect tensile strength test could be appreciated in assessing the tensile properties of the asphalt mixes which can be correlated with the cracking of the pavement. A high value of indirect tensile strength is an indication of higher resistance to low temperature cracking. Moreover, a higher value of indirect tensile strength at failure would also imply that the asphalt mix is capable of withstanding larger tensile strains prior to cracking.

Figure 7.8 and Table 7.8 presents the ITS results for the three types of mixes prepared using different binders. The results revealed that, modified binders have higher values as compared to mixes prepared with conventional binders. Dense graded mixes such as BC displayed higher values as compared to gap- graded SMA. Though the ITS values for BC and DBM mixes are higher than SMA, they will develop cracks due to lower binder content. It is hence necessary to determine the resistance to cracking for different mixes from repeated bending test. The tensile strength ratio (TSR) values were also plotted on the secondary axis. MoRT&H requires a minimum of 80% TSR to make the mix resistive to moisture damage. Marshall stability of compacted specimens was determined after conditioning them by keeping in water maintained at 60 °C for 24 h prior to testing. This stability, expressed as percentage of the stability of Marshall specimens determined under standard conditions, is the retained stability of the mix. Tensile strength ratio (TSR) is the average static indirect tensile strength of the conditioned specimens expressed as percentage of the average static indirect tensile strength of unconditioned specimens. Conditioning was done by keeping the specimens in water maintained at 60 °C for 24 h and by curing at 25 °C for 2 h before commencing the test. The test was conducted at 25 °C. Modified binders were found to be least susceptible to moisture damage. The minimum specification criteria of 80% TSR was not satisfied for mixes prepared with VG 10. For DBM, VG 30 also displayed slightly lower value than the minimum required. Hence for these mixes anti-stripping agent should be used to protect it from being vulnerable to moisture effects.

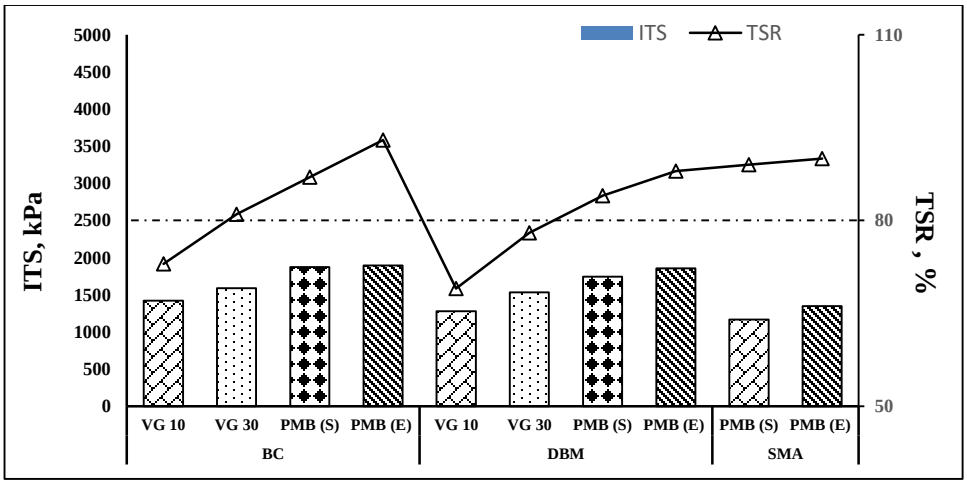

Figure 7.8 ITS and TSR values for different mixes

Table 7.8 Indirect Tensile Strength of mixes

Mix Type	Binder Type	Indirect Tensile Strength @ 25°C (kPa)
BC	VG-10	814.15
	VG-30	949.74
	PMB (S)	1237.54
	PMB (E)	1395.68
DBM	VG-10	755.99
	VG-30	872.30
	PMB (S)	1110.85
	PMB (E)	1279.37
SMA	PMB (S)	748.28
	PMB (E)	959.53

7.3.6 *Asphalt Film Thickness*

For the calculation of asphalt film thickness of different asphalt mixes, surface area method as proposed by Kandhal et. al. ([142]) was used in the study. The equivalent surface area of different aggregate sizes was calculated using the surface area factor for each sieve size. Using the effective volume of bitumen/kilogram of aggregate, the asphalt film thickness was evaluated as follows:

$$\text{Asphalt film thickness} = \frac{\text{effective volume of bitumen per Kg of aggregate}}{\text{surface area of the mix gradation}} \quad (7.10)$$

The following surface area factors given in Asphalt Institute (MS-2) were used in this study.

Table 7.9 Surface area factors

IS Sieve (mm)	Maximum size of aggregate	4.75	2.36	1.18	0.600	0.300	0.150	0.075
Surface area factor (m^2/kg)	0.41	0.41	0.82	1.64	2.87	6.14	12.29	32.77

A minimum film thickness of 8 µm has been reported in many studies for production of a durable asphalt mix. An effort was made in this study for the determination of the asphalt film thickness of different asphalt mixes. Table 7.10 presents the calculation of the surface area factors for different mixes. Figure 7.9 shows the variation of film thickness with variation of binder content for all the mixes used in the study. The film thickness at the design asphalt content is also depicted in Table 7.11. Evidently all the mixes prepared in this study had a film thickness above 8 µ, indicating that all the mixes would perform satisfactorily with respect to durability. As can be seen in the table that SMA has the highest film thickness and would tend to produce the most durable pavement, followed by DBM and BC.

Table 7.10 Surface area of mixes

IS sieve Size (mm)	**% passing**			**Surface area factor (m^2/kg)**	**Surface area (m^2/kg)**		
	BC	**DBM**	**SMA**		**BC**	**DBM**	**SMA**
37.5		100		0.41		0.41	
26.5	100	95	100	0.41	0.410		0.410
19	95	83	95				
13.2	69	68	57.5				
9.5	62		42.5				
4.75	45	46	24	0.41	0.184	0.189	0.098

2.36	36	35	20	0.82	0.295	0.287	0.164
1.18	27		17	1.64	0.443		0.279
0.6	21		15	2.87	0.603		0.431
0.3	15	14	15	6.14	0.921	0.860	
0.15	9			12.23	1.101		
0.075	5	5	10	32.77	1.638	1.638	3.277
Surface area (m^2/Kg)					**5.601**	**3.384**	**4.659**

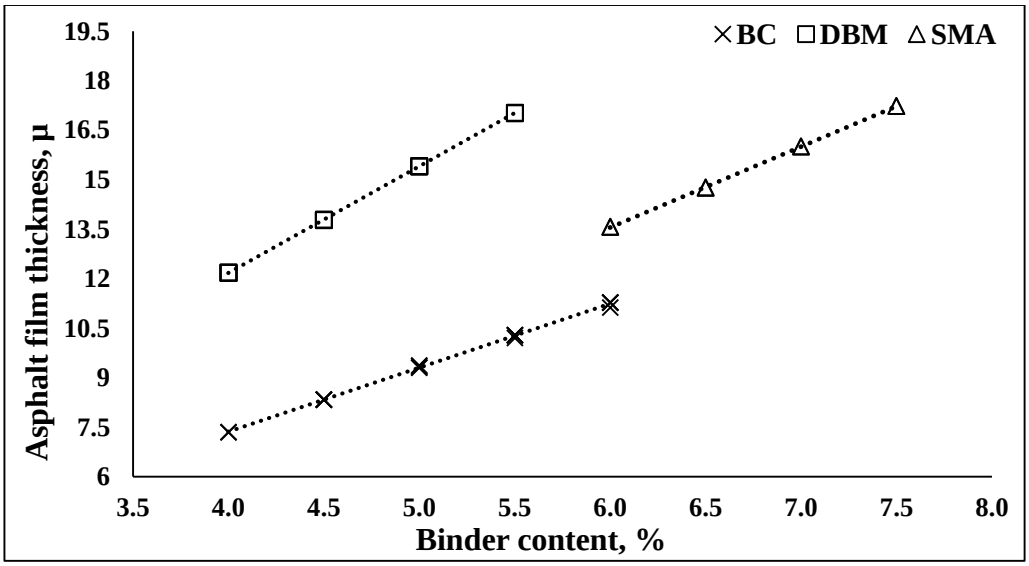

Figure 7.9 Asphalt film thickness of mixes

Table 7.11 Asphalt film thickness of mixes at design asphalt content

Mix type	Binder type	Vol. of binder (%)	Wt. of binder (Kg)	Wt of aggregate (Kg)	Wt of binder/ kg of Aggregate	Film thickness (µ)
BC	VG-10	10.91	110.14	2007.94	0.055	9.68
	VG-30	8.40	84.86	1547.13	0.0545	9.63
	PMB (S)	10.98	110.93	2022.38	0.055	9.70
	PMB (E)	8.44	85.29	1554.92	0.055	9.76
DBM	VG-10	7.13	72.05	1529.13	0.047	13.78

	VG-30	8.53	86.17	1787.04	0.048	14.10
	PMB (S)	7.54	76.11	1543.25	0.049	14.43
	PMB (E)	9.17	92.61	1877.82	0.049	14.43
SMA	PMB (S)	15.70	158.57	2244.01	0.071	15.02
	PMB (E)	15.03	151.80	2113.91	0.072	15.26

7.4 Conclusions

This chapter presented the study on mix design of bituminous mixes using Marshall mix design method. Strength evaluation of Marshall samples was conducted using tests like indirect tension test, retained Marshall stability and tensile strength ratio. The film thickness of different mixes using various binders were also assessed to check for the appropriate film thickness required for durability. The Marshall test results indicated higher stability for dense graded mixtures prepared with polymer modified bitumen. SMA mixes displayed lower stability values attributed to high VMA and increased binder content. The moisture susceptibility as shown by the retained Marshall stability test was higher for conventional binders. The retained Marshall stability values for SMA mixes were found to be higher than the dense graded mixes. This is attributable to the higher binder content which increases the film thickness making the mix water resistant. ITS values for BC and DBM were found to be higher than SMA. Mixes prepared with modified binders displayed higher strength values in comparison to viscosity graded binders. VG 10 did not satisfy the minimum TSR criteria required to satisfy the moisture susceptibility criteria. All the mixes prepared in this study had a film thickness above 8 μ, indicating that all the mixes would perform satisfactorily with respect to durability. As can be seen in the table that SMA has the highest film thickness and would tend to produce the most durable pavement, followed by DBM and BC.

Chapter 8
Performance Evaluation of Asphalt Mixes

8.1 Introduction

The pavements over time suffer failure due to passing traffic loads and exposure to different environmental conditions. Among the most important of these failures, we can mention rutting which is considered as the main concern of transportation agencies in the field of pavement. The permanent deformation (rutting) of asphalt pavements has an important impact on the performance of the pavements during their lifetimes [62, 97, 134, 171]. Rutting is the load-induced permanent deformation of asphalt pavements and may occur in any layer of a pavement structure [188, 189]. It is one of the main distresses occurring in asphalt pavements and badly affects the comfort-ability, ride-ability, motorist safety, and general performance. The temperature and stress-induced by loading can be named as two main parameters that lead to permanent deformation in asphalt pavements. When the traffic loading increases and temperatures are high, rutting failure are more likely to occur. Research in the field of improving the constituent materials of hot mix asphalt (HMA), mix designs and methods of analysis and pavements design, including laboratory and field tests are needed to provide more service life for pavements and as a result, the loss of costs which are set to be spent to repair pavement failures is prevented [13, 60, 67, 122, 123].

In developing an experimental testing method for evaluating the rutting resistance of asphalt mixtures, most researchers have used wheel tracking test, the uniaxial compressive creep test, the triaxial repeated load test (TRT), the indirect tension test, and the bending creep test [140]. The wheel tracking test simulates traffic loading on pavements by applying a wheel load on a slab specimen [117, 139, 151, 187]. The testing conditions are similar to pavements in service and the rut depth is measured after a specific number of loading cycles. The wheel tracking test has been proven to be an effective method to evaluate the rutting potential in asphalt pavements.

Fatigue is one of the three (rutting, fatigue cracking and low temperature cracking) major failure modes in flexible pavements which results in degradation of the pavement

materials and finally the pavement structure [201]. The materials in pavement are subjected to short time load amplitudes upon passage of a vehicle. Higher amplitudes of this repeated loading results in reduction of material stiffness and its subsequent accumulation with time may lead to complete failure [32]. Fatigue initiated cracks occurs at points where critical tensile strains and stresses occur. The critical strain on the other hand is also a function of the stiffness of the mix. Since the stiffness of an asphalt mix in a pavement layered system varies with depth, the location of the critical strain will also change. Once the crack/damage initiates at the critical location, the action of traffic eventually causes these cracks to propagate through the entire bound layer leading to the failure of the pavement. Most commonly it is assumed that the fatigue cracking initiates at the bottom of the bound layer attributed to the bending action of the pavement layer. This stress induced micro-crack propagates to the surface due to the repeated movement of vehicles, leading to what is known as “bottom-up-cracking”. However, a plethora of studies have also clearly demonstrated that fatigue cracking may also be initiated from the top and propagate downwards (top-down cracking). In general, it is hypothesized that critical tensile and/or shear stresses develop at the surface and cause extremely large contact pressures at the tire edges-pavement interface. This stress coupled with highly aged (oxidized) thin surface layer is responsible for the surface cracking. Another view of fatigue failure may be given through energy concepts [88]. Any energy (in the form of loading) supplied to the pavement results in accumulation of strain. The area under the stress-strain curve represents the energy being input into the material. Upon removal of the load, the stress is removed and the strain is recovered. If the loading and unloading curves coincide, all the energy put into the material is recovered or the material returns to its original position after the load is removed. If the two curves do not coincide, energy is lost in the material, which may be in the form of mechanical work, heat generation, or damage in such a manner that it could not be used to return the material to its original shape. This energy difference defined as the dissipated energy of the material caused by the load cycle is responsible for the fatigue failure of the material.

Over the past 40 years, different test methods have been developed to simulate the fatigue behavior of hot mix asphalt (HMA) materials, with varying success [5, 35, 70, 94, 114, 164, 167, 193]. Tangella et al. [170] listed the general categories of different test methodologies which included: simple flexure, supported flexure, diametral test, triaxial test,

direct axial test, fracture test, and wheel tracking test. In the SHRP-A-404 report [115], a comprehensive evaluation was performed based on which the repeated flexure beam test (third/four–point bending) was given the highest rank. Usually two types of loading modes are adopted in laboratory fatigue testing: constant stress (controlled–stress) mode and constant strain (controlled–strain) mode. In the constant stress loading mode, the stress is kept constant and the strain increases with load cycles. Whereas, in the constant strain mode of loading, the strain is maintained constant in all the loading cycles and the stress decreases subsequently. In the field, the loading conditions are more complex and are usually combined modes of loading [156]. Researchers [76, 170] have suggested that controlled strain testing might be used for relatively thin pavements with HMA less than 50 mm (2 in.), because the strain in thin asphalt layer is governed by the underneath layers and is merely affected by the decrease in stiffness of the asphalt mix. The controlled-stress testing might be more appropriate for thicker pavements of more than 152 mm (6 in.) where the main load – carrying component is the top layer. For intermediate thicknesses, a combination of constant stress and constant strain exists. It has been found that the fatigue life obtained from constant stress testing condition is shorter than the life obtained from constant strain testing condition [115]. In this study, constant strain mode has been adopted assuming that the thickness of the wearing course is not high.

This chapter focusses on quantifying the performance of unmodified and modified asphalt mixes using wheel rut testing and four point beam bending test. Rut testing was conducted at 60 °C, while 4PBBT was conducted at 20 °C. The suitability of different test methods for quantifying rutting is also presented and discussed. A new phenomenological model has been proposed to quantify the fatigue life of asphalt mixes. At the end correlation between fatigue and rutting of binders and mixes has been established.

8.2 Experimental Investigation

8.2.1 *Wheel rut testing*

Laboratory wheel-tracking device was used to measure the pavement quality by running simulative tests on hot mix asphalt (HMA) samples. The testing assembly used in this study is shown in Figure 8.1.

In this test (BS 2004) a small loaded wheel is rolled repeatedly across a prepared HMA specimen to measure parameters like rut depth, moisture susceptibility and stripping predictions. Square sizes slabs were prepared to carry out the testing and representative samples before and after the test is shown in Figure 8.2.The test can be done both in air and water control modes. In this study water control mode was used to simulate the effect of moisture on the pavement.

Result of the test specimen can be correlated to actual in-service pavement performance [40, 87]. Samples of 300 mm x 300 mm x 50 mm were prepared adopting a new method of loading and unloading. All the specimens were prepared to achieve a target air void content of 4% by weight of the total mix. As the height of beam was fixed, the weight of the mixture required to achieve the target air void was pre-calculated. The aggregates and bitumen were mixed at the required mixing temperature and were placed in the pre-heated mould. A compression testing machine was used for applying load till the desired height was achieved. The loading was accompanied by an unloading process to avoid breaking of aggregates due to static loading. After compaction the specimen was allowed to cool for 24 hours. The sample was extracted from the mould and the air void content was measured using the saturated surface-dry procedure (AASHTO T166). Compacting the specimens is one of the most difficult task, when the target air void content is fixed. This may be possible, but would require many trials. As the height of the sample is fixed, it might happen that, due to different orientation of aggregate particles within the mix, for different specimens, slight variation in the fixed air void content of 4% may result. So an allowance of ±0.2% was given to the required air void content. A wheel load of 700 ±5 N with tyre pressure of about 0.56 MPa was applied on the sample. The loaded wheel had a total travel distance of 230 ± 10 mm with a speed of 42 passes per minute. Each sample was tested at 60 °C up to 10, 000 load cycle or 25mm rut depth whichever was earlier. LVDT was used to measure the vertical displacement of the slab specimen per cycle.

Figure 8.1 Wheel rut tester

a b

Figure 8.2 (a,b) Wheel tracking test samples, (a) before, (b) after

8.2.2 *Four point beam bending test (4PBBT)*

The flexural fatigue testing protocol of AASHTO T321-2003 and SHRP M-009 requires preparation of oversized beam specimens that have to be sawed to the required dimensions. The final required dimensions are 380 ± 6 mm (15 ± 1/4 in.) in length, 50 ± 6 mm (2 ± 1/4 in.) in height, and 63 ± 6 mm (2.5 ± 1/4 in.) in width. No specific procedure is mentioned for beam preparation. However, several methods including full scale rolling wheel compaction, miniature rolling wheel compaction, and vibratory loading have been used over years.

In this study, the beams were prepared adopting a new method of loading and unloading. The mould used for beam preparation had an inside dimension of 382 mm x 50 mm x 70 mm. The final dimension was fixed as 382 mm x 50 mm x 50 mm to achieve uniform beam sizes for all the type of mixtures. All the specimens were prepared to achieve a target air void content of 4% by weight of the total mix. The beam was prepared using a similar procedure

as adopted in wheel rut testing. Similar to samples prepared in wheel rut test, an allowance of ±0.2% was given to the required air void content. The testing protocol mentioned in Table 8.1 was adopted for conducting the four point beam bending (4PBB) test. Figure 8.3 (a,b) shows the 4PBB apparatus used in this study.

a b

Figure 8.3 (a,b) Four point beam bending apparatus

Table 8.1 Test condition adopted for 4PBB test

S. No.	Test Parameter	Test Condition
1	Test temperature (°C)	20 ± 0.5
2	Strain amplitude (10^{-6} m)	200-1000
3	Loading frequency (Hz)	10
4	Air void content (%)	4 ± 0.2
5	Type of loading	Sinusoidal
6	Failure condition	When the flexural stiffness is reduced to 50% of the initial flexural stiffness or 200000 loading cycles have been applied, whichever occurs first.

The maximum tensile stress and strain were calculated using the following equations

$$\sigma_t = \frac{0.382.P}{b.h^2} \tag{8.1}$$

$$\varepsilon_t = \frac{12.\delta.h}{3.L^2 - 4.a^2} \tag{8.2}$$

Where,

σ_t = Maximum tensile stress, Pa.

ε_t = Maximum tensile strain, m/m

P =Applied load, N

b = Average specimen width, m

h = Average specimen height, m

δ = Maximum deflection at the center of the beam

L = Length of the specimen, 382 mm.

a = Length between the clamps *(L/3 = 127.33 mm)*

The flexural stiffness, phase angle, dissipated energy and cumulative dissipated energy are calculated as follows

$$S = \frac{\sigma_t}{\varepsilon_t} \tag{8.3}$$

$$\phi = 360.f.s \tag{8.4}$$

$$D = \pi.\sigma_t.\varepsilon_t.\sin(\phi) \tag{8.5}$$

$$C.D.E = \sum_{i=1}^{N} D_i \tag{8.6}$$

Where,

S = Flexural stiffness, Pa

ϕ = Phase angle, degrees

f = Load frequency, Hz

s = Time lag, seconds

D = Dissipated energy per cycle, J/m^3

$C.D.E$ = Cumulative dissipated energy, J/m^3

8.3 Results and Analysis

8.3.1 *Analysis of wheel rut testing*

Figure 8.4 (a-c) shows the variation of rut depth with increase in number of cycles for the three different mixes at 60 °C. The rut depth increases with increase in number of cycles. Mixes prepared with polymer modified binders have lower rut depth as compared to mixes prepared using viscosity graded binders. Initially all the curves were found to be close to each other for lower cycle numbers. As the cycle number increased (typically after 500 cycles), the difference in rut depth became more prominent. Figure 8.4 (d) presents the rut depth obtained at the end of 10000 loading cycles for different mixes prepared using the four binders. SMA was found to be the most rut resistant mix among the three mixes studied, followed by BC. The poor performance of the mixes prepared using viscosity graded binders are analogous to the result obtained in bitumen testing.

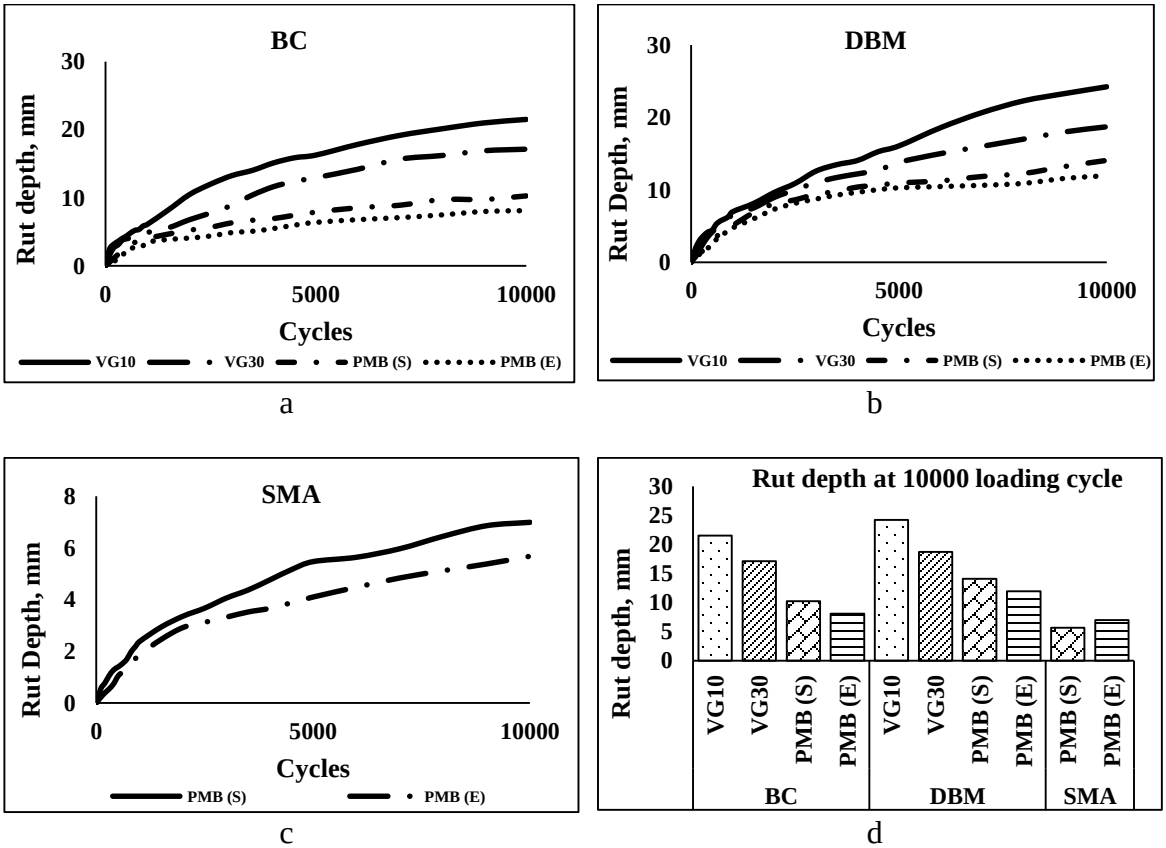

Figure 8.4 Variation of rut depth (a) with loading cycles for BC; (b) with loading cycles for DBM; (c) with loading cycles for SMA and (d) at 10000th loading cycle.

8.3.2 *Fatigue life from 4PBBT*

Figure 8.5 (a-d) presents the comparison of the fatigue life of different mixes for each binder type. The results of 200 micro strain are not shown because all the mixes exhibited fatigue life higher than $2x10^5$ cycles. At 400 micro strain SMA mixes prepared with PMB (S) and PMB (E) also had higher fatigue life. It was found that, at lower strain levels (<600 micro strain) mixes prepared with polymer modified binders exhibited higher fatigue life than those prepared using conventional binders. Amongst the polymer modified binder, PMB (S) gave superior results. As the strain level increased, the fatigue life of PMB (E) reduced drastically, and was almost close to the behavior shown by conventional binders. PMB (S) on the other hand, displayed the best performance at all the strain levels. Amongst all the mixes, SMA had the highest fatigue life, which was almost 5 times of the fatigue life of BC and DBM. This may be attributed to the volumetric of the bituminous mixture. SMA being a gap graded mix, has high VMA (17-22%), which can accommodate ample amount of bitumen for a fixed air void content of 4%. This increases the film thickness inside the mix, making the mix more durable to the induced strain.

Figure 8.6 (a-c) illustrates the fatigue life as a function of strain. The slope of the curve indicates the sensitivity of the binders to the change in the magnitude of strain. PMB (E) showed highest susceptibility to this change while PMB (S) was found to be least susceptible. It was found that at lower strain levels (≤400 μm) PMB (E) had fatigue life very close to PMB (S). But as the strain increased the fatigue life of PMB (E) decreased very sharply. At higher strain amplitudes (≥800 μm), the fatigue life of PMB (E) mixes was even lower than that of the mixes prepared using conventional binders. This behavior of PMB (E) may be explained as follows. In PMB (E) the crystalline nature of the polymer stiffens the binder inducing viscous behavior. At low strains, due to high stiffness the binder can take higher number of load repetition without any damage. But due to the rigid nature, it cannot be stretched to higher strain which will result in formation of cracks. On the other hand in PMB (S), the polymers are cross linked into a three dimensional network. The polystyrene end-block impart strength while the butadiene mid-blocks impart exceptional elasticity. This makes the binder more flexible and increases its capability to resist higher strains.

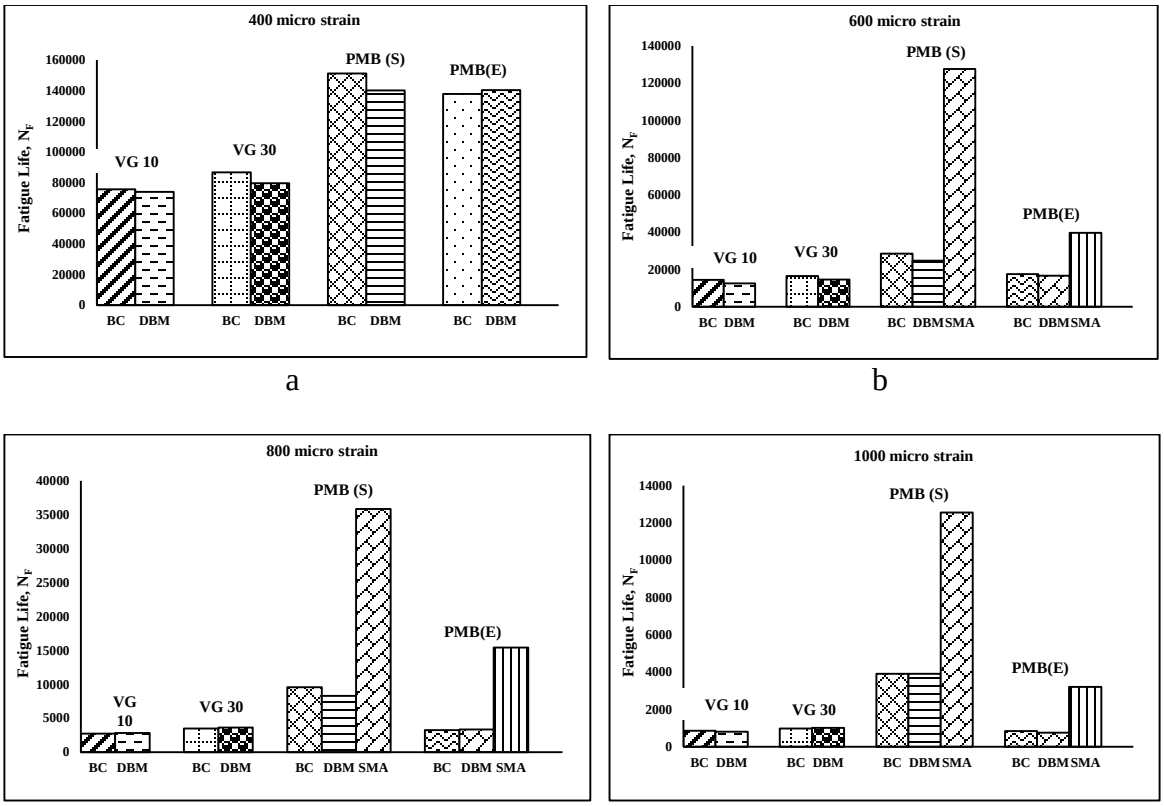

a b

c d

Figure 8.5 (a-d) Fatigue life at different strain levels.

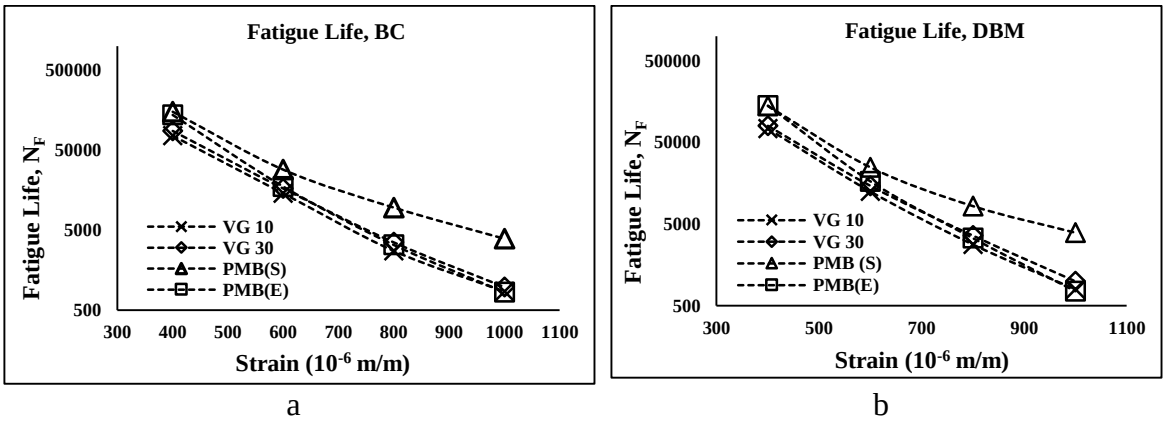

a b

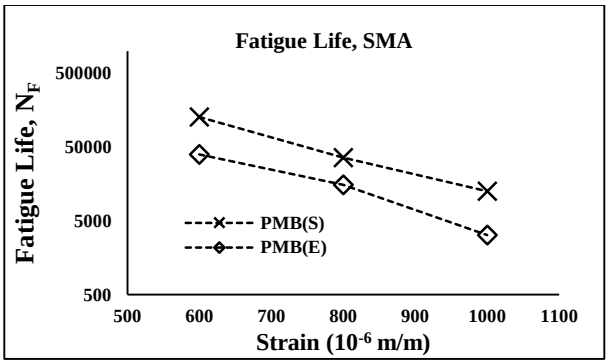

C

Figure 8.6 (a-c) Fatigue life of different type of bituminous mixes.

8.3.3 *Correlating binder and mix performance*

8.3.3.1 Correlating fatigue

It was attempted to correlate the fatigue results of asphalt binders with the fatigue life of asphalt mixtures. Assuming that the strain in binder is about 50 times the strain in mixtures, four strain levels (2,3,4,5 %) of LAS test were chosen corresponding to four similar strain levels (400, 600, 800, 1000 micro-strain) of 4PBBT. Table 8.2 shows the fatigue life of each binder with respect to different mixes. Plotting the results of the binders against the fatigue life of mixes, it can be seen from Figure 8.7 (a-d) that linear correlation is achieved for all the mixes. For PMB (E) and PMB (S) the fatigue life for SMA is also shown. It can be seen that the slope for SMA deviates considerably than that of BC and DBM. This may attributed to the higher VMA for SMA mixes as compared to BC and DBM. The correlation equation however varies with the type of mix for each binder.

Table 8.2 Fatigue life of asphalt binders and mixes at four similar strain amplitudes.

Fatigue life (number of cycles)													
VG 10			VG 30			PMB (S)				PMB (S)			
Binder	BC	DBM	Binder	BC	DBM	Binder	BC	DBM	SMA	Binder	BC	DBM	SMA
4958	75620	73850	5612	86795	79549	29547	151208	140205		10598	137845	140451	
1520	14366	12553	1484	16548	14675	6650	28501	24782	127582	2415	17478	16657	39668
657	2745	2814	578	3505	3615	2308	9565	8293	35856	846	3255	3361	15413
343	853	795	278	970	998	1016	3900	3915	12565	375	835	755	3198

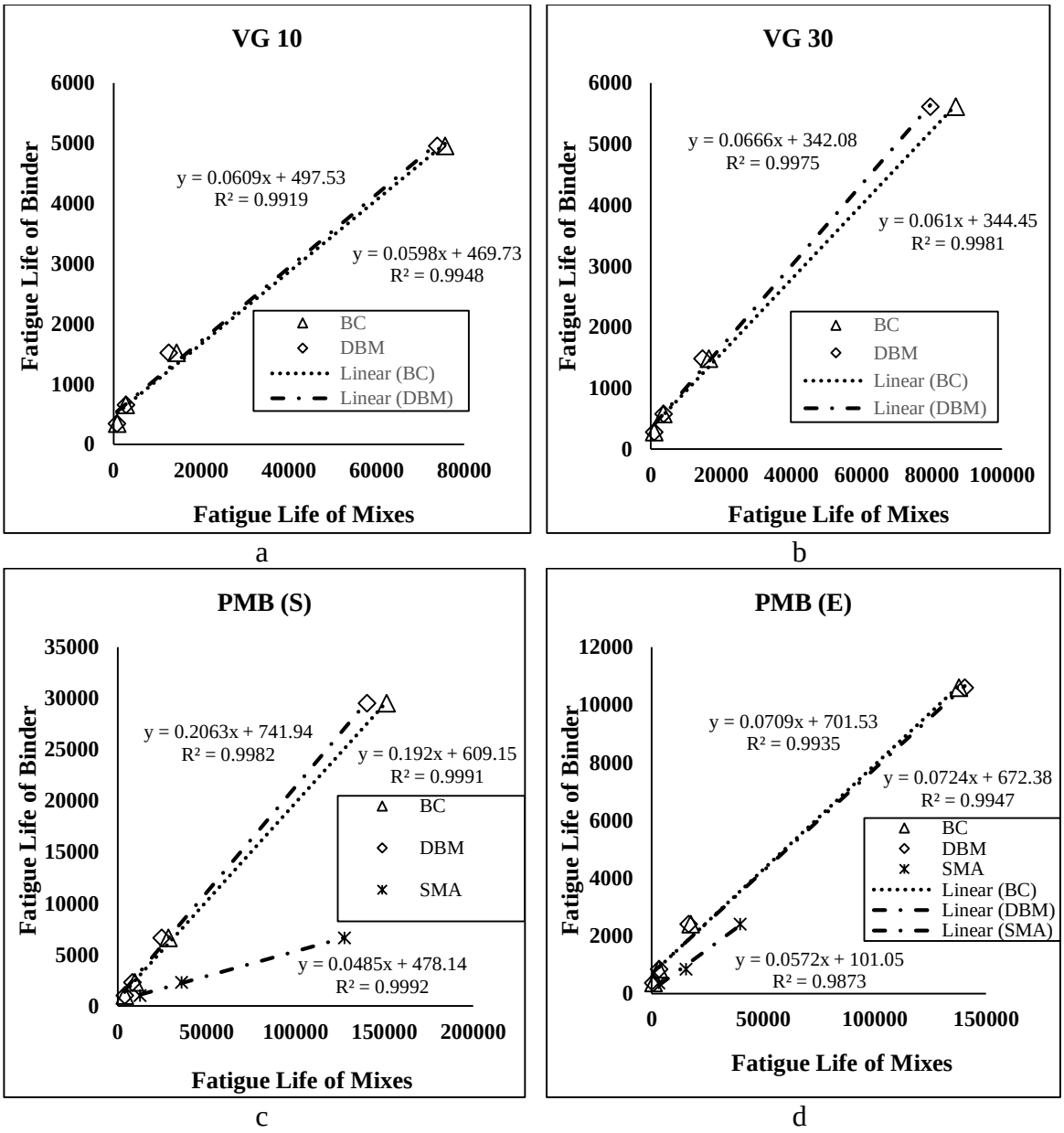

Figure 8.7 (a-d) Correlation of fatigue life of asphalt binders and mixes

8.3.3.2 Correlating rutting

Various test methods as discussed in section 2.8 of chapter 2 were used to compare and correlate the binders rutting performance to the rut depth obtained in wheel rut testing.

Fig. 8.8 (a) shows the values of $|G^*|/\sin\delta$ at all the temperatures at a frequency of 10 rad/sec. On a general note, modified binders had higher values as compared to the VG binders. Plastomeric modified binders displayed the highest value while VG 10 had the least.

The values for all the binders decreased with increase in temperature. However, the rate of this decrement was found higher for conventional binders. Amongst the modified binders, PMB (S) displayed lower decrement in $|G^*|/\sin\delta$ with increase in temperature. Hence, the temperature susceptibility of elastomeric modification can be said to be lower as compared to plastomeric modified bitumen. This phenomena can also be attributed to the melt of EVA crystallites in PMB (E) at higher temperature. This argument is supported by the study done by Airey [6] on behavior of aged and unaged polymer modified binders.

Fig. 8.8 (b) displays the value of ZSV obtained for the unmodified and modified bitumen. Similar to $|G^*|/\sin\delta$, ZSV also decreased with increase in temperature. Modified binders were found to give higher values than the conventional binders at all the test temperatures. Unlike in $|G^*|/\sin\delta$, the temperature susceptibility of plastomeric modified binders was found to be lower in comparison to elastomeric modified binders. This may be attributed to the test condition, in which, at lower shear rates (corresponding to the ZSV), PMB (E), due to its stiff nature, offers more resistance to the micro flow as compared to other binders.

The effect of temperature on the parameter suggested by Shenoy ($\frac{|G^*|}{(1-1/\tan\delta\sin\delta)}$) for all the asphalt binders is presented in Fig. 8.8 (c). The ranking of binders with respect to the rutting susceptibility are found to be similar to the other two parameters discussed above.

Fig. 8.8 (d) displays the values for J_{nr} at a stress level of 3.2 kPa for all the four binders. A higher value of J_{nr} is an indication of higher rut sensitiveness. For a binder to be rut effective a lower value is desired. It was found that PMB (E) had the lowest values at all the temperatures. From Table 2.1 and values shown by Fig. 8.8 (d), it was concluded that VG 10 is not suitable for extremely heavy loading conditions (represented as E) even at 50 °C. Moreover at 60 °C, the value for VG 10 is 2.76 kPa^{-1}, which is less than 2 kPa^{-1}, the minimum required for traffic with heavy loading conditions (designated as H). VG 30 on the other hand is not suitable for very heavy (V in table) and extremely heavy loading conditions at places where the average maximum temperature of pavement is greater than or equal to 60 °C. However, polymer modified binders were found to be suitable for all the loading conditions

at 60 °C. Fig. 8.8 (e) also shows the percent recovery for all the binders at different temperatures at 3.2 kPa^{-1} shear stress. For VG 10 and VG 30, irrespective of any temperature, the percent recovery was found to be less than 30%, which is the minimum required, as specified in Table 2.2. The study strongly suggests that these conventional binders should be avoided at places where rutting is the major failure mode. Polymer modified binders (both elastomer and plastomer) are found to have high recovery values even at 60 °C. Hence they will tend to recover when subjected to cyclic loading typically seen in actual pavement conditions. Nevertheless, the ranking of binder corresponding to rutting susceptibility is found to be same as the other methods.

All the methods discussed above give the same binder ranking as far as rutting performance is concerned. The MSCR method however throws light on fundamental viscoelastic properties of the binder which is impeded in the other methods. The degree to which each method effects the strength properties of the binder with change in temperature is different. Moreover, the amount by which one binder is superior to the other at a particular temperature also varies with the type of method.

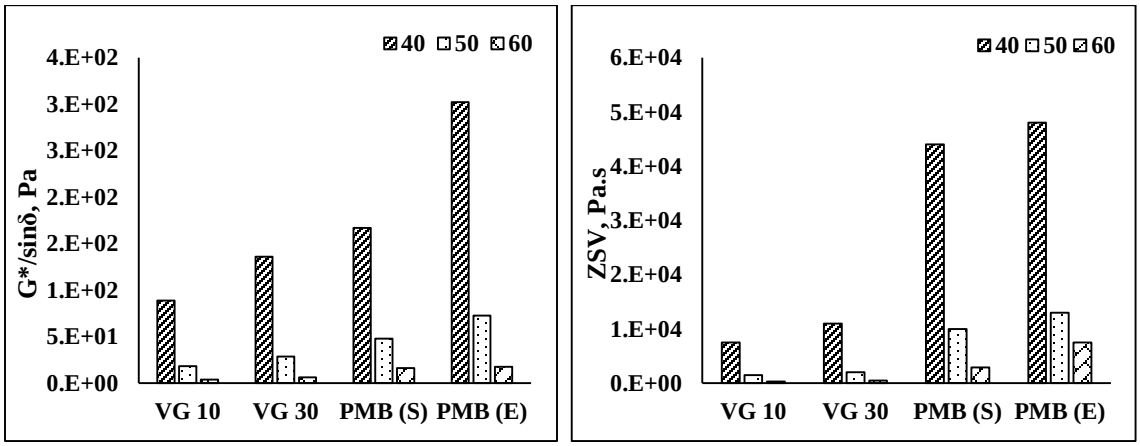

(a) (b)

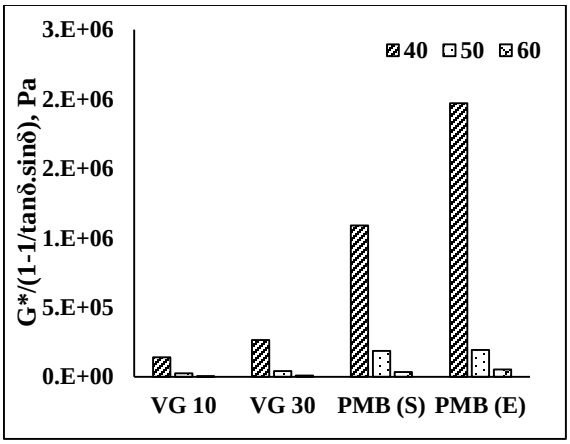

(c)

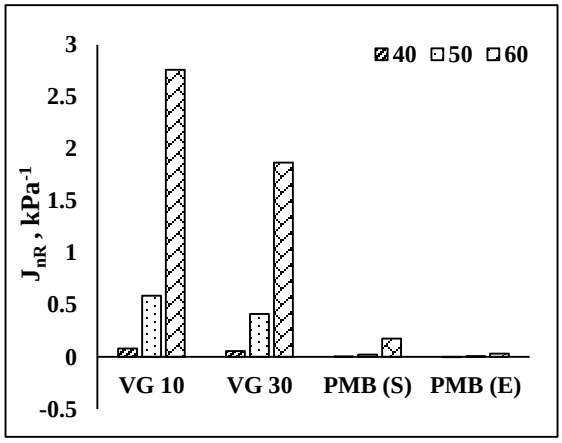

(d)

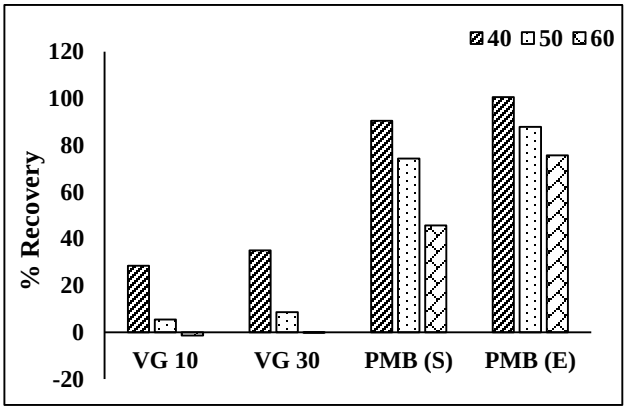

(e)

Figure 8.8 (a-e) Rutting susceptibility parameter with respect to (a) G*/sinδ; (b) ZSV; (c) Shenoy method; (d) MSCR (J_{nr}) and (e) MSCR (% recovery).

To evaluate the suitability of different binder testing methods as a rutting susceptibility parameter, it was necessary to correlate the performance of binder with the result obtained for different mixes. As different binder test methods gave the same ranking of the binder, it was difficult to justify the best test parameter just by analyzing the trend of the results. To delineate this incongruity, the values from all the test methods, including the rut depth values were normalized. After normalizing all the values for different binders, the root mean squared error (RMSE) values were calculated. A lower RMSE value will indicated closer correlation between binder and mix results. The following equations were used to calculate the normalized values (NV) and RMSE.

$$NV = \frac{y - \bar{y}}{SD} \tag{8.7}$$

Where,

NV= Normalized value

y= Actual value (here fatigue life)

$\bar{y}$ = Mean of the values

SD= Standard deviation

$$RMSE = \sqrt{\frac{\sum_{i=1}^{n}(X_{binder,i} - X_{\text{mix},i})^2}{n}} \tag{8.8}$$

Where, X_{binder} is value for the binder and X_{mix} is the value obtained from asphalt mixture testing for the i^{th} binder.

Table 8.3 and Table 8.4 present the NV and RMSE for BC and DBM using different methods. As SMA was prepared using only two binders the results are not shown. It was found at for both BC and DBM, RMSE values were minimum for MSCR method. The other methods were found to have comparatively higher values. The parameter proposed by Shenoy was found to have highest deviation followed by G*/sinδ method. Hence MSCR can be concluded to be the best available parameter to quantify the rutting susceptibility of asphalt binders.

Table 8.3 NV for different methods

Binders	**Normalized Values**					
	Methods				**Mixes**	
	G*/sinδ	**ZSV**	**Shenoy**	**MSCR**	**RD (BC)**	**RD (DBM)**
VG 10	-1.0198	-0.7402	-0.8855	1.1677	1.17368	1.2841038
VG 30	-0.6897	-0.6924	-0.74	0.49622	0.46609	0.2668114
PMB (S)	0.74709	0.02841	0.39623	-0.7775	-0.6455	-0.578963
PMB (E)	0.96239	1.40422	1.22932	-0.8864	-0.9942	-0.971952

Table 8.4 RMSE value for different methods

RMSE values		
Method	**Mixes**	
	BC	**DBM**
G*/sinδ	1.71205	1.69688
ZSV	1.67422	1.66081
Shenoy	1.72591	1.71194
MSCR	0.08659	0.16802

The correlation equation of J_{nr} with respect to rut depth achieved with the measured data for BC and DBM is shown in Figure 8.9(a,b). Though correlating using only four data points might be misleading, the obtained equations are analogous to equations found by other researchers.

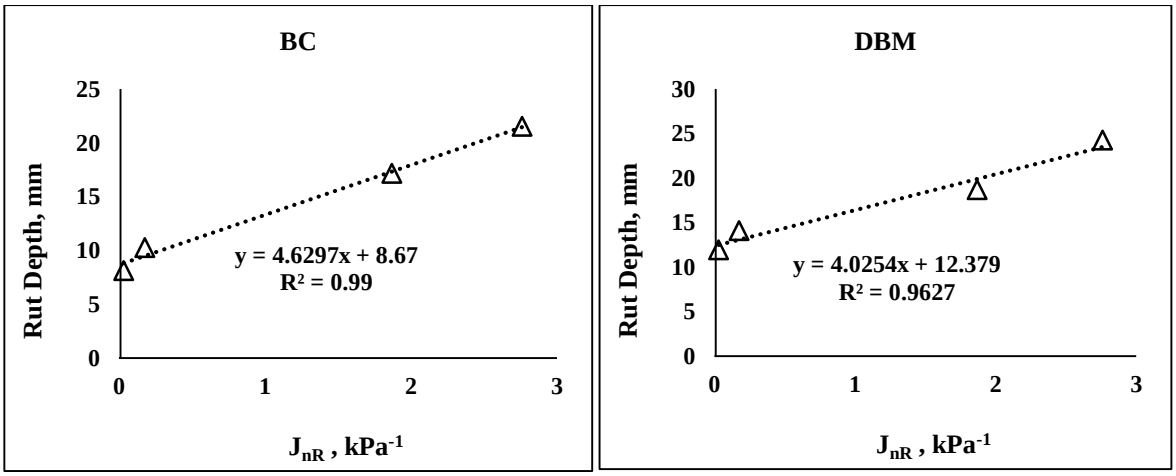

a b

Figure 8.9 (a,b) Correlation of J_{nr} and rut depth (a) for BC and (b) DBM

8.3.4 *Modelling fatigue*

Fatigue cracking prediction is normally based on the cumulative damage concept developed by Miner [112]. The allowable number of load repetitions is related to the tensile strain at the bottom of the asphalt pavement layer. The damage is calculated by the ratio of the predicted number of load repetitions to the allowable number of those repetitions. The overall history of the development of fatigue can be subdivided into five main categories/approaches as follows

- The phenomenological approach
- The continuum damage mechanics approach
- The fracture mechanics approach
- The energy and dissipated energy approach.

This study focusses on analyzing the phenomenological approach. Traditionally the failure in this approach is defined to be reduction in 50% of the initial stiffness of the material. The fatigue life is quantified by N_f, which is the number of load repetition to failure. For a controlled strain mode, N_f can be modelled in one of the following ways.

- Fatigue models relating N_f with strain.
- Fatigue models relating N_f with strain and stiffness.
- Fatigue models relating N_f with strain, stiffness and volumetric parameters.

Though the simplest approach, this method has been criticized mainly due to the inability in providing an accurate mechanism of damage accumulation in the mixture under repetitive load. This study emphasizes on analyzing the previously developed models and providing a more fundamental way which could be applied directly to the complex loading scenarios that are actually common to in-service pavements.

8.3.4.1 Fatigue models relating N_f with strain

This is the simplest fatigue model which could be mathematically represented as

$$N_f = k_1.(\frac{1}{\varepsilon_t})^{k_2} \tag{8.9}$$

Where

ε_t =tensile strain at the bottom of the specimen

k_1, k_2 =experimentally determined coefficients

The coefficients k_1 and k_2 are determined by fitting a power law regression function with the test data on a log scale. At higher strain levels and for modified binders, the sensitivity of the mix is not same at all the strain levels. Hence, a constant value of k_2 to characterize the fatigue response of the mix might be misleading.

8.3.4.2 Fatigue models relating N_f with strain and stiffness.

The basic equation governing the fatigue life using this form of model can be written as

$$N_f = k_1.(\frac{1}{\varepsilon_t})^{k_2}.(\frac{1}{E})^{k_3} \quad (8.10)$$

Where,

N_f =Fatigue life (cycles)

ε_t =Tensile strain at critical location

k_1, k_2, k_3 =laboratory regression coefficients

E =stiffness of the material

Several modification and generalization of the model parameters (k_1, k_2, and k_3) have been made to fit the experimental data [115, 155, 173]. The above given equations works fairly well for low strain amplitudes, where the stiffness of the mixture does not vary with the strain amplitude [156]. But at higher strains, the value of E is not constant, which imposes restriction in using the second term $(\frac{1}{E})^{k_3}$. Harvey and Tsai from their study also suggested that modulus/stiffness values should not be used in fatigue models.

8.3.4.3 Fatigue models relating N_f with strain, stiffness and volumetric parameters.

Pell and cooper [130] incorporated the volumetric of asphalt mixture (volumetric binder content V_b (%); AV, the air void content (%) for calculation of fatigue life of bituminous mix.

$$N_f = k_1(\frac{1}{\varepsilon_t})^{k_2}(\frac{1}{E})^{k_3}(\frac{V_b}{V_b + AV})^{k_4} \quad (8.11)$$

k_1, k_2, k_3, k_4 = experimentally determined parameters

E=Asphalt concrete initial modulus, psi.

The model suffers from a drawback similar to the first and second approach. Nevertheless, the volumetric parameter seems to be a likely indicator of the fatigue damage. It has been proved in many studies that a higher binder film (achieved by increasing the binder content), reduces the stress concentration between the aggregate particles which results in increment of fatigue life. So, using a volumetric parameter as an independent variable might add more accuracy in quantifying the fatigue life of asphalt mixtures.

If the third term ($(\frac{1}{E})^{k_3}$) in equation 9 is avoided assuming the strain dependent reduction in the value of E, then the equation can be modified and written as

$$N_f = k_1(\frac{1}{\varepsilon_t})^{k_2}(\frac{V_b}{V_b + AV})^{k_3} \tag{8.12}$$

8.4 Proposed model

A bituminous mix comprises two main components: aggregates and bitumen. The aggregates of different sizes are mixed, which provides the shear strength and the bitumen holding the particles together imparts cohesion to the structure. So, the response to any loading condition, whether it be flexure or compression is affected mainly due to two mix attributes: the way the aggregates are combined i.e. the aggregate gradation and the type and amount of binder. Other factor including type and mineralogical properties of aggregate may also influence the strength of the mix. However, in this study a single source of aggregates was chosen. Considering that the air void content in the mix is fixed, the aggregate gradation and the binder properties will only be the influential factors.

It is hypothesized in this study that the degree to which a single binder influences the mix properties remains same for different types of mixes. Also, the extent to which the aggregate gradation affects the strength of the mix remains unaltered, irrespective of the type of binder used. Aggregates are generally considered linear materials whose response do not vary with the change in load amplitudes (strain level). The change in material (here bituminous mix) strength/stiffness with change in strain/stress levels can be attributed to the rheological characteristics of the bitumen which is the non-linear component in a bituminous mixture. This point will become clearer by considering the proposed model which is mathematically represented as

$$N_f = k_1.(\frac{1}{\varepsilon})^{k_2}.(VFB)^{k_3} \quad (8.13)$$

Where

k_1 =experimentally determined parameter

k_2 =parameter determining the sensitivity of the binder to the strain level.

k_3 =parameter determining the sensitivity of the mix to the fatigue.

VFB = voids filled with bitumen (%).

As discussed above, the binder is the main component which is sensitive to the change in strain level. So, the value of parameter k_2 cannot remain constant when the mix is subjected to varying strain amplitudes. This variation should relate to the degradation of the material property (such as stiffness) with increase in strain level. Studies have shown that the stiffness of a mix decreases exponentially with increase in strain amplitude. Considering this statement to be true, it has been assumed that k_2 decreases exponentially with increase in strain level as follows

$$k_2 = A.\exp^{-B\varepsilon} \quad (8.14)$$

Where A and B are model parameter which are binder specific and will remain same for each binder across different types of mixes. The parameter k_1 and k_3 are assumed to be constant for a particular aggregate gradation (type of mix) irrespective of any binder used. Substituting the value of k_2 in the above equation and taking log both sides, we get

$$\log N_f = \log k_1 - A\exp^{-B\varepsilon}.\log\varepsilon + k_3 \log(VFB) \quad (8.15)$$

The above model was used and was compared with the equations 8.12 and 8.15 to check its applicability in modelling the fatigue response of different types of mixes prepared with unmodified and modified bitumen.

8.4.1 *Validation of the proposed model*

In order to validate the applicability of the proposed model (equation 8.18) the experimental values were fitted with the modelled values. For comparison, equations 8.12 &

8.15 were also used to observe the deviation of the calculated and experimental results. These models are denoted as Model 2 and Model 1. The model parameters were optimized using SOLVER function in MS excel to obtain the best fit. For the proposed model all the assumptions (as explained in section 8.4) were considered.

Figure 8.10 demonstrates the curve fit of all the three models with the experimental value. It can be seen that the proposed model fits best to the experimental results. The other two models, deviate, especially at higher strain levels. Model 2 showed the highest deviation followed by Model 1. This deviation can be attributed to the constant value of the model parameter used, which delineates the inclusion of strain sensitivity. The highest deviation of Model 1 and Model 2 was found for mixes containing PMB (E). This may be due to the high strain sensitivity of the plastomer. For mixes prepared with PMB (S), Model 1 showed good fit. This is due to the less susceptibility of PMB (S) to change in strain amplitude. However the proposed model displayed excellent correlation with the experimentally obtained values. Hence the assumption of the exponential decrease of the value of k_2 in the proposed model stands true. Also the excellent model fit proved that the parameters k_1 and k_3 are only mix dependent and same values may be used irrespective of the type of binder. The parameters A and B used to define k_2 was solely binder dependent. The values remained constant for different binders irrespective of the type of mix. Table 8.5 presents the value of the model parameters obtained in the study. The proposed model was also compared with Model 1 and Model 2 statistically using the RMSE values as discussed in the previous section.

Table 8.5 displays the values of RMSE obtained in the study upto three significant digits. A higher RMSE value would indicate higher deviation from the experimental values. It can be seen that in all the cases the error is minimum for the proposed model. Amongst model 1 and model 2, model 1 gave better results. Model 1 was found to be close to the proposed model for mixes prepared with PMB (S). This may be attributed to the low sensitivity of PMB (S) to change in strain making the proposed model behave close to Model 1.

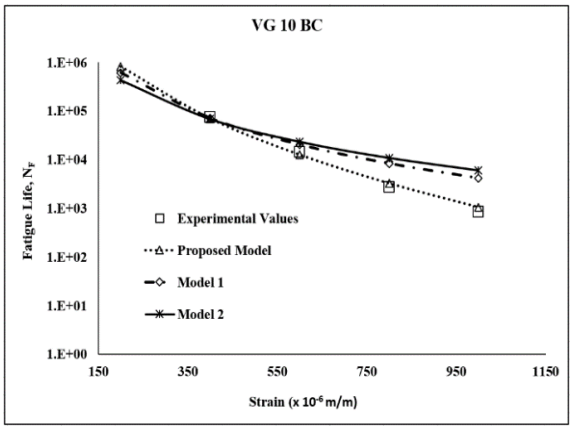
VG 10 BC
Fatigue Life, N_F
1.E+06
1.E+05
1.E+04
1.E+03
1.E+02
1.E+01
1.E+00
150
350
550
750
950
1150
Strain (x 10^{-6} m/m)
Experimental Values
Proposed Model
Model 1
Model 2

a

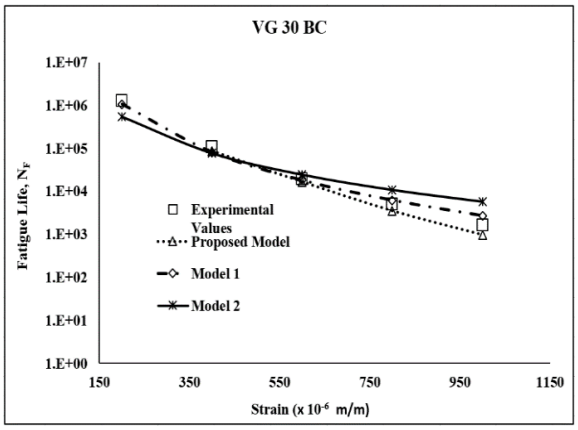
VG 30 BC
Fatigue Life, N_F
1.E+07
1.E+06
1.E+05
1.E+04
1.E+03
1.E+02
1.E+01
1.E+00
150
350
550
750
950
1150
Strain (x 10^{-6} m/m)
Experimental Values
Proposed Model
Model 1
Model 2

b

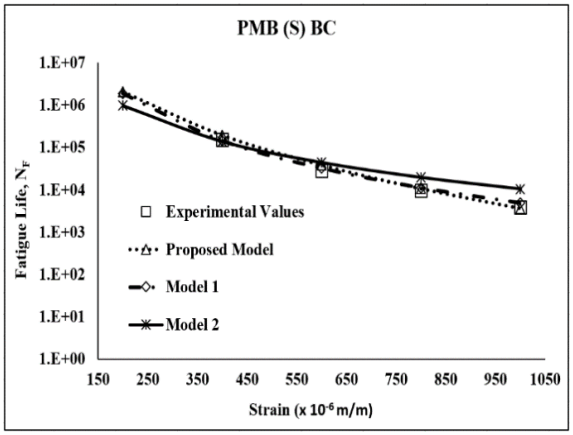
PMB (S) BC
Fatigue Life, N_F
1.E+07
1.E+06
1.E+05
1.E+04
1.E+03
1.E+02
1.E+01
1.E+00
150
250
350
450
550
650
750
850
950
1050
Strain (x 10^{-6} m/m)
Experimental Values
Proposed Model
Model 1
Model 2

c

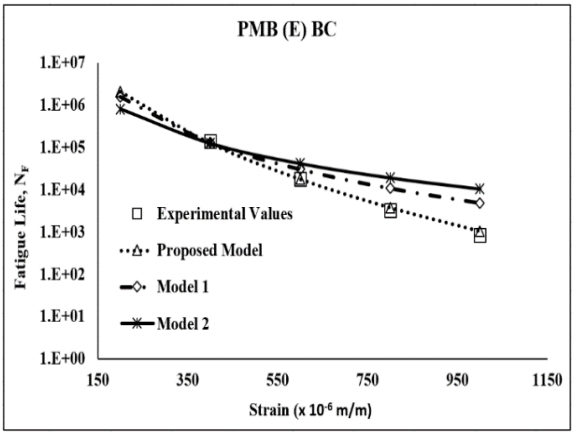
PMB (E) BC
Fatigue Life, N_F
1.E+07
1.E+06
1.E+05
1.E+04
1.E+03
1.E+02
1.E+01
1.E+00
150
350
550
750
950
1150
Strain (x 10^{-6} m/m)
Experimental Values
Proposed Model
Model 1
Model 2

d

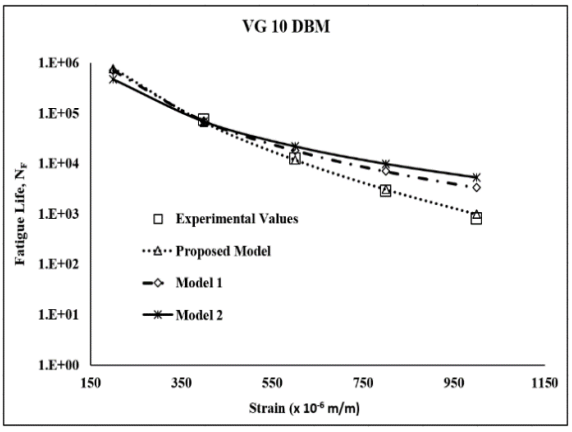
VG 10 DBM
Fatigue Life, N_F
1.E+06
1.E+05
1.E+04
1.E+03
1.E+02
1.E+01
1.E+00
150
350
550
750
950
1150
Strain (x 10^{-6} m/m)
Experimental Values
Proposed Model
Model 1
Model 2

e

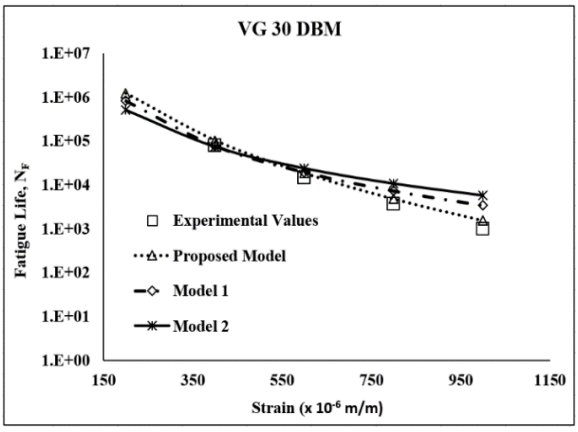
VG 30 DBM
Fatigue Life, N_F
1.E+07
1.E+06
1.E+05
1.E+04
1.E+03
1.E+02
1.E+01
1.E+00
150
350
550
750
950
1150
Strain (x 10^{-6} m/m)
Experimental Values
Proposed Model
Model 1
Model 2

f

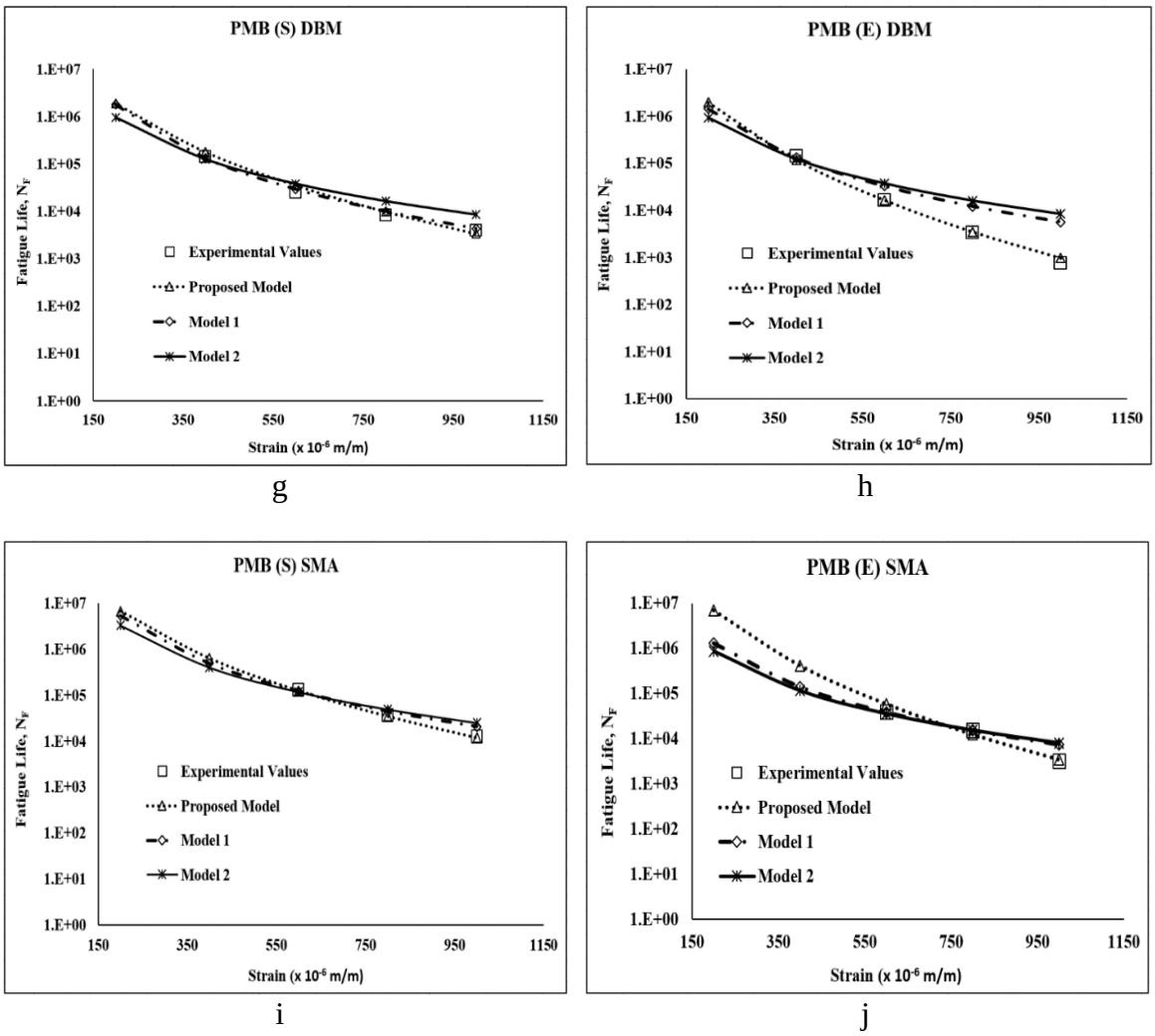

g h

i j

Figure 8.10 (a-j) Comparison of different model fit with the experimental results

Table 8.5 Model parameters obtained through SOLVER function.

Mix Type	Binder	Model 1			Model 2		Proposed Model			
		k_1	k_2	k_3	k_1	k_2	k_1	k_3	A	B
BC	VG 10	3.7E-05	3.5E+00	1.7E+01	6.5E-05	2.7E+00	0.07	0.9	2.1	3.80E-04
	VG 30	2.1E-05	3.7E+00	2.0E+01	1.6E-05	2.8E+00	0.07	0.9	2.15	3.60E-04
	PMB (S)	3.0E-05	3.7E+00	2.0E+01	3.6E-05	2.8E+00	0.07	0.9	2.18	3.00E-04
	PMB (E)	3.1E-05	3.6E+00	1.8E+01	8.2E-05	2.7E+00	0.07	0.9	2.25	4.50E-04
DBM	VG 10	6.6E-05	3.3E+00	1.5E+01	2.4E-05	2.8E+00	0.065	0.85	2.1	3.80E-04
	VG 30	6.1E-05	3.4E+00	1.6E+01	2.2E-05	2.8E+00	0.065	0.85	2.15	3.60E-04
	PMB (S)	2.9E-05	3.7E+00	2.0E+01	1.4E-05	2.9E+00	0.065	0.85	2.18	3.00E-04
	PMB (E)	4.4E-05	3.4E+00	1.5E+01	1.4E-05	2.9E+00	0.065	0.85	2.25	4.50E-04
SMA	PMB (S)	2.2E-05	3.5E+00	1.4E+01	1.9E-05	3.0E+00	0.2	0.7	2.18	3.00E-04
	PMB (E)	5.8E-05	3.2E+00	1.5E+01	1.6E-05	2.9E+00	0.2	0.7	2.25	4.50E-04

Table 8.6 Root mean squared error (RMSE) for different models.

Binder	RMSE								
	BC			DBM			SMA		
	Model 1	Model 2	Proposed Model	Model 1	Model 2	Proposed Model	Model 1	Model 2	Proposed Model
VG 10	0.027	0.081	0.015	0.051	0.088	0.006			
VG 30	0.014	0.066	0.013	0.035	0.076	0.005			
PMB (S)	0.024	0.081	0.015	0.033	0.084	0.025	0.032	0.050	0.000
PMB (E)	0.066	0.125	0.009	0.082	0.116	0.016	0.015	0.060	0.073

8.5 Conclusions

In wheel rut test, SMA was found to be the most rut resistant mix followed by BC. Mixes prepared with modified binders had lower rut depths as compared to mixes prepared using viscosity graded binders. For lower cycle numbers the variation of rut depth with cycle was found to be close to each other for different binders. As the cycle number increased (typically after 500 cycles), the difference in rut depth became more prominent. To determine the best binder testing method which correlates most closely to rut depth of bituminous mixes, statistical parameter, root mean square error (RMSE) was calculated for each method. It was found that MSCR gave the best results out of all the four methods, followed by ZSV. Correlation equations between J_{nr} and rut depth were also established for BC and DBM.

At lower strain levels mixes prepared with polymer modified binders had higher fatigue life as compared to mixes prepared with conventional viscosity graded binders. At high strain amplitude mixes prepared with PMB (E) gave poor performance in fatigue. The fatigue life PMB (E) mixes were even lower than the mixes prepared using conventional binders. This is attributed to the high strain sensitivity of PMB (E). PMB (S) on the other had gave best results in comparison to other binders.

Amongst all the mixes, SMA gave the best performance in fatigue. The fatigue life of SMA mixes were almost five times higher as compared to other bituminous mixtures. This is attributed to the high VMA percentage, which can accommodate large amount of binder for a fixed air void content. This increases the film thickness which reduces the stress and increases the durability.

It was found that for similar strain levels the fatigue life of asphalt binders could be linearly correlated with the fatigue life of asphalt mixes. The correlation equation varies with the type of mix for each binder.

The new proposed model gave excellent fit with the experimentally obtained values. The traditional models were found to deviate from the experimentally obtained values especially for mixes prepared with plastomeric modified binder. The use of constant model parameter was found to be the reason for such deviation. The new proposed model was also found to be statistically reliable as shown by the lower RMSE.

The assumption that the model parameter k_2 of the proposed model will vary exponentially with strain level was found to be true. Moreover, the model parameter k_2 was found to be dependent only on the type of binder, irrespective of any aggregate gradation. Similarly, the parameters k_1 and k_3 were found to be dependent on the type of gradation irrespective of any binder used.

Chapter 9
Conclusions and Recommendations

9.1 Conclusions

Based upon the study presented in the previous chapters the following conclusions were drawn

1. It is important to obtain the proper blending requirement for modifying bitumen with any additive. The importance of different blending parameters depends on the type of modifier used. It was found that for EVA modification temperature plays the most crucial role while for SBS the effect of shear rate is crucial. It was found that SBS could be incorporated in the base binder at a temperature of 180 °C using a high shear mixture operated at 1500 rpm for 60 minutes. The corresponding temperature, shear rate and time for EVA were 190 °C, 600 rpm and 30 minutes. Storage stability test showed that optimum modifier content for EVA is 5% while for SBS is 3%. This result was also validated by the study of morphology using Fluorescence microscopy.

2. Polymer modified binders were found to be more shear thinning as compared to normal binders. At higher temperatures, normal binders also show tendency of shear thinning, but at very high shear rates. The concept of Rheogram for plotting master curve of viscosity versus shear rate was found to be applicable to all the binders, with little deviation observed for PMB (E). C-Y model fitted well with the master curve of all the binders. Steady shear viscosity measurement using DSR and Brookfield viscometer were found to be in good alignment with each other. Mixing temperature for modified binder were found to be lower for practical shear rates varying from laboratory to field. The mixing temperature requirements decreased with increase in shear rate.

3. The LVE strain increased with increase in temperature and reduction in frequency. At higher frequency and for low temperatures the LVE strain limits were low, owing

to the higher stiffness of bitumen. The variation of LVE strain with frequency was not as much significant as with temperature. It was also found that PMB (S) gave more stable values with variation in both frequency and temperature. This strain susceptibility was found highest for PMB (E).

4. At higher temperatures spindle diameter 8 mm gave higher values for complex modulus and phase angle of the asphalt binders as compared to 25 mm diameter spindle. This difference reduced with reduction in temperature with the curves coinciding at intermediate temperatures. With further reduction (at lower temperatures) the curve reversed its direction with 8 mm diameter tending to give lower values than 25 mm spindle diameter. At higher temperatures higher plate gap gave lower values of complex modulus as compared to lower gap width. The difference in the measurements decreased with decrease in temperature with similar values at intermediate temperatures. At lower temperatures smaller gap width gave higher values. A change in spindle diameter and plate gap changes the value of the rheological parameter. The changes were more pronounced at lower and higher temperatures. One conclusion which could be drawn from the study was that 8 mm spindle geometry cannot be used for higher temperatures and is suitable for temperature range of 10- 30 °C typically. The study of thermorheological simplicity cannot be made only on the basis of complex modulus master curves. Phase angle curves are more sensitive to change in chemical nature of the bitumen.

5. The shift factor obtained by the equivalent slope method which was developed in the study gave better results in plotting master curves as compared to WLF and Arrhenius equation. The shift factor for all the binders at different reference temperature was found to obey exponential law.

6. It was found that Cox-Merz rule can be successfully applied in the zero shear viscosity domain. The critical shear rate was lower for modified binders, which indicated higher dependence of modified binders on shear rate. At very high shear rate of the order of 10^5 s^{-1}, the viscosity of modified binders were found to be lower

than the conventional binder. The simple C-Y model was found to be successfully applicable in modelling the rheological properties of both conventional and modified bitumen. The model however is sensitive to the determination of ZSV values. So, accurate determination of ZSV is recommended to gain more confidence in using the equation.

7. It was found that the conventional binders are highly sensitive to change in stress level and temperatures and are not suitable at locations with extreme temperature and loading conditions. The average percent recovery of modified binders were subsequently higher than the conventional binders. PMB (S) showed higher recovery than PMB (E) at 60 °C for higher stress levels.

8. Burgers model was found to be weak in characterizing the delayed elastic response of modified bitumen. The model parameter η_M had good correlation with the unrecoverable creep compliance J_{nR} and the average % recovery. The value of η_M was affected by the level of stress only after a certain temperature. This temperature was binder specific and was found to be the point from where the viscous flow dominates. The Boltzmann superposition was not valid for recovery potion of MSCR test. The deviations mainly occurred at lower stress levels and temperatures. The power law was modified to include the nonlinearity associated with bitumen. The factor α correlated well with the J_{nR} and average % recovery. Critical values of η_M and α were assigned, which should be achieved at the desired temperature of study. This temperature should correspond to the maximum average temperature of the study area. A minimum value of 2000 Pa.s and a maximum value of 0.92 was assigned for J_{nR} and α, so as to trace the presence of delayed elastic response in any bitumen. The parameter B of the power law model showed a linear relationship with temperature. The ratio of the averages, was almost constant irrespective of any temperature. The ratio was found to be same as the ratio of the corresponding softening point for the binders. The parameter A was found to be function of both stress level and the temperature. It displayed a power law behavior with respect to the stress level. For a particular temperature the ratio of A was found to be invariant with stress level. This

ratio was at a particular temperature showed excellent correlation with the inverse of the ratio of Zero Shear Viscosity (ZSV) of the binders. The parameter *B.n* (considered as α) in the recovery model was found to have similar correlation as the factor *B.* The equations relating the model parameters with the intrinsic binder properties is presented and could be very useful to establish the creep and recovery behavior of any binder through simple measurements of conventional properties.

9. LAS test was found to be more practical than the existing intermediate performance criteria of $G^*.sin\delta$. By LAS test it was possible to evaluate the complex behavior of the binder at a wide range of loading level. Elastomeric polymer modified binder (PMB (S)) displayed the highest fatigue life at all the test temperatures. PMB (E) was found to susceptible to strain amplitudes at 10 and 20 ºC at which the performance degraded at higher strain levels. VG 10 and VG 30 had lower fatigue lives at lower strain amplitudes. But the rate of decrease in fatigue life with increase in strain level was lower than the modified binders. VG 10 had the lowest strain susceptibility and gave better results than PMB (E) and VG 30 at higher strain amplitudes. However at 30 ºC PMB (E) performed better than the conventional binders. A lower value of α and a higher value of *A* is desirable for superior performance in fatigue. The increased in fatigue life with increase in temperature was found to be highest for VG 10.

10. PMB (S) gave the best overall performance in both the test methods. PMB (E), though performs well at higher temperature, but at intermediate pavement temperature it may be susceptible to fatigue cracking attributed to higher sensitivity to strain amplitudes. Among the conventional binders both VG 10 and VG 30 were found to be suitable for resisting fatigue cracking at intermediate pavement temperatures. Nevertheless, at higher temperatures both VG 10 and VG 30 showed poor performance. These detailed information about the performance of the binders are impeded in the traditional Superpave performance criteria. Hence the study finds both LAS and MSCR to be more fundamental in characterizing the rutting and fatigue performance of asphalt binders. It has to be mentioned that the results of this study is

based solely on binder testing and must be verified using validation with mixture performance testing.

11. The Marshall test results indicated higher stability for dense graded mixtures prepared with polymer modified bitumen. SMA mixes displayed lower stability values attributed to high VMA and increased binder content. The moisture susceptibility as shown by the retained Marshall stability test was higher for conventional binders. The retained Marshall stability values for SMA mixes were found to be higher than the dense graded mixes. ITS values for BC and DBM were found to be higher than SMA. Mixes prepared with modified binders displayed higher strength values in comparison to viscosity graded binders. VG 10 did not satisfy the minimum TSR criteria required to satisfy the moisture susceptibility criteria. All the mixes prepared in this study had a film thickness above 8 μ, indicating that all the mixes would perform satisfactorily with respect to durability.

12. In wheel rut test, SMA was found to be the most rut resistant mix followed by BC. Mixes prepared with modified binders had lower rut depths as compared to mixes prepared using viscosity graded binders. For lower cycle numbers the variation of rut depth with cycle was found to be close to each other for different binders. As the cycle number increased (typically after 500 cycles), the difference in rut depth became more prominent. To determine the best binder testing method which correlates most closely to rut depth of bituminous mixes, statistical parameter, root mean square error (RMSE) was calculated for each methods. It was found that MSCR gave the best results out of all the four methods, followed by ZSV. Correlation equations between J_{nr} and rut depth were also established for BC and DBM. At lower strain levels mixes prepared with polymer modified binders had higher fatigue life as compared to mixes prepared with conventional viscosity graded binders. At high strain amplitude mixes prepared with PMB (E) gave poor performance in fatigue. The fatigue life PMB (E) mixes were even lower than the mixes prepared using conventional binders. This is attributed to the high strain sensitivity of PMB (E). PMB (S) on the other had gave best results in comparison to other binders.

13. Amongst all the mixes, SMA gave the best performance in fatigue. The fatigue life of SMA mixes were almost five times higher as compared to other bituminous mixtures. This is attributed to the high VMA percentage, which can accommodate large amount of binder for a fixed air void content. This increases the film thickness which reduces the stress and increases the durability. It was found that for similar strain levels the fatigue life of asphalt binders could be linearly correlated with the fatigue life of asphalt mixes. The correlation equation varies with the type of mix for each binder.

14. The new proposed model gave excellent fit with the experimentally obtained values. The traditional models were found to deviate from the experimentally obtained values especially for mixes prepared with plastomeric modified binder. The use of constant model parameter was found to be the reason for such deviation. The new proposed model was also found to be statistically reliable as shown by the lower RMSE. The assumption that the model parameter k_2 of the proposed model will vary exponentially with strain level was found to be true. Moreover, the model parameter k_2 was found to be dependent only on the type of binder, irrespective of any aggregate gradation. Similarly, the parameters k_1 and k_3 were found to be dependent on the type of gradation irrespective of any binder used.

9.2 Recommendations

The following are the recommendations laid out by the study conducted of unmodified and modified asphalt binders and mixes.

1. The optimum modifier and the requirements for its blending should be wisely selected. Tests like storage stability and fluorescence microscopy should be used to find the optimum modifier content for the base binder.
2. New technique proposed for evaluation of mixing compaction temperatures can be employed for modified binders. Role of shear rate should be taken into account for modified binders.
3. Virgin binder, VG 10 and VG 30 should not be used at locations with high temperature and loading conditions, especially when permanent deformation is the

main failure mode. PMB (E) should be avoided at locations with lower temperatures. PMB (S) can be successfully used for all types of loading and temperature conditions.

4. Gap graded mixes like stone mastic asphalt prepared with modified binders are capable of resisting more stresses and hence should be employed in highways where extreme situation prevails.

9.3 Future Scope of the Study

Future research may be conducted in the following areas:

1. The outcome of this research was based on testing and analysis done on four types of binders and three types of mixes. Study can be extended to more number and types of binders and mixes to validate the study.
2. The technique proposed in this study for obtaining mixing temperatures for bitumen is analytical and should be validated in field so that more confidence can be gained in using modified binders.

References

1. AASHTO. (2010). "Specification For Performance-Graded Asphalt Binder Using Multiple Stress Creep Recovery (Mscr) Test." *MP19* , Washington, DC.

2. AASHTO. (2012). "Standard method of test for determining the rheological properties of asphalt binder using dynamic shear rheometer." *T 315*, Washington, DC

3. AASHTO. (2013). "Method of Test for Viscosity Determination of Asphalt Binder Using Rotational Viscometer." *T316,* Washington, DC.

4. AASHTO. (2014). "Standard Method of Test for Estimating Damage Tolerance of Asphalt Binders Using the Linear Amplitude Sweep." *TP 10,* Washington, DC

5. Adhikari, S., Shen, S., & You, Z. (2010). "Evaluation of Fatigue Models of Hot-Mix Asphalt Through Laboratory Testing." *Transportation Research Record: Journal of the Transportation Research Board, 2127*, 36–42.

6. Airey, G. D. (1997). "Rheological Characteristics of Polymer Modified and Aged Bitumens." *PhD Thesis*, The University of Nottingham.

7. Airey, G. D. (2002). "Rheological evaluation of ethylene vinyl acetate polymer modified bitumens." *Construction and Building Materials*, 16(8), 473–487.

8. Airey, G. D. (2002). "Use of Black Diagrams to Identify Inconsistencies in Rheological Data." *Road Materials and Pavement Design*, 3(4), 403–424.

9. Airey, G. D. , and Hunter, A. E. (2003). "Dynamic mechanical testing of bitumen—Sample preparation methods." ICE Transport , 156 (2), 85–92.

10. Airey, G. D., Rahimzadeh, B., and Collop, A. C. (2003). "Viscoelastic linearity limits for bituminous materials." *Materials and Structures*, 36, 643–647.

11. Airey, G.D., Rahimzadeh, B. & Collop, A.C. (2003). "Viscoelastic linearity limits for bituminous materials." *Mater Struct, 36*, 643–647.

12. Airey, G. D., Rahimzadeh, B., and Collop, A. C. (2004). “Linear Rheological Behavior of Bituminous Paving Materials.” *Journal of Materials in Civil Engineering*, 16(3), 212–220.

13. Alam, S., Kumar, A., & Dawes, L. (2013). "Life Cycle Analysis for Sustainibility aseesment of Road Projects." *In 19th CIB World Building Congress*. Brisbane: Construction and Society, Queensland.

14. Al-shalout, I., Miro, O., and Stas, R. (2007). “Effects of Moisture , Compaction Temperature and Gradation Types on Durability of Asphalt.” *Damascus univ. Journal*, (23), 7–35.

15. Anderson, D., Hir, Y., Marasteanu, M., Planche, J.-P., Martin, D., and Gauthier, G. (2001). “Evaluation of Fatigue Criteria for Asphalt Binders.” *Transportation Research Record*, 1766(01), 48–56.

16. Anderson, D. A., Christensen, D. ., Bahia, H. U., Dongre, R., Sharma, M. G., and Antle, C. E. (1994). “SHRP-A-369: Binder Characterization and Evaluation-Physical Characterization.” *Strategic Highway Research Program*, Washington, DC.

17. Anderson, D. A., and Kennedy, T. W. (1993). “Development of SHRP Binder Specification.” *Journal of the Association of Asphalt Paving Technologists*, 62, 481–507.

18. Anjan Kumar, S., Sarvanan, U., Murali Krishnan, J., and Veeraragavan, a. (2014). “Rheological characterisation of modified binders at mixing and compaction temperature.” *International Journal of Pavement Engineering*, 15(9), 767–785.

19. ASTM. (2008). "Standard Test Method for Effect of Heat and Air on a Moving Film of Asphalt (Rolling Thin-Film Oven Test)." *D 2872*

20. ASTM. (2013). "Standard Practice for Accelerated Aging of Asphalt Binder Using a Pressurized Aging Vessel." *D 6521*

21. ASTM. (2012). "Standard Test Method for Multiple Stress Creep and Recovery (MSCR) of Asphalt Binder Using a Dynamic Shear Rheometer." *D7405-10a.*

22. Awanti, S. S., Amarnath, M. S., and Veeraragavan, A. (2008). “Laboratory evaluation

of SBS modified bituminous paving mix." *Journal of Materials in Civil Engineering*, 20(4), 327–330

23. Awanti, S.S., Amarnath, M.S. & Veeraragavan A. (2007). "Influence of rest periods on fatigue characteristics of SBS polymer modified bituminous concrete mixtures." *Int J Pavement Eng., 8*, 177–186.

24. Azari, H., McCuen, R. H., and Stuart, K. D. (2003). "Optimum Compaction Temperature for Modified Binders." *Journal of Transportation Engineering*, 129, 531–537.

25. Bahia, H. U., Zhai, H., Zeng, M., HU, Y., & Turner, P. (2001). "Development of binder specification parameters based on characterization of damage behavior." *Journal of the Association of Asphalt Paving Technologists*, *70*, 442–470.

26. Bai, F., Yang, X., & Zeng, G. (2014). "Creep and recovery behavior characterization of asphalt mixture in compression." *Construction and Building Materials*, *54*, 504–511.

27. Bari, J., and Witczak, M. (2007). "New Predictive Models for Viscosity and Complex Shear Modulus of Asphalt Binders: For Use with Mechanistic-Empirical Pavement Design Guide." *Transportation Research Record*, 2001(2001), 9–19.

28. Becker, Y., and Méndez, M. P. (2001). "Polymer Modified Asphalt." *Vision Technologica*, 9, 39–50.

29. Behzadfar, E., and Hatzikiriakos, S. G. (2014). "Rheology of bitumen: Effects of temperature, pressure, CO_2 concentration and shear rate." *Fuel*, 116, 578–587.

30. Di Benedetto, H., Olard, F., Sauzéat, C. & Delaporte, B. (2004). "Linear viscoelastic behaviour of bituminous materials: From binders to mixes." *Road Mater Pavement Des, 5*, 163–202.

31. Di Benedetto, H., Sauzeat, C., Bilodeau, K., Buannic, M., Mangiafico, S., Nguyen, QT., Pouget, S., Tapsoba, N. & Van Rompu, J. (2011). "General overview of the time-temperature superposition principle validity for materials containing bituminous binder." *Int J Roads Airports, 1*, 35–52.

32. Benedetto, H., Roche, C., Baaj, H., Pronk, A., & Lundström, R. (2004). "Fatigue of bituminous mixtures." *Materials and Structures*, *37*, 202–216.

33. Bird, R. B., and Carreau, P. (1968). "A nonlinear viscoelastic model for polymer solutions and melts - 1." *Chemical Engineering Science*, 23(2), 427–434.

34. Biro, S., Gandhi, T., & Amirkhanian, S. (2009). "Determination of zero shear viscosity of warm asphalt binders." *Construction and Building Materials*, *23*(5), 2080–2086.

35. Bodin, D., de La Roche, C., & Chabot, A. (2004). "Prediction of Bituminous Mixes Fatigue Behavior During Laboratory Fatigue Tests". In *3rd Eurasphalt & Eurobitume Congress* (pp. 1935–1945). Vienna.

36. de Carcer, Í. A., Masegosa, R. M., Teresa Viñas, M., Sanchez-Cabezudo, M., Salom, C., Prolongo, M. G., Contreras, V., Barceló, F., and Páez, A. (2014). "Storage stability of SBS/sulfur modified bitumens at high temperature: Influence of bitumen composition and structure." *Construction and Building Materials*, 52, 245–252.

37. Castro, M., & Sánchez, J. a. (2008). "Estimation of asphalt concrete fatigue curves - A damage theory approach." *Construction and Building Materials*, *22*, 1232–1238.

38. Celauro, C., Fecarotti, C., Pirrotta, a., & Collop, a. C. (2012). "Experimental validation of a fractional model for creep/recovery testing of asphalt mixtures." *Construction and Building Materials*, *36*, 458–466.

39. Chandra, S., and Choudhary, R. (2013). "Performance Characteristics of Bituminous Concrete with Industrial Wastes as Filler." *Journal of Materials in Civil Engineering*, 25(11), 1666–1673.

40. Chen, X. ., Huang, B., and Xu, Z. (2007). "Comaprison Between Flat Rubber Wheeled Loaded Wheel Tester and Asphalt Pavement Analyzer." *Road Materials and Pavement Design*, 3, 595–604.

41. Cox, W. P., and Merz, E. H. (1958). "Correlation of dynamic and steady flow viscosities." *Journal of Polymer Science*, 28(118), 619–622.

42. Cross, M. M. (1965). “Rheology of non-Newtonian fluids: A new flow equation for pseudoplastic systems.” *Journal of Colloid Science*, 20, 417–437.

43. D’Angelo, J. (2009). "Current Status of Superpave Binder Specification." *Road Materials and Pavement Design, 10*(11), 13–24.

44. D’Angelo, J. (2009). T"he Relationship of the MSCR Test to Rutting." *Road Materials and Pavement Design, 10*(11), 61–80.

45. D’Angelo, J., Kluttz, R., Dongre, R. N., Stephens, K., and Zanzotto, L. (2007). “Revision of the Superpave High Temperature Binder Specification: The Multiple Stress Creep Recovery Test (With Discussion).” *Journal of the Association of Asphalt Paving Technologists,*76, 123–162.

46. D’Angelo, J., Reinke, G., Bahia, H., Wen, H., Johnson, C. M., & Marasteanu, M. (2010). "*Development in Asphalt Binder Specifications*." Transportation Research Circular E-C147, 1-13.

47. Dash, S. S., and Panda, M. (2015). “Effect of Aggregate Gradation on Cold Bituminous Mix Performance.” *Advances in Civil Engineering Materials*, 4(1), 20140047.

48. Dealy, J., and Plazek, D. (2009). “Time-Temperature Superposition- A Users Guide.” *Rheology Bulletin*.

49. Delgadillo, R., & Bahia, H. U. (2010). "The Relationship between Nonlinearity of Asphalt Binders and Asphalt Mixture Permanent Deformation." *Road Materials and Pavement Design, 11*(3), 653–680.

50. Delgadillo, R., & Bahia, H. U. (2010). The Relationship between Nonlinearity of Asphalt Binders and Asphalt Mixture Permanent Deformation. *Road Materials and Pavement Design*, *11*(3), 653–680.

51. Delgadillo, R., Bahia, H. U., & Lakes, R. (2012). "A nonlinear constitutive relationship for asphalt binders." *Materials and Structures*, *45*, 457–473.

52. Domingos, M. D. I., Faxina, A. L., and Sc, D. (2009). “Susceptibility of Asphalt Binders to Rutting : Literature Review.” *Journal of Materials in Civil Engineering*, 1–8.

53. Dongre, R., D’Angelo, J., Reinke, G., and Shenoy, A. (2007). “New Criterion for Superpave High-Temperature Binder Specification.” *Transportation Research Record:Journal of Transportation Research Board*, 1875, 22-32.

54. Doraiswamy, D. (1991). “The Cox–Merz rule extended: A rheological model for concentrated suspensions and other materials with a yield stress.” *Journal of Rheology*, 35(4), 647–685.

55. Doraiswamy, D. (2002). “The origins of rheology: a short historical excursion.” *Rheology Bulletin*, 71, 1–9.

56. Dubois, E., Mehta, D. Y., & Nolan, A. (2014). "Correlation between multiple stress creep recovery (MSCR) results and polymer modification of binder." *Construction and Building Materials*, *65*, 184–190.

57. Eyring, H. (1935). “The Activated Complex in Chemical Reactions.” *The Journal of Chemical Physics*, 3(2), 107.

58. Fecarotti, C., Celauro, C., and Pirrotta, A. (2012). “Linear ViscoElastic (LVE) Behaviour of Pure Bitumen via Fractional Model.” *Procedia - Social and Behavioral Sciences*, SIIV-5th International Congress - Sustainability of Road Infrastructures , 53, 450–461.

59. Ferry, J.D. (1980). "*Viscoelastic Properties of Polymers."*, 3rd ed., JW, NY.

60. Fwa, T.F. & Kumar, C. (1991). "Pavement Performance and Life-Cycle Cost Analysis.", *J Transp Eng*, *117*, 33–46.

61. Fwa, T. F., Pasindu, H. R., and Ong, G. P. (2012). “Critical Rut Depth for Pavement Maintenance Based on Vehicle Skidding and Hydroplaning Consideration.” *Journal of Transportation Engineering*, 138(4), 423–429.

62. Fwa, T. F., Tan, S. A., & Zhu, L. Y. (2004). "Rutting Prediction of Asphalt Pavement Layer Using Model". *Journal of Transportation Engineering*, *130*(5), 675–683.

63. García-Morales, M., Partal, P., Navarro, F. J., and Gallegos, C. (2006). "Effect of waste polymer addition on the rheology of modified bitumen." *Fuel*, 85(7-8), 936–943.

64. García-Morales, M., Partal, P., Navarro, F. J., Martínez-Boza, F., Gallegos, C., González, N., González, O., and Muñoz, M. E. (2004). "Viscous properties and microstructure of recycled eva modified bitumen." *Fuel*, 83(1), 31–38.

65. González, O., Muñoz, M. E., Santamaría, a., García-Morales, M., Navarro, F. J., and Partal, P. (2004). "Rheology and stability of bitumen/EVA blends." *European Polymer Journal*, 40(10), 2365–2372.

66. Goodrich, J.L. (1988). "Asphalt and Polymer Modified Asphalt Properties Related to the Performance of Asphalt Concrete Mixes." *Proceedings of the Association of Asphalt Paving Technologists*, Vol. 57, pp. 116 – 175.

67. Gul, W. A., & Guler, M. (2014). "Rutting susceptibility of asphalt concrete with recycled concrete aggregate using revised Marshall procedure". *Construction and Building Materials*, *55*, 341–349.

68. Hafeez, I., & Ahmed, M. (2014). "Creep Compliance : A Parameter to Predict Rut Performance of Asphalt Binders and Mixtures." *Arabian Journal for Science and Engineering*, *39*(8), 5971–5978.

69. Hafeez, I., and Kamal, M. . (2014). "An Experimental-Based Approach to Predict Asphalt Mixtures Permanent Deformation Behavior." *Arabian Journal for Science and Engineering*, 39(12), 8681–8690.

70. Harvey, J. T., Deacon, J. A., Tsai, B., & Monismith, C. L. (1995). "*Fatigue Performance of Asphalt Concrete Mixes and its Relationship to Asphalt Concrete Pavement Performance in California"*. Report: RTA-65W485-2, California Department of Transportation,Berkley.

71. Hintz, C., and Bahia, H. (2013). “Understanding Mechanisms Leading to Asphalt Binder Fatigue in Dynamic Shear Rheometer.” *Road Materials and Pavement Design*, 14(2).

72. Hintz, C., & Bahia, H. (2013). "Simplification of Linear Amplitude Sweep Test and Specification Parameters." *Transportation Research Record:Journal of Transportation Research Board*, 2370, 10-16.

73. Hintz, C., Velasquez, R., Johnson, C., and Bahia, H. (2011). “Modification and Validation of Linear Amplitude Sweep Test for Binder Fatigue Specification.” *Transportation Research Record: Journal of the Transportation Research Board*, 2207, 99–106.

74. Huang, H. W. (1990). “The use of bottom ash in highway embankments, subgrade and subbases.” *Joint Highway Research Project, Final Report, FHWA/IN/JHRP-90/4*.

75. Huang, W., & Tang, N. (2015). "Characterizing SBS modified asphalt with sulfur using multiple stress creep recovery test." *Construction and Building Materials, 93*, 514–521.

76. Huang, Y. H. (2010). "*Pavement Analysis and Design* (second edition)." Pearson Education.

77. Huner, M. H., & Brown, E. R. (2001). "*Effects of re-heating and compaction temperature on hot mix asphalt volumetric*". North Central Association Technology Report, 01-04.

78. IRC (2010). "Guidlines on Use of Modified Bitumen in Road Construction.", *SP-53*, Indian Roads Congress, New Delhi.

79. IRC (2008). "Tentative Specifications for Stone Matrix Asphalt", *SP-79*, Indian Roads Congress, New Delhi.

80. Isacsson, U. L. F., & Lu, X. (1999). "Characterization of bitumens modified with SEBS , EVA and EBA polymers", *Journal of Material Science, 4*, 3737–3745.

81. Jayakody, S., Chaminda, G., and Kumar, A. (2014). “Assessment of recycled concrete aggregates as a pavement material.” *Geomechanics and Engineering*, 6(3), 235–248.

82. Jayakody, S., Chaminda, G., Ramanujam, J., and Kumar, A., 2013. "Laboratory study on performance of recycled concrete aggregates blended with reclaimed asphalt pavement as pavement granular material." *In*: *Third International Conference-Geotechnique,Construction,Materials and Environment*: The Geomate International Society, 389–393, Nagoya, Japan.

83. John, R., & Whiteoak, D. (2003). "*Shell Bitumen Handbook* (Fifth Edition)." Thomas Telford.

84. Johnson, C., Bahia, H., & Wen, H. (2009). "Practical Application of Viscoelastic Continuum Damage Theory to Asphalt Binder Fatigue Characterization." *Journal of the Association of Pavemnent Technologists, 78*, 597-638.

85. Johnson, C. M., Bahia, H. U., & Coenen, A. (2009). "Comparison of Bitumen Fatigue Testing Procedures Measured in Shear and Correlations with Four-Point Bending Mixture Fatigue." *2nd Workshop on Four Point Bending, Guimaraes, Portugal*, (1).

86. Kakade, V. B., Reddy, I. S., & Reddy, M. A. (2013). "Identification of rheological parameters of modified binders to predict rutting behavior of bituminous concrete mixes." *Indian Highways*, *41*(11), 9-18

87. Kandhal, P. S., and Cooley, L. (2003). "Accelerated Laboratory Rutting Test: Evaluation of the Asphalt Pavement Analyzer", *National Cooperative Highway Research Program*, Report 508, Washington, DC.

88. Khalid, H. A. (2000). "A comparison between bending and diametral fatigue tests for bituminous materials." *Materials and Structures*, *33*(7), 457–465.

89. Khan, M. A., Mehrotra, A., and Svrcek, W. (1984). “Viscosity models for gas-free Athabasca bitumen.” *Journal of canadian petroleum technology*, 23 , pp. 47–53.

90. Kim, Y. R. (2008). “*Modeling of asphalt concrete”* , 1st Ed., 11, McGraw-Hill, New York.

91. Kim, Y.-R., and Little, D. N. (2004). “Linear Viscoelastic Analysis of Asphalt Mastics.” *Journal of Materials in Civil Engineering*, 16(2), 122–132.

92. Kumar, A., and S.Veeraragavan, A. (2012). “Rheological and Rutting Characterization of Asphalt Mixes with Modified Binders.” *Journal of Testing and Evaluation*, 40(1), 103713.

93. Kumar, S., Amarnath, M. S., & Udayakumar, L. (2010). "Applications of Scrap Steel in High Performance Cement Concrete Pavements - An Experimental Study and Life Cycle Cost Analysis." *International Journal of Pavements*, *9*(1-2-3), 110-119.

94. Kutay, M. E. "VECD (Visco-Elastic Continuum Damage): State-of-the-art technique to evaluate fatigue damage in asphalt pavements." *Online Presentation*, Michigan State University.

95. Lakes, R. S. (2009). *Viscoelastic Materials*. Cambridge University Press.

96. Lekha, B. M., Ravi Shankar, a. U., and Sarang, G. (2013). “Fatigue and Engineering Properties of Chemically Stabilized Soil for Pavements.” *Indian Geotechnical Journal*, 43(1), 96–104.

97. Li, Q., Ni, F., Gao, L., Yuan, Q., & Xiao, Y. (2014). "Evaluating the rutting resistance of asphalt mixtures using an advanced repeated load permanent deformation test under field conditions". *Construction and Building Materials*, *61*, 241–251.

98. Li , S.C., Jarvela , P.K., & Jarvela , P.A. (1997). "A comparison between apparent viscosity and dynamic complex viscosity for polypropylene/maleated polypropylene blends" . *Polym. Eng. Sci.*, 37 , 18 – 23.

99. Liu, G., Nielsen, E., Komacka, J., Greet, L., and Ven, M. van de. (2014). “Rheological and chemical evaluation on the ageing properties of SBS polymer modified bitumen: From the laboratory to the field.” *Construction and Building Materials*, 51, 244–248.

100. Lu, X. , Isacsson, U. , and Ekblad, J. (1999). “Rheological properties of SEBS, EVA and EBA polymer modified bitumens.” *Mater. Struct. ,* 32 (2), 131–139.

101. Lu, X., Isacsson, U. (2000). "Modification of road bitumens with thermoplastic

polymers.", *Polym Test, 20*, 77–86.

102. Lu, X., and Isacsson, U. (2002). “Effect of ageing on bitumen chemistry and rheology.” *Construction and Building Materials*, 16(1), 15–22.

103. Marasteanu, M., Clyne, T., McGraw, J., Li, X., and Velasquez, R. (2005). “High-Temperature Rheological Properties of Asphalt Binders.” *Transportation Research Record*, 1901(1), 52–59

104. Marasteanu, M. , and Anderson, D. (1996). “Time-temperature dependency of asphalt binders—An improved model.” *Electron. J. Assoc. Asph. Paving Technol.* , **65** , 408–448.

105. Martínez-Boza, F., Partal, P., Conde, B., and Gallegos, C. (2001). “Steady-state flow behaviour of synthetic binders.” *Fuel*, 80, 357–365.

106. Mas, R., and Magnin, A. (1997). “Experimental validation of steady shear and dynamic viscosity relation for yield stress fluids.” *Rheologica Acta*, 55, 49–55.

107. Masad, E., Somadevan, N., Bahia, H. U., & Kose, S. (2001). "Modeling and Experimental Measurements of Strain Distribution in Asphalt Mixes." *Journal of Transportation Engineering*, *127*(6), 477–485.

108. Mastrofini, D., and Scarsella, M. (2000). “Application of rheology to the evaluation of bitumen ageing.” *Fuel*, 79(9), 1005–1015.

109. Maxwell, J. C. (1866). "*Linear Viscoelasticity."* Shear Rheometry-Drag Flows, 109-209.

110. Merusi, F. (2012). "Delayed mechanical response in modified asphalt binders. Characteristics, modeling and engineering implications." *Road Materials and Pavement Design*, *13*(2), 321–345.

111. Merusi, F., Giuliani, F., and Polacco, G. (2012). “Linear Viscoelastic Behaviour of Asphalt Binders Modified with Polymer/clay Nanocomposites.” *Procedia - Social and Behavioral Sciences*, Elsevier B.V., 53, 335–345.

112. Miner, M. A. (1945). "Cumulative Damage in Fatigue." *Journal of Applied Mechanics*, *12*(9), A159–A164.

113. Moalla Hamed, F. K. (2010). "*Evaluation of Fatigue Resistance for Modified Asphalt Concrete Mixtures Based on Dissipated Energy Concept*." The University of Darmstadt, PhD Thesis.

114. Molenaar, A. (2007). "Prediction of Fatigue Cracking in Asphalt Pavements: Do We Follow the Right Approach?" *Transportation Research Record: Journal of the Transportation Research Board*, *2001*, 155–162.

115. Monismith, C. L., Tangella, S. C. S., Craus, J., & Deacon, J. A. (1990). "Summary Report on Fatigue Response of Asphalt Mixtures." *Report TM-UCB-A-003A-89-3*,University of California Berkley.

116. Morea, F., Agnusdei, J. O., and Zerbino, R. (2010). "Comparison of methods for measuring zero shear viscosity in asphalts." *Materials and Structures*, 43, 499–507.

117. Morea, F., Zerbino, R., & Agnusdei, J. (2013). "Wheel tracking rutting performance estimation based on bitumen Low Shear Viscosity (LSV), loading and temperature conditions". *Materials and Structures*, *47*(4), 683–692.

118. Mui, J. (2008). "*Viscoelastic-viscoplastic model to predict creep in a random chopped mat thermoplastic composite."* University of Waterloo, Masters Thesis.

119. Munera, J. C., and Ossa, E. A. (2014). "Polymer modified bitumen: Optimization and selection." *Materials & Design*, 62, 91–97.

120. Naskar, M., Reddy, K. S., Chaki, T. K., Divya, M. K., and Deshpande, a. P. (2012). "Effect of ageing on different modified bituminous binders: comparison between RTFOT and radiation ageing." *Materials and Structures*, 46(7), 1227–1241.

121. Navarro, F. J., Partal, P., Martínez-Boza, F., and Gallegos, C. (2004). "Thermo-rheological behaviour and storage stability of ground tire rubber-modified bitumens." *Fuel*, 83(14-15), 2041–2049.

122. Nuñez, J. Y. M., Domingos, M. D. I., & Faxina, A. L. (2014). "Susceptibility of low-density polyethylene and polyphosphoric acid-modified asphalt binders to rutting and fatigue cracking." *Construction and Building Materials*, *73*, 509–514.

123. Özen, H. (2011). "Rutting evaluation of hydrated lime and SBS modified asphalt mixtures for laboratory and field compacted samples." *Construction and Building Materials*, 25(2), 756–765.

124. Panda, M., and Mazumdar, M. (1999). "Engineering Properties of EVA-Modified Bitumen Binder for Paving Mixes." *Journal of Materials in Civil Engineering*, 11(2), 131–137.

125. Panda, M., & Mazumdar, M. (2002). "Utilization of Reclaimed Polyethylene in Bituminous Paving Mixes." *Journal of Materials in Civil Engineering*, *14*(6), 527–530.

126. Papanicolaou, G. C., Zaoutsos, S. P., & Cardon, A. H. (1999). "Further development of a data reduction method for the nonlinear viscoelastic characterization of FRPs." *Composites Part A: Applied Science and Manufacturing*, *30*(7), 839–848.

127. Park, S., Kim, Y., and Schapery, R. (1996). "A viscoelastic continuum damage model and its application to uniaxial behaviour of asphalt concrete." *Mechanics of Materials;*, 24, 241–255.

128. Partal, P., Martínez-Boza, F., Conde, B., and Gallegos, C. (1999). "Rheological characterisation of synthetic binders and unmodified bitumens." *Fuel*, 78, 1–10.

129. Pasquini, E., Canestrari, F., Cardone, F., and Santagata, F. a. (2011). "Performance evaluation of gap graded Asphalt Rubber mixtures." *Construction and Building Materials*, Elsevier Ltd, 25(4), 2014–2022.

130. Pell, P., & Cooper, K. (1975). "The Effect of Testing and Mix Variables on the Fatigue Performance of Bituminous Materials." *Journal of the Association of Asphalt Paving Technologists*, *44*, 1–37.

131. Perez-Lepe, A. P. , Martinez-Boza, F. J. , Gallegos, C. , Gonzales, O. , Munoz, M. E. , and Santamaria, A. (2003). "Influence of the processing conditions on the rheological

behaviour of polymer-modified bitumen." *Fuel* , 82 (11), 1339–1348.

132. Petersen J.C., Robertson J.F., Branthaver J.F., Harnsberger P.M ., Duvall JJ Kim S.S. (1994). "*Binder characterization and evaluation",* SHRP-A-367, Strategic Highways Research Program, National Research Council Washington, D.C.

133. Punith, V. S., Veeraragavan, A., and Amirkhanian, S. N. (2011). "Evaluation of reclaimed polyethylene modified asphalt concrete mixtures." *International Journal of Pavement Research and Technology*, 4(1), 1–10.

134. Qi-sen, Z., Yu-liang, C., and Xue-lian, L. (2009). "Rutting in Asphalt Pavement under Heavy Load and High Temperature." *GeoHunan International Conference*, 39–48.

135. Rahi, M., Fini, E.H., Asce, M., Hajikarimi, P., & Nejad, F.M. (2014). "Rutting Characteristics of Styrene-Ethylene / Propylene-Styrene Polymer Modified Asphalt." *J Mater Civ Eng*, *27*, 1–5.

136. Rahi, M., Fini, E.H., Asce, M., Hajikarimi, P., & Nejad, F.M. (2014). "Rutting Characteristics of Styrene-Ethylene / Propylene-Styrene Polymer Modified Asphalt." *J Mater Civ Eng*, *27*, 1–5.

137. Rahimzadeh, B. (2002). "Linear and Non-Linear Viscoelastic Behaviour of Binders and Asphalts." , *PhD Thesis*, The University of Nottingham.

138. Rahi M., Hajikarni, P., Fereidoon, M.N. (2015). "Comparing different rutting specification parameters using high temperature characteristics of rubber-modified asphalt binders", *Road Materials and Pavement Design, 16*(4), 751-766.

139. Reddy, I. S., Reddy, M. A., & Pandey, B. B. (2011). "Development of rutting criteria for bituminous mixes using wheel tracking device." *Highway Research Journal*, *4*(2), 1-8.

140. Reddy, S., & Reddy, M. A. (2011). "Low cost device for evaluating rutting characteristics of bituminous mixes." *Indian Highways*, *39*(3). 51-58.

141. Rek, V., Jurkas, K., Ocelic, V., & Rakus, J. (2013). "Rheological Properties and Stability of Ethylene Vinyl Acetate Polymer-Modified Bitumen." *Polymer Engineering Science, 53* (2013), 2276-2283.

142. Roberts, F. L., Kandhal, P. S., Brown, E. R., Lee, D.-Y., & Kennedy, T. W. (1996). "*Hot Mix Asphalt Materials, Mixture Design and Cinstruction* (Second Edition)." Lanham, Maryland: NAPA Research and Education Foundation.

143. Rowe, G. M., D'Angelo, J. A., & Sharrock, M. J. (2002). "Use of the zero shear viscosity as a parameter for the high temperature binder specification parameter." Journal of Applied Asphalt Binder Technology, 2(2). 29-51.

144. Roylance, D. (2001). "Stress-Strain Curves." *MIT Press,* Cambridge, MA.

145. Saal, R. , and Labout, W. (1940). "Rheological properties of asphaltic bitumen." *J. Phys. Chem.* , 44 (2), 149–165.

146. Safaei, F., Lee, J. S., Nascimento, L., Hintz, C., & Kim, Y. R. (2014). "Implications of warm-mix asphalt on long-term oxidative ageing and fatigue performance of asphalt binders and mixtures." *Road Materials and Pavement Design*, 15(Special Issue), 45–61.

147. Santagata, E., Baglieri, O., Dalmazzo, D., & Tsantilis, L. (2013). "Evaluation of the anti-rutting potential of polymer-modified binders by means of creep-recovery shear tests." *Materials and Structures*, *46*(10), 1673–1682.

148. Schapery, R. A. (1997). "Nonlinear Viscoelastic and Viscoplastic Constitutive Equations Based on Thermodynamics." *Mechanics of Time-Dependent Materials, 1*, 209–240.

149. Selvamohan, S., Zaman, M., and Laguros, J. . (2007). "A Laboratory Evaluation of Unmodified and Polymer Modified Performance-Grade Binders with Anti-Stripping Additives." *Journal of Engineering, Computing and Architechture*, 1(2), 1–11.

150. Sengoz, B., and Isikyakar, G. (2008). "Evaluation of the properties and microstructure of SBS and EVA polymer modified bitumen." *Construction and Building Materials*, 22(9), 1897–1905.

151. Shafabakhsh, G. H., Sadeghnejad, M., & Sajed, Y. (2014). "Case study of rutting performance of HMA modified with waste rubber powder." *Case Studies in Construction Materials, 1*, 69–76.

152. Shan, L., Tan, Y., and Richard Kim, Y. (2012). “Applicability of the Cox–Merz relationship for asphalt binder.” *Construction and Building Materials*, 37, 716–722.

153. Shankar, A. U. R., and Suresha, S. N. (2006). “Strength Behaviour of Geogrid Reinforced Shedi Soil Subgrade and Aggregate System.” *Road Materials and Pavement Design*, 7(3), 313–330.

154. Sharma, V., Chandra, S., and Choudhary, R. (2010). “Characterization of Fly Ash Bituminous Concrete Mixes.” *Journal of Materials in Civil Engineering*, 22(12), 1209–1216.

155. Shell. (1978). "*Shell Pavement Design Manual: Asphalt Pavements and Overlays for Road Traffic*." London: Shell International Petroleum Co., Ltd.

156. Shen, S. (2006). "*Dissipated Energy Concepts for HMA Performance: Fatigue and Healing."* University of Illinois at Urbana-Champaign, PhD Thesis.

157. Shenoy, A. (2001). "Refinement of the Superpave Specification Parameter for Performance Grading of Asphalt." *Journal of Materials in Civil Engineering*, *127*(8), 357–362.

158. Shenoy, A. (2004). “High Temperature Performance Grading of Asphalts through a Specification Criterion that Could Capture Field Performance.” *Journal of Transportation Engineering*, American Society of Civil Engineers, 130(1), 132–137

159. Shenoy, A. V, Saini, D. R., & Nadkarni, V. M. (1982). "Rheograms for asphalt from single viscosity measurement." *Rheologica Acta*, *339*, 333–339.

160. Singh, M. (2012). "*Strength Characteristics of Modified Bitumen With Various Aggregates."* Indian Institute of Technology, Roorkee, (PhD Thesis).

161. Singh, M., Kumar, P., & Anupam, A.K. (2012). "Effect of type of aggregate on permanent deformation of bituminous concrete mixes.", *Road Materials and Pavement Design*, *8*, 1-17.

162. Singh, P., & Choudhary, R. (2014). "Determination of Mixing and Compaction Temperatures of Asphalt Concrete Mixes by Density Analysis." In *International*

Conference on Sustainable Civil Infrastructure (pp. 17–18). Hyderabad: ASCE India Section.

163. Soenen, H., Visscher, J.D., Tanghe, T., Vanelstraete, A., Redelius, P. (2014). "Selection of Binder Performance Indicators for Asphalt Rutting Based on Triaxial and Wheel Tracking Tests", *Journal of the Association of Asphalt Paving Technologists, 75,* 165-201

164. Sousa, J., Pais, J., Prates, M., Barros, R., Langlois, P., & Leclerc, A.-M. (1998). "Effect of Aggregate Gradation on Fatigue Life of Asphalt Concrete Mixes." *Transportation Research Record: Journal of the Transportation Research Board, 1630*(1), 62–68.

165. Stastna, J., Zanzotto, L., and Vacin, O. J. (2003). "Viscosity function in polymer-modified asphalts." *Journal of Colloid and Interface Science*, 259, 200–207.

166. Stuart, K. D., Mogawer, W. S., & Romero, P. (1999). "Validation of asphalt binder and mixture tests that measure rutting susceptibility using the accelerated loading facility." *Federal Highway Administration*. Washington, DC.

167. Suo, Z., & Wong, W. G. (2009). "Analysis of fatigue crack growth behavior in asphalt concrete material in wearing course." *Construction and Building Materials*, *23*(1), 462–468.

168. Suresha, S. N., Asce, S. M., George, V., and Shankar, A. U. R. (2009). "Evaluation of Properties of Porous Friction Course Mixes for Different Gyration Levels." *Journal of Materials in Civil Engineering*, 21(12), 789–796.

169. Sybilski, D. (2015). "Zero-Shear Viscosity of Bituminous Binder and Its Relation to Bituminous Mixture's Rutting Resistance." *Transportation Research Record: Journal of the Transportation Research Board*. *1535,* 15-21

170. Tangella, S. C. S., Craus, J., Deacon, J. A, & Monismith, C. L. (1990). "Summary Report on Fatigue Response of Asphalt Mixtures." *Report TM-UCB-A-003A-89-3*,University of California Berkley.

171. Tarefder, R. A., Zaman, M., & Hobson, K. (2003). A Laboratory and Statistical Evaluation of Factors Affecting Rutting. *International Journal of Pavement Engineering*, *4*(1), 59–68.

172. Tarefder, R., White, L., & Zaman, M. (2006). "Development and Application of a Rut Prediction Model for Flexible Pavement." *Transportation Research Record: Journal of the Transportation Research Board*.

173. The Asphalt Institute. (1982). Research and Development of Asphalt Institute's Thickness Design Manual. Ninth Edition, *Research Report No. 82-2.*

174. Uddin, W. (2003). "Viscoelastic Chracterization of Polymer-Modified Asphalt Binders of Pavement Applications." *Applied Rheology*, 13, 191–199.

175. Uddin, W., and Garza, S. (2004). "Pavement Construction Effects on Subgrade Resilient Modulus and Validation by 3D-FE Simulation." *Road Materials and Pavement Design*, 5(3), 355–371.

176. Uddin, W., and Nanagiri, Y. (2002). "Performance of Polymer-Modified Asphalt Overlays in Mississipi Based on Mechanistic Analysis and Field Evaluation." *International Journal of Pavements*, 1(1).

177. Ukwuoma, O., and Ademodi, B. (1999). "The effects of temperature and shear rate on the apparent viscosity of Nigerian oil sand bitumen." *Fuel Processing Technology*.

178. De Visscher, J., Soenen, H., Vanelstraete, a, and Redelius, P. (2004). "A Comparison of the Zero Shear Viscosity From Oscillation Tests and the Repeated Creep Test." *Proceedings of the 3Rd Eurasphalt and Eurobitume Congress Held Vienna*, 2, 1501–13.

179. Vlachovicova, Z., Wekumbura, C., Stastna, J., and Zanzotto, L. (2007). "Creep characteristics of asphalt modified by radial styrene-butadiene-styrene copolymer." *Construction and Building Materials*, 21, 567–577.

180. Wang, C., and Zhang, J. (2014). "Evaluation of Rutting Parameters of Asphalt Binder Based on Rheological Test." *International Journal of Engineering and Technology*, 6(1), 30–33.

181. Ward, I. ., & Sweeney, J. (2013). *Mechanical Properties of Solid Polymers*. Wiley-Interscience, New York.

182. Wen, G., Zhang, Y., Zhang, Y., Sun, K., and Fan, Y. (2002). "Rheological characterization of storage-stable SBS-modified asphalts." *Polymer Testing*, 21(3), 295–302.

183. West, R. C., Watson, D. E., & Turner, P. A. (2010). "Mixing and Compaction Temperatures of Asphalt Binders in Hot-Mix Asphalt." NCHRP *Report-648.*

184. Williams, M. L., Landel, R. F., and Ferry, J. D. (1955). "The Temperature Dependence of Relaxation Mechanisms in Amorphous Polymers and Other Glass-forming Liquids1." *Journal of the American Society*, 77(7), 3701–3707.

185. Winter, H. H. (2008). "Three views of viscoelasticity for Cox–Merz materials." *Rheologica Acta*, 48(3), 241–243.

186. Wu, H., Huang, B., and Shu, X. (2014). "Characterizing fatigue behavior of asphalt mixtures utilizing loaded wheel testers." *Journal of Materials in Civil Engineering*, 26(1), 152–159.

187. Xu, T., Wang, H., Li, Z., & Zhao, Y. (2014). "Evaluation of permanent deformation of asphalt mixtures using different laboratory performance tests." *Construction and Building Materials*, *53*, 561–567.

188. Yang, R. R., Huang, W. H., & Tai, Y. T. (2005). "Variation of Resilient Modulus with Soil Suction for Compacted Subgrade Soils." *Transportation Research Record:Journal of Transportation Research Board*, *1913*, 99–106.

189. Yang, S. R., & Huang, H. W. (2007). "Permanent deformatiom and critical stress of cohesive soil under repeated loading." *Transportation Research Record:Journal of Transportation Research Board*, *2016*, 23–30.

190. Yang, X., & You, Z. (2015). "High temperature performance evaluation of bio-oil modified asphalt binders using the DSR and MSCR tests." *Construction and Building Materials*, *76*, 380–387.

191. Ye, Y., Yang, X., & Chen, C. (2010). "Modified Schapery's Model for Asphalt Sand."

Journal of Engineering Mechanics, *136*, 448–454.

192. Yero, S., and Hainin, M. (2011). “Viscosity Characteristics of Modified Bitumen.” *ARPN Journal of Science and Technology*, 2(5), 500–503.

193. Yoo, P. J., & Al-Qadi, I. L. (2010). "A strain-controlled hot-mix asphalt fatigue model considering low and high cycles.", *International Journal of Pavement Engineering*, *11*(6), 565–574.

194. Yusoff, N. I. M. (2012). “Modelling the Linear Viscoelastic Rheological Properties of Bituminous Binders.” *PhD Thesis*, The University of Nottingham.

195. Yusoff, N. I. M., Jakarni, F. M., Nguyen, V. H., Hainin, M. R., and Airey, G. D. (2013). “Modelling the rheological properties of bituminous binders using mathematical equations.” *Construction and Building Materials*, 40, 174–188.

196. Yusoff, N. I. M., Shaw, M. T., and Airey, G. D. (2011). “Modelling the linear viscoelastic rheological properties of bituminous binders.” *Construction and Building Materials*, 25(5), 2171–2189.

197. Yut, I., and Zofka, A. (2014). “Correlation between rheology and chemical composition of aged polymer-modified asphalts.” *Construction and Building Materials*, 62, 109–117.

198. Zhang, J., Sabouri, M., Guddati, M. N., & Kim, Y. R. (2013). "Development of a failure criterion for asphalt mixtures under fatigue loading.", *Road Materials and Pavement Design*, *14*(3), 1–15.

199. Zhou, F., Mogawer, W., and Li, H. (2012). “Evaluation of Fatigue Tests for Characterizing Asphalt Binders.” *Journal of Materials in civil Engineering*, *25*(5), 610–617.

200. Zhu, J., Birgisson, B., and Kringos, N. (2014). “Polymer modification of bitumen: Advances and challenges.” *European Polymer Journal*, *54*, 18–38.

201. Ziari, H., Babagoli, R., & Akbari, A. (2014). "Investigation of fatigue and rutting performance of hot mix asphalt mixtures prepared by bentonite-modified bitumen.", *Road Materials and Pavement Design*, *16*(3), 101–118.

202. Zoorob, S. E., Castro-Gomes, J. P., and Pereira Oliveira, L. a. (2012). “Assessing low shear viscosity as the new bitumen Softening Point test.” *Construction and Building Materials*, *27*(1), 357–367.

203. Zoorob, S.E., Castro-Gomes, J.P., Pereira Oliveira, L. a., & O’Connell, J. (2012). "Investigating the Multiple Stress Creep Recovery bitumen characterisation test." *Constr Build Mater*, *30*, 734–745.

204. Zupančič, A., and Žumer, M. (2002). “Rheological examination of temperature dependence of conventional and polymer-modified road bitumens.” *The Canadian Journal of Chemical Engineering*, *80* (2), 253–263.

List of Publications

Published in Journals

1. **Saboo, N.** and Kumar, P. (2015) *"Optimum Blending Requirements for EVA Modified Binder"*, **International Journal of Pavement Research and Technology, Chinese Society of Pavement Engineering,** Vol. 8, No. 3, pp 172-178.
2. **Saboo, N.** and Kumar, P. (2015) *"Study of flow behaviour for predicting mixing temperature of bitumen"*, **Construction and Building Materials, Elsevier,** Vol. 87, No. 15, pp 38-44.
3. **Saboo, N.** and Kumar, P. (2015) *"A study on creep and recovery behaviour of asphalt binders"*, **Construction and Building Materials, Elsevier,** Vol. 96, No. 2015, pp 632-640.
4. Kumar, P., Mishra S., **Saboo N. (2013) "***A laboratory study on short term and long term ageing of bitumen using modifiers"*, **Indian Highways, Indian Roads Congress**, Vol. 41, No. 12, pp 41-52.

Accepted for Journals

5. **Saboo, N.** and Kumar, P. *"Analysis of Different Test Methods for Quantifying Rutting Susceptibility of Asphalt Binders"*, **Journal of Materials in Civil Engineering, ASCE** (accepted).
6. **Saboo, N.** and Kumar, P. (2015) *"Rheological Study on Mixing Temperatures of Modified Bitumen"*, **Transportation in Developing Economics, Springer** (accepted).
7. **Saboo, N.** and Kumar, P. (2015) *"Equivalent Slope Method for Construction of Master Curves"*, **Indian Highways, Indian Roads Congress** (accepted).

Under Review in Journals

8. **Saboo, N.** and Kumar, P. *"Rheological investigation of SBS and EVA modified bitumen using MSCR and LAS test"*, **Materials and Structures, Springer.**
9. **Saboo, N.,** Pratim Das, B., Praveen Kumar. *"New Phenomenological Approach for Modelling Fatigue Life of Bituminous Mixes"*, **Construction and Building Materials, Elsevier.**

10. **Saboo, N.** and Kumar, P. *"Study of Flow Behavior for Rheological Modelling of Bitumen"*, **International Journal of Pavement Research and Technology, Chinese Society of Pavement Engineering.**
11. **Saboo, N.** and Kumar P. *"Study of Creep and Recovery for Modified Binders"* **Indian Highways, Indian Roads Congress.**
12. Kumar, P., **Saboo, N.,** Radhika *"Effect of Sulphur Mixing on Storage Modulus of SBS Modified Bitumen"*, **Indian Highways, Indian Roads Congress.**
13. Kumar, P., **Saboo, N.,** Pratim Das, B. *"A Comparative Study of Dense and Gap Graded Mixes prepared using Modified binders"*, **Indian Highways, Indian Roads Congress.**
14. Kumar P., Tiwari, S., **Saboo, N.** *"Effect of Temperature on Deflection values obtained using Falling Weight Deflectometer"*, **Indian Highways, Indian Roads Congress.**
15. Kumar, P., Ransinchung, G.D.R., Mehta, M., **Saboo, N.** *"A study on Performance of Bituminous Mixes using Falling Weight Deflectometer (FWD)"*, **Indian Highways, Indian Roads Congress.**

In Pipeline for Journals

16. **Saboo, N.** and Kumar, P. *"Effect of Spindle Geometry on Rheological Measurements in Dynamic Shear Rheometer"*, **Road Materials and Pavement Design, Taylor & Francis.**
17. **Saboo, N.** and Kumar, P. *"Performance Evaluation of SBS and EVA Modified Asphalt Binders and Mixes"*, **Journal of Materials in Civil Engineering, ASCE.**
18. **Saboo, N.** and Kumar, P. *"Performance Characteristics of Modified Binders at Different Temperatures"*, **International Journal of Pavement Engineering, Taylor & Francis.**
19. **Saboo, N.** and Kumar, P. *"Shift Factor Analysis for Construction of Master Curves for Asphalt Binders"*, **Construction and Building Materials, Elsevier.**
20. Singh, B., **Saboo, N.,** Kumar, P. *"Modelling the Non-linear Rheological Characteristics of Asphalt Binders: A Theoretical Approach"*, **Construction and Building Materials, Elsevier.**

Conferences

21. **Saboo, N.** and Kumar, P. *"Rheological Investigations of Sulfur Modified Bitumen"*, **ICSCI, ASCE India Section**, Oct 17-18, Hyderabad India, 2014, pp 703-713.
22. **Saboo, N.** and Kumar, P. *"Creep and Recovery as a Function of Conventional Binder Properties"*, **3rd Conference of the Transportation Research Group of India** (accepted).